COUNTERACTION OF ANTIVIRAL MEMBRANE PROTEINS BY PRIMATE LENTIVIRUSES

Weinelt, Julia

Awarding institution:
King's College London

COUNTERACTION OF ANTIVIRAL MEMBRANE PROTEINS BY PRIMATE LENTIVIRUSES

Julia Weinelt

A thesis submitted to the University of London for the degree of Doctor of Philosophy

Department of Infectious Diseases
King's College London
School of Medicine

Declaration

I, Julia Weinelt, confirm that the work presented in this thesis is my own. Where information has been derived from other sources, I confirm that this has been indicated in the thesis.

London, 4th January 2016

Julia Weinelt

Abstract

During viral infection, HIV encounters a number of cellular proteins, so-called restriction factors, that inhibit its replication at different stages of the viral life cycle. One such factor is tetherin (CD317/BST2), which is an interferon inducible transmembrane protein that inhibits virus release from infected cells by tethering budding virions to the plasma membrane. Tetherin antagonism is highly conserved and various enveloped viruses encode antagonist proteins including HIV-1 Vpu, HIV-2 Env, SIV Nef or KSHV K5. Tetherin is expressed as two isoforms that differ in the length of their cytoplasmic tail. The longer isoform contains an important tyrosine based endocytic and signalling motif that is not present in the shorter one. The data presented in this thesis show that Vpu proteins from the pandemic HIV-1 group M were the only lentiviral tetherin antagonists tested that exhibited differential activity against the two isoforms. These Vpu alleles are considerably more active against the long, signalling form of human tetherin. In addition, this group of Vpu proteins target human long tetherin for endosomal degradation. This adaption of Vpu may have implications for the recent evolution of HIV-1 and the role of tetherin in the pathogenesis of pandemic HIV/AIDS.

Vpu binds to and antagonises tetherin by preventing it from reaching the cell surface and re-routing it for endosomal degradation. This requires the phosphorylation of two serines in the cytoplasmic tail of Vpu that recruit the $SCF^{\beta TRCP1/2}$ ubiquitin ligase complex. However, whether the final ubiquitin-dependent degradation of tetherin is essential for Vpu to counteract its antiviral activity is unclear. Data presented in this thesis aims to re-evaluated this question and indicates that Vpu phosphorylation can be decoupled from $SCF^{\beta TRCP1/2}$ recruitment and tetherin degradation. The phospho-mutant phenocopies a Vpu trafficking mutant and both are unable to bind to clathrin adaptors AP-1 or AP-2 in the presence of tetherin. Direct linkage of the Vpu mutants to the clathrin machinery rescues their function without restoring β-TrCP interaction of the phospho-mutant. Altogether, these data suggest that the phosphorylation of Vpu and its interaction with tetherin regulate its binding to clathrin adapters, which may be the crucial step in tetherin counteraction prior to ubiquitin-dependent degradation.

Recently, the multispanning transmembrane proteins serine incorporator (SERINC) 3 and 5, have been identified to potently restrict HIV-1 virion infectivity and both are targeted by the accessory protein Nef. The data presented here confirm previous findings and further characterize determinants in SERINC5 required for restriction.

Table of Contents

Table of Figures

Table of Tables

Table of Abbreviations

6HB	Six-helix bundle
AAA ATPase	ATPase-associated with various cellular activities
Ab	Antibody
ADCC	Antibody-dependent cell-mediated cytotoxicity
AGS	Aicardi-Goutières syndrome
AICD	Activation-induced cell death
AIDS	Acquired immunodeficiency syndrome
ALIX	Apoptosis-linked gene-2-interacting protein X
Amp	Ampicillin
AMSH	Associated molecule with the SH3 domain of STAM
AP	Adaptor protein
APC	Antigen-presenting cell
APOBEC3	Apolipoprotein B messenger RNA (mRNA)-editing enzyme catalytic polypeptide-like 3
APS	Ammonium persulfate
Arf	ADP ribosylation factor
ATCC	American Type Culture Collection
ATM	Ataxia-telangiectasia-mutated kinase
ATR	ATM and Rad3-related kinase
AZT	Azidothymidine
BAF	Barrier to auto-integration factor
BFA	Brefeldin A
BGH	Bovine Growth Hormone
BioID	Proximity dependent biotin identification
BirA	Biotin ligase
Bro1	BCK1-like resistance to osmotic shock protein-1
BROX	BRO1 domain and CAAX motif-containing protein
BSA	Bovineserum albumine
BST-2	Bone marrow stromal antigen 2
C-HR	Carboxyl terminal helical region
C-terminus	Carboxyl-terminus
CA	Capsid
CB	Clathrin box
CCD	Catalytic core domain
CCR5	C-C chemokine receptor type 5
CCV	Clathrin-coated vesicle
CDK7	Cyclin-dependent kinase 7
CEP55	Centrosomal protein 55kDa
cGAS	Cyclic guanosine monophosphate-adenosine monophosphate (cGAMP) synthase
CHC	Clathrin heavy chain

CHMPs	Charged multivesicular body proteins
CLC	Clathrin light chain
CPSF6	Cleavage and polyadenylation specificity factor subunit 6
CTD	Carboxyl-terminal domain
cpz	Chimpanzee
CTL	Cytotoxic T cell
CXCR4	CXC chemokine receptor type 4
CycT1	Cyclin T1
CypA	Cyclophilin A
DC	Dendritic cell
DMSO	Dimethyl sulfoxide
DNA	Deoxyribonucleic acid
dNTP	Deoxynucleotide triphosphate
DTT	Dithiothreitol
E.*coli*	E*scherichia coli*
ECL	Enhanced chemiluminescence
EDTA	Ethyleneadiaminetetraacetic acid
Env	Envelope
ER	Endoplasmic reticulum
ERAD	Endoplasmic-reticulum-associated protein degradation
ESCRT	Endosomal sorting complex required for transport
EST	Expression sequence tag
FACS	Fluorescence-activated cell sorting
FBS	Fetal bovine serum
FDA	Food and drug administration
FIV	Feline immunodeficiency virus
FRET	Fluorescence resonance energy transfer
Fv1	Friend virus susceptibility 1
GABA	ɣ-Aminobutyric acid
Gag	Group-specific antigen
GALT	Gut-associated lymphoid tissue
GFP	Green fluorescent antigen
Gln	Glutamine
gor	Gorilla
gp	Glycoprotein
GPI	Glycosylphosphatidylinositol
gsn	Greater spot-nosed monkey
H	Hour
HA	Hamagglutinin (Influenza A)
HAART	Highly active antiretroviral therapy
HHV-8	Human Herpesvirus 8
HIV-1	Human immunodeficiency virus type 1
HIV-2	Human immunodeficiency virus type 2

HLA	Human leukocyte antigen
HRP	Horseradish peroxidase
HSC	Hematopoietic stem cell
Hsp90	Heat shock protein 90
HTLV	Human T-lymphotropic virus
hu	Human
IFN	Interferon
Ig	Immunoglobulin
IN	Integrase
IRES	Internal ribosome entry site
ISG	Interferon-stimulated gene
IU	Infectious unit
Kb	Kilobase
kDa	Kilo Dalton
KSHV	Kaposi's sarcoma-associated virus
LAV	Lymphadenopathy-associated virus
LB	Luria Broth
LEDGF	Lens epithelium derived growth factor
LTR	Long terminal repeat
MA	Matrix
mAB	Monoclonal antibody
mac	Macaque
MARCH	Membrane-associated RING-CH
MFI	Mean fluorescence intensity
mg	Milligram
MHC	Major histocompatibility complex
Min	Minute
ml	Milliliter
MLV	Murine leukemia virus
mM	Millimolar
MOI	Multiplicity of infection
mRNA	Messenger RNA
MVB	Multivesicular body
NC	Nucleocapsid
NES	Nuclear export signal
NFAT	Nuclear factor of activated T-cell
NF-κB	Nuclear factor kappa B
ng	Nanogram
NK	Natural killer
NKT	Natural killer T cell
NLS	Nulcear localization signal
nM	Nanomolar
NMR	Nuclear magnetic resonance

NNRTI	Non-nucleoside reverse transcriptase inhibitor
NPC	Nuclear pore complex
NRTI	Nucleoside reverse transcriptase inhibitor
NWM	New world monkey
OD	Optical Density
ORF	Open reading frame
OWM	Old world monkey
PAMP	Pathogen-associated molecular pattern
PBMC	Peripheral blood mononuclear cell
PBS	Phosphate-buffered saline
pbs	Primer binding site
PCR	Polymerase chain reaction
pDC	Plasmacytoid dendritic cell
PDI	Protein disulphide-isomerase
PE	Phycoerythrin
PEI	Polyethylenimine
pH	Potential hydrogen
PIC	Pre-integration complex
PM	Plasma membrane
Pol	Polymerase
PPT	Polypurine tract
PR	Protease
PRR	Pattern-recognition receptor
Pts	Pan troglodytes schweinfurthii
Ptt	Pan troglodytes troglodytes
rcm	Red-capped mangabey
rh	Rhesus
RING	Really interesting new gene
RLU	Relative light unit
RNA	Ribonucleic acid
rpm	Revolution per minute
RRE	Rev response element
RT	Reverse transcriptase
SAMHD1	Sterile alpha motif- and metal-dependent phosphohydrolase domain-containing protein 1
SDS-PAGE	Sodium dodecyl sulfate polyacrylamide gel electrophoresis
Sec	Second
SEM	Standard error of the mean
SERINC	Serine incorporator
shRNA	Small hairpin RNA
SILAC	Stable isotope labelling by amino acids in cell culture
siRNA	Small interfering RNA
SIV	Simian immunodeficiency virus
sm	Sooty mangabey
SNAT-1	Sodium coupled neutral amino acid transporter 1
SU	Surface

tan	Tantalus monkey
TAR	Trans-activation response
Tat	Trans-activator of transcription
TCR	T-cell receptor
TEM	Transmission electron microscopy
TGN	Trans-Golgi network
THN	Tetherin
TLR	Toll-like receptor
TM	Transmembrane
TRIM	Tripartite motif
Tsg101	Tumor susceptibility gene 101
Ub	Ubiquitin
UBAP1	Ubiquitin-associated protein 1
UPS	Ubiquitin-proteasome system
v/v	Volume/volume
Vif	Viral infectivity factor
VLP	Virus-like particle
Vpr	Viral protein R
Vpu	Viral protein U
VS	Virological synapse
VSV-G	Vesicular stomatitis virus G glycoprotein
w/v	Weight/volume
WT	Wild-type
YFP	Yellow fluorescent protein
µg	Microgram
µl	Microliter
µM	Micromolar

Acknowledgements

Firstly, I would like to express my sincere gratitude to my supervisor **Stuart Neil** for his support during these four years, his patience, motivation, and immense knowledge. He guided me through easy and less easy times of my PhD studies and through the process of writing publications and this thesis. I could not have imagined having a better and also more fun mentor for my PhD. I look forward to working with him and continuing to learn from him.

I would like to thank my thesis committee, **Tim Tree**, **John Cason, Michael Linden**, and my second supervisor **Michael Malim** for their scientific advice and support.

I would like to thank **Suzy Pickering** and **Toshana Foster** for their incredible help throughout my PhD and especially for their advice during the process of writing this thesis. A special thank you goes to **Rui Galão** for being my go-to person and the best bench-mate I could have wished for. Also, **Tonya Kueck** has been immensely helpful and a pleasure to work with. I learned so much from all of you. In the lab, on the gym floor and in the pub. I am grateful to be surrounded by such smart, kind and amazing people.

A big thank you goes to all the past and present Team Neil members **Raphael Vigan**, **Gregory Berger**, **Jonny Sumner**, **Harry Wilson**, **Franka Debeljak**, **Pedro Matos**, **Max Handley** and **Kristina Schierhorn**.

Last but not least, I would like to thank my family: My parents **Marita** and **Frank Weinelt**, my sisters **Susann** and **Anja Weinelt**, **Michl Krenner**, **Thaiana Cervi**, **Daniel Sayer**, **Agrippina** and **Henry**. They provided me with personal advice, hugs, support and nutrition. All this played an essential role in finishing my PhD successfully. I am deeply thankful to have you all in my life.

Chapter 1 Introduction

1.1 The HIV Pandemic

Almost thirty-five years ago in 1981, acquired immunodeficiency syndrome (AIDS) was first described in the United States in homosexual men presenting with unusual opportunistic infections and a compromised immune system (Gottlieb et al. 1981). Two years later, the virus now known as human immunodeficiency virus 1 (HIV-1) was isolated from patient samples and identified as the causative agent (Barré-Sinoussi et al. 1983; Gallo et al. 1983). In 2008, the Noble Prize in Physiology or Medicine was awarded to Françoise Barré-Sinoussi and Luc Montagnier for their discovery of HIV-1. Five years after the first reports of HIV-1, another virus causing AIDS was isolated from patients in western Africa and named human immunodeficiency virus 2 (HIV-2) (Clavel et al. 1986). While it was only distantly related to HIV-1, it was more closely related to a simian immunodeficiency virus (SIV) infecting and causing immunodeficiency in captive macaques, SIVmac. Later, it was found that this infection was not a natural infection of macaques, which may explain its pathogenicity in this host (Apetrei et al. 2006; Apetrei et al. 2005). Subsequently, SIVs were identified in a broad range of primates from sub-Saharan Africa including African green monkeys, sooty mangabeys and chimpanzees. However, in most natural hosts SIV infections were non-pathogenic. HIV-1 and HIV-2 cluster together with SIVs in a phylogenetic lineage. It has been suggested that cross-species transmission occurred most likely due to hunting and handling of infected bushmeat (Peeters et al. 2002).

HIV-1 is the result of the zoonotic transmission of chimpanzee SIV (SIVcpz) to humans. There have been at least four independent cross-species transmissions that led to the emergence of HIV-1 group M, N, O and P. Group M is responsible for the vast majority of HIV-1 infections world-wide, while groups N, O and P are non-pandemic and confined to central Africa. Group O (outlier) was discovered in 1990 as the causative agent of tens of thousands of infections and is confined to Cameroon, Gabon and surrounding countries (Mauclère et al. 1997; Peeters et al. 1997). For group N (non-M and non-O) only thirteen cases have been reported, all but one discovered in Cameroon (Simon et al. 1998; Vallari et al. 2010). Group P is the least prevalent with only two isolates found to date that both originated in Cameroon (Plantier et al. 2009; Vallari et al. 2011). Group M and N are very closely related to SIVcpz found in the central chimpanzee subspecies *Pan troglodytes troglodytes* from south Cameroon (SIVcpz*Ptt*), indicating that these virus groups are of SIVcpz*Ptt* origin (Keele et al. 2006; Van Heuverswyn & Peeters 2007). In contrast, SIVcpz*Pts* infecting eastern

chimpanzees (*Pan troglodytes schweinfurthii*, Pts) has so far not been found to be transmitted to humans. SIVcpz itself is a recombinant of SIVs infecting red-capped mangabeys and Cercopithecus species, including greater spot-nosed, mustached and mona monkeys (Bailes et al. 2003). Although all four HIV-1 groups are closely related to SIVcpz*Ptt*, due to greater sequence similarity to SIV infecting gorillas (SIVgor), HIV-1 groups P and O were potentially transmitted to humans via gorillas from southern and central Cameroon, respectively (D'arc et al. 2015).

HIV-2, which is restricted to western Africa, is more closely related to SIVs infecting sooty mangabeys (SIVsmm) and multiple cross-species transmissions have occurred (Huet et al. 1990; Hirsch et al. 1989; Gao et al. 1992; Chen et al. 1996). Infection is associated with lower viral loads, which may explain the lower transmission rates. Compared to HIV-1 infection, a greater proportion of people infected with HIV-2 do not progress to AIDS.

Of all the HIV zoonoses, it was HIV-1 group M that spread most efficiently in humans and is responsible for the HIV pandemic, accounting for over 98% of all HIV infections worldwide. Genetic evidence suggests that HIV-1 group M emerged from the region around Kinshasa, the capital of the Democratic Republic of Congo (DRC), formerly known as Zaire, and it was estimated that the group M common ancestor dates back to the 1920s (Korber et al. 2000; Worobey et al. 2008; Faria et al. 2014). Transportation and migration in and around Kinshasa facilitated the spread of HIV-1 group M to other regions in central Africa (Gray et al. 2009). Group M has diversified in humans to form nine subtypes or clades: A, B, C, D, F, G, H, J and K. Clade B is responsible for most of the infections found in Europe and the United States. Phylogenetic studies suggest that a single African strain of clade B was transferred to Haiti and subsequently the United States in the 1960s where it spread internationally, becoming the most geographically dispersed subtype (Gilbert et al. 2007; Hemelaar et al. 2011). In contrast, subtype C, which accounts for around 50% of all HIV-1 infections worldwide, spread efficiently especially in southern Africa.

HIV is transmitted via body fluids such as blood, semen, vaginal secretions or breast milk, and it is primarily a sexually transmitted disease (Hladik & McElrath 2008; Cohen et al. 2011). In 2014, 36.9 million people were living with HIV worldwide, most of them in sub-Saharan Africa. Since 2000, 25.3 million people have died of AIDS related illnesses (www.UNAIDS.org). Even though infection rates have decreased in recent years there were still approximately two million new infections reported in 2014. Highly active antiretroviral therapy (HAART) has become more and more

accessible even in developing countries, which is one of the reasons for the reduced number of AIDS-related deaths. However, there is neither an efficient vaccine nor a broadly applicable cure for HIV infection.

1.2 HIV Genome and Structure

HIV-1 belongs to the family of the *Retroviridae*. These are enveloped viruses with a positive-sense single-stranded RNA (ssRNA) genome that have a similar structure and genomic organisation. Characteristically, the retroviral genomic RNA is converted into DNA by the virally-encoded reverse transcriptase (RT) and is integrated into the host genome by the virally-encoded integrase (IN). HIV-1 belongs to the retroviral genus of lentiviruses ('lente-', latin for slow) and these viruses cause chronic persistent infections in different mammalian species.

The 9.7 kb HIV-1 proviral DNA encodes nine viral genes. Common to all replicating retroviruses are the *gag*, *pol* and *env* genes (Figure 1.1 A). *Pol* encodes three enzymes: RT that converts the genomic HIV RNA into the proviral DNA, IN that integrates the proviral DNA into the host cell genome to form the provirus and the protease (PR) that is responsible for the maturation of budding viral particles by cleaving the Gag poly-protein into the main structural components of the virus. These are matrix (MA), capsid (CA), nucleocapsid (NC) and p6. *Env* encodes for the two glycoproteins, the surface (SU) gp120 and the transmembrane (TM) gp41. Gp120 binds to CD4 on the target cell, which induces conformational changes in the Env spike and enables co-receptor CCR5/CXCR4 binding. This is followed by the fusion of the virion with the host cell membrane mediated by gp41 (Wilen et al. 2012). HIV-1 encodes six more regulatory and accessory proteins Tat, Rev, Vif, Vpr, Vpu and Nef. Tat is a regulatory protein that interacts with cellular proteins and binds the trans-activation response (TAR) sequence in the viral RNA. This promotes viral transcription elongation. Rev, also a regulatory protein, binds to the Rev responsive element (RRE), which is a cis-acting RNA sequence in the *env* gene. Rev binding to RRE facilitates efficient nuclear export of unspliced or partially spliced viral mRNAs. Vif, Vpr, Vpu and Nef are proteins that regulate innate and adaptive host cell immune functions (Swanson & Malim 2008). The proviral DNA is flanked at each end by a long terminal repeat (LTR). The 5' LTR serves as a promoter for the initiation of transcription of the viral genome. The 3' LTR is required for the polyadenylation signal (polyA tail). Like cellular mRNAs, the viral RNA is polyadenylated at the 3' end and capped with 7-

methylguanosine at the 5' end. Further important elements in the viral genome include the primer binding site (PBS) that is required for the annealing of the cellular $tRNA^{Lys3}$, which initiates reverse transcription, the ψ packaging signal that is responsible for the incorporation of the viral RNA into the budding virion through interaction with the NC, the polypurine tracts (PPT) for plus strand DNA synthesis, a dimerization sequence, splice donor and splice acceptor sites.

The HIV-1 particle has a diameter of approximately 100 nm. It contains two copies of the viral genomic RNA. RT and the genomic RNA are enclosed by NC and together with IN and PR surrounded by the conically shaped capsid (Figure 1.1 B). The capsid is made up of hexameric CA subunits and is surrounded by the MA, which in turn is connected to the envelope formed by the host cell lipid bilayer (Sundquist & Kräusslich 2012).

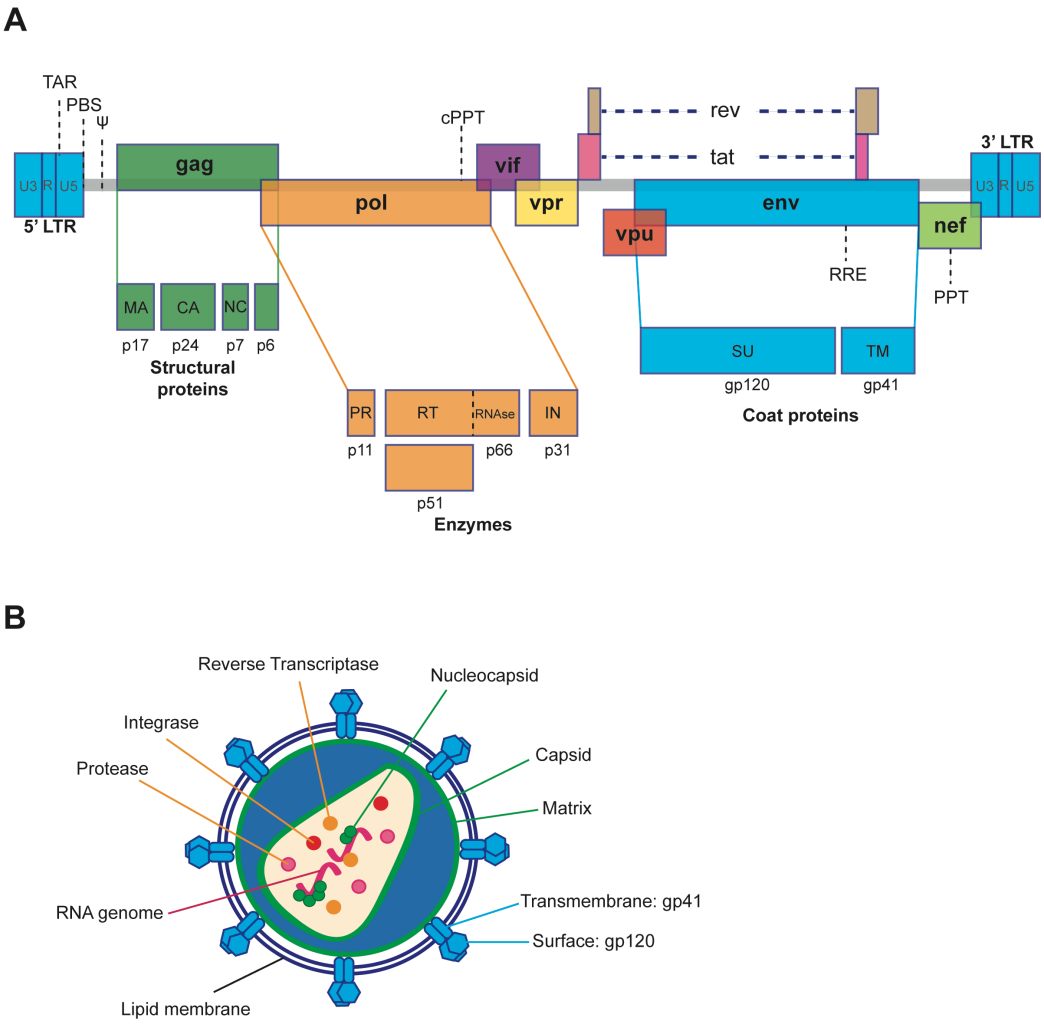

Figure 1.1 HIV-1 proviral genome and particle structure. (**A**) Schematic representation of the proviral HIV-1 genome containing the nine open reading frames of HIV-1: *gag*, *pol*, *vif*, *vpr*, *tat*, *rev*, *vpu*, *env* and *nef*. Abbreviations: LTR (long terminal repeat), U5 (5' untranslated region), R (repeat element), U3 (3' untranslated region), MA (matrix), CA (capsid), NC (nucleocapsid), PR (protease), RT (reverse transcriptase), IN (integrase), SU (surface), TM (transmembrane), TAT (trans-activator of transcription), ψ (packaging signal), PBS (primer-binding site for $tRNA^{Lys3}$), RRE (rev response element), PPT (polypurine tract). (**B**) Schematic representation of the HIV-1 virus particle.

1.3 The HIV Replication Cycle

The HIV-1 replication cycle starts with the binding of the viral envelope protein subunit gp120 to the cellular receptor CD4, expressed primarily on helper T cells and macrophages. Conformational changes in gp120/41 then facilitate co-receptor CC-chemokine receptor 5 (CCR5) or C-X-C chemokine receptor type 4 (CXCR4) binding followed by the fusion of the viral particle with the target cell and the translocation of the viral core into the cytoplasm. The single-stranded RNA is then reverse transcribed into double-stranded DNA (dsDNA) and forms the pre-integration complex (PIC) together with the viral MA (p17), CA (p24), viral IN, viral RT, the accessory protein viral protein R (Vpr) and several host cell-derived proteins. The PIC travels to the nucleus utilising the cellular microtubules for anterograde transport and there is evidence that the capsid is still associated with the PIC upon arrival at the nuclear pore (Matreyek & Engelman 2011; Peng et al. 2014; Hulme et al. 2015). This is followed by nuclear import and integration of the dsDNA into the host cell genome or dead-end formation of 2-LTR circles. Importantly, while most retroviruses cannot enter the nucleus until the nuclear membrane breaks down during cell division, lentiviruses infect non-dividing cells by hijacking cellular nuclear import pathways (Matreyek & Engelman 2011). The transcription of the viral genes depends on cellular transcription factors such as NF-κB and specificity factor 1 (SP1). They initiate the binding of the cellular RNA polymerase II to the TATA box at the 5' LTR and initiate mRNA transcription. Tat binding is required for efficient elongation and the subsequently produced mRNA is exported from the nucleus. Translation and protein processing occurs in the cytoplasm by the cellular machinery. Proteins and genomic RNA are then trafficked to the plasma membrane where they assemble into viral particles and bud from the host cell membrane. Maturation of the particle is mediated by the viral protease to form the fully infectious particle. A schematic of the viral life cycle is depicted in Figure 1.2 and in the following sections of the Introduction the steps of the HIV-1 life cycle will be discussed in more detail.

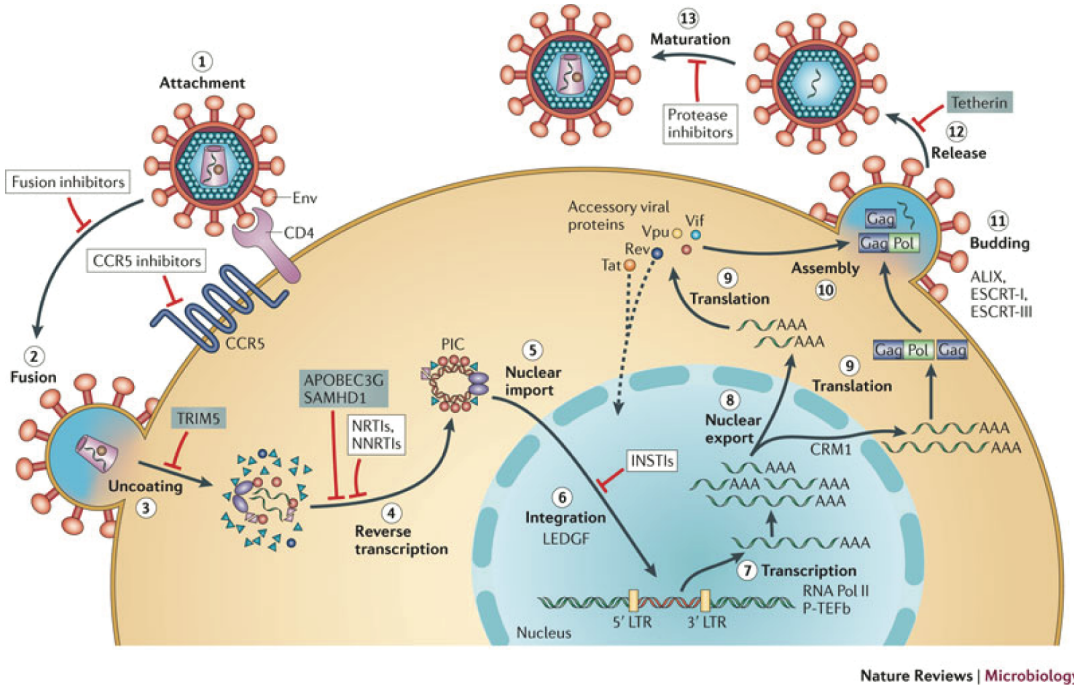

Figure 1.2 HIV-1 replication cycle. The infection begins when the envelope (Env) glycoprotein trimers engage the target cell receptor CD4 and the membrane-spanning co-receptor CCR5 (step 1), leading to fusion of the viral and cellular membranes and entry of the viral particle into the cell (step 2). Partial core shell uncoating (step 3) facilitates reverse transcription (step 4), which yields the PIC. Following import into the cell nucleus (step 5), PIC-associated IN orchestrates the formation of the integrated provirus, aided by the host chromatin-binding protein lens epithelium-derived growth factor (LEDGF) (step 6). Proviral transcription (step 7), mediated by host RNA polymerase II (RNA Pol II) and positive transcription elongation factor b (P-TEFb), yields viral mRNAs of different sizes. Partially spliced and unspliced mRNAs require the viral Rev protein and the host protein CRM1 for nuclear export (step 8). mRNAs serve as templates for protein production (step 9), and genome-length RNA is incorporated into viral particles with protein components (step 10). Viral-particle budding (step 11) and release (step 12) from the cell is mediated by ESCRT (endosomal sorting complex required for transport) complexes and ALIX and is accompanied or soon followed by protease-mediated maturation (step 13) to create an infectious viral particle. Each step in the HIV-1 life cycle is a potential target for antiviral intervention; the sites of action of clinical inhibitors (white boxes) and cellular restriction factors (blue boxes) are indicated. INSTI, integrase strand transfer inhibitor; LTR, long terminal repeat; NNRTI, non-nucleoside reverse transcriptase inhibitor; NRTI, nucleoside reverse transcriptase inhibitor. (Figure from Engelman & Cherepanov 2012).

1.3.1 Attachment and Entry

The first step of the viral life cycle consists of binding to and entering the target cell. Figure 1.3 depicts a schematic of the important steps in this process. Initial viral attachment to the cell can be rather non-specific through host cell proteins such as heparin sulphate proteoglycans, α4β7 integrins or pattern recognition receptors (PRR), like the dendritic cell-specific intercellular adhesion molecule 3-grabbing non-integrin (DC-SIGN) (Geijtenbeek et al. 2000; Saphire et al. 2001; Arthos et al. 2008). These attachment factors are cell type dependent and are not essential for HIV entry,

but can enhance infection of target cells. Also, viruses can move along the cell plasma membrane using host cell transport pathways, before reaching sites on the target cell with increased receptor expression that are favourable for HIV entry (Lehmann et al. 2005; Sherer et al. 2010). The first essential step is the binding of the the viral Env gp120 subunit to the main receptor of HIV entry, CD4 (Figure 1.3).

HIV-1 Env is a glycosylated trimer comprised of heterodimers formed by gp120 and gp41. The gp120 subunit is responsible for receptor binding. It contains five relatively conserved domains (C1-C5) and five variable regions (V1-V5) that all contain a loop structure, apart from V5. The variable regions have a fundamental role in co-receptor binding and immune evasion, particularly V3 (Hartley et al. 2005). The number of Env trimers that is required to facilitate entry, known as the entry stoichiometry, is currently under debate, with reports ranging from 1 to 19 trimers (Reviewed by Brandenberg et al. 2015).

It was known for a long time that CD4 is the main receptor used for HIV-1 entry. HIV-1 preferentially infects $CD4^+$ T cells, blocking antibodies to CD4 inhibit infection and Env can be co-immunoprecipitated with CD4. Moreover, CD4 expression promotes infection in non-permissive human cells (Dalgleish et al. 1984; Klatzmann et al. 1984; Maddon et al. 1986; McDougal et al. 1986). CD4 is a member of the immunoglobulin superfamily and its cellular function is to enhance T cell receptor (TCR) signalling. The binding of CD4 and HIV gp120 is followed by rearrangements in the V1/V2 regions of gp120 and, subsequently, leads to the formation of the bridging sheet (Kwong et al. 1998). These events are critical for the second step of HIV-1 entry: binding of Env to the co-receptor.

HIV-1 can either use CCR5 or CXCR4 as a co-receptor for entry. Depending on the co-receptor usage, there are R5 (CCR5 user), X4 (CXCR4 user) or R5X4 (where both co-receptors can be used) HIV strains (Berger et al. 1998). Interestingly, only R5 and R5X4 viruses are transmitted efficiently and X4 or R5X4 viral species are mainly found late in infection, even though target cells express high levels of CXCR4 (Keele et al. 2008; Schuitemaker et al. 1992; Connor et al. 1997). This may potentially be due to host restriction on X4 HIV transmission (reviewed by Margolis & Shattock 2006). A switch in co-receptor usage over the course of infection occurs in nearly 50% of untreated infected individuals and was implicated in disease progression (Scarlatti et al. 1997; Connor et al. 1997). Differences in co-receptor tropism among different HIV-1 clades may be a

result of differing host biology or environmental differences such as co-infections. This may depend on the geographical area an infected individual lives in (Wilen et al. 2012).

The final step of HIV-1 entry is the fusion of the viral membrane with the host cell. Upon binding to the co-receptor, the hydrophobic fusion peptide in gp41 is exposed and inserted into the host cell membrane, thereby, tethering both host and viral membranes. Each gp41 fusion peptide in the Env trimer folds at a hinge region, which brings the amino-terminal helical region (HR-N) and the carboxy-terminal helical region (HR-C) together to form a six helical bundle (6HB) (Chan et al. 1997; Weissenhorn et al. 1997). Subsequently, the fusion pore is formed and the viral contents are released into the host cell cytoplasm (Reviewed by Melikyan 2008).

HIV-1 does not require a low pH to promote host cell entry (McClure et al. 1988). This does not necessarily mean that HIV fuses at the plasma membrane. Whilst there is evidence for cell surface fusion, it has also been demonstrated that complete fusion can require endocytosis, which may be dependent on the viral strain or cell type (Stein et al. 1987; Miyauchi et al. 2009; Uchil & Mothes 2009). Furthermore, host cell entry via cell-cell transmission was shown to be enabled via formation of the so-called virological synapse between an infected cell and a target cell, which is characterized by recruitment of CD4, CCR5 and CXCR4. Infected dendritic cells (DCs) catalysed infection of co-cultured T cells without being productively infected themselves and HIV was shown to be able to migrate to the DC-T cell interface (Cameron et al. 1992; McDonald et al. 2003).

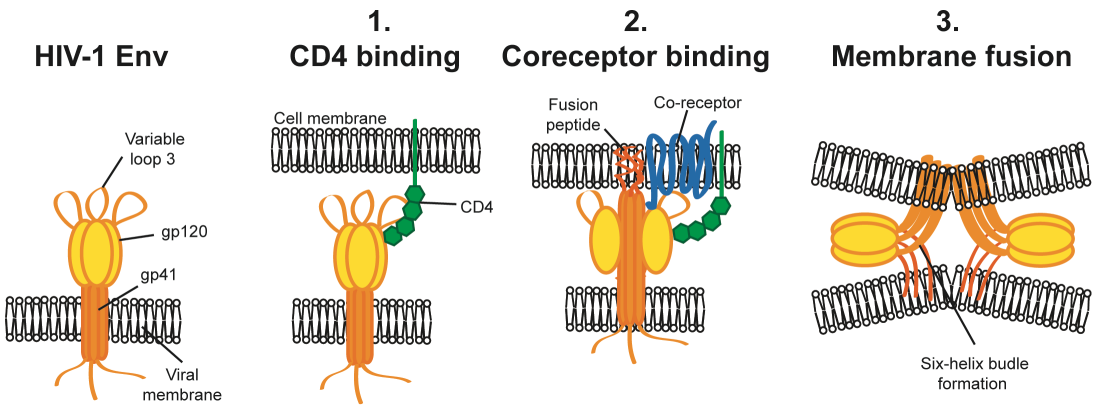

Figure 1.3 Schematic representation of HIV binding and entry. HIV Env, comprised of gp120 and gp41 subunits, first attaches to the host cell, binding CD4 (1). This causes conformational changes in Env, allowing co-receptor binding, which is mediated in part by the V3 loop of Env (2). This initiates the membrane fusion process as the fusion peptide of gp41 inserts into the target membrane, followed by six-helix bundle formation and complete membrane fusion (3).

1.3.2 Reverse Transcription

Once the viral core has reached the cytoplasm, the viral RNA genome needs to be reverse transcribed into DNA to enable integration into the host genome. This is a common feature of all retroviruses, thus all of them encode a RT and IN. The discovery that some viruses have an enzymatic activity that copies RNA into DNA, reverse transcription, was made more than a decade before the identification of HIV-1 (Baltimore 1970; Mizutani et al. 1970). The first anti-HIV drug to be approved by the U.S. Food and Drug Administration (FDA), azidothymidine (AZT), is an inhibitor of RT and today a large proportion of the anti-HIV drugs in use inhibit this viral enzyme.

RT is produced from the Gag-Pol polyprotein that is cleaved by the viral PR. On the one hand, this enzyme acts as a DNA polymerase, copying either RNA or DNA into DNA and on the other, it has RNase H function and degrades RNA that is part of an RNA-DNA duplex. The mature lentiviral RT is a heterodimer. One RT subunit is the 560 amino acid long p66. The smaller subunit, p51, contains the first 440 amino acids from p66 (Lightfoote et al. 1986). There are two domains in p66: a polymerase and a RNase H domain and both are enzymatically active in the mature RT. The structure of the polymerase domain resembles a human right hand with fingers, a palm, a thumb and connecting subdomains (Kohlstaedt et al. 1992). The structure of p51 is similar to that of p66 as it contains the same four subdomains. Their arrangement, however, differs and while p66 plays a catalytic role, p51 is a structural component of the RT (Kohlstaedt et al. 1992; Jacobo-Molina et al. 1993). However

The majority of the reverse transcription of the viral genomic RNA into DNA takes place in the newly infected cell. Nevertheless, there have been reports that the synthesis of the viral DNA starts already before infection of the target cell due to the limited presence of nucleotides in viral particles (Lori et al. 1992; Trono 1992; Huang et al. 1997). Reverse transcription takes place in the so-called reverse transcription complex (RTC), which contains several viral proteins including MA, CA, NC, IN and Vpr (Fassati & Goff 2001). The roles of these components are not yet fully understood. In later stages of the DNA synthesis process the RTC transitions into the preintegration complex (PIC) and is transported to the nucleus. The capsid shell is at least partially lost at some stage before nuclear entry and this process is called uncoating. In what order all these events take place is still unclear. The requirement for CA in nuclear entry and possibly integration suggests that capsid uncoating is not completed before nuclear entry (Matreyek & Engelman 2011; Peng et al. 2014; Hilditch & Towers 2014; Hulme et al. 2015). The timing of these processes also impacts on the

immune sensing of HIV-1 reverse transcription intermediates in the cytoplasm (Reviewed by Jakobsen et al. 2015).

A schematic representation of reverse transcription is depicted in Figure 1.4. For reverse transcription to occur, two components are required. Firstly, a template, which is provided by the HIV genomic plus strand RNA. Secondly, a primer, which is the host cell-derived $tRNA^{Lys3}$ that is complementary to a sequence near the 5' end of the viral genomic RNA called the primer binding site (PBS) and is incorporated into budding HIV virions. The tRNA hybridises to the PBS and RT-mediated DNA polymerisation occurs to create a DNA-RNA duplex. The RNA in a DNA-RNA duplex serves as a substrate for the RNase H that cleaves off the 5' end of the viral RNA and exposes the newly synthesized minus strand DNA (Figure 1.4 B). As both ends of the genomic viral RNA are direct repeats (R), the newly synthesized minus strand DNA can transfer to the 3' end of the viral RNA. Importantly, this can be either of the two copies of single stranded RNA that are packaged into the virion (Hu & Temin 1990; van Wamel & Berkhout 1998). Minus strand DNA synthesis then continues across the full length of the viral RNA, accompanied by RNA degradation by RNase H. However, RNase H is unable to degrade a resistant purin-rich sequence in the genomic RNA called the polypurine tract (PPT). The PPT serves as a primer for the initiation of plus strand DNA synthesis. There are two PPTs in the HIV genome, one located near the 3' end of the RNA and one in the middle of the genome, the central PPT. In contrast to the central PPT, the 3' PPT is essential for plus strand DNA synthesis initiation, but the central PPT increases the ability to complete plus-strand synthesis (Charneau et al. 1992). The minus strand is copied from the 3' PPT onwards, including the 18 nucleotides of the $tRNA^{Lys3}$ primer. The tRNA is then degraded by RNase H, however, HIV-1 RT cleaves all but one nucleotide off, leaving one A at the 5' end of the minus strand (Pullen et al. 1992; Smith & Roth 1992). Then the second, plus strand transfer occurs. As the 3' end of the plus strand contains the 18 nucleotides from the tRNA primer that are complimentary to the minus strand 3' end, both sequences anneal and DNA synthesis continues with both the minus and the plus strand extended to the end of both templates. The reverse transcription DNA product is longer than the genomic RNA as the ends of the DNA contain parts from both ends of the genomic RNA meaning that each end of the viral DNA has the same sequence, U3-R-U5. These so-called long terminal repeats (LTR) determine the ends of the provirus and are the substrate for integration by the viral IN.

Most patients are productively infected by only one single HIV virus as determined by phylogenetic reconstruction of the founder virus sequence (Salazar-Gonzalez et al. 2009). There is a high level of variation in viral sequences within patients, suggesting that mutations occur during the viral life cycle (Coffin 1995; Keele et al. 2008). Being able to mutate quickly plays a key role in the virus' ability to evade the host immune system and also in the development of resistance to anti-HIV drugs. The high level of variability of HIV has made vaccine development difficult. One explanation for the number of mutations occurring in HIV during replication is that the viral RT has no proofreading function and therefore, mutations are not corrected. It has so far not been possible to separate the contribution of the viral RT and the host cell RNA polymerase II, which transcribes the integrated provirus, to the virus mutation rate (O'Neil et al. 2002). The combined error rate for RT and RNA pol II is approximately 2×10^{-5} per bp per replication cycle (Mansky & Temin 1995; Abram et al. 2010). Furthermore, HIV-1 also exhibits a higher level of recombination compared to other retroviruses (Onafuwa et al. 2003). The viral RT can switch between the two packaged genomic RNA templates during minus strand DNA synthesis. For a sequence change to occur, it is required that the virus producing cell is infected with more than one virus. Double infection, for example due to transfer of multiple viruses across the virological synapse, occurs more frequently than expected from random events (Dang et al. 2004).

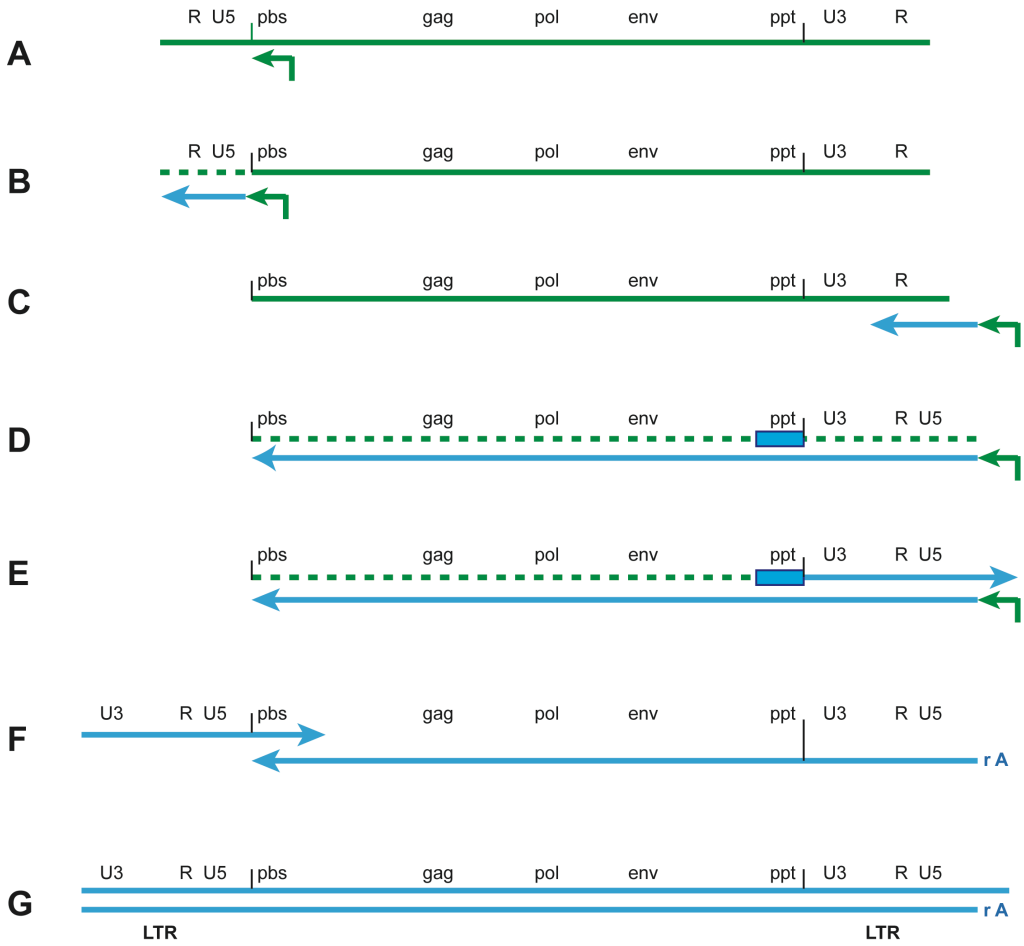

Figure 1.4 Retroviral reverse transcription converts the single-stranded RNA genome into double-stranded DNA. (**A**) The viral RNA genome (blue) with a tRNA primer annealed near the 5′ end. (**B**) RT initiates reverse transcription and generates a minus-strand DNA (orange). RNase H activity of RT degrades the RNA template (dashed line). (**C**) Minus-strand transfer occurs between the R sequences at both ends of the genome allowing minus-strand DNA synthesis to continue. (**D**) This is accompanied by RNA degradation. A purine-rich sequence (PPT), adjacent to U3, is resistant to RNase H cleavage and serves as the primer for the synthesis of plus-strand DNA. (**E**) Plus-strand synthesis continues until the first 18 nucleotides of the tRNA are copied, allowing RNase H cleavage to remove the tRNA primer. The RNase H of HIV-1 RT leaves the rA from the 3′ end of the tRNA attached to minus-strand DNA. (**F**) Second (plus-strand) transfer. (**G**) Extension of the plus and minus strands leads to the synthesis of the complete double-stranded linear viral DNA.

1.3.3 Nuclear Import and Integration

Once the HIV-1 dsDNA is synthesized it is transported into the nucleus where it can be integrated into the host cell genome to serve as a template for transcription of viral genes and viral genomic RNA. The viral DNA associates with IN, and forms the preintegration complex (PIC), which contains a range of viral and host cell proteins. Lentiviruses are able to infect non-dividing cells, which separates them from simpler retroviruses. The PIC must be able to cross the nuclear membrane to deliver the proviral DNA and proteins that are essential for integration into the nucleus. The viral component that is absolutely crucial in this process is CA (Yamashita & Emerman 2004;

Yamashita et al. 2007). However, the process of nuclear entry is still not fully understood. There are several proteins in the PIC that exhibit nuclear localization properties, including MA, CA and IN. Cellular proteins have also been implicated in the nuclear import of the PIC, such as transportin 3 (TNPO3), or the nucleoporins 358 (NUP358) and 153 (NUP153) and cleavage and polyadenylation specificity factor 6 (CPSF6) (Reviewed by Hilditch & Towers 2014). Interestingly, CA mutants show altered cellular co-factor dependence for nuclear entry as well as a retargeted integration site preference.

A schematic representation of viral DNA integration into the host genome is shown in Figure 1.5. The first step involves the 3' end processing of the viral DNA. Two nucleotides are removed from each 3' end of the blunt ended viral DNA (Figure 1.5 A-B). This is followed by the DNA-strand transfer. The 3' ends of the viral DNA attack phosphodiester bonds on opposite strands of the host cell target DNA (Figure 1.5 C). The gaps and two-nucleotide overhangs are then repaired by cellular enzymes and the integration is completed. This leads to a five base pair duplication of the target DNA flanking the proviral DNA (Figure 1.5 D-E). For integration *in vitro* only the viral IN and the terminal sequences in the viral DNA are absolutely required (Bushman et al. 1990).

IN has three domains that are structurally distinct. A catalytically active central core domain and N- and C-terminal domains. While a full structure of HIV IN binding to DNA is not available, the structure of the prototype foamy virus (PFV) intasome was solved (Maertens et al. 2010). Structural data show that PFV IN forms a homotetramer and binds to and deforms target DNA, which correlates with reports that DNA distortion promotes HIV DNA integration (Bor et al. 1995). Raltegravir was approved in 2007 by the FDA as the first integrase inhibitor used in anti-HIV therapy. Structural data revealed that it blocks the access of target DNA to the viral IN and also displaces the viral DNA 3' ends from the IN active site, thereby disrupting catalysis.

Integration site selection does not appear to be random. Development of high-throughput screens enabled the analysis of HIV integration sites in infected cells and showed that HIV favours integration into active transcription units that are characterized by high G/C content, a high gene density, high CpG island density, short introns, high frequency of Alu repeats, but also certain epigenetic modifications such as histone modifications (Wang et al. 2007; Brady et al. 2009). The efficiency of integration is also determined by cellular proteins such as LEDGF, a protein that contains a chromatin binding domain and an A/T hook domain potentially for DNA binding

(Cherepanov et al. 2003). LEDGF tightly binds IN via its C-terminus and tethers IN and the viral DNA to the chromatin, targeting them to transcription units for integration. Knockdown of LEDGF leads to an infectivity defect at the integration step, which is demonstrated by inhibited provirus formation and concomitant increased formation of 2-LTR circles, which are unintegrated, dead end products of viral DNA (Farnet & Haseltine 1991; Llano et al. 2006; Shun et al. 2007). An increase in 2-LTR circle formation can also be observed in the presence of an integration inhibitor, suggesting this may be the reason for the inhibitory effect of a LEDGF knockdown (Arts & Hazuda 2012). Recently it was reported that HIV-1 integration preferentially occurs in peripheral regions of the nucleus, proximal to the nuclear pore in areas of open chromatin (Marini et al. 2015). These findings correlate with the important role of NPC components in HIV-1 infection, because these co-factors are enriched for HIV integration sites in chromatin immunoprecipitations (Brass et al. 2008; König et al. 2008; Matreyek et al. 2013).

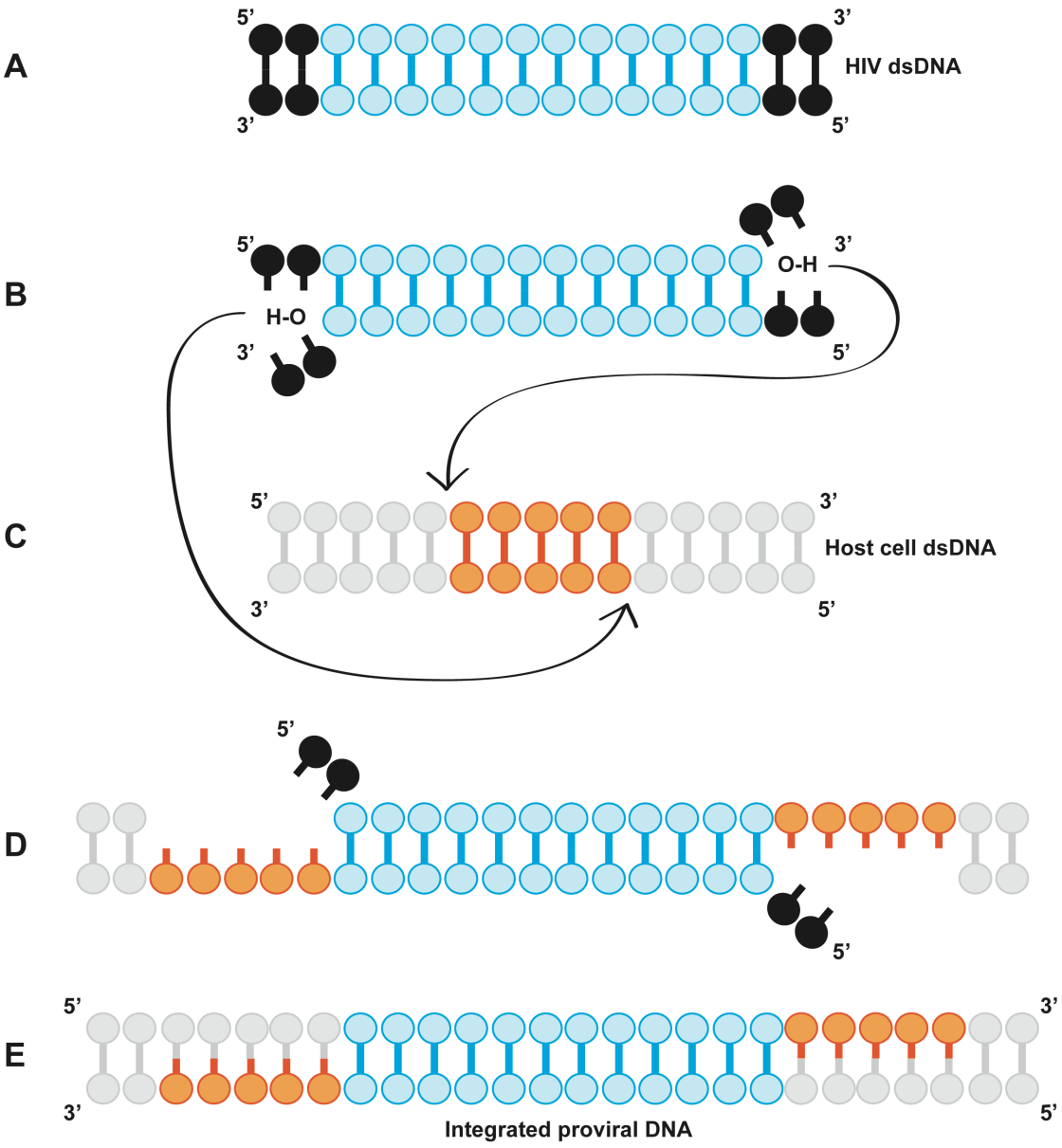

Figure 1.5 Integration of the HIV proviral DNA into the host genome. (**A**) HIV-1 proviral dsDNA. (**B**) IN catalyses 3' terminus processing, generating reactive 3′-hydroxyl groups at both ends of the viral DNA. (**C**) The two 3′-hydroxyl viral DNA ends mediate the strand transfer and ligatiion with the host DNA. (**D**) Strand transfer results in a five-base, single-stranded gap and a two-base overhang at the 5′-ends of the viral DNA. (**E**) 5' trimming and DNA repair by cellular repair enzymes.

1.3.4 Transcription and Nuclear Export

Once the proviral DNA is integrated into the host genome it can serve as a template for the transcription of viral mRNAs and genomic RNA. Like all other retroviruses, HIV-1 uses the 5' LTR as the promoter for the initiation of transcription. The HIV-1 LTR contains several regulatory elements that serve as binding sites for cellular transcription initiation factors (Rittner et al. 1995). The core promoter contains three tandem SP1 binding sites, a TATA box and a highly active initiator sequence (Jones et al. 1986; Garcia et al. 1989). The transcription factor IID (TFIID) and its associated co-factor TBP-associated factor (TAF) bind to the TATA box and recruit RNA polymerase II (RNAP II) to the LTR. In addition, there are enhancer regions in the LTR that contain NF-κB binding motifs. These can be engaged by both NF-κB and nuclear factor of activated T cell (NFAT) to enhance transcription (Nabel & Baltimore 1987; Liu et al. 1992). This is particularly important for virus replication in primary T cells (Alcamí et al. 1995). HIV-1 also requires the transactivating factor Tat for transcription, which regulates transcription elongation (Kao et al. 1987). In the absence of this factor, RNAP II pauses at the promoter and transcription elongation fails. Tat recognizes a regulatory viral RNA element downstream of the transcription initiation site, the transactivation-responsive region (TAR). This region forms a highly stable, nuclease-resistant stem-loop structure (Berkhout et al. 1989; Selby et al. 1989). The cellular positive acting elongation factor P-TEFb is an important co-factor for Tat and plays an essential role in transactivation. It contains a cyclin component (CycT1) that forms a stable complex with the cyclin-dependent kinase 9 (CDK9), Tat and the TAR RNA (Wei et al. 1998). The binding of Tat to P-TEFb leads to conformational changes in the CDK9 subunit, which activates the enzyme (Tahirov et al. 2010). The kinase then phosphorylates the negative elongation factor (NELF), which leads to its dissociation from the TAR RNA (Fujinaga et al. 2004). Furthermore, Spt5, a subunit of the DRB sensitivity-inducing factor (DSIF), is phosphorylated, which converts this elongation inhibitor into a positive elongation factor (Bourgeois et al. 2002; Yamada et al. 2006). In addition to the removal of these blocks to elongation, CDK9 also hyperphosphorylates the C-terminal domain (CTD) of the RNAP II, which enhances its processivity (Isel & Karn 1999). Protein complexes containing Tat and P-TEFb also contain a range of other cellular transcription activators or co-activators including AFF4, ENL, AD9 or ELL2 (He et al. 2010; Sobhian et al. 2010). Figure 1.6 shows a schematic representation of the processes described.

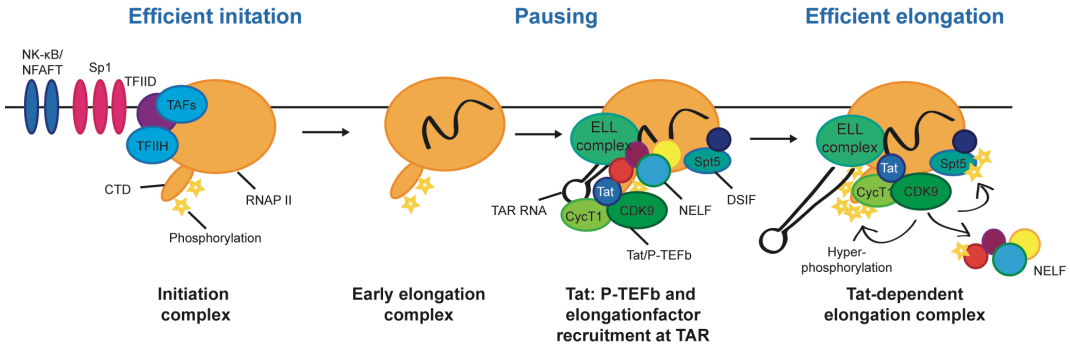

Figure 1.6 HIV-1 transcription transactivation by Tat. Transcription initiation is strongly induced by NF-kB. The Tat/P-TEFb complex (including CDK9 and CycT1 and the accessory elongation factors including ELL2) is recruited to the elongation complex via binding interactions with TAR RNA. This activates the CDK9 kinase and leads to hyperphosphorylation of RNAP II, Spt5, and NELF. The phosphorylation of NELF leads to its release. The presence of hyperphosphorylated RNAP II and Spt5 allows enhanced transcription of the full HIV-1 genome.

The HIV-1 primary transcripts are subjected to extensive splicing events to generate more than 40 different spliced mRNAs that can be found in infected cells. These are completely spliced ~1.8 kb mRNAs that encode for Tat, Rev and Nef, but there are also unspliced (~9 kb) and partially spliced (~4 kb) mRNAs encoding Vif, Vpr, Vpu, Env, Gag and Pol (Figure 1.7). The pre-mRNA is associated with a large complex of cellular factors that facilitate RNA splicing, the so-called spliceosome. Exonic and intronic splicing enhancers (ESEs and ISEs respectively) facilitate splice site recognition and interact with SR proteins. Exonic and intronic splicing silencers (ESSs and ISSs respectively) repress splicing and are bound by members of the heterogenous ribonuclear protein (hnRNP) family. For optimal virus replication the viral mRNA splicing needs to be tightly regulated to balance mRNA and genomic RNA production (reviewed by Karn & Stoltzfus 2012). Unspliced and incompletely spliced transcripts are usually degraded in the nucleus. However, some of the HIV-1 coding mRNAs are not fully spliced, but still needed for viral protein production. Therefore, HIV-1 expresses the regulator of expression of virion proteins (Rev) that facilitates the transport of intron-containing viral RNAs out of the nucleus.

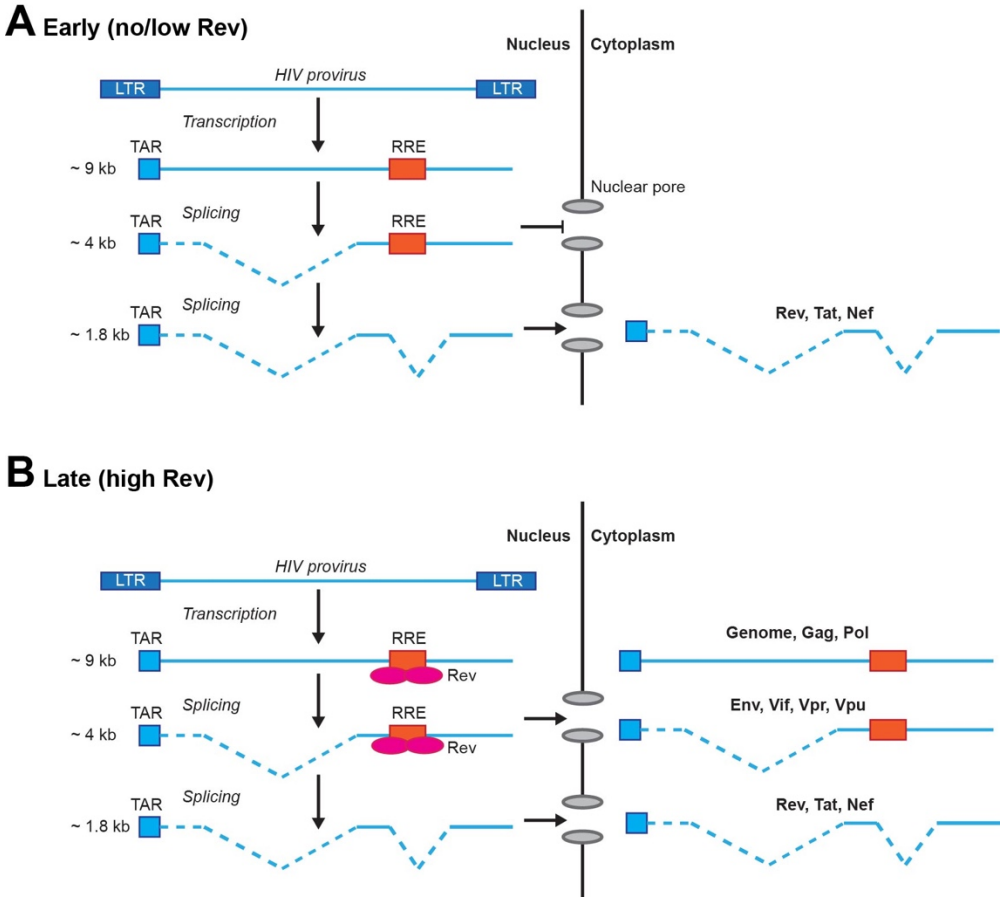

Figure 1.7 HIV-1 mRNA splicing. (**A**) Early phase of mRNA expression. Only the completely spliced ~1.8 kb mRNA encoding Tat, Rev and Nef is exported into the cytoplasm by the normal nuclear export cellular pathway and translated. The unspliced ~9 kb and incompletely spliced ~4 kb mRNAs are retained in the nucleus where they undergo splicing or degradation. (**B**) Late phase of mRNA expression. When Rev concentrations in the nucleus exceed a threshold, Rev binds to the RRE in the *env* gene to mediate export to the cytoplasm and translation of ~9 kb and ~4 kb mRNAs.

A schematic of the nuclear transport process is depicted in Figure 1.8. Rev interacts with a highly structured stem loop RNA element that is located in the *env* gene and the RRE (Malim et al. 1989). All mRNA species that are incompletely or unspliced, such as those encoding Gag, Pol and Env, require Rev for nuclear export and expression. The fully spliced mRNAs that encode Tat, Rev and Nef are exported to the cytoplasm even in the absence of Rev by the cellular transport pathways that also transport cellular mRNAs. In the fully spliced mRNAs the region that contains the RRE is removed. In the case of the unspliced/partially spliced mRNAs Rev binds the RRE, which is followed by additional binding of Rev monomers to the complex (Malim & Cullen 1991; Zapp et al. 1991). The export occurs via the nuclear pore complex (NPC). RRE-bound Rev interacts with the karyopherin family member Crm1 through its C-terminal nuclear export signal (NES)

(Köhler & Hurt 2007). Members of the karyopherin family bind their cargo in the presence of the GTP-bound form of Ran GTPase. After export, the GTP hydrolyses to GDP through RanGAP and RanBP1. This destabilizes the Rev complex and leads to its dissociation from the RRE (Fischer et al. 1995). Rev is then transported back into the nucleus through binding to the nuclear import factor importin-β (Henderson & Percipalle 1997).

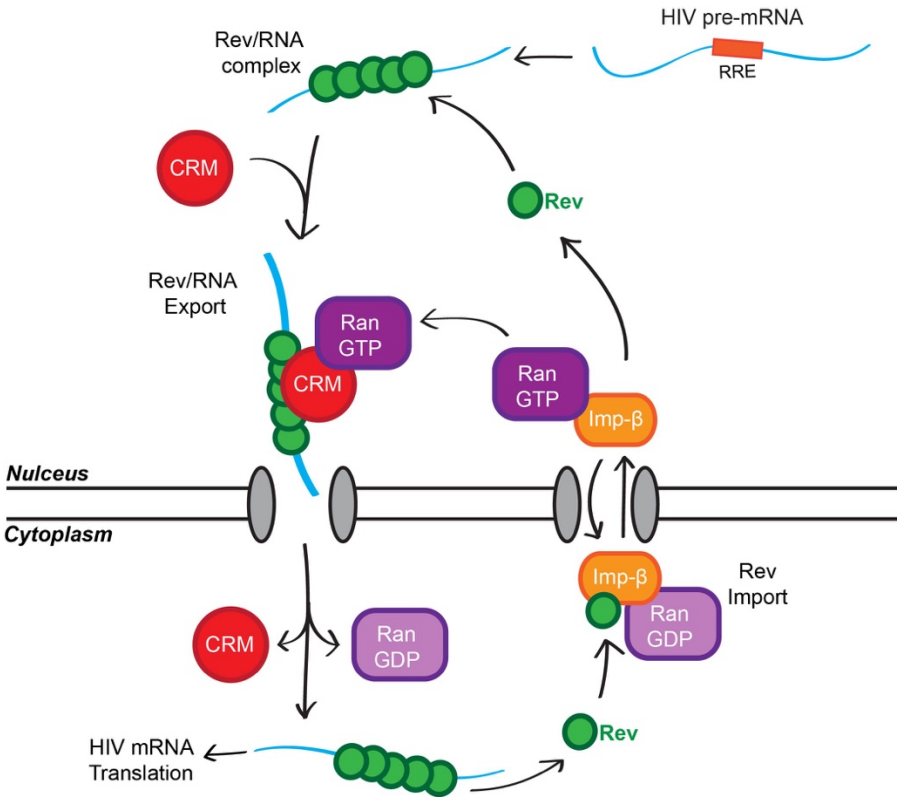

Figure 1.8 HIV-1 Rev transport cycle. Rev binds unspliced or incompletely spliced mRNA transcripts through RRE and interacts with Crm1. This complex crosses the nuclear membrane by interaction with nuclear pore proteins. In the cytoplasm, Ran-GTP is converted into Ran-GDP leading to the release of Rev, Crm1 and viral mRNA. Crm1 is transported back into the nucleus and Rev binds to importin-β together with Ran-GDP to facilitate transport back into the nucleus. Once in the nucleus Ran-GDP is converted into Ran-GTP and Rev is released to initiate another nuclear export cycle of viral mRNA.

1.3.5 Translation and Viral Assembly

Once the mRNAs are transported into the cytoplasm, the cellular translation machinery produces the viral proteins. All viral mRNAs contain a poly(A) tail at their 3' end and a 7-methyl-guanosine cap at their 5' end. Translation can be initiated when the small 40S ribosomal subunit and eukaryotic initiation factors (eIFs) are recruited to the viral mRNA, followed by scanning until the ribosome encounters an authentic AUG translation initiation codon. The 60S subunit is then

recruited to form the 80S ribosomal complex and the mRNA is translated into the according amino acids. Once the termination codon is reached the protein is released and the ribosome is recycled for another round of translation. Translation initiation, however, can be difficult in the highly structured regions of the HIV-1 mRNA that include the TAR, PBS, poly(A) hairpin and RNA packaging sequences, as these interfere with the cellular ribosomal scanning process. Several mechanisms have been reported to overcome this problem. Posttranscriptional control elements (PCEs) that bind RNA enhance translation initiation. Examples are the DEIH helicase RHA and RNA binding proteins SRp40 and SRp55 that enhance the translation of Gag (Bolinger et al. 2010; Swanson et al. 2010). Internal ribosome entry sites (IRES) in viral mRNAs have been described for *Picornaviridae*. They promote the recruitment of the 43S ribosome independently of 5' cap binding. Whether IRES activity exists in the HIV-1 genome is under debate (Reviewed by Bolinger & Boris-Lawrie 2009). The mRNA encoding Env is bicistronic and contains an overlapping upstream open reading frame encoding Vpu. For efficient Env expression a mechanism is employed that is called 5' cap-dependent ribosome shunting. The scanning ribosome can jump over large regions of the mRNA before it recognises the correct AUG codon (Krummheuer et al. 2007). Another mechanism evolved by retroviruses is programmed frameshifting that ensures translation of certain viral proteins. This is facilitated by specific sequence and structural signals in the mRNA. HIV-1 requires a -1 frameshift to shift from the *gag* reading frame to the *pro* and *pol* reading frame, which occurs around 5% of the times that Gag is translated. Two cis-acting elements are required for this process. The 'UUUUUUA' "slippery" sequence that leads to a slippage during translation and a stem-loop pseudoknot structure that increases the time that the ribosome is associated with the slippery sequence (Brierley & Dos Ramos 2006).

HIV-1 assembly occurs at the host cell plasma membrane and is orchestrated by the HIV-1 Gag and Gag-Pro-Pol polyproteins. They induce the required steps for plasma membrane binding, protein-protein interactions that are necessary to form a spherical particle, concentrating HIV-1 Env on the plasma membrane and packaging the genomic RNA via its packaging signal. All these events take place simultaneously at the plasma membrane through conformational changes in Gag and eventually lead to the budding of the viral particle using the cellular endosomal sorting complexes required for transport (ESCRT), and the maturation of the virion (Figure 1.9).

Gag molecules assemble to form an immature virus particle at the plasma membrane. The polyproteins traffic to the PM and sort into detergent-resistant, lipid raft membrane microdomains

(Ono & Freed 2001). Membrane targeting requires the myristoylation of the MA domain in Gag and specific lipids in the plasma membrane, phosphatidyl inositol biphosphate ($PI(4,5)P_2$) (Ono et al. 2004). Binding of MA to these lipids leads to the exposure of the N-terminal myristoyl group that can then mediate stable anchoring of Gag to the PM. This so called myristoyl switch is furthermore facilitated by Gag multimerization and was proposed to be regulated by tRNA binding to MA (Tang et al. 2004; Kutluay et al. 2014).

HIV-1 Env traffics to the PM independently of Gag. Both Env and Vpu are translated on the rough endoplasmic reticulum (ER). Env is sorted to the PM through the cellular secretory pathway where it is glycosylated. It assembles into trimeric complexes that are processed into the transmembrane (TM, gp41) and surface (SU, gp120) subunits by the cellular protease furin, before the complexes are delivered to the PM via cellular vesicular transport pathways. The intracellular tail of gp41 is responsible for the sorting of Env into “raft”-like domains and mediates the interaction with the Gag subunit MA to promote the incorporation. On average, 7-14 Env trimers are found on a mature HIV-1 virion (Zhu et al. 2006). Therefore, Gag MA mediates plasma membrane binding and recruitment of Env to sites of viral budding. The central Gag domain CA mediates all protein-protein interactions that are required to assemble the immature lattice of the virion and will later form the conical capsid shell of the mature viral core. The NC domain of Gag is responsible for capturing the two copies of the full length HIV-1 genomic RNA. This requires two zinc-finger motifs in NC as well as the Ψ packaging site in the genomic RNA that is located in the 5’ region spanning the major splice donor site and the Gag initiation codon (Reviewed by D’Souza & Summers 2005). The C-terminal p6 domain of Gag has binding sites for several proteins and mediates the packaging of the HIV-1 Vpr protein. Furthermore, this domain contains two late assembly domains that bind to the ESCRT components TSG101 or ALIX and are essential for the budding of the virion as detailed in section 1.3.6. In addition to the viral components, there are also cellular molecules that are packaged into the budding virion, such as the $tRNA^{Lys3}$ that anneals to the PBS in the viral genome and serves as the primer for the next round of reverse transcription. The virus membrane is acquired during budding and is derived from the host cell plasma membrane. It is enriched for raft lipids such as sphingomyelin, cholesterol, saturated fatty acids and phosphatidyl serine (Brügger et al. 2006).

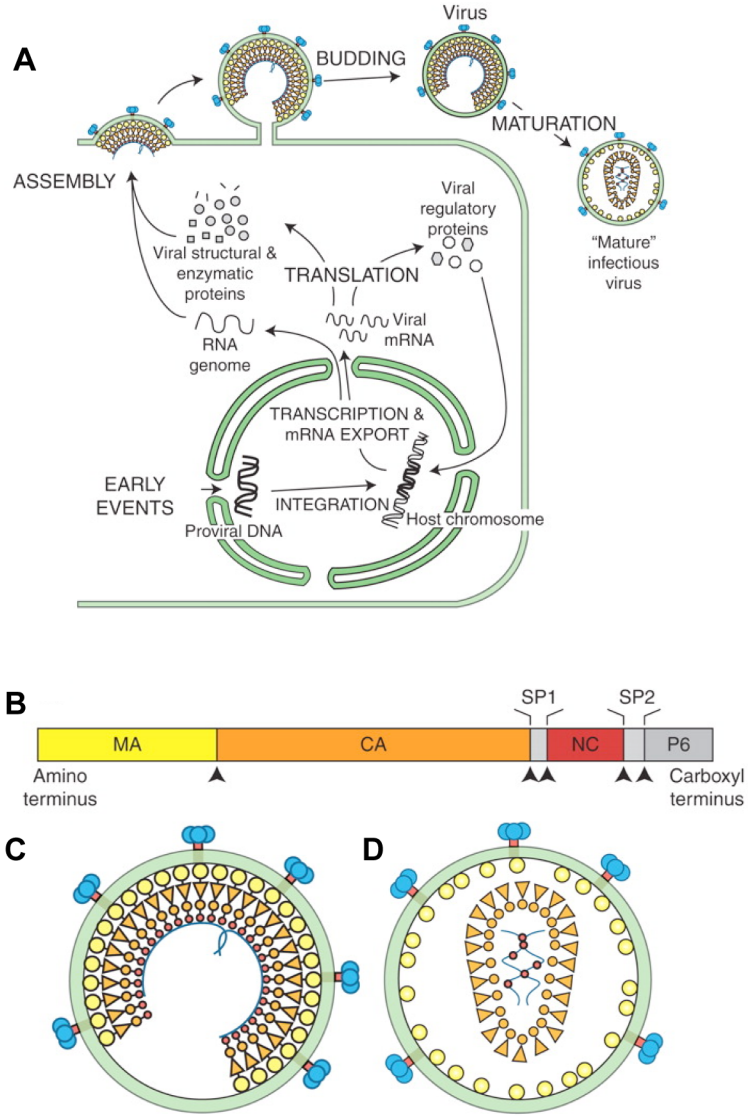

Figure 1.9 HIV-1 assembly, budding and maturation. (**A**) Schematic illustration showing the different stages of HIV-1 assembly, budding, and maturation. (**B**) The HIV-1 Gag polyprotein and its different domains; arrows indicate the five sites that are cleaved by the viral PR during maturation. (**C**) Schematic model showing the organization of the immature HIV-1 virion. (**D**) Schematic model showing the organization of the mature HIV-1 virion. (Adapted from (Sundquist & Kräusslich 2012)).

1.3.6 Viral Budding and Release

During assembly of all the required HIV components at the plasma membrane and HIV-1 Gag polymerization, the budding and release of the new virion is induced. These events are mediated by the cellular ESCRT machinery that is recruited by the HIV-1 p6 late domains. Late domains are not restricted to HIV-1, but are used by a broad range of enveloped viruses to recruit the ESCRT machinery for viral release (Martin-Serrano & Neil 2011). Apart from facilitating viral budding, ESCRT pathways are responsible for cellular processes involving membrane fission events, such

as releasing vesicles into endosomal multivesicular bodies and abscission of two separating daughter cells during cytokinesis (Reviewed by Hurley & Hanson 2010). The HIV-1 Gag subunit p6, responsible for recruiting the ESCRT machinery, contains two different late domain motifs that bind and recruit early acting ESCRT factors. The primary late domain is a four amino acid sequence PTAP (Pro-Thr/Ser-Ala-Pro) that interacts with the N-terminal ubiquitin E2 variant (UEV) domain in the TSG101 subunit, which belongs to one of the ESCRT complexes, ESCRT-I (Martin-Serrano et al. 2001; Garrus et al. 2001; VerPlank et al. 2001). PTAP motifs can also be found in cellular proteins such as HRS that recruit ESCRT to endosomal membranes (Ren & Hurley 2011). Therefore, HIV-1 p6 appears to mimic a cellular ESCRT recruiting motif of membrane-specific adaptors (Pornillos et al. 2003). Additionally, there is a second late domain in HIV-1 p6, YPXL (Tyr-Pro-X-Leu, "X" can vary in sequence and length). It interacts with a conserved hydrophobic groove in the V domain of the ESCRT-associated factor ALIX. This late domain however, appears to be less critical for HIV-1 replication than PTAP (Strack et al. 2003; Fujii et al. 2009). Furthermore, the Bro domain found at the N-terminus of ALIX can interact with NC, which is involved in virus release (Popov et al. 2008). Also, the E3 ubiquitin ligase NEDD4L has been implicated in viral release through its interaction with the C-terminus of HIV-1 CA. This suggests that ubiquitination of Gag through NEDD4L may facilitate late domain recruitment of the ESCRT machinery. However, the effect of NEDD4L on release is modest (Chung et al. 2008).

The human ESCRT pathway contains more than thirty proteins. The minimal core set of ESCRT proteins required for HIV-1 budding is depicted in Figure 1.10. Both TSG101 and ALIX recruit another ESCRT complex, ESCRT-III and VPS4 complexes that then mediate the membrane fission necessary for virus budding, before ESCRT components are recycled. The human ESCRT-III complex comprises the charged multivesicular body protein (CHMP) families. Particularly important for HIV-1 budding are CHMP2 and CHMP4 (Morita et al. 2011). How TSG101/ ESCRT-I recruits the core ESCRT-III and VPS4 complex is not fully understood, but it is well characterized for ALIX. Late domain binding induces conformational changes in ALIX and leads to its dimerization and activation and subsequent ESCRT-III recruitment. The ALIX Bro domain binds to C-terminal helices of CHMP4 proteins, which is thought to induce CHMP4 polymerization into filaments within the virion neck. Recruitment and polymerization of CHMP2 exposes C-terminal motifs that bind the N-terminal MIT domain of the VPS4 ATPase. VPS4 molecules assemble into a complex of two stacked hexamer rings that are linked through CHMP5/LIP5 and that is enzymatically active. There

are three models of how membrane fission occurs: the spiral, the tube and the dome model, whereas the dome model is the most accepted. CHMP4 filaments, possibly in complex with CHMP2 and other ESCRT-III components, spiral into the neck of the budding virion and form a closed dome that constricts and promotes fission. Hydrolysis of ATP by VPS4 assists in fission completion and mediates the disassembly of the filaments and release of ESCRT-III subunits into the cytoplasm (Reviewed by Sundquist & Kräusslich 2012). The different ESCRT complexes will be discussed in more detail in section 1.8.

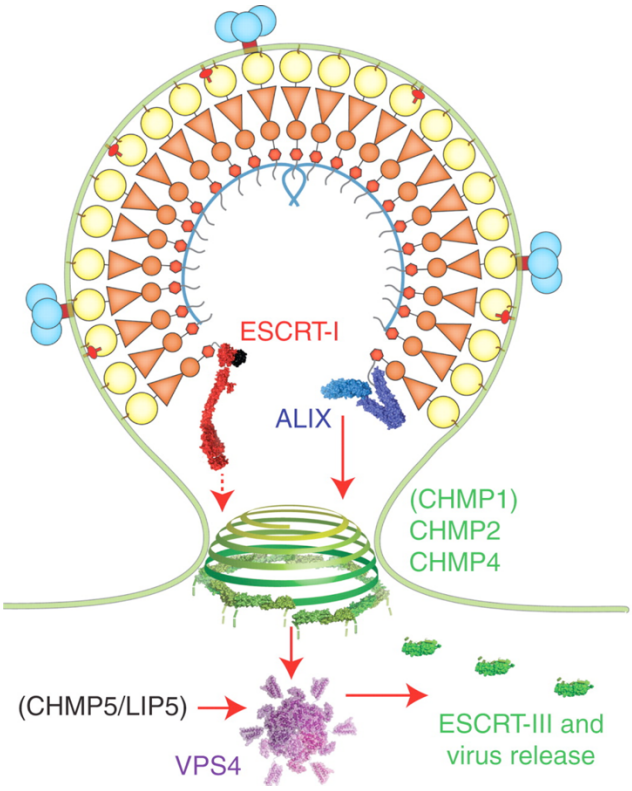

Figure 1.10 Recruitment of the cellular ESCRT machinery for HIV-1 budding. Late domain motifs within $p6_{Gag}$ bind directly to the UEV domain of the TSG101 subunit of the heterotetrameric ESCRT-I complex (red, with bound ubiquitin in black) and the V domain of ALIX (blue). These interactions result in the recruitment of the ESCRT-III proteins of the CHMP2 and CHMP4 families (green), which apparently polymerize into a "dome" that promotes closure of the membrane neck. They also recruit the VPS4 ATPases (purple), which completes the membrane fission reaction and uses the energy of ATPase to release the ESCRT-III from the membrane and back into the cytoplasm. Auxiliary factors shown in parentheses. (Adapted from Sundquist & Kräusslich 2012).

1.3.7 Maturation

The final step of the viral life cycle is the maturation of the virus into a fully infectious particle that is able to infect another target cell. This requires the proteolytic processing of the Gag and Gag-Pro-Pol polyproteins by the viral PR. This is a multistep process that involves conformational changes and subunit rearrangements and starts simultaneously with the budding of the virion. Both polyproteins are cleaved at five sites each to create MA, CA, NC, p6, PR, RT and IN. MA remains associated with the inner leaflet of the viral membrane, whereas CA forms the typical HIV-1 conical core structure that consists of around 1200 CA molecules that form a net of hexagons and pentagons called the “fullerene cone”. The capsid core is closed at both ends, which is facilitated through the addition of twelve pentagonal defects. The CA subunits interact via their N- and C-terminal domains. The C-terminal domains also make inter-ring contacts (Ganser et al. 1999; Briggs et al. 2006; Ganser-Pornillos et al. 2008). The HIV-1 capsid plays essential roles at various steps of the viral life cycle such as in reverse transcription and nuclear entry, and capsid stability is crucial for these processes. The capsid also surrounds and encases the nucleocapsid and genomic RNA (Reviewed by Sundquist & Kräusslich 2012).

The HIV-1 protease is an aspartic acid protease that forms a homodimer wherein the active site traverses the dimer interface. In the context of the Gag-Pro-Pol polyprotein PR is inactive. Unprocessed PR constructs dimerize only very weakly, but can form transient complexes with catalytic activity. This can induce auto-processing of the N-termini and leads to the formation of a stable dimer with full catalytic activity (Tang et al. 2008). Once active, PR appears to recognise the overall structure of its substrate rather than a specific sequence (Prabu-Jeyabalan et al. 2002). The PR-induced cleavage events in the viral particle lead to the activation of the fusogenic acivity of Env (Murakami et al. 2004; Wyma et al. 2004), the stabilization of the RNA dimer and its chaperoning by the nucleocapsid (Moore et al. 2009; Rein 2010) and the disassembly of the immature lattice to form the conical capsid. The fully infectious virus is then equipped to infect a new target cell.

1.4 HIV Pathogenesis and the Host Innate Immune Response

HIV is mainly transmitted via the mucosal surfaces of genital or rectal tissue during sexual contact. It is thought that infection originates from only one virus, the transmitted/founder virus, that then disseminates to other lymphoid tissues (Keele et al. 2008).

The course of HIV infection can be divided into different stages. During the initial phase (~1-2 weeks), also known as the eclipse phase, the virus starts to replicate and spreads from the initial site of infection to other tissues and organs. At this stage, viremia and antiviral immune response are still low. In the first few weeks of infection the virus causes considerable damage to the host. In particular, $CD4^+$ T cells are dramatically depleted in tissues other than the peripheral blood, such as the gut-associated lymphoid tissue (GALT). Within the next weeks, during the acute phase, viremia increases considerably (commonly up to 10^7 copies of RNA per ml) and many infected $CD4^+$ T cells can be found in the blood and lymph nodes. Infected individuals may exhibit flu-like symptoms including fever and enlarged lymph nodes. The immune response starts to generate antibodies against all viral proteins and mounts a $CD8^+$ T cell response that is directed against viral antigens. At the end of the acute phase, viremia starts to decline due to a certain degree of immune control, to reach what is known as the viral set point (1-10^5 copies/ml). The next phase of HIV infection, the chronic phase, is characterized by a stable or slowly increasing viremia. Simultaneously, $CD4^+$ T cell levels in the blood fall gradually. This phase can persist for years or even decades and is usually asymptomatic, which means that patients may not be aware of their infection. When $CD4^+$ T cell counts drop below a certain level (~200 cells/µl) defining the onset of AIDS, the host immune system is so compromised that viremia rises and opportunistic infections start to occur, which eventually lead to the death of the patient. If left untreated, the mortality rate of HIV-1 infection is 95% (Reviewed by Coffin & Swanstrom 2013).

The two major drivers of HIV-1 pathogenesis are $CD4^+$ T cell depletion and systemic inflammation. Interestingly, only a small proportion of the host's $CD4^+$ T cells are productively infected and further, direct killing by HIV does not explain the death of bystander cells, which accounts for the majority of $CD4^+$ T cell death. It was shown that infection of naïve T cells is aborted early after entry, before reverse transcription is completed (Doitsh et al. 2010). This leads to the accumulation of DNA in the cytoplasm, which is sensed as a danger signal by the interferon gamma inducible protein 16 (IFI16) in infected $CD4^+$ T cells. As a result, the cell starts a proinflammatory defence program, which leads to caspase-1-induced pyroptosis of the cell. In addition, this programed cell death leads to the release of interleukin-1β to trigger further immune responses (Monroe et al. 2013; Doitsh et al. 2014). Therefore, this host immune response may contribute to the pathogenic, systemic inflammation and $CD4^+$ T cell loss characteristic of HIV-1 infection.

Upon viral infection, the host's immune system reacts to the intruding pathogen with an early, nonspecific innate response and, at a later point during infection, with a highly specific adaptive immune response. Early events during acute infection have been proposed to be critical for the course of HIV infection. The antiviral immune response comprises proinflammatory cytokines, certain innate immune cells, the complement system and interferon-inducible, cellular antiviral proteins (Reviewed by Carrington & Alter 2012; Guha & Ayyavoo 2013). The main cell types involved in the early immune response and proinflammatory cytokine production are dendritic cells (DCs), macrophages, natural killer (NK) cells and neutrophils. They express various pattern recognition receptors (PRRs) that enable them to sense pathogen-associated molecular patterns (PAMPs) such as protein motifs, carbohydrates or nucleic acids that are unique to pathogens and usually not present in the host cell. The sensing of PAMPs by PRRs induces downstream signalling and the induction of transcription factors that then mediate the expression of proinflammatory cytokines and type I IFN. DCs are the major source of high levels of IFN during early infection and they express diverse PRRs.

One group of PRRs are Toll-like receptors (TLRs) that are present on the cell surface or in intracellular compartments and are able to sense viral PAMPs such as glycoproteins, nucleic acids or unmethylated CpG DNA. RNA viruses, like HIV-1, trigger an innate immune response through TLR7/TLR8, which leads to the activation of DCs and the release of type-I IFN and TNF-α (Beignon et al. 2005). Additionally, TLR2 and 4 have been implicated in innate responses to HIV-1. Due to differential induction of type-I IFN they are associated with increased or decreased HIV transmission, respectively (Thibault et al. 2009). Furthermore, TLR9 has been reported to directly bind to gp120 to induce DC activation and type-I IFN secretion, which leads to the activation of NK cells (Martinelli et al. 2007). Another example of PRRs are the RIG-I-like receptors (RLRs) that recognize HIV RNA in the cytoplasm (Solis et al. 2011).

Other cellular proteins that can sense viral, cytoplasmic DNA, such as retroviral RT products, are the aforementioned IFI16 and the cyclic guanosine monophosphate-adenosine monophosphate (cGAMP) synthase (cGAS) (Gao et al. 2013; Jakobsen et al. 2013). Both activate the adaptor protein stimulator of interferon genes (STING) that then mediates the expression of type-I IFN and other cytokines. It has been shown that cGAS can sense HIV-1 infection in dendritic cells and macrophages and that this was dependent on the viral capsid (Rasaiyaah et al. 2013; Lahaye et al. 2013). Capsid interaction with CPSF6 or cyclophilins was shown to be required for

avoiding sensing by cGAS. While the CPSF6 or cyclophilin binding mutants N74D or P90A, respectively, in capsid triggered innate sensors and led to an inhibition of viral replication (Rasaiyaah et al. 2013). Interestingly, the cellular protein TREX1 has been shown to inhibit HIV sensing in infected cells (Yan et al. 2010a). This 3' exonuclease binds to cytosolic viral DNA and digests it, thereby preventing its recognition by cellular PRRs and subsequent interferon induction that would inhibit viral replication.

Among the most important innate immune cells in the response to viral pathogens are NK cells, which are activated and expand upon stimulation by IFN-α and IL-15. They express inhibitory killer immunoglobulin-like receptors (KIR) that interact with MHC-I molecules on other host cells, which leads to the inhibition of the NK cell. Many viruses have been shown to downmodulate MHC-I from the surface of the infected cell to avoid viral antigen presentation and detection by $CD8^+$ T cells. The lack of surface MHC-I expression is an activation signal for NK cells, but additional activating signals are required before killing of the infected cell is induced. Stress ligands such as MIC-A and ULBP-1/2 that are usually upregulated upon viral infection are recognised by the C-type lectin NK-cell (NKG2D) receptor. Expression of these stress ligands can even be sufficient to overcome the inhibitory effect of MHC-I recognition by NK cells (Raulet 2003; Zhang et al. 2005). HIV-1 Nef induces the downregulation of MHC-I molecules from the cell surface in a selective manner. While MHC-I HLA-A and HLA-B are removed, other MHC-I molecules remain on the cell surface, and this is thought to be a mechanism of avoiding NK cell killing. In addition, Nef downmodulates the expression of some NK cell activating NKG2D ligands (Cerboni et al. 2007). Thus, HIV is able to overcome NK cell mediated killing of the infected cell.

During acute infection, HIV-1 infected individuals produce high levels of circulating type-I IFN. Importantly, IFN expression leads to the induction of interferon stimulated genes (ISGs). Various restriction factors such as APOBEC3G, TRIM5α, tetherin, SAMHD1 and MX2 belong to this group of proteins and are able to inhibit viral replication at distinct steps of the viral life cycle. They will be discussed in more detail in the following section.

1.5 Cellular Restriction Factors and the Role of HIV-1 Accessory Proteins

HIV-1 encodes several accessory proteins including Vif, Nef, Vpu and Vpr. Whilst they are dispensable in some *in vitro* experimental settings, there is accumulating evidence for their essential role in viral replication *in vivo*. In particular, they modulate the host cell environment in a variety of ways that allow the virus to evade the antiviral immune response. This includes the antagonism of cellular antiviral factors. Whilst various host cell proteins are required for efficient HIV-1 replication, the host cell expresses a range of proteins that are detrimental for the virus. Viral infectivity varies greatly depending on the cell line used under experimental conditions and so does the requirement for HIV-1 accessory proteins. Analysis and comparison of permissive and non-permissive cells led to the discovery of restriction factors for HIV-1 that inhibit at various steps of the viral life cycle and are antagonised by HIV-1 accessory proteins. Most of these restriction factors are induced by IFN to some degree (Reviewed by Malim & Bieniasz 2012).

The first retroviral restriction factor to be identified was a protein encoded in mice, known as Friend virus susceptibility factor-1 (Fv1), that can block murine leukemia virus (MLV) replication (Best et al. 1996). There are two allelic variants in inbred mice, $Fv1^{n}$ and $Fv1^{b}$ that inhibit infection with B-tropic or N-tropic MLV, respectively, whereas heterozygous $Fv1^{n/b}$ mice are resistant to both MLVs. Fv1 is similar to an endogenous retroviral *gag* gene and the mechanism of inhibition is thought to require viral capsid binding to block the transit of proviral DNA to the nucleus (Hilditch et al. 2011). However, its precise mode of action remains to be determined.

In the following section the cellular restriction factors APOBEC3G, TRIM5α, tetherin, SAMHD1, Mx2, and SERINC5/3 and their antagonism by HIV and/or SIV accessory proteins will be discussed in more detail.

1.5.1 APOBEC3G and HIV Vif

The virion infectivity factor (Vif) is a 23 kDa protein that is required for viral replication in primary cells such as $CD4^{+}$ T cells, but is dispensable in other cell lines. Cell fusion experiments between permissive and non-permissive cell types suggested the existence of a dominantly acting restriction factor and a cDNA subtraction-based screen revealed Apolipoprotein B messenger RNA editing

enzyme catalytic polypeptide-like 3G (APOBEC3G) to be the restriction factor of Vif-deficient HIV-1 (Simon et al. 1998; Sheehy et al. 2002).

APOBEC3G (A3G) belongs to a family of proteins comprising eleven members in humans. It is expressed widely in human tissues and particularly in hematopoetic cells where it is partially inducible by type 1 interferon (Koning et al. 2009; Refsland et al. 2010). All APOBEC proteins have one or two zinc-coordinating domains with polynucleotide (RNA or DNA) cytidine deaminase activity (Z domains) that mediate the post-synthetic editing of cytidine residues to uridines, and therefore, change the nucleotide sequence. A3G has two of these domains. The C-terminal Z domain mediates the deamination with a sequence specificity of 5'CCCA (deaminated C underlined), whereas the N-terminal Z domain does not have catalytic activity, but mediates the packaging of A3G into assembling virions and is also recognised by HIV Vif (reviewed by Malim 2009). In the absence of Vif, A3G is incorporated into budding virions through RNA and nucleocapsid interaction of the N-terminal Z-domain (Bogerd & Cullen 2008). A3G forms dimers in an RNA-dependent manner, however, the relevance of dimerization for its antiviral function is unclear (Huthoff et al. 2009). It associates with the RTC and induces the deamination of up to 10% of the cytidines in the newly synthesized single-stranded negative-strand viral DNA, which leads to the loss of genetic integrity and functional inactivity (Harris et al. 2003; Mangeat et al. 2003; Zhang et al. 2003; Yu et al. 2004). A certain low level of APOBEC3 induced viral mutation has also been reported to contribute to viral diversification and was implicated in immune escape and development of drug resistance (Wood et al. 2009; Kim et al. 2010; Sadler et al. 2010). Additionally, it was suggested that A3G leads to a general decrease in viral cDNA levels in infected cells (Iwatani et al. 2007; Bishop et al. 2008).

Other members of the APOBEC3 family that have antiviral activity are APOBEC3D (A3D), APOBEC3F (A3F) and APOBEC3H (A3H). They share A3G's mechanism of action and are counteracted by Vif. However, they have different target site preferences for deamination: 5'TC or 5'GC.

HIV-1 Vif efficiently counteracts A3G by recruiting a cellular ubiquitin ligase complex including cullin 5 (CUL5), elongins B and C, RING-box protein 2 (Rbx2), and also the transcription co-factor core binding factor β (CBFβ) (Yu et al. 2003; Jäger et al. 2012; Zhang et al. 2012). This leads to the polyubiquitination and proteasomal degradation of A3G and prevents incorporation into

assembling virions. Furthermore, counteraction of APOBEC3 is species-specific for HIV and SIV Vif proteins and was suggested to be an important barrier to zoonotic transmission in primates (Gaddis et al. 2004; Compton & Emerman 2013; Etienne et al. 2013).

1.5.2 TRIM5α and the HIV Capsid

In many non-human primate cells, HIV-1 replication is blocked even though virus entry does occur. It became apparent that a dominant cellular antiviral factor targeted the HIV-1 capsid protein with similarity to the murine Fv1 protein and that this factor was present in primate cells (Hofmann et al. 1999; Towers et al. 2000; Cowan et al. 2002; Besnier et al. 2002). It was identified as the cellular tripartite motif (TRIM)-containing protein 5α (TRIM5α) and was discovered when rhesus macaque genes were screened for their ability to restrict HIV-1 in human cells (Stremlau et al. 2004).

TRIM5α belongs to a family of proteins that contains around 70 members of which several have been implicated to have antiviral function, including TRIM5, TRIM11, TRIM15, TRIM19, TRIM22, TRIM28 and TRIM31. Most research however, focuses on TRIM5 and only the TRIM5α isoform has antiretroviral activity in humans. All TRIM family members have a similar domain organization (Nisole et al. 2005). They contain an N-terminal RING domain with E3 ubiquitin ligase activity, one or two B-box type 2 domains required for the formation of higher order multimers and a central coiled-coil domain that, in the case of TRIM5, is required for dimerization. The C-terminal domain can vary and in TRIM5α this domain is called B30.2 or PRYSPRY and mediates protein-protein interactions. The SPRY domain is responsible for recognising the substrate, i.e. viral capsid, in the cytoplasm of infected cells. Interestingly, this domain shows signs of rapid evolution among species' sequences (Sawyer et al. 2005; Song et al. 2005; Johnson & Sawyer 2009). It is comprised of three hypervariable segments (V1-V3), where V1 determines the antiretroviral specificity (Perez-Caballero et al. 2005; Sawyer et al. 2005; Stremlau et al. 2005). While human TRIM5α is very potent in blocking N-MLV or equine infectious anaemia virus (EIAV) infection it is inactive against wild type HIV-1, although this may depend on the HIV isolate (Hatziioannou et al. 2004; Keckesova et al. 2004; Perron et al. 2004; Battivelli et al. 2010). However, HIV-1 replication is potently inhibited by old world monkey TRIM5α. In general, a certain species' TRIM5α is inactive against viruses that

have adapted to the host, but potently restricts viruses infecting other hosts, which indicates that it can be an effective barrier to cross-species transmission (Hatziioannou et al. 2006).

Cyclophilin A (CypA), a host cell chaperone protein, has been shown to be able to bind lentiviral capsid via a surface loop. Whilst the role of this binding is unclear, it can affect the sensitivity of capsid to TRIM5α (Berthoux et al. 2005; Keckesova et al. 2006; Stremlau, Song, et al. 2006). In owl monkeys and some species of macaque a retro-transposition event placed CypA into the TRIM5 locus, which resulted in the expression of a chimeric TRIM-CypA fusion protein called TRIMCyp. The CypA domain replaced the PRYSPRY domain in this protein (Sayah et al. 2004; Liao et al. 2007; Brennan et al. 2008; Newman et al. 2008; Virgen et al. 2008; Wilson et al. 2008). Capsids from lentiviruses that bind to CypA are restricted by TRIMCyp.

Both TRIM5α and TRIMCyp inhibit viral replication by directly binding the capsid of restriction-sensitive virus and inducing premature uncoating, thereby disrupting the RTC and blocking reverse transcription (Stremlau et al. 2006). TRIM5α assembles into hexagonal structures that interact with the hexagonal lattice of the capsid (Ganser-Pornillos et al. 2011). The formation of higher order multimers mediated by the B-box domain was suggested to increase the efficiency of the interaction between TRIM5α and capsid and therefore enhance antiviral activity (Perez-Caballero et al. 2005). The disassembled viral components are then degraded by the proteasome, which depends on the E3 ubiquitin ligase activity of the RING domain and also leads to a faster turnover of TRIM5α itself (Kutluay et al. 2013; Diaz-Griffero et al. 2006).

Neither ubiquitin nor proteasomal degradation are essential for the antiviral function of TRIM5α. In fact, no function of TRIM5α has been shown to be absolutely crucial for its antiviral activity, apart from its ability to bind capsid and to form multimers. It may be possible that TRIM5α inhibits viral replication in more than one way, which could result in redundancy. It was also suggested that TRIM5α inhibits reverse transcription and nuclear import independent of its role in uncoating (Roa et al. 2012; Wu et al. 2006). Importantly, no virally encoded antagonist of TRIM5α has been identified, but evasion of restriction is achieved by capsid mutations.

TRIM5α was shown to be an innate sensor of retroviral infection, triggering immune activation upon capsid binding (Pertel et al. 2011). This was suggested to be connected to its restriction of retroviral reverse transcription (Fletcher et al. 2015). The TRIM5α RING E3 ubiquitin ligase together with the UBC13-UEV1A E2 ubiquitin ligase complex mediate the synthesis of Lys63-linked ubiquitin

chains that recruit the TAK-1 kinase complex. This leads to the activation of transcription factors NF-κB and activator protein 1 (AP1) and subsequently proinflammatory cytokine and type-I IFN production, further stimulating the antiviral state. In addition, other TRIM family members have also been implicated in stimulating the innate, antiretroviral immune response (Uchil et al. 2013).

1.5.3 SAMHD1 and Vpx

Infection of certain resting primary cells such as monocytes, dendritic cells (DCs) or quiescent $CD4^+$ T cells by HIV-1 is relatively inefficient. However, it can be enhanced *in vitro* by the expression of the HIV-2 or SIVmac viral protein X (Vpx), which increases the number of reverse transcription products and has also been found to associate with an E3 ubiquitin ligase complex containing DCAF1, CUL4A and DDB1 (Goujon et al. 2008; Srivastava et al. 2008). Therefore, it was suggested that Vpx antagonises a cellular restriction factor present in cells that are non-permissive to HIV-1 infection. The sterile alpha motif domain and histidine-aspartate domain-containing protein 1 (SAMHD1) was shown to be a Vpx-interacting protein in co-immunoprecipitates and identified as a HIV-1 restriction factor (Laguette et al. 2011; Hrecka et al. 2011).

SAMHD1 plays a role in the cell-intrinsic innate immune response and regulation of IFN production. Polymorphisms in this protein in humans are associated with the Aicardi-Goutières syndrome (AGS), a neurological condition characterized by high levels of type-I interferon expression and upregulation of IFN-stimulated genes, which mimics congenital viral infections (Rice et al. 2009; Crow & Rehwinkel 2009). SAMHD1 contains a conserved N-terminal sterile alpha motif (SAM) domain and a C-terminal region that is required for the Vpx-induced recruitment of the E3 ubiquitin ligase complex and subsequent proteasomal degradation and inactivation of SAMDH1 (Ahn et al. 2012). Furthermore, it has a catalytic histidine-aspartate (HD) domain that exhibits triphosphohydrolase activity that is responsible for converting dNTPs into deoxynucleosides and triphosphate (Goldstone et al. 2011; Lahouassa et al. 2012; Powell et al. 2011; Goncalves et al. 2012; Franzolin et al. 2013). This decreases the level of dNTPS in the cytoplasm and it was suggested that this would limit the availability of dNTPs for viral reverse transcription and thereby inhibit viral replication. This is supported by the fact that HIV-2 Vpx increases the cellular levels of dNTPs and that exogenous addition of dNTPs to the culture medium bypasses SAMHD1-induced viral restriction (Lahouassa et al. 2012).

Whether the NTPase activity is the main antiviral activity of SAMHD1 was challenged by the observation that phosphorylation of residue T592 in SAMHD1 inhibited antiviral function without affecting NTPase activity and thus there may be an alternative mode of action (White et al. 2013; Welbourn et al. 2013; Yan et al. 2015). SAMHD1 also contains a nucleic acid binding domain overlapping the HD domain and has been reported to have nuclease activity towards single-stranded RNA or RNA in DNA/RNA hybrids (Beloglazova et al. 2013; Ryoo et al. 2014). It was proposed that SAMHD1 targets the viral RNA for degradation before reverse transcription can occur.

Structural data suggests that SAMHD1 forms dimers and, upon dGTP binding, tetramers (Goldstone et al. 2011; Ji et al. 2013; Hansen et al. 2014; Miazzi et al. 2014). While tetramerization does not seem to be required for the proposed nuclease activity of SAMHD1, it is essential for its dNTPase activity (Brandariz-Nuñez et al. 2013; Ryoo et al. 2014). The relative importance of dNTPase and nuclease activity of SAMHD1 and whether they are relevant for its antiviral function is a matter of debate. Conflicting reports supply evidence for the importance of both, but it is difficult to combine them in a single model (Reviewed by Ballana & Esté 2015).

Vpx is derived from a duplication or recombination event of the lentiviral *vpr* gene. HIV-2 and some SIVs encode both Vpx and Vpr, whereas HIV-1 only encodes the Vpr protein. Only a few Vpr proteins from SIVs infecting Sykes' monkeys, De Brazza's monkeys and African green monkeys and the Vpx proteins from HIV-2 and some SIVs, including SIVmac (macaque) and SIVsmm (sooty mangabey), have been found to be able to counteract SAMHD1(Lim et al. 2012). Why HIV-1 does not encode a countermeasure for SAMHD1 is so far unknown. It was suggested that SAMHD1-mediated restriction could be beneficial in the context of reduced recognition of viral reverse transcription products by cellular innate sensors such as cGAS and therefore, counteraction of this restriction factor by HIV-1 may not be essential (Gao et al. 2013; Lahaye & Manel 2015).

1.5.4 The Role of HIV-1 Vpr

The small 14 kDa protein Vpr is conserved among all primate lentiviruses. It became apparent that Vpr is essential for efficient viral replication *in vivo* when rhesus macaques were infected with a *vpr*-mutated SIVmac, where it was associated with attenuated pathogenesis (Lang et al. 1993; Hoch et al. 1995). Furthermore, it is required for efficient *in vitro* replication in macrophages (Connor

et al. 1995). Various roles have been ascribed to Vpr, including influencing reverse transcription, nuclear import of the PIC, interfering with cell cycle progression, regulation of apoptosis and transactivation of the HIV-1 LTR (Reviewed by Guenzel et al. 2014). As mentioned previously, some SIV Vpr proteins are able to induce the degradation of SAMHD1, however, HIV-1 Vpr is unable to do so. Vpr is packaged into assembling and budding virions via interaction with Gag p6, which indicates that it may be involved in early steps of the viral life cycle after host cell entry. It comprises a flexible N-terminus, a three alpha-helical domain and a flexible C-terminus and localizes to the nucleus and the nuclear membrane in infected cells.

The most established function of Vpr is its ability to induce cell cycle arrest in the G2/M transition phase, which is supported by the fact that HIV-1 infected individuals have higher numbers of $CD4^+$ T cells in the G2 phase. It was suggested that this function may be beneficial for the virus, as there is increased transcription during the G2 phase (Goh et al. 1998). To induce cell-cycle arrest, Vpr recruits a DDB1-CUL4 E3 ubiquitin ligase complex that was suggested to interfere with the DNA replication machinery (Wen et al. 2007; Hrecka et al. 2007). It was proposed that Vpr induces the degradation of a cellular factor that is required for the progression of the cell cycle into the M phase. Recently, the structure-specific endonuclease (SSE) regulator SLX4 complex, containing DCAF1, MUS81-EME1 and SLX4, was shown to interact with Vpr (Laguette et al. 2014). Vpr and DCAF1 recruit the polo-like kinase 1 (PLK1), which then activates the SLX4-associated endonuclease MUS81-EME1 that can cleave DNA. This inappropriate activation of the SLX4 complex that leads to chromosome instability and cell cycle arrest was suggested to be the mode of action of Vpr. The ability of various Vpr proteins to interact with SLX4 positively correlates with their ability to induce cell cycle arrest (Berger et al. 2015).

SLX4 belongs to the Fanconi Anemia (FA) protein family and mutations in these proteins have been associated with susceptibility to cancer and abnormal IFN production. In addition to cell cycle arrest induction, the SLX4 complex is also thought to be involved in the degradation of HIV-1 reverse transcripts. Around 90% of all viral reverse transcripts do not integrate and it has been demonstrated that degradation of these transcripts by cellular proteins such as TREX1 prevents recognition by the innate immune system and IFN induction (Suspène & Meyerhans 2012; Yan et al. 2010). The components of the SLX4 complex have been shown to be essential in the prevention of IFN induction upon infection and this has been attributed to reverse transcript degradation (Laguette et al. 2014).

1.5.5 MX2 Inhibits Early Stages of HIV Replication

The human myxovirus resistance protein 2 (MX2 or MXB) was recently identified as an IFN-inducible inhibitor of early post-entry HIV-1 infection (Goujon et al. 2013; Kane et al. 2013; Liu et al. 2013). It induces a block prior to nuclear import, but after reverse transcription. The viral determinant of restriction was proposed to be viral CA, however, the mechanism of antiviral action is still unclear. Mutations in CA that relieve the sensitivity to MX2 restriction do also interfere with binding to cyclophilin A, nucleoporins NUP153 and NUP358, and CPSF6, but do not abrogate binding to the MX2 (Fribourgh et al. 2014; Fricke et al. 2014; Liu et al. 2015).

MX proteins are highly conserved among vertebrates. Most mammals, including humans, have two *mx* genes encoding MX1/MXA and MX2/MXB. They are members of a family of dynamin-like GTPases. Neither are constitutively expressed, but are IFN-inducible and share 63% sequence identity as well as a similar structure (Gao et al. 2011; Fribourgh et al. 2014). They have an N-terminal GTPase (G) domain and a C-terminal stalk domain. Both domains are connected via a tripartite bundle signalling element (BSE). In the case of MX1, the stalk domain is essential for oligomerization and the BSE domain transmits conformational changes between C- and N-terminal domain upon GTP binding and hydrolysis (Haller et al. 2010; Gao et al. 2010; Gao et al. 2011). It localises to the cytoplasm and was shown to interact with intracellular membranes such as the membranes of the smooth endoplasmic reticulum/Golgi intermediate compartment. MX1 inhibits a broad range of RNA and DNA viruses, such as avian influenza A viruses (FLUAV), La Crosse virus, Thogoto virus, measles virus, VSV, or hepatitis B virus, but not HIV-1, by blocking diverse steps of the viral life cycle (Reviewed by Haller et al. 2015). While GTPase activity and oligomerization beyond dimerization are required for MX1 induced inhibition of viruses, they are dispensable for the anti-HIV-1 function of MX2 (Pitossi et al. 1993; Ponten et al. 1997; Gao et al. 2010; Dicks et al. 2015).

MX2 is expressed as two isoforms that differ in the length of their N-terminus (Melén et al. 1996). The shorter 76 kDa isoform lacks an N-terminal nuclear localization signal (NLS)-like motif that is required for antiviral function (Busnadiego et al. 2014; Goujon et al. 2014). This motif is required for the localization of long 78 kDa MX2 to the cytoplasmic face of the nuclear pore. Furthermore, the N-terminal region contains a triple arginine motif (residues 11 to 13) that is essential for antiviral function, potentially due to the ability to bind capsid (Goujon et al. 2015; Schulte et al. 2015). In fact, the N-terminal 91 amino acids of MX2 are sufficient for its anti-HIV-1

activity and this can be transferred to MX1 in chimeric proteins (Goujon et al. 2014; Busnadiego et al. 2014; Matreyek et al. 2014; Goujon et al. 2015). The mechanism of MX2's antiviral action remains to be determined. Whether it inhibits nuclear import of viral components or interferes with cellular factors that are required for viral capsid stability is still unclear.

1.5.6 HIV-1 Nef

When a full length sequence for the HIV-1 genome became first available it was discovered that an additional unknown open reading frame existed close to the 3' end of the viral genome, partially overlapping with the U3 region (Ratner et al. 1985; Wain-Hobson et al. 1985; Muesing et al. 1985). This open reading frame was shown to encode the 27-32 kDa viral protein Nef (for negative factor) that is common to all primate lentiviruses. Its name originates from reports that it suppresses viral transcription and replication upon overexpression in cell culture (Luciw et al. 1987; Ahmad & Venkatesan 1988; Niederman et al. 1989). This was, however, contradicted by later reports (Hammes et al. 1989; Kim et al. 1989). Nef seems to play an essential role *in vivo* for the maintenance of high viral loads as well as the development of AIDS. This became apparent in rhesus macaques infected with a Nef deficient SIVmac239 or patients infected with a Nef-deleted version of HIV-1, which was characterized by the absence of disease progression (Kestler et al. 1991; Deacon et al. 1995; Kirchhoff et al. 1995).

Nef comprises a structured, globular core domain that is flanked by a flexible N-terminal arm and a C-terminal disordered loop. All of those regions contain important motifs for protein-protein interactions or protein trafficking. Nef predominantly localises to perinuclear regions and associates with cellular membranes due to its myristoylation, but this also requires two basic leucine and arginine clusters close to its N-terminus (Greenberg et al. 1997; Bentham et al. 2006). It is incorporated into assembling virions, probably due to its association with cellular membranes, and gets cleaved by the viral protease, but the role of these events remains unclear (Pandori et al. 1996; Welker et al. 1996; Bukovsky et al. 1997; Chen et al. 1998). Nef interacts with numerous host factors and various roles have been ascribed to this accessory protein including downregulation of host cell molecules such as CD4, MHC-I and tetherin from the plasma membrane, modification of T cell signalling and activation, and enhancement of viral infectivity.

Nef achieves the downregulation of CD4 from the surface of infected cells by direct binding to CD4 and recruitment of clathrin adaptor protein 2 (AP-2) via its canonical dileucine $_{160}$ExxxLL$_{165}$ motif and additional stabilizing acidic residues $_{174}$(E/D)D$_{175}$ (Lindwasser et al. 2008; Ren et al. 2014). This induces the endocytosis of surface CD4, followed by lysosomal degradation of the protein. Nef binds to the membrane proximal region of CD4's cytoplasmic tail, which involves W57 and L58 residues in Nef (Anderson et al. 1994; Grzesiek et al. 1996). However, this function of Nef is independent of serine phosphorylation in the CD4 cytoplasmic tail (Garcia & Miller 1991). Nef is not the only HIV-1 protein that affects CD4. In addition, HIV-1 Vpu is able to mediate the lysosomal degradation of newly synthesized CD4, which it encounters in the ER. There have been numerous explanations suggested for the benefits of CD4 downmodulation by HIV-1. It increases virion release and infectivity of viral particles, enhances viral replication and prevents cytotoxic superinfection (Argañaraz et al. 2003; Wildum et al. 2006). Furthermore, binding of CD4 to Env gp120 leads to conformational changes that result in the interaction with the co-receptor and in the exposure of the helical heptad repeat (HR1) of the gp41 ectodomain, which can serve as an epitope for antibody-dependent cell-mediated cytotoxicity (ADCC). Downmodulation of CD4 by HIV-1 Nef and Vpu has been reported to prevent this (Veillette et al. 2014; Pham et al. 2014). The downregulation of CD4 by Nef seems to be a crucial function as it is highly conserved among Nef proteins and also maintained throughout disease progression (Basmaciogullari & Pizzato 2014).

Another surface molecule that is modulated by Nef is the major histocompatibility complex I (MHC-I). This Nef function is only maintained under strong selection pressure in the acute phase of infection and is supposed to protect the infected cell from killing by cytotoxic T lymphocytes (CTLs) at a stage of infection when the host is still immuno-competent (Collins et al. 1998; Carl et al. 2001). Two models for Nef-mediated downmodulation of surface MHC-I have been suggested. One proposes that Nef enhances the endocytosis of surface MHC-I, whereas the other model states that Nef induces the mis-trafficking of newly synthesized MHC-I. In the first model, Nef binds directly to the membrane trafficking proteins phosphofurin acidic cluster sorting proteins 1 or 2 (PACS-1/-2), which mediates trafficking of Nef to the TGN where Nef interacts with Src family kinases (SFK) (Atkins et al. 2008). This activates the SFKs Kck, Lyn and c-Src, which trigger a phosphorylation cascade and the formation of a protein complex comprised of tyrosine kinase zeta-chain-associated protein kinase 70 (ZAP-70) and the signalling kinase phosphoinositide 3-kinase (PI3K). This activates PI3K, which leads to the production of phosphatidylinositol (3,4,5)-triphosphate (PIP3) on

the inner leaflet of the membrane. How this process mediates the internalization of MHC-I is so far unclear (Reviewed by Pawlak & Dikeakos 2015). Internalized MHC-I is also inhibited from recycling back to the PM. This is achieved by the formation of a ternary complex between Nef, the cytoplasmic tail of MHC-I and the μ1 subunit of AP-1 (Figure 1.11) (Jia et al. 2012). The second model proposes that Nef blocks the trafficking of newly synthesized MHC-I from the TGN to the PM. Nef binds to immature, hyperphosphorylated MHC-I in the TGN and sequesters it, thereby inhibiting trafficking to the PM (Kasper et al. 2005). This also requires a ternary complex between Nef, MHC-I and AP-1, and the sorting into coatomer protein complex subunit beta (β-COPI) coated vesicles followed by lysosomal degradation (Schaefer et al. 2008). Both models are not mutually exclusive and may occur at different time points and further depend on the cell type. The importance of downmodulating MHC-I from the cell surface may be explained by its function in presenting viral peptides to $CD8^+$ cytotoxic T lymphocytes (CTLs). Consistent with this hypothesis, cells that are infected with a virus bearing a functional Nef are less efficiently killed by CTLs (Collins et al. 1998; Yang et al. 2002). On the other hand, cells lacking any MHC-I are targeted by natural killer (NK) cells for destruction (Kusunoki et al. 2000). To avoid this, Nef primarily targets MHC-I classes HLA-A and HLA-B, while leaving HLA-C, HLA-E and HLA-G unaffected (Cohen et al. 1999; Pizzato et al. 2004; Specht et al. 2008).

Apart from CD4 and MHC-I, some SIV and HIV Nefs also downregulate tetherin to enhance viral release. This will be discussed in more detail in section 1.6.

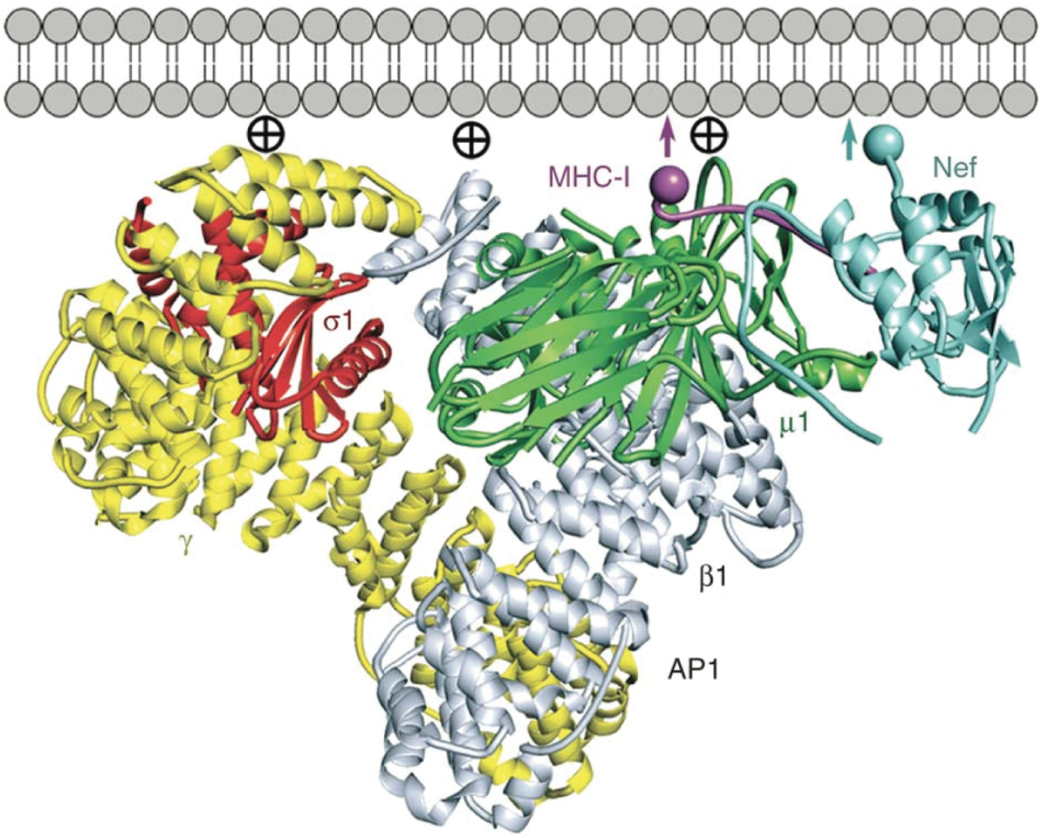

Figure 1.11 Model of Nef binding to MHC-I and AP-1 at a lipid membrane. Circled crosses represent PIP_2-binding sites and arrows indicate membrane-anchoring sites. (From Jia et al. 2012).

Nef proteins from SIVs that are non-pathogenic in their natural host as well as the Nef encoded by HIV-2 have the ability to efficiently downmodulate the TCR-CD3 complex from infected cells. This results in the suppression of T cell activation and inhibits activation-induced cell death (AICD). This correlates with the lower pathogenicity of these viruses in their natural host and was suggested to allow them to persist in the presence of an intact immune system. This activity of Nef was lost in SIVcpz prior to transmission to humans and the emergence of HIV-1 and it has been proposed that this is a determinant of the higher pathogenicity of HIV-1 in humans (Schindler et al. 2006).

In addition to influencing the surface levels of certain cellular proteins, Nef also modulates the activation threshold of T lymphocytes (Schrager & Marsh 1999; Simmons et al. 2001). It does so by hijacking signalling pathways and interacting with Src family tyrosine kinases, p21-activated serine/threonine kinases and Vav (Saksela et al. 1995; Fackler et al. 1999). This alters the transcriptional program in infected T cells, potentially creating a favourable environment for HIV replication. Moreover, this interference with signalling pathways also mediates the inactivation of cofilin, an actin depolymerizing factor, which leads to restriction of cell motility and migration of

infected cells (Stolp et al. 2009). Residues in Nef required for these activities are a proline-rich motif PxxP, an amphiphatic α-helix in the N-terminal region and a hydrophobic surface in the C-terminal loop (Saksela et al. 1995; Baur et al. 1997; Agopian et al. 2006).

Another important function of Nef is its positive effect on the infectivity of virions independent of its function of increasing infectivity by inducing the degradation of CD4 (Chowers et al. 1994; Miller et al. 1995; Goldsmith et al. 1995). This activity of Nef is highly conserved among various Nef proteins from HIV and SIV and is maintained during disease progression by strong selective pressure, but the precise role and mechanism were not understood until recently (Carl et al. 2001; Münch et al. 2007).

Infectivity enhancement by Nef requires AP-2 interaction via the ExxxLL or YxxL motif in HIV or SIV Nef, respectively (Chowers et al. 1994; Lock et al. 1999). Furthermore, dynamin 2 interaction and clathrin-mediated endocytosis are crucial for this function and it was suggested that it induces the endocytosis of a cellular factor (Pizzato et al. 2007). Comparative analysis of the protein composition of Nef-positive and Nef-deficient virus revealed that the cellular proteins Ezrin and EHD4 were more abundant in nascent virions produced in the absence of Nef (Bregnard et al. 2013). Although no direct inhibitory effect of these proteins was shown they were suggested to be co-factors for the infectivity enhancement by Nef. In addition, the lipid composition of viral particles did not correlate with virion infectivity (Brügger et al. 2007).

It was clear that Nef needed to be expressed in producer cells to overcome the restriction. However, it does not alter the incorporation of viral Env into budding virions (Aiken & Trono 1995; Miller et al. 1995; Lai et al. 2011). Nevertheless, the requirement for Nef to enhance infectivity depends on the envelope used to pseudotype the HIV particle. Env from viruses that require endocytosis and endosome acidification for fusion, such as VSV, are not responsive to Nef expression, i.e. Nef does not enhance the infectivity of HIV bearing these envelopes (Miller et al. 1995; Aiken 1997; Luo et al. 1998; Pizzato et al. 2008). In contrast, envelopes from viruses that fuse at neutral pH at the plasma membrane, such as HIV, require Nef for infectivity enhancement. Although, this has been a matter of debate, as HIV has been shown to also be able to fuse in early endosomes after endocytosis, but before acidification (Miyauchi et al. 2009; van Wilgenburg et al. 2014). Some HIV envelopes are more responsive to Nef's action than others and co-receptor usage does not seem to determine this requirement (Papkalla et al. 2002; Lai et al. 2011; Usami &

Göttlinger 2013). The differences in Nef responsiveness were mapped to a variable region of gp120, V2, that is also involved in neutralization sensitivity and trimer association. In fact, Nef has been shown to decrease the sensitivity to neutralizing antibodies that are directed against the membrane-proximal extracellular region of gp41 (Lai et al. 2011).

Reports about a possible Nef interference with the process of fusion of the the viral particle with the host cell membrane are conflicting, but it was suggested that Nef may interfere with the enlargement of the fusion pore that is required for efficient translocation of the viral core (Zhou & Aiken 2001; Tobiume et al. 2003; Cavrois et al. 2004). Differential results have been ascribed to different experimental set ups and the potentially easier diffusion of small molecules through the fusion pore compared to the large viral core.

Interestingly, an unrelated protein to Nef that is expressed by MLV, glycoGag, has been shown to have identical effects on HIV infectivity. GlycoGag is expressed from an unspliced MLV RNA that is translated from a CUG initiation codon upstream from the Gag initiation codon, resulting in a chimeric protein where the N-terminus constitutes a transmembrane domain (Pizzato 2010; Usami & Göttlinger 2013; Usami et al. 2014). It similarly increased infectivity of Nef-deficient virus and as for Nef, the V2 region of gp120 dictates the responsiveness to glycoGag. Envelopes such as VSV-G are, however, not affected. Importantly, the effect of Nef and glycoGag on infectivity are not additive.

Recently, it was found that Nef's enhancement of particle infectivity was due to its counteraction of the cellular membrane proteins serine incorporator 3 and 5 (SERINC3/5) (Usami et al. 2015; Rosa et al. 2015; Matheson et al. 2015). SERINC's mechanism of action in reducing infectivity of nascent virions is still unclear and several questions remain. The antiviral function of SERINC proteins and counteraction by HIV-1 Nef will be further addressed in chapter 5.

1.5.7 HIV-1 Vpu

The viral protein unique (Vpu) was identified in 1988 when an additional HIV-1 open reading frame, overlapping with the *tat* and *env* genes, was identified (Cohen et al. 1988; Strebel et al. 1988). Vpu is expressed by HIV-1, SIVgor and their precursor SIVcpz. Furthermore, SIVgsn, SIVmon, SIVmus and Dent's monkey SIV (SIVden) also express a Vpu protein. SIVcpz originates from successive cross-species transmission and recombination events involving the precursors of

SIVgsn/mon/mus/den and SIVrcm (Bailes et al. 2003). Therefore, it is likely that all Vpu proteins originate from the SIVgsn/mon/mus/den lineage of lentiviruses.

It was clear early on that Vpu was essential for the efficient release of virions from infected cells and it was reported later that this was due to the counteraction of tetherin (Terwilliger et al. 1989; Klimkait et al. 1990; Neil et al. 2008). This Vpu function will be discussed in more detail in section 1.6.4.1. Importantly, Vpu also induces the downregulation of CD4, and other surface molecules such as CD1d, NTB-A and SNAT1 (Klimkait et al. 1990; Willey et al. 1992; Shah et al. 2010; Moll et al. 2010; Matheson et al. 2015).

The 16 kDa phosphoprotein Vpu is translated from a bicistronic mRNA that also encodes for the HIV-1 envelope glycoprotein (Schwartz et al. 1990). It contains a short N-terminal domain, a transmembrane domain and C-terminal cytoplasmic tail (Figure 1.12) (Maldarelli et al. 1993; Bour & Strebel 2003). NMR data indicates that the transmembrane domain of Vpu is tilted between 15° and 30° in a lipid environment and is required for oligomerization of Vpu and ion-channel formation (Park et al. 2003; Park & Opella 2005; Schubert et al. 1996; Lopez et al. 2002). However, ion channel activity does not appear to be required for tetherin counteraction and virus release (Skasko et al. 2011; Bolduan et al. 2011). The cytoplasmic portion of Vpu comprises two alpha helices and has conformational flexibility. A recent study solved the Vpu full-length structure and showed that the two cytoplasmic helices form a U-shape (Zhang et al. 2015). The length of the inter-helical loop and the orientation of the third helix depend on the lipid composition. The relative flexibility of the C-terminal helix was suggested to support accessibility for the interaction with various proteins.

Two highly conserved serine residues in the cytoplasmic tail (S52 and S56) are constitutively phosphorylated by casein kinase II (CKII) (Schubert et al. 1992; Schubert & Strebel 1994; Friborg et al. 1995). This serine modification is required for the direct interaction with β-TrCP and the recruitment of the E3 ubiquitin ligase SCF complex (SCF^{TrCP}), which mediates CD4 and tetherin degradation (Margottin et al. 1998; Douglas et al. 2009).

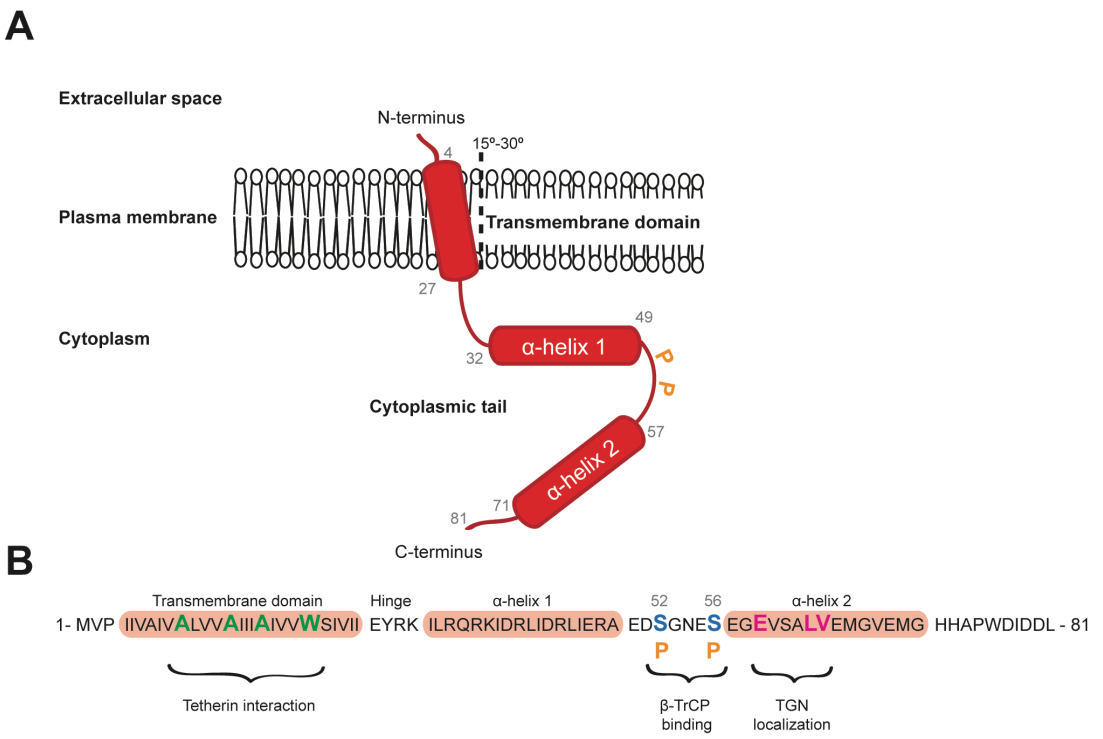

Figure 1.12 The topology of HIV-1 Vpu. (**A**) secondary structure of NL4.3 Vpu. The N-terminal transmembrane domain is predicted to be tilted by 13°. The cytoplasmic tail contains two alpha helices and is phosphorylated (P) at two serines at position 52 and 56. (**B**) Amino acid sequence of HIV-1 NL4.3 Vpu. Domains are indicated. Important residues are highlighted. Green: alanine face in the TM domain, required for direct interaction with tetherin. Blue: phosphorylated serine residues required for β-TrCP interaction. Pink: ExxxLV trafficking motif.

Vpu predominantly localizes to the TGN, endosomes and the ER (Varthakavi et al. 2003; Dubé et al. 2009). A dileucine-based sorting motif, ExxxLV, in the second alpha helix of the cytoplasmic tail of Vpu has been shown to be essential for this localization (Dubé et al. 2009; Kueck & Neil 2012). HIV-1 subtype C Vpus have a dileucine-based motif proximal to the transmembrane domain. These Vpus, however, localize mainly to the plasma membrane (Ruiz et al. 2008).

1.5.7.1 Vpu and CD4 Degradation

HIV-1 encodes two accessory proteins that are able to induce the degradation of CD4: Nef and Vpu. This indicates that removal of CD4 plays a crucial role in HIV-1 replication. CD4 can reduce the infectivity of viral particles by binding to the envelope precursor gp160 in the ER and preventing it from being processed and reaching the cell surface (Willey et al. 1992). This results in reduced Env-incorporation and infectivity of the budding particles. Additionally, CD4 surface expression can lead to super-infection of the cell, which is associated with increased cytotoxicity and reduced viral

spread (Wildum et al. 2006). Furthermore, binding of HIV-1 Env to CD4 exposes epitopes that are targeted by ADCC-mediating antibodies (Veillette et al. 2014). Nef and Vpu do not share the same anti-CD4 mechanism. Whilst Nef is expressed early in the viral life cycle and induces the enhanced AP-2 dependent endocytosis of surface CD4 followed by lysosomal degradation, Vpu is expressed at the same time as Env and induces the degradation of newly synthesized CD4 in the ER (Reviewed by Dubé et al. 2010).

Vpu and CD4 interact directly via their cytoplasmic tails and the hydrophobic transmembrane domains were suggested to stabilize the contact (Bour et al. 1995; Magadán et al. 2010). Residues in the cytoplasmic tail of CD4, $_{414}$LSEKKT$_{419}$, and a membrane proximal α-helix are sufficient to confer sensitivity to Vpu. Both cytoplasmic α-helices in Vpu have been found to be important for CD4 binding (Tiganos et al. 1997; Schubert et al. 2010; Singh et al. 2012). The phosphorylated serine motif is required for direct interaction with a WD-repeat in β-TrCP and formation of a ternary complex consisting of Vpu, CD4 and β-TrCP, which recruits the SCF E3 ubiquitin ligase (Margottin et al. 1998). This induces the ubiquitination of CD4 lysine, serine and threonine residues, which is followed by extraction from the ER and a form of endoplasmic reticulum-associated protein degradation (ERAD) (Binette et al. 2007; Magadán et al. 2010). This Vpu-mediated ERAD of CD4 differs from the classical process, because it does not use the ER membrane-associated E3 ubiquitin ligases. The VCP-UFD1L-NPL4 complex, including AAA-ATPase p97/VCP, that is involved in extraction of ERAD substrates from the ER, however, is required for Vpu-induced CD4 degradation (Binette et al. 2007).

1.5.7.2 Vpu and the Innate Immune Response

NK cells play a major role in the innate immune response to HIV-1 infection as discussed in section 1.4. The activation of NK cells is achieved by recognition of stress-induced molecules through the NK cell receptor NKG2D, but further signals are required to induce degranulation of NK cells (Cerwenka & Lanier 2001). One such signal can be the activation of co-receptors like the NK-T and B cell antigen (NTB-A), which belongs to the signalling lymphocytic activation molecule (SLAM) family and is found on blood-derived NK, T and B cells. Interestingly, HIV-1 Vpr was shown to increase NKG2D ligand expression levels (Ward et al. 2009). Also, HIV-1 Nef induces the downmodulation of MHC-I molecules from the surface of infected cells, which could potentially

enhance NK cell response (Cohen et al. 1999). In contrast, Vpu was shown to inhibit NK cell activation by downregulating surface levels of NTB-A in infected T cells (Shah et al. 2010). This Vpu function appears to be mechanistically different to its anti-tetherin and anti-CD4 function. Direct binding to NTB-A involves the transmembrane domain of Vpu. However, Vpu does not enhance the endocytosis of surface NTB-A and it was proposed that Vpu induces differential trafficking and sequestration of NTB-A. Counteraction is not dependent on β-TrCP recruitment and Vpu does not induce the degradation of NTB-A. Rather, Vpu interferes with the glycosylation pattern of newly synthesized NTB-A , which results in aberrant transport (Bolduan et al. 2013). Whether this Vpu function is essential *in vivo* is, however, unclear. In humanized, infected mice NTB-A was not found to be downregulated in a Vpu-dependent manner (Sato et al. 2012; Dave et al. 2013). While NK cell activation may be highly regulated by different HIV-1 proteins, further investigation is needed to understand the interference with NK cell activation by HIV-1.

Another surface molecule that has been shown to be downmodulated from HIV-1 infected dendritic cells is CD1d (Moll et al. 2010). As an MHC-I-like protein, CD1d presents antigens to natural killer T (NKT) cells. This results in the activation of immune cells and cytokine secretion, which further stimulates the antiviral immune response. Vpu does not induce enhanced endocytosis or degradation of CD1d, but rather sequesters it in early endosomes and prevents it from recycling back to the cell surface. As a result, CD1d is unable to present antigens to the immune system.

Recently, Vpu was found to downregulate the amino acid transporter SNAT1 from the cell surface of infected cells and to induce its ESCRT-dependent endolysosomal degradation via recruitment of β-TrCP (Matheson et al. 2015). This requires the phospho-serines in the Vpu cytoplasmic tail, but also W22 in the Vpu TM has been shown to be required. SNAT1 regulates the uptake of alanine into primary human $CD4^+$ T cells and alanine has been shown to be essential for T cell mitogenesis. Therefore, Vpu-mediated SNAT1 downregulation may represent a strategy to regulate immune cell activation (Matheson et al. 2015).

Recent data suggest that Vpu plays an additional important role in regulating the proinflammatory immune response. Vpu was shown to limit immune activation by NF-κB by antagonising tetherin-mediated signalling as discussed in section 1.6.8, but also by directly interfering with downstream NF-κB activation (Bour et al. 2001; Sauter et al. 2015). Whilst not all Vpu proteins antagonise tetherin, direct NF-κB inhibition is a conserved function among various

primate Vpus. Interestingly, primary Vpus from patient isolates were highly efficient in inhibiting NF-κB activation, compared to the lab-adapted strain NL4.3 Vpu (Pickering et al. 2014). It was suggested that Vpu achieves the direct inhibition of signalling by sequestration of β-TrCP and thereby stabilization of the NF-κB inhibitor IκB, which is a target of the SCF-β–TrCP ligase (Besnard-Guerin et al. 2004; Hotter et al. 2013). Interestingly, HIV-1 Nef induces NF-κB early in infection, presumably to promote viral replication. NF-κB inhibition by late expression of Vpu is dominant over the stimulating effects mediated by Nef, at a stage of infection when viral replication is efficiently driven by Tat, thereby independent of NF-κB (Sauter et al. 2015).

In addition, Vpu has been implicated in reducing TLR7-mediated type-I IFN production by pDCs (Bego et al. 2015). Through downmodulation and relocation of surface tetherin, it was suggested to promote tetherin/ILT-7 interaction upon cell-to-cell contact, which then results in the suppression of type-I IFN production by pDCs.

1.6 Tetherin and its Counteraction by Viruses

Tetherin, also known as CD317, HM1.24 or bone marrow stromal cell antigen 2 (BST-2), was discovered in a proteomic screen as a plasma membrane protein that was downregulated from the surface of cells expressing K5, a membrane-associated RING CH ubiquitin ligase encoded by Kaposi's sarcoma-associated herpesvirus (KSHV; also human herpesvirus 8 (HHV8)) (Bartee et al. 2006). Shortly after, tetherin was shown to be the target of HIV-1 Vpu (Neil et al. 2008; Van Damme et al. 2008).

It was long known that Vpu was able to enhance the release of virions from the plasma membrane of infected cells and that in the absence of Vpu virions would accumulate at the cell surface and in endosomes (Klimkait et al. 1990; Göttlinger et al. 1993). This requirement for Vpu was cell type dependent and species-specific (Varthakavi et al. 2003; Neil et al. 2006; Neil et al. 2007). Efficient HIV-1 release from permissive cell lines such as 293T, HT1080 or HOS cells did not require Vpu expression. In non-permissive cell lines such as Hela cells, HIV-1 release was restricted in the absence of Vpu. Heterokaryon experiments between permissive and non-permissive cells suggested a dominantly acting cellular factor was inhibiting the release of HIV-1 particles in the absence of Vpu (Varthakavi et al. 2003; Neil et al. 2006). Vpu was also able to rescue the release of a range of retroviral and filovirus-like particles and the restrictive phenotype

could be induced in permissive cells by type-I interferon treatment (Göttlinger et al. 1993; Neil et al. 2007). Fully mature virions were retained at the cell surface of Vpu-deficient HIV-1 infected cells. These virions could be released by protease treatment, in particular, when endocytosis was blocked using a Rab5 dominant negative mutant (Neil et al. 2006; Neil et al. 2007). Therefore, it was concluded that the inhibitor was a cellular, IFN-inducible protein that retained virions on the cell surface. It was constitutively expressed in some cell types such as Hela cells and was antagonised by HIV-1 Vpu.

BST-2 was identified as this restriction factor in 2008 (Neil et al. 2008; Van Damme et al. 2008). It was first described to be expressed on bone marrow stromal cells (hence the name), terminally differentiated B cells and plasmacytoid dendritic cells, and it was suggested to be involved in B cell growth (Goto et al. 1994; Ishikawa et al. 1995; Blasius et al. 2006). Comparing gene arrays from cell types that require Vpu expression for HIV-1 release or not revealed that BST-2 was expressed at levels 20-fold higher in Hela cells compared to HOS cells and it was upregulated to the same level by IFN-α treatment in permissive cell types such as 293T or HT1080 cells. It was subsequently called tetherin due to its 'tethering' mechanism of action (Neil et al. 2008).

It was soon clear that tetherin was capable of inhibiting diverse enveloped DNA and RNA viruses and that viruses had co-evolved to encode species-specific countermeasures, such as Vpu or K5. The anti-tetherin activity of a virus was suggested to play a crucial role in cross-species transmission of HIV-1 and HIV-2 (Sharp & Hahn 2011a). Importantly, tetherin was also suggested to play a role in retroviral pathogenesis and the anti-viral immune response *in vivo* (Liberatore & Bieniasz 2011; Barrett et al. 2012; Swiecki et al. 2012). Additionally, it is now clear that tetherin possesses antiviral function in addition to its physical function of virion retention. The following sections will describe the role of tetherin and its viral antagonism in more detail.

1.6.1 Tetherin Topology and Subcellular Localization

Tetherin is a type-II transmembrane protein with an unusual topology. It comprises a short N-terminal cytoplasmic tail, a transmembrane domain and an extracellular domain with a glycosylphosphatidylinositol (GPI)-anchor that covalently anchors the C-terminus to the outer leaflet of the PM (Figure 1.13) (Kupzig et al. 2003; Hinz et al. 2010; Schubert et al. 2010; H. Yang et al. 2010; Swiecki et al. 2011). Thus, tetherin is anchored to the PM at both ends, which is essential for

its anti-viral function. The GPI anchor is added to the protein posttranslationally in the ER through the enzymatic activity of PIG-L (Nakamura et al. 1997). In cells that lack PIG-L, no GPI anchor is added to proteins, resulting in their ER retention and failure to enter the secretory pathway. In the case of tetherin, this leads to a loss of antiviral function (Perez-Caballero et al. 2009). In addition, the GPI anchor is responsible for the association with lipid rafts (Kupzig et al. 2003). Two conserved asparagine residues in the ectodomain of tetherin (N-65 and N-92) are glycosylated, which explains the variable running size of 30-40 kDa of the mature protein in Western blots. While glycosylation has been shown to contribute to the transport and folding of tetherin, it is dispensable for antiviral function (Andrew et al. 2009; Perez-Caballero et al. 2009).Three cysteine residues in the ectodomain (C-53, C-63 and C-91) are required for the formation of a disulphide-linked tetherin dimer. The extracellular helix forms a parallel, dimeric, disulphide-linked coiled coil domain (residues 47 to 152), resulting in a 17nm alpha-helical rod-like structure. The dimer is hinged at two positions (A88 and G109 in human tetherin) that provides it with rotational flexibility and allows it to accommodate membrane curvature (Schubert et al. 2010; H. Yang et al. 2010). Although two tetherin dimers can form head-to-head tetramers under reducing conditions, this does not seem to be relevant for tetherin's anti-viral function and are unlikely to form *in vivo* due to steric hindrance of the disulphide bonds (Schubert et al. 2010). However, tetrameric structures of murine tetherin have been reported to resemble BAR domains that are involved in generation or stabilization of membrane curvature (Swiecki et al. 2013).

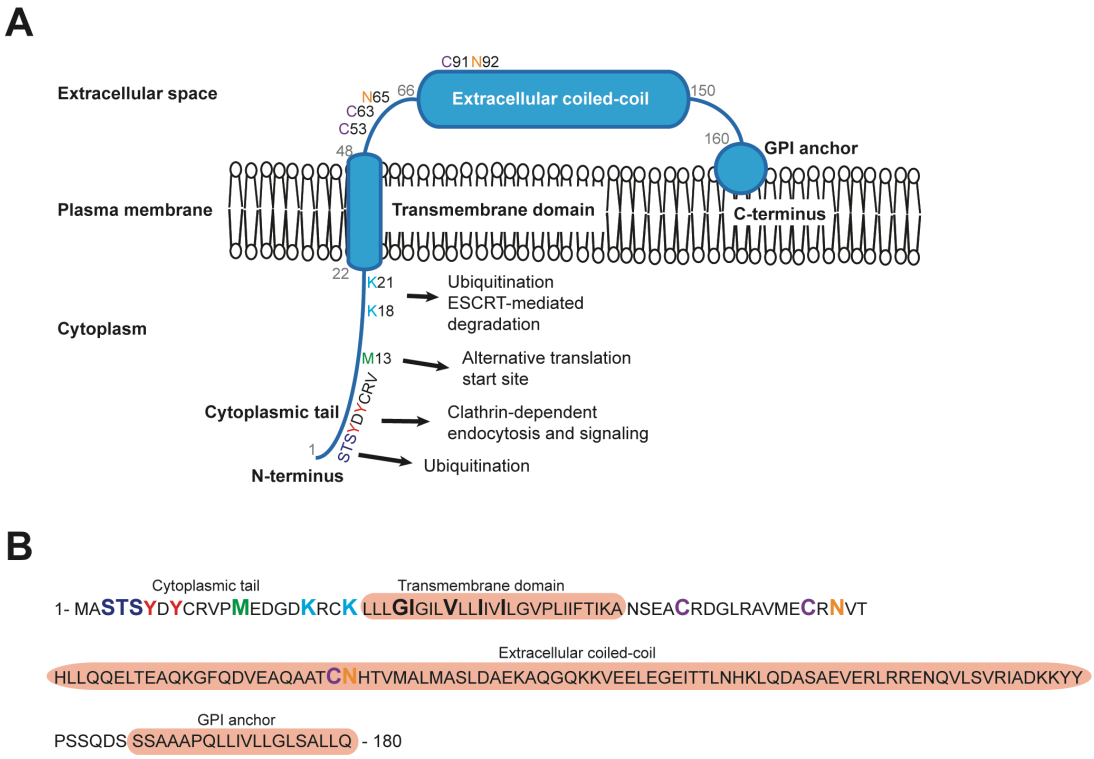

Figure 1.13 Tetherin topology. (**A**) Schematic representation of a tetherin monomer at the plasma membrane. The major domains are indicated: the N-terminal cytoplasmic tail, the transmembrane domain, the long α-helical extracellular coiled-coil domain, and the C-terminal GPI anchor. Important residues are marked. The dual-tyrosine motif (YDYCRV) required for endocytosis and signaling. Potential ubiquitin-acceptor residues include two lysines (K18 and K21) and an STS motif at the N-terminus. An additional M at position 13 can serve as an alternative translation start site. Three cysteine residues (C53, C63 and C91) are involved in dimerization and two glycosylation sites (N65 and N92) are indicated in the extracellular domain. (**B**) The amino acid sequence of human tetherin with the molecular features described in (**A**). Additionally, residues in the transmembrane domain that are required for Vpu binding are highlighted.

Tetherin predominantly localises to the PM, but also to the TGN and early/recycling endosomes (Kupzig et al. 2003). It is endocytosed from the PM in a clathrin-dependent manner that involves binding of clathrin adaptor AP-2 via the highly conserved, non-canonical dual-tyrosine motif YxYxxΦ in the cytoplasmic tail of tetherin (Figure 1.14) (Rollason et al. 2007; Masuyama et al. 2009). It then recycles from endosomes to the TGN, which requires interaction with the clathrin adaptor AP-1, before it is transported back to the PM. Clathrin-mediated, cellular transport pathways will be described in more detail in section 1.8.

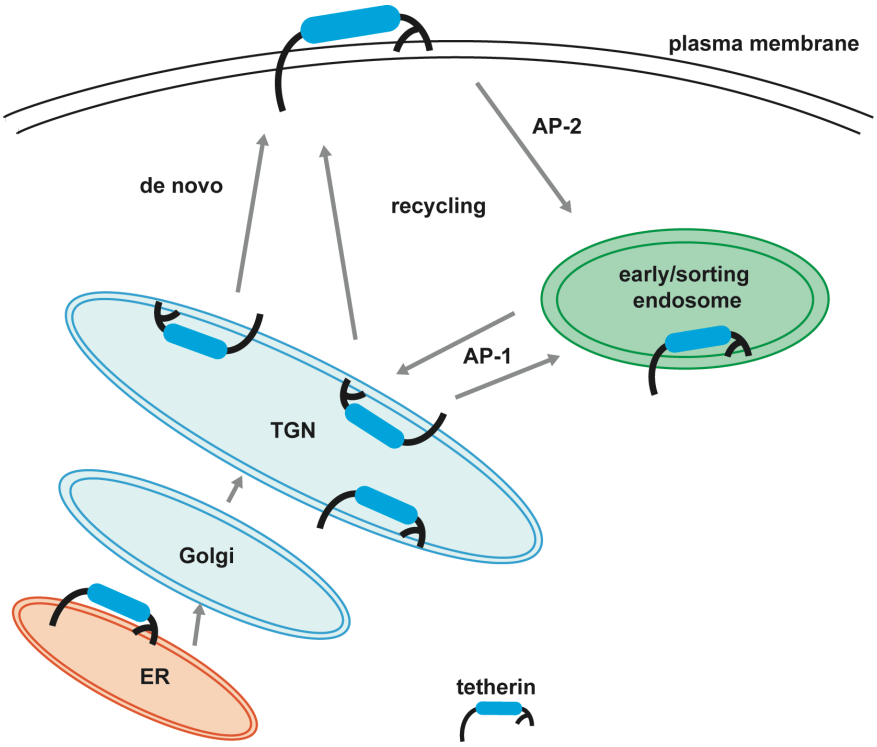

Figure 1.14 Model of tetherin recycling. Tetherin trafficking in the absence of Vpu. Newly synthesized tetherin traffics to the plasma membrane. AP-2 mediates the endocytosis of tetherin in clathrin-coated pits. It then traffics to the TGN, mediated by AP-1, and recycles back to the plasma membrane.

At the PM, tetherin associates with cholesterol-rich lipid rafts via its GPI anchor and it has been suggested that tetherin may regulate membrane protein distribution in these micro-domains (Kupzig et al. 2003; Billcliff et al. 2013). In addition, tetherin is involved in the polarization of epithelial cells where it interacts with the subapical actin cytoskeleton (Rollason et al. 2009). This is mediated through interaction with RICH2, EBP50 and ezrin. Interestingly, tetherin knock-out mice do not show developmental defects and the role of this tetherin function *in vivo* is unclear (Rollason et al. 2009; Liberatore & Bieniasz 2011). Interaction of tetherin with RICH2 also has implications for the signalling capacity of tetherin upon virion restriction, which will be explained in more detail in section 1.6.8.

Tetherin is constitutively expressed in many tissues and cell types including vascular endothelium, hepatocytes, monocytes, plasma cells and epithelia (Erikson et al. 2011). Tetherin expression can be induced by IFN-I treatment, but also by IFN-II and other proinflammatory cytokines to varying degrees in different cell types (Blasius et al. 2006; Neil et al. 2008; Van Damme et al. 2008; Homann et al. 2011; Bego et al. 2012). The tetherin promoter harbours several putative

NFAT, STAT and NF-κB binding sites 1.5 kb upstream of the transcriptional start site. An overlapping sequence containing an interferon-stimulated response element (ISRE), gamma-interferon activation site (GAS) and interferon regulatory factor (IRF) binding site is also present in the promoter region that is conserved across species (Bego et al. 2012). Tetherin expression can be directly induced by IRF 1, 3 and 7 independently of autocrine IFN-I, suggesting that tetherin can be induced by PRR signalling, as has been shown for TLR3 and TLR8 in human lymphoid and myeloid cells, respectively (Homann et al. 2011; Bego et al. 2012).

1.6.2 Genetic Diversity of Tetherin

Orthologues of tetherin exist in vertebrates including fish, birds, reptiles and mammals (Heusinger et al. 2015). Two unrelated proteins of the slime mold *Dictyostelium discoideum* have an organization similar to tetherin, but no evidence for convergent evolution or antiviral activity was detected. Human tetherin is encoded on chromosome 19 and can be expressed as two isoforms (Ishikawa et al. 1995; Cocka & Bates 2012). Like all mammalian tetherins that have been sequenced to date, human tetherin contains a second methionine in the cytoplasmic tail. In human tetherin it is located at position 13 and has, like the methionine at position 1, a weak Kozak consensus sequence in front of it. This results in leaky ribosomal scanning during translation and the expression of both a long and short isoform (Cocka & Bates 2012). The twelve amino acids that are missing in the short isoform contain important motifs for trafficking, but also ubiquitination and tetherin signalling. The latter will be explained in more detail in section 1.6.8. Whilst both human isoforms restrict HIV-1 release they are differentially sensitive to HIV-1 Vpu. Data presented in chapter 3 of this thesis addresses the differential role of human tetherin isoforms in the context of viral antagonism.

Polymorphic initiation codons for the long tetherin isoform have been described in domestic cats and NZW mice (Celestino et al. 2012; Barrett et al. 2012). Both lack the first AUG start codon in the *bst-2* gene and only express the shorter version of tetherin. In the case of NZW mice this has been associated with decreased pathogenesis of Friend virus infection *in vivo*. During the evolution of ruminants and before sheep, goats and cows diverged, their *bst2* gene was duplicated, which resulted in the expression of two tetherin isoforms. Both sheep tetherins, oBST2A and oBST2B, have antiviral activity with varying efficiency and potentially cell type specificity (Arnaud et al. 2010).

1.6.3 Tetherin's Antiviral Activity

Tetherin restricts the release of enveloped viruses by physically cross-linking budding virions to the plasma membrane (Figure 1.15 A-B). This non-specific mechanism of inhibition allows it to prevent the release of a broad range of viruses including all members of the *Retroviridae* family, Paramyxoviruses (Nipah, Hendra), Filoviruses (Ebola virua, Marburg virus), Rhabdoviruses (VSV), Arenaviruses (Lassa), Flaviviruses (Dengue virus) and some Herpesviruses (Herpes simplex virus 1 and 2, Human herpes virus 8). This also indicates that it is unlikely that tetherin executes its function through direct specific interaction with viral proteins. There are several lines of evidence supporting the role of tetherin in cross-linking virions to the PM. Restricted virions can be released by protease treatment and tetherin fragments can be detected in the liberated particle (Neil et al. 2008; Perez-Caballero et al. 2009; Venkatesh & Bieniasz 2013). Furthermore, tetherin colocalizes with HIV-1 Gag in immunofluorescence assays and immunoelectron micrographs show tetherin between budding virions and the PM (Figure 1.15 A and B) (Neil et al. 2008; Jolly et al. 2010; Fitzpatrick et al. 2010; Hammonds et al. 2010).

The topology of tetherin is essential for its antiviral function. However, it is not the specific sequence of tetherin, but rather the overall structure that is required. An artificial molecule mimicking the topology of tetherin was almost as potent in inhibiting virus release as tetherin (Perez-Caballero et al. 2009). This suggests that tetherin does not require a co-factor for its antiviral activity. Theoretically, several models of tetherin cross-links between virion and PM are possible. An equatorial model was proposed, where both ends of one tetherin molecule are inserted into the same lipid membrane and virion tethering would occur through dimer formation. Another model is the axial model, where both N-termini or C-termini of the dimer are either inserted together in the PM or the virion (Figure 1.15 C). Accumulating evidence supports the axial model of tetherin insertion (Perez-Caballero et al. 2009; Venkatesh & Bieniasz 2013). Site specific proteolytic cleavage and quantification of tethered virions showed that the C-termini of tetherin dimers were incorporated into budding virions three to five times more often than the N-termini (Venkatesh & Bieniasz 2013). One study suggested that 4-7 tetherin dimers are inserted per virion, while another study proposed that each particle was associated with 80-400 dimers (Lehmann et al. 2011; Venkatesh & Bieniasz 2013). The distinct experimental setup of these two studies may explain these differences and the number of tetherin dimers inserted into budding virions for restriction is not entirely clear.

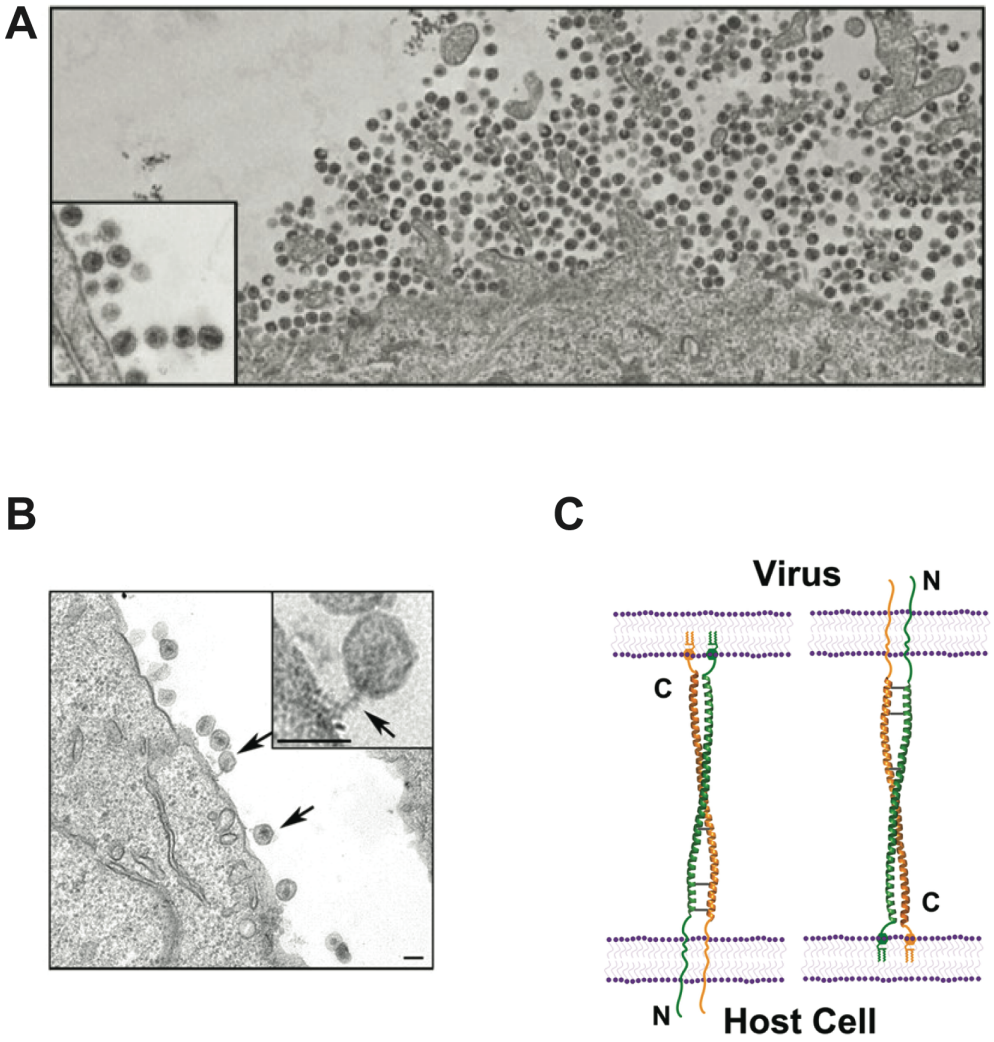

Figure 1.15 Restriction of viral particles by tetherin. (**A**) Electron micrographs: Vpu-deficient HIV-1 accumulate at the cell surface of infected HT1080 cells expressing tetherin. (From Neil et al. 2008) (**B**) Jurkat cells infected with HIV-1 NL4.3 ΔVpu were fixed and prepared for TEM. Virions tethered to the PM are indicated with an arrow. Scale bar, 100 nm. (From (Jolly et al. 2010) (**C**) Schematic representation virion restriction by tetherin. Tetherin monomers are in parallel orientation. Either the GPI anchors or the N-terminal transmembrane domains are inserted into the virion. (From Venkatesh & Bieniasz 2013).

Virion retention is followed by endocytosis of the particles that then accumulate in endosomal compartments. Potentially, this can lead to the degradation of the virions and release of viral antigens for presentation to the immune system. This would have implications for an augmented antiviral immune response induced by tetherin-mediated virion restriction. The process of endocytosis and endosomal accumulation is dependent on the dual-tyrosine motif in the cytoplasmic tail of tetherin and the cellular GTPase Rab5 and E3 ubiquitin ligase Rabring7 (BCA-2) (Neil et al. 2006; Miyakawa et al. 2009). Whether the association of tetherin with the cortical actin network via RICH2 plays a role in virion internalization is unclear.

1.6.4 Viral Antagonists

As mentioned previously, tetherin restricts a broad range of viruses. To overcome this restriction, several viruses have evolved antagonists. These virally encoded proteins remove tetherin from its site of viral budding, thereby preventing its insertion and virion retention. Antagonism often involves the mis-trafficking of tetherin, either preventing it from reaching the plasma membrane or inducing its endocytosis (Le Tortorec et al. 2011). Tetherin counteraction is species-specific and different viruses evolved different countermeasures and mechanisms that will be discussed in the following section. Examples of tetherin antagonists and a short description of their mechanism is depicted in Figure 1.16.

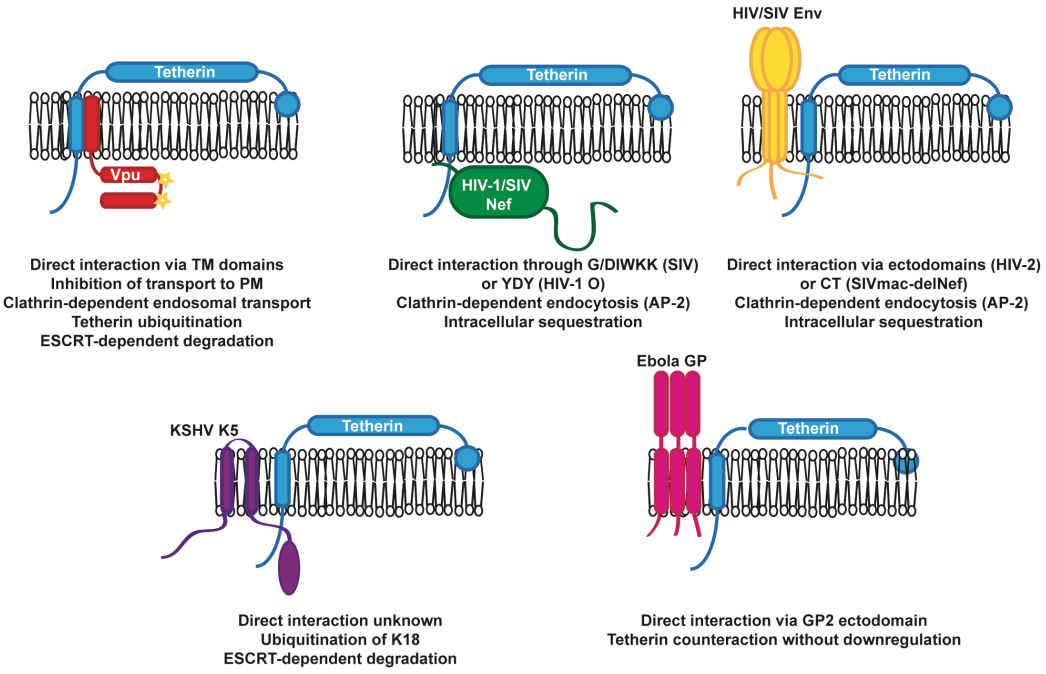

Figure 1.16 Viral tetherin antagonists. Schematic representation of well characterized tetherin antagonists HIV-1 Vpu, SIV/HIV-1 Nef, HIV-SIV Env, KSHV K5 and Ebola GP with a short summary of their mechanism of action.

1.6.4.1 HIV-1 Vpu

HIV-1 Vpu is the prototypic tetherin antagonist and has been studied extensively. It induces the downmodulation of tetherin from the surface, which is achieved by re-routing newly synthesized and recycling tetherin and preventing it from reaching the cell surface. It also reduces total cellular levels of tetherin by inducing its ESCRT-dependent lysosomal degradation. This process is

mechanistically different to Vpu-mediated CD4 degradation (Van Damme et al. 2008; Douglas et al. 2009; Iwabu et al. 2009; Mitchell et al. 2009).

Tetherin and Vpu interact directly via their transmembrane domains and this is essential for counteraction and determines species-specificity (Figure 1.17) (Iwabu et al. 2009; Mangeat et al. 2009; Perez-Caballero et al. 2009; Dubé, Roy, et al. 2010; Vigan & Neil 2010; McNatt et al. 2013). Whilst HIV-1 Vpu efficiently antagonises human tetherin it is inactive against non-human primate tetherins other than chimpanzee or gorilla (McNatt et al. 2009). Residues that are essential for Vpu-sensitivity lie along one face in the transmembrane α-helix and include I34, L37 and L41. Additionally, a threonine at position 45 has been implicated. In Vpu, a conserved alanine face, $A_{10}xxx(A/V)_{14}xxxA_{18}xxxW_{22}$, was found to be crucial for direct interaction with tetherin (Gupta et al. 2009; Vigan & Neil 2010; Kobayashi et al. 2011; Skasko et al. 2011; Matthew W. McNatt et al. 2013). Interestingly, these residues are conserved in the Vpu proteins from HIV-1 groups M and N, but not in the Vpu proteins of group O that have no anti-tetherin activity (Sauter et al. 2009; Vigan & Neil 2010). The requirements for tetherin/Vpu interaction furthermore suggest that Vpu binds tetherin as a monomer, as a Vpu multimer would not allow binding via this face (Park et al. 2003; Vigan & Neil 2010). Tryptophan 22 in Vpu's transmembrane domain has also been suggested to regulate multimerization of Vpu and therefore, substrate accessibility (Magadán & Bonifacino 2012).

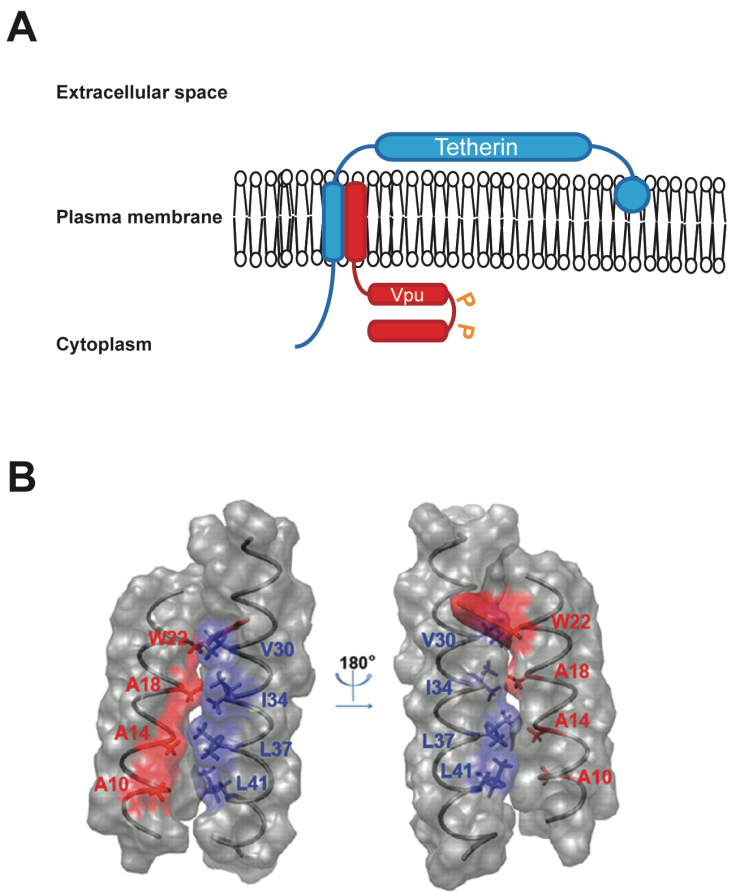

Figure 1.17 Interaction between tetherin and Vpu. (**A**) Vpu and tetherin interact via their transmembrane domains. (**B**) NMR structural model of Vpu and tetherin transmembrane domains interacting. Important residues for interaction are annotated for Vpu (red) and tetherin (blue) (from Skasko et al. 2012).

To antagonise restriction, Vpu removes tetherin from the cell surface, the site of its action. However, Vpu does not induce enhanced endocytosis of tetherin or its removal from lipid rafts (Mitchell et al. 2009; Miyagi et al. 2009; Dubé et al. 2010; Schmidt et al. 2011). Rather, Vpu prevents the trafficking of tetherin to the plasma membrane and mediates its sequestration in TGN-associated and/or endosomal compartments, which is followed by lysosomal degradation (Van Damme et al. 2008; Douglas et al. 2009; Iwabu et al. 2009; Mitchell et al. 2009) (Figure 1.18). Whether the final degradation step is required for tetherin antagonism by Vpu is a matter of debate and it has been further proposed that the mis-trafficking of tetherin may be sufficient for counteraction (Schubert & Strebel 1994; Mangeat et al. 2009; Mitchell et al. 2009). In agreement with tetherin sequestration, Vpu and tetherin co-localize predominantly to the TGN and endosomal compartments. Moreover, mutations in Vpu that inhibit its TGN localization also confer a defect in promoting virus release from tetherin expressing cells (Dubé et al. 2009).

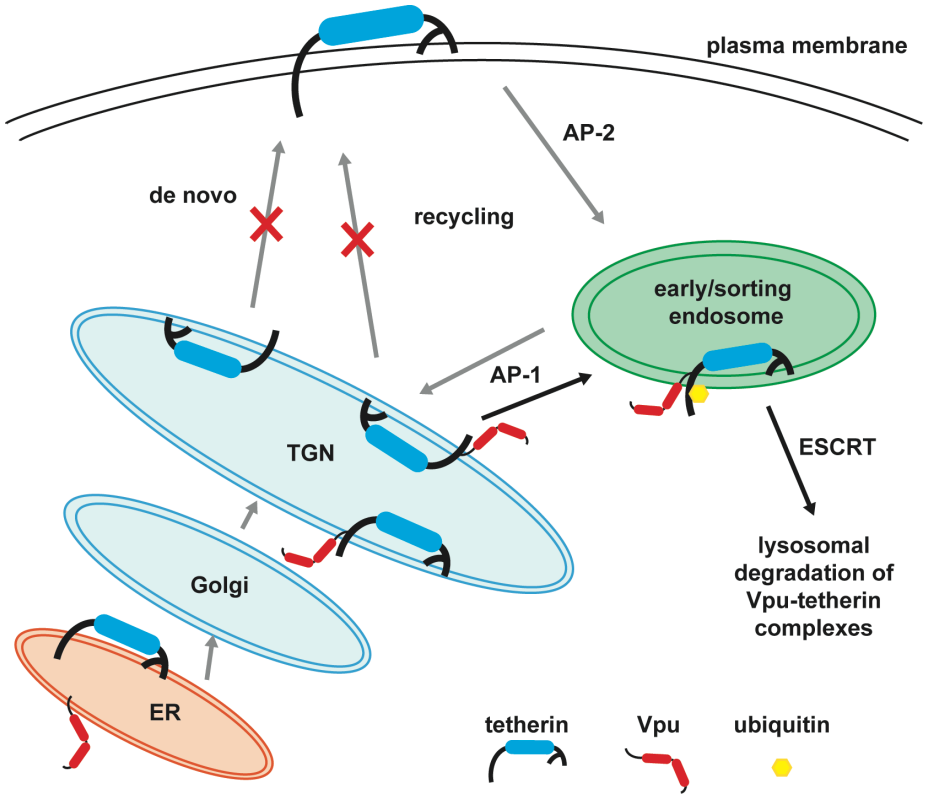

Figure 1.18 Model of Vpu-mediated mis-trafficking of tetherin. In an uninfected cell, newly synthesized tetherin traffics to the plasma membrane. AP-2 mediates the endocytosis of tetherin in clathrin-coated pits. It then traffics to the TGN, mediated by AP-1, and recycles back to the plasma membrane. In HIV-1 infected cells, Vpu interacts with newly synthesized or recycling tetherin in the endoplasmic reticulum (ER) or the Golgi apparatus. Instead of reaching the plasma membrane, the Vpu/tetherin complexes are sorted into endosomal compartments. Furthermore, Vpu recruits SCF-β-TrCP, which ubiquitinates tetherin's cytoplasmic tail. Ubiquitin-dependent recruitment of HRS then induces ESCRT-dependent degradation in lysosomes.

Inhibition of the fast recycling pathway through monensin had no effect on tetherin surface levels and revealed that tetherin recycles through a slow pathway (Dubé et al. 2011). Thus, it was suggested that Vpu has to counteract both newly synthesized and slow-recycling tetherin to promote virus release. Interestingly, the anti-malaria drug primaquine was shown to mimic Vpu's anti-tetherin function. Whilst not inducing tetherin endocytosis, it interferes with cellular transport pathways and is able to overcome tetherin restriction, further indicating that mis-trafficking of tetherin may be sufficient for antagonism (Schmidt et al. 2011). Additionally, evidence for antagonism of recycling tetherin by Vpu comes from a study using brefeldin A (BFA), which inhibits protein transport from the ER to the Golgi apparatus. BFA treatment did not affect tetherin downmodulation in the presence of Vpu, contributing to the evidence that Vpu inhibits the endosomal recycling of tetherin in addition (Lau et al. 2011).

Tetherin antagonism by Vpu is dependent on clathrin, which was demonstrated by overexpression of the C-terminal fragment of AP180 that disrupts clathrin-mediated endocytosis (Lau et al. 2011; Kueck & Neil 2012). This is determined by an acidic dileucine sorting motif, ExxxLV, in the second alpha helix of the Vpu cytoplasmic tail. The subcellular localization of Vpu suggested that the mis-trafficking of tetherin may involve the clathrin adaptor AP-1. However, individual knockdown of clathrin adaptors AP-1, AP-2 or AP-3 did not lead to reduced counteraction of tetherin by Vpu and it was suggested that this may be due to redundancy in clathrin adaptor usage (Mitchell et al. 2009; Kueck & Neil 2012). Recently, binding of a Vpu-tetherin fusion protein to AP-1 has been demonstrated structurally (Jia et al. 2014). While tetherin binds to the μ subunit of AP-1 via its dual-tyrosine motif, Vpu binds the σ subunit via the ExxxLV trafficking motif. The ExxxLV motif in Vpu is required for correct subcellular localization of Vpu and also tetherin counteraction. Mutation of these residues leads to increased tetherin surface levels and inhibits tetherin degradation (Kueck & Neil 2012). Interestingly, this trafficking motif is absent in the Vpu proteins of HIV-1 group M subtype C. However, they contain a di-leucine motif, ExxxLL, in the first cytoplasmic alpha-helix (Ruiz et al. 2008). Whether this motif plays a role in trafficking and tetherin antagonism remains to be determined. In chapter 4 of this thesis, Vpu trafficking, the role of the phospho-serines in tetherin antagonism and clathrin adaptor binding will be analysed further.

Vpu mediates the degradation of tetherin by sorting it into an endo-lysosomal pathway, which involves Rab GTPases that mediate intracellular membrane trafficking. The late endosome-associated Rab7a is involved in fusion of endosomal and lysosomal compartments and was also shown to be required for the processing of HIV-1 Env and Env incorporation into assembling virions, which is important for virion infectivity (Caillet et al. 2011). In addition, knockdown of this GTPase resulted in a release defect of HIV-1 in tetherin expressing cells. It was suggested that Rab7a-mediated trafficking processes are essential for the activity of Vpu to overcome tetherin restriction.

Tetherin degradation is dependent on ubiquitination and several residues in tetherin have been proposed to be ubiquitin acceptor sites. Lysine 18 and/or 21 were shown to be mono-ubiquitinated and their mutation blocks tetherin degradation (Pardieu et al. 2010; Goffinet et al. 2010). Furthermore, serine and threonine residues were reported to be poly-ubiquitinated and implicated in Vpu-mediated antagonism (Tokarev et al. 2011). In contrast, another study indicated that none of theses residues were required and a mutated tetherin was still ubiquitinated and antagonised (Gustin et al. 2012). In this study, it was suggested that tetherin may be ubiquitinated at the

cytoplasmic tyrosine residues or the NH_2 terminus of tetherin. The ubiquitination of tetherin depends on the phosphorylation of the two serine residues in the DSGNES motif in Vpu's cytoplasmic tail that are required for the recruitment of the E3 ubiquitin ligase complex SCF^{TrCP} (Margottin et al. 1998; Mangeat et al. 2009; Douglas et al. 2009; Mitchell et al. 2009; Iwabu et al. 2009; Goffinet et al. 2009). Mutation of the two serines completely abrogates the interaction between Vpu and β-TrCP, but only partially reduces virus release from tetherin expressing cells (Van Damme et al. 2008; Mitchell et al. 2009). This indicates that the β-TrCP-mediated degradation of tetherin may not be solely responsible for the anti-tetherin activity of Vpu. However, there are discrepant data on the role of tetherin degradation in Vpu-mediated antagonism and it is still unclear whether this last step is essential for promoting virus release from infected cells. The role of tetherin degradation in tetherin antagonism by HIV-1 Vpu is re-evaluated in chapter 4 of this thesis.

The ESCRT machinery is involved in the natural turnover of tetherin. ESCRT-0 component HRS binds to ubiquitinated cargo and induces its sorting for lysosomal degradation. It was reported that HRS was required for the downregulation and degradation of tetherin by Vpu and efficient particle release (Janvier et al. 2011). Moreover, ESCRT-I subunit UBAP1 was shown to be essential for tetherin degradation (Agromayor et al. 2012). UBAP1 knockdown resulted in the accumulation of ubiquitinated tetherin, which suggests that Vpu-mediated sorting of tetherin for degradation requires the ubiquitin-dependent multivesicular body pathway. However, UBAP1 depletion had no effect on virus release, further indicating that the trafficking of tetherin to endosomal compartments from which it cannot escape is required for virus release, but tetherin degradation may be dispensable.

As mentioned earlier, Vpu proteins are also expressed by the SIVgsn/mon/mus/den lineage and SIVcpz and SIVgor. While SIVcpz and SIVgor Vpus have no anti-tetherin activity, the Vpu proteins from SIVgsn/mon/mus/den have activity against their host species tetherin (Sauter et al. 2009). SIV cross-species transmission resulted in the emergence of HIV-1 groups M, N, O and P. While group M Vpu is an efficient tetherin antagonist, the Vpu proteins encoded by group N have moderate, if any activity, while group O and P encoded Vpus are completely inactive. In the case of group O, Vpu lacks the important transmembrane residues required for interaction with tetherin, which is essential for antagonism (Yang et al. 2011; Vigan & Neil 2011). However, its Nef protein has adapted to moderately counteract human tetherin (Kluge et al. 2014). While group N Vpus are still able to interact with tetherin, most of them lack the crucial phospho-serine and ExxxLV motifs

in the cytoplasmic tail, which also inhibits their anti-CD4 function (Sauter et al. 2012). One exception is a highly pathogenic variant of HIV-1 group N that was isolated from an individual returning to France from Togo. The Vpu from this isolate shows an intact phospho-serine and ExxxLV motif and is able to efficiently counteract tetherin. Only two isolates of group P have been identified to date. Vpu, Nef and Env proteins from these viruses do not counteract tetherin (Yang et al. 2011; Sauter et al. 2011).

1.6.4.2 SIV Nef and HIV-1 Group O Nef

Most SIVs do not encode a Vpu and instead use their Nef protein to counteract the tetherin of their host species (Jia et al. 2009; Sauter et al. 2009; Zhang et al. 2009). These include SIVmac (rhesus macaque), SIVagm (African green monkey), SIVsmm (sooty mangabey), and SIVrcm (red capped mangabey). To evade tetherin restriction, SIV Nef induces the enhanced internalization of tetherin from the cell surface, which is dependent on interaction with AP-2, but, of note, does not induce the degradation of tetherin (Zhang et al. 2011a). Depletion of AP-2 by RNAi or mutation of the AP-2 binding site in Nef abrogates its anti-tetherin function. Furthermore, myristoylation and membrane association of Nef is required for this function.

SIV Nef counteracts tetherin in a species-specific manner and human tetherin is resistant to its antagonism. This maps to a five amino acid deletion in (G/DIWKK) in the cytoplasmic tail of human tetherin. Insertion of these residues into human tetherin renders it sensitive to SIV Nef antagonism (Zhang et al. 2009). It was suggested that Nef-like activity may have exerted strong selective pressure on tetherin, which resulted in the loss of this motif on human tetherin (Lim et al. 2010). SIVcpz and SIVgor encode a Vpu protein, but they do not possess anti-tetherin activity. Instead they use their Nef protein for antagonism (Yang et al. 2010; Sauter & Kirchhoff 2011). This may be explained by the fact that SIVcpz is the product of cross-species transmission and recombination events that involves precursors of the SIVgsn/mus/mon/den lineage and SIVrcm (Bailes et al. 2003). The 5' portion of the SIVcpz genome, including *vpu*, originates from an SIV infecting guenons and the 3' portion, including *nef*, from an SIV most similar to SIVrcm, which lacks *vpu* (Sharp & Hahn 2011a). As two different tetherin antagonists were present in SIVcpz, this function may have been lost in Vpu, but preserved in Nef (Sauter et al. 2010).

There are several examples that provide evidence that tetherin exerts high selective pressure on SIV replication *in vivo*. When a chimpanzee experimentally infected with HIV-1 developed disease, it was found that the Vpu-deficient virus re-acquired anti-tetherin function in Nef (Götz et al. 2012). In a separate study, attenuated Nef-deficient SIVmac was shown to regain pathogenesis by adapting its Env protein to counteract rhesus tetherin (Serra-Moreno et al. 2011).

Similarly to SIVcpz and SIVgor, HIV-1 group O encodes a Vpu that does not exhibit anti-tetherin function. Recently, it was shown that the Nef protein of HIV-1 group O has some capacity to counteract human tetherin (Kluge et al. 2014). Due to the five amino acid deletion in human tetherin, group O Nef seems to have adapted to target adjacent residues and was suggested to prevent the transport of long tetherin to the cell surface instead of enhancing endocytosis.

1.6.4.3 Retroviral Envelope Proteins

While HIV-1 Vpu readapted to compensate for the lack of Nef activity against human tetherin, HIV-2, which does not encode a Vpu, uses its Env to remove tetherin from its site of action (Sharp & Hahn 2011a). Interaction between Env and tetherin is essential for the downregulation of tetherin and this is determined by the Env ectodomain (Le Tortorec & Neil 2009). Differences in these regions account for the lack of anti-tetherin activity of HIV-1 ROD14, compared to HIV-2 ROD10 or HIV-2 ST (Jia et al. 2009; Le Tortorec & Neil 2009; Hauser et al. 2010; Exline et al. 2015). In the case of tetherin, an alanine face in the coiled-coil ectodomain was found to confer sensitivity to HIV-2 Env (Exline et al. 2015). In addition, proteolytic processing of the Env gp140 precursor to gp105 and gp41 is essential for tetherin counteractivity, as well as AP-2 binding via a GYxxΦ motif in the cytoplasmic tail that is common to all HIV and SIV Envs (Abada et al. 2005; Noble et al. 2006; Le Tortorec & Neil 2009). There is no evidence of Env-induced tetherin degradation, but tetherin is sequestered away from the PM and accumulates in TGN-associated compartments. HIV-2 Env is a less efficient tetherin antagonist than HIV-1 Vpu or SIV Nef, but shows a broader species-specificity (Hauser et al. 2010). As Env is a major determinant of viral infectivity, it is possible that adaption of Env to tetherin antagonism may come with a fitness cost (Evans et al. 2010).

Several other lentiviral envelopes have been described to have anti-tetherin activity. There is the Env from tantalus monkey SIV (SIVtan) that is able to counteract several primate tetherins. Again, the AP-2 binding site as well as interaction with tetherin via its ectodomain are required for

its function (Gupta et al. 2009). However, as the infectious molecular clone of SIVtan has been passaged in human T cells it is unclear what role SIVtan Env or Nef may play in infection of the natural host. A further example of a primate lentivirus using Env to counteract tetherin is a Nef-deleted SIVmac that reverted back to its pathogenicity in infected Rhesus macaques (Serra-Moreno et al. 2011). Interestingly, in this virus amino acid changes in the cytoplasmic tail of gp41 confer tetherin-counteractivity. Antagonism is also determined by species-specific differences in the cytoplasmic tail of tetherin surrounding the dual-tyrosine motif (PIL**YDY**(R/C)KM versus STS**YDY**CRV in Rhesus macaque and human tetherin, respectively). Another virus that uses Env to counteract tetherin is FIV against feline tetherin (Dietrich, McMonagle, et al. 2011; Celestino et al. 2012; Morrison et al. 2014). Interestingly, it does not induce downmodulation of tetherin from the cell surface, yet is required for optimal release. Furthermore, FIV Env only rescues the release of FIV, but not other viral particles (Morrison et al. 2014). Therefore, FIV Env seems to employ a so far unknown mechanism of tetherin antagonism.

The human endogenous retrovirus K (HERV-K) has recently been described to possess anti-tetherin activity, mediated by its envelope protein (Lemaître et al. 2014). Two out of six HERV-K Envs tested exhibited tetherin counteractivity, but due to the extremely polymorphic nature of these elements in humans, variability in antagonistic activity is likely. HERV-K Env does not induce the removal of tetherin from the cell surface or its degradation and the mechanism of counteraction is so far unknown.

1.6.4.4 Herpesviruses

Kaposi's sarcoma-associated herpesvirus (KSHV; also human herpesvirus 8, HHV8) encodes two MARCH E3 ubiquitin ligases, K3 and K5 (Boname & Lehner 2011). Both contain two transmembrane domains that are linked by a short extra-cellular loop, a C-terminal cytoplasmic tail that contains residues required for subcellular trafficking and endosomal targeting, and an N-terminal cytoplasmic tail that contains the RING-CH domain that is crucial for the protein's function. K5 induces the ubiquitination and endosomal degradation of a range of cellular membrane proteins such as MHC-I, NK-receptor ligands, adhesion molecules and cytokine receptors. Tetherin was identified as a target of K5 in a mass-spectrometry-based proteomic screen and it was shown that K5 was required to enhance KSHV, but also Vpu-deficient HIV-1 release from tetherin expressing

cells (Bartee et al. 2006; Mansouri et al. 2009; Pardieu et al. 2010). The assembly process of herpesviruses differs from HIV in that there are several envelopment phases that eventually lead to the release of virions through the secretory pathway. It is still unclear at which step tetherin inhibits K5-deficient KSHV release (Pardieu et al. 2010).

The substrate specificity of K3 and K5 is determined by their transmembrane domains, but no direct interaction with target molecules has so far been demonstrated (Ishido et al. 2000). Rhesus and murine tetherin are insensitive to K5. Human tetherin that contains macaque-specific mutations in the transmembrane domain that render it insensitive to HIV-1 Vpu is still downregulated. This implies different determinants of species-specificity for both antagonists (Pardieu et al. 2010). K5 induces the ubiquitination of its target molecules on membrane-proximal lysine residues, which in the case of tetherin is lysine 18, whereas lysine 21 seems to be dispensable (Mansouri et al. 2009; Pardieu et al. 2010). This is followed by ESCRT-dependent lysosomal degradation. K5 was suggested to mediate tetherin degradation similarly to MHC-I degradation. This involves ubiquitination during transport to the PM, which then induces enhanced uptake and endosomal targeting. The addition of ubiquitin is mediated by E2-ligases of the UbcH5 family and Ubc13 then promotes poly-Ub chain formation (Duncan et al. 2006). For K5 activity it was suggested that K63 ubiquitin linkages, but also branched poly-Ub chains with K11 linkages are important (Boname et al. 2010).

K3 or K5 homologues can be found in other mammalian ɣ2-herpesviruses and MARCH-ligases are also encoded by mammalian poxviruses. Although, whether they have anti-tetherin function is unclear (Lehner et al. 2005). The cellular K5 homologue MARCH-VIII is able to promote tetherin degradation and it is possible that this may regulate cellular tetherin expression in an ESCRT-dependent manner (Bartee et al. 2006).

Other herpesviruses that were reported to be restricted by tetherin are herpes simplex virus 1 and 2 (HSV-1, HSV-2) (Zenner et al. 2013; Blondeau et al. 2013; Liu et al. 2014). While HSV-1 glycoprotein M (gM) has been demonstrated to have moderate anti-tetherin activity, HSV-1 gB or gD do not. gM induces tetherin accumulation in TGN46-positive compartments, but tetherin degradation seems to be independent of gM (Blondeau et al. 2013). Another group identified the virion host shut-off (Vhs) protein, an endoribonuclease, as a tetherin antagonist and suggested it reduces mRNA levels of a range of transcripts, including that of tetherin (Zenner et al. 2013). For

HSV-2 it was suggested that gB, gD, gH and gL exhibited anti-tetherin activity and they were able to downregulate tetherin to a certain extent (Liu et al. 2014).

One interesting example is the β-herpesvirus human cytomegalovirus (HCMV). Not only does it seem to be resistant to tetherin restriction in infected cells, but tetherin was reported to enhance entry of HCMV into cells expressing high levels of tetherin (Viswanathan et al. 2011). As tetherin is incorporated into released HCMV it was proposed that tetherin facilitates the interaction with other tetherin molecules in the target cell membrane.

1.6.4.5 Ebolavirus GP

Filoviruses, such as Eboalvirus (EBOV) and Marburg virus (MARV) are sensitive to tetherin restriction and the glycoproteins (GPs) encoded by both viruses have been implicated in tetherin antagonism (Kaletsky et al. 2009; Lopez et al. 2010; Kühl et al. 2011). Another report however, suggests that infectious EBOV replication is not negatively affected by tetherin and it was suggested that the role of GP may be cell-type specific (Radoshitzky et al. 2010; Kühl et al. 2011). Despite this discrepancy, GP is able to enhance the release of Vpu-defective HIV-1 from tetherin expressing cells. In addition to human tetherin, it also antagonises primate and murine tetherins. However, it is still unclear how, or even if GP mediates the exclusion of tetherin from assembling virions. It does not appear to induce the downmodulation of tetherin from the cell surface or its association with lipid rafts (Lopez et al. 2012). Sequences in the membrane spanning domain (msd) of GP as well as its glycan cap and mucin domain have been shown to be crucial for anti-tetherin function (Vande Burgt et al. 2015).

1.6.4.6 Other Viral Tetherin Antagonists

Tetherin restricts a broad range of viruses due to its ability to target the lipid membrane. Some viruses may be sensitive to tetherin restriction, but do not encode a countermeasure. This may not be required if tetherin is not expressed in the tissue that is infected or if the virus is capable of interfering with the host immune response and interferon-induced gene expression. Depending on the mode of assembly, some viruses may also be intrinsically insensitive. In addition to the viruses and viral antagonists described above, tetherin restriction has also been investigated in the context of other viruses.

Influenza A virus (FLUAV) is released from the plasma membrane of infected cells. However, the role of tetherin restriction is a matter of debate. Whilst earlier studies suggest FLUAV is only modestly restricted by tetherin, the release of FLUAV VLPs produced by expressing virion components *in trans* is markedly inhibited (Watanabe et al. 2011; Bruce et al. 2012; Winkler et al. 2012). Additionally, no effect of tetherin on viral replication was found in FLUAV infected mice (Londrigan et al.). In contrast, other studies demonstrated that FLUAV release is inhibited by tetherin (Mangeat et al. 2012; Leyva-Grado et al. 2014; Dittmann et al. 2015). The viral neuraminidase (NA) has been implicated in tetherin antagonism and a recent study suggests that tetherin sensitivity depends on the FLUAV strain used and that both NA and hemagglutinin (HA) are required for tetherin antagonism (Yondola et al. 2011; Gnirß et al. 2015).

Hepatitis B virus (HBV) is a member of the Hepadnaviridae family of enveloped DNA viruses. Tetherin seems to only have a minimal effect on HBV release, although it was suggested that this is cell type dependent (Miyakawa et al. 2015; Lv et al. 2015). The HBV surface protein (HBs) was implicated in tetherin antagonism. It can interact with tetherin via its fourth transmembrane domain and is supposed to inhibit tetherin dimerization, which is essential for its restrictive activity.

Alphaviruses are small enveloped RNA viruses that bud from the plasma membrane and include Chikungunya virus (CHIKV) and Semliki Forest virus (SFV). Both are restricted by tetherin and CHIKV was reported to counteract this restriction via its nsP1 protein that induces the downregulation of tetherin from the cell surface (Jones et al. 2013; Mahauad-Fernandez et al. 2014; Ooi et al. 2015). Interestingly, SFV seems to be restricted by long tetherin only, but not by short tetherin (Ooi et al. 2015).

Tetherin can also restrict coronaviruses, including the severe acute respiratory coronavirus (SARS-CoV), that does not bud from the plasma membrane, but in the ER-Golgi apparatus intermediate compartment and reaches the cell surface in vesicles (Wang et al. 2014; Taylor et al. 2015). A novel mechanism of tetherin counteraction was suggested to be employed by SARS-CoV. Its ORF7a was proposed to interfere with tetherin glycosylation to overcome restriction (Taylor et al. 2015).

1.6.5 Tetherin in the Context of Primate Lentiviral Evolution

As described above, tetherin counteraction by primate lentiviruses is not mediated by the same protein for each virus (Sauter et al. 2009). Whilst encoding both Vpu and Nef, SIVcpz Nef has anti-tetherin activity, but Vpu has not. Evolutionary analyses suggested that SIVcpz is the result from cross-species transmission and recombination events (Figure 1.19 B). The 5' region of its genome including the *vpu* gene originates from the SIVgsn/mus/mon lineage. The 3' region including the *nef* gene from SIVrcm (Bailes et al. 2003). Both Vpu and Nef were functional against the original host and related monkey tetherins. In SIVcpz, only the Nef gene adapted to counteract tetherin, while both Vpu and Nef are able to downregulate CD4 (Sauter et al. 2009).

Upon cross-species transmission to humans Nef was unable to antagonise human tetherin, due to a five amino acid deletion in the cytoplasmic tail of human tetherin (Figure 1.19 A). This deletion occurred before the separation of Neanderthal, Denisovian and homo sapiens, approximately 1 Mya (Sauter et al. 2011). However, in the case of pandemic HIV-1 group M, Vpu readapted to efficiently counteract human tetherin. The other three independent cross-species transmissions to humans resulting in HIV-1 groups N, O and P did not lead to successful readaption of this function in Vpu. Group N Vpus have moderate anti-tetherin activity, but group O and P lack it completely (Sauter et al. 2009). Instead, group O adapted its Nef protein to counteract tetherin by targeting residues in the cytoplasmic tail adjacent to the deletion (Kluge et al. 2014).

The species-specificity of tetherin counteraction maps to residues in the TM domain of the protein. One amino acid change is sufficient to render it resistant to HIV-1 Vpu (Gupta et al. 2009). It can counteract human and also great ape tetherins including chimpanzee and gorilla proteins, but is inefficient against the monkey variant (Jia et al. 2009; Sauter et al. 2009). Switching the African green monkey or rhesus macaque tetherin TM with that of the human protein, however, restores counteractivity by HIV-1 Vpu (McNatt et al. 2009).

HIV-2 does not encode a Vpu protein due to its origin from the SIVsmm lineage that also does not encode it. Whilst SIVsmm has a Nef that counteracts its host species tetherin, again, this protein was inefficient against human tetherin due to the five amino acid deletion (Figure 1.19). Therefore, HIV-2 Env adapted to counteract human tetherin (Le Tortorec & Neil 2009).

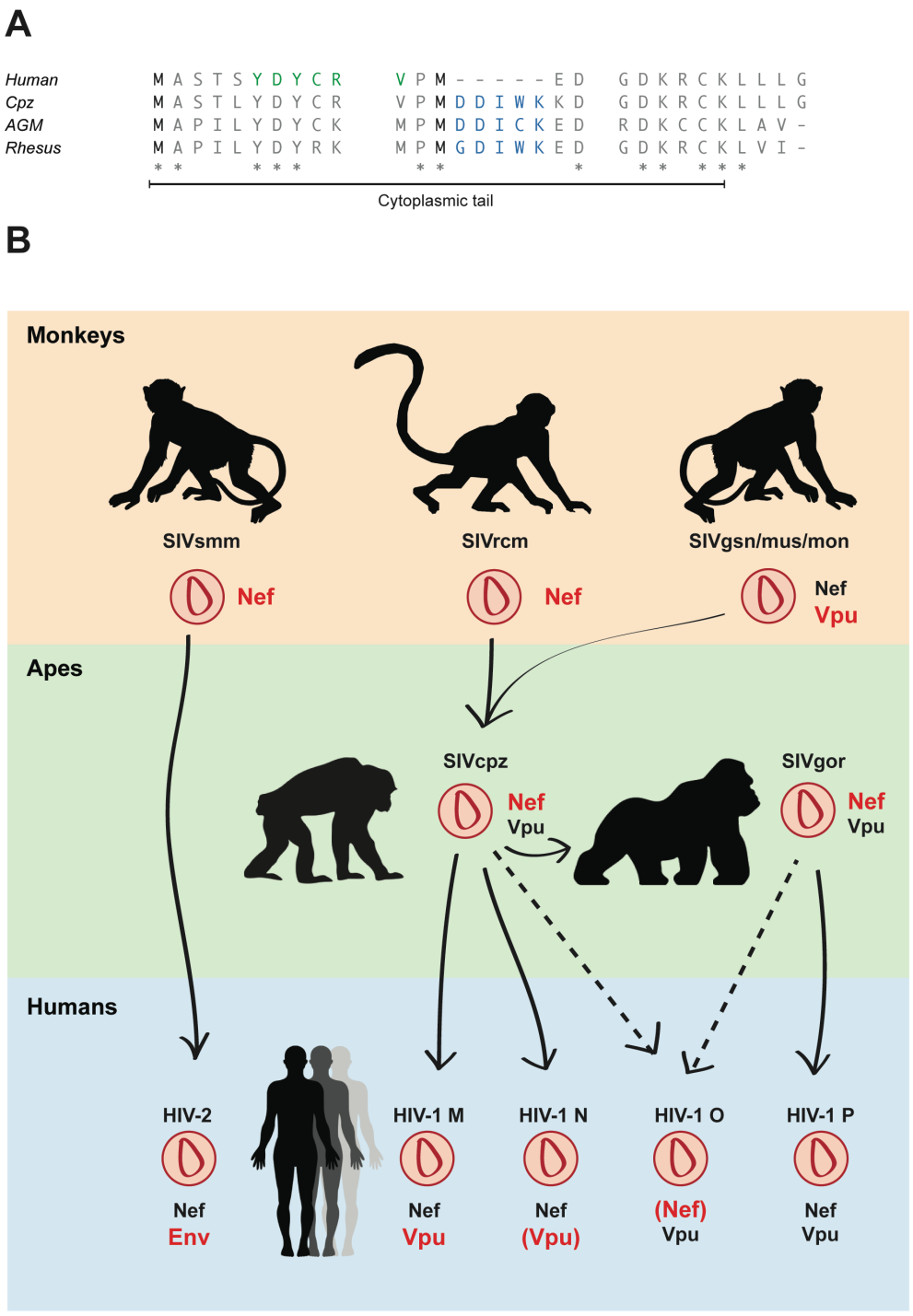

Figure 1.19 Co-evolution of tetherin and its primate lentiviral antagonists. (**A**) Amino acid alignment of the cytoplasmic tail of primate tetherins. Identical amino acids between all four sequences are indicated by an asterisk. The dual-tyrosine motif important for endocytosis and signaling is marked green. The five amino acid stretch that was deleted in human tetherin and is supposed to be targetted by SIV Nef is marked in blue. (**B**) SIVcpz acquired *vpu* and *nef* from two different monkey SIV lineages, SIVgsn/mus/mon and SIVrcm, respectively, and SIVcpz Nef adapted to counteract chimpanzee tetherin SIVgor and SIVsmm also use Nef to counteract tetherin. Upon cross-species SIV Nefs were unable to antagonise human tetherin, because of the deletion of the target amino acid motif in tetherin's cytoplasmic tail.

There is evidence that tetherin exerts strong selective pressure on viruses and that changes in the protein sequence have driven the evolution of Nef, Env and Vpu to adapt to counteraction. Being able to switch between these accessory proteins to fulfil this function may have been a key to cross-species transmission to humans (Sharp & Hahn 2011b). Further examples indicating the selective pressure of tetherin *in vivo* come from a Nef-deleted SIVmac that regained pathogenicity and was show to have readapted to tetherin antagonism using its Env protein (Serra-Moreno et al. 2011). Furthermore, Nef reacquired anti-tetherin function in HIV-1 passaged in a chimpanzee (Götz et al. 2012). Also, a highly pathogenic HIV-1 group N virus was isolated that harboured a Vpu protein with enhanced anti-tetherin activity (Sauter et al. 2012).

While efficient tetherin antagonism is clearly not the only determinant of enhanced pathogenicity and viral spread, it can be speculated that this function contributes to it. Importantly, the pandemic HIV-1 group M encodes the most efficient antagonists for human tetherin, while other HIV-1 groups N, O and P, and HIV-2 remain largely geographically restricted.

1.6.6 Tetherin and Cell-to-Cell Transmission

Replication of HIV-1 is more rapid when infected cells are co-cultured with target cells as compared to when infection occurs through cell-free virus and it has been suggested that cell-to-cell transmission may be the major route of HIV-1 dissemination *in vivo* (Sattentau 2008). Cell-to-cell transfer of virus occurs through a polarized physical interaction between a donor and a target cell that is known as the virological synapse (VS). This cell contact does not only promote HIV-1, but also human T-lymphotropic virus type 1 (HTLV-1) transmission, the latter spreading almost exclusively via this mode (Igakura et al. 2003; Jolly et al. 2004). The VS is formed by viral envelope and receptor interactions and is stabilized by cytoskeletal rearrangements and adhesion molecules. Before the discovery of tetherin as the cellular target of Vpu, it was clear that Vpu-deficient HIV-1 was able to replicate efficiently in T cells without being released into the supernatant from the infected cell (Strebel et al. 1989; Terwilliger et al. 1989; Klimkait et al. 1990; Yao et al. 1992; Schubert et al. 1995). In fact, HIV-1 was shown to lose its functional Vpu when selected for variants that exhibit enhanced cell-to-cell transmission efficiency (Gummuluru et al. 2000). Furthermore, more synaptic contacts can be observed in T cells infected with a Vpu-deficient HIV-1. However, the role of tetherin in cell-to-cell transmission remains unclear. Correlating with the earlier data,

Vpu-deficient virus spreads more efficiently via the VS between Jurkat cells and primary $CD4^+$ T cells and siRNA knockdown of tetherin reduces this spread (Jolly et al. 2010). In contrast, other studies using co-culture assays and various cell types found that tetherin inhibits the efficient spread via the VS (Casartelli et al. 2010; Kuhl et al. 2010; Giese & Marsh 2014). Interestingly, HTLV-1 cell-to-cell transmission is not sensitive to tetherin (Ilinskaya et al. 2013). Discrepant results on the role of tetherin in cell-to-cell transfer of HIV-1 may be explained by cell type-specific differences in tetherin expression levels, but also by differences in the speed of tethered virion endocytosis, which removes viruses from the site of transfer (Zhong et al. 2013). Altogether, where an effect of tetherin expression on cell-to-cell transmission was observed, it was weak and the role of tetherin in this process remains elusive.

1.6.7 Tetherin and Viral Pathogenesis

Various examples indicate that tetherin is a potent anti-viral factor *in vivo*. Homozygous tetherin knockout mice show no developmental defects or abnormalities in the lymphoid and myeloid cell population. However, when fibroblasts from these mice were infected with Moloney MLV (Mo-MLV) the virus was less sensitive to inhibition by type-I IFN. When the tetherin knockout mice were infected with the IFN inducing MLV variant LP-BM5 viral loads were increased and pathogenesis was more severe, pointing to an important anti-viral role of tetherin *in vivo* (Liberatore & Bieniasz 2011). Another example comes from NZW mice that only harbour a truncated version of tetherin, similar to short human tetherin. Lymphoid and myeloid cells from these mice show increased tetherin surface levels and Friend MLV infection was characterized by reduced viral loads and pathogenesis (Barrett et al. 2012). Accordingly, *in vivo* RNAi knockdown of tetherin in mice infected with mouse mammary tumor virus (MMTV) resulted in increased viral loads (Jones et al. 2012). In contrast, when tetherin knockout mice were infected with influenza virus, viral titers were reduced and $CD8^+$ T cell response increased (Swiecki et al. 2013). The role of tetherin in influenza infection is still unclear and these results may indicate that the role of tetherin *in vivo* is more complex.

The adaptation of HIV-1 group M Vpu to efficiently counteract tetherin is an indicator that tetherin plays an essential anti-viral role *in vivo*, considering that HIV-1 group M is primarily responsible for the HIV pandemic (Sauter et al. 2009). Furthermore, there is evidence that anti-tetherin function is selected for in HIV-1 infected individuals even many years after initial infection

(Pickering et al. 2014). Pegylated-IFNα treatment of HIV-1/HCV co-infected individuals leads to an increase in tetherin and APOBEC3G, correlating with reduction of HIV-1 viral loads, and emergence of Vpu sequence changes that confer enhanced tetherin antagonism (Pillai et al. 2012). Moreover, polymorphisms in the promoter region of tetherin have been correlated with disease progression (Laplana et al. 2013).

1.6.8 Tetherin and Anti-Viral Innate Immunity

The restriction of cell-free virus release by tetherin is not the only anti-viral function of tetherin. It has been suggested that it plays a broader role in the antiviral immune response *in vivo*. Tetherin-mediated virion retention may have several consequences that are summarized in Figure 1.20. Restricted virions accumulate on the cell surface and may trigger an antiviral immune response due to antibody opsonisation and complement- or phagocyte-mediated destruction through Fc-receptor recognition. Antibody-dependent cell-mediated cytotoxicity (ADCC) has been shown to be enhanced by tetherin-restricted virions. Binding of gp120 to CD4 exposes epitopes in gp120 that are targeted by ADCC. Increased abundance of HIV-1 Env at the surface through tetherin restriction may therefore enhance the exposure of these epitopes upon CD4 binding. Importantly, HIV-1 Vpu and Nef antagonism of tetherin inhibit the ADCC response (Veillette et al. 2014; Arias et al. 2014; Alvarez et al. 2014a; Pham et al. 2014). Tetherin also mediates the endocytosis of restricted virions that accumulate in endosomes. These may then be subject to endosomal processing and generation of viral PAMPs that can be recognised by endosomal PRRs such as TLRs. Furthermore, in antigen-presenting cells virion degradation may lead to the liberation of antigens that can be presented via MHC-II to further stimulate an antiviral T cell response.

Tetherin can also directly induce NF-κB activation (Matsuda et al. 2003; Galão et al. 2012; Cocka & Bates 2012; Tokarev et al. 2013). This can be achieved by overexpression of tetherin, antibody crosslinking of surface tetherin and, importantly, via the retention of tetherin-sensitive retroviral and filoviral particles on tetherin-expressing cells, which also induces cross-linking. Therefore, tetherin can be seen as an innate sensor of budding virions. NF-κB activation results in increased proinflammatory gene expression and promotes an antiviral state. Primary human $CD4^+$ T cells infected with tetherin-sensitive HIV-1 produce higher levels of the chemokines/cytokines CXCL10, IL-6 and also type-I IFN in a tetherin-dependent manner (Galão et al. 2012). This function

requires the structural determinants in tetherin that are also essential for virion restriction, but additionally the tyrosine-based motif in the cytoplasmic tail of long tetherin has been found to be crucial. While this motif is also responsible for endocytosis, virion internalization is not required for tetherin to induce NF-κB signalling. The YDYCRV motifs of a long tetherin homodimer have been described to act as a hemITAM that can be found in C-type lectins (Galão et al. 2014). Phosphorylation of the tyrosines by Src family kinases allows the recruitment of Syk, which then promotes NF-κB activation dependent on TRAF2 and 6 and TAK1. Interaction with RICH2 and indirect connection of tetherin to the cortical actin cytoskeleton is also essential for induction of signalling, even though it is not required for inhibition of virus release. Whether RICH2 is required for the internalization of restricted virions for endosomal degradation is so far unclear.

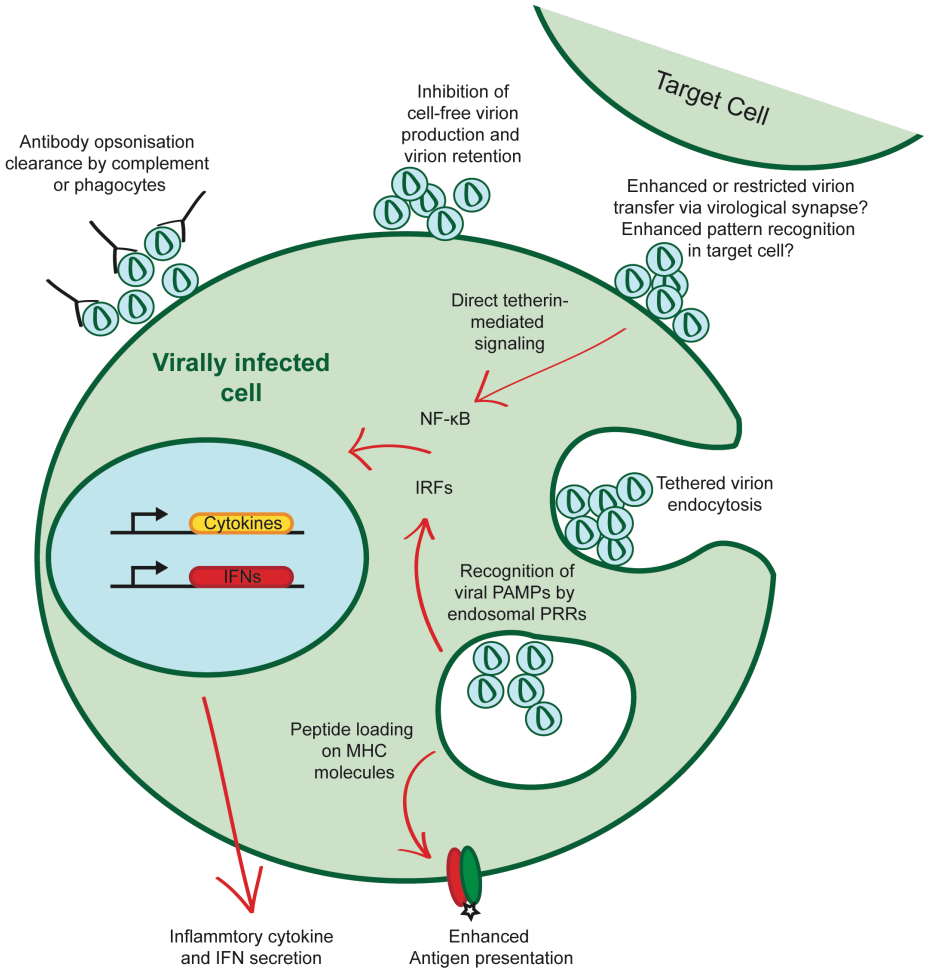

Figure 1.20 Potential tetherin-mediated immunological consequences of virion retention. Tetherin physically blocks cell-free virion release. Accumulations of virus may promote opsonisation by specific antiviral antibodies and results in clearance of the virus infected cell by complement deposition and/or killing by phagocytes expressing Fc receptors. In addition, tetherin induces NF-κB activation upon aggregation and synthesis of proinflammatory cytokines. Internalization of tetherin-retained virions into late endosomes may further lead to degradation of the particle, potentially releasing PAMPs for recognition by other endosomal PRRs, promoting type 1 IFN expression. Endosomal processing of viral proteins in myeloid cells may also lead to enhanced presentation of viral antigens on class II MHC molecules to CD4+ T cells. Moreover, increased transfer of tetherin-retained viral particles across VSs may enhance exposure of viral components to PRRs in target cells.

While chimpanzee tetherin is able to induce NF-κB moderately, tetherin proteins from rhesus macaques, African green monkeys or gorillas are not able to induce signalling at all. These differences are determined by amino acid residues in the cytoplasmic tail, specifically the RV in the YDYCRV motif and also the five amino acid deletion (G/DIWKK) in human tetherin (Galão et al. 2012). While the tyrosines are conserved across species, monkey tetherins are not phosphorylated at these positions and fail to recruit Syk. This may be due to structural differences and lack of accessibility to Src family kinases (Galão et al. 2014). Importantly, human tetherin seems to have evolved this function specifically. Due to the lack of required residues in the cytoplasmic tail of short human tetherin, this isoform does not induce NF-κB signalling, but rather dominantly interferes with it (Cocka & Bates 2012; Galão et al. 2012). As HIV-1 group M efficiently antagonises and degrades the human long, but not short, isoform, it was speculated that tetherin signalling affected the adaptation of Vpu during zoonotic transmission of this group, perhaps influencing the ability of HIV to become pandemic (Weinelt & Neil 2014). Whether tetherin signalling is regulated at the level of differential isoform expression remains to be determined.

Tetherin also induces type-I IFN production in primary $CD4^+$ T cells. However, this process may be indirect. It involves IRF3 activation and can be blocked by inhibition of the TLR3 adaptor TRIF (Galão et al. 2012). These findings suggest that restricted and endocytosed virions may become available to PRR sensing.

Additionally, tetherin has been shown to interact with the immunoglobulin-like transcript 7 (ILT-7) (Cao et al. 2009). ILT-7 is a leukocyte inhibitory receptor that is expressed on pDCs and suppresses TLR7- and TLR9-induced type-I IFN production upon cross-linking. pDCs sense HIV infected cells mainly through TLR7 and this involves Env-dependent transfer of virus across cells (Lepelley et al. 2011; Beignon et al. 2005). It was suggested that binding of tetherin to ILT-7 would induce this inhibitory effect on TLR signalling (Cao et al. 2009). However, another study contradicted these findings (Tavano et al. 2013). A recently published report may have elucidated this discrepancy (Bego et al. 2015). It confirms that the tetherin and ILT-7 interaction induces an inhibitory effect on type-I IFN production in pDCs. Tetherin-restricted virions are efficiently sensed by pDCs and it was suggested that this was due to inefficient interaction between tetherin and ILT-7 in this scenario. Vpu reduces tetherin surface expression. However, it was shown that some pools

of tetherin remain on the surface and are sequestered away from the site of viral budding. Thereby, Vpu promotes virus release from infected cells and enables the remaining surface tetherin to interact with ILT-7, which then results in reduced levels of type-I IFN (Bego et al. 2015). Whether the remaining tetherin on the surface is comprised of the short isoform that cannot be downregulated by Vpu remains to be confirmed. However, it may explain the benefit of preferentially targeting the long, signalling isoform and leaving the short one on the surface.

1.7 The Clathrin Machinery and Vesicle Trafficking

Vesicular transport in the cell mediates the trafficking of cargo between different subcellular compartments. Vesicles bud from specialized coated regions. This coat is required for directing specific membrane proteins to the membrane patch from which the vesicle will bud, but is also required to form the curved basket-like lattice that shapes the vesicle. There are clathrin-, COPI- and COPII-coated vesicles. While COPI/COPII coated vesicles mediate the transport from the ER and the Golgi cisternae, clathrin mediates the transport between the Golgi apparatus, the plasma membrane and endosomes. Viruses have been shown to hijack clathrin-mediated trafficking to induce the mis-localization and sometimes degradation of cellular proteins. Clathrin forms triskelions that contain three heavy chains that assemble at their C-termini and each bind a clathrin light chain. The triskelions then form the basket-like structure made up of pentagonal and hexagonal faces. Spherical clathrin-coated vesicles then bud from membranes and the GTPase dynamin 2 pinches the vesicle off by forming a spiral around the neck of the vesicle and restraining it through GTP hydrolysis (Bonifacino & Traub 2003).

Membrane sites where clathrin assembles are characterized by phosphoinositides and Arf GTPases. These recruit clathrin adaptor proteins, which are responsible for cargo protein binding, to the site of vesicle formation. Several clathrin binding proteins have been described, including clathrin adaptor proteins (APs), HRS, AP180 and gamma adaptin ear-containing ARF-binding (GGA) proteins. All contain a long unstructured region that is able to interact with the β-propeller head of clathrin located at the N-terminus of the heavy chain. This unstructured region contains a peptide called clathrin box with a consensus sequence of ρLφρφρ (ρ=polar residue, φ=aliphatic hydrophobic residue) (Lafer 2002).

APs are a family of heterotetrameric proteins that comprises AP-1, AP-2, AP-3, AP-4 and AP-5 and are components of clathrin coats. They consist of a globular core formed by two large subunits (α and β2 in AP-2, γ and β1 in AP-1), a medium-sized subunit (μ2 in AP-2, μ1 in AP-1) and one small subunit (σ2 in AP-2, σ1 in AP-1). The C-terminal region of the large subunits projects from the core and contains a disordered “hinge” and a globular “ear” or “appendage” domain. While the core is responsible for the recognition of sorting signals in cargo proteins and recruitment to membranes, the hinge/appendage region interacts with clathrin or other adaptor proteins. Each adaptor protein mediates the transport between different cellular compartments. AP-1 mainly mediates the bi-directional transport between the TGN and endosomes and AP-2 induces the endocytosis of transmembrane proteins from the plasma membrane for sorting into endosomes (Figure 1.21). The roles of AP-3, AP-4 and AP-5 are less clear. AP-4 and AP-5 have been proposed to be components of non-clathrin coats mediating TGN/endosomal and endosomal sorting, respectively. The function of AP-3 and whether it is clathrin-dependent is unclear, but it has been suggested to play a role in sorting between endosomes and lysosomes (Lafer 2002; Hirst et al. 2011; Canagarajah et al. 2013).

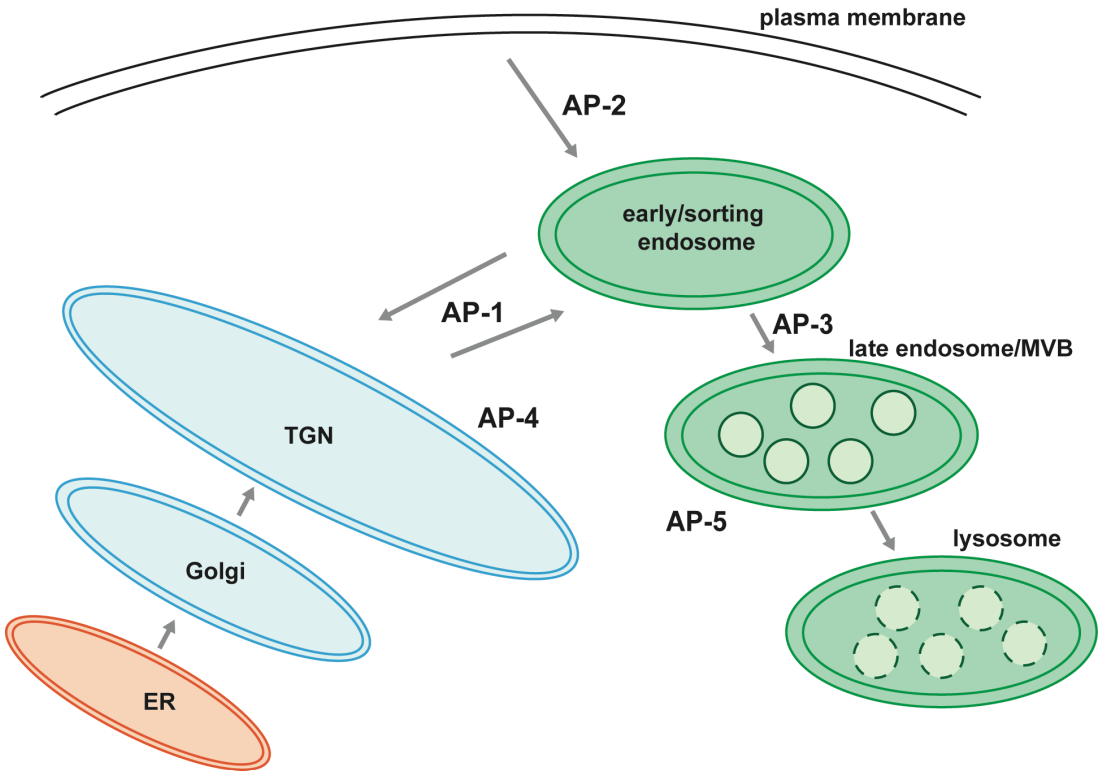

Figure 1.21 Clathrin adaptor proteins and membrane trafficking. Schematic representation of sorting pathways between TGN, plasma membrane and endosomal compartments. AP-1 mainly mediates sorting between the TGN and endosomes, while AP-2 exclusively induces the endocytosis of membrane proteins from

the plasma membrane. AP-3 is thought to be involved in sorting between endosomes and lysosomes. AP-4 and AP-5 are not associated with clathrin coats, but have been implicated in TGN to endosome and late endosomal sorting, respectively.

Clathrin adapter proteins AP-1 and AP-2 are able to recognize their cargo proteins through specific linear sequences that are present in cytoplasmic regions. These are either tyrosine-based motifs Yxxφ or dileucine-based motifs (D/E)xxxL(L/I) (Bonifacino & Traub 2003). In the case of tyrosine-based motifs, the Y is indispensable and the φ represents a bulky hydrophobic residue. Residues 2 and 3 are variable, but tend to be hydrophilic. Flanking residues can also influence the strength and specificity of binding. These motifs bind to the core μ subunit of adaptor proteins and induce rapid endocytosis from the PM as well as targeting to lysosomes and sorting between TGN and endosomes. Tetherin comprises a variant of this motif with its sequence YxYxxφ that interacts with the AP-2 α subunit and can also bind the μ subunits of AP-1 and AP-2 (Masuyama et al. 2009; Rollason et al. 2007). For the dileucine motif (D/E)xxxL(L/I), the first leucine is essential, while the second leucine can also be replaced by an isoleucine. An acidic residue is placed at position one and is required for targeting the cargo to late endosomes and lysosomes. Dileucine motifs can be recognized by core small σ and the large γ subunit interface of AP-1 or the large α subunit of AP-2, but also by μ subunits of AP-1 and AP-2 at different sites than tyrosine-based signals. These motifs mediate rapid endocytosis and transport to endosomal and lysosomal compartments. HIV-1 Nef has been demonstrated to contain two dileucine motifs that interact with the μ subunit of AP-1 and -2 and the σ- α hemi-complex of AP-2. Interaction of Nef with AP-1 and -2 is required for the downregulation of cellular proteins CD4 and MHC-I (Janvier et al. 2003; Chaudhuri et al. 2007; Lindwasser et al. 2008; Ren et al. 2014). HIV-1 Vpu also contains a variant of a dileucine motif in its cytoplasmic tail, ExxxLV, that has been demonstrated to be essential for the correct localisation and anti-tetherin function of Vpu, and for interaction with the σ-subunit of AP-1 (Kueck & Neil 2012; Jia et al. 2014).

1.8 The ESCRT Pathway

The endosomal sorting complex required for transport (ESCRT) system is involved in remodelling and scission of membranes. The initial function was described to be the sorting of membrane proteins from endosomes to lysosomes via the formation of multivesicular bodies

(MVBs) (Katzmann et al. 2001). Biogenesis of MVBs are formed from endosomes when the membrane buds into the lumen. Ubiquitinated membrane proteins can be sorted into these budding vesicles by ESCRT proteins. In addition to this role, two more functions of ESCRT have been investigated extensively. These are the budding off of HIV-1 and other enveloped viruses from the infected cell and membrane abscission during cytokinesis (Figure 1.22). All these functions involve invaginations that bud off, away from the cytoplasm (Henne et al. 2011).

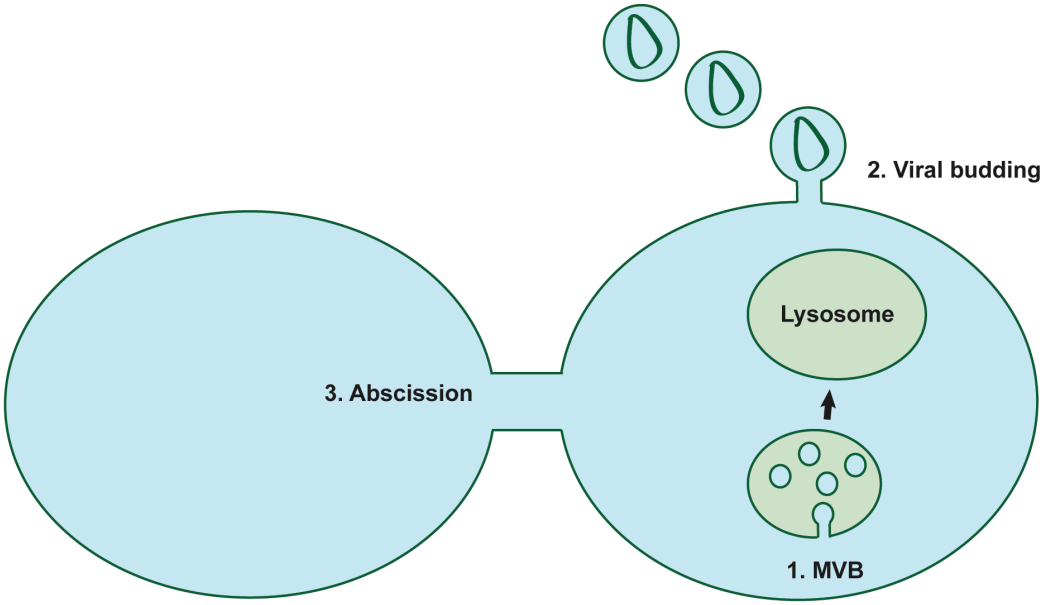

Figure 1.22 Roles of the ECSRT machinery. Main functions of ESCRT include 1. MVB biogenesis, 2. viral budding and 3. abscission.

There are five ESCRT complexes that comprise different proteins that are recruited in a sequential manner. The ESCRT-0 complex contains the hepatocyte growth factor-regulated tyrosine kinase substrate (HRS) and the signal transducing adaptor molecule 1/2 (STAM1/2) and both interact via their coiled coil domains in a 1:1 ratio. HRS has a zinc finger domain, FYVE (Fab-1, YGL023, VPS27 and EEA1), that binds to the endosomal lipid phosphatidylinositol 3-phosphate (PtdIn(3)P) and is important for specificity and membrane recruitment. Both HRS and STAM1/2 contain several ubiquitin binding motifs. HRS, for example, is supposed to bind to mono- and lysine 63-linked ubiquitinated proteins via its double-sided ubiquitin-interacting motif (DUIM) and the N-terminal VHS domain (VPS27, HRS, STAM). Several ubiquitin binding domains have been suggested to allow the sequestration of multiple proteins simultaneously. Additionally, both HRS

and STAM1/2 have clathrin binding regions. HRS interacts with clathrin's heavy chain at endosomal membranes and recruits cargo into flat clathrin lattice microdomains (Raiborg et al. 2006). It is unclear whether HRS and STAM1/2 are the only ESCRT-0 components and other proteins such as GGA proteins have been suggested due to similar domain organization.

The ESCRT-I complex consists of TSG101, VPS28, VPS37 and either MVB12 or UBAP1 that assemble in a 1:1:1:1 ratio. This complex is recruited to endosomes by HRS, which is essential for the sorting of cargo proteins for lysosomal degradation as ESCRT-I cannot bind to membrane lipids directly. Specifically, the HRS PSAP motif binds to the ubiquitin E2 variant domain (UEV) of TSG101. The ESCRT-I proteins TSG101, MVB12 and UBAP1 are able to bind to ubiquitin through hydrophobic isoleucine 44. However, unlike ESCRT-0, they are not involved in capturing the ubiquitinated cargo.

The ESCRT-II complex consists of EAP45, EAP30 and EAP20, that assemble in a 1:1:2 ratio. The recruitment of ESCRT-II depends on VPS28. The GRAM-like ubiquitin binding in EAP45 (GLUE) domain in EAP45 is able to bind to ubiquitin and also PtdIn(3)P, which mediates localization to cellular membranes.

The ESCRT-III complex consist of four major subunits termed charged multivesicular body proteins, CHMP2, 3, 4 and 6 and their isoforms and also ALIX (apoptosis-linked gene-2 interacting protein X), CHMP1, and IST1 (increased salt tolerance-1). When membranes sculpt for budding, the components of this complex recruit each other to endosomes transiently and the physical contact between the components induces conformational changes that activate the subunits that are usually auto-inhibited. Apart from ALIX, none of the ESCRT-III components has been shown to interact with ubiquitin. ALIX and CHMP1 are also required for MVB sorting and cytokinesis, whereas IST1 is only implicated in cytokinesis. When the ESCRT-III complex assembles at the endosomal membrane, the energy to separate the membranes is delivered by the AAA ATPase VPS4 that binds to ESCRT-III via its microtubule-interacting and trafficking (MIT) domain. VPS4 was also proposed to be involved in the recycling of ESCRT-III subunits after completion of abscission or possibly the removal of ESCRT-III to generate constrictive forces that may be required for abscission. During the final steps of abscission the centrosomal protein 55 (CEP55) is recruited to the midbody, which then leads to the recruitment of ESCRT-I and ALIX and subsequently ESCRT-II for abscission.

HIV-1 has hijacked the cellular ESCRT pathways to mediate budding from the plasma membrane. As mentioned earlier, Gag recruits ESCRT-I and –III complexes via its P(S/T)AP motif in the p6 domain that specifically interacts with TSG101 and recruits further ESCRT-III components. Additionally, the (L)YPXnL motif in p6 is able to bind ALIX and recruit ESCRT components.

1.9 Aim of Thesis

HIV-1 interferes with host cellular processes to promote an optimal environment for virus replication. Virally encoded proteins have a broad range of functions to overcome restrictions imposed by the host. The counteraction of so-called cellular restriction factors by HIV-1 accessory proteins plays a crucial role in the fitness of a virus and is a major field of scientific investigation. Understanding these host-virus interactions may provide us with new strategies in antiviral therapy in the future.

The data presented in this thesis aims to clarify aspects of restriction factor antagonism by HIV-1 and other primate lentiviruses. In particular, this work focuses on the antiviral function of two cellular transmembrane proteins, tetherin and SERINC3/5. The results section of this thesis is divided into three chapters:

1. The cellular restriction factor tetherin is expressed as two isoforms in humans, which exhibit differential sensitivity to HIV-1 group M Vpu proteins, but not other tetherin antagonists.
2. Mis-trafficking of tetherin is sufficient for Vpu to overcome release restriction. Motifs in Vpu's cytoplasmic tail and serine phosphorylation are required for this function and mediate clathrin adaptor interaction.
3. HIV-1 Nef enhances virion infectivity by counteraction of the recently identified restriction factors SERINC3 and 5.

Chapter 2 Materials and Methods

2.1 Polymerase Chain Reaction (PCR)

Primers for all PCR reactions were synthesized by MWG Eurofins. Primers were designed to contain EcoRI, NotI or XhoI restriction enzyme cleavage sites. A Kozak consensus sequence was also included in the forward primers and a TAG or TGA stop codon was included in the reverse primer or not, depending on whether a C-terminal HA-tag was added.

The **standard PCR** was used for subcloning of DNA fragments into vectors with different multiple cloning sites. All tetherin constructs were generated with the natural Kozak consensus sequence (ATC TGG or GTG CCC), all other proteins were generated to contain an optimal Kozak consensus sequence (GCC ACC) immediately upstream of the ATG start codon. The PCR mix was prepared as described in table 1 and the thermo cycler (Eppendorf Mastercycler) was programmed as shown in table 2.

Overlapping PCR was used to generate Vpu mutants in pCRV1 and mutants in the NL4.3 proviral plasmid. Two reverse complementary primers were designed containing the desired mutation and two separate PCR reactions were conducted all using the standard PCR conditions. The mutation-containing primers (primer 1, forward, and 2, reverse) were used in combination with full-length outer Vpu primers or, in the case of NL4.3 provirus, a forward primer annealing upstream of the *vpr* gene (CAT AAT AAG AAT TCT GCA ACA ACT GC) and a reverse primer annealing in the *env* gene (CTT AAT TTG CTA GCT ATC TGT TTT AAA GTG). The forward primer and primer 2, and the reverse primer and primer 1 were used in separate reactions. Amplified products were purified and both combined in a third PCR mix using the outer forward and reverse primer only to generate a full-length construct.

Site directed mutagenesis (QuickChange) was used to generate Vpu mutants in pCR3.1. Reverse complementary primers containing the desired mutation in the middle were designed. 125 ng of each primer and 20 ng of template PCR were mixed in the otherwise standard PCR mix and the cycler was programmed as described in table 2. The PCR product was then treated with the DpnI restriction enzyme to digest the methylated template DNA, before being transformed.

For construct **synthesis**, overlapping primers for the full coding sequence were designed for greater spot-nosed and mona monkey tetherin as well as N1.FR.2011 Vpu. The outer primers contained the desired restriction sites. All primers were added to the same standard PCR mix and PCR conditions were the same as for the standard PCR, however, with only 10 cycle repeats. 1 µl from this reaction was then added to another standard PCR mix containing only the outer primers and this second PCR was done with 30 cycles.

Table 1. PCR mix

Reagent	Final concentration
Phusion® High-Fidelity DNA Polymerase (NEB)	0.5 µl (1 unit)
Phusion® HF buffer (NEB)	1 x
dNTPs (Sigma)	500 µM
DNA template	200 ng (standard PCR) 20 ng (QuickChange)
Primer (reverse and forward)	0.5 µM each
ddH_2O	x µl
Total	20 µl (standard PCR) 50 µl (QuickChange)

Table 2. PCR conditions

Step	Temperature	Time	Cycle repeats
Denaturation	95°C	30 sec	1 x
Denaturation	95°C	30 sec	30 x (standard PCR) 16 x (QuickChange)
Primer annealing	58°C	30 sec (standard PCR) 60 sec (QuickChange)	
Extension	72°C	60 sec (standard PCR) 1 min per kb (QuickChange)	
Extension	72°C	10 min	1 x
Cooling	4°C	Until stopped	

2.2 Extraction and Purification of DNA

The PCR products were separated using agarose gel electrophoresis. For a 1% agarose gel, 1 g electrophoresis grade agarose (Invitrogen) was dissolved while heating in 100 ml 1 x TAE buffer (1x TAE: 40 mM Tris-acetate, 1 mM EDTA, 0.114% glacial acetic acid, pH 8.2-8.3). After cooling, 2 µl ethidium bromide (Sigma) was added and the gel was poured into a gel cast. Once the gel set, the samples were loaded next to a 2-log DNA ladder (NEB). Samples were separated in the electric field at 100 V for around 30 min. To visualize the bands, the Chemi Doc UV system (Bio-Rad) was used. DNA fragments of the right size were cut out of the agarose gel and DNA was extracted using the QIAquick Gel Extraction Kit (QIAGEN) following the manufacturers instructions.

2.3 Restriction Endonuclease Digestion

To clone DNA fragments into vectors, the DNA fragment and vector backbone were cleaved using restriction endonucleases. Restriction enzymes commonly used in these studies include EcoRI, NotI, XhoI, NheI and DpnI (all NEB). The digestion mix was prepared as shown in table 3 and incubated at 37°C for 2 h. If required, self-ligation was prevented using Antarctic Phosphatase (NEB), which removes the 5' phosphate group of the linearized vector. Antarctic Phosphatase reaction buffer (1 x final concentration) was mixed with 5 units of the enzyme, added to the digestion mix and incubated for additional 30 min.

Table 3. Restriction endonuclease digestion

Reagent	Final volume
Buffer (depending on enzyme, e.g. CutSmart)	2 µl
BSA (not with CutSmart buffer)	1 x
Restriction enzyme(s)	20 units
DNA (1-2 µg)	x µl
ddH_2O	x µl
Total	Up to 20 µl

2.4 Ligation and Transformation of Plasmid DNA into Competent Cells

A ligation reaction mix was prepared as shown in table 4 using T4 DNA ligase (NEB). The mix was then incubated for 30 min at room temperature or at 16°C overnight. A negative control was treated the same way, but sterile water instead of the DNA insert was added to the mix. This was done to check the background level of vector self-ligation.

Table 4. DNA ligation

Reagent	Final volume
Vector	x µl
DNA Insert	x µl (3 x of vector)
T4 ligase buffer 10 x	1 µl
T4 DNA ligase	1 µl
ddH_2O	x µl
Total	10 µl

The ligation mix was then added to 50 µl of chemically competent DH10 *Escherichia coli (E.coli)* cells and incubated for 20 min on ice. The cells were then heat-shocked for 45 sec at 42°C before going back on ice. Then 750 µl fresh Luria-Bertani (LB) broth without antibiotics was added to the cells and they were incubate in a shaker at 30°C or 37°C for 1 h. Cells were then spread on LB agar plates containing ampicillin (100 µg/ml) and incubated at 30°C or 37°C overnight. All retroviral vectors were grown at 30°C to avoid recombination. Single colonies were picked and grown overnight in 3 ml LB broth containing ampicillin. The culture was then used to purify plasmid DNA for restriction enzyme digest or sequencing, or to inoculate a bigger culture (100 ml) for incubation overnight.

2.5 Preparation of Chemically Competent Cells

DH10 *E.coli* cells (Invitrogen) were grown in LB broth in a shaker (220rpm) at 37°C for 16 h. Then 500 µl of the overnight culture were added to 50 ml LB broth and incubated at 37°C in a shaker until the OD_{550} reached 0.45. Cells were put on ice for 10 min and pelleted in a pre-chilled bench top centrifuge at 3000 x g. the pellet was resuspended in 20 ml buffer 1 (table 5) and incubated for 5 min on ice. Cells were pelleted again and resuspended in buffer 2. After 10 min on ice cells were snap-frozen on dry ice in aliquots and stored at -80°C until used further.

Table 5. Buffers used for making chemically competent cells. All filter-sterilized.

Buffer 1	Buffer 2
30 mM KAc	10 mM PIPES
100 mM RbCl	75 mM $CaCl_2$
10 mM $CaCl_2$	10 mM RbCl
50 mM $MnCl_2$	15% glycerol
15% glycerol	

2.6 Plasmid Amplification and Purification

From a 3 ml bacterial overnight mini-culture, 100 µl were added to 100 ml LB broth containing ampicillin and incubated overnight at 30°C or 37°C in a shaker. Cells were pelleted at 6000 x g for 15 min at 4°C. Plasmid DNA was extracted using the endotoxin free NucleoBond® Xtra Midi kit (Macherey-Nagel). Bacterial cells were lysed and the lysate was cleared and loaded onto an equilibrated column where the DNA binds to the silica-based membrane. The membrane was washed twice and the DNA was eluted in a high salt buffer and precipitated by centrifugation using isopropanol. The precipitated DNA was washed again in 70% ethanol before being eluted in endotoxin free water.

Plasmids from a 3 ml bacterial mini-cultures were purified by the same principle using the QIAprep Spin Miniprep Kit (QIAGEN) and following the manufacturer's instructions.

2.7 DNA Sequencing and Vectors

The Nanodrop ND-100 Spectrophotometer (Labtech International) was used to determine the DNA concentrations of purified plasmid DNA before being sent off for sequencing to Eurofins MWG Operon. For sequencing of pCR3.1 the T7 forward primer or BGH reverse primer were used. For the other vectors, primers directed to down- or upstream sequences of the multiple cloning site were used. A list of plasmids used in these studies is shown in table 6 and 7 and important features are indicated.

Table 6. Vectors and proviruses

Vector	Source	Description
pCR3.1	Invitrogen	Mammalian expression vector, cytomegalovirus (CMV) promoter
pCRV1	Paul Bieniasz	HIV-based, Rev-dependent expression vector (Zennou et al. 2004)
pLHCX	Clontech	Retroviral vector derived from moloney murine leukemia virus (MMLV), hygromycin resistance, CMV promoter
pCMS28	Michael Malim	Retroviral vector derived from pMigR1, puromycin resistance via IRES
HIV-1 NL4.3	NIH AIDS Reagent Program	Full length, replication competent HIV-1 molecular clone
HIV-1 NL4.3 ΔVpu	Stuart Neil	As WT NL4.3, but ATG start codon of vpu ORF replaced with BamHI restriction site that introduces frameshift (Neil et al. 2006)
HIV-1 NL4.3 ΔNef and ΔNefΔVpu	Anna Le Tortorec	ATG of Nef mutated or both Nef and Vpu ATG mutated
HIV-1 NL4.3 Vpu 2/6, ELV, LILI mutants	Tonya Kueck	
Other HIV-1 NL4.3 Vpu mutants	Generated using overlapping PCR	
HIV-2 pRod10	Centre for AIDS Research (NIBSC, Potters Bar, UK)	Full length, replication competent HIV-2 molecular clone
SIVmac239	Theodora Hatziioannou	Assembled from plasmids p239SpSp5′ and p239SpE3′ (Kestler et al. 1990) (NIH AIDS Reagent Program) into a low copy number (pXF3) backbone (Zhang et al. 2009)
SIVmac239 ΔNef	Theodora Hatziioannou	Premature stop codon at codons 58 and 59 of Nef 3' to the Env stop codon.

Table 7. List of plasmids

Gene	Vector	Restriction sites	Tag	Stable cell lines	Source
Human tetherin WT/long/short (natural Kozak)	pCR3.1 pLHCX pCMS28	XhoI/NotI XhoI/NotI BglII/BamHI/NotI	- - -	- 293, HT1080 Jurkat Tag	Stuart Neil and standard PCR
Human tetherin mutants	pCR3.1 pLHCX	XhoI/NotI XhoI/NotI	- -	- 293	Standard PCR
Rhesus macaque tetherin WT/long/short	pCR3.1 pLHCX	XhoI/NotI XhoI/NotI	- -	- 293	Stuart Neil
Greater spot-nosed monkey tetherin WT/long/short	pCR3.1 pLHCX	XhoI/NotI XhoI/NotI	- -	- -	Synthesized
Mona monkey tetherin WT/long/short	pCR3.1 pLHCX	XhoI/NotI XhoI/NotI	- -	- -	Synthesized
HIV-1 NL4.3 Vpu	pCR3.1 pCRV1 pCMS28		+/- HA -	- - 293 tetherin	Tonya Kueck Suzy Pickering
HIV-1 group M Vpus (T/F)	pCRV1		-	-	Suzy Pickering
HIV-1 group M Vpus (clades)	pCG		-	-	Michael Schindler
N1.FR.2011 Vpu	pCRV1 pCMS28	EcoRI/NotI EcoRI/NotI	-	- 293 tetherin	Synthesized
YBF30 Vpu	pCRV1 pCMS28	EcoRI/NotI EcoRI/NotI	-	- 293 tetherin	Michael Schindler
SIVgsn/mon/cpz Vpu	pCG		-	-	Michael Schindler
HIV-2 Env IRES GFP or mutant	pCRV1		-	-	Anna LeTortorec
K5 or mutant	pCMS28	EcoRI/XhoI	-	HT1080	Rafael Vigan
HIV-1 NL4.3 Vpu and mutants	pCR3.1	EcoRI/NotI	+/- HA	-	Klaus Strebel, Tonya Kueck, subcloning
HIV-1 NL4.3 Vpu and mutants +CB/CBmut	pCR3.1	EcoRI/NotI	+/- HA	-	Tonya Kueck, QuickChange, Overlapping PCR
HIV-1 2_87 Vpu and mutants	pCR3.1	EcoRI/NotI	+/- HA	-	synthesized, Overlapping PCR
SERINC3/5	pCR3.1	XhoI/NotI	HA	-	Toshana Foster, Amplified from $CD4^+$ T cells
SERINC3/5 isoforms	pCR3.1	XhoI/NotI	HA	-	Standard PCR
VSV-G	pMDG		-	-	Stuart Neil
Ebola GP	pCAGGS		-	-	Ed Wright
XMRV Env	pCRV1		-	-	Rui Galao
Measles Env			-	-	Michael Malim
MLV Gag-Pol	pCRV1		-	-	Stuart Neil
HIV Gag-Pol	pCRV1		-	-	Paul Bieniasz
LentiCRISPRv2			-	-	Zhang lab
YFP	pCR3.1		-	-	Paul Bieniasz
GFP	pCR3.1		-	-	Paul Bieniasz

2.8 Cell Culture

Adherent cells were incubated at 37°C and 5% CO_2 in Dulbecco's Modified Eagle Medium (DMEM; Invitrogen) that was supplemented with 10% heat-inactivated fetal calf serum (FCS; Invitrogen) and 0.02 mg/ml gentamycin (Invitrogen). Suspension cells were maintained at 37°C and

5% CO_2 in Roswell Park Memorial Institute (RPMI) medium (Invitrogen) supplemented with 10% FCS and 0.02 mg/ml gentamycin. Cells were passaged every two days or when required. Adherent cells were detached from the tissue culture plate using Trypsin (TrpLE Expres + phenol red, Invitrogen), resuspended in pre-warmed DMEM and added to a fresh tissue culture plate. Suspension cells were aspirated and fresh RPMI medium was added to the tissue culture flask. A list of cells used in these studies can be found in table 8.

To generate frozen stocks of cell lines, cells were pelleted by centrifugation at 3000 x g and resuspended in 90% FCS supplemented with 10% DMSO (Sigma). Cells were then placed at -80°C before transferring them to liquid nitrogen.

Table 8. Cell lines used in this study

Cell line	Origin	Source	Culture medium	Details
Hela	Human adenocarcinoma cell line	American Type Culture Collection (ATCC)	DMEM	Endogenous tetherin expression
Hela-TZMbl	Human adenocarcinoma cell line	NIH AIDS Reagents Repository Program	DMEM	Endogenous tetherin expression; expression of CD4 and CCR5; β-Galactosidase reporter gene under HIV-1 promoter
HEK-293T	Human embryonic kidney cells	ATCC	DMEM	Tetherin expression is IFN-inducible
HEK-293	Human embryonic kidney cells	ATCC	DMEM	Tetherin expression is IFN-inducible
HT1080	Human fibrosarcoma cell line	ATCC	DMEM	No tetherin
Jurkat	CD4+ T lymphocyte (leukemia)	ATCC	RPMI	Endogenous tetherin expression
Jurkat TAg	CD4+ T lymphocyte (leukemia)	Marie-Jose Bijlmakers, KCL	RPMI	Tetherin expression is IFN-inducible

2.9 Transient Transfection

Cells were plated the day before at a density of 1.2 x 10^5 cells per well of a 24 well plate or 3 x 10^5 cells per well of a 6 well plate. The right amount of pCR3.1 or pCRV1 expression vector was diluted in serum free medium. The transfection reagent was mixed with with serum free medium and incubated for 5 min at room temperature before being added to the DNA and gently mixed. Either polyethylenimine (PEI; 1 mg/ml in ddH_2O, filtered, pH 7.0; Polyscience) or, for Hela cells, Lipofectamine 2000 (2 mg/ml; Invitrogen) was used as a transfection reagent. The mix was incubated for 20 min and then added onto the cells. Six hours post transfection the medium was changed. 48 h post transfection cells and supernatants were analysed for protein expression or infectious virus release. In the case of transfection for microscopy, cells were fixed 16 h post transfection.

2.10 Generation of Stable Cell Lines

To produce virus-like particles, 293T packaging cells in a 6 well plate were transfected with 600 ng MLV Gag-Pol expression vector, 300 ng VSV-G expression vector and 1 µg of a MLV-based retroviral vector, pLHCX or pCMS28 (containing selection markers for hygromycin or puromycin, respectively), encoding the gene of interest such as tetherin, K5 or Vpu. The 293T cells then produce replication-incompetent retroviral particles, so called virus-like particles (VLPs). The retroviral vector containing the gene of interest is packaged into the particle comprised of MLV structural proteins and the VSV-G envelope. When tetherin stable cell lines were produced, 200 ng of Vpu expression vector were co-transfected to enable VLP release. 48 h post transfection the VLPs were harvested and filtered through a 0.45 µm filter. This supernatant was then added to 293T, HT1080 or Jurkat cells for transduction. Target cells were spinoculated with VLP supernatant for 1 h at 3000 g to increase delivery of viral particles to target cells. The cells were then incubated at 37°C for 48 hours before they were split into 10 cm tissue culture plates. Antibiotic selection was added to the cells (100 µg/ml hygromycin B or 1 µg/ml puromycin) and they were incubated at 37°C until non-transduced cells had died and stably expressing cells were selected for.

2.11 Generating Stable Knockout Cell Lines Using the CRISPR-Cas9 System

Three sets of guide RNAs targeting the SERINC3 or SERINC5 locus were designed using the Zhang lab website (http://crispr.mit.edu) and cloned into a lentiCRISPRv2 plasmid (AddGene, Cambridge, MA) (Shalem et al. 2014). Guide sequences for SERINC3 (Genbank accession number NM_006811.2): 1. GTG TCT TCT CCC TCG CCA GC, 2. ATA AAT GAG GCG AGT CAC CG and 3. AAC ATG AGG CAC CGC TGC AG, targeting exon 1 or 2. Guide sequences for SERINC5 (Genbank accession number NM_001174072.2): 1. ATG TCA GCT CAG TGC TGT GC, 2. GCT GAG GGA CTG CCG AAT CC and 3. CTG AGG GAC TGC CGA ATC CT, targeting exon 1 or 2. Guide sequences targeting Luciferase were used as a non-target control. 293T cells in a 6 well plate were transfected with 600 ng HIV Gag-pol, 300 ng VSV-G and 1 µg lentiCRISPRv2 carrying the guide sequence per well to generate VLPs. 48 post transfection VLPs were harvested. 293T cells (4×10^5 per well) or Jurkat Tag cells (4×10^6 per well) were split into a 6 well plate and spinoculated with the VLP supernatants for 1 hour at 3000 x g. Puromycin selection (1 µg/ml) was added two days post transduction and was maintained until single cell clones had been obtained by limiting dilution (for 293T cells) or fluorescence activated cell sorting (FACS; for Jurkat TAg cells). The SERINC knockout was confirmed by sequencing.

2.12 Isolation of CD4+ T Lymphocytes From Blood

Total peripheral blood mononuclear cells (PBMCs) were isolated from the blood of healthy individuals using density gradient centrifugation. Blood was collected in heparin-coated tubes (BD Bioscience) and diluted with an equal amount of 1 x PBS. 30 ml of blood were then layered onto 15 ml of Lymphoprep (Axis-Shield) in a 50 ml falcon tube and centrifuged at 1000 x g at room temperature for 30 min without brakes. PBMCs form a separate layer, the buffy coat, at the border between blood and lymphoprep and can be aspirated using a Pasteur pipette. PBMCs were then diluted in 40 ml of 1 x PBS and pelleted at 300 x g for 10 min. This was repeated three times. The

$CD4^+$ T cells were isolated from the total PBMCs by negative isolation using the Dynabeads Untouched Human CD4 T Cells kit (Invitrogen) following the manufacturer's instructions. Total $CD8^+$ T cells, B cells, NK cells, monocytes, platelets, dendritic cells granulocytes and erythrocytes were depleted from total PBMCs using a mixture if mouse IgG antibodies directed against non-$CD4^+$ T cells that were captured by magnetic Dynabeads. The remaining CD4+ T cells were then activated using Dynabeads Human T-Activator CD3/CD28 for T cell expansion and activiation (Invitrogen) following the manufacturer's instructions. The Dynabeads provide both TCR and co-stimulating signals for T cell activation. The beads were then removed and the cells were kept in rhIL-2 (30 U/ml; Roche) before they were infected with VSV-G pseudotyped HIV-1.

2.13 SDS-PAGE and Western Blotting

For the detection of proteins in cell lysates and culture supernatants from experimental assays were subjected to sodium dodecyl sulfate polyacrylamide gel electrophoresis (SDS-PAGE) and Western blotting.

The resolving gel was mixed containing all the ingredients shown in table 9 and poured into a glass plate sandwich and casting frame. Where indicated, 25 µM Phos-tag (Wako Chemicals, Japan) and 50 µM MnCl2 (Sigma) were added to an 8% polyacrylamide gel to induce a mobility shift of phosphorylated proteins. The gel was then topped with isopropanol and allowed to set before it was rinsed with ddH_2O. The stacking gel was mixed as mentioned in table 9 and poured on top of the resolving gel. A plastic comb was inserted and the gel was allowed to set. The gel was then placed into a Mini-PROTEAN Tetra Cell electrophoresis system (Bio-Rad) and filled with running buffer (0.1% SDS, 25 mM Tris-Base, 200 mM glycine pH 8.8). Samples were diluted with 2 x Laemmli buffer (LB; 20% glycerol, 4% SDS, 100 mM Tris-HCL pH 6.8, 200 mM β-mercaptoethanol, 0.2% bromophenol blue) and boiled for 10 min at 100°C for denaturation before being loaded onto the gel, next to a protein marker (Prestained Protein marker, broad range 7-175 kDa; NEB). The gel was then run for about 2 h at 80 V.

The separated proteins were transferred onto a nitrocellulose membrane (Amersham Protran 0.45 NC) in a Criterion Blotter (Bio-Rad) in transfer buffer (20% ethanol, 25 mM Tris-base, 200 mM glycine pH 8.8) for 1 h at 100 V or 16 h at 18 V. The membrane was then blocked using 5% Marvel milk dissolved in 1 x PBS/0.1% Tween 20. The primary antibody in 5% milk was incubated with the membrane for 1 h at room temperature, followed by three 10 min washing steps in 1 x PBS/0.1% Tween 20. The membrane was then incubated with the secondary antibody for 1 hour, followed by three wash steps. Membranes incubated with a IRDye conjugated secondary antibody were analysed on the LI-COR Odyssey infrared imaging system (LI-COR Bioscience). Membranes that were incubated with a horseradish peroxidase (HRP) conjugated secondary antibody were additionally incubated with SuperSignal West Pico Chemiluminescent solutions (Thermo Scientific) for 2 min before being visualised using the ImageQuant LAS 400 mini system (GE Healthcare).

Table 9. SDS-PAGE gel ingredients

Separating gel	8%	10%	12%	Stacking gel	
ddH_2O	5.5 ml	5 ml	4.5 ml	ddH_2O	3.25 ml
1.5 M Tris pH 8.8	2.5 ml	2.5 ml	2.5 ml	0.5 M Tris pH 6.8	1.25 ml
Acrylamide (40%)	2 ml	2.5 ml	3 ml	Acrylamide (40%)	465 µl
APS (10%)	50 µl	50 µl	50 µl	APS (10%)	25 µl
TEMED	10 µl	10 µl	10 µl	TEMED	5 µl
SDS (10%)	100 µl	100 µl	100 µl	SDS (10%)	50 µl

Table 10. Primary antibodies used for Western blotting

Antibody	Species	Antigen	Source	Dilution
α-Hsp90	Rabbit	Human HSP90; polyclonal	Santa Cruz Biotechnology	1:5000
α-Vpu	Rabbit	NL4.3 Vpu (amino acids 33-81); polyclonal	NIH AIDS Reagent Program	1:5000
α-p24CA (HIV-1)	Mouse	183-H12-5C (Hybridoma supernatant); monoclonal	NIH AIDS Reagent Program	1:75
α-HA	Rabbit	HA epitope tag; polyclonal	Rockland	1:5000
α-HA	Mouse	CYP**YDVPDYA**SL HA.11 clone 16B12; monoclonal	Covance	1:5000
α-BST2	Rabbit	Human tetherin; polyclonal	NIH AIDS Reagent Program	1:1000
α-βTrCP	Rabbit	Residues surrounding I69 of human β-TrCP; monoclonal	Cell Signaling Technology	1:1000 (1% milk)
α-myc	Mouse	Clone 9E10; monoclonal	Covance	1:1000
α-AP-1 γ1	Mouse	Derived from 100/3 hybridoma, AP-1 adaptor from bovine brain was used as immunogen; monoclonal	Sigma	1:1000
α-AP-2 α	Mouse	AP2a 8G8/5; monoclonal	Sigma	1:1000

Table 11. Secondary antibodies used for Western blotting

Antibody	Conjugate	Source	Dilution
Goat α-mouse	IRDye 680	LI-COR Bioscience	1:5000
Goat α-rabbit	IRDye 800	LI-COR Bioscience	1:5000
Goat α-mouse	HRP	Cell signalling	1:5000
Goat α-rabbit	HRP	Cell signalling	1:5000

2.14 Gene Knockdown Using siRNA

293T or 293T tetherin cells were plated at 2 x 10^5 cells per well of a 12 well plate. For each well, 2 µl Dharmafect (Thermo Scientific) was mixed with 98 µl Opti-MEM (Life Technologies) and added to 5 µl of the 20 µM siRNA oligonucleotide mixed with 95 µl Opti-MEM. Both β-TrCP1 and 2 were knocked down using the SMARTpool siRNA against human BTRC and FBXW11 (Thermo

Scientific). Non-targeting siRNA was used as a control (Thermo Scientific). Two days post transfection cells were reseeded into 24 well plates and a second siRNA transfection was performed following manufacturers instructions. 4 h post transfection cells were infected with VSV-G pseudotyped HIV-1 or mutants thereof at an MOI of 0.8. Supernatants and cell lysates were harvested 48 h later and infectivity of viral supernatants was determined on Hela TZMbl cells as described in 2.23. Cell lysates and pelleted viral supernatants were subjected to SDS-PAGE and Western blotting for analysis of β-TrCP, Hsp90, Pr55 and p24CA expression as described in 2.13.

2.15 NF-κB Reporter Assay

For the transient reporter gene assay, 293 cells were plated into a 24 well plate at a density of 10^5 cells per well. They were transfected with 50 ng of pCR3.1 tetherin plasmid or control pCR3.1 YFP in combination with 10 ng of 3xκB-pCONA-FLuc reporter (NF-κB-dependent firefly luciferase reporter construct) and 5 ng pCMV-RLuc (for determination of the background signal). 48 h post transfection, firefly and renilla luciferase activity in cell lysates was assayed using the Dual-Luciferase Reporter Assay System (Promega). Cells were first lysed in 100 µl 1 x passive lysis buffer for 10 min. Lysates were transferred into Eppendorf tubes and cleared for 10 min at high speed. 10 µl of the cleared lysate were added to a white luminescence 96 well plate and 50 µl luciferase assay reagent II. The signal was measured immediately in a luminescence counter (Victor Light 1420-Perkin Elmer; Wallac software). Then, 50 µl of the Stop&Glo substrate diluted in Stop&Glo buffer 1:50 was added to each well and the signal was measured in the same luminescence counter. Values of the luciferase reading were then normalized to the Stop&Glo Renilla read-out.

2.16 Immunoprecipitation (IP)

Jurkat cells were treated with IFN (1,000 U/ml) or left untreated, Jurkat-TAg L-tetherin, Jurkat-TAg S-tetherin, and Jurkat- TAg empty-vector control cells were lysed on ice for 20 min in buffer containing 50 mM Tris (pH 7.4), 150 mM NaCl, 200 µM sodium orthovanadate, 1% NP-40, 0.5% sodium deoxycholate, 5 mM N-ethylmaleimide, and complete protease inhibitors (Roche). Lysates were cleared by centrifugation, and supernatants were incubated with 5 µg/ml mouse α-BST2 monoclonal antibody (eBioscience) for 1.5 h at 4°C. Sepharose-protein G beads were washed in lysis buffer before they were added to the samples and incubated for another 3 h. Beads were washed five times in lysis buffer before the peptide–N-glycosidase mixture for deglycosylation was added (New England BioLabs). Samples were incubated at 37°C overnight and resuspended in SDS-PAGE loading buffer. Cell lysates and immunoprecipitates were subjected to SDS-PAGE and Western blotting for tetherin and Hsp90 as described in 2.13.

2.17 Cross-Linking IP

293T tetherin, 293T tetherin Y6,8A or 293 Rhesus tetherin cells were transfected with 8 µg GFP expression construct, pCR3.1 Vpu-HA or mutant thereof. Transfection media was changed 6 hours post transfection and cells incubated with 50 nM concanamycin. In the case of CKII inhibitor treatment, cells were treated with 50 µM final Tyrphostin 24 hours prior to harvesting. 48 hours post transfection, cells were trypsinised and washed in PBS. Cells were cross-linked with 0.05%

HCHO/PBS for 10 min at 37°C. The cross-linking reaction was then quenched by incubating cells in 0.25M glycine for 5 min. Cells were washed once in PBS before resuspension in lysis buffer (10mMHepes pH 7, 150mMNaCl, 6mMMgCl2, 2mMDTT, 10% glycerol, 0.5% NP40, 200 µM sodium orthvanadate and 1x Complete protease inhibitors (Roche)). Cells were lysed on ice for 10 min followed by repeated sonication (3 x 10 s cycles with 20 s rests). The cell lysates were clarified by centrifugation at 1000 x g for 10 min and supernatants were immunoprecipitated with 5 µg/ml mouse monoclonal anti-HA.11 antibody (Covance) or rabbit polyclonal anti-HA antibody (Rockland) on Dynabeads protein G beads (Life Technologies) for 4 hours at 4°C. Beads were collected post incubation and washed 5 times in lysis buffer before cross-links were reversed in 1% SDS, 10mM EDTA and 5mm DTT at 65°C for 45 min. Samples were then analysed for HA, AP-1 and AP-2 by SDS-PAGE and Western blotting as described in 2.13.

For the β-TrCP IP, 293T cells were co-transfected with 700 ng of pCR3.1 myc β-TrCP 2 and pCR3.1 Vpu-HA/mutant or pCR3.1 YFP expression plasmids. 48 h post transfection, Crosslinking Immunoprecipitation was performed as previously described above. Cell lysates and immunoprecipitates were analysed for Vpu and myc by SDS-PAGE and Western blotting assays as described in 2.13.

2.18 Immunofluorescence Microscopy

Cells were plated on poly-L-lysine (Sigma) treated coverslips and transfected with 100 ng of a tetherin, Vpu or 500 ng Gag-GFP expression vector. 16 h post transfection cells were fixed in 4% paraformaldehyde for 15 min and washed with 10 mM glycine. Cells were permeabilized in 1% BSA/0.1% Triton-X100 for 15 min. Then the primary antibodies (table 12) diluted in 1% BSA/0.01%Triton-X100 were added and incubated for 45 min at room temperature. Cells were washed twice and the secondary antibodies (table 13) were added and incubated for 45 min. After two more wash steps, the coverslips were mounted onto glass slides using ProLong AntiFace-49,6-diamidino-2-phenylindole (DAPI; Molecular Probes, Invitrogen). The cells were then visualised either on a Leica DM-IRE2 confocal microscope (63 x oil immersion lens) and images analysed using the Leica Confocal Software and ImageJ; or Z stacks were taken on a Nikon ECLIPSE Ti inverted microscope (100 x oil immersion lens) and images were deconvolved using AutoQuant X3 and analysed using ImageJ software.

Table 12. Primary antibodies used for immunofluorescence microscopy

Antibody	Species	Antigen	Source	Dilution
α-HA	Mouse	CYP**YDVPDYA**SL HA.11 clone 16B12	Covance	1:1000
α-HA	Rabbit	HA epitope tag	Rockland	1:1000
α-BST2	Mouse	Human tetherin, residues 40-181	Abnova	1:200
α-TGN46	Sheep	Human TGN46	AbD Serotec	1:100
α-CD63	Mouse	Human CD63 (Hybridoma Supernatant)	Developmental Studies Hybridoma Bank, University of Iowa	1:10

Table 13. Secondary antibodies used for immunofluorescence microscopy

Antibody	Conjugation	Source	Dilution
Donkey α-mouse	Alexa Fluor 488 Alexa Fluor 594 Alexa Fluor 630	Molecular Probes (Invitrogen)	1:500
Donnkey α-rabbit	Alexa Fluor 488 Alexa Fluor 594 Alexa Fluor 630	Molecular Probes (Invitrogen)	1:500
Donkey α-sheep	Alexa Fluor 488 Alexa Fluor 594 Alexa Fluor 630	Molecular Probes (Invitrogen)	1:500

2.19 Detection of Surface Proteins by Flow Cytometry

293 cells stably expressing tetherin isoforms were transfected with 500 ng pCRV1 HIV-2 Env-IRES-GFP or the indicated mutant. 48 h post transfection cells were stained for surface tetherin using a monoclonal α-BST IgG2a antibody (Abnova) and a goat α-mouse IgG2a-Alexa 633 conjugated secondary antibody (Molecular Probes, Invitrogen). Alternatively, a PE conjugated monoclonal α-BST2 antibody (eBioscience) was used to stain untransfected stably tetherin expressing 293 cells. The cells were detached from the tissue culture plate using 5 mM EDTA and washed in ice cold FACS buffer (1% BSA, 0.1% sodium azide in 1 x PBS). The primary antibody was diluted in FACS buffer and added to the cells for 1 hour on ice. Cells were then washed three times with FACS buffer, before the secondary antibody was added for 1 hour on ice. Cells were then washed three times in FACS buffer and resuspended in 1 x PBS. Tetherin and GFP expression were then assessed on a FACSCanto II flow-cytometer (Becton Dickinson) and results were analysed using the FlowJo software.

2.20 Generating Infectious Virus Stocks and Virus Stock Titration on Hela-TZMbl Cells

293T cells in a 6 well plate were transfected using PEI with 2 µg of a provirus and 200 ng pCMV-VSV-G, if pseudotyped. This allows the additional expression of VSV-G on the virus particle and infection of CD4 negative cells. 6 h post transfection the medium was replaced and 48 h post transfection the culture supernatant containing the viral particles was filtered through a 0.45 µm filter, aliquoted and stored at -80°C.

To determine the infectious titer of the virus stock, Hela TZMbl cells were plated in a 96 well plate (10^4 cells per well) and infected with 25 µl of a serial dilution of the virus stock (10^0 to 10^{-6}). 48 h later cells were fixed in 0.5% glutaraldehyde for 15 min and washed in 1 x PBS. Then the X-Gal substrate solution (1 mg/ml X-gal-dimethylformamide, 5 mM K ferrocyanide, 5 mM ferricyanide, 2 mM $MgCl_2$, 0.02% NP40 and 0.015 Triton-X100 in 1 x PBS) was added and the fixed cells were incubated at 37°C for 2 hours or overnight. Infected cells will turn blue due to Tat-activated β-galactosidase expression and X-Gal cleavage, which then forms an intense blue product. The blue colonies were counted with a light microscope and the end point titer was determined as infectious units per ml.

Cells were then infected at different multiplicities of infection (MOI) depending on the assay. A MOI of 1 means that the amount of infectious particles is the same as the amount of cells infected. However, the amount of cells that are infected is defined by the Poisson distribution:

$$P(n) = \frac{m^n \times e^{-m}}{n!}$$

Where P(n) is the probability that a cell will be infected by n viruses and m being the MOI. That means that the probability for a cell to be infected at an MOI of 1 is around 63% and at an MOI of 2 around 87%. An MOI of 2 was used in assays looking at the degradation of tetherin. A lower MOI of 0.5-1 was used in single round infection assays.

2.21 Virus Release Assay

293T cells were plated in a 24 well plate at a density of 1.2 x 10^5 cells per well. Cells were transfected with 500 ng proviral plasmid and increasing concentrations of tetherin or SERINC expression vector using PEI. Alternatively, 293T cells transfected with 50 ng of tetherin or 293T tetherin cells were transfected with increasing amounts of Vpu or mutants in addition to 500 ng proviral plasmid.

For infection assays, adherent cells were plated in a 24 well plate at a density of 1.2 x 10^5 cells per well or 1 x 10^6 suspension cells were infected at an MOI of 0.8-1 with VSV-G pseudotyped virus. In the case of CKII inhibitor treatment, cells were treated with 50 µM final Tyrphostin or DMSO 24 h prior to harvesting.

The medium was changed 6 h later and cells and supernatants were harvested 48 h post transfection/infection. The supernatant was analysed for infectious virus release as described in 2.23 and for physical virus particle release as described in 2.22. Cell lysates were analysed by Western blotting as described in 2.13.

2.22 Determining Physical Virus Release

The supernatant was harvested from each well and filtered through a 0.22 µm filter (Millipore) into a fresh plate. 700 µl of the filtered supernatant was layered on top of 500 µl cold 20% sucrose in 1 x PBS in a microfuge tube. The tubes were then centrifuged for 1 h at 4°C and 17,900 x g. Then the supernatant was aspirated and the invisible pellet was resuspended in 20 µl 2 x loading buffer. Samples were then boiled for 10 min and analysed by Western blotting for p24CA as described in 2.13.

2.23 Determining Infectious Virus Release

The infectious virus release in supernatants was determined using Hela-TZMbl cells that were plated in a 96 well plate (10^4 cells per well). 25 µl of the supernatant was added to one well of Hela-TZMbl cells and the plate was incubated for 48 h at 37°C. Cells were then lysed using 50 µl Tropix Galacto-Star Lysis solution (Applied Biosystems) for at least 15 min at room temperature. 10 µl of the lysate was transferred into a white luminescence 96 well plate and incubated for 15 min with 45 µl Tropix Galacto-Star substrate diluted in Reaction Buffer Diluent 1:50 (Applied Biosystems). β-

galactosidase activity was then measured in a luminescence counter (Victor Light 1420-Perkin Elmer; Wallac software).

2.24 Tetherin Degradation Assay

To assess tetherin degradation, 293T tetherin cells or Jurkat TAg cells were infected with the indicated VSV-G pseudotyped virus at an MOI of 2. The medium was replaced 6 h later and cells were harvested 48 h post infection and analysed for total tetherin expression by Western blotting as described in 2.13.

Alternatively, stably tetherin expressing cells were transfected with a Vpu expression construct and harvested 48 h later or transduced with VLPs containing Vpu or K5 and harvested after selection. Total tetherin in cell lysates was then determined by Western blotting as described in 2.13.

2.25 Intracellular p24 Staining for FACS

Cells were infected with a VSV-G pseudotyped virus at an MOI of 1 and stained 48 h later. Cells were first stained for tetherin as described in 2.19. Then they were fixed and permeabilized for 20 min using Fixation/Permeabilization solution (Cytofix/cytoperm Fixation/Permeabilization kit, BD Bioscience) and stained for intracellular HIV-1 p24CA using the KC57 PE-conjugated antibody (Beckman-Coulter) diluted in Perm/Wash buffer (Cytofix/cytoperm Fixation/Permeabilization kit, BD Bioscience). Cells were then washed in Perm/Wash buffer and analysed on a FACSCalibur flow-cytometer (Becton Dickinson) and FlowJo software.

Chapter 3 Differential Sensitivities of Tetherin Isoforms to Counteraction by Primate Lentiviruses

The data presented in this chapter have been published as “Differential sensitivities of tetherin isoforms to counteraction by primate lentiviruses” (Weinelt & Neil 2014).

3.1 Introduction

Tetherin (BST-2/CD317) is an interferon-induced transmembrane protein that has antiviral activity against a broad range of enveloped viruses including members of the families *Retroviridae* (Neil et al. 2008; Jouvenet et al. 2009) and *Herpesviridae* (Zenner et al. 2013; Pardieu et al. 2010; Mansouri et al. 2009; Blondeau et al. 2013) and negative-strand RNA viruses (Sakuma et al. 2009). It crosslinks budding virions to the plasma membrane and thereby restricts virus release from the infected cells, facilitated by its unique topology that is crucial for its function (Perez-Caballero et al. 2009). Tetherin is a dimeric glycoprotein with an N-terminal cytoplasmic tail (CT), a transmembrane domain, a coiled-coil extracellular domain and a C-terminal glycosylphosphatidylinositol (GPI) anchor (Neil 2013). The GPI anchor is inserted into budding virions and parallel tetherin dimers physically restrict their release (Venkatesh & Bieniasz 2013). Tetherin targets a viral determinant, the host-derived viral envelope, which the virus cannot mutate and it also explains tetherin’s wide activity against various virus families. Tethered virus is eventually endocytosed and trafficked to late endosomes (Neil et al. 2008), possibly for degradation. Recently, human tetherin has also been shown to induce NF-κB signalling upon virus retention, acting as an innate sensor of viral release (Cocka & Bates 2012; Galão et al. 2012; Tokarev et al. 2013). There is genetic evidence from primate lentiviruses that the ability of a virus to overcome tetherin is essential for its *in vivo* spread. Tetherin exerts a high evolutionary pressure on enveloped viruses. This is highlighted by the fact that various viruses have evolved diverse proteins with anti-tetherin activity that often act in a species-specific manner (Neil 2013). Examples include HIV-1 Vpu (Neil et al. 2008; Van Damme et al. 2008), SIV Nef (Jia et al. 2009; Zhang et al. 2009), HIV-2 Env (Le Tortorec & Neil 2009), Ebola GP (Kaletsky et al. 2009), Herpes gM (Blondeau et al. 2013) and KSHV K5 (Pardieu et al. 2010; Mansouri et al. 2009). It has been suggested that efficient tetherin counteraction by the Vpu protein of the major HIV-1 group M is a reason for its pandemic spread compared to other HIV-1 groups with less efficient antagonists (Sauter et al. 2009).

HIV-1 Vpu is a membrane phosphoprotein that interacts with human and chimpanzee tetherin (Dubé, Roy, et al. 2010; Skasko et al. 2012; Vigan & Neil 2010; Matthew W McNatt et al. 2013). It antagonises tetherin by rerouting the newly synthesized and recycling protein, eventually leading to its endosomal degradation (Dubé et al. 2011; Schmidt et al. 2011; Kueck & Neil 2012). This trafficking event is dependent on clathrin and requires an acidic dileucine motif (ExxxLV) in Vpu's CT as well as a tyrosine based sorting motif (YDY) in tetherin's CT (Kueck & Neil 2012). The requirements in tetherin for counteraction and degradation are still not completely clear. Degradation is dependent on ubiquitination of potentially multiple residues in tetherin's CT, including an STS motif (Tokarev et al. 2011). This process also requires the ESCRT machinery, as well as the recruitment of the $SCF^{\beta TrCP1/2}$ E3 ligase by a phosphoserine motif (DSGNES) in Vpu (Agromayor et al. 2012; Janvier et al. 2011; Tokarev et al. 2011; Gustin et al. 2012; Mitchell et al. 2009; Douglas et al. 2009). Tetherin antagonists other than HIV-1 Vpu do not mediate degradation, but induce endocytosis of tetherin from the cell surface and lead to its sequestration (Jia et al. 2009; Le Tortorec & Neil 2009; Zhang et al. 2011b; Serra-Moreno et al. 2013a; Lau et al. 2011).

Recently, it has been shown that two isoforms of human tetherin can be expressed (Cocka & Bates 2012). They differ in the length of their cytoplasmic tail, with the shorter isoform lacking the first twelve amino acids compared to the long isoform. Those residues include the tyrosine based (YDY) sorting motif that is also important for induction of signalling as well as the STS motif that is potentially ubiquitinated. Both isoforms are thought to be expressed due to leaky ribosomal scanning, which results from suboptimal Kozak sequences flanking two AUGs. The presence of these two start codons is highly conserved among tetherin sequences from different species (Figure 3.1 A and B). It has been reported that short human tetherin (S-tetherin) is less sensitive to HIV-1 NL4.3 Vpu than long tetherin (L-tetherin) (Cocka & Bates 2012).

In this chapter the findings of Cocka and Bates are extended, with further investigation into the differences in antagonism of short and long primate tetherins by various viral countermeasures. It is confirmed that short human tetherin is less efficiently counteracted, downregulated and degraded by HIV-1 Vpu at physiological tetherin expression levels. This is dependent on the tyrosine and serine based motifs in tetherin's CT. Furthermore, the data show that S-tetherin is less sensitive to a range of HIV-1 group M Vpus. In contrast, Vpu proteins from a highly pathogenic HIV-1 group N virus as well as from greater spot-nosed monkey or mona monkey SIV antagonised both isoforms of their respective hosts with equivalent efficiency. Additionally, tetherin isoforms did not exhibit

differential sensitivity to other tetherin countermeasures such as SIVmac Nef, HIV-2 Env or KSHV K5. These data suggest that the differential sensitivity of tetherin isoforms is a conserved feature of HIV-1 group M Vpus only.

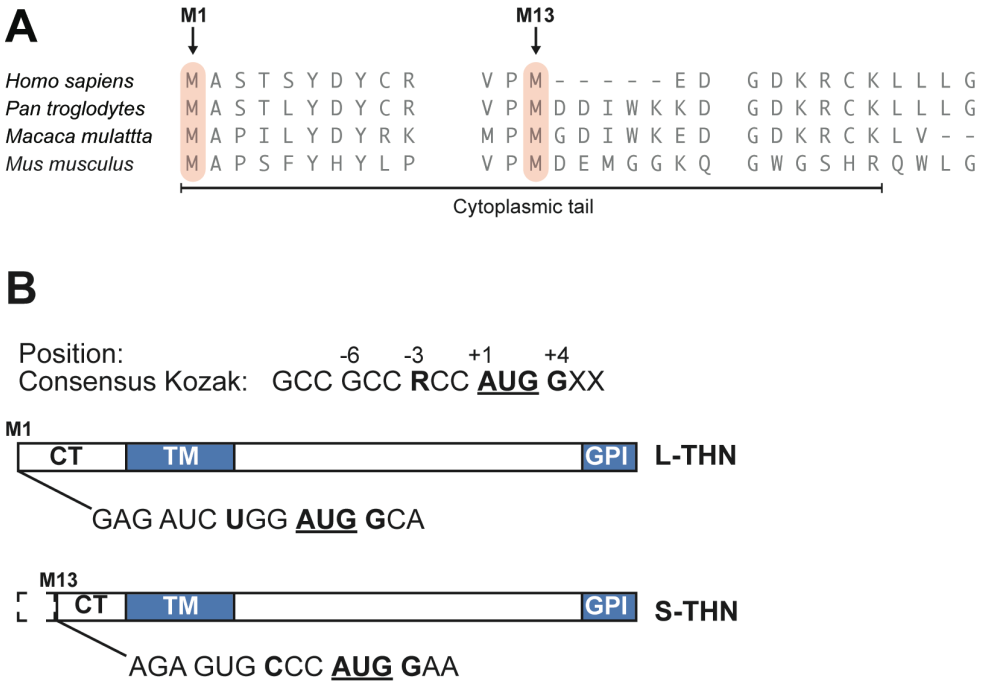

Figure 3.1 The tetherin cytoplasmic tail amino acid sequence is highly conserved among species. (A) Alignment of the amino acid sequences of the cytoplasmic tail of tetherin of different mammalian species. Methionines M1 and M13 are highly conserved. Accession numbers: Homo sapiens (NP_004326); Pan troglodytes (NP_001177409); Macaca mulatta (ACV96781); Mus musculus (NP_932763). (B) Nucleotide sequences in front of the M1 and M13 AUGs in human tetherin mRNA differ from the consensus Kozak translation initiation sequence. Positions -3 and +1 to +4 are highlighted and particularly important for translation initiation. L-THN and S-THN refer to proteins initiated at M1 or M13 respectively. R=Purine. (Adapted from Cocka and Bates, 2012.)

3.2 Results

3.2.1 Long and Short Tetherin Isoforms are Differentially Sensitive to HIV-1 Vpu

To further investigate the differences in counteraction of the two tetherin isoforms, constructs were generated encoding human tetherin containing the naturally occurring Kozak sequence (WT tetherin) and either the first (M1A, S-tetherin) or the methionine at position thirteen (M13I, L-tetherin) were mutated (Figure 3.2 A). First, the findings of Cocka and Bates that HIV-1 Vpu was less efficient in counteracting short tetherin were confirmed. 293T cells were transiently transfected with WT NL4.3 HIV-1 or a Vpu-deficient version (ΔVpu; with a frame shift mutation in the start codon of Vpu; Neil et al. 2006) and increasing amounts of the tetherin expression vectors. Increasing amounts of all tetherin constructs led to similarly reduced virus release of the Vpu deficient virus (Figure 3.2 B). All tetherins were well expressed with the WT construct expressing both isoforms (Figure 3.2 C). WT NL4.3 HIV-1 was unaffected by all concentrations of long tetherin. However, above moderate expression levels of short tetherin partially restricted WT virus release. The expression of both isoforms from the WT tetherin vector had a weaker, but notable effect on WT HIV-1 release. Four times more WT tetherin was needed to restrict WT virus release to a similar level as short tetherin. Assuming that L- and S-tetherin assort randomly into homo- and heterodimers, this suggests that heterodimers are sensitive to counteraction by Vpu and it is the S-tetherin homodimers that are responsible for increased restriction.

Next, it was tested whether there was a difference in Vpu-mediated degradation of the two isoforms. For this, 293 cells stably expressing L-tetherin or S-tetherin were infected. Both tetherin isoforms were expressed to similar levels at the cell surface of 293 cells as determined by flow cytometry (Figure 3.2 D). As 293 cells do not express CD4, they were infected with VSV-G pseudotyped HIV-1 NL4.3 WT or ΔVpu HIV-1 at an MOI of 2 for 48 h. Analysis of tetherin expression by Western blotting showed that, as expected, WT virus was potently degrading L-tetherin (Figure 3.2 E). Under the same conditions S-tetherin was not degraded, but infection led to a molecular mass shift in tetherin. This could be a Vpu mediated modification of tetherin, potentially ubiquitination, which could explain the residual activity of HIV-1 Vpu against S-tetherin.

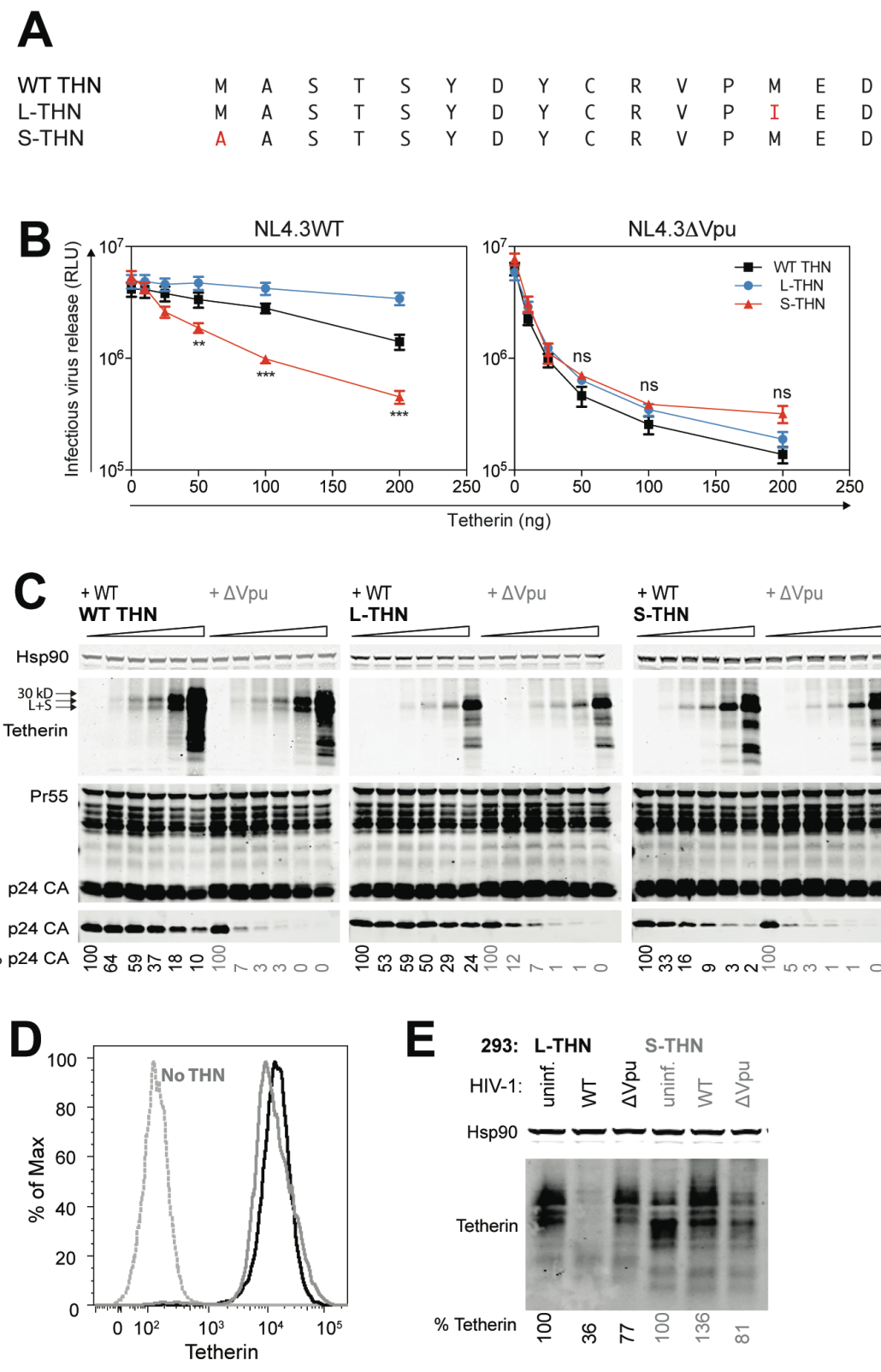
A
WT THN M A S T S Y D Y C R V P M E D
L-THN M A S T S Y D Y C R V P I E D
S-THN A A S T S Y D Y C R V P M E D
B
NL4.3WT
NL4.3ΔVpu
Infectious virus release (RLU)
Tetherin (ng)
WT THN
L-THN
S-THN
ns
**
***
C
+ WT
+ ΔVpu
WT THN
L-THN
S-THN
Hsp90
30 kD
L+S
Tetherin
Pr55
p24 CA
cells
virions
% p24 CA
100 64 59 37 18 10 100 7 3 3 0 0
100 53 59 50 29 24 100 12 7 1 1 0
100 33 16 9 3 2 100 5 3 1 1 0
D
No THN
% of Max
Tetherin
E
293: L-THN S-THN
HIV-1: uninf. WT ΔVpu uninf. WT ΔVpu
Hsp90
Tetherin
% Tetherin
100 36 77 100 136 81

Figure 3.2 Tetherin isoforms are differentially sensitive to HIV-1 NL4.3 Vpu. (**A**) Schematic representation of the wild type tetherin amino acid sequence (WT THN) and mutants for long (L-THN) and short tetherin (S-THN). (**B**) and (**C**) 293T cells were transfected with increasing amounts of WT THN, L-THN or S-THN and NL4.3 WT or ΔVpu proviral plasmid. (**B**) 48 h post transfection infectious virus release was determined using Hela-TZMbl reporter cells. Error bars represent standard deviations of the means of three independent experiments. Asterisks represent the p value for the difference in virus release from L-tetherin and S-tetherin expressing cells at 50 ng, 100 ng or 200 ng of tetherin expression vector. ns, not significant; **p<0.01, ***p<0.001 as determined by two-tailed t test (**C**) Cell lysates and pelleted viral supernatants from (**B**) were subjected to SDS-PAGE and analyzed by Western blotting for Hsp90, tetherin and p-24CA. Percent of p24 release into the supernatant indicated below are relative to the release of NL4.3WT or NL4.3ΔVpu in the absence of tetherin. (**D**) 293 cells stably expressing the tetherin isoforms were analyzed for their tetherin surface expression (PE conjugated monoclonal α-BST2 antibody (eBioscience)) by flow cytometry. (long tetherin, solid black line; short tetherin, solid grey line; empty vector 293 cells, dashed grey line No THN). (**E**) 293 cells stably expressing tetherin isoforms were infected with VSV-G-pseudotyped NL4.3WT or NL4.3ΔVpu virus at an MOI of 2. 48 h post infection, cells were harvested and subjected to SDS-PAGE and analyzed by Western blotting for tetherin and Hsp90, and analyzed by LiCor quantitative imager. Percent of tetherin levels indicated below each lane are relative to tetherin levels in the corresponding uninfected cell line.

A tyrosine based sorting signal (YDYCRV) as well as a potential ubiquitination motif (STS) in tetherin's CT have been implicated in tetherin antagonism by HIV-1 Vpu (Kueck & Neil 2012; Tokarev et al. 2011). Both motifs are absent in S-tetherin and mutation of those residues reduces the sensitivity of tetherin to Vpu (Figure 3.3 A and B). Mutation of both motifs simultaneously seemed to have a slightly additive effect, which could be the result of reduced natural turnover due to the lack of the required sorting motifs (Figure 3.3 B and C). Replacing the tyrosines with phenylalanine (YDY → FDF) retains tetherin's sensitivity to Vpu as this substitution retains the endocytic sorting signal to a certain extent (Figure 3.3 B). This reduced sensitivity of the YDY, STS or double mutant does not correlate with total cellular expression or surface levels of tetherin (Figure 3.3 C and D). This was determined by flow cytometry analysis of 293 cells stably expressing the different isoforms (Figure 3.3 D). This demonstrates that these residues are required for Vpu's enhanced anti-tetherin function against the long isoform.

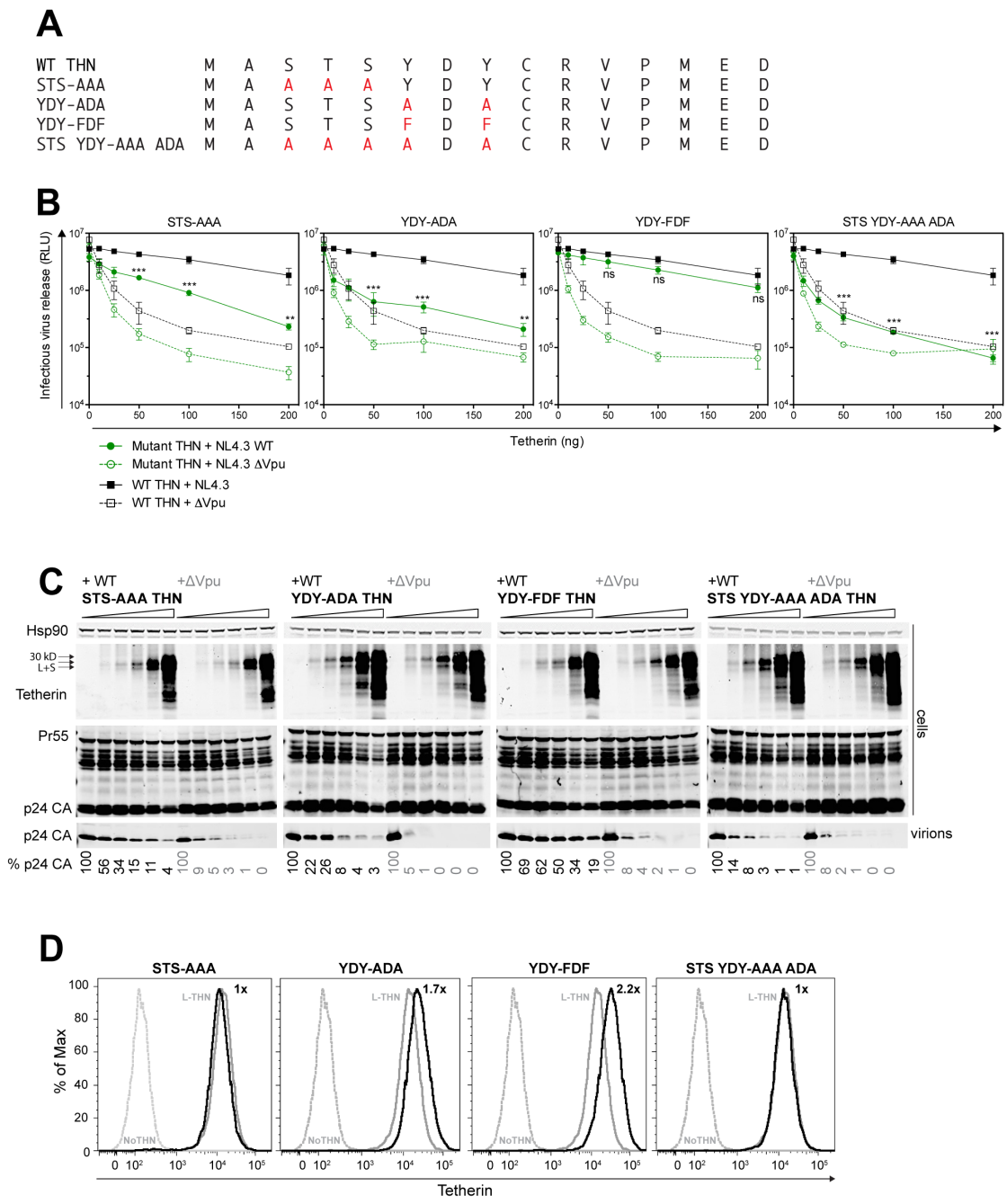

Figure 3.3 The sensitivity of tetherin to Vpu is dependent on serines, a threonine and tyrosines. (**A**) Cytoplasmic tail amino acid sequence of tetherin mutants used to determine required residues for the sensitivity to NL4.3 HIV-1 Vpu. (**B** and **C**) 293T cells were transfected with increasing amounts of different tetherin mutants and NL4.3 WT or ΔVpu proviral plasmid. (**B**) 48 h post transfection infectious virus release was determined using Hela-TZMbl reporter cells. Error bars represent standard deviations of the means of three independent experiments. Black: WT tetherin; green: mutant tetherin; solid lines, NL4.3 wild type provirus; dashed lines, NL4.3 ΔVpu provirus. Asterisks represent the p value for the difference in virus release from WT tetherin and mutant tetherin expressing cells at 50 ng, 100 ng or 200 ng of tetherin expression vector. ns, not significant; **p<0.01, ***p<0.001 as determined by two-tailed t test. (**C**) Cell lysates and pelleted viral supernatants from (**B**) were subjected to SDS-PAGE and analyzed by Western blotting for Hsp90, tetherin and p-24CA. Percent of p24 release into the supernatant indicated below are relative to the release of NL4.3WT or NL4.3ΔVpu in the absence of tetherin. (**D**) 293 cells stably expressing the tetherin mutants (solid black line) were analyzed for their tetherin surface expression by flow cytometry (PE conjugated monoclonal α-BST2 antibody (eBioscience)) and are shown in comparison to 293 cells expressing long tetherin (L-THN; solid grey line) and empty vector 293 cells (dashed grey line). Numbers indicate the fold median fluorescence intensity compared to L-tetherin expressing cells.

Next this phenotype was confirmed in a cell type that is more relevant to HIV infection. A $CD4^+$ T cell line, Jurkat TAg, was used, which expresses the SV40 large T antigen and no detectable levels of tetherin. Bulk populations of Jurkat TAg cells stably expressing L- or S-tetherin had similar tetherin surface levels as Jurkat cells treated with interferon for 24 h as determined by flow cytometry (Figure 3.4 A). Immunoprecipitation of tetherin from these cell lines showed that Jurkat cells express both isoforms and both L- and S-tetherin are induced equally by Interferon treatment. Jurkat TAg cells do not express any detectable tetherin, whereas the stable Jurkat TAg cell lines only express either L- or S-tetherin, which means that they were useful for further experiments (Figure 3.4 B). L- or S-tetherin expressing Jurkat TAg cells were infected with either WT NL4.3 virus or the ΔVpu version for 48 h and tetherin surface levels and intracellular p24 expression were assessed. As expected, the Vpu deficient virus was unable to downregulate any tetherin isoform from the cell surface (Figure 3.4 C and D). Rather, tetherin levels appeared to be enhanced in p24 positive cells, which could potentially be due to accumulating virions on the cell surface and was observed before (Kueck et al. 2012). The WT virus was able to efficiently downregulate L-tetherin from infected cells. However, it was much less efficient in similarly downregulating S-tetherin (Figure 3.4 C and D). This was in keeping with the infectious virus released from the same cells. There was a significant reduction in WT virus release expressing S-tetherin compared to that from L-tetherin expressing cells (Figure 3.4 E). The same phenotype could be observed for the physical particle release from the same infected cells (Figure 3.4 F). To rule out that WT tetherin was induced by infection, immunoprecipitates of infected cells for tetherin were analysed for tetherin expression levels. However, WT tetherin expression was not induced upon infection in this system (Figure 3.4 G).

These data confirm that S-tetherin is less sensitive to HIV-1 NL4.3 Vpu, possibly because it is lacking important sorting motifs in its cytoplasmic tail that are required for HIV-1 Vpu's ability to counteract tetherin potently. S-tetherin is less efficiently downregulated from the cell surface and is not degraded. The residual activity that is observed against S-tetherin is consistent with data from others showing that Vpu is capable of promoting virus release without downregulating tetherin from the cell surface, but rather by excluding it from sites of viral budding (Matthew W McNatt et al. 2013; Miyagi et al. 2009).

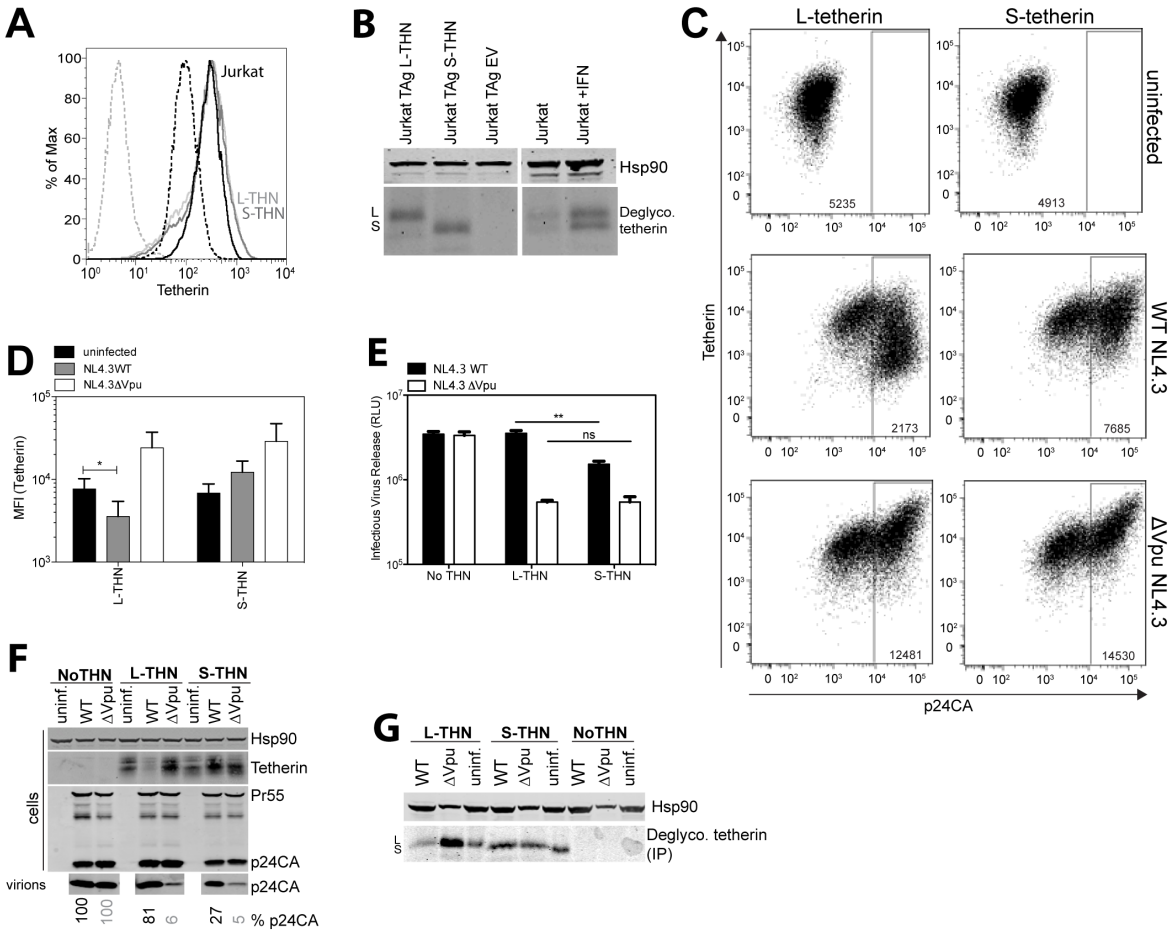

Figure 3.4 Differential sensitivity of tetherin isoforms to Vpu in CD4+ T cell lines. (**A**) Jurkat TAg cells stably expressing long (solid light-grey line) or short (solid dark grey line) tetherin were analyzed for their tetherin surface expression compared to Jurkat cells treated with interferon for 24h (solid black line) or left untreated (dashed black line) and to Jurkat TAg cells (dashed grey line) not expressing tetherin. (**B**) Jurkat TAg cells expressing tetherin isoforms and Jurkat cells treated with interferon or left untreated were lysed and immunoprecipitated with anti-tetherin antibody and deglycosylated. Lysates and precipitates were subjected to SDS-PAGE and analyzed by Western blotting for Hsp90 and tetherin. (**C**) to (**D**) Jurkat TAg cells expressing long or short tetherin were infected with VSV-G pseudotyped HIV-1 NL4.3 WT or ΔVpu at an MOI of 2 for 48 h. (**C**) Cells were analyzed by flow cytometry for their intracellular p24 and surface tetherin expression. Median fluorescence intensities (MFI) are indicated. (**D**) Quantification of C. median fluorescent intensities of three independent experiments are represented. *p<0.05 as determined by two-tailed t test. (**E**) Supernatants from infected cells were titered for infectious virus on TZMbl cells. Data are from four different experiments and error bars show the SEMs. **p<0.01 as determined by two-tailed t test. (**F**) Cell lysates and pelleted viral supernatants from (**C**) were subjected to SDS-PAGE and analyzed by Western blotting for HIV-1 Hsp90, tetherin and p-24CA. Percent p24 release relative to NL4.3WT or NL4.3ΔVpu release in the absence of tetherin is indicated below. (**G**) 293 cells expressing no THN, L-THN or S-THN were infected at an MOI of 2. 48 h post infection cells were lysed and immunoprecipitated with anti-tetherin antibody and deglycosylated. Lysates and precipitates were subjected to SDS-PAGE and analyzed by Western blotting for Hsp90 and tetherin.

3.2.2 Tetherin Isoforms Show a Similar Subcellular Localization

To see whether the differential sensitivity of L- and S-tetherin was due to differential distribution of the proteins in the cell, the subcellular localization of both isoforms was analysed. It was shown that tetherin localizes to the plasma membrane but also to intracellular endocytic compartments and the TGN. HT1080 cells do not express tetherin and are flat and easy to image. Therefore, they were transduced with L- or S-tetherin, immunostained for tetherin and a TGN marker (TGN46) and analysed by confocal microscopy. However, no apparent difference in localization between the long and the short isoform of tetherin could be observed and both seemed to be expressed on the cell surface and in TGN46 positive intracellular compartments (Figure 3.5 A). In addition, both isoforms were expressed to equal levels on the cell surface of the same cells (Figure 3.5 B).

Even though the isoforms do not show a differential subcellular localization themselves, we were wondering whether retained virions would localize distinctly depending on the tetherin isoform expressed. Tetherin-restricted virions are endocytosed and accumulate in late endosomal compartments (Neil et al. 2006). As S-tetherin lacks an important tyrosine-based sorting signal that is required for AP-1 and AP-2 mediated trafficking, endocytosis of virions would be expected to be inhibited as well. This has been reported before by our group for the tyrosine mutant of tetherin (Galão et al. 2012). To confirm these results for human S-tetherin, 293 cells stably expressing L- or S-tetherin were transfected with HIV-1 Gag-GFP, as a surrogate for viral particles, and analysed for whether Gag localized to the plasma membrane only or to the plasma membrane as well as distinctly to endosomal compartments (Neil et al. 2006). As expected, in cells expressing no tetherin Gag localized predominantly to the plasma membrane only (Figure 3.6 A and B). In contrast, cells expressing L-tetherin showed distinct accumulation of Gag in intracellular compartments. Cells expressing S-tetherin exhibited a lower proportion of cells with this distinct endosomal accumulations compared to L-tetherin expressing cells (41% versus 70%). This indicates that residues in the cytoplasmic tail of tetherin play a role in endocytosis. This data confirm previous findings implicating the dual-tyrosine motif in the cytoplasmic tail of tetherin in this partial phenotype (Lau et al. 2011; Galão et al. 2012). Even though enhanced endocytosis of virions by L-tetherin is not relevant for L-tetherin's signalling capacity, this process may have subsequent detrimental effects for virus replication (Galão et al. 2012). For example, endocytosed virions may be sorted into endosomal pathways for degradation, which can potentially result in increased pattern

recognition or antigen presentation, followed by increased proinflammatory signalling. Therefore, counteracting L-tetherin more efficiently may be a way to overcome this.

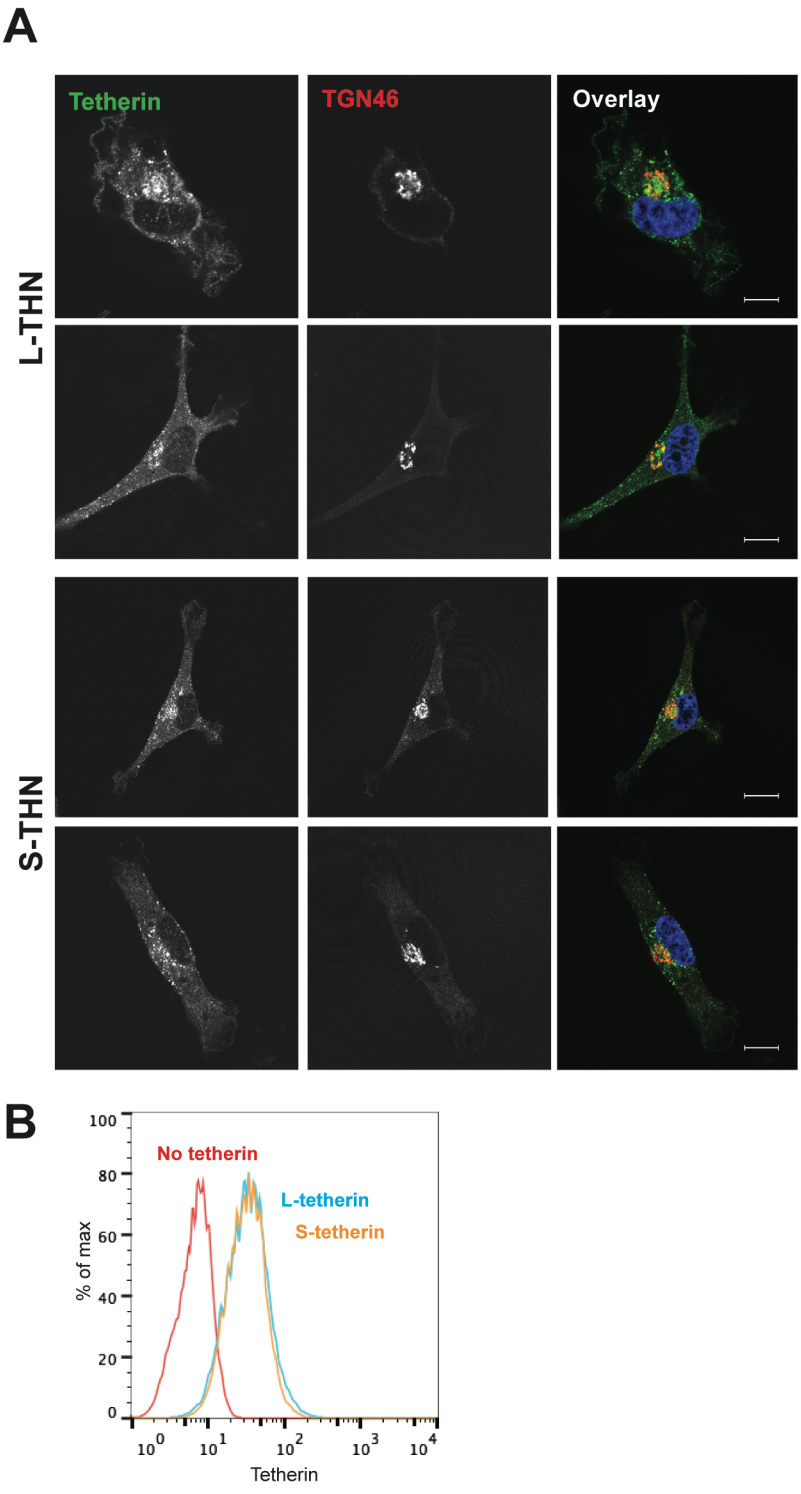

Figure 3.5 Subcellular localization of tetherin isoforms. (**A**) HT1080 cells expressing human L- or S-tetherin were fixed, stained for tetherin (green) and TGN46 and examined by confocal microscopy. Nuclei were counterstained with DAPI (blue). Panels are representative examples. Bars = 10 µm. (**B**) The same cells were cell surface stained for tetherin and analysed by flow cytometry and compared to HT1080 cells not expressing tetherin (red).

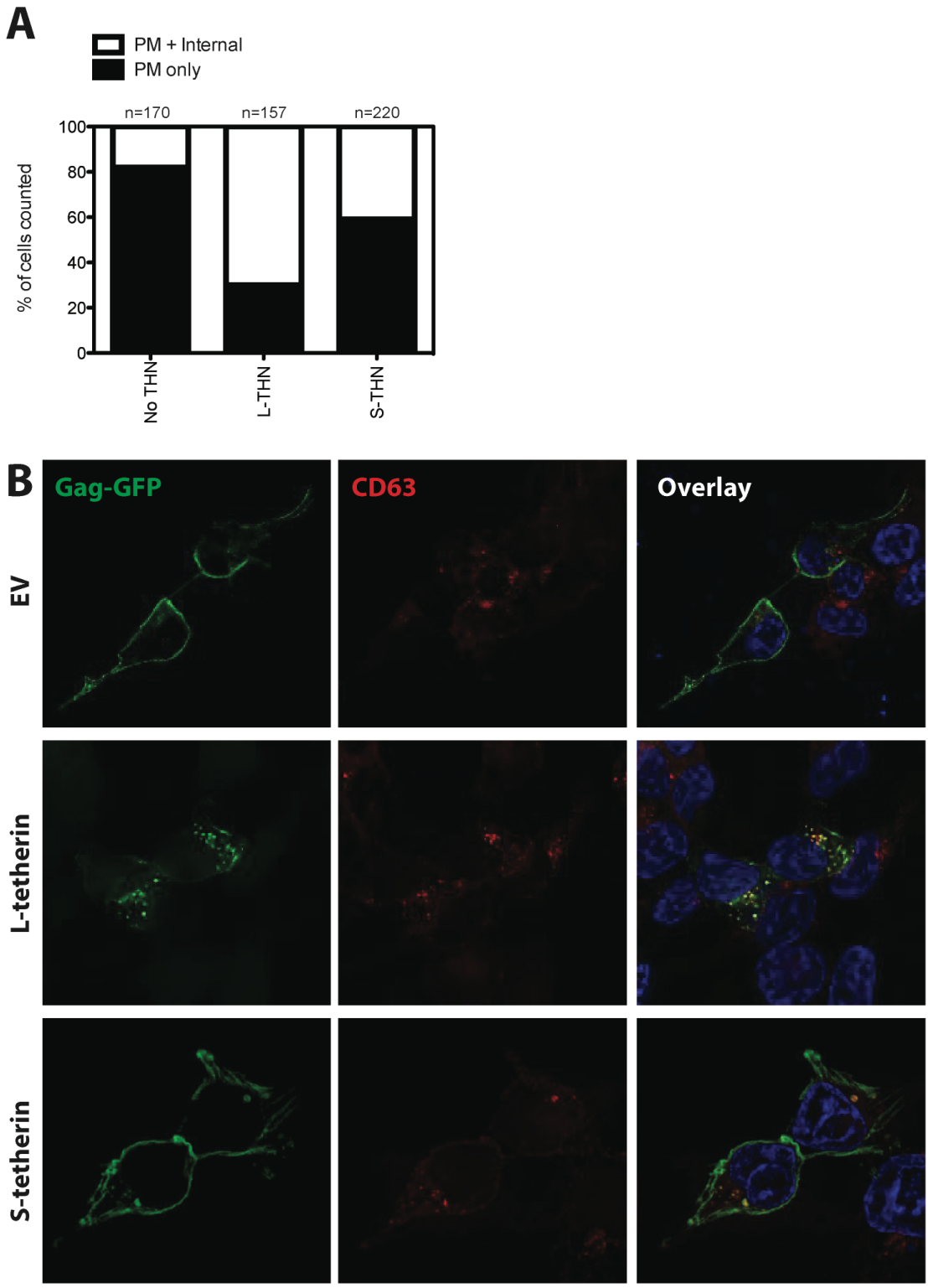

Figure 3.6 HIV-1 gag accumulation in endosomes is reduced in S-tetherin expressing cells (A and B) Tetherin-expressing 293 cell lines were transfected with an HIV-1 gag-GFP expression vector. 24 h later cells were fixed, stained for late endosomal marker CD63 and examined by widefield fluorescent microscopy. (A) Random fields were enumerated on the basis of whether transfected cells displayed plasma-membrane only Gag-GFP localization or PM and distinct endsomal accumulation of Gag-GFP. (B) Panels are representative examples. Bars = 10 μm. Z stacks were taken of all cells (n = 15), images were deconvolved using the AutoQuant X3 software.

3.2.3 The Differential Sensitivity of Tetherin Isoforms is a Feature of HIV-1 Group M Vpu Proteins

Another study that has been conducted in our lab analysed the efficiency of primary Vpu proteins from HIV-1-infected patients and found that the lab-adapted HIV-1 strain NL4.3 encodes a Vpu that is less potent in antagonising tetherin compared to most primary Vpus (Pickering et al. 2014). This prompted us to look at the ability of other HIV-1 group M Vpus to antagonise tetherin isoforms since the differential effect might have been limited to NL4.3 Vpu, and therefore not be representative. One patient Vpu from the Pickering et al. study that has been found to be superior to NL4.3 Vpu for tetherin counteraction, RP2v16_287i (2_87), and Vpus from several transmitted/founder viruses were tested for their isoform antagonism (Figure 3.7 A). Increasing amounts of Vpu expression construct were co-transfected with the NL4.3 ΔVpu provirus and a fixed dose of tetherin (50 ng). All Vpus were able to potently counteract L-tetherin even at low concentrations (Figure 3.7 B). They also counteracted WT tetherin equally well at higher Vpu expression levels. In contrast, they were all less efficient in counteracting S-tetherin, independent of Vpu concentration. Similar data were obtained for Vpus from other HIV-1 clades A1, A2, C, F and H (Figure 3.8 A). Where Vpu was active against tetherin (clade C MJ4 and F seemed to be defective for all isoforms), L-tetherin was antagonised efficiently at low Vpu expression levels (Figure 3.7 B). As seen with the other Vpus tested, counteraction of S-tetherin was much reduced for those Vpus. Altogether, these data show that the differential sensitivity of tetherin isoforms is a feature of all HIV-1 group M Vpus tested.

A

```
NL4.3       MQPI-IVAIVALVVAIIIAIVVWSIVIIEYRKILRQRKIDRLIDRLIERAEDSGNESEGE
CHO58       MQPLN-IAIGALIVAAILAIIVWTIVFIEYRKILKQRKIDRLIERISERAEDSGNESDGD
TRJO        MSPLVIASIVALVVAAIIVIVIWSIVFIEYRKILRQRKIDRLVDRILERAEDSGNESDGD
WITO        MQPLEILAVVALVVALILAIVVWTIVYIEYRKIQKQKKIDRLIDRIRERAEDSGNESDGD
CHO77       MQSLYILGIVALVVAAILAIVVWTIVYIEYRKIVRQRKIDRLLDRIIDRAEDSGNESEGD
2_87        MKSLETLAIVALVVAAILAIVVWSIVFIEYRKILRQRKIDRLIDRIRERAEDSGNESEGD
REJO        MQTLQILAIVALVIAGIIAIVVWTIVFIEYKKILRQRKIDRLIDRIRDRAEDSGNESEGD
            *. :   .: **::* *:.*::*:** ***:** :*:******::*: :*********:*:

NL4.3       VS---ALVEMGVEMGHHAPWDIDDL
CHO58       QEELSKLMEMGH-H---APWDVNDL
TRJO        QEELSALVEMGH-HGHDAPWDIDDL
WITO        QEELSALVEMGH-H---APWDVNDE
CHO77       QEELSALMEMGH-H---APWVIDDQ
2_87        QEELSALVERGH-L---APWDIDDL
REJO        QEELSALVEMGH-H---APWDIDDL
             .    *:* *      *** ::*
```

B

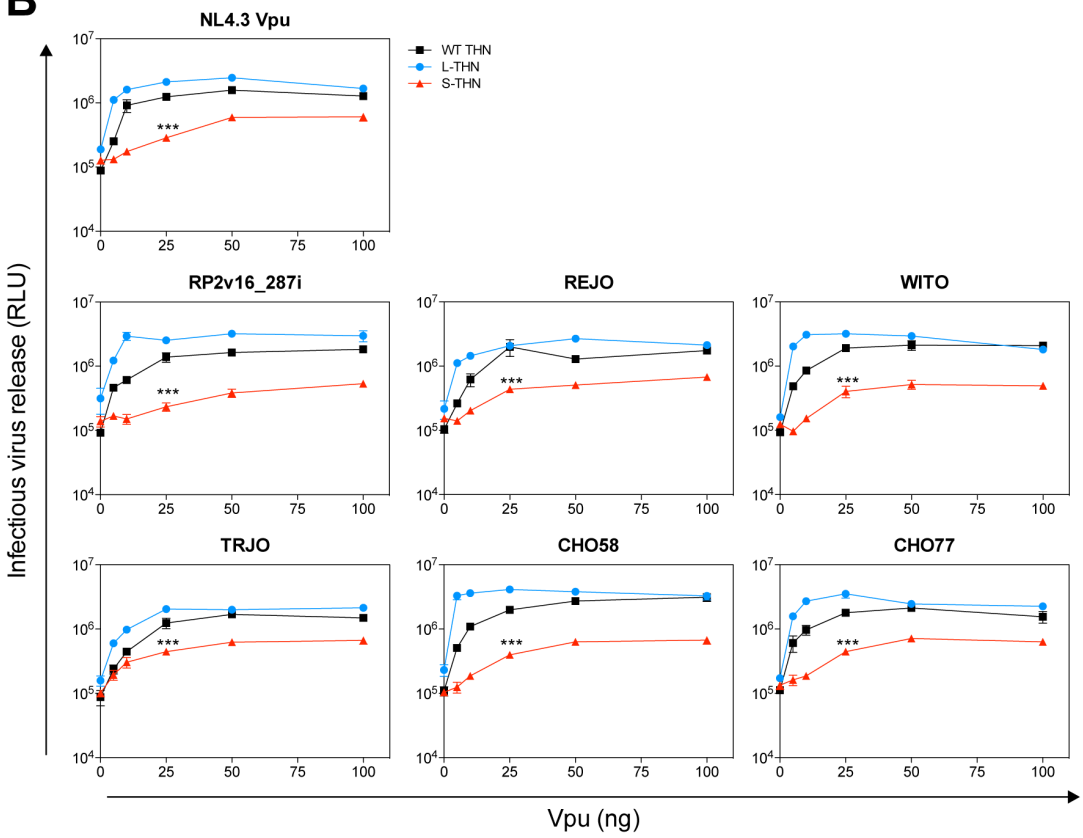

Figure 3.7 Differential sensitivity of human tetherin isoforms is a feature HIV-1 Group M Vpu proteins. (**A**) Alignment of HIV-1 Vpu amino acid sequences. Vpus used and their GenBank accession numbers: NL4.3 (KC913697.1), RP2v16_287i (2_87; Pickering et al. 2012), REJO (JN944911.1), WITO (JN944938.1), TRJO (JN944936.1), CHO58 (JN944940.1) and CHO77 (JN944941.1). Alignment was generated using Clustal Omega. (**B**) 293T cells were transfected with increasing amounts of Vpu, ΔVpu proviral plasmid and 50 ng of human WT THN, L-THN or S-THN. 48 h post transfection infectious virus release was determined using Hela-TZMbl reporter cells. Error bars represent standard deviations of the means of three independent experiments. Asterisks represent the p value for the difference in virus release from L- tetherin and S-tetherin expressing cells at 25 ng of Vpu expression vector. ***p<0.001 as determined by two-tailed t test.

A

```
NL4.3       ------MQPIIVAIVALVVAIIIAIVVWSIVIIEYRKILRQRKIDRLIDRLIERAEDSGN
C(MJ4)      MIDLLARVDYRIGLAAFVVALLIAIIVWTIVYLEYRKLVRQRKIDWLIKRIRERAEDSGN
C(Bro)      MLELIGRIDYRLGVGALIVALIIVIIVWTIAYIEYRKLVRQRRIDWLVKRIKERAEDSGN
H           -MYI-----LGLGIGALVVTFIIAVIVWTIVYIEYKKLVRQKKIDRLIERIGERAEDSGN
F           MSNL-----LAIGIAALIVALIITIVVWTIAYIEYKKLVRQRKINRLYKRISERAEDSGN
A1          MTPL-----EIWAIVGLVVVSIIAIVVWTIVGIEYKKLLKQRKIDRLIRRISERAEDSGN
A2          MLPL-----VILAIVGLIVALILAIVVWTIVFIEYKKIKKQRKIDWLIKRISERAEDSGN
                          .: .::*. ::.::**:*. :**:*: :*::*: *  *: ********

NL4.3       ESEGEVSALVEMGVEMGHHAPWDIDDL
C(MJ4)      ESEGDTEELATM-VDMGQLRLLDNL--
C(Bro)      ESGGDTEELETM-VDMGHLRLLDGNDL
H           ESDGDTEELSKL-MEMGHLNLGYVADL
F           ESEGDAEELAAL-GEVGPFIPGDINNL
A1          ESDGDTDELAKL-VEMGNYDLGDNNNL
A2          ESDGDTEELSAL-VERGHLDFGDVNNV
            ** *:.. *  :  : *
```

B

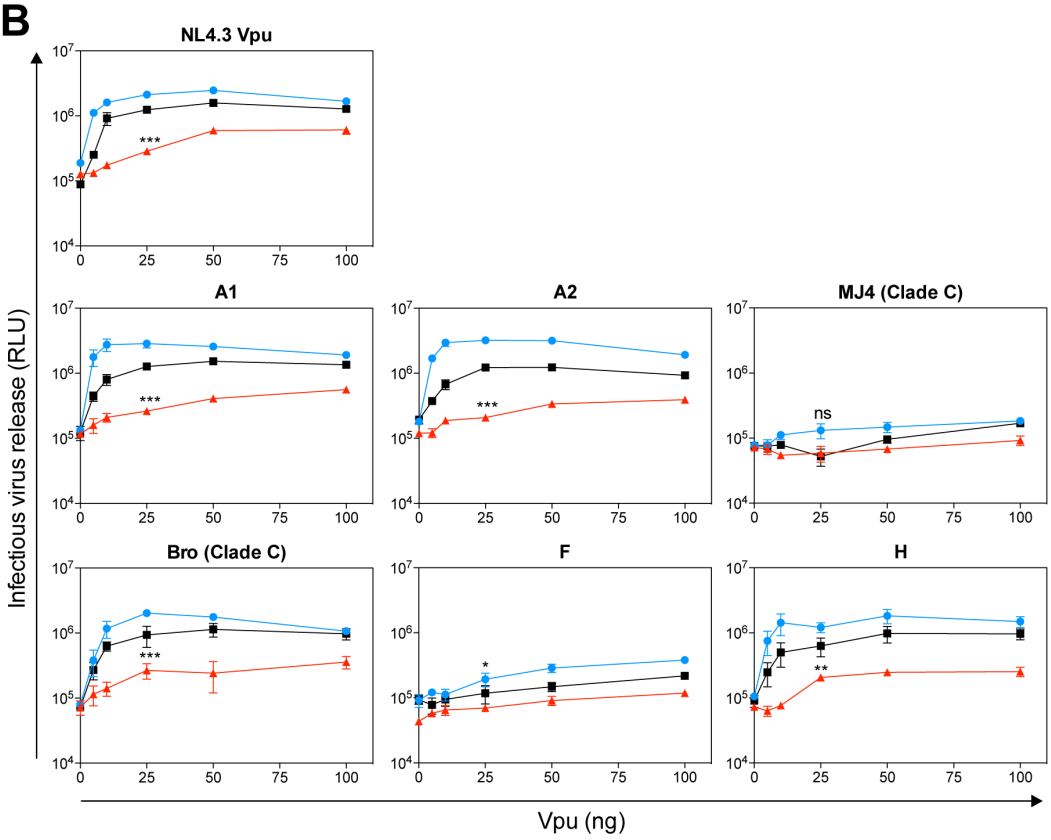

Figure 3.8 Differential sensitivity of human tetherin isoforms is a feature HIV-1 Group M Vpu proteins. (**A**) Alignment of HIV-1 Vpu amino acid sequences. Vpus used and their GenBank accession numbers: NL4.3 (KC913697.1), A1 (AF069673.1), A2 (AF286237.1), MJ4 (C) (AF321523.1), Bro (C) (U52953.1), F (AF005494.1) and H (AF005496.1). Alignment was generated using Clustal Omega. (**B**) 293T cells were transfected with increasing amounts of Vpu, ΔVpu proviral plasmid and 50 ng of human WT THN, L-THN or S-THN. 48 h post transfection infectious virus release was determined using Hela-TZMbl reporter cells. Error bars represent standard deviations of the means of three independent experiments. Asterisks represent the p value for the difference in virus release from L- tetherin and S-tetherin expressing cells at 25 ng of Vpu expression vector. ns, not significant; *p<0.05, **p<0.01, ***p<0.001 as determined by two-tailed t test.

3.2.4 An HIV-1 Group N Vpu From Togo is More Efficient in Counteracting Both Isoforms

Apart from HIV-1 group M, HIV-1 group N as well as some simian immunodeficiency viruses (SIVs) also utilise their Vpu proteins to counteract tetherin. Vpus from HIV-1 group N have been reported to be very poor tetherin antagonists. However, there is one exception of a highly pathogenic group N virus (N1.FR.2011) isolated from a patient who acquired infection in Togo in western Africa (Sauter et al. 2012). Compared to other group N Vpus, this Vpu acquired a trafficking motif in the second alpha helix (ExxxLV) that can also be found in group M Vpus and has been shown to be crucial for promoting tetherin rerouting to endosomes and therefore counteraction (Figure 3.9 A). This particular group N Vpu has been reported to be able to induce tetherin surface downregulation as well as increase virus release as potently as group M NL4.3 Vpu. Therefore, it was tested whether the two human tetherin isoforms were also differentially sensitive to this group N Vpu. NL4.3 ΔVpu virus, a fixed dose of human tetherin (50 ng) and increasing amounts of Vpu were co-transfected and infectious virus release was assessed 48 h later. As shown before by others, the group N YBF30 Vpu was unable to promote virus release from cells expressing any isoform (Figure 3.9 B). N1.FR.2011 however, was very potent in counteracting L-tetherin. Additionally, it counteracted S-tetherin equally well at higher Vpu expression levels, which could be seen both for infectious virus release and physical particle yield (Figure 3.9 B and C). This ability of N1.FR.2011 Vpu to promote virus release from S-tetherin-expressing cells led us to investigate whether this Vpu was also able to induce surface downregulation and degradation of both tetherin isoforms.

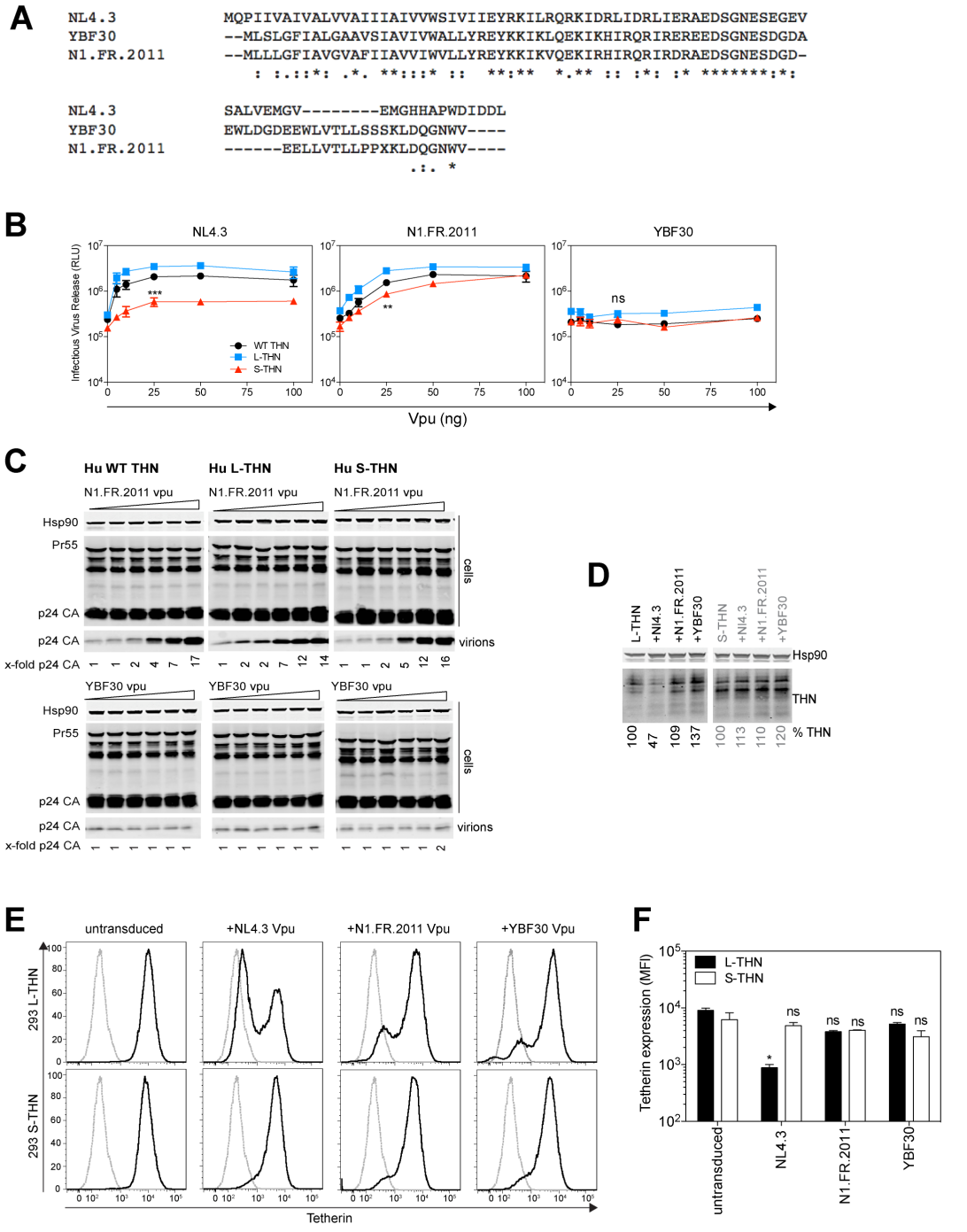

Figure 3.9 HIV-1 group N Vpu from Togo is more efficient in targeting of both tetherin isoforms. (**A**) Alignment of HIV-1 Vpu amino acid sequences. Vpus used and their GenBank accession numbers: NL4.3 (KC913697.1), N1.FR.2011 (JN572926.1) and YBF30 (AJ006022.1). Alignment was generated using Clustal Omega. (**B**) 293T cells were transiently transfected with increasing amounts of Vpu, ΔVpu proviral plasmid and 50 ng of human WT THN, L-THN or S-THN. 48 h post transfection infectious virus release was determined using Hela-TZMbl reporter cells. Error bars represent standard deviations of the means of three independent experiments. Asterisks represent the p value for the difference in virus release from L- tetherin and S-tetherin expressing cells at 25 ng of Vpu expression vector. ns, not significant; **p<0.01, ***p<0.001 as determined by two-tailed t test. (**C**) Cell lysates and pelleted viral supernatants from (**B**) were subjected to SDS-PAGE and analyzed by Western blotting for Hsp90 and p-24CA. Fold increase of p24 release into the supernatant indicated below are relative to the release of NL4.3ΔVpu in the absence of vpu. (**D**) 293 cells stably expressing L- or S-tetherin were transduced with retroviral vectors encoding different Vpus. Cell lysates were analysed for their tetherin expression using SDS PAGE and Western blotting. (**E**) Vpu transduced cells from (**D**) were stained for surface tetherin and analysed by flow cytometry. 293 empty vector cells (not expressing tetherin), dashed grey line. (**F**) Median fluorescence intensity for tetherin of cells from (**E**) is shown. Asterisks represent the p value for the difference in tetherin surface expression (MFI) on non-transduced or Vpu transduced cells. ns, not significant; *p<0.05, **p<0.01, ***p<0.001 as determined by two-tailed t test.

To see whether any of the group N Vpus were able to degrade the tetherin isoforms, stable tetherin-expressing 293 cells were transduced with retroviral vectors encoding the Vpus and selected for puromycin resistance. Whereas NL4.3 Vpu was able to induce the degradation of L-tetherin, but not S-tetherin as expected, both N1.FR.2011 and YBF30 Vpus were unable to mediate the degradation of either of the two isoforms (Figure 3.9 D). Similarly, N1.FR.2011 was unable to induce the more than 2-fold surface downregulation of L-tetherin seen with NL4.3 Vpu in the same transduced cells. No downregulation of S-tetherin was seen for any of the group N Vpus either (Figure 3.9 E and F). These results suggest that the mechanism of action of the N1.FR.2011 Vpu might rather be exclusion of tetherin molecules from budding virions at the cell surface.

3.2.5 Long and Short Monkey Tetherins are Equally Targeted by Vpu Proteins From SIVgsn and SIVmon

As mentioned before, HIV-1 is not the only primate lentivirus that uses its Vpu protein to target tetherin. The HIV-1 Vpu originates from the SIVcpz Vpu, which itself has the Vpu proteins of greater spot-nosed (gsn) monkey and mona (mon) monkey SIV as ancestors. Both of these viruses use their Vpu to counteract their host species' tetherin as well as other primate tetherins, such as rhesus macaque tetherin. To see whether the differential sensitivity of tetherin isoforms was an ancestral feature of Vpu, a fixed dose of rhesus macaque tetherin isoforms was co-transfected with NL4.3 ΔVpu virus and increasing amounts of SIVgsn or SIVmon Vpu. In contrast to HIV-1 group M Vpu, both SIV Vpus were able to counteract all rhesus macaque tetherin isoforms with equal efficiency (Figure 3.10 A and B). Furthermore, similarly to N1.FR.2011 Vpu, both SIV Vpus were unable to mediate degradation of either L- or S-tetherin (Figure 3.10 C). To rule out species-specific effects, it was tested whether a different phenotype could be observed when the host species' tetherins of gsn and mon rather than rhesus macaque tetherin were used. Again, all isoforms were antagonised with equal efficiency, taking into account that WT and S-tetherin were more highly expressed (Figure 3.10 D-G). These data show that the differential sensitivity of tetherin isoforms to Vpu is not an ancestral feature of these proteins. Rather, this suggests that when Vpu was readapting to counteract human tetherin during zoonotic transmission of SIVcpz to humans to form HIV-1 group M, it evolved to predominantly antagonise L-tetherin.

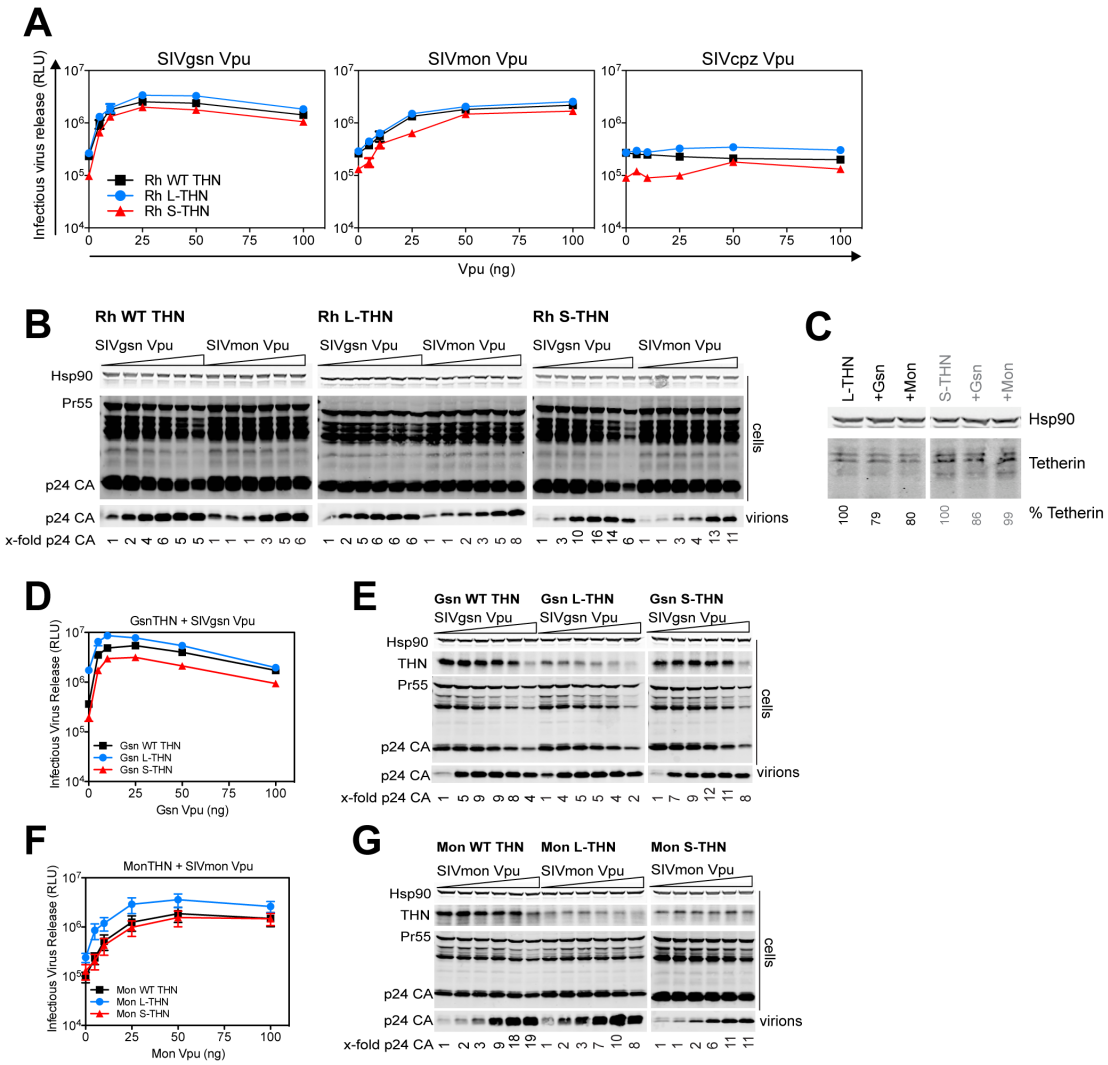

Figure 3.10 Targeting of both tetherin isoforms by ancestral Vpu proteins from SIVgsn and SIVmon. (**A**) 293T cells were transiently transfected with increasing amounts of Vpu, ΔVpu proviral plasmid and 50 ng of rhesus macaque WT THN, L-THN or S-THN. 48 h post transfection infectious virus release was determined using Hela-TZMbl reporter cells. Error bars represent standard deviations of the means of three independent experiments. (**B**) Cell lysates and pelleted viral supernatants from (**A**) were subjected to SDS-PAGE and analyzed by Western blotting for Hsp90 and p-24CA. Fold increase of p24 release into the supernatant indicated below are relative to the release of NL4.3ΔVpu in the absence of Vpu. (**C**) 293 cells stably expressing L- or S-tetherin were transduced with retroviral vectors encoding different Vpus. Cell lysates were analysed for their tetherin expression using SDS PAGE and Western blotting. (**D**) and (**F**) 293T cells were transiently transfected with increasing amounts of SIVgsn Vpu (**D**) or SIVmon Vpu (**F**), ΔVpu proviral plasmid and 50 ng of gsn (**D**) or mon (**F**) WT THN, L-THN or S-THN. 48 h post transfection infectious virus release was determined using Hela-TZMbl reporter cells. Error bars represent standard deviations of the means of three independent experiments. (**E**) and (**G**) Cell lysates and pelleted viral supernatants from (**D**) and (**F**) were subjected to SDS-PAGE and analyzed by Western blotting for Hsp90, tetherin and p-24CA. Fold increase of p24 release into the supernatant indicated below are relative to the release of NL4.3ΔVpu in the absence of Vpu. GenBank accession numbers: Vpu gsn (AF468659), Vpu mon (AY340701), Vpu cpz (AY418255), gsn tetherin (GQ925923.1), mon tetherin (GQ925924.1), rhesus macaque tetherin (NM_001161666.1).

3.2.6 Both Tetherin Isoforms are Equally Targeted by HIV-2 Envelope, SIVmac Nef and KSHV K5

Next, it was further investigated whether tetherin antagonists other than Vpu might show differential efficiency against tetherin isoforms. As mentioned before, tetherin exerts high evolutionary pressure on enveloped viruses and therefore various viruses have evolved different countermeasures. HIV-2 uses its envelope (Env) to counteract tetherin by enhancing its endocytosis from the cell surface, dependent on the clathrin adaptor protein complex 2 (AP-2) (Lau et al. 2011; Le Tortorec & Neil 2009). HIV-2 Env binds to AP-2 via a GYXXθ motif in Env's cytoplasmic tail. Mutation of the GY to AA renders the already weak tetherin antagonist completely non-functional. To see how efficiently HIV-2 Env counteracts the two human tetherin isoforms, we co-transfected the HIV-2 ROD10 provirus or the GY-AA Env mutant thereof with increasing amounts of WT, L- or S-tetherin and analysed the amount of physical virus particles released into the supernatant. Infectious release of the GY-AA mutant was completely abolished by any concentration of any of the tetherin isoforms. Even though HIV-2 ROD10 was rather weak in promoting virus release, it did not distinguish between L- and S-tetherin (Figure 4.10 A). The same was seen when looking at Env's ability to downregulate tetherin from the cell surface. 293 cells stably expressing L- or S-tetherin were transfected with HIV-2 ROD10 Env IRES GFP or the GY-AA mutant of it. As expected, the GY-AA mutant was unable to downregulate any tetherin from the surface. However, the WT Env downregulated both isoforms equally well (Figure 4.10 B). This shows that the mechanism HIV-2 Env uses to counteract tetherin is independent of ubiquitination and sorting motifs in tetherin's cytoplasmic tail that are crucial for Vpu's anti-tetherin function.

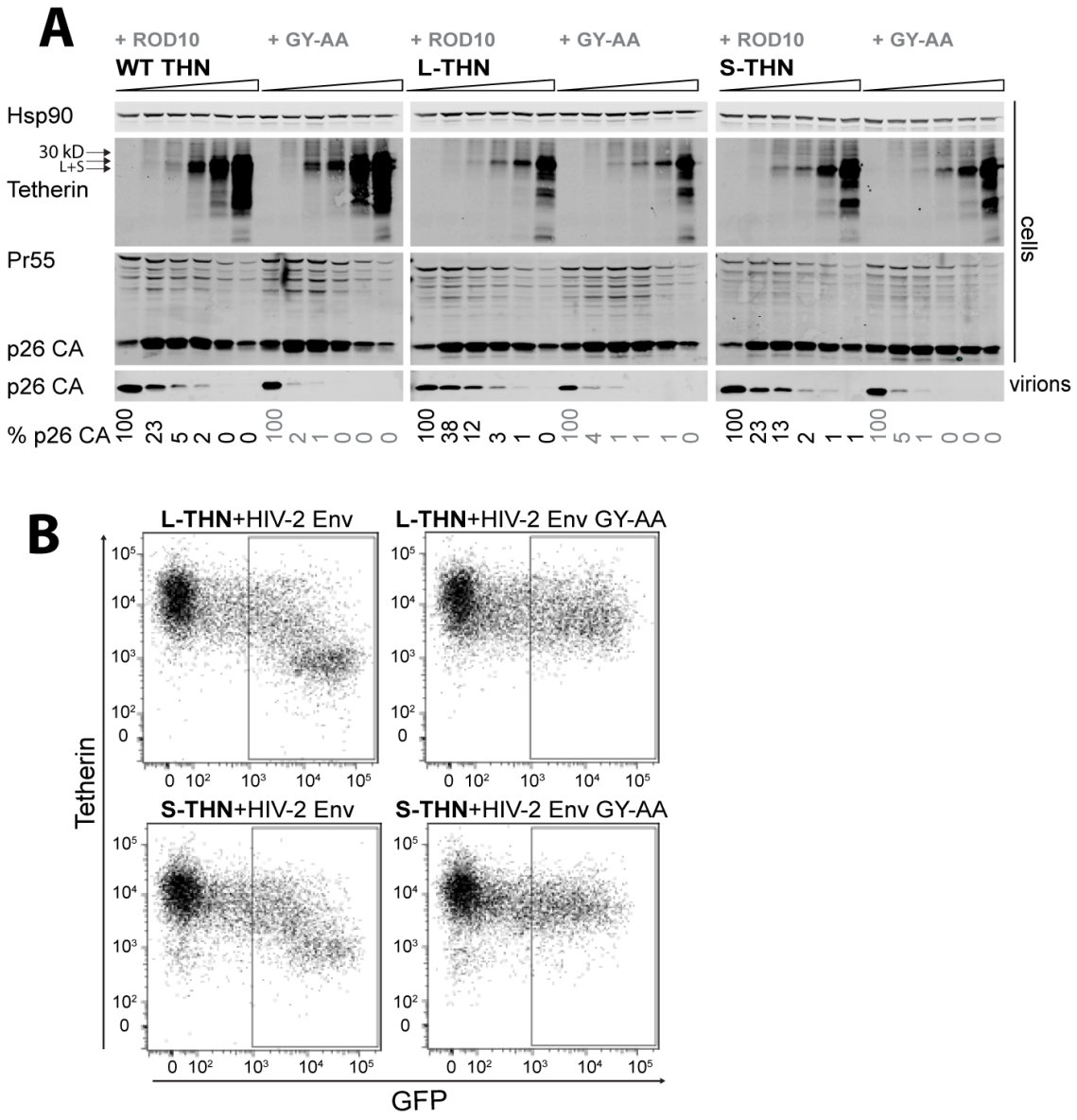

Figure 3.11 HIV-2 Envelope targets human tetherin isoforms with equal efficiency. (**A**) 293T cells were transfected with increasing amounts of human WT-, L- or S-THN and HIV-2 ROD10 or the ROD10 GY-AA mutant proviral plasmid. Cell lysates and pelleted virions were subjected to SDS-PAGE and analyzed by Western blotting for Hsp90, tetherin and p26CA expression. Percent of p26CA in the supernatant are indicated below, relative to virus release in the absence of tetherin. This blot is a representative example of three independent experiments. (**B**) 293 cells stably expressing L-THN or S-THN were transfected with HIV-2 ROD10 Env IRES GFP or HIV-2 ROD10 GY-AA mutant Env IRES GFP. 48 h post transfection cells were analyzed by flow cytometry for their GFP and tetherin surface expression. Panels are representative examples of three independent experiments.

Most SIVs use their Nef protein to counteract tetherin as they do not encode a Vpu. One example is the rhesus macaque SIV. SIVmac Nef binds to the cytoplasmic tail of rhesus macaque tetherin and recruits AP-2 to induce tetherin's endocytosis and intracellular sequestration similarly to the effect of HIV-2 Env (Zhang et al. 2011a; Serra-Moreno et al. 2013a). Nef is thought to bind to a five amino acid stretch ((G/D)DIWK) in primate tetherin's cytoplasmic tail that is not present in

both human tetherin isoforms. The short isoform of macaque tetherin lacks twelve amino acids of its cytoplasmic tail, however, it still contains this five amino acid motif. We tested the ability of SIVmac Nef to counteract the macaque tetherin isoforms by co-transfecting SIVmac239 WT virus or a Nef deficient version (ΔNef) with increasing amounts of rhesus macaque tetherin isoforms. The Nef deficient virus exhibits an infectivity defect in 293T cells. To overcome this we also co-transfected VSV-G. Like HIV-1 ΔVpu virus, SIVmac ΔNef virus release was restricted with increasing amounts of any tetherin isoform (Figure 3.12 A and B). The WT virus was relatively insensitive to any of the tetherin isoform and counteracted them with comparable efficiency. These data show that the lack of twelve amino acids in macaque tetherin's cytoplasmic tail does not impact on its sensitivity to SIVmac Nef.

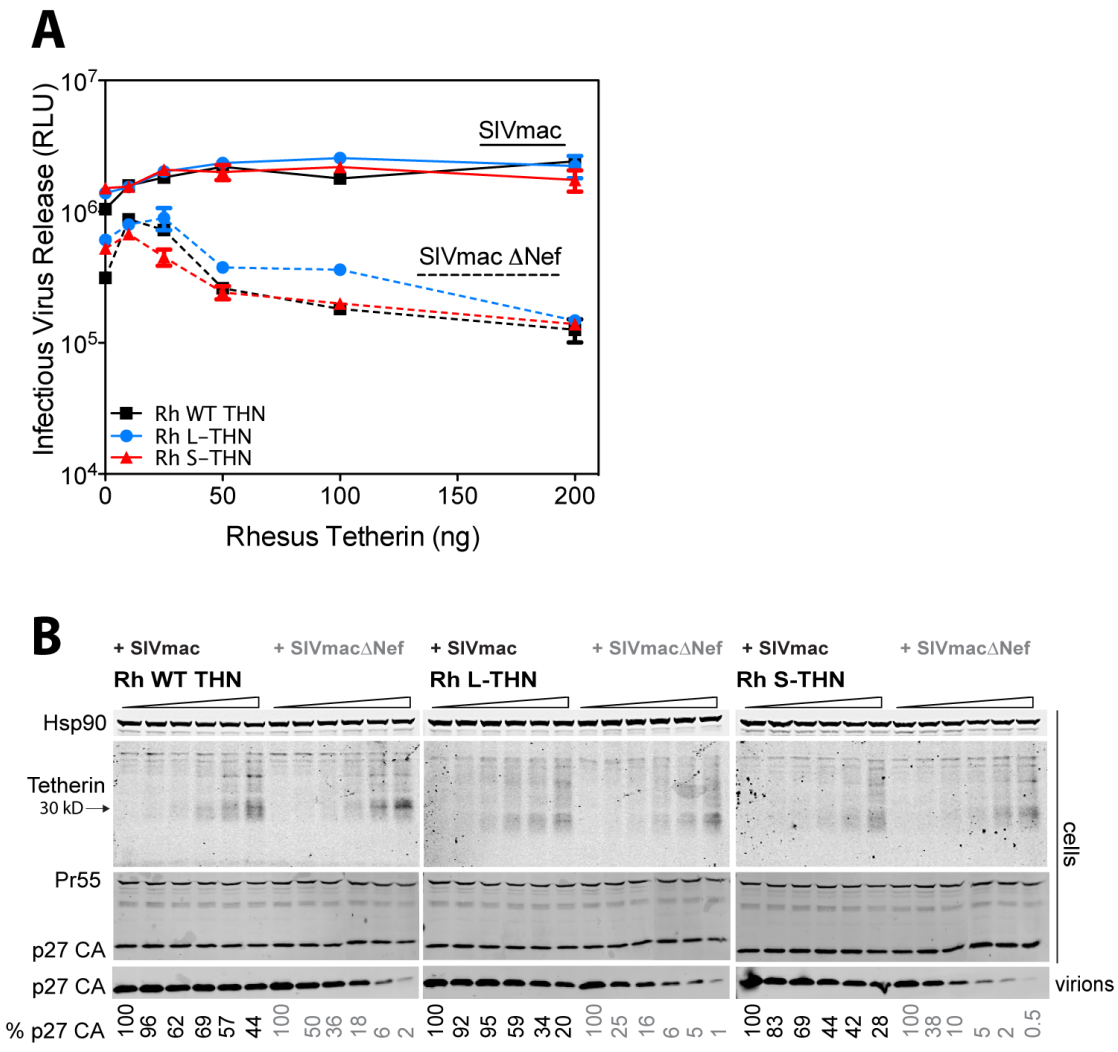

Figure 3.12 SIVmac Nef targets rhesus macaque tetherin isoforms with equal efficiency. (**A**) and (**B**) 293T cells were transfected with increasing amounts of rhesus macaque WT-, L- or S-THN and SIVmac or SIVmac ΔNef proviral plasmid. (**A**) Infectious virus release from transfected cells was titered on Hela-TZMbl reporter cells. Solid lines, SIVmac; Dashed lines, SIVmac ΔNef. (**B**) Cell lysates and pelleted supernatant virions were subjected to SDS-PAGE and analyzed by Western blotting for Hsp90, rhesus tetherin and p27CA expression. Percent of p27CA in the supernatant are indicated below, relative to virus release in the absence of tetherin. This is a representative blot of three independent experiments.

The next antagonist tested was the Kaposi's sarcoma-associated herpesvirus (KSHV) encoded K5 ubiquitin ligase. K5 targets a lysine residue at position 18 in the cytoplasmic tail of human tetherin and induces ESCRT-dependent endosomal degradation of tetherin. This lysine is present in both L- and S-tetherin. However, K5 is not able to counteract rhesus macaque tetherin, which suggests that residues in the cytoplasmic tail of tetherin might play a role in this specificity. HT1080 cells were used for the following experiments as 293Ts do not support K5 function efficiently (Pardieu et al. 2010). HT1080 cells stably expressing human tetherin isoforms were transduced with puromycin-resistant lentiviral vectors encoding K5 or a mutant of K5, K5NTR. This mutant harbours a lesion in it's C-terminal cytoplasmic tail that eliminates its function (Means et al. 2007). Resistant cells were selected for and tetherin surface expression was assessed. Transduction with the mutant K5NTR protein did not change tetherin surface levels. However, K5 WT transduced cells showed potent tetherin downregulation from the cell surface both for L- and S-tetherin (Figure 3.13 A). Examining the total tetherin levels in the same cells revealed that both isoforms were also equally well degraded by WT K5 (Figure 3.13 B).

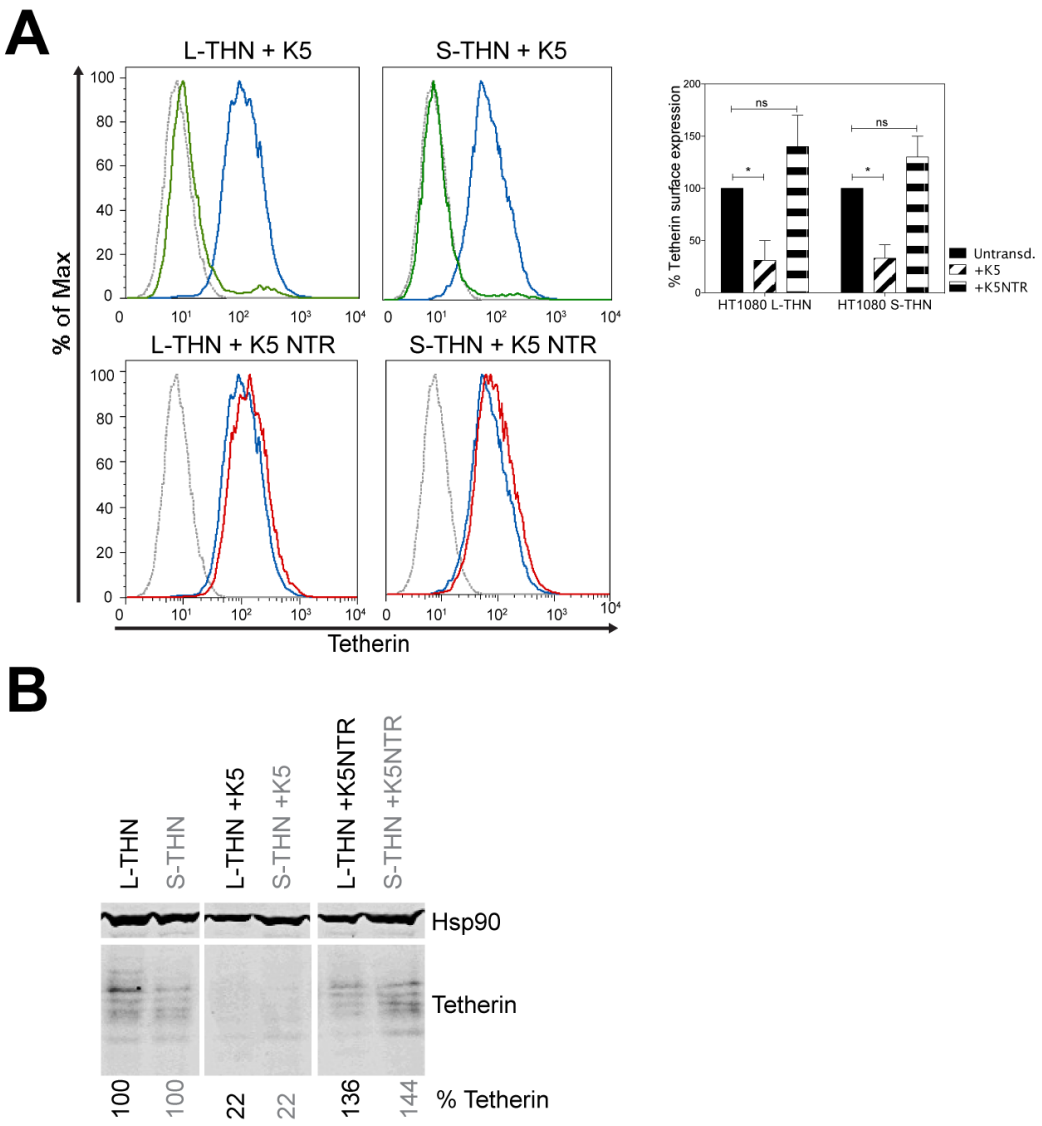

Figure 3.13 KSHV K5 targets human tetherin isoforms with equal efficiency. (**A**) HT1080 cells stably expressing tetherin isoforms were transduced with K5 or a K5 mutant (K5NTR) defective for tetherin antagonism and selected. Cells were then analysed by flow cytometry for surface tetherin expression. Dotted grey, tetherin negative HT1080 cells; grey, non-transduced tetherin expressing HT1080 cells; black, tetherin expressing cells transduced with wt K5 (upper panel) or a mutant (K5NTR; lower panel). Graph indicates the tetherin surface expression on transduced cell lines, shown in percent relative to the fluorescence of the corresponding non-transduced tetherin expressing cell line. Asterisks represent the p value for the difference in tetherin surface expression (MFI) on non-transduced or K5/K5NTR transduced cells. ns, not significant; *p<0.05 as determined by two-tailed t test. (**B**) Cell lysates of transduced and non-transduced cells were subjected to SDS-PAGE and analyzed by Western blotting for Hsp90 and tetherin expression. Percentage of tetherin expression in lysates compared to non-transduced cells is shown below.

In summary, these data indicate that the first twelve amino acids that are absent in S-tetherin are dispensable for its sensitivity to viral antagonists other than HIV-1 group M Vpu. Both isoforms are equally counteracted by all other antagonists tested here. This also suggests that the mechanisms of counteraction used by those antagonists are independent of the trafficking of tetherin itself, which is dependent on residues that are missing from S-tetherin.

3.2.7 Human L- Tetherin is Able to Induce NF-κB Signalling Whereas S-Tetherin and Both GSN and MON Tetherin Isoforms are Not

Apart from its function of physically tethering virions to the plasma membrane of infected cells, tetherin has recently been shown to be a potent inducer of NF-κB, not only upon virus retention, but also following tetherin overexpression (Cocka & Bates 2012; Galão et al. 2012; Tokarev et al. 2013). Determinants in tetherin's cytoplasmic tail have been found to be important for its signalling capacity including the two tyrosines at position six and eight as well as the adjacent CRV residues and mutation of those motifs has been shown to abolish NF-κB induction. All of the aforementioned residues are absent in S-tetherin and, therefore, it is not surprising that S-tetherin is unable to induce proinflammatory signalling (Cocka & Bates 2012). These data were confirmed by co-transfecting 293 cells with human tetherin isoforms and an NF-κB-dependent firefly luciferase reporter construct. Cells transfected with L-tetherin showed a 24-fold induction of NF-κB whereas cells transfected with WT-tetherin showed a 16-fold induction compared to non-tetherin transfected cells (Figure 3.14 A). As expected, cells overexpressing S-tetherin did not show any NF-κB induction as S-tetherin is lacking essential residues. This is interesting, considering that HIV-1 group M Vpus seem to have evolved to efficiently counteract the signalling, long form of human tetherin.

Tetherins from other species have been shown to only have limited signalling capacity. Whereas chimpanzee tetherin can induce NF-κB to a certain extent, rhesus, African green monkey and mouse tetherin are completely non-functional in this respect, even though they potently inhibit virus release (Galão et al. 2012). As the Vpu proteins of SIVgsn and SIVmon counteracted both isoforms of their host's tetherin very efficiently we wondered whether those tetherin proteins were also able to induce NF-κB signalling. As before, increasing amounts of tetherin were transfected with the reporter construct. However, none of the gsn nor the mon tetherin isoforms were able to induce NF-κB (Figure 3.14 A).

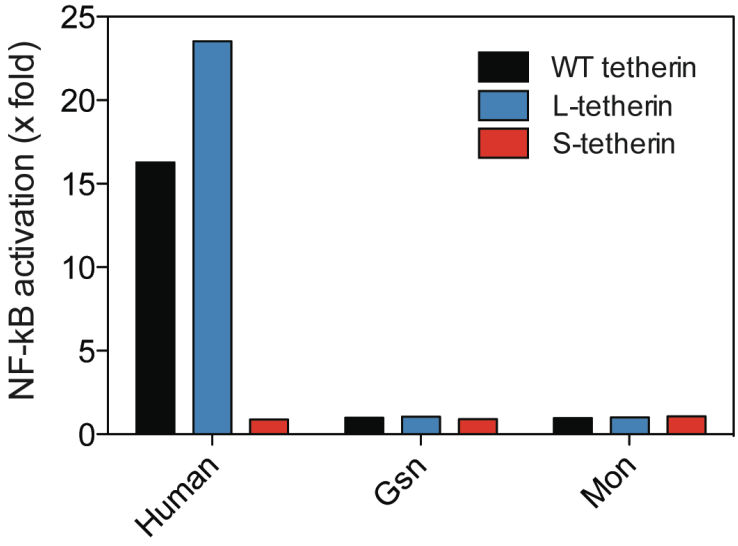

Figure 3.14 NF- κB activation by different primate tetherin isoforms. 293 cells were transfected with 50 ng of human, gsn or mon tetherin isoforms and a firefly-luciferase NF-κB reporter plasmid. 48 h post transfection fold increase of reporter activity relative to non-tetherin transfected cells was determined. Solid lines, human tetherin; dashed lines, gsn or mon tetherin. This experiment was only done once.

3.3 Discussion

In this chapter I examined the differential sensitivity of two tetherin isoforms to a range of lentiviral antagonists. I was able to show that the Vpu proteins of the pandemic HIV-1 group M were the only tetherin antagonists tested here that exhibit a difference in their ability to counteract human L- and S-tetherin. They antagonised the long version of tetherin more efficiently than S-tetherin, with L-tetherin being downregulated from the cell surface and degraded. All the other countermeasures tested in this study were equally efficient against both isoforms of their host species. Examples are SIVmac Nef and HIV-2 envelope, which do not induce degradation, but rather lead to endocytosis of tetherin and its sequestration, which occurs in an AP-2 dependent manner (Le Tortorec & Neil 2009; Zhang et al. 2011b; Serra-Moreno et al. 2013b; Lau et al. 2011; Noble et al. 2006). Also, Vpu proteins from HIV-1 group N or SIVgsn and SIVmon were equally efficient against their host species tetherin. These proteins, however, were unable to induce either downregulation or degradation of the tetherin, suggesting that their mode of action might be different to the other antagonists.

Human tetherin is expressed as two isoforms. Two ATG start codons exist in its coding sequence with suboptimal Kozak sequences in front of them, which can potentially lead to leaky ribosomal scanning and the expression of both isoforms. These two ATGs are highly conserved among mammalian tetherins (Cocka & Bates 2012). According to our data both isoforms are expressed and interferon-induced to equal amounts in CD4 positive T cells. Assuming that they assemble independently there would be a ratio of homo- to heterodimers of 1:2:1. This is in agreement with our data showing that four times as much wild type tetherin (expressing both isoforms) is needed to restrict virus to a similar level as S-tetherin expression only and shows that only S-tetherin homodimers are less sensitive to HIV-1 Vpu. Whether the expression of the different tetherin isoforms is regulated in any way remains an open question. Even though interferon seems to be able to induce both human isoforms to comparable levels, differential regulation cannot be completely ruled out. There have been several cases reported for different species, which possess a polymorphism in the first ATG of tetherin. Similar to a human S-tetherin, domestic cats (Dietrich et al. 2011; Celestino et al. 2012), horses (Yin et al. 2014) and at least one inbred mouse strain, NZW, express a truncated version of tetherin lacking N-terminal residues (Barrett et al. 2012). In the latter case, this has been correlated with decreased Friend retrovirus replication and pathogenesis and increased levels of tetherin on $CD4^+$ lymphocytes.

The main question that arises is why HIV-1 group M Vpus differentiate between the human tetherin isoforms whereas other antagonists do not. This HIV-1 group M emerged from a zoonotic transmission of SIVcpz, which itself has its ancestors in guenon SIVs, including SIVgsn and SIVmon (Sharp & Hahn 2011). Both those ancestors use their Vpu protein against both host species tetherin isoforms, as our data show. SIVcpz, however, uses its Nef protein to counteract chimpanzee tetherin. Upon zoonotic transmission of SIVcpz to humans, Vpu readapted to counteract tetherin and this was a crucial step in transmission of the virus. As human tetherin has a deletion of five amino acids (G/DDIWK) in its cytoplasmic tail it is insensitive to SIVcpz Nef (Sauter et al. 2011; Serra-Moreno et al. 2013a). Therefore, Vpu reacquired anti-tetherin function in HIV-1 while still maintaining its anti-CD4 function (Sauter et al. 2009). It is important to note that this five amino acid deletion in human tetherin is also a determinant of its increased signalling capacity (Galão et al. 2012). HIV-1 group M is the group that is responsible for the world wide HIV pandemic and its success has been partially ascribed to its efficient tetherin-antagonising Vpu protein (Sauter et al. 2009). There are three key features that make HIV-1 group M Vpu the most efficient at downregulating, but also at degrading human tetherin. There is the AxxxAxxxAxxxW transmembrane interface that is required for direct tetherin binding (Vigan & Neil 2010; Skasko et al. 2012). Furthermore, there are two important motifs in the cytoplasmic tail of Vpu. One acidic dileucine trafficking motif (ExxxLV) that has been shown to interact with clathrin adaptor AP-1 in a tetherin dependent manner and the E3 ubiquitin ligase binding site, DSGNES, that contains two phosphorylated serines (Kueck & Neil 2012; Jia et al. 2014; Kueck et al. 2015; Mitchell et al. 2009; Sauter et al. 2012). Vpu proteins from other HIV-1 groups differ from group M in these motifs. HIV-1 group O Vpus, for example, are unable to bind directly to tetherin via their transmembrane domain and are hence non-functional against it (Sauter et al. 2009). However, this group of HIV-1 has recently been shown to use its Nef protein to counteract tetherin to some extent (Kluge et al. 2014). Group N Vpu proteins are able to bind to tetherin, however, fail to efficiently counteract it or induce its downregulation or degradation, with one exception being N1.FR.2011 (Sauter et al. 2009; Sauter et al. 2012). Since efficient anti-tetherin function seems to be crucial for successful transmission this might explain why those groups of HIV-1 remained geographically restricted. The Vpu protein from the pathogenic group N N1.FR.2011 reacquired the essential cytoplasmic tail determinants and our data show that it is capable to counteract both human tetherin isoforms equally well, without inducing downregulation or degradation of the proteins. This suggests that there must be cell biological differences in the mechanism of action. One possibility is that it is excluding tetherin from

budding virions, which would require the acidic dileucine motif in Vpu, but not the sorting signal in tetherin (McNatt et al. 2013; Sauter et al. 2012). Similarly, SIVgsn and SIVmon Vpus do counteract both their host species tetherin isoforms very efficiently without leading to their downregulation or degradation, as data presented in this chapter show. In contrast to N1.FR.2011 however, they do not have the ExxxLV trafficking motif (Sauter et al. 2009). The mode of action of those proteins still needs clarification.

The question that still remains is: Why do only HIV-1 group M Vpus differentiate between the isoforms? In addition to its ability to physically restrict virions, another function of tetherin has recently been shown to be the induction of NF-κB and proinflammatory signalling (Galão et al. 2012; Tokarev et al. 2013). This function also depends on the YDYCRV motif in tetherin's cytoplasmic tail. Virion retention and clustering of tetherin leads to the phosphorylation of the tyrosines and the recruitment of a TRAF2/TRAF6/TAK1 complex that then activates NF-κB in an endocytosis-independent manner (Galão et al. 2012; Galão et al. 2014). However, only human tetherin and to a lesser extent chimpanzee tetherin have been shown to be able to induce robust NF-κB signalling. This is due to species-specific changes in tetherin's cytoplasmic tail, importantly, the deletion of five amino acids in human tetherin that also renders it insensitive to SIV Nef (Galão et al. 2012). Furthermore, it has been shown that only human L-tetherin is able to induce signalling but not S-tetherin. S-tetherin even dominantly interferes with signal induction, suggesting that only L-tetherin homodimers are able to mediate proinflammatory signalling (Cocka & Bates 2012). This is in keeping with the suggestion that the two YDYCRV motifs of a L-tetherin homodimer can act as a noncanonical hemi-immunoreceptor tyrosine-based activation motif (hemITAM) (Galão et al. 2014). To be able to function, both tyrosine motifs need to be intact. The lack of the YDYCRV signalling and sorting motif in S-tetherin also means it is endocytosed and recycled much less than L-tetherin. Accordingly, restricted HIV-1 virions are not trafficked to late endosomes as much in the presence of S-tetherin or a tetherin YDY mutant (Galão et al. 2012) compared to L-tetherin, as our data confirm. The delivery of virions to endosomes by L-tetherin may have, additionally, important immunological consequences. Restricted and endocytosed virus is potentially degraded and subjected to enhanced antigen presentation or might serve as a pathogen-associated molecular pattern (PAMP). This PAMP can be sensed by a pattern recognition receptor (PRR) and would induce proinflammatory signalling. The increased accumulation of virions on the cell surface possibly mediated by S-tetherin on the other hand, is leading to enhanced opsonisation and

antibody-dependent cellular cytotoxicity (ADCC) (Pham et al. 2014; Arias et al. 2014; Alvarez et al. 2014). Furthermore, tetherin has been reported to regulate PRR function in plasmacytoid dendritic cells via the inhibitory leukocyte receptor ILT7. This has been, however, a matter of debate (Cao et al. 2009; Tavano et al. 2013; Bego et al. 2015). Moreover, the role of tetherin in restricting cell-to-cell transfer of virus at the virological synapse (VS) is controversial. Differential representation of tetherin isoforms at the VS could potentially explain the different results obtained in those studies (Casartelli et al. 2010; Jolly et al. 2010; Kuhl et al. 2010). In both cases, the role of tetherin isoforms is unclear and requires further investigation.

Altogether, the data presented in this chapter show clearly that the differential sensitivity of tetherin isoforms is restricted to HIV-1 group M, which is also the only group of tetherin antagonists that is able to induce efficient downregulation and degradation of L-tetherin. Considering the successful pandemic spread of this group of viruses, being able to specifically target L-tetherin very efficiently must have an evolutionary benefit. The proinflammatory signalling capacity of human L-tetherin upon virus retention is likely to have detrimental effects on a virus *in vivo* and the ability to overcome this might, therefore, be crucial for successful virus replication.

Chapter 4 Serine Phosphorylation of HIV-1 Vpu and its Binding to Tetherin Regulates Interaction with Clathrin Adaptors

Most of the data presented in this chapter have been published as “Serine Phosphorylation of HIV-1 Vpu and Its Binding to Tetherin Regulates Interaction with Clathrin Adaptors” (Kueck et al. 2015). This was a co-first authored manuscript by myself, Tonya Kueck and Toshana Foster. Where data are presented from others they are referred to appropriately.

4.1 Introduction

Tetherin physically restricts viral release by cross-linking budding virions to the infected cell, which induces proinflammatory signalling (Neil et al. 2008; Van Damme et al. 2008; Galão et al. 2012). In uninfected cells, endocytosed tetherin is recycled back to the plasma membrane via the TGN (Figure 4.1 A). This is dependent on its cytoplasmic dual tyrosine sorting motif (YDYCRV) that has been shown to interact with the clathrin adaptor AP-1 (Rollason et al. 2007; Jia et al. 2014). Counteraction of tetherin by viral accessory proteins such as Vpu or Nef is a crucial feature of successfully transmitted viruses. These antagonists act by removing tetherin from its site of action, the plasma membrane (PM). HIV-1 Vpu directly interacts with tetherin via both their transmembrane domains and targets it into an ESCRT-dependent endosomal degradation pathway, thereby preventing newly synthesized and recycling tetherin from trafficking to the PM (Figure 4.1 B) (McNatt et al. 2013; Skasko et al. 2012; Vigan & Neil 2010).

The degradation of tetherin requires a highly conserved DSGNES motif in Vpu’s cytoplasmic tail (Douglas et al. 2009; Mangeat et al. 2009; Mitchell et al. 2009). The two serines in this motif are phosphorylated constitutively (S52/53 and S56/57 in subtype B depending on the isolate) by CKII, which mediates the recruitment of the β-TrCP 1/2 subunits of the Skp1-Cullin1-F-Box (SCF) E3 ubiquitin ligase complex (Schubert et al. 1992; Schubert & Strebel 1994; Margottin et al. 1998). Tetherin can be ubiquitinated at several cytoplasmic residues including an STS motif (Tokarev et al. 2011). However, whether recruitment of β-TrCP and the subsequent degradation of tetherin are crucial steps in antagonism by Vpu is a matter of debate and depends on the assay used. Mutation of the serines in the conserved DSGNES motif in Vpu (the so-called 2/6A mutant) leads to a partial defect in counteraction that cannot be fully explained by the lack of tetherin degradation (Mangeat

et al. 2009; Mitchell et al. 2009; Schubert & Strebel 1994). It has been proposed previously that β-TrCP recruitment is not essential for tetherin counteraction and that the DSGNES motif in Vpu might play an additional role (Tervo et al. 2011). This notion is supported by naturally occurring Vpu variants that have been examined by our lab. Mutation of the N or the E in the DSGNES motif led to reduced anti-tetherin activity without losing anti-CD4 function, which is dependent on the recruitment of β-TrCP (Pickering et al. 2014). These data indicate that mis-trafficking of tetherin may be sufficient to overcome its restriction.

Antagonism of tetherin by Vpu has been shown to be clathrin dependent (Lau et al. 2011; Kueck & Neil 2012). While AP-1 has been proposed to be the major clathrin adaptor involved in Vpu-mediated tetherin mis-trafficking, knock down of AP-1 does not result in loss of Vpu function (Kueck & Neil 2012). Recently, it has been reported that tetherin and Vpu can form a ternary complex with AP-1 where Vpu's ExxxLV motif binds the σ-subunit and tetherin's YXXθ binds the μ-subunit of AP-1 (Jia et al. 2014). This acidic dileucine variant ExxxLV in the second α-helix of the cytoplasmic tail of Vpu has been shown to be required for the mis-trafficking of tetherin (Schmidt et al. 2011; Dubé et al. 2011; Kueck & Neil 2012). Mutation of this motif results in aberrant localization of Vpu and reduced virus release from tetherin expressing cells. Tetherin degradation by this Vpu mutant is completely abolished, without the loss of tetherin-Vpu binding. The residual anti-tetherin activity of this mutant is fully dependent on the dual-tyrosine motif in tetherin (Kueck & Neil 2012).

Two isoleucine residues (I43 and I46 in B Vpu; this mutant is referred to as LILI) and a tryptophan residue (W76) have been newly identified as important for Vpu's anti-tetherin activity (Pickering et al. 2014). Whilst the two isoleucine residues are also required for CD4 downregulation, the tryptophan is not. Both the LILI and the tryptophan mutant will be further analysed in the following chapter.

Dr Tonya Kueck, a former PhD student in our lab was able to show that the ESCRT components UBAP1 and HRS are required for tetherin degradation, but have only little to no effect on Vpu's function to promote virus release (Kueck et al. 2015; see appendix). Dr Kueck along with Dr Toshana Foster have been involved in some of the data presented in this chapter and this will be indicated accordingly.

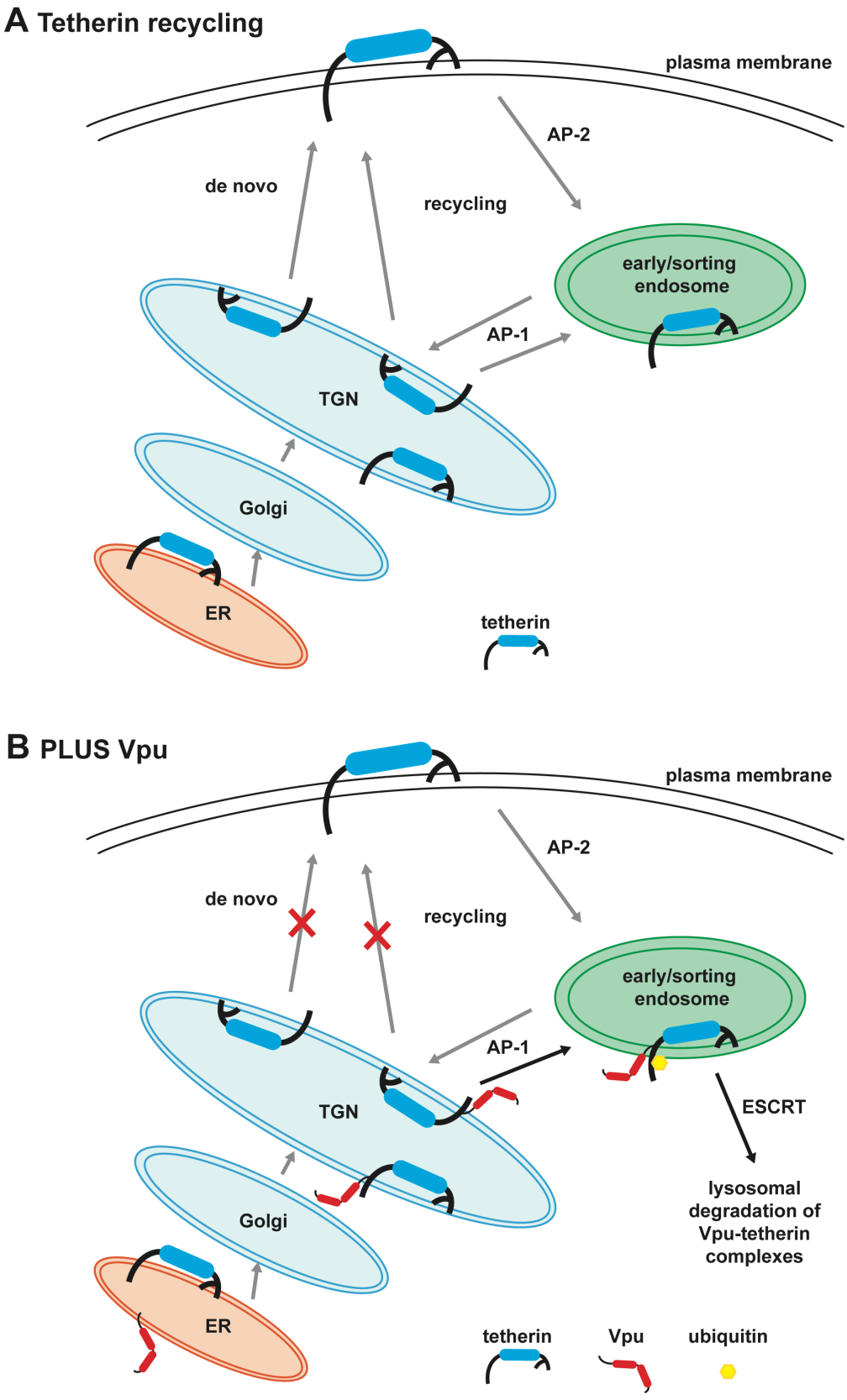

Figure 4.1 Model of tetherin trafficking and Vpu-mediated mis-trafficking. (**A**) Tetherin trafficking in the absence of Vpu. Newly synthesized tetherin traffics to the plasma membrane. AP-2 mediates the endocytosis of tetherin in clathrin-coated pits. It then traffics to the TGN, mediated by AP-1, and recycles back to the plasma membrane. (**B**) Tetherin trafficking in the presence of Vpu. Vpu interacts with newly synthesized or recycling tetherin in the endoplasmic reticulum (ER) or the Golgi apparatus. Instead of reaching the plasma membrane, the Vpu/tetherin complexes are sorted into endosomal compartments. Vpu recruits SCF-β-TrCP, which ubiquitinates tetherin's cytoplasmic tail. Ubiquitin-dependent recruitment of HRS then induces ESCRT-dependent degradation in lysosomes.

In this chapter the importance of β-TrCP recruitment in tetherin counteraction was re-evaluated. The data presented here suggest that Vpu phosphorylation is required for counteraction, whereas β-TrCP binding is not and they confirm the idea of a dual function of the phosphorylated serine motif. The Vpu phospho-mutant 2/6A as well as various other Vpu mutants exhibit defects that show similarity to the ExxxLV mutant in terms of virus release and subcellular localization of Vpu. This could also be confirmed for the same mutants generated in a primary Vpu. Addition of the clathrin binding box of the ESCRT-0 component HRS to the C-terminus of the Vpu mutants rescues virus release, tetherin downregulation as well as Vpu localization, but not β-TrCP interaction of the 2/6A mutant. For the first time, we are able to demonstrate binding of Vpu to AP-1 in a tetherin-dependent manner. Altogether, the data support a model where phosphorylation of Vpu mediates clathrin adaptor binding and subsequent mis-trafficking of tetherin, which seems to be the essential step in counteraction of the physical restriction.

4.2 Results

4.2.1 Recruitment of β-TrCP is Not Required for HIV-1 Release

Recruitment of the $SCF^{\beta TRCP1/2}$ E3 ubiquitin ligase by the phosphorylated DSGNES motif in the cytoplasmic tail of Vpu is crucial for the degradation of tetherin. However, whether this degradation step is required for counteraction of virus restriction has been a matter of debate. Most of the studies in this area have been done under transient transfection conditions. Therefore, this question was re-evaluated using viral infection of 293T cells stably expressing tetherin. To ensure these cells expressed tetherin at physiological levels, cells stably expressing tetherin were analysed for their surface tetherin by flow cytometry and compared to 293T cells that were treated with interferon for 24 h to induce endogenous tetherin expression. This showed that tetherin was expressed to comparable, but slightly higher levels in the stable cell line (Figure 4.2 A). It was previously shown that knockdown of UBAP1 (ESCRT-1) resulted in the block of tetherin degradation, but had only an insignificant effect on infectious virus release (Agromayor et al. 2012). Similarly, Tonya Kueck showed that the ESCRT-0 component HRS was required for tetherin degradation but not virus release (Kueck et al. 2015; see appendix). To reinvestigate the role of ubiquitin ligase recruitment, β-TrCP 1 and 2 were simultaneously knocked down in 293T or 293T THN cells and infected with HIV-1 WT, ΔVpu or the phospho-mutant (2/6A). In Vpu 2/6A two serine residues, 52 and 56, are mutated to alanines, which leads to the loss of serine-phosphorylation. This Vpu mutant is unable to interact with β-TrCP and has a defect in counteracting tetherin and in inducing its degradation (Mitchell et al. 2009; Margottin et al. 1998; Mangeat et al. 2009). Efficient siRNA knock down of β-TrCP in 293T and 293T tetherin cells had only a minor effect on the release of WT virus and did not recapitulate the defect of the 2/6A mutant in tetherin-expressing cells (Figure 4.2 B and C). Under the same conditions, the degradation of tetherin was completely abolished in cells infected at an MOI of 2. This indicates that not only core ESCRT components are dispensable for tetherin counteraction, but also recruitment of the $SCF^{\beta TRCP1/2}$ E3 ubiquitin ligase by Vpu is not required for promoting virus release from infected cells under conditions where β-TrCP depletion blocks tetherin degradation completely.

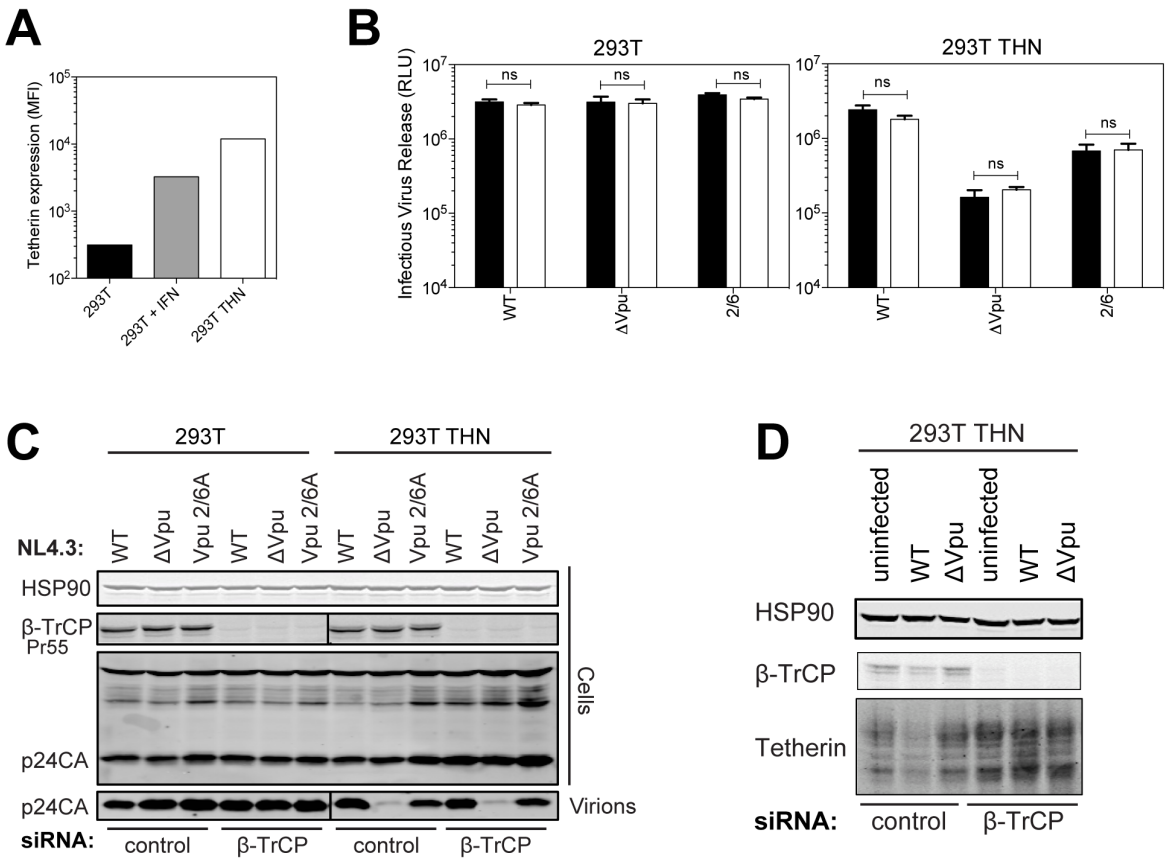

Figure 4.2 Recruitment of β-TrCP is required for tetherin degradation, but not for tetherin counteraction. (**A**) The graph indicates the median fluorescence intensity of tetherin surface expression for 293T cells, 293T cells treated with 1000 U/ml universal type-I interferon for 24 h or the same cells stably expressing tetherin. (**B-D**) 293T or 293T tetherin cells were transfected with siRNA oligonucleotide directed against β-TrCP1 and 2 or non-targeting control. Cells were infected with VSV-G pseudotyped NL4.3 HIV-1 WT, ΔVpu or Vpu 2/6A mutant at an MOI of 0.8. (**B**) Infectivity of viral supernatants was assayed on HeLa-TZMbl reporter cells. Infectious virus release was plotted as β-galactosidase activity in relative light units (RLU). Error bars represent the standard deviation of three independent experiments. Asterisks represent the p value for the difference in infectious virus release from β-TrCP siRNA or control siRNA transfected cells. ns, not significant as determined by two-tailed t test. (**C**) Cell lysates and sucrose purified viral supernatants from (**B**) were subjected to SDS-PAGE and analyzed by Western blotting for HSP90, β-TrCP and HIV-1 p24CA, and analyzed by LiCor quantitative imager. (**D**) Cells were treated as in (**B**) but infected at an MOI of 2. Cell lysates were subjected to SDS-PAGE and analyzed by Western blotting for HSP90, β-TrCP and tetherin.

4.2.2 The 2/6A Phosphorylation Mutant Phenocopies the ExxxLV Trafficking Mutant

Recently, it has been shown by our group that a conserved ExxxLV sorting signal was required for tetherin counteraction and that mutation of this motif to alanines resulted in a virus release and Vpu localization defect (Kueck & Neil 2012). Residual activity of the ELV mutant was dependent on the presence of the dual tyrosine motif in tetherin (Kueck & Neil 2012). Another study showed that Vpu and tetherin form a ternary complex with AP-1, which requires both the ExxxLV in Vpu and the YDYCRV in tetherin. Additionally, residues 42 and 43 in Vpu's first alpha helix were proposed to make a non-canonical contact with AP-1μ (Jia et al. 2014). A study conducted in our lab analysing patient-derived HIV-1 Vpu sequences also identified similar residues to be important for anti-tetherin activity (Pickering et al. 2014). Mutation of the conserved $L_{41}I_{42}/L_{45}I_{46}$ (LILI) residues to alanines reduced virus release from infected tetherin-expressing cells to the levels of the ELV mutant and also the phospho-mutant 2/6A showed a comparable defect. (Figure 4.3 A-C). Infection of 293T cells expressing the tyrosine mutant of tetherin (Y6,8A) resulted in the loss of the residual activity of the Vpu mutants. All mutants were also similarly defective for downregulating tetherin from the cell surface (Kueck et al. 2015; see appendix). The two serine residues are located in an acidic patch between the LILI and the ELV motifs. We therefore hypothesized that the 2/6A mutant may be similarly defective for mis-trafficking tetherin like the ELV mutant. WT Vpu predominantly associates with the TGN marker TGN46 and it was shown that this localization was significantly reduced for the ELV trafficking mutant in tetherin expressing cells (Kueck & Neil 2012). Hela cells were transfected with HA-tagged versions of WT Vpu or the 2/6A, ELV and LILI mutants. Like the ELV mutant, 2/6A and LILI mainly localized to peripheral endosomal compartments rather than only to the TGN (Figure 4.4 A). Quantification of the coincidence of Vpu-HA and TGN46 showed that all mutants presented a significantly reduced TGN co-localization compared to WT Vpu (Figure 4.4 B). This suggests that the 2/6A and LILI mutants exhibit the same trafficking defect as the ELV mutant and that their residual anti-tetherin activity depends on an intact sorting signal in the cytoplasmic tail of tetherin.

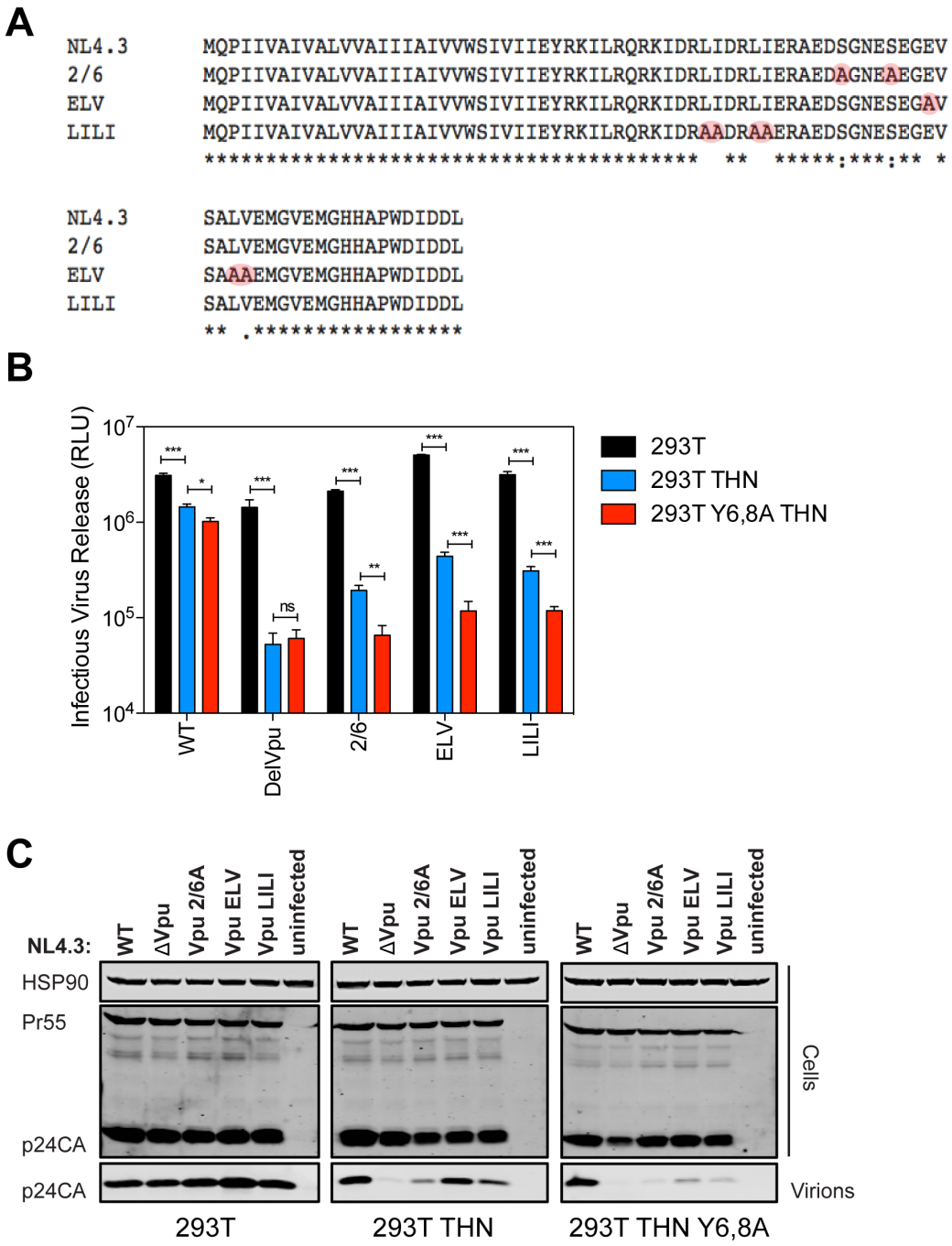

Figure 4.3 The 2/6 Vpu phospho-mutant phenocopies the Vpu trafficking mutant. (**A**) Alignment of amino acid sequences of HIV-1 NL4.3 Vpu and mutants. Mutations are highlighted in red. Alignment was generated using Clustal Omega. (**B and C**) 293T, 293T tetherin or Y6,8A tetherin cells were infected with VSV-G pseudotyped NL4.3 WT or mutant virus at an MOI of 0.8. (**B**) 48 hours post infection viral supernatants were assayed for infectivity using HeLa-TZMbl reporter cells as in Fig 1. Error bars represent the standard deviation of three independent experiments. Asterisks represent the p value for the difference in infectious virus release from 293T cells and tetherin expressing 293T cells. ns, not significant; *p<0.05, **p<0.01, ***p<0.001 as determined by two-tailed t test. (**C**) Cell lysates and sucrose purified viral supernatants were subjected to SDS-PAGE and analyzed by Western blotting as in figure 4.2.

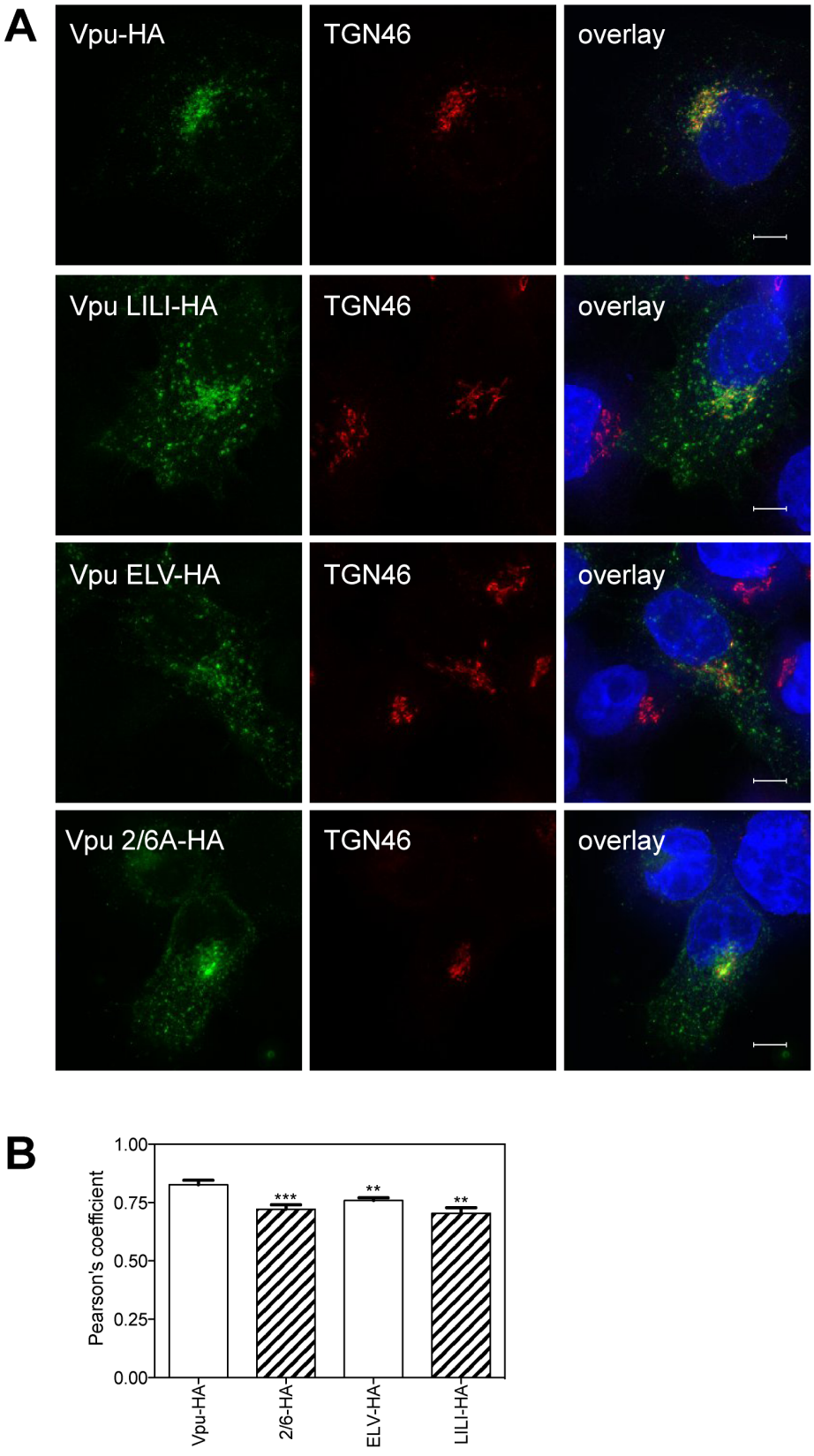

Figure 4.4 The 2/6 Vpu phospho-mutant has a similar localization defect to the Vpu trafficking mutant. (**A**) Hela-TZMbl cells were transfected with 100 ng of pCR3.1 Vpu-HA or indicated mutants. 16 hours post transfection cells were fixed and stained for HA (green) and the TGN marker TGN46 (red) and examined by widefield fluorescent microscopy. Panels are of representative examples. Bars = 10 μm. (**B**) Z stacks were taken of all cells (n=15), images were deconvolved using the AutoQuant X3 software and Pearson's correlations were calculated for all Z stacks using ImageJ. Results were analyzed by unpaired 2-tailed t-test - **p<0.01, *** p<0.001.

If the 2/6A and the ELV mutants are defective for the same reason we might expect that a 2/6A-ELV double mutant would not have an additive anti-tetherin defect. In keeping with this hypothesis, there was no significant additive reduction of virus release in the case of the double-mutant from infected 293T tetherin cells, even though virus release seemed to be slightly reduced in all cell types (Figure 4.5). Another DSGNES motif mutant, NE, was also examined for its ability to counteract tetherin. N54 and E55 are highly conserved and while these residues are not required for β-TrCP interaction, patient-derived mutants (N55H/E56G) have been found to have impaired anti-tetherin activity (Pickering et al. 2014). Mutation of these residues in NL4.3 led to reduced virus release similar to all the other mutants tested (Figure 4.5). Furthermore, all mutants exhibited the same phenotype in primary $CD4^+$ T-cells treated with type-I interferon, which induces tetherin expression (Figure 4.6). Of note, the apparent molecular weight of the LILI Vpu mutant in figure 4.5 B and 4.6 does not correlate with the amino acid length of the protein. The anomalous migration could be due to amino acid changes resulting in gel shifting.

These data further indicate that the DSGNES motif plays a role in anti-tetherin activity independent of its β-TrCP recruitment function. Altogether, these data suggest that the 2/6A mutant is defective in tetherin counteraction, potentially because serine phosphorylation regulates trafficking of Vpu and that this function can be decoupled from its role in ubiquitin ligase recruitment.

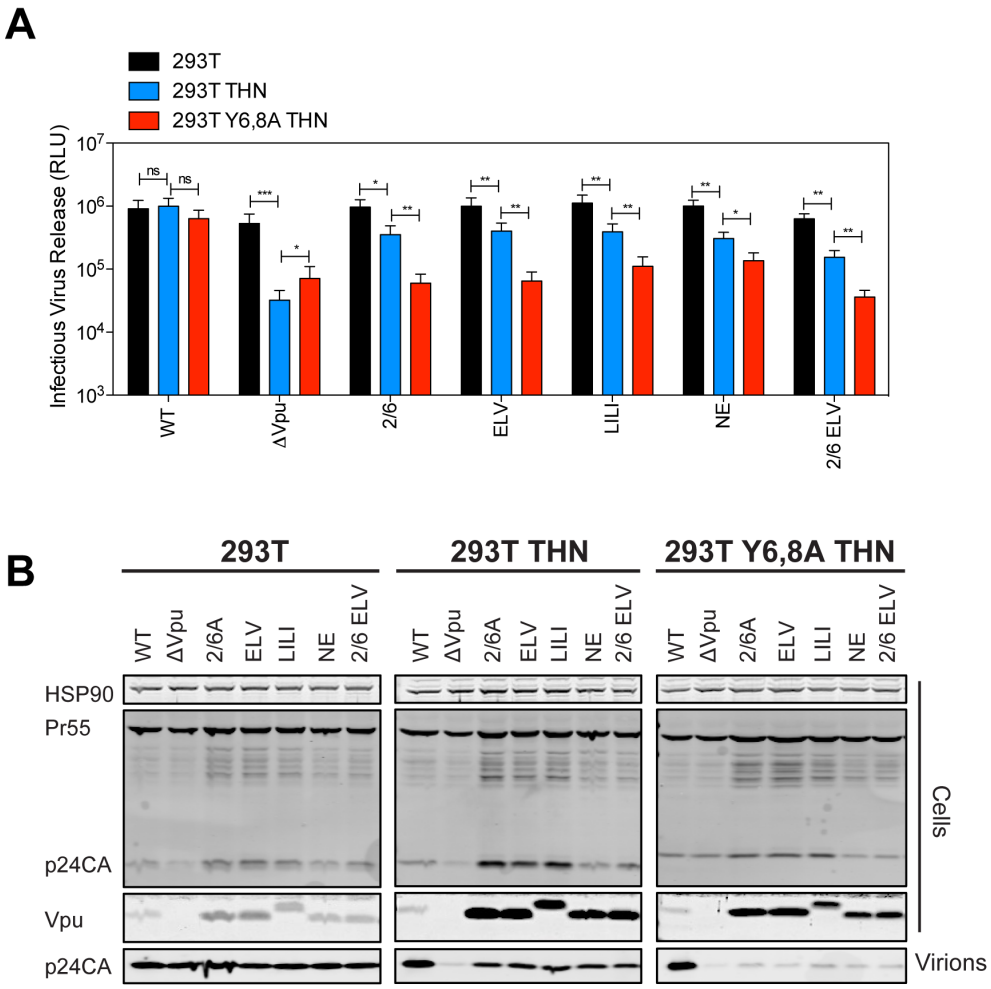

Figure 4.5 Additional Vpu mutants have a similar virus release defect in 293T tetherin cells. (**A and B**) 293T, 293T tetherin or Y6,8A tetherin cells were infected with VSV-G pseudotyped NL4.3 WT or mutant virus at an MOI of 0.8. (**A**) 48 hours post infection viral supernatants were assayed for infectivity using HeLa-TZMbl reporter cells as in Figure 1. Error bars represent the standard deviation of three independent experiments. Asterisks represent the p value for the difference in infectious virus release from 293T cells and tetherin expressing 293T cells. ns, not significant; *p<0.05, **p<0.01, ***p<0.001 as determined by two-tailed t test. (**B**) Cell lysates and sucrose purified viral supernatants were subjected to SDS-PAGE and analysed by Western blotting as as in figure 4.2.

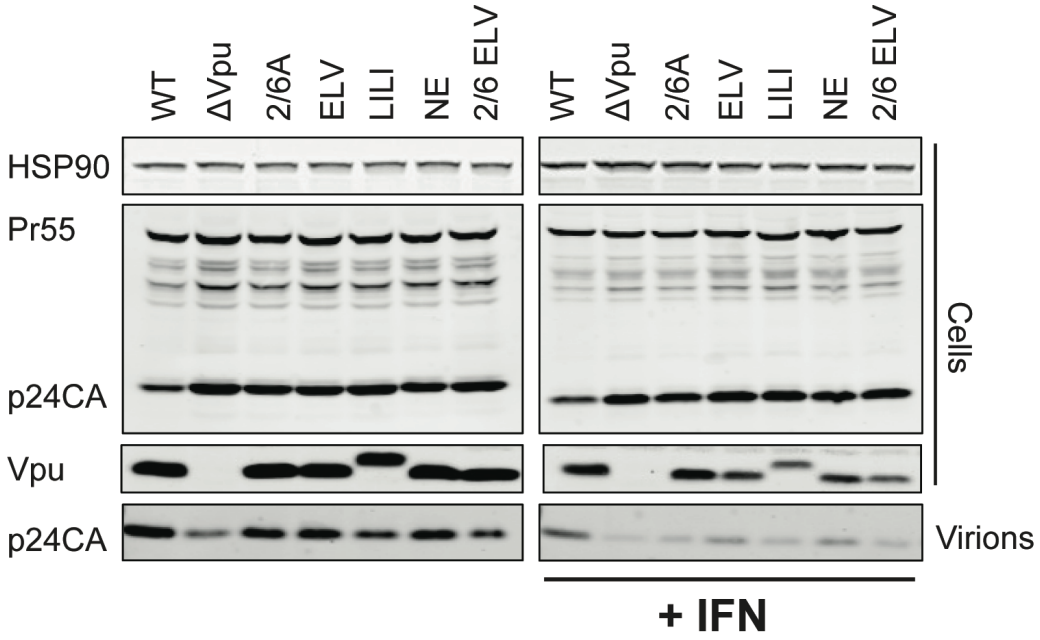

Figure 4.6 Additional Vpu mutants have a similar virus release defect in primary CD4+ T cells. (A) Primary human CD4+ T cells were infected with the indicated HIV-1 mutant at an MOI of 0.8. 16 h later the cells were treated or not with 5000 U/ml universal type-I interferon. Cell lysates and viral supernatants were harvested a further 24 h later and analysed cellular viral expression and physical particle yield by quantitative Western blotting.

4.2.3 Equivalent Mutants in a Highly Active Primary Vpu Show the Same Phenotypes as the NL4.3 Vpu Mutants

As mentioned before, a previous study conducted by members of our group found that the lab strain NL4.3 Vpu is inferior in its anti-tetherin activity to most Vpus isolated from patient samples (Pickering et al. 2014). To be sure that the defects seen with the different mutants are not limited to NL4.3, the same mutations were introduced in a highly active patient-derived Vpu (Vpu 2_87) and tested for their tetherin counteractivity and subcellular localization. The 2/6A phospho-mutant is named 3/7A here, because in this isolate the two serines are at positions 53 and 57. 293T cells expressing WT tetherin or the tyrosine mutant (Y6,8A) were co-transfected with increasing amounts of Vpu and a Vpu-defective NL4.3 provirus. At lower concentrations 2_87 Vpu WT was counteracting tetherin more efficiently than NL4.3 Vpu WT (Figure 4.7 A black versus grey lines, all panels). Similar to the mutants in NL4.3 Vpu all 2_87 Vpu mutants were partially defective in antagonizing WT tetherin compared to 2_87 Vpu WT (Figure 4.7A red triangle) and lost any residual activity against the tyrosine mutant of tetherin Y6,8A (Figure 4.7 A red open circle). Also, the localization of all mutants was comparable to that of the NL4.3 Vpu mutants with more Vpu being present in peripheral endosomal compartments. Quantification revealed that there was a significant

reduction in co-localization of Vpu with TGN46 for all the mutants compared to WT 2_87 Vpu (Figure 4.8 A and B). This demonstrates that the defects of the Vpu mutants are not restricted to the lab strain NL4.3 Vpu and shows that these residues are essential for Vpu trafficking and tetherin antagonism in a patient-derived Vpu protein.

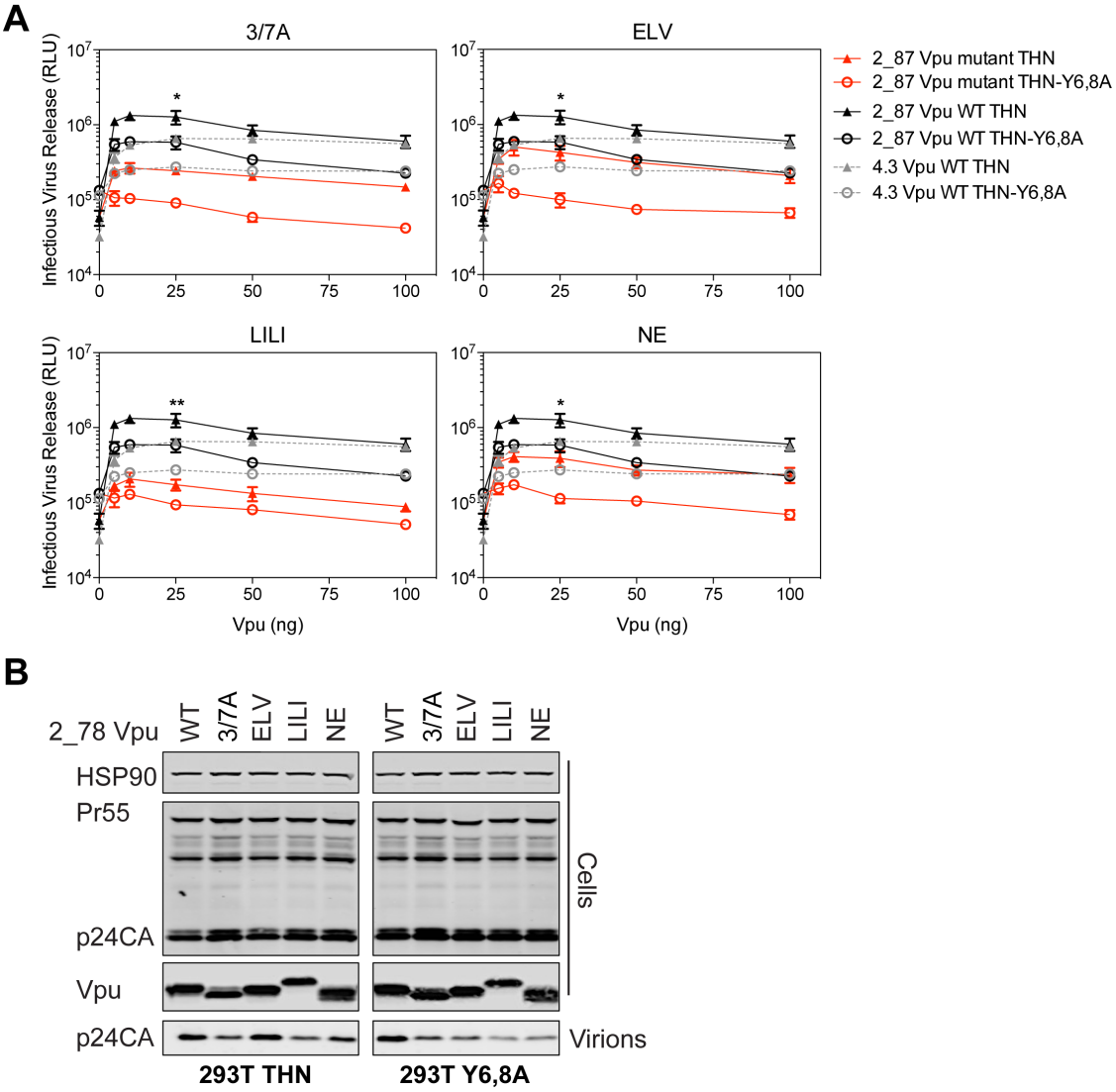

Figure 4.7 Mutants of a primary isolate Vpu exhibit a comparable virus release defect to NL4.3 Vpu mutants. (**A**) 293T tetherin cells were transfected with NL4.3 ΔVpu proviral plasmid in combination with YFP expression vector and pCR3.1 2_87 Vpu or mutants thereof. 48 hours post transfection infectivity of viral supernatants was determined on HeLa-TZMbl cells as in figure 4.2. Error bars represent standard deviation of two independent experiments. Red, 2_87 Vpu mutant; black, 2_87 Vpu WT; grey, NL4.3 Vpu WT; Triangle, 293T THN cells; open circle, 293T THN Y6,8A. Asterisks represent the p value for the difference in virus release from 293T THN cells between 2_87 Vpu WT and Vpu mutant at 25ng of Vpu expression vector. *p > 0.05, **p > 0.01, as determined by two-tailed t test (**B**) Cell lysates and pelleted supernatant virions from (**A**) were harvested and subjected to SDS-PAGE and analysed by Western blotting for HIV-1 p24CA, Vpu and HSP90, and analysed by LiCor quantitative imager.

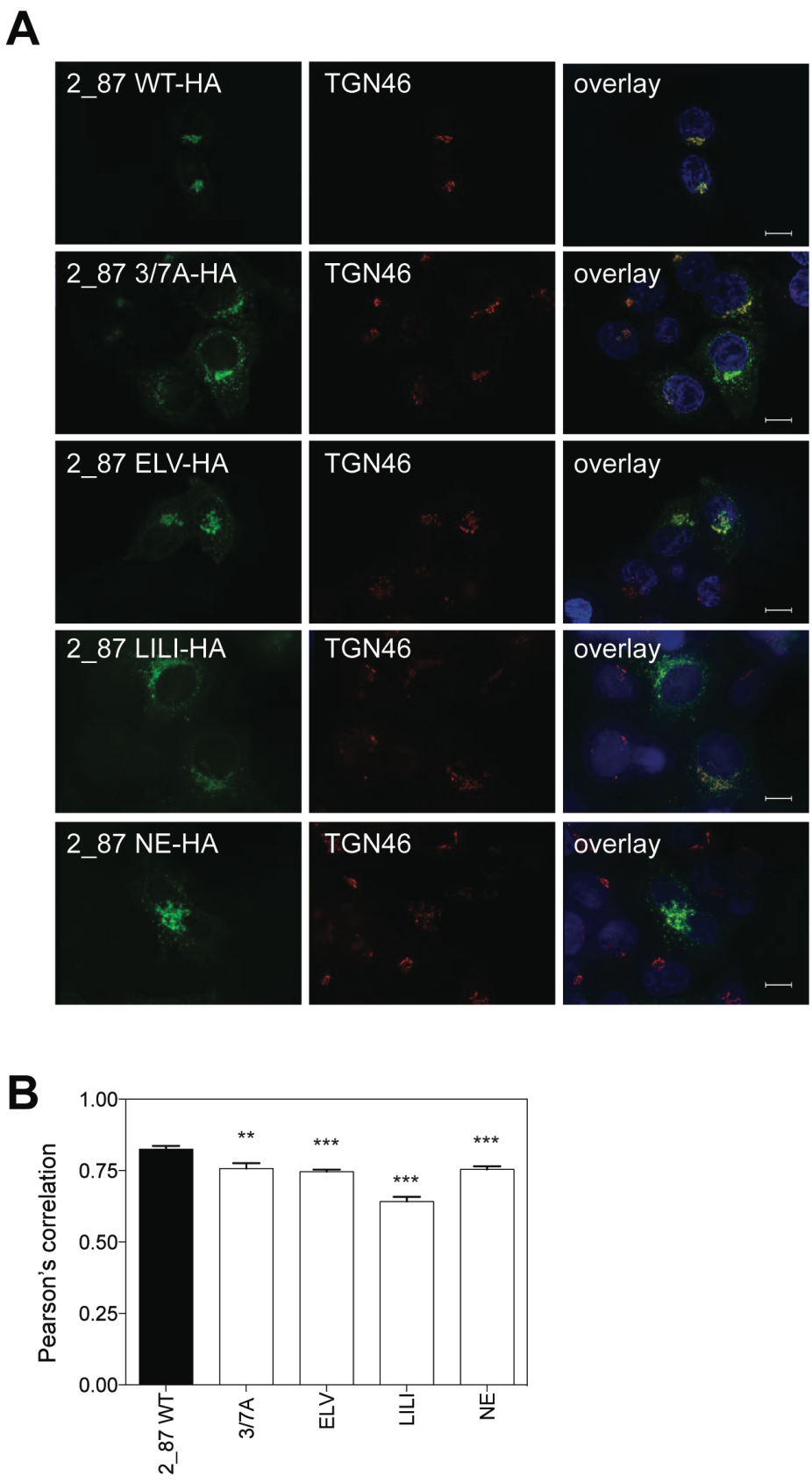

Figure 4.8 Mutants of a primary isolate Vpu exhibit a comparable localization phenotype to NL4.3 Vpu mutants. (**A**) Hela cells were transfected with 100 ng of pCR3.1 2_87 Vpu-HA or indicated mutants. 16 hours post transfection cells were fixed and stained for HA (green) and the TGN marker TGN46 (red) and examined by widefield fluorescent microscopy. Panels are of representative examples. Bars = 10 µm. (**B**) Z stacks were taken of all cells (n=15), images were deconvolved using the AutoQuant X3 software and Pearson's correlations were calculated for all Z stacks using ImageJ. Results were analyzed by unpaired 2-tailed t-test - *** P = 10-5 or lower.

4.2.4 Vpu Phosphorylation is Required for Tetherin Counteraction

The HIV-1 Vpu 2/6A mutant shows a defect in virus release that cannot be completely attributed to its inability to recruit β-TrCP and this suggests that Vpu phosphorylation potentially plays another role in tetherin antagonism. Both serines are phosphorylated by casein kinase II (CKII) (Schubert et al. 1994). To test the requirement of Vpu serine phosphorylation for tetherin antagonism the CK-II inhibitor Tyrphostin AG 1112 was used, which has been implicated in inhibition of Vpu-mediated tetherin degradation (Schindler et al. 2010). Therefore, WT HIV-1 infected cells were treated with Tyrphostin AG 1112 to see whether this would recapitulate the 2/6A defect. The treatment resulted in the inhibition of WT HIV-1 release in tetherin-expressing cells, especially in those expressing the Y6,8A mutant (Figure 4.9 A). Lysates from cells transfected with HA-tagged Vpu expression vectors were run on an 8% PhosTag gel and analysed for Vpu by Western blotting. Phosphorylated WT Vpu appeared as a smear in contrast to the unphosphorylated 2/6A Vpu (Figure 4.9 C). WT Vpu from cells treated with Tyrphostin, however, appeared as a significantly reduced smear, consistent with loss of phosphorylation. These data further demonstrate that phosphorylation of serine residues in the cytoplasmic tail of Vpu is required for efficient virus release. Importantly, while these data correlate with the previous findings, it needs to be mentioned that Tyrphostin AG 1112 may have additional effects on the overall experimental system and is toxic at concentrations higher that the one used here. It would also be beneficial to include the 2/6 Vpu mutant in further experiments.

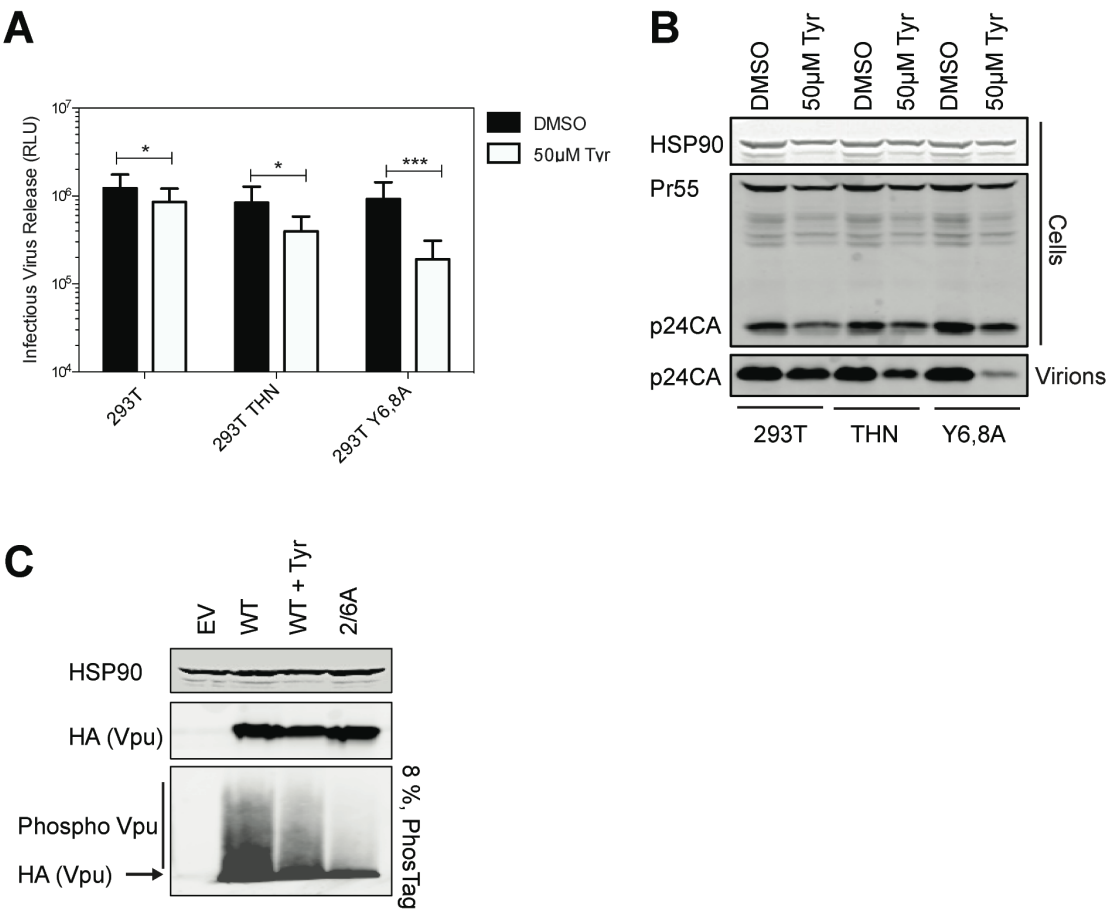

Figure 4.9 Serine phosphorylation of Vpu is required for tetherin counteraction. (**A**) 293T, 293T tetherin or Y6,8A tetherin cells were infected with VSV-G pseudotyped NL4.3WT at an MOI of 0.8. 6 hours post infection DMSO or 50 μM Tyrphostin was added to the medium. 48 hours post infection viral supernatants were assayed for infectivity using HeLa-TZMbl reporter cells as in figure 4.2. Error bars represent the standard deviation of three independent experiments. Asterisks represent the p value for the difference in virus release from 293T or 293T THN cells treated with DMSO or Tyrphostin AG 1112. *p > 0.05, ***p > 0.001, as determined by two-tailed t test (**B**) Cell lysates and sucrose purified viral supernatants were subjected to SDS-PAGE and analyzed by Western blotting as in figure 4.2. (**C**) 293T tetherin cells were transfected with 2 μg pCR3.1Vpu-HA or 2/6 Vpu-HA and treated with DMSO or 50 μM Tyrphostin for 24 h. Cell lysates were electrophoresed as before, or on an 8%, 50 μMPhos-tag gel to separate the phosphorylated species.

4.2.5 Addition of the HRS Clathrin Binding Box Rescues Vpu Mutants in Tetherin-Expressing Cells, Which is Dependent on Tetherin's YDY Motif

Vpu counteracts tetherin by preventing it from reaching the cell surface and rerouting it into a clathrin-dependent endosomal trafficking pathway. All mutants tested in this study exhibit a defect in their anti-tetherin activity and subcellular localization comparable to the ELV trafficking mutant that has been suggested to be impaired in its ability to bind AP-1 (Jia et al. 2014). The next question

was whether this defect could be rescued when clathrin adaptors were bypassed. To test this, the clathrin box (CB) from ESCRT-0 component HRS (AQLISFD) or a clathrin-interaction mutant thereof (AQAASFD) was added to the C-terminus of all the Vpu mutants (Figure 4.10 A). All constructs were transiently co-transfected with a Vpu-deficient provirus into 293T cells stably expressing WT tetherin or Y6,8A tetherin. WT Vpu rescued virus release efficiently with or without CB addition in 293T tetherin cells and also remained active in 293T cells expressing the tyrosine mutant Y6,8A (Figure 4.10 B and C). As expected, all mutants showed reduced tetherin counteractivity in tetherin expressing cells. They were all expressed well, although the molecular weight of the chimeras in SDS-PAGE did not reflect their amino acid length (Figure 4.10 C). The residual anti-tetherin-activity of all mutants was completely abolished in Y6,8A tetherin cells (Figure 4.10 B). The addition of the HRS CB rescued virus release efficiently for all mutants in tetherin-expressing cells (Figure 4.10 B). In contrast, CB addition did not rescue virus release in Y6,8A tetherin cells and all chimeras remained defective (Figure 4.11). This shows that addition of a clathrin binding box to a Vpu trafficking mutant is not sufficient to reconstitute WT Vpu function in Y6,8A tetherin cells. Tetherin sorting into clathrin-rich domains in the recycling compartment is crucial for the CB chimera rescue and subsequent anchoring of the Vpu/tetherin complex to clathrin and further endosomal trafficking.

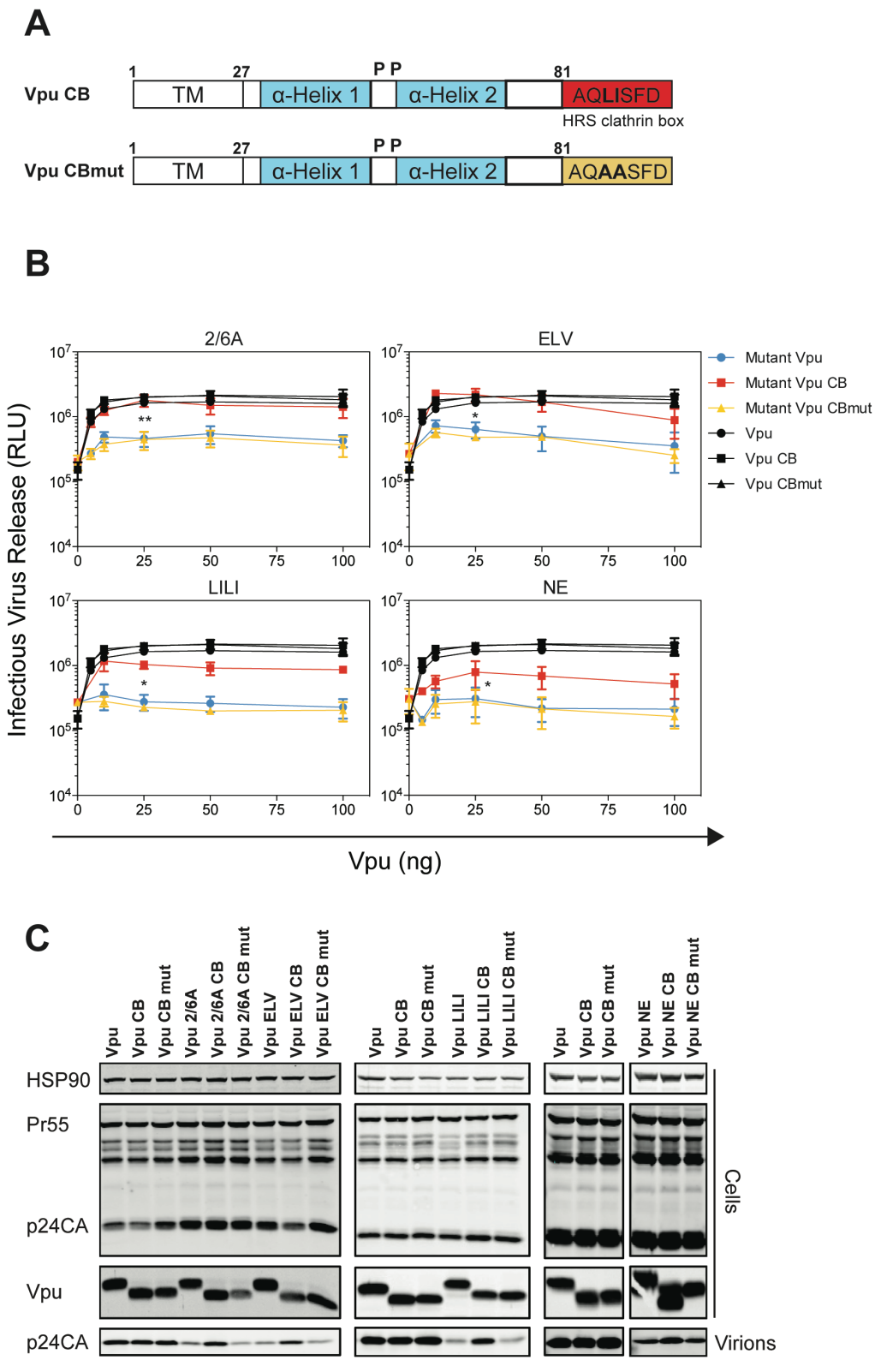

Figure 4.10 Functional rescue of Vpu phospho- and trafficking mutants by direct interaction with clathrin. (**A**) Schematic representation of Vpu CB chimera constructs. (**B**) 293T tetherin cells were transfected with NL4.3 ΔVpu proviral plasmid in combination with YFP expression vector and pCR3.1 Vpu, pCR3.1 Vpu CB or Vpu CB mut or Vpu mutants thereof. 48 hours post transfection infectivity of viral supernatants was determined on HeLa-TZMbl cells as in figure 4.3. Error bars represent standard deviation of three independent experiments. Asterisks represent the p value for the difference in virus release from 293T cells between Vpu mutants and Vpu mutants with CB at 25ng of Vpu expression vector. *p > 0.05, **p > 0.01, as determined by two-tailed t test (**C**) Cell lysates and pelleted supernatant virions from (**B**) were harvested and subjected to SDS-PAGE and analyzed by Western blotting for HIV-1 p24CA, Vpu and HSP90, and analyzed by LiCor quantitative imager.

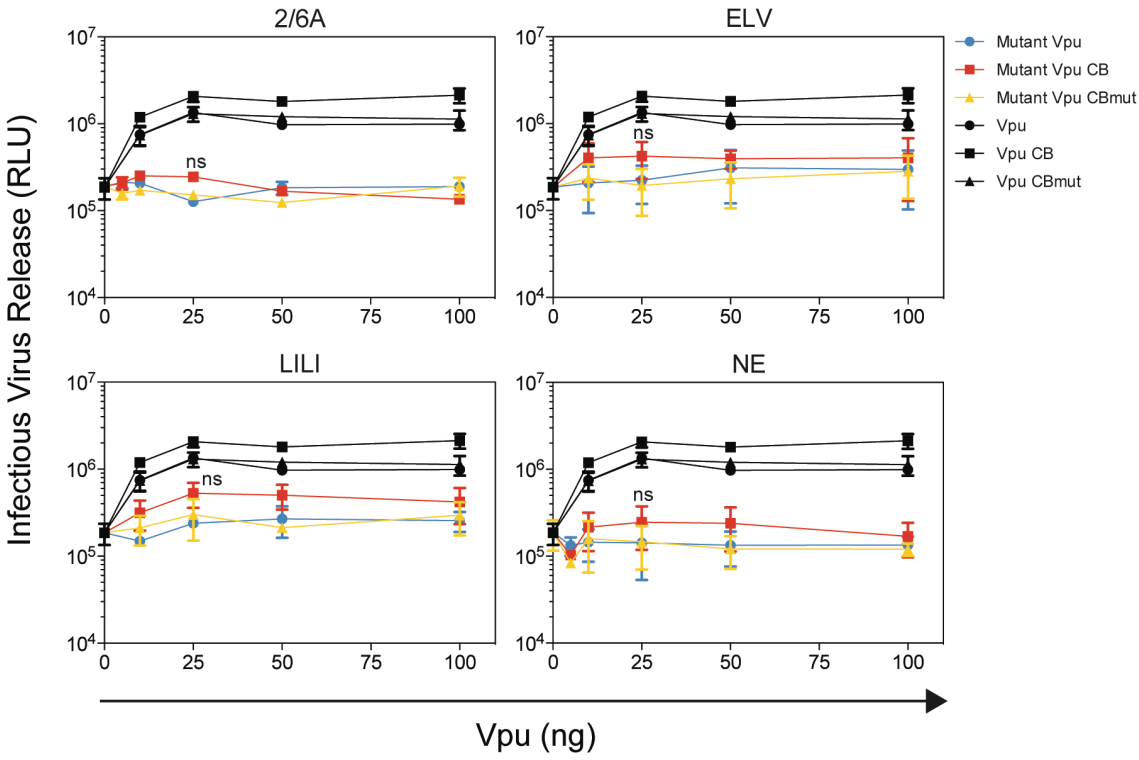

Figure 4.11 The rescue of trafficking mutants by direct clathrin interaction is dependent on tetherin's dual tyrosine motif. 293T Y6,8A tetherin cells were transfected with NL4.3 ΔVpu proviral plasmid in combination with YFP expression vector and pCR3.1 Vpu, pCR3.1 Vpu CB or Vpu CBmut or Vpu mutants thereof. 48 hours post transfection infectivity of viral supernatants was determined on HeLa-TZMbl cells as in figure 4.2. Error bars represent standard deviation of three independent experiments. Asterisks represent the p value for the difference in virus release from 293T THN cells between 2_87 Vpu WT and Vpu mutant at 25ng of Vpu expression vector. ns, not significant; as determined by two-tailed t test.

As CB addition to the Vpu mutants restored their tetherin counteractivity, Tonya Kueck also investigated whether it would also rescue tetherin downregulation from the cell surface. Hela-TZMbl cells were therefore transfected with the different Vpu constructs and analysed for their tetherin surface expression 48 h later. This revealed that the CB addition enabled the Vpu mutants to downregulate tetherin from the surface as efficiently as WT Vpu (Figure 4.12 A). In contrast, tetherin degradation was not restored in the same cells when the CB was present (Figure 4.12 B). Moreover, it was tested whether direct clathrin linkage would restore binding of the Vpu 2/6A mutant to β-TrCP. All Vpu mutants with CB or CBmut could be immunoprecipitated with a myc-tagged β-TrCP2, except the Vpu 2/6A mutant (Figure 4.13). This further supports the notion that Vpu's anti-tetherin function can be decoupled from ubiquitin ligase recruitment by the phospho-serines.

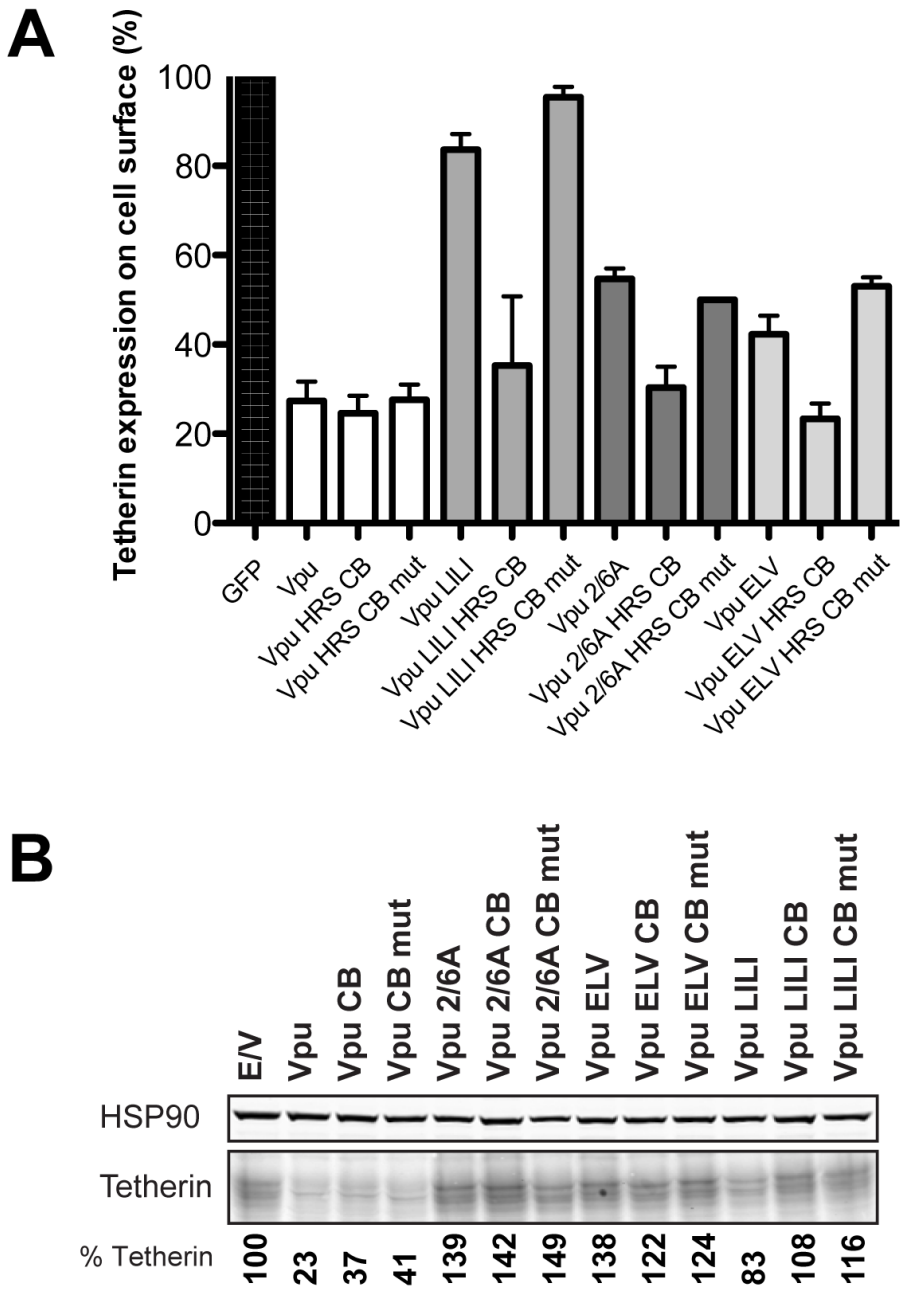

Figure 4.12 Clathrin binding rescues tetherin downregulation, but not tetherin degradation. (**A**) HeLa-TZMbl cells were co-transfected with pCR3.1 Vpu or indicated mutant and a GFP expression vector. Cell-surface tetherin levels were analysed 48 hours post transfection by flow cytometry in the GFP positive cells. The percentages of tetherin surface expression levels are calculated from median fluorescence intensities. Error bars represent standard deviation of two independent experiments. (**B**) 293T tetherin cells were transfected with pCR3.1 Vpu or indicated mutant. 48 hours post transfection cell lysates were subjected to SDS-PAGE and analyzed by Western blotting for HSP90 and tetherin, and analyzed by LiCor quantitative imager. The panel is representative for two independent experiments. All data by Tonya Kueck.

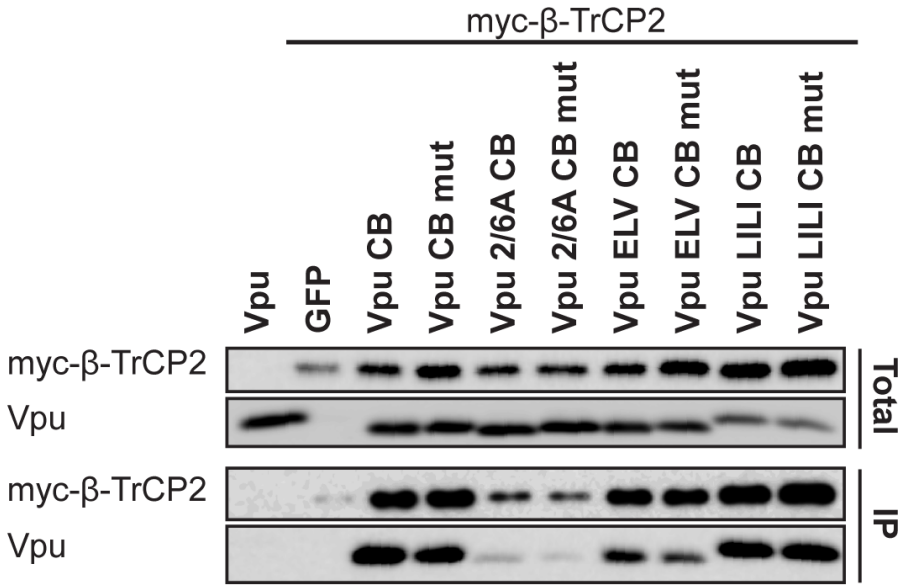

Figure 4.13 Clathrin binding does not restore β-TrCP binding. 293T cells were transfected with pCR3.1 Vpu or indicated mutant in combination with a pCR3.1 myc-β-TrCP2 expression vector. 48 hours post transfection cells were lysed and immunoprecipitated with anti-myc antibody, using PFA (0.05% w/v) as a cross-linking agent. Total cell lysates and precipitates were subjected to SDS-PAGE and analysed by Western blotting for myc-β-TrCP2 and Vpu-HA, and analysed by ImageQuant. All data by Tonya Kueck.

As CB addition to mutant Vpus is able to rescue virus release from transfected cells it was next investigated whether there was also a change in subcellular localization of the chimeric Vpus. Hela-TZMbl cells were transfected with HA-tagged versions of the Vpu mutants and the Vpu-CB chimeric constructs. As described before, all mutants showed significantly reduced co-localization to TGN46 positive compartments (Figure 4.14 A). Adding the CB restored the localization of all mutants to a WT Vpu phenotype and peripheral endosomal localization was remarkably reduced. Quantification confirmed that there was a significant difference in co-localization of Vpu with TGN46 between mutant Vpus and their Vpu-CB chimeras (Figure 4.14 B).

These data strengthen our hypothesis that the anti-tetherin defect of the 2/6A mutant and all the other trafficking mutants is due to a deficiency in clathrin-dependent sorting upstream of ubiquitin ligase recruitment.

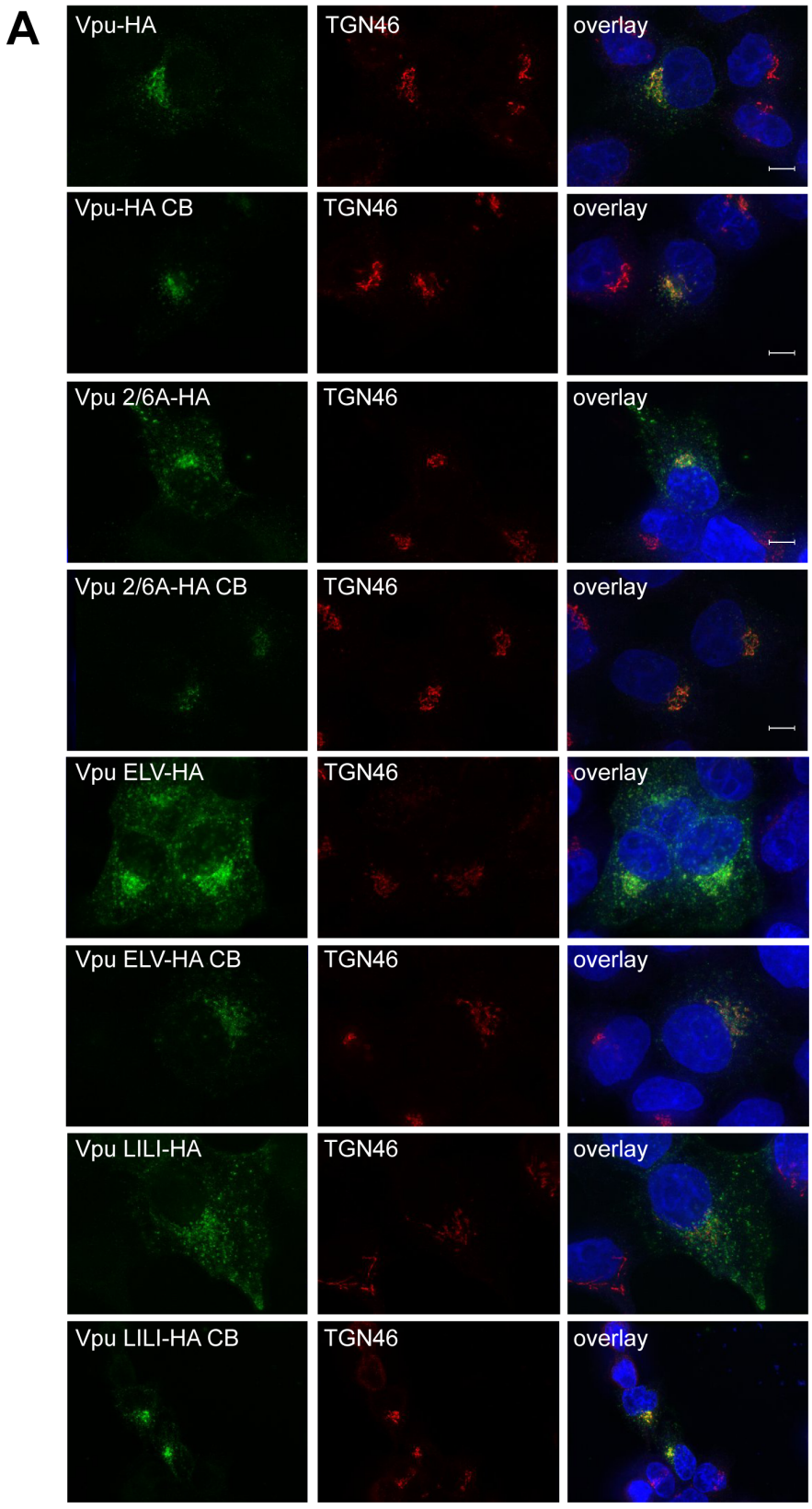
A
Vpu-HA
TGN46
overlay
Vpu-HA CB
TGN46
overlay
Vpu 2/6A-HA
TGN46
overlay
Vpu 2/6A-HA CB
TGN46
overlay
Vpu ELV-HA
TGN46
overlay
Vpu ELV-HA CB
TGN46
overlay
Vpu LILI-HA
TGN46
overlay
Vpu LILI-HA CB
TGN46
overlay

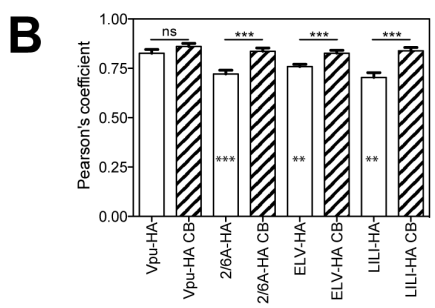
B
Pearson's coefficient
1.00
0.75
0.50
0.25
0.00
ns
***
***
***
***
**
**
Vpu-HA
Vpu-HA CB
2/6A-HA
2/6A-HA CB
ELV-HA
ELV-HA CB
LILI-HA
LILI-HA CB

Figure 4.14 Addition of a clathrin box to Vpu mutants rescues subcellular localization. (**A and B**) Hela cells were transfected with 100 ng of pCR3.1 Vpu-HA or Vpu-HA CB or indicated mutants and processed as in Figure 2. Vpu-HA (green); TGN marker TGN46 (red). (**A**) Bars = 10 µm. (**B**) Asterisks inside the bars represent significant localization differences between the mutant and WT Vpu, those above between mutant and mutant clathrin box fusion.

4.2.6 Vpu Interacts with Clathrin Adaptors AP-1 and AP-2 in Tetherin-Expressing Cells in a Phosphorylation-Dependent Manner

Clathrin-dependent sorting of Vpu/tetherin complexes has been proposed to be the first essential step in Vpu-mediated tetherin antagonism (Kueck & Neil 2012). Furthermore, it has been suggested that Vpu inhibits trafficking of recycling and newly synthesised tetherin to the plasma membrane rather than enhancing tetherin endocytosis, which indicates the involvement of AP-1 (Schmidt et al. 2011; Dubé et al. 2011). This is in keeping with structural data suggesting that tetherin and Vpu form a ternary complex with AP-1, wherein Vpu binds the σ-subunit of AP-1 via its ExxxLV motif and tetherin the µ-subunit via its YDYCRV motif (Jia et al. 2014). However, neither siRNA knockdown of AP-1 nor mouse AP-1ɣ1a -/- fibroblasts have any effect on Vpu-mediated antagonism (Kueck & Neil 2012). Due to the relatively weak affinities of clathrin adaptors to their cargoes it has been difficult to demonstrate binding by conventional immunoprecipitation in living cells. Dr Toshana Foster, a postdoc in our group, performed cross-linking immunoprecipitations in 293T tetherin cells that were transfected with HA-tagged Vpu or mutants. Results from these experiments demonstrated an interaction between AP-1ɣ and WT Vpu-HA (Figure 4.15 A). In contrast, AP-1ɣ was not detectable in immunoprecipitates of the A14L/W22A Vpu, a mutant that is unable to interact with tetherin's transmembrane domain (Vigan & Neil 2010). This suggests that the interaction of Vpu and tetherin via their transmembrane domains is crucial for AP-1 binding and anti-tetherin activity. This idea was further supported by the finding that no AP-1ɣ could be pulled down with WT Vpu in 293T cells not expressing tetherin (Kueck et al. 2015; see appendix). For all the other Vpu mutants the amount of AP-1 ɣ was reduced in the immunoprecipitates (Figure 4.15 A). When the same assay was done in 293T cells expressing Y6,8A tetherin all residual AP-1ɣ interaction was abolished (Figure 4.15 B). This shows that AP-1/tetherin interaction is important for the residual binding of the Vpu mutants. Additionally, there was no binding to AP-1 of any Vpu, including WT Vpu, in cells expressing rhesus macaque tetherin (Figure 4.15 C). As HIV-1 Vpu is unable to bind to rhesus macaque tetherin, this result confirms that direct interaction of Vpu and tetherin is crucial for AP-1 binding.

As mentioned before, AP-1 knockdown does not have any effect on tetherin antagonism. However, Vpu's ExxxLV motif could potentially interact with other clathrin adaptors such as AP-2, which could serve as an alternative route of clathrin machinery interaction. Therefore, we analysed the immunoprecipitates of the 293T tetherin and Y6,8A tetherin cells also for the presence of AP-2. We found that AP-2 could be pulled down with WT Vpu, but none of the mutants in both cell lines (Figure 4.15 A and B). Therefore, the ExxxLV trafficking motif is likely to also mediate AP-2 interaction. Since WT Vpu can interact with both major clathrin adaptors and knockdown of one adaptor has no effect on tetherin antagonism, it might be possible that they compensate for the lack of the other.

We wanted to further investigate the role of serine phosphorylation in clathrin adaptor binding. Therefore, immunoprecipitation in 293T Y6,8A tetherin was repeated, but cells were treated with the CK-II inhibitor Tyrphostin. Binding of WT Vpu to AP-1 and AP-2 was completely abolished under these conditions, supporting the hypothesis that Vpu phosphorylation is required for the interaction with the clathrin machinery (Figure 4.15 D).

Together, these data demonstrate an interaction between Vpu and endogenous AP-1 in living cells and transmembrane domain interaction of tetherin and Vpu is essential. Importantly, the 2/6A mutant was unable to bind to AP-1, which emphasizes the potential role of serine phosphorylation in mediating clathrin adaptor binding and subsequent trafficking events.

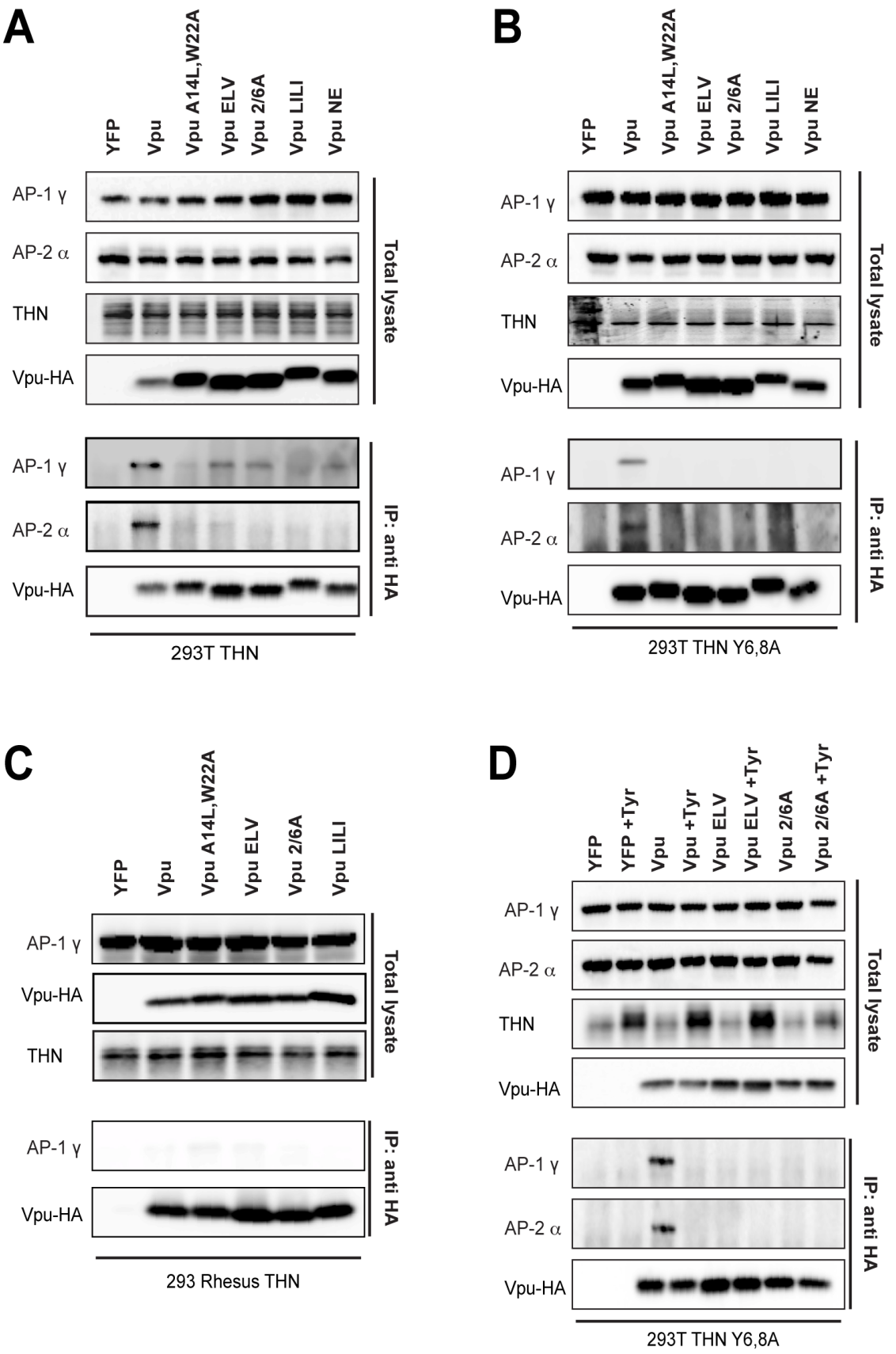

Figure 4.15 Vpu interacts with clathrin adaptors AP-1 and AP-2 in tetherin-expressing cells in a phosphorylation dependent manner. (**A-C**) 293T tetherin (**A**), 293T tetherin Y6,8A (**B**) or 293 rhesus tetherin (**C**) cells were transfected with pCR3.1 Vpu-HA, Vpu A14L/W22A-HA, Vpu ELV-HA, Vpu 2/6A-HA, Vpu LILI-HA or Vpu NE-HA mutants. 48 h post transfection, cells were lysed and cross-linked using PFA (0.05% w/v) and immunoprecipitated with anti-HA antibody. Total cell lysates and precipitates were subjected to SDS-PAGE and analyzed by Western blotting for Vpu-HA, tetherin, AP-1γ or AP-2α. Panels are of representative experiments. All data by Toshana Foster.

4.2.7 A Highly Conserved C-Terminal Tryptophan in the Cytoplasmic Tail of Vpu Has a Context Dependent Phenotype

A highly conserved tryptophan residue in the C-terminal part of the cytoplasmic tail of Vpu was proposed to be important in tetherin antagonism and has been ascribed a role in membrane anchoring (Pickering et al. 2014; Lewinski et al. 2015; Jafari et al. 2014; Zhang et al. 2015). A naturally occurring polymorphism at position 76 (W76G) was described to reduce viral release from tetherin-expressing cells whereas tetherin downregulation and degradation were not affected. Therefore, this W76G substitution in NL4.3 Vpu was tested with the addition of the HRS clathrin box or mutant as described in Figure 4.10. 293T tetherin or Y6,8A tetherin cells were co-transfected with increasing amounts of Vpu or the W mutant and a Vpu deficient NL4.3 provirus. In contrast to the previous findings the NL4.3 Vpu W76G mutant was highly active against WT tetherin in this assay (Figure 4.16 A and B). However, W76G lost its activity almost completely against the Y6,8A mutant of tetherin, similar to the results obtained with the Vpu trafficking mutants. Interestingly, addition of the HRS clathrin box to W76G was able to rescue virus release in Y6,8A tetherin cells. It should be noted that the W76G Vpu was not recognized well by the NIH Vpu antibody (Figure 4.16 B). When HA-tagged Vpu constructs were transfected into 293T cells, the difference in detection between the NIH Vpu antibody and an HA antibody was apparent (Figure 4.16 C). Wild type Vpu or the W76G Vpu mutant appeared to run at a higher molecular weight then the same Vpus with the added clathrin box. These gel shifts could be due to the nature of the amino acids added and do not correlate with the amino acid length of the proteins.

Furthermore, the subcellular localization of this Vpu mutant was investigated by transfecting Hela cells with the W76G-HA construct and staining the fixed cells for HA and the TGN marker TGN46. This mutant appeared to localize to peripheral compartments to a certain extent, although this was less pronounced than the trafficking mutants (Figure 4.16 D). However, no quantification of the co-localization of W76G Vpu with TGN46 has been conducted to confirm a difference to WT Vpu. These data indicate that the W76G mutant has an intermediate phenotype. While it is not acting like WT Vpu it also is not as defective as the trafficking mutants in terms of promoting virus release and subcellular localization. Furthermore, the data here presented does not correlated with the previous reports. Further investigation is needed to explain the varying and unusual phenotypes described. Whether W76 plays a role in tetherin mis-trafficking and clathrin adaptor binding is so far unclear.

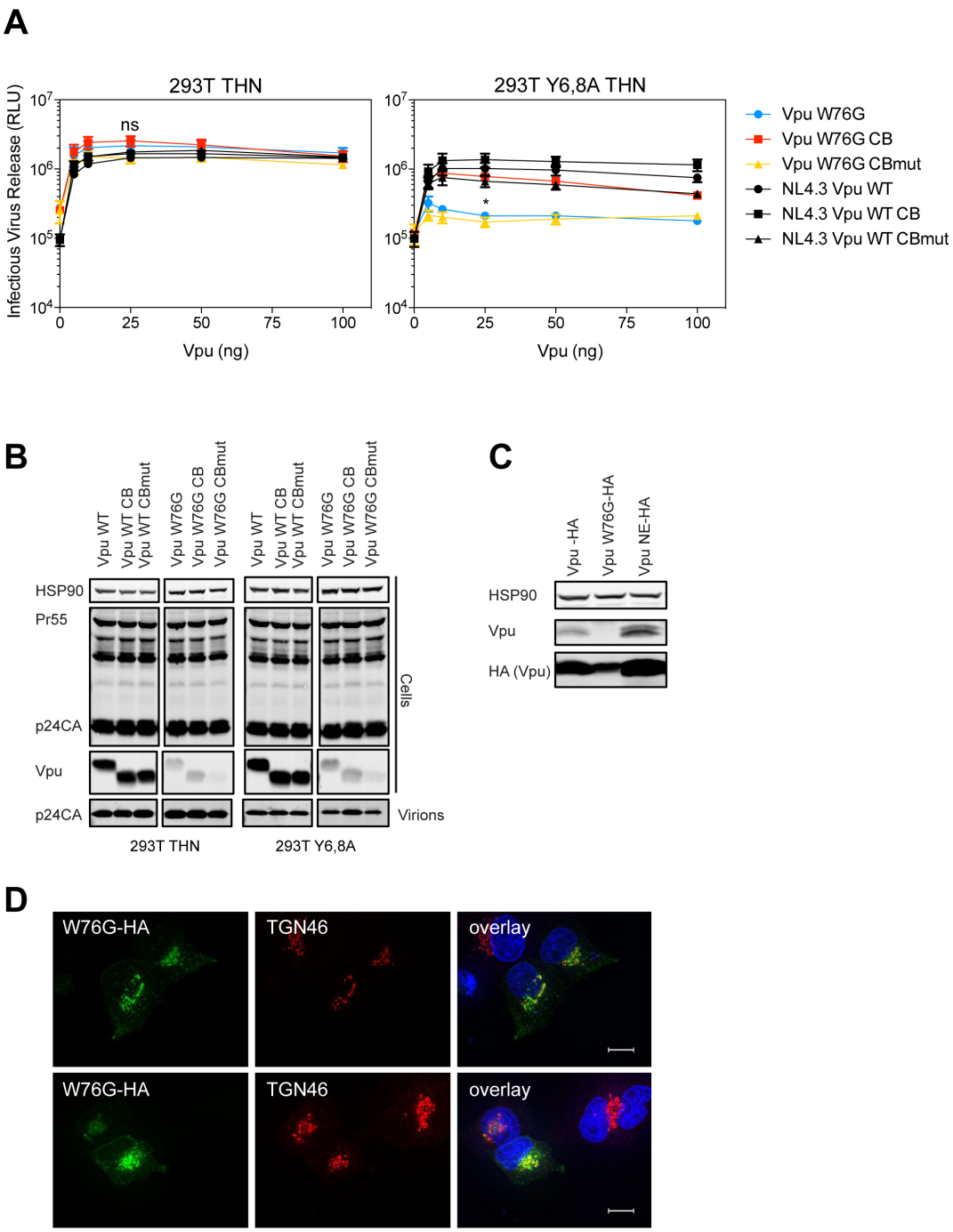

Figure 4.16 A highly conserved tryptophan in Vpu's cytoplasmic tail has a context dependent phenotype. (**A**) 293T tetherin cells were transfected with NL4.3 ΔVpu proviral plasmid in combination with YFP expression vector and pCR3.1 Vpu, pCR3.1 Vpu CB or Vpu CB mut or the Vpu W76G mutant thereof. 48 hours post transfection infectivity of viral supernatants was determined on HeLa-TZMbl cells as in Figure 4.3. Error bars represent standard deviation of three independent experiments. Asterisks represent the p value for the difference in virus release from 293T cells between Vpu W76G and Vpu W76G CB transfected cells at 25ng of Vpu expression vector. ns, not significant; *p > 0.05, as determined by two-tailed t test (**B**) Cell lysates and pelleted supernatant virions from (**A**) were harvested and subjected to SDS-PAGE and analyzed by Western blotting for HIV-1 p24CA, Vpu and HSP90, and analyzed by LiCor quantitative imager. (**C**) 293T cells were transfected with 700 ng pCR3.1 Vpu-HA or the indicated mutant. 48 h later cell lysates were harvested and subjected to SDS-PAGE and analysed by Western blotting for Hsp90, HIV-1 Vpu and HA. (**D**) Hela cells were transfected with 100 ng of pCR3.1 2_87 Vpu-HA or indicated mutants. 16 hours post transfection cells were fixed and stained for HA (green) and the TGN marker TGN46 (red) and examined by widefield fluorescent microscopy. Panels are of representative examples. Bars = 10 μm.

4.3 Discussion

In this chapter the role of $SCF^{\beta TrCP1/2}$ recruitment in Vpu-mediated tetherin antagonism has been re-evaluated. β-TrCP binding to the phosphorylated serines in the cytoplasmic tail of Vpu has been shown to be essential for CD4 and tetherin degradation. However, whether this process is required for counteraction of the physical restriction imposed by tetherin has been a matter of debate. Here, it has been demonstrated that the Vpu phospho-mutant (2/6A) is partially defective for tetherin counteraction and that this is likely due to its inability to interact with the clathrin trafficking machinery rather than the lack of β-TrCP recruitment. For the first time we were able to show that Vpu interacts with AP-1 and AP-2 *in cellulo* and that this is dependent on transmembrane interaction of Vpu and tetherin. The data discussed support recent structural observations showing that Vpu and tetherin form a ternary complex with AP-1 (Jia et al. 2014). This is dependent on the YDYCRV sorting signal in tetherin and the ExxxLV trafficking motif in Vpu. It was demonstrated that the Vpu ELV, 2/6A and other trafficking mutants are unable to bind AP-1 efficiently in the presence of tetherin and that direct linkage to the clathrin machinery rescues all Vpu trafficking mutants. This is dependent on the intact YDY motif in tetherin, but does not restore β-TrCP interaction of 2/6A. The data clarify the role of the DSGNES motif in tetherin antagonism by Vpu and we therefore propose that sorting of Vpu/tetherin complexes into clathrin-rich domains is the crucial step in tetherin antagonism.

So far, many studies investigating the mechanism of Vpu-mediated tetherin counteraction have been done under conditions wherein tetherin, Vpu and/or provirus have been transiently transfected into cells. This, however, can lead to artefacts such as overexpression induced ER-associated degradation (Andrew et al. 2011). Furthermore, transfection leads to a high variability in expression levels of the transfected constructs between cells. In contrast, under infection conditions tetherin is degraded in endosomes. When strong blocks to degradation are imposed, however, tetherin accumulates due to potentially overwhelmed endosomes, which can lead to an artificial block to counteraction. Performing infection assays at a relevant multiplicity of infection enabled us to separate the role of Vpu phosphorylation in $SCF^{\beta TrCP1/2}$ recruitment and counteraction of physical tetherin restriction. The biochemical data presented in this chapter confirms recent structural data (Jia et al. 2014). The ExxxLV motif in Vpu has been suggested to interact with the acidic dileucine binding site in the AP-1 σ-subunit and is essential in AP-1 binding. Additionally, our LILI mutant phenotype correlates with a proposed non-canonical interaction of R44/L45 with AP-1 μ. However,

the structural data have been obtained using artificial Vpu/tetherin fusions that may not necessarily reflect the biological role of clathrin adaptor recruitment. Therefore, our data demonstrate, for the first time in living cells, the involvement of the DSGNES motif and Vpu-tetherin transmembrane interaction in the recruitment of the clathrin trafficking machinery. We propose a model where phosphorylation regulates the interaction of the ExxxLV motif with clathrin adaptors (Figure 4.17). Although we cannot exclude the direct binding of the phosphorylated motif to clathrin adaptors, this explanation is more consistent with the data presented here, as there is no significant additive effect for the 2/6A-ELV double mutant on virus release.

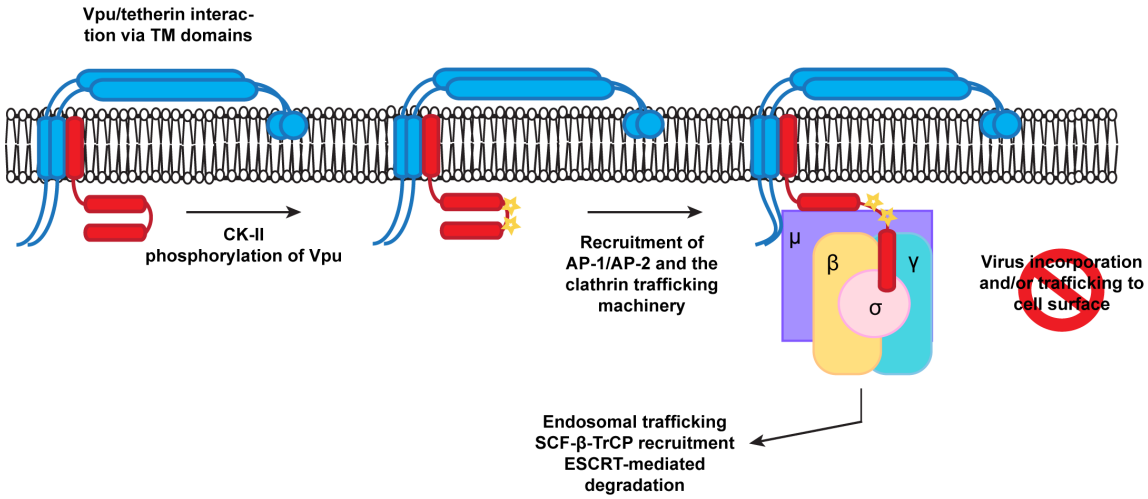

Figure 4.17 A proposed model for Vpu engagement of clathrin adaptors during tetherin counteraction. Vpu and tetherin interactions via TM/TM domain interactions and casein kinase II phosphorylation promote Vpu recruitment of AP-1 or AP-2. This allows the EXXXLV motif to bind to the σ subunit, and potentially through non-canonical interactions between its first alpha helix with the AP-1 or 2 μ subunits. In addition, the YDY motif in tetherin binds to the AP1μ. Thus tetherin/Vpu complexes are sorted into clathrin rich domains of the TGN or PM for subsequent trafficking and ubiquitination.

Phosphorylated motifs upstream of acidic dileucine motifs have been described before to regulate interaction with the clathrin machinery. An example is the CK-II-mediated phosphorylation upstream of a non-canonical AP-1 binding site in the cation-dependent mannose-6-phosphate receptor that regulates their interaction (Mauxion et al. 1996). Additionally, adjacent acidic patches have been implicated to be important. Such a patch exists in HIV-1 Vpu between the DSGNES and the ExxxLV motif and has been shown to be shorter in the laboratory-adapted strain NL4.3 Vpu

compared to patient derived isolates with superior anti-tetherin activity (Pickering et al. 2014). Vpu/tetherin interaction and Vpu phosphorylation could potentially induce conformational changes that allow the complex to interact with clathrin adaptors. Whereas clathrin adaptor binding requires tetherin to be present, β-TrCP binding does not, which indicates that Vpu phosphorylation is an independent event with additional function. SCY1-like protein 2 (SCYL2), a clathrin associated protein that modulates protein phosphatase 2A (PP2A), has been reported to induce the de-phosphorylation of Vpu and thereby inhibit its function (Miyakawa et al. 2012). Regulated phosphorylation/de-phosphorylation of Vpu could therefore potentially regulate Vpu activity at the level of clathrin-dependent trafficking.

Partial NMR structures of Vpu in solution or associated with lipid show that the ExxxLV motif is embedded within the structure in lipids. However, it adapts an extended conformation when in solution (Figure 4.18) (Wittlich et al. 2009; Willbold et al. 1997). Vpu phosphorylation has been shown to induce conformational changes in the C-terminal region of Vpu's cytoplasmic tail that are important for β-TrCP binding. However, there is discrepancy in the literature whether these changes correlate with an opening up of the ExxxLV site (Coadou et al. 2002; Coadou et al. 2003; Wittlich et al. 2008). A full length Vpu NMR structure has recently been reported and confirms the previously reported results (Zhang et al. 2015). Importantly, all these studies have been conducted in the absence of target binding and therefore it is uncertain how representative they are.

In lipid-associated structures, a highly conserved tryptophan residue (W76) at the C-terminus of Vpu's cytoplasmic tail has been shown to pack against the DSGNES motif, as if it were locking the structure. Alternatively, W76 has been implicated in displacing tetherin from sites of viral assembly due to its potential role in membrane anchoring (Lewinski et al. 2015; Zhang et al. 2015). However, data presented in this chapter suggest that mutation of this residue to a glycine reduces viral release dramatically only in cells expressing the tetherin mutant Y6,8A and this can be rescued by direct clathrin linkage. Furthermore, this Vpu mutant does not seem to exhibit a localization defect as dramatic as, for example, that of an ExxxLV mutant. The role of this residue in trafficking Vpu/tetherin complexes, potentially into clathrin-rich domains, remains therefore elusive due to conflicting results. Further investigation is necessary and might show a potential trafficking and/or AP-1/2 interaction defect of this mutant.

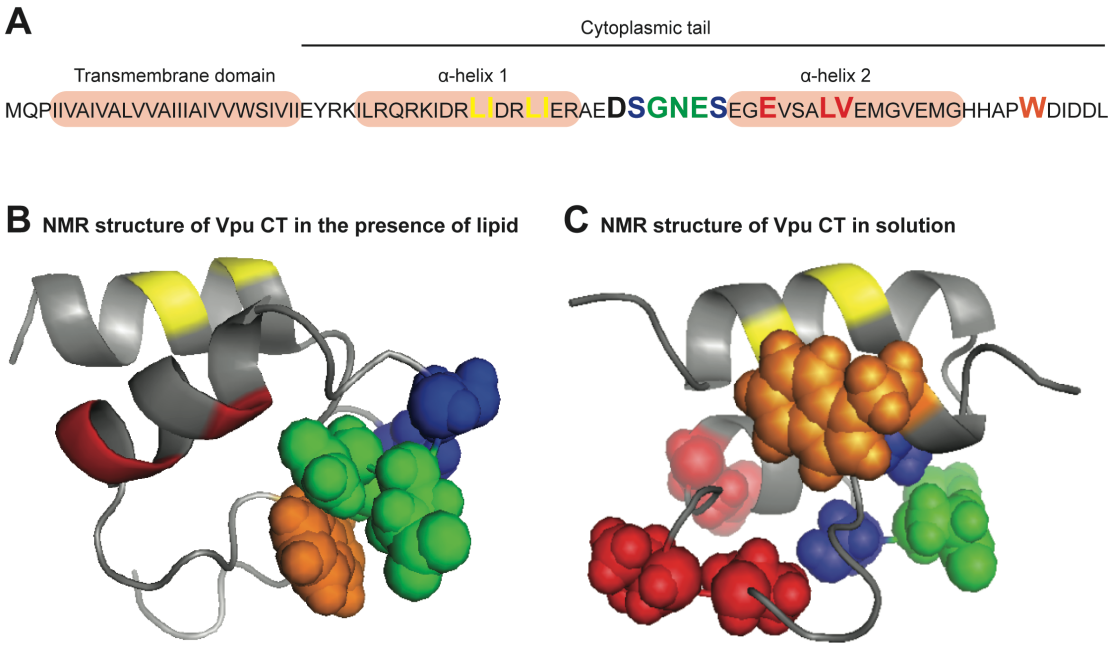

Figure 4.18 Important residues for the anti-tetherin function of Vpu. (**A**) Amino acid sequence of HIV-1 NL4.3 Vpu. Conserved residues that are required for tetherin counteraction are highlighted. (**B**) Structure of the cytoplasmic tail of Vpu in the presence of membrane simulating dodecylphosphatidylcholine (DPC) micelles obtained by high-resolution liquid state NMR. (**C**) Structure of the cytoplasmic tail of Vpu in aqueous buffer obtained by high-resolution liquid state NMR. (**B**) and (**C**) adapted from Wittlich et al., 2009. Highlighted motifs are colour-coordinated with (**A**), (Images were produced by Stuart Neil using PyMol version 1.7).

There is much indirect evidence that AP-1 is the major clathrin adaptor involved in Vpu-mediated tetherin antagonism. Vpu localizes predominantly to the TGN and blocks the transport of recycling tetherin to the plasma membrane (Schmidt et al. 2011; Dubé et al. 2011; Kueck & Neil 2012). Additionally, recently published structural data suggests that Vpu and tetherin can form a ternary complex with AP-1 (Jia et al. 2014). However, knockdown of AP-1 or other clathrin adaptors has no effect on Vpu function (Kueck & Neil 2012). Several orthologs exist for some subunits of AP-1 and there is potential redundancy in clathrin adaptor usage (Bonifacino & Traub 2003). Therefore, our observation that Vpu can also bind to AP-2 in an ExxxLV dependent manner is important. It potentially explains why neither of the clathrin adaptors have been identified as being essential for tetherin antagonism by Vpu, as lack of one clathrin adaptor might be compensated for by another (Mitchell et al. 2009; Kueck & Neil 2012). It also correlates with the weakly enhanced endocytosis of tetherin that has been reported (Dubé et al. 2011). Also, Vpu/tetherin chimeric proteins have been shown to be excluded from sites of viral budding at the cell surface, which is dependent on the ExxxLV motif. This may indicate AP-2-mediated trafficking and anchoring to

clathrin-rich domains at the plasma membrane (McNatt et al. 2013). However, tetherin's YDY motif cannot bind the AP-2 μ subunit because of a steric clash of Y6 in the binding pocket (Jia et al. 2014). This motif on the other hand has been shown to be essential in AP-1-mediated trafficking to the plasma membrane via the TGN and this is where Vpu most likely encounters the majority of the tetherin molecules (Rollason et al. 2007; Schmidt et al. 2011). AP-1 also mediates the transport between the TGN and endosomes and therefore it is likely to be the major clathrin adaptor involved in tetherin antagonism (Bonifacino & Traub 2003). Since the Vpu ExxxLV motif is dominant over the YDY tetherin motif it may be possible that Vpu/tetherin complexes that escape the transport from the TGN to endosomes and traffic to the plasma membrane would be endocytosed. This could be mediated by AP-2 as it has been shown for SIV Nef and HIV-2 Env (Zhang et al. 2011; Lau et al. 2011; Serra-Moreno et al. 2013). AP-2 binding can also possibly be the explanation for the residual activity of Vpu against short tetherin in the absence of surface downregulation that has been discussed in chapter 3 (Cocka & Bates 2012; Weinelt & Neil 2014). A combination of the events discussed above may be the reason for variable observations in the importance of surface downregulation in tetherin.

Even though degradation may be decoupled from counteracting tetherin's physical restriction, that does not mean that tetherin degradation does not play an important role for HIV-1 *in vivo*. Long human tetherin is able to induce NF-κB signalling upon virion retention and can lead to endocytosis and possibly virion degradation. This is potentially followed by enhanced antigen presentation and/or detection by pattern recognition receptors, which could explain the highly efficient antagonism of the long tetherin isoform by HIV-1 group M Vpus. Additionally, tetherin has been suggested to enhance antibody-dependent cell-mediated cytotoxicity (ADCC) and to be involved in modulating immune activation via interaction with the immunoglobulin-like transcript 7 (ILT7), both detrimental processes for a virus (Arias et al. 2014; Alvarez et al. 2014; Pham et al. 2014; Cao et al. 2009; Tavano et al. 2013; Bego et al. 2015). The LILI and ELV mutants remain able to bind β-TrCP so that ubiquitination of the STS motif would still occur. However, all Vpu trafficking mutants can still be rescued by clathrin box addition in cells expressing the STS tetherin mutant (Kueck et al. 2015). This suggests that clathrin-dependent mis-trafficking is the essential antagonistic step and is likely to occur before ubiquitination. Tetherin degradation could possibly be essential for HIV-1 *in vivo* to prevent recognition by the host, rather than to counteract the physical restriction imposed by tetherin.

Chapter 5 HIV-1 Nef Counteracts Serine Incorporators 5 and 3 That Restrict Virion Infectivity

Selected data presented in this chapter are part of the collaborative publication “Cell Surface Proteomic Map of HIV Infection Reveals Antagonism of Amino Acid Metabolism by Vpu and Nef” (Matheson et al. 2015).

5.1 Introduction

Nef is an accessory protein encoded by all primate lentiviruses including HIV-1. It is a 27 kDa protein that is myristoylated at its N-terminus and localizes predominantly to peri-nuclear compartments. Whilst it does not seem to be a crucial factor for replication in cell culture, it is required in primary cells and plays a fundamental role *in vivo* as a determinant of viral pathogenicity and in the development of AIDS (Kestler et al. 1991; Deacon et al. 1995; Kirchhoff et al. 1995). A range of functions have been ascribed to Nef. It is responsible for the downregulation of CD4 from the cell surface, which is dependent on clathrin-mediated endocytosis and is followed by its lysosomal degradation (Garcia & Miller 1991; Aiken et al. 1994; Rhee & Marsh 1994; Chaudhuri et al. 2007). Downregulation of CD4 has been suggested to prevent the exposure of HIV-1 Env epitopes and limit their susceptibility to ADCC (Veillette et al. 2014). Furthermore, Nef also induces the downregulation of other surface molecules such as HLA-A and HLA–B, but not HLA-C (Schwartz et al. 1996; Collins et al. 1998; Cohen et al. 1999). This protects infected cells from being targeted by cytotoxic T cells that recognize viral peptides presented by HLA-A or HLA-B. At the same time, natural killer (NK) cells are prevented from killing the infected cell due to inhibitory signals they receive from HLA-C still being expressed on the surface. Many primate lentiviral Nef proteins, including that of HIV-2, are also able to downregulate the T cell receptor complex, which protects infected cells from activation-induced cell death and has been correlated with non-pathogenic natural infections (Schindler et al. 2006). However, this function was lost in HIV-1 Nef, which potentially accounts for HIV-1’s increased pathogenicity. Another highly conserved function of Nef is its ability to increase the infectivity of virions (Chowers et al. 1995; Münch et al. 2007). This function seems to be important as it is highly conserved among lentiviruses and is maintained throughout disease progression (Münch et al. 2007; Carl et al. 2001). Similarly, the MLV protein glycoGag enhances the infectivity of Nef-deficient HIV-1 virions without any sequence homology to

Nef (Pizzato 2010). The requirement for both proteins depends on the cell type in which virus is produced (Pizzato 2010). Also, clathrin-mediated endocytosis and dynamin 2 have been shown to be essential for the infectivity-enhancing function in the producing cells suggesting a factor is removed from the plasma membrane (Craig et al. 1998; Pizzato et al. 2007). Furthermore, the Nef effect also depends on the envelope of the virus. Variable regions in HIV-1 Env determine the responsiveness to Nef, but it is independent of co-receptor usage and there is no Nef effect on Env abundance in virions (Lai et al. 2011; Usami & Göttlinger 2013; Miller et al. 1995). In addition, the pathway of virus entry determines the Nef responsiveness. Pseudotyping HIV-1 with envelopes from viruses that fuse at low pH, such as vesicular stomatitis virus G protein (VSV-G) or ebola virus glycoprotein (EBOV GP), has been reported to overcome the the infectivity block (Pizzato 2010; Miller et al. 1995; Aiken 1997; Chazal et al. 2001; Pizzato et al. 2008; Luo et al. 1998). Moreover, the effect of Nef on virus-cell fusion is limited and has been a matter of debate (Cavrois et al. 2004; Tobiume et al. 2003; Day et al. 2004).

Recent reports by two independent groups show that the cellular factor responsible for the infectivity block that is counteracted by Nef and glycoGag is SERINC5 (S5), and to a lesser extent SERINC3 (S3) (Usami et al. 2015; Rosa et al. 2015). Both proteins were also identified as targets of Nef in a SILAC-based plasma membrane profiling study conducted by our collaborators (Matheson et al. 2015). The data presented in this chapter were generated before the publication of those manuscripts, but after SERINC5/3 were revealed to be targets of HIV-1 Nef at the Cold Spring Harbor Laboratory Retroviruses meeting in May 2015.

SERINC3 and 5 belong to the SERINC family of transmembrane proteins, which is comprised of five members. They have been reported to be involved in the incorporation of serine into membrane lipids such as phosphatidylserine and sphingolipids (Inuzuka et al. 2005). However, their function is still largely unknown. S5 is highly expressed in T cell lines such as Jurkat TAg cells and primary CD4+ T cells, which impose an infectivity block on Nef-deficient HIV-1. Nef and glycoGag inhibit the incorporation of S5 into budding virions by downregulating it from the cell surface. However, the mechanism of S5-induced restriction remains unknown (Usami et al. 2015; Rosa et al. 2015).

In this chapter, the reported inhibitory effect of exogenous and endogenous SERINC5/3 on Nef-deficient virus was confirmed and the role of this newly identified antiviral factor was further

investigated. Four isoforms of SERINC5 and two isoforms of SERINC3 have been predicted. S5 isoforms differ at their C-terminus whereas S3 isoform 2 lacks 55 N-terminal residues compared to isoform 1. Only S5 isoform 4, however, seems to be able to induce a block to Nef-deficient virus. Furthermore, I examined a potential role of interferon-induced transmembrane (IFITM) proteins in SERINC function. This group of proteins has recently been shown to also restrict HIV-1 at the level of entry. However, the data generated so far do not suggest any synergistic effect.

5.2 Results

5.2.1 Exogenous SERINC5 Potently Reduces the Infectivity of Nef-Deficient Viral Particles

As mentioned before, our collaborators identified SERINC5 (S5) and 3 (S3) as targets of Nef in a stable isotope labelling with amino acids in cell culture (SILAC)-based proteomic screen (Matheson et al. 2015). CEM-T4 cells grown in the presence of heavy isotope labelled lysine and arginine were infected with WT, ΔVpu or ΔNef HIV-1 or transduced with single genes (Vpu or Nef). The peptides obtained from the different conditions were analysed by mass spectrometry and compared to mock infected or GFP transduced control cells grown in medium containing medium or light isotope labelled lysine or arginine. They found changes in the expression of known and unknown proteins on the plasma membrane, including S5 and S3, which are downregulated specifically in Nef expressing cells (Figure 5.1A).

Different assays were used to further investigate the effect of SERINC on HIV-1 infectivity (Figure 5.1 B). 293T cells with low endogenous levels of SERINC5/3 were transfected with HIV-1 NL4.3 proviral plasmid, SERINC5/3 expression vector and, where stated, various Env expression vectors. Alternatively, Jurkat TAg cells, which express high levels of SERINC5, were infected with infectious VSV-G pseudotyped HIV-1 NL4.3 virus. Cells were then incubated for 48 h before the infectivity of the virions in the supernatant was titered on target cells, TZMbl reporter cells. Depending on the Env expressed on and the presence of SERINC in the released virions infectivity is expected to be altered (Usami et al. 2015, Rosa et al. 2015).

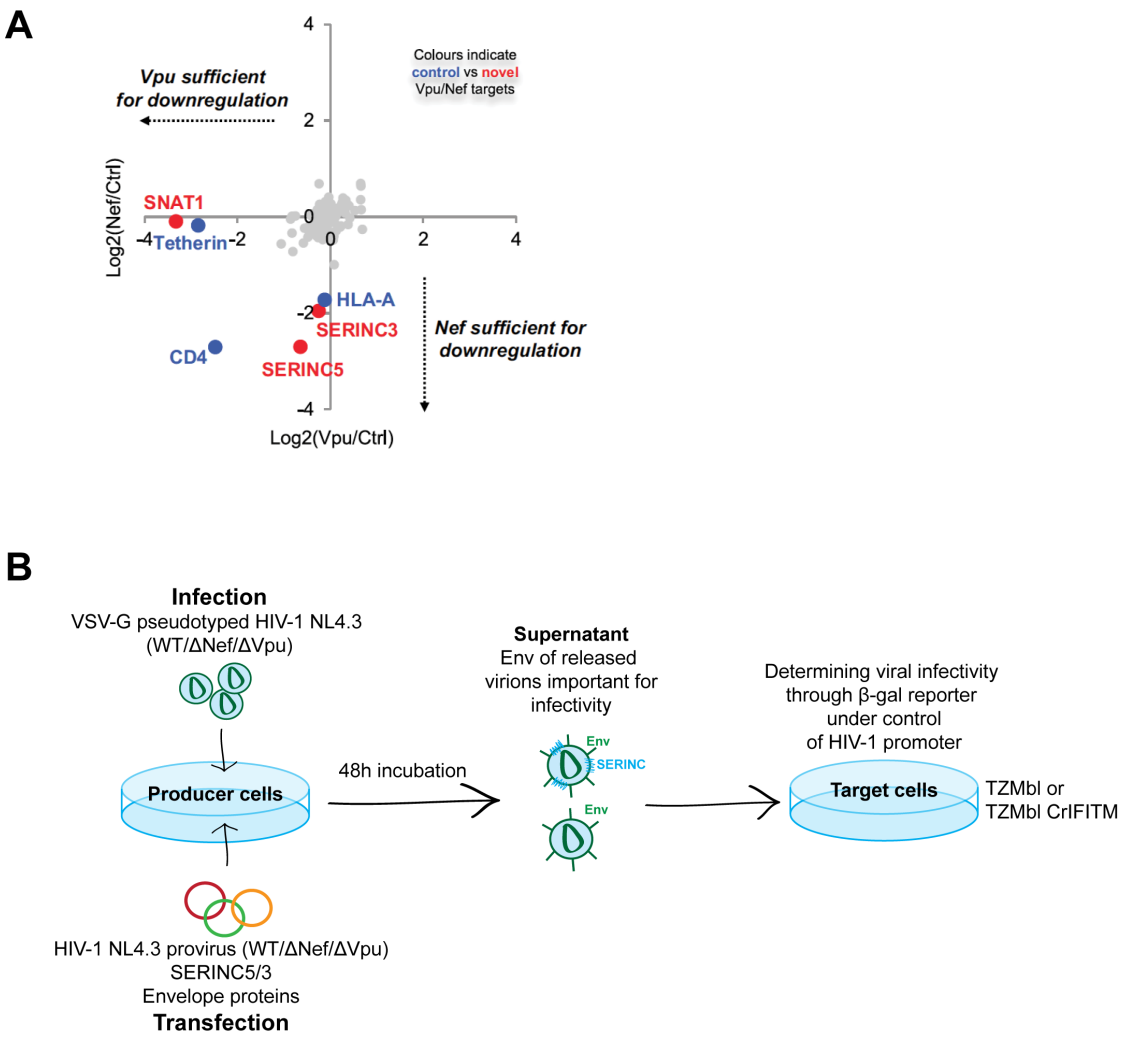

Figure 5.1 Identification of SERINC5/3 as a target of HIV-1 Nef and assay design. (**A**) Plasma membrane proteins in CEM-T4 cells transduced with Vpu (x axis) versus Nef (y axis) as single genes or CEM-T4 cells infected with Vpu-deficient versus Nef-deficient HIV-1 viruses (not shown) were quantified in a stable isotope labelling with amino acids in cell culture (SILAC)-based screen and compared to GFP-transduced or uninfected CEM-T4 cells. Known and novel plasma membrane proteins that are modulated by both HIV-1 Vpu and Nef (CD4) or by HIV-1 Vpu (tetherin, SNAT1) or HIV-1 Nef (HLA-A, SERINC3, SERINC5) only were identified (Matheson et al. 2015). (**B**) Design of assays conducted in this chapter. Producer cells, such as 293T or Jurkat TAg cells, were either infected with VSV-G pseudotyped HIV-1 NL4.3 or transfected with proviral constructs, SERINC expression vector and various envelope expression vectors, where applicable. Cells were then incubated for 48 h before the amount of infectious virus in the supernatant was determined using TZMbl reporter cells as target cells. Infectivity will be influenced by the Env expressed on the released virions and the presence of SERINC in virions.

To test the effect of exogenous S5 expression on infectious particle release of HIV-1, 293T cells were transiently transfected with a WT, Nef-deficient (ΔNef, mutation of start codon of Nef open reading frame), Vpu-deficient (ΔVpu) or Nef- and Vpu-deficient (ΔNefΔVpu) HIV-1 NL4.3 proviral construct and increasing amounts of S5 expression vector. The progeny virus from the 293T producer cells was then titered for infectivity on TZMbl reporter cells. 293T cells have been shown to express low levels of S5 and also S3 (Rosa et al. 2015). Even at 0 ng exogenous S5, ΔNef and ΔNefΔVpu exhibited reduced infectious virus yield compared to WT HIV-1 or the Vpu-

deficient virus (Figure 5.2 A and B). When exogenous S5 was expressed, the inhibition of ΔNef virus by S5 increased from 5-fold at 0 ng to 23-fold at only 10 ng of S5 expression vector. With increasing S5 expression levels the infectivity of WT virus also decreased slightly. There was, however, no difference in infectivity when Vpu was or or not expressed. This indicates that the SERINC effect is Nef-specific and independent of Vpu. This also suggests that the anti-SERINC activity of Nef is saturable, as WT infectivity was also reduced, but not to the same extent as ΔNef. S5 expression had no effect on intracellular virus protein production and physical virion release did not differ significantly between the different viruses (Figure 5.2 A and C). These results confirm the recently published data reporting that SERINC5 reduces viral infectivity, which can be overcome by Nef (Usami et al. 2015; Rosa et al. 2015).

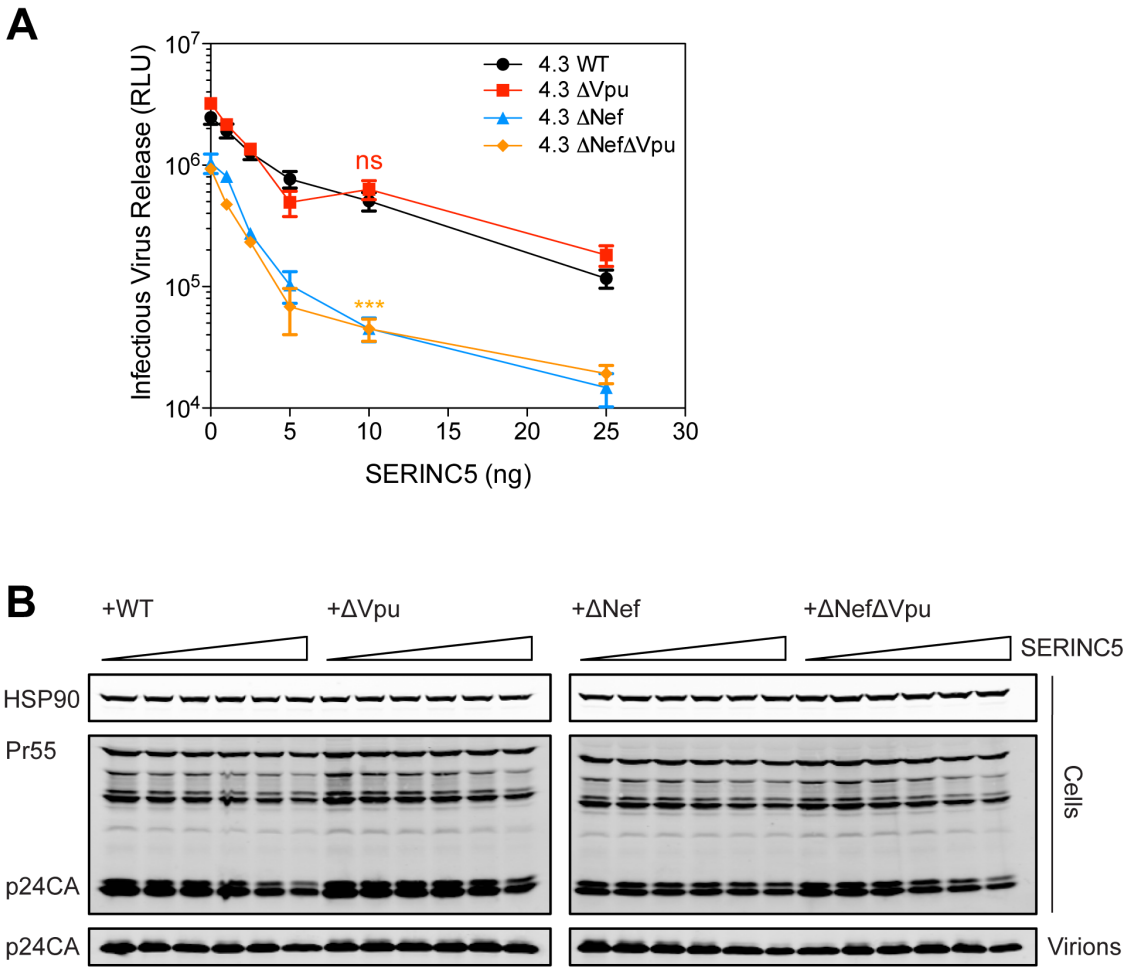

Figure 5.2 SERINC5 potently reduces the virion infectivity and is antagonised by Nef. (**A-B**) 293T producer cells were transfected with increasing amounts of SERINC5 and NL4.3WT, ΔVpu, ΔNef or ΔNefΔVpu proviral plasmid. (**A**) At 48 h posttransfection, infectious virus release was determined with TZM-bl HeLa reporter cells as target cells. Error bars represent standard deviations of the means of three independent experiments. RLU, relative light units. Asterisks represent the p value for the difference in virus infectivity of a Nef-deficient HIV-1 (ΔNef; orange) or Vpu-deficient HIV-1 (ΔVpu; red) compared to WT HIV-1 NL4.3 in the presence of 10 ng SERINC5 expression vector as titered on TZMbl reporter cells. ns, not significant; ***p<0.001 as determined by two-tailed t test. (**B**) Cell lysates and pelleted viral supernatants from panel A were subjected to SDS-PAGE and analyzed by Western blotting for Hsp90 and p24 CA.

5.2.2 Knockout of Endogenous SERINC3 and SERINC5 Rescues the Infectivity of Nef-Deficient Virus

Primary T cells as well as many T cell lines, including Jurkat TAg (JTAg), have been reported to express high levels of S5 and also S3. It was next tested whether knockout of S5 or S3 in JTAg cells would relieve the inhibiting effect on ΔNef virus. Using the clustered regularly interspaced short palindromic repeat (CRISPR)-Cas9 system, JTAg knockout cells for S5 or S3 were generated (Mali et al. 2013). The guide RNAs for both S5 and S3 targeted the first exon of the genes (S5 (GenBank NM_001174072.2) guide sequence: ATGTCAGCTCAGTGCTGTGC; S3 (GenBank NM_006811.2) guide sequence: GTGTCTTCTCCCTCGCCAGC). A guide RNA targeting luciferase (Luc) served as a non-targeting control. JTAg cells were transduced with virus-like particles containing the lentiCRISPR with expression cassettes for Cas9 and the guide RNAs followed by puromycin selection. JTAg parental cells and bulk populations of the surviving Luc, S3 or S5 knockout cells were infected with VSV-G pseudotyped HIV-1 NL4.3 WT or a Nef and/or Vpu deficient virus at an MOI of 1. Viral supernatants were titered 48 h later on TZMbl reporter cells. A 37-fold reduction in infectious virus release of the Nef-deficient virus in parental JTAg and Luc control cells could be observed compared to WT virus (Figure 5.3 A). When S5 was knocked out, viral infectivity of ΔNef increased 17-fold whereas it only increased 3-fold for WT HIV-1. In keeping with previous reports, S3 knockout had a milder 4-fold effect on ΔNef infectious virus release. Again, no difference in infectivity was observed between WT and ΔVpu virus in all cell lines, confirming that Vpu has no role in S5/3 counteraction. As with the transient expression of S5, S3 and S5 knockout had no effect on intracellular virus production or physical virion release (Figure 5.3 B).

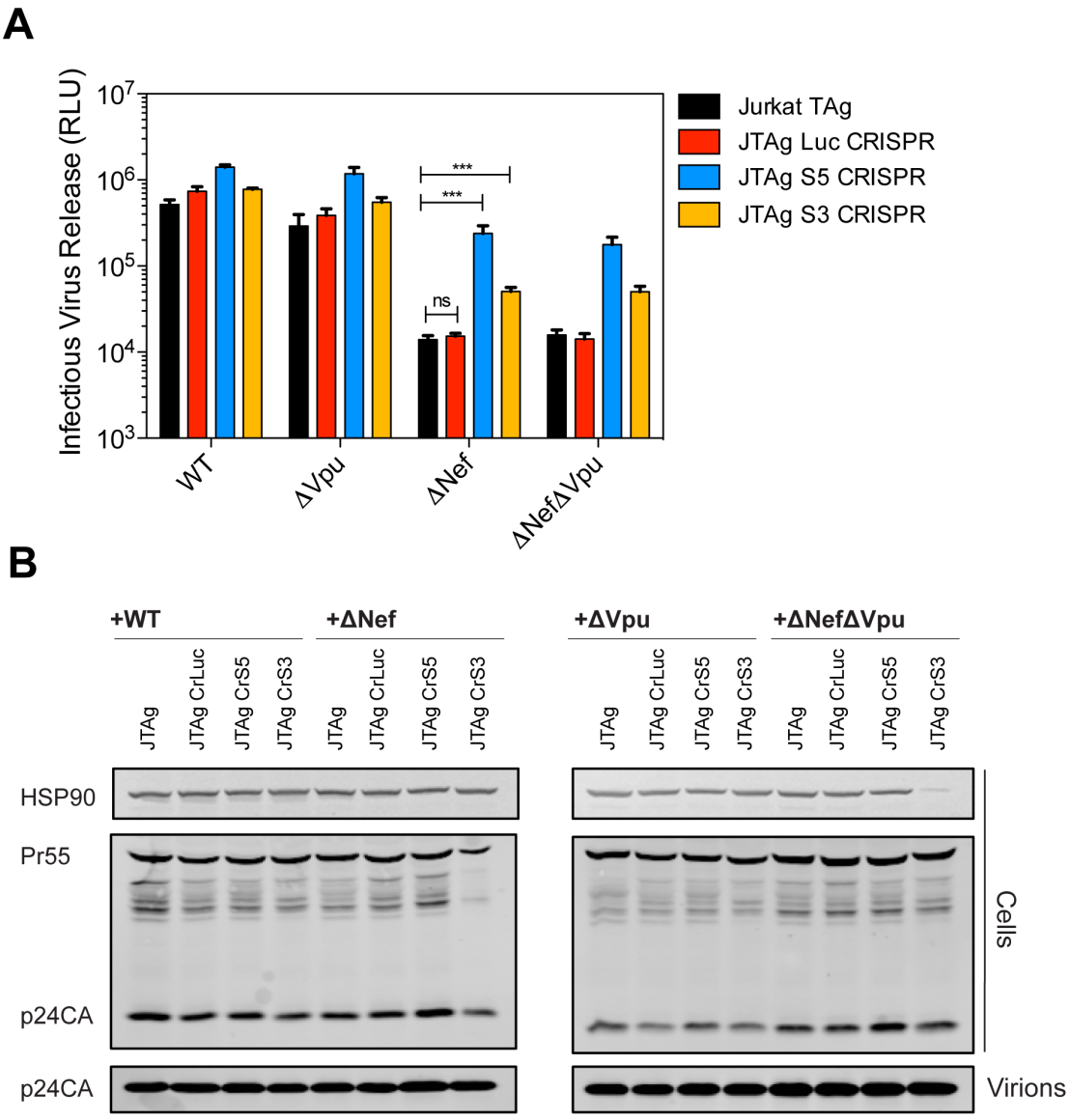

Figure 5.3 Endogenous SERINC5 and SERINC3 restrict viral infectivity in infected CD4+ T cells (**A and B**) Jurkat TAg cells or Jurkat TAg cells stably expressing a lentiviral vector containing CRISPR-Cas9 with a guide RNA sequence targeting the SERINC5 or SERINC3 or a control guide RNA (luciferase; Luc) were infected with VSV-G pseudotyped HIV-1 NL4.3WT, ΔNef, ΔVpu or ΔNefΔVpu at an MOI of 1 for 48 h. (**A**) Infectious virus release into the supernatant of the JTAg cells was determined using TZM-bl HeLa reporter cells as target cells. Error bars represent standard deviations of the means of four independent experiments. RLU, relative light units. Asterisks represent the p value for the difference in virus infectivity of a Nef-deficient HIV-1 (ΔNef) in the presence or absence of SERINC5/3 as titered on TZMbl cells. ns, not significant; ***p<0.001 as determined by two-tailed t test. (**B**) Cell lysates and pelleted viral supernatants from panel A were subjected to SDS-PAGE and analyzed by Western blotting for Hsp90 and p24 CA.

Single cell clones were generated from the bulk knockout cell populations by flow cytometry single cell sorting. Nine (Luc) or ten (S5 and S3) clones were infected as described for Figure 5.3. with VSV-G pseudotyped WT or ΔNef NL4.3 virus and infectious virus release was titered on TZMbl cells. As expected, ΔNef infectivity was reduced in all Luc-knockout control JTAg cell clones (Figure 5.4 A upper panel). This restriction was relieved by knocking out S5 or S3 in all single cell clones (Figure 5.4 A middle and lower panel). However, the difference in ΔNef release between parental cells and S5/3 knockout cells seemed to be smaller in this experiment. None of the knockouts had a significant effect on WT HIV-1. The single cell clones can now be used to verify the CRISPR-Cas9 knockout on a genomic level.

Altogether, these data confirm that endogenous SERINC5 and SERINC3 restrict the release of infectious virus, which is counteracted by Nef.

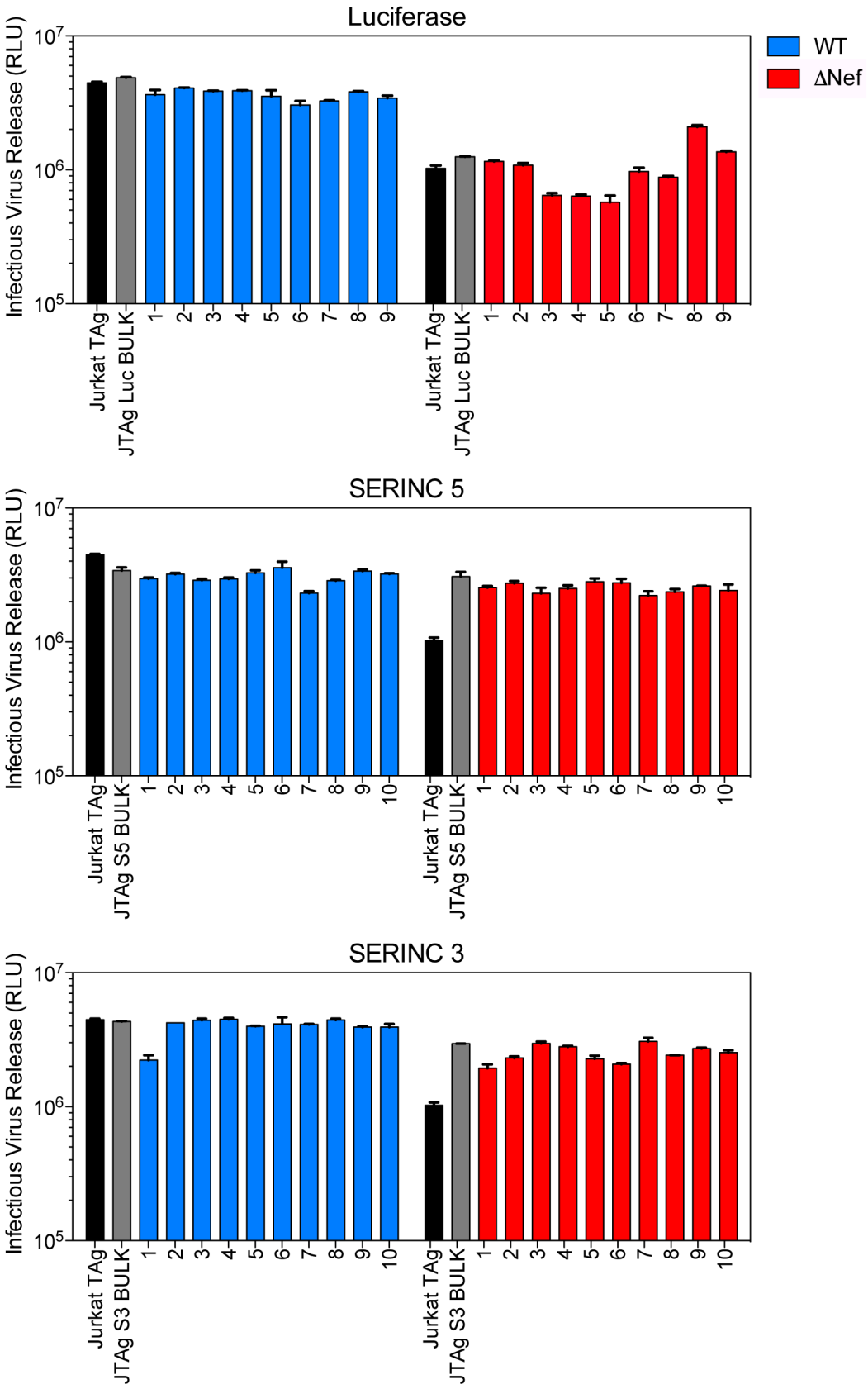

Figure 5.4 Infection of single cell clones of SERINC depleted Jurkat TAg cells. Jurkat TAg cells or Jurkat TAg cells stably expressing a lentiviral vector containing CRISPR-Cas9 with a guide RNA sequence targeting the SERINC5 or SERINC3 or a control guide RNA (luciferase; Luc) and single cell clones thereof were infected with VSV-G- pseudotyped HIV-1 NL4.3WT, ΔNef, ΔVpu or ΔNefΔVpu at an MOI of 1 for 48 h. Infectious virus release was determined with TZM-bl HeLa reporter cells. Error bars represent standard deviations of the means of duplicates from one experiment. RLU, relative light units.

5.2.3 Envelopes From Viruses That Fuse at Low pH Are Insensitive to SERINC5

Envelopes from viruses that fuse at a low pH, such as VSV-G or EBOV GP, have been reported to be resistant to the block to infectivity that is relieved by Nef (Aiken 1997; Chazal et al. 2001; Luo et al. 1998). To test whether those envelope proteins were also resistant to SERINC5 expression, WT and Nef-deficient provirus were transiently co-transfected with increasing amounts of SERINC5 expression vector. Additionally, VSV-G envelope expression or empty vector were transfected and infectious virus was titered on TZMbl cells. Again, viral infectivity of ΔNef decreased considerably with increasing amounts of S5, whereas WT NL4.3 was less affected (Figure 5.5 A). Physical particle release from 293T cells did not change significantly for any virus (Figure 5.5 B). When VSV-G was added, the restricting effect of S5 was completely absent at all S5 expression levels (Figure 5.5 A (dashed lines) and B). Also, for this level of VSV-G expression, no saturation was observed, compared to non-pseudotyped WT HIV-1. Similarly to the effect of VSV-G, EBOV GP pseudotyping rendered both WT and Nef-defective HIV-1 NL4.3 completely resistant to SERINC5 expression (Figure 5.6 A). These findings are in keeping with the recently published results. Nef does not provide the same level of resistance to S5 as VSV-G or EBOV GP pseudotypes. Whether this resistance is for example conferred by the route of entry or the amount and property of envelope proteins on the surface is unknown and requires further investigation.

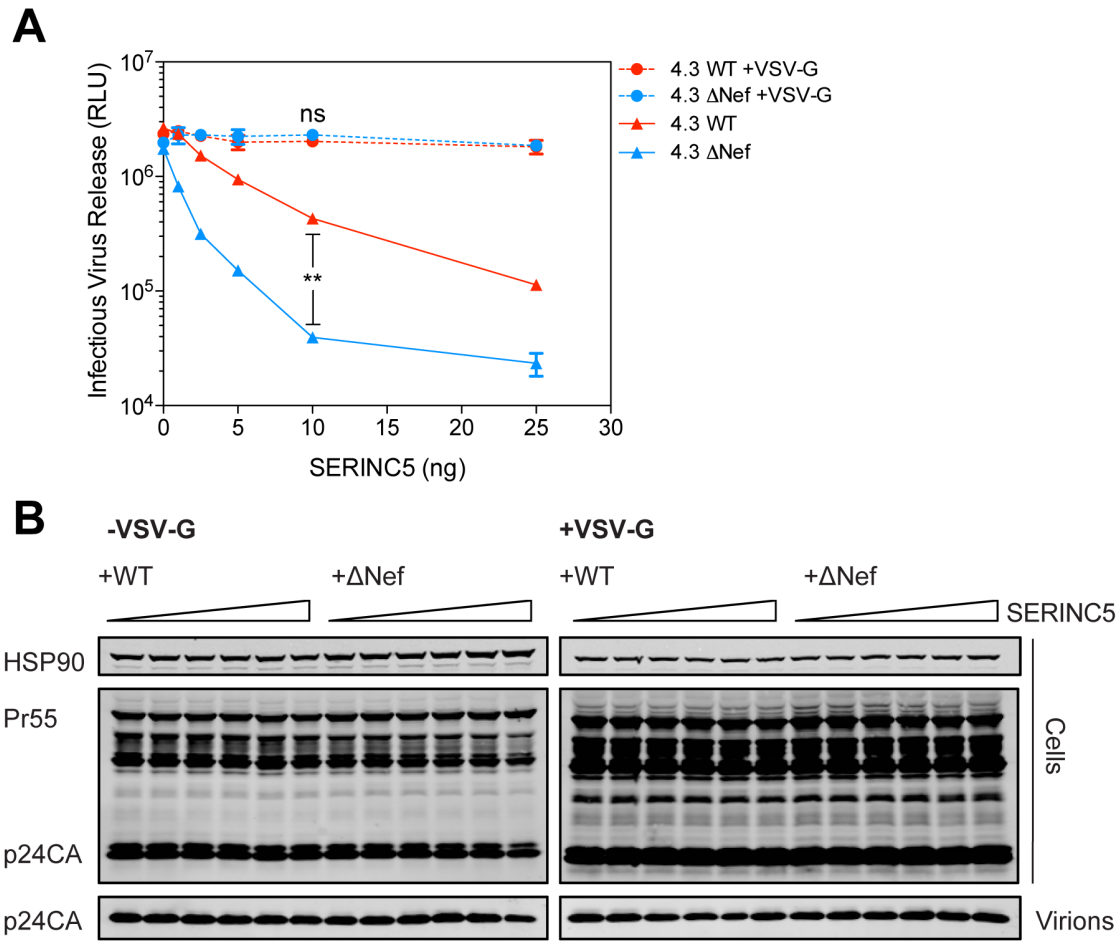

Figure 5.5 VSV-G pseudotyping rescues the infectivity defect of Nef-deficient virus. (**A-B**) 293T producer cells were transfected with increasing amounts of SERINC5 expression vector and NL4.3WT or a ΔNef proviral plasmid plus or minus 200 ng VSV-G expression vector. (**A**) At 48 h post transfection, infectious virus release was determined on TZM-bl target cells. Dashed lines, plus VSV-G; solid lines, without VSV-G. Error bars represent standard deviations of the means of duplicates from one experiment. RLU, relative light units. Asterisks represent the p value for the difference in virus infectivity of WT HIV-1 NL4.3 and the Nef-deficient HIV-1 NL4.3 (ΔNef) plus or minus VSV-G pseudotyping at 10 ng SERINC5 expression vector as titered on TZMbl target cells. ns, not significant; **p<0.01 as determined by two-tailed t test. (**B**) Cell lysates and pelleted viral supernatants from panel A were subjected to SDS-PAGE and analyzed by Western blotting for Hsp90 and p24 CA.

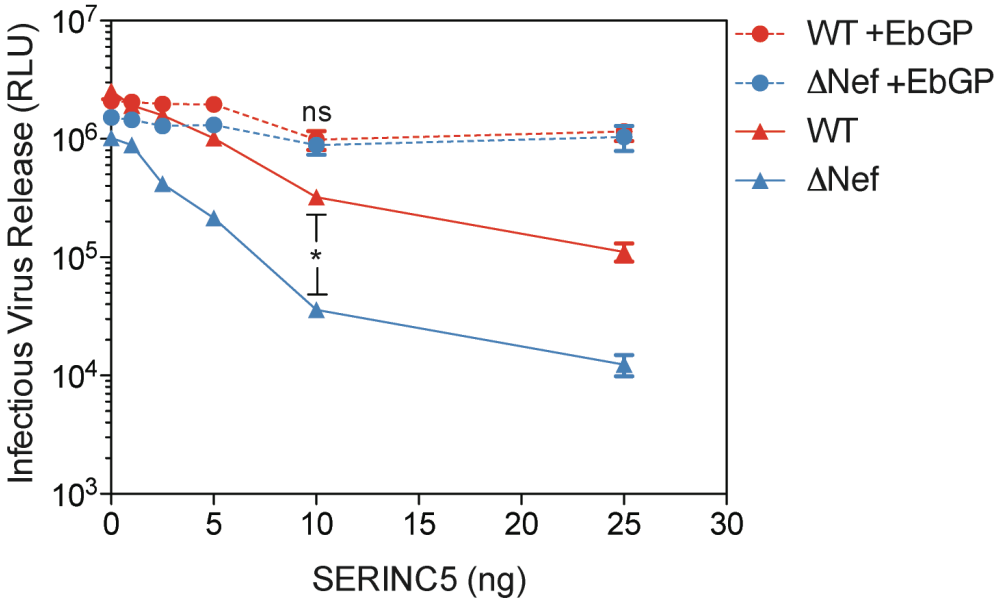

Figure 5.6 EBOV GP pseudotyping rescues the infectivity defect of Nef-deficient virus. 293T cells were transfected with increasing amounts of SERINC5 expression vector and NL4.3WT or a ΔNef proviral plasmid plus or minus 200 ng EBOV GP expression vector. At 48 h post transfection, infectious virus release was determined with TZM-bl HeLa reporter cells. Error bars represent standard deviations of the means of duplicates from one experiment. RLU, relative light units. Asterisks represent the p value for the difference in virus infectivity of WT HIV-1 NL4.3 and the Nef-deficient HIV-1 NL4.3 (ΔNef) plus or minus EbGP pseudotyping at 10 ng SERINC5 expression vector as titered on TZMbl target cells. ns, not significant; **p<0.01 as determined by two-tailed t test.

Viruses that fuse with the target cell in a pH-independent manner, such as HIV, have been reported to be responsive to Nef expression. Therefore, the effect of SERINC5 on other pH-independent envelopes was tested using measles virus (MV) and xenotropic murine leukemia virus-related virus (XMRV) envelopes (Lamb 1993; Côté et al. 2012). XMRV is a recombinant gammaretrovirus that was probably generated during passages of human prostate tumors in nude mice harbouring endogenous MLV proviruses, and its envelope shares significant sequence homology with xenotropic and polytropic MLVs (Paprotka et al. 2011). XMRV envelope expression or empty vector were transfected into 293T cells with provirus and increasing amounts of S5, and infectious virus release was titered 48 h later on TZMbl reporter cells. Whereas ΔNef HIV-1 infectivity decreased with increasing amounts of S5, co-expression of XMRV Env seemed to counteract this effect to a certain extent and also appeared to increase the infectivity of WT virus. However, XMRV Env did not overcome the S5 induced difference in infectivity between WT and ΔNef virus (Figure 5.7 A). Potentially, this may be an effect of XMRV Env overexpression rather than this Env's ability to counteract S5 function. Expression of Nef and XMRV Env at the same time

abrogated the saturating effect of S5 compared to when WT HIV-1 Nef only was expressed. This assay will be repeated, to confirm this result.

For MV, both the fusion (F) protein and hemagglutinin (H) are required to induce fusion with the target cell. Both components were co-transfected to equal amounts into 293T cells along with provirus and increasing amounts of S5 expression vector. In contrast to XMRV Env, the expression of MV F and H increased the inhibitory effect of S5 even further for both WT and ΔNef HIV-1, although, the additional effect on infectious virus release of the ΔNef virus was larger (Figure 5.7 B).

These results indicate that the lack of Nef-responsiveness reported for pH-dependent viruses, correlates with their envelopes' resistance to S5. The two other envelope proteins from pH-independent viruses tested here, seem to be differentially affected by S5. Whereas measles envelopes increased the restrictive effect of S5 on infectivity, XMRV Env relieved the inhibitory effect to a certain extent. However, it was not able to overcome the difference in infectivity between WT and ΔNef HIV-1.

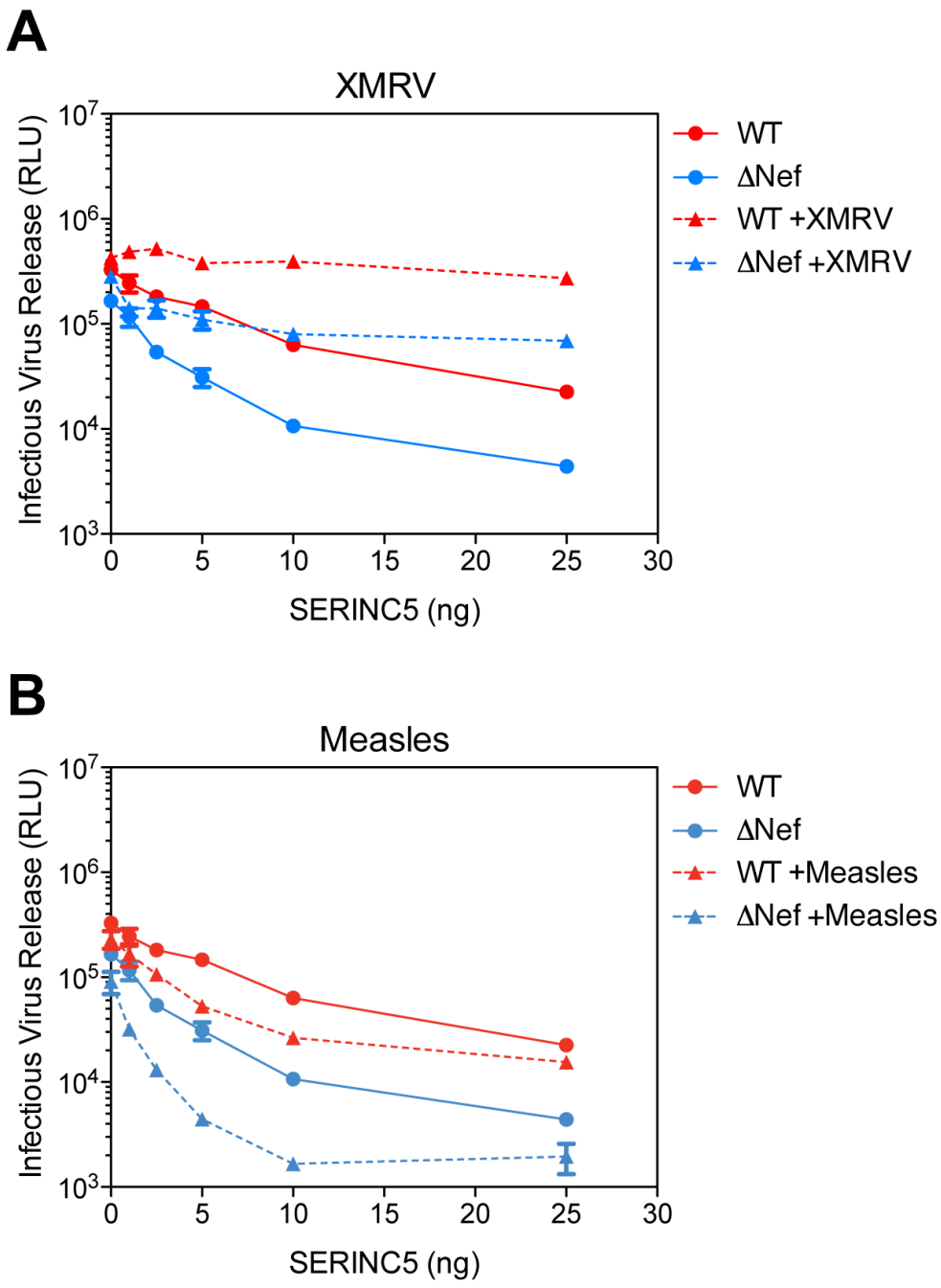

Figure 5.7 XMRV and MV envelopes do not overcome the S5-imposed restriction on Nef-deficient virus. (**A**) 293T cells were transfected with increasing amounts of SERINC5 expression vector and NL4.3WT or a ΔNef proviral plasmid plus or minus 200 ng XMRV Env expression vector. At 48 h post transfection, infectious virus release was determined with TZM-bl HeLa reporter cells. RLU, relative light units. (**B**) 293T cells were transfected as in (**A**) plus or minus 100 ng measles hemagglutinin and 100 ng fusion protein expression vector. Infectious virus was titered as in (**A**).

5.2.4 SERINC3 and SERINC5 Isoforms Have Differential Effects on HIV-1 Infectivity

Several isoforms of SERINC5 and SERINC3 have been proposed (Gerhard et al. 2004, Ota et al. 2004). Four isoforms of S5 are predicted that differ in their C-terminus (Figure 5.8). In all previous experiments, isoform 4 has been used. This is the longest of all predicted S5 isoforms and, according to Uniprot.org (accession number: Q86VE9), contains an extra transmembrane domain culminating in a total of ten. For S3, two isoforms have been predicted that differ in the first 55 N-terminal amino acids with isoform 2 lacking the first 55 amino acids, compared to isoform 1 (Figure 5.9). All 55 residues are predicted to be in an extracellular domain (Uniprot.org, accession number: Q13530).

Different isoforms may potentially have different antiviral roles, as observed in Chapter 3 with tetherin. Therefore, all SERINC isoforms were tested for their ability to block the infectivity of Nef-deficient virus.

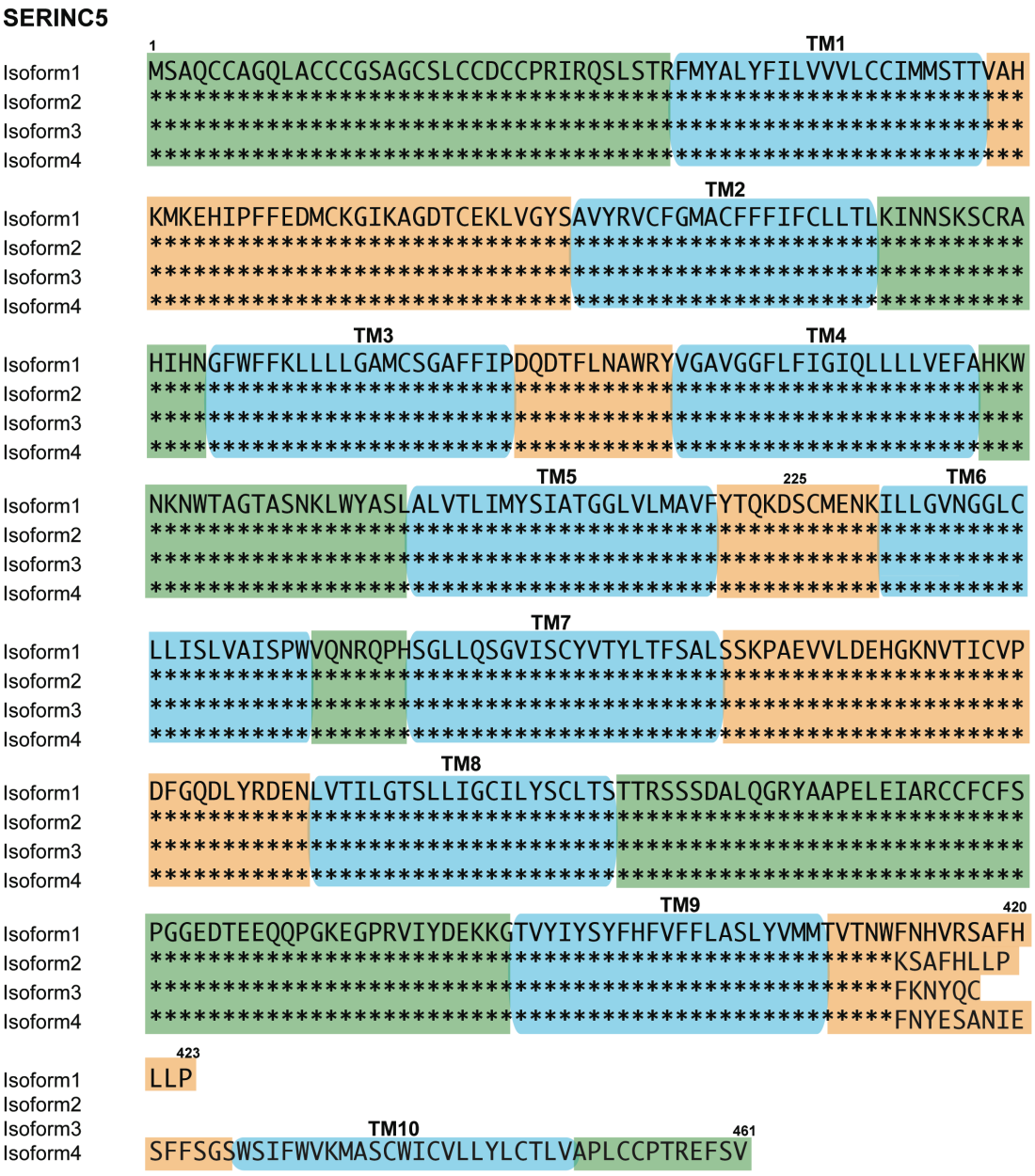

Figure 5.8 Amino acid sequence alignment of SERINC5 isoforms. Four isoforms have been predicted for SERINC5 (GenBank accession numbers for I1: NM_178276.6, I2: NM_001174071.2, I3: BC101281.3, I4: NM_001174072.2). They differ in the length and sequence of their C-terminus. Topology indicated according to Uniprot.org. Green, extracellular domain; orange, cytoplasmic domain; blue, transmembrane (TM) domain, number of TM domain is indicated. Numbers indicate amino acid position. Asterisks indicate sequence identity.

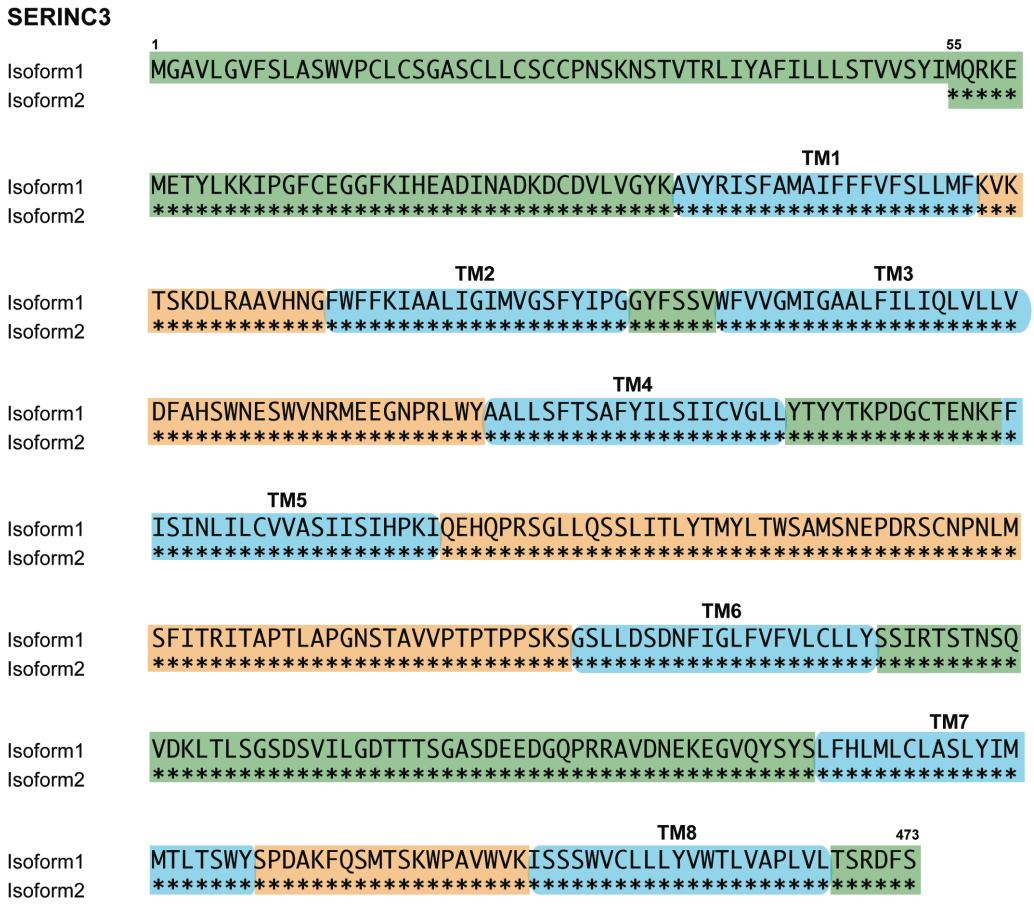

Figure 5.9 Amino acid sequence alignment of SERINC3 isoforms. Two isoforms have been predicted for SERINC3 (GenBank accession numbers for I1: NM_006811.2, I2: AK300618.1). They differ in the length of their N-terminus. Topology indicated according to Uniprot.org. Green, extracellular domain; orange, cytoplasmic domain; blue, transmembrane (TM) domain, number of TM domain is indicated. Numbers indicate amino acid position. Asterisks indicate sequence identity.

Similar to the assays performed previously, WT or ΔNef NL4.3 provirus were transiently co-transfected with increasing amounts of the SERINC isoforms into 293T cells. Infectious virus release was then assessed 48 h later on TZMbl cells. As expected, increasing amounts of S5 isoform 4, which has already been used throughout this chapter, decreased virion infectivity of Nef-deficient virus in a dose-dependent manner and also had some effect on WT HIV-1 (Figure 5.10 A). In contrast, all other S5 isoforms seemed to have little to no effect on the infectivity of Nef-deficient or WT virus. Included in this assay was a mutant of S5 isoform 4, S225G. SERINC5 proteins are very well conserved among primates including chimpanzees, gorillas, rhesus macaques and sooty mangabeys. Amino acid sequence alignment of their S5 proteins showed that there is a highly conserved glycine at position 225 in a cytoplasmic domain of all the non-human primate sequences mentioned before (Figure 5.11). However, in humans this residue has changed

to a serine. To assess whether mutation of this residue to a glycine would alter its antiviral activity, this mutant was included in this assay. However, mutation of G225 had no effect on viral infectivity (Figure 5.10 A). S3 isoforms were also tested for their effect on infectious virus release. S3 is reported to play only a limited role in the infectivity defect of Nef-deficient virus and T cell lines and primary T cells express less S3 than S5. 293T cells, on the other hand, intrinsically express more S3 than S5. Transient, exogenous expression of S3 isoforms in 293T cells had no effect on WT HIV-1 and only limited effect on ΔNef infectivity (Figure 5.10 B). All S5 and S3 isoforms were N-terminally HA-tagged and were well expressed (Figure 5.10 C).

These data suggest that there is differential sensitivity of ΔNef virus to the different SERINC isoforms. They further indicate that the inhibitory function of S5 isoform 4, that has been used throughout this chapter and also in the recent publications, is determined by residues in the C-terminus of the protein that are absent in all other S5 isoforms. Isoform 4 is predicted to have one additional transmembrane domain and a C-terminal extracellular domain. Truncation of these domains will aid in finding the determinants of S5 function. Furthermore, it will be interesting to see whether the difference in inhibition is perhaps due to differential localization of the proteins or incorporation into virions.

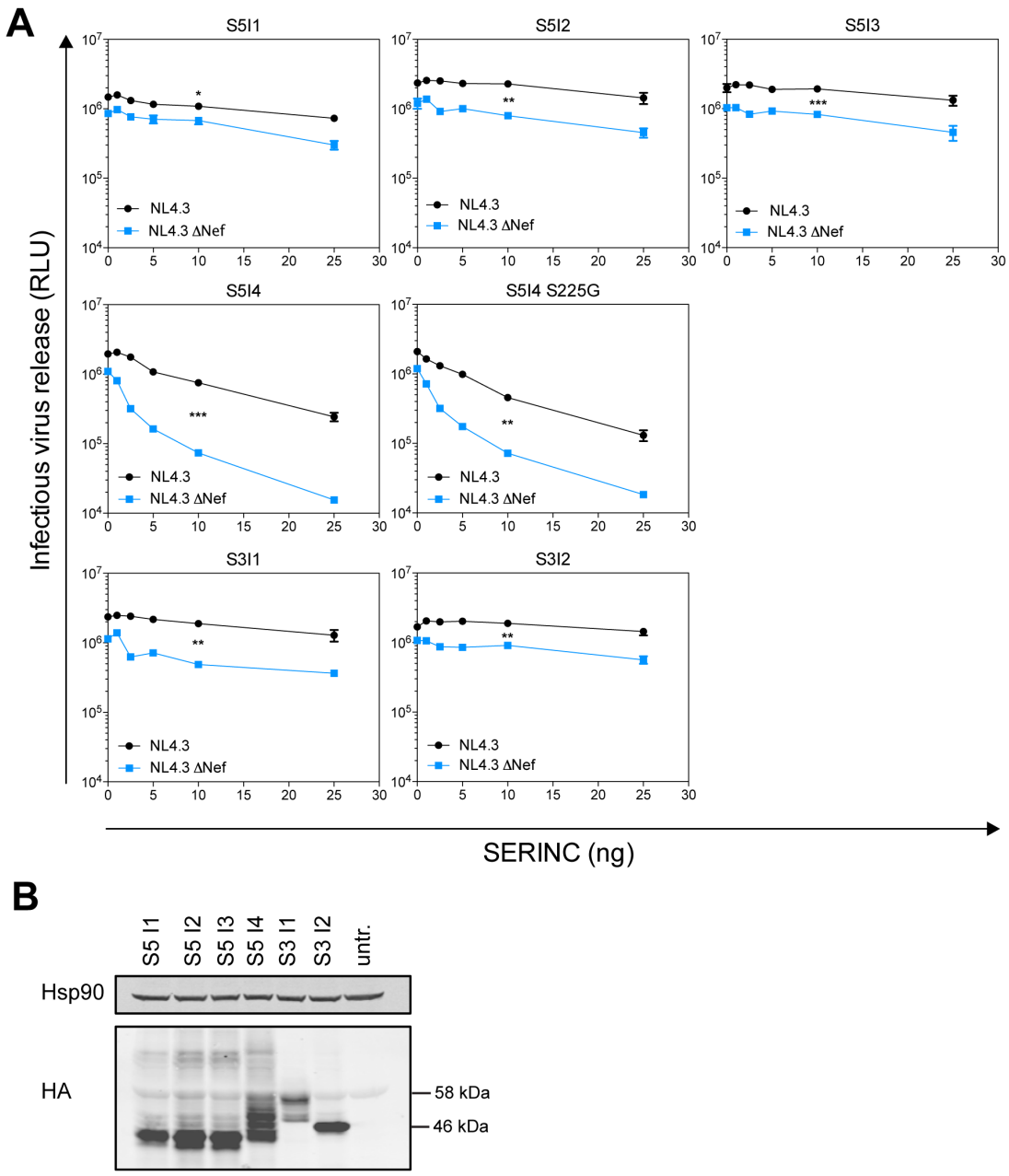

Figure 5.10 SERINC Isoforms have differential effects on virion infectivity. (**A and B**) 293T producer cells were transfected with increasing amounts of S5 isoforms and NL4.3WT or ΔNef proviral plasmid. (**A**) At 48 h post transfection, infectious virus release was determined with TZM-bl HeLa reporter cells as target cells. RLU, relative light units. Asterisks represent the p value for the difference in virus infectivity between WT and ΔNef virions at 10 ng SERINC expression vector titered on TZMbl cells. *p<0.05, **p<0.01, ***p<0.001 as determined by two-tailed t test. (**B**) Cell lysates from 293T cells transfected with HA-SERINC constructs for 24 h were subjected to SDS-PAGE and analyzed by Western blotting for Hsp90 and HA-SERINC.

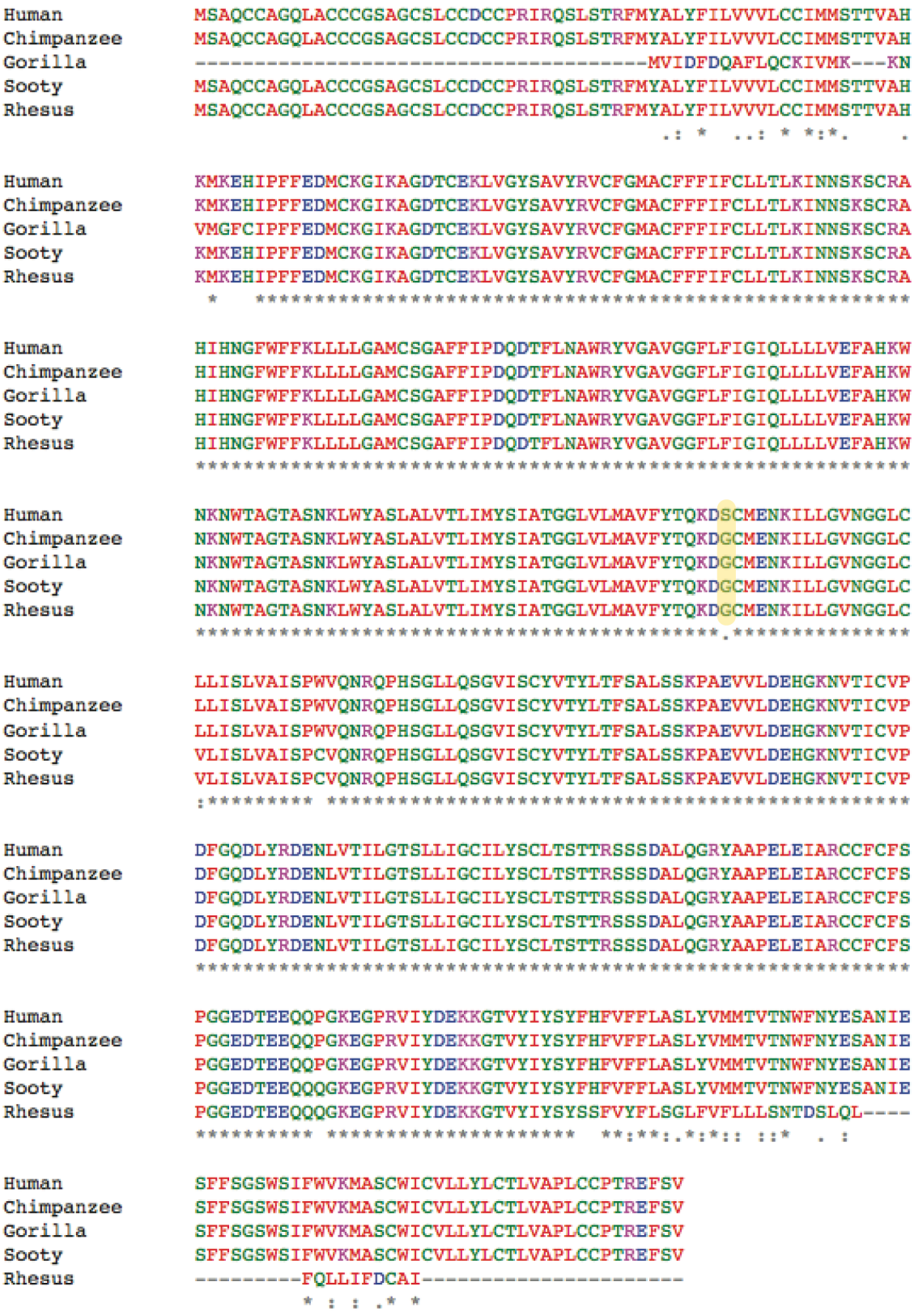

Figure 5.11 Alignment of primate SERINC5 amino acid sequences. Human (NP_001167543.1), chimpanzee (XP_001136963.1), gorilla (XP_004058691.1), sooty mangabey (XP_011944576.1) and rhesus macaque (XP_001109947.2) SERINC5 amino acid sequences were aligned. Serine/glycine 225 is highlighted in yellow. Alignment was generated using Clustal Omega.

5.2.5 IFITM Proteins Do Not Influence the SERINC5-Induced Infectivity Defect

Interferon-induced transmembrane (IFITM) proteins have been shown to inhibit a broad range of viruses including influenza A, hepatitis C virus, Ebola virus, Dengue virus, VSV and HIV-1 (Perreira et al. 2013; Weidner et al. 2010; Lu et al. 2011). Their mechanism of action is still not understood. However, it has been suggested that they inhibit virus-cell fusion in target cells expressing IFITMs (Lu, 2010, JVI). Furthermore, it has been shown that IFITMs get incorporated into budding HIV-1 virions, which then potentially inhibit the infection of target cells (Compton et al. 2014; Tartour et al. 2014). In contrast, it was also recently proposed that it is not the incorporation that reduces infectivity, but rather the effect of IFITMs on Env processing and the inhibition of cell-to-cell transmission (Yu et al. 2015). S5 was shown to be incorporated into Nef-deficient virions and it was suggested that this incorporation is responsible for the inhibition of infection of target cells at early stages (Usami et al. 2015; Rosa et al. 2015). Both protein families have been proposed to inhibit viruses at the entry stage, and therefore it seemed reasonable to hypothesize that there was a synergistic effect of S5 and IFITMs on viral infectivity. To test this, producer 293T cells were transiently transfected as before with different proviral constructs and increasing amounts of S5 expression vector. 48 h post transfection the infectivity of viral supernatants was determined on target cells, TZMbl reporter cells (TZM) or TZMbl reporter cells knocked out for IFITM1, 2 and 3 (TZM CrIFITM) simultaneously, using the CRISPR-Cas9 system. Infectious virus titers revealed that there was no additional effect on viral infectivity when target cells expressed IFITMs or not (Figure 5.12 A, solid lines versus dashed lines). Similarly, the SERINC5/3 positive or negative Jurkat TAg cells were infected as described in Figure 5.3 and viral titers were analysed for infectivity on TZMbl or TZMbl IFITM negative cells. Again, no significant difference in infectivity was seen between supernatants titered on TZMbl cells or TZMbl cells containing the IFITM knockout (TZM CrIFITM) (Figure 5.12 B).

These data suggest that there is no synergistic effect on viral infectivity of SERINC5 or 3 and IFITMs expressed on target cells. However, these experiments do not rule out that there may be an effect of IFITMs expressed in the producer Jurkat TAg cells. Furthermore, the inhibitory effects seen for IFITMs are generally not more than 2-fold. Due to the significantly larger SERINC effect the IFITM effects might therefore be masked.

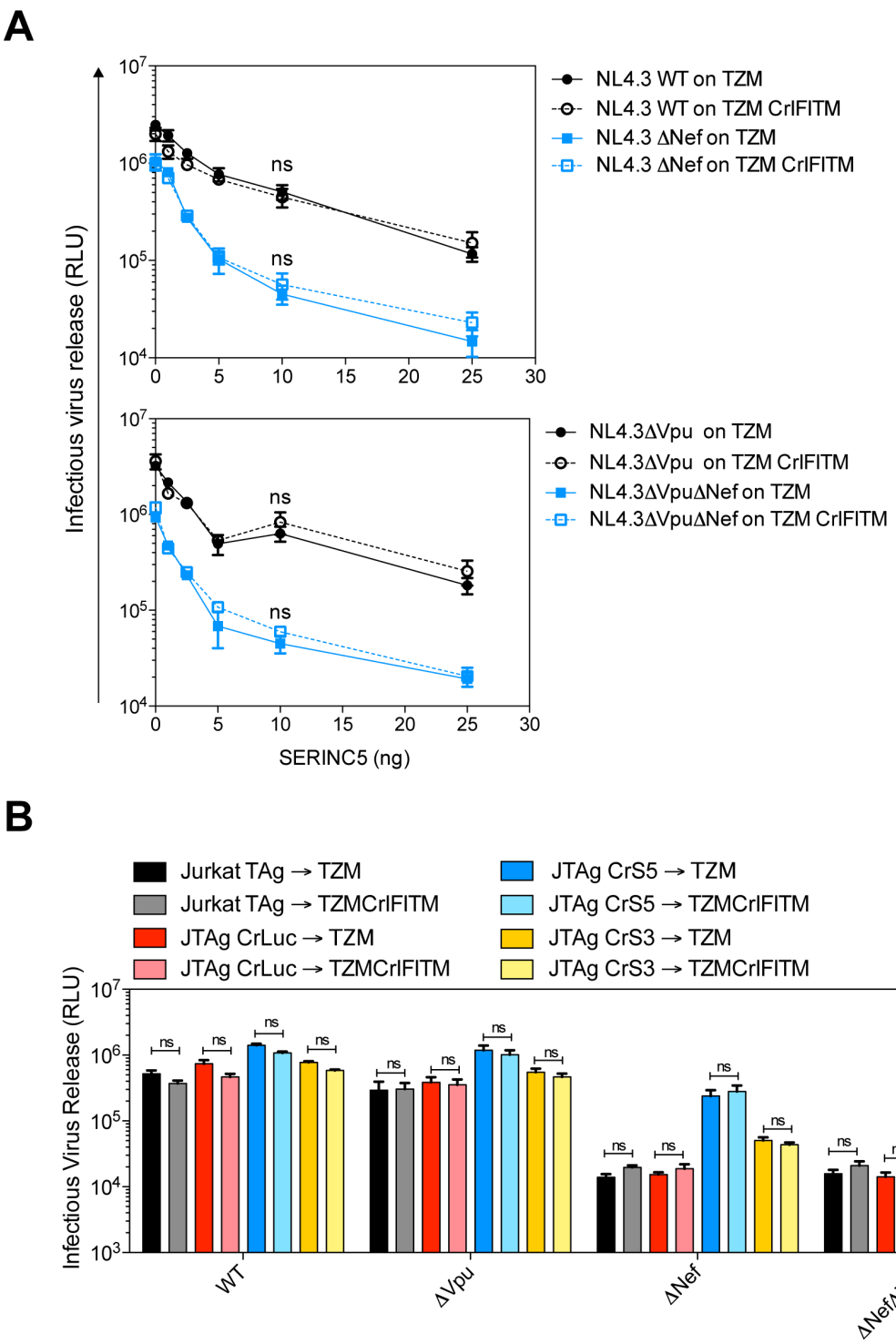

Figure 5.12 Role of IFITMs in SERINC mediated restriction. (**A**) 293T cells were transfected with increasing amounts of S5 and NL4.3WT, ΔVpu, ΔNef or ΔNefΔVpu proviral plasmid. At 48 h post transfection, infectious virus release was determined using TZM-bl reporter cells or the same cells stably expressing lentiviral vectors containing CRISPR-Cas9 with a guide RNA sequence targeting IFITM1, 2 and 3. Error bars represent standard deviations of the means of four independent experiments. RLU, relative light units. Solid lines, TZMbl (TZM); dashed lines, TZMbl CRISPR IFITM (TZM CrIFITM). Asterisks represent the p value for the difference in virus infectivity titered on TZMbl cells or TZMbl CrIFITM cells. ns, not significant as determined by two-tailed t test (**B**) Jurkat TAg cells or Jurkat TAg cells stably expressing a lentiviral vector containing CRISPR-Cas9 with a guide RNA sequence targeting the SERINC5 or SERINC3 or a control guide RNA (Luciferase; Luc) were infected with VSV-G- pseudotyped HIV-1 NL4.3WT, ΔNef, ΔVpu or ΔNefΔVpu at an MOI of 1 for 48 h. Infectious virus release into the supernatant of the JTAg cells was determined as in (**A**). Error bars represent standard deviations of the means of four independent experiments. RLU, relative light units. Supernatants titered on TZMbl CRISPR IFITM are indicated (TZMCr). Asterisks represent the p value for the difference in virus infectivity titered on TZMbl cells TZMbl CrIFITM. ns, not significant as determined by two-tailed t test.

5.3 Discussion

In this chapter I discuss the antiviral activity of SERINC5 and SERINC3, which have recently been identified as targets of HIV-1 Nef (Usami et al. 2015; Rosa et al. 2015; Matheson et al. 2015). My data confirm the recent findings and extend the characterization of these newly recognized restriction factors.

SERINC5 and 3 have recently been shown to be targets of HIV-1 and MLV glycoGag and are responsible for the decreased infectivity of Nef-deficient HIV-1 (Usami et al. 2015; Rosa et al. 2015; Matheson et al. 2015). They belong to a family of transmembrane proteins that contains five members and is highly conserved in all eukaryotes. Their function is largely unknown, but they were reported to facilitate the incorporation of serine into phophatidylserine and sphingolipids (Inuzuka et al. 2005). Therefore, they may potentially be able to alter the lipid composition of the cellular plasma membrane domain where the virus assembles, thereby affecting viral infectivity (Waheed & Freed 2010). In contrast to other restriction factors such as tetherin, SERINC expression is not induced by type I interferon, but S5 and 3 are constitutively expressed at different levels depending on the cell type. Four S5 and two S3 isoforms have been predicted. Different isoforms can have differential functions and varying effects on a Nef-deficient virus. The data presented in this chapter show that S5 isoform 4 has a significantly stronger inhibitory effect on viral infectivity than all the other S5 and 3 isoforms. The determinants responsible for the increased efficiency can be found in the C-terminal portion of the protein that is absent from the other S5 isoforms. Further experiments are required to confirm this phenotype and define the residues required for SERINC's function. Furthermore, it remains to be determined whether SERINC isoform function correlates with localization and/or virion incorporation or not.

It was shown that S5 almost exclusively localizes to the plasma membrane where it gets incorporated into budding virions and that Nef counteracts S5 by preventing its incorporation. Interestingly, human S5 is antagonised by various Nef proteins, including SIV Nefs, and also glycoGag, suggesting that there is a low species specificity (Usami et al. 2015; Rosa et al. 2015). Pseudotyping Nef-deficient HIV-1 with VSV-G or EBOV GP made the virus completely resistant to S5, however, it did not prevent its incorporation into the budding virions. Therefore, these envelopes must differ from Nef in the manner in which they overcome the inhibiting effect of S5. HIV-1 Nef induces the downregulation of S5 from the cell surface, which could explain why enhancement of infectivity by Nef is dependent on dynamin 2 and clathrin adaptor AP-2 (Usami et al. 2014; Pizzato

et al. 2007). It was suggested that S5 acts by inhibiting virus entry into target cells, as production of reverse transcription products is strongly inhibited in its presence and fusion with target cells is reduced to a certain extent (Usami et al. 2015; Rosa et al. 2015). Notably, the inhibitory effect of SERINC on fusion seemed to be much lower than its effect on infectious virus release. Also, the role of Nef on virus-cell fusion is a controversial matter (Day et al. 2004; Tobiume et al. 2003; Cavrois et al. 2004). It was therefore proposed that the effect of SERINC on infectivity may potentially be due to the inhibition of fusion pore expansion, which is the highest energy requiring step in the fusion process (Cohen & Melikyan 2004). Whilst small molecules may still be able to pass through the formed fusion pore, the translocation of the much bigger viral core could be prevented, which would explain the discrepant data. This would be in keeping with data showing that Nef enhances the translocation of the viral core (Schaeffer et al. 2001).

Interestingly, different HIV-1 envelope proteins vary in their Nef responsiveness, which also correlates with their sensitivity to S5. For example, the primary HIV-1 isolate JRFL is less Nef-responsive and less sensitive to S5 than another primary HIV-1 isolate, SF162. The determinants for this difference have been attributed to the V1/V2 loop of gp120 (Usami & Göttlinger 2013; Rosa et al. 2015). This region is also involved in the neutralization sensitivity of an envelope and this sensitivity has been found to correlate with an envelope's Nef responsiveness (Lai et al. 2011; Pinter et al. 2004). Additionally, the entry stoichiometry differs between envelopes and the number of envelope trimers on the surface of a virus determines its infectivity (Brandenberg et al. 2015). Furthermore, different HIV-1 envelopes may deliver different energies towards fusion, which could also potentially explain the difference in infectivity and requirement for Nef. It was hypothesized that S5 acts by inhibiting the clustering of envelope trimers (Usami et al. 2015). Envelopes from viruses that fuse in a pH-dependent manner, such as VSV-G and EBOV GP, are resistant to S5 without the requirement for Nef (Chazal et al. 2001; Usami et al. 2015; Rosa et al. 2015). Whether this is due to an increased amount of envelope protein on the viral surface or fusion at low pH is yet unknown.

IFITM proteins have recently been shown to inhibit virus entry (Lu et al. 2011; Compton et al. 2014; Yu et al. 2015). Whether IFITM proteins have any involvement in SERINC function or if both have a synergistic effect on viral infectivity is unclear. Data presented in this chapter indicates that there is no involvement of IFITM proteins in the effect of SERINC when IFITMs are expressed in target cells. However, whether IFITM expression in producer cells and potentially simultaneous

incorporation of SERINC and IFITM proteins into virions has an influence on viral infectivity is so far unclear and requires further experimentation.

Altogether, further investigation is needed to determine the mode of action of S5. Considering that this restriction factor is counteracted by two evolutionarily distant viruses (HIV-1 with Nef and MLV with glycoGag) suggests that it has an important role in antiviral immunity. Future work will focus on determining the requirements in S5 for its antiviral function and whether SERINC isoforms have differential effects due to differences in localization and/or incorporation. In addition, whether IFITM proteins have any role in SERINC function or whether there is a synergistic effect remains to be answered. It will also be interesting to investigate why some envelope pseudotypes are much less sensitive or even resistant to S5 expression.

Chapter 6 General Conclusion

More than 30 years after the discovery of HIV-1 and extensive research, the worldwide HIV-1 pandemic still persists. Our understanding of primate lentiviral replication increased immensely over the years, but many questions remain to be answered. Antiviral, cellular restriction factors have become a broad field of research with new factors being discovered constantly. It is clear that many of these factors evolved under selective pressure from pathogens and their functions shaped during host/virus co-evolution. Simultaneously, primate lentiviruses evolved accessory proteins to combat these host restrictions. Accessory proteins such as Vpu and Nef are essential for efficient viral replication *in vivo*. It becomes more and more apparent that these proteins have various functions and interact with diverse proteins to create an environment most favourable for viral replication. This involves the antagonism of physical restrictions as well as the evasion of systemic host immunity. Interestingly, Nef and Vpu have shared some of their cellular targets during the evolution of primate lentiviruses. They both downregulate CD4 from the surface and affect proinflammatory NF-κB signalling. While Nef is expressed early on in the replication cycle, Vpu appears later. A picture emerges where the timing of viral protein expression may be a key to the regulation of opposing effects and differing mechanisms of counteraction. Other cellular targets are unique to HIV-1 Vpu or Nef such as tetherin counteraction by Vpu (with the exception of some SIV Nefs) and the recently reported SERINC3/5 antagonism of Nef. Both of these cellular restriction factors are expressed in the primary target of HIV-1, $CD4^+$ T cells, and they have a strong inhibitory effect on HIV-1 lacking their countermeasure. Advancing the knowledge of the interplay between viral accessory proteins and restricting host cell factors may provide us with new opportunities for antiviral therapy. This results presented in this thesis focused on aspects of tetherin antagonism by Vpu and other primate lentiviruses as well as Nef-mediated counteraction of SERINC3/5.

In chapter 3 the differential sensitivity of the two human tetherin isoforms was addressed. The existence of two human isoforms was described recently and it was suggested that S-tetherin is less sensitive to HIV-1 NL4.3 Vpu (Cocka & Bates 2012). In the study presented in this thesis, a range of HIV and KSHV encoded tetherin antagonists were tested against human L- and S-tetherin. SIV Nef and Vpu proteins were analysed for their antagonism of monkey tetherin isoforms. In summary, all antagonists tested in this study were able to overcome the restriction of both L- and S-tetherin to equal levels with one exception. The Vpu proteins from HIV-1 group M efficiently antagonised L-tetherin, but S-tetherin was considerably less sensitive to their counteraction. The

increased sensitivity of L-tetherin mapped to serine, threonine and tyrosine residues in the cytoplasmic tail that are missing in S-tetherin. These are residues that were implicated in ubiquitination, endocytosis and signalling (Tokarev et al. 2011; Cocka & Bates 2012; Galão et al. 2012). The major group M is responsible for the worldwide pandemic and interestingly, this is the only group of HIV that evolved an efficient tetherin countermeasure that is also able to induce tetherin degradation. The reason why group M Vpu is the only tetherin antagonist out of the ones tested here that differentiates between the human tetherin isoforms and only counteracts and degrades L-tetherin is unclear. However, one hypothetical explanation may be the immunological pressure imposed by L-tetherin. As described earlier, restriction by both tetherin isoforms potentially has several immunological consequences, with some limited to L-tetherin (Figure 1.20). Human L-tetherin homodimers directly induce NF-κB signalling, while S-tetherin dominantly interferes with this function. In addition, only L-tetherin is efficiently endocytosed and delivers restricted virions to endosomes, potentially mediating their degradation and liberation of viral antigens for PRR recognition. Importantly, the *in vivo* relevance of tetherin isoforms, surface expression and endocytosis has been demonstrated in infected mice (Barrett et al. 2012; Li et al. 2014). A polymorphism in the *bst-2* gene of NZW mice leads to the expression of a truncated tetherin, similar to the short version in humans. This was associated with increased surface expression of tetherin and reduced Friend retrovirus (FV) acute viremia and pathogenesis (Barrett et al. 2012). Later however, using mice with a different MHC haplotype, it was shown that endocytosis competent tetherin correlated with better control of FV replication and disease *in vivo*, because it was able to promote a stronger cell-mediated immune response (Li et al. 2014). In addition, tetherin was recently confirmed to have an inhibitory effect on type-I IFN production through interaction with ILT-7 (Bego et al. 2015). Virus restriction relieves this inhibitory effect and enhances IFN production. Interestingly, Vpu was reported to mediate the downregulation of tetherin and to relocate remaining pools of the protein away from the site of viral budding. Thus, Vpu promotes virion release and the inhibition of pDC signalling through tetherin/ILT7 interaction (Bego et al. 2015). Whether the tetherin pools that remain at the surface are comprised of short tetherin that cannot be downregulated by Vpu is unclear. However, these studies exemplify potential functions for both L- and S-tetherin *in vivo* and may be an explanation for the maintenance of both isoforms in mammals. The pandemic HIV-1 group M Vpu proteins evolved to specifically antagonise L-tetherin efficiently. One might speculate that the signalling function of L-tetherin had a major effect on the adaption of Vpu during zoonotic transmission. Also, the findings by Bego et al. indicate that it can be immunologically

beneficial for a virus to leave some levels of tetherin on the cell surface, similar to what has been reported for MHC-I downregulation by HIV-1 Nef where surface expression of HLA-A and –B is modulated, whilst HLA-C, -E and -G remain at the plasma membrane (Cohen et al. 1999; Pizzato et al. 2004; Specht et al. 2008).

The antagonism of tetherin by Vpu requires clathrin-dependent aberrant trafficking of the protein away from the plasma membrane and site of viral assembly, and subsequent delivery for endo-lysosomal degradation. This requires the formation of a ternary complex between Vpu, clathrin adaptor AP-1 and tetherin (Jia et al. 2014). The dual-tyrosine motif in tetherin and the ExxxLV motif in Vpu are essential for this interaction and additionally, residues in the first alpha helix of Vpu (R44/L45; corresponding to the LILI mutant) have been shown to make a non-canonical contact. Whether the final degradation step of tetherin is required to promote virus release was a matter of debate (Mangeat et al. 2009; Mitchell et al. 2009; Tervo et al. 2011). Chapter 4 of this thesis aims to elucidate this discrepancy for the role of serine phosphorylation of Vpu, β-TrCP recruitment and tetherin degradation in the counteraction of tetherin restriction. The data presented here show evidence that β-TrCP recruitment is required for Vpu-induced tetherin degradation, but dispensable for counteracting the restriction on virus release. The Vpu phospho-mutant, although unable to bind to β-TrCP, has residual anti-tetherin activity that is lost in the context of a tyrosine mutant tetherin. The phospho-mutant shares this phenotype with the ELV and the LILI mutant and all have a similar peripheral rather than TGN-associated subcellular localization. Interestingly, ELV, LILI and the phospho-mutant could be rescued by direct clathrin linkage, bypassing clathrin adaptors. Importantly, this did not restore β-TrCP binding of the phospho-mutant. In addition, data presented here demonstrate that all three motifs are required for efficient binding of Vpu to clathrin adaptors AP-1 and AP-2 in tetherin expressing cells. This is consistent with the structural data reported by Jia et al. and suggests a new role for Vpu phosphorylation in regulating binding of Vpu to the clathrin machinery. So far the partial and full length structural data on Vpu has been limited to studies investigating the protein in isolation or as an tetherin-fused chimeric protein (Willbold et al. 1997; Wittlich et al. 2009; Jia et al. 2014; Zhang et al. 2015). However, to gain better insight into the conformational changes Vpu is capable of, it will be important to analyse its structure in complex with its targets. This will be crucial in the context of exploiting these interactions between Vpu and cellular factors as a target for antiviral drug design.

Recently, the transmembrane proteins SERINC3 and 5 have been described as new restriction factors for HIV-1 that are counteracted by HIV-1 Nef and MLV glycoGag (Usami et al. 2015; Rosa et al. 2015; Matheson et al. 2015). Particularly SERINC5 decreases the infectivity of Nef-deficient virus due to its incorporation into budding virions. Nef prevents this by downregulating SERINC5 from the cell surface. Pseudotyping Nef-deficient HIV-1 with VSV-G or EBOV GP overcomes SERINC5 restriction. Furthermore, some HIV-1 envelopes have been shown to be less sensitive. The data presented in chapter 5 of this thesis confirms recently published data. Furthermore, it shows that out of several predicted isoforms for SERINC3 and 5, only SERINC5 isoform 4 has an inhibiting effect on virion infectivity and this maps to the C-terminus of the protein. Further investigation will show the exact requirements in SERINC5 and whether its function depends on subcellular localization and/or incorporation. Another group of antiviral proteins that recently received more attention are IFITMs. They also act at early stages of the viral life cycle and have been proposed to affect HIV-1 entry (Lu et al. 2011; Compton et al. 2014; Yu et al. 2015). The data presented in this thesis does not show a synergistic effect between SERINC3/5 function and IFITM expression on target cells. However, the effect of IFITM incorporation into virions in the context of SERINC will be investigated before a role of IFITMs will be ruled out.

Both HIV-1 Vpu and Nef fulfil a broad range of functions in the infected cell that allows efficient viral replication and escape from the immune system. The counteraction of host cell factors can be essential to facilitate this and has been implicated in pathogenesis of HIV-1. Understanding the interplay between host and viral proteins can therefore be an important tool for the discovery of future drug targets. So far there is no broadly applicable cure for HIV and infected individuals are forced to adhere to a drug regime for the rest of their lives. HIV reservoirs persist in the body even in the face of combined antiretroviral therapy (cART) and this is what poses a barrier to curing HIV infection. Discontinuing the anti-retroviral treatment results in a rebound of virus. Reducing the viral reservoir is the essential step to the eradication of the virus. Triggering the right immune responses in an infected individual may allow the body to clear infection gradually and potentially reduce the reservoir in the context of compounds that reactivate latent viral pools. However, approaches using latency-reversing agents (LRAs) in the context of cART, referred to as ‘shock and kill’ were so far unsuccessful in reducing the latent HIV-1 reservoir (Reviewed by Rasmussen et al. 2015). This may be attributed to insufficient activation of tissue-associated HIV-1 reservoirs and also CTL responses. It was suggested that enhancing the innate and adaptive immune response towards

infected cells may boost current shock-and-kill approaches. Inhibiting specific virus-host interactions between Vpu, Nef and their targets could have immense immunological consequences for the virus *in vivo* and may be beneficial in this context. For example, hindering Vpu-mediated counteraction of tetherin would not simply result in the reduced release of virions into the extracellular space. Furthermore, presentation of tethered virions to the immunes system, ADCC recognition upon CD4 binding and opsonisation would be enhanced. Endocytosed virions may be degraded and the antigens may induce PRR signalling in addition to the NF-κB activation of tetherin itself. ILT7 inhibition may be relieved and pDCs would produce more type-I IFN. Altogether, the antiviral state of the host would be augmented considerably. These are potential outcomes of the disruption of only one of Vpu's functions. Understanding the effects of HIV-1 accessory proteins on the host, will therefore provide a starting point for the search for specific and effective antiviral intervention towards a cure.

References

Abada, P., Noble, B. & Cannon, P.M., 2005. Functional domains within the human immunodeficiency virus type 2 envelope protein required to enhance virus production. *Journal of virology*, 79(6), pp.3627–38.

Abram, M.E. et al., 2010. Nature, position, and frequency of mutations made in a single cycle of HIV-1 replication. *Journal of virology*, 84(19), pp.9864–78.

Agopian, K. et al., 2006. A hydrophobic binding surface on the human immunodeficiency virus type 1 Nef core is critical for association with p21-activated kinase 2. *Journal of virology*, 80(6), pp.3050–61.

Agromayor, M. et al., 2012. The UBAP1 Subunit of ESCRT-I Interacts with Ubiquitin via a SOUBA Domain. *Structure (London, England : 1993)*, 20(3), pp.414–28.

Ahmad, N. & Venkatesan, S., 1988. Nef protein of HIV-1 is a transcriptional repressor of HIV-1 LTR. *Science (New York, N.Y.)*, 241(4872), pp.1481–5.

Ahn, J. et al., 2012. HIV/simian immunodeficiency virus (SIV) accessory virulence factor Vpx loads the host cell restriction factor SAMHD1 onto the E3 ubiquitin ligase complex CRL4DCAF1. *The Journal of biological chemistry*, 287(15), pp.12550–8.

Aiken, C. et al., 1994. Nef induces CD4 endocytosis: requirement for a critical dileucine motif in the membrane-proximal CD4 cytoplasmic domain. *Cell*, 76(5), pp.853–64.

Aiken, C., 1997. Pseudotyping human immunodeficiency virus type 1 (HIV-1) by the glycoprotein of vesicular stomatitis virus targets HIV-1 entry to an endocytic pathway and suppresses both the requirement for Nef and the sensitivity to cyclosporin A. *Journal of virology*, 71(8), pp.5871–7.

Aiken, C. & Trono, D., 1995. Nef stimulates human immunodeficiency virus type 1 proviral DNA synthesis. *Journal of virology*, 69(8), pp.5048–56.

Alcamí, J. et al., 1995. Absolute dependence on kappa B responsive elements for initiation and Tat-mediated amplification of HIV transcription in blood CD4 T lymphocytes. *The EMBO journal*, 14(7), pp.1552–60.

Alvarez, R.A. et al., 2014. HIV-1 Vpu antagonism of tetherin inhibits antibody-dependent cellular cytotoxic responses by natural killer cells. *Journal of virology*, 88(11), pp.6031–46.

Anderson, S.J. et al., 1994. The cytoplasmic domain of CD4 is sufficient for its down-regulation from the cell surface by human immunodeficiency virus type 1 Nef. *Journal of virology*, 68(5), pp.3092–101.

Andrew, A.J. et al., 2009. The formation of cysteine-linked dimers of BST-2/tetherin is important for inhibition of HIV-1 virus release but not for sensitivity to Vpu. *Retrovirology*, 6, p.80.

Andrew, A.J., Miyagi, E. & Strebel, K., 2011. Differential effects of human immunodeficiency virus type 1 Vpu on the stability of BST-2/tetherin. *Journal of virology*, 85(6), pp.2611–9.

Apetrei, C. et al., 2006. Kuru experiments triggered the emergence of pathogenic SIVmac. *AIDS (London, England)*, 20(3), pp.317–21.

Apetrei, C. et al., 2005. Molecular epidemiology of simian immunodeficiency virus SIVsm in U.S. primate centers unravels the origin of SIVmac and SIVstm. *Journal of virology*, 79(14), pp.8991–9005.

Argañaraz, E.R. et al., 2003. Enhanced CD4 down-modulation by late stage HIV-1 nef alleles is associated with increased Env incorporation and viral replication. *The Journal of biological chemistry*, 278(36), pp.33912–9.

Arias, J.F. et al., 2014. Tetherin antagonism by Vpu protects HIV-infected cells from antibody-dependent cell-mediated cytotoxicity. *Proceedings of the National Academy of Sciences of the United States of America*.

Arnaud, F. et al., 2010. Interplay between ovine bone marrow stromal cell antigen 2/tetherin and endogenous retroviruses. *Journal of virology*, 84(9), pp.4415–25.

Arthos, J. et al., 2008. HIV-1 envelope protein binds to and signals through integrin alpha4beta7, the gut mucosal homing receptor for peripheral T cells. *Nature immunology*, 9(3), pp.301–9.

Arts, E.J. & Hazuda, D.J., 2012. HIV-1 Antiretroviral Drug Therapy. *Cold Spring Harbor Perspectives in Medicine*, 2(4), pp.a007161–a007161.

Atkins, K.M. et al., 2008. HIV-1 Nef binds PACS-2 to assemble a multikinase cascade that triggers major histocompatibility complex class I (MHC-I) down-regulation: analysis using short interfering RNA and knock-out mice. *The Journal of biological chemistry*, 283(17), pp.11772–84.

Bailes, E. et al., 2003. Hybrid origin of SIV in chimpanzees. *Science (New York, N.Y.)*, 300(5626), p.1713.

Ballana, E. & Esté, J.A., 2015. SAMHD1: At the Crossroads of Cell Proliferation, Immune Responses, and Virus Restriction. *Trends in Microbiology*, 23(11), pp.680–92.

Baltimore, D., 1970. RNA-dependent DNA polymerase in virions of RNA tumour viruses. *Nature*, 226(5252), pp.1209–11.

Barré-Sinoussi, F. et al., 1983. Isolation of a T-lymphotropic retrovirus from a patient at risk for acquired immune deficiency syndrome (AIDS). *Science (New York, N.Y.)*, 220(4599), pp.868–71.

Barrett, B.S. et al., 2012. A Single Nucleotide Polymorphism in Tetherin Promotes Retrovirus Restriction In Vivo. *PLoS pathogens*, 8(3), p.e1002596.

Bartee, E., McCormack, A. & Früh, K., 2006. Quantitative membrane proteomics reveals new cellular targets of viral immune modulators. *PLoS pathogens*, 2(10), p.e107.

Basmaciogullari, S. & Pizzato, M., 2014. The activity of Nef on HIV-1 infectivity. *Frontiers in microbiology*, 5, p.232.

Battivelli, E. et al., 2010. Strain-specific differences in the impact of human TRIM5alpha, different TRIM5alpha alleles, and the inhibition of capsid-cyclophilin A interactions on the infectivity of HIV-1. *Journal of virology*, 84(21), pp.11010–9.

Baur, A.S. et al., 1994. HIV-1 Nef leads to inhibition or activation of T cells depending on its intracellular localization. *Immunity*, 1(5), pp.373–84.

Baur, A.S. et al., 1997. The N-terminus of Nef from HIV-1/SIV associates with a protein complex containing Lck and a serine kinase. *Immunity*, 6(3), pp.283–91.

Bego, M.G. et al., 2015. Vpu Exploits the Cross-Talk between BST2 and the ILT7 Receptor to Suppress Anti-HIV-1 Responses by Plasmacytoid Dendritic Cells. *PLoS pathogens*, 11(7), p.e1005024.

Bego, M.G., Mercier, J. & Cohen, E.A., 2012. Virus-activated interferon regulatory factor 7 upregulates expression of the interferon-regulated BST2 gene independently of interferon signaling. *Journal of virology*, 86(7), pp.3513–27.

Beignon, A.-S. et al., 2005. Endocytosis of HIV-1 activates plasmacytoid dendritic cells via Toll-like receptor-viral RNA interactions. *The Journal of clinical investigation*, 115(11), pp.3265–75.

Beloglazova, N. et al., 2013. Nuclease activity of the human SAMHD1 protein implicated in the Aicardi-Goutieres syndrome and HIV-1 restriction. *The Journal of biological chemistry*, 288(12), pp.8101–10.

Bentham, M., Mazaleyrat, S. & Harris, M., 2006. Role of myristoylation and N-terminal basic residues in membrane association of the human immunodeficiency virus type 1 Nef protein. *The Journal of general virology*, 87(Pt 3), pp.563–71.

Berger, E.A. et al., 1998. A new classification for HIV-1. *Nature*, 391(6664), p.240.

Berger, G. et al., 2015. G2/M Cell Cycle Arrest Correlates with Primate Lentiviral Vpr Interaction with the SLX4 Complex. *Journal of virology*, 89(1), pp.230–40.

Berkhout, B., Silverman, R.H. & Jeang, K.T., 1989. Tat trans-activates the human immunodeficiency virus through a nascent RNA target. *Cell*, 59(2), pp.273–82.

Berthoux, L. et al., 2005. Cyclophilin A is required for TRIM5{alpha}-mediated resistance to HIV-1 in Old World monkey cells. *Proceedings of the National Academy of Sciences of the United States of America*, 102(41), pp.14849–53.

Besnard-Guerin, C. et al., 2004. HIV-1 Vpu sequesters beta-transducin repeat-containing protein (betaTrCP) in the cytoplasm and provokes the accumulation of beta-catenin and other SCFbetaTrCP substrates. *The Journal of biological chemistry*, 279(1), pp.788–95.

Besnier, C., Takeuchi, Y. & Towers, G., 2002. Restriction of lentivirus in monkeys. *Proceedings of the National Academy of Sciences of the United States of America*, 99(18), pp.11920–5.

Best, S. et al., 1996. Positional cloning of the mouse retrovirus restriction gene Fv1. *Nature*, 382(6594), pp.826–9.

Billcliff, P.G. et al., 2013. CD317/tetherin is an organiser of membrane microdomains. *Journal of cell science*, 126(Pt 7), pp.1553–64.

Binette, J. et al., 2007. Requirements for the selective degradation of CD4 receptor molecules by the human immunodeficiency virus type 1 Vpu protein in the endoplasmic reticulum. *Retrovirology*, 4, p.75.

Bishop, K.N. et al., 2008. APOBEC3G inhibits elongation of HIV-1 reverse transcripts. *PLoS pathogens*, 4(12), p.e1000231.

Blasius, A.L. et al., 2006. Bone marrow stromal cell antigen 2 is a specific marker of type I IFN-producing cells in the naive mouse, but a promiscuous cell surface antigen following IFN stimulation. *Journal of immunology (Baltimore, Md. : 1950)*, 177(5), pp.3260–5.

Blondeau, C. et al., 2013. Tetherin Restricts Herpes Simplex Virus Type 1 and is Antagonised by Glycoprotein M. *Journal of virology*.

Bogerd, H.P. & Cullen, B.R., 2008. Single-stranded RNA facilitates nucleocapsid: APOBEC3G complex formation. *RNA (New York, N.Y.)*, 14(6), pp.1228–36.

Bolduan, S. et al., 2013. HIV-1 Vpu affects the anterograde transport and the glycosylation pattern of NTB-A. *Virology*, 440(2), pp.190–203.

Bolduan, S. et al., 2011. Ion channel activity of HIV-1 Vpu is dispensable for counteraction of CD317. *Virology*, 416(1-2), pp.75–85.

Bolinger, C. et al., 2010. RNA helicase A modulates translation of HIV-1 and infectivity of progeny virions. *Nucleic acids research*, 38(5), pp.1686–96.

Bolinger, C. & Boris-Lawrie, K., 2009. Mechanisms employed by retroviruses to exploit host factors for translational control of a complicated proteome. *Retrovirology*, 6, p.8.

Boname, J.M. et al., 2010. Efficient internalization of MHC I requires lysine-11 and lysine-63 mixed linkage polyubiquitin chains. *Traffic (Copenhagen, Denmark)*, 11(2), pp.210–20.

Boname, J.M. & Lehner, P.J., 2011. What has the study of the K3 and K5 viral ubiquitin E3 ligases taught us about ubiquitin-mediated receptor regulation? *Viruses*, 3(2), pp.118–31.

Bonifacino, J.S. & Traub, L.M., 2003. Signals for sorting of transmembrane proteins to endosomes and lysosomes. *Annual review of biochemistry*, 72, pp.395–447.

Bor, Y.C., Bushman, F.D. & Orgel, L.E., 1995. In vitro integration of human immunodeficiency virus type 1 cDNA into targets containing protein-induced bends. *Proceedings of the National Academy of Sciences of the United States of America*, 92(22), pp.10334–8.

Bour, S. et al., 2001. The human immunodeficiency virus type 1 Vpu protein inhibits NF-kappa B activation by interfering with beta TrCP-mediated degradation of Ikappa B. *The Journal of biological chemistry*, 276(19), pp.15920–8.

Bour, S., Schubert, U. & Strebel, K., 1995. The human immunodeficiency virus type 1 Vpu protein specifically binds to the cytoplasmic domain oBour, S., Schubert, U. & Strebel, K., 1995. The human immunodeficiency virus type 1 Vpu protein specifically binds to the cytoplasmic domain of CD4: implicat. *Journal of virology*, 69(3), pp.1510–20.

Bour, S. & Strebel, K., 2003. The HIV-1 Vpu protein: a multifunctional enhancer of viral particle release. *Microbes and infection / Institut Pasteur*, 5(11), pp.1029–39.

Bourgeois, C.F. et al., 2002. Spt5 cooperates with human immunodeficiency virus type 1 Tat by preventing premature RNA release at terminator sequences. *Molecular and cellular biology*, 22(4), pp.1079–93.

Brady, T. et al., 2009. HIV integration site distributions in resting and activated CD4+ T cells infected in culture. *AIDS (London, England)*, 23(12), pp.1461–71.

Brandariz-Nuñez, A. et al., 2013. Contribution of oligomerization to the anti-HIV-1 properties of SAMHD1. *Retrovirology*, 10, p.131.

Brandenberg, O.F., Magnus, C., Rusert, P., et al., 2015. Different infectivity of HIV-1 strains is linked to number of envelope trimers required for entry. *PLoS pathogens*, 11(1), p.e1004595.

Brandenberg, O.F., Magnus, C., Regoes, R.R., et al., 2015. The HIV-1 Entry Process: A Stoichiometric View. *Trends in microbiology*, 23(12), pp.763–74.

Brass, A.L. et al., 2008. Identification of host proteins required for HIV infection through a functional genomic screen. *Science (New York, N.Y.)*, 319(5865), pp.921–6.

Bregnard, C. et al., 2013. Comparative Proteomic Analysis of HIV-1 Particles Reveals a Role for Ezrin and EHD4 in the Nef-Dependent Increase of Virus Infectivity. *Journal of Virology*, 87(7), pp.3729–3740.

Brennan, G., Kozyrev, Y. & Hu, S.-L., 2008. TRIMCyp expression in Old World primates Macaca nemestrina and Macaca fascicularis. *Proceedings of the National Academy of Sciences of the United States of America*, 105(9), pp.3569–74.

Brierley, I. & Dos Ramos, F.J., 2006. Programmed ribosomal frameshifting in HIV-1 and the SARS-CoV. *Virus research*, 119(1), pp.29–42.

Briggs, J.A.G. et al., 2006. Cryo-electron microscopy reveals conserved and divergent features of gag packing in immature particles of Rous sarcoma virus and human immunodeficiency virus. *Journal of molecular biology*, 355(1), pp.157–68.

Bruce, E.A. et al., 2012. Release of filamentous and spherical influenza A virus is not restricted by tetherin. *The Journal of general virology*, 93(Pt 5), pp.963–9.

Brügger, B. et al., 2007. Human immunodeficiency virus type 1 Nef protein modulates the lipid composition of virions and host cell membrane microdomains. *Retrovirology*, 4, p.70.

Brügger, B. et al., 2006. The HIV lipidome: a raft with an unusual composition. *Proceedings of the National Academy of Sciences of the United States of America*, 103(8), pp.2641–6.

Bukovsky, A.A. et al., 1997. Nef association with human immunodeficiency virus type 1 virions and cleavage by the viral protease. *Journal of virology*, 71(2), pp.1013–8.

Vande Burgt, N., Kaletsky, R. & Bates, P., 2015. Requirements within the Ebola Viral Glycoprotein for Tetherin Antagonism. *Viruses*, 7(10), pp.5587–5602.

Bushman, F.D., Fujiwara, T. & Craigie, R., 1990. Retroviral DNA integration directed by HIV integration protein in vitro. *Science (New York, N.Y.)*, 249(4976), pp.1555–8.

Busnadiego, I. et al., 2014. Host and viral determinants of Mx2 antiretroviral activity. *Journal of virology*, 88(14), pp.7738–52.

Caillet, M. et al., 2011. Rab7A is required for efficient production of infectious HIV-1. *PLoS pathogens*, 7(11), p.e1002347.

Cameron, P.U. et al., 1992. During HIV-1 infection most blood dendritic cells are not productively infected and can induce allogeneic CD4+ T cells clonal expansion. *Clinical and experimental immunology*, 88(2), pp.226–36.

Canagarajah, B.J. et al., 2013. The clathrin adaptor complexes as a paradigm for membrane-associated allostery. *Protein science : a publication of the Protein Society*, 22(5), pp.517–29.

Cao, W. et al., 2009. Regulation of TLR7/9 responses in plasmacytoid dendritic cells by BST2 and ILT7 receptor interaction. *The Journal of experimental medicine*, 206(7), pp.1603–14.

Carl, S. et al., 2001. Modulation of different human immunodeficiency virus type 1 Nef functions during progression to AIDS. *Journal of virology*, 75(8), pp.3657–65.

Carrington, M. & Alter, G., 2012. Innate immune control of HIV. *Cold Spring Harbor perspectives in medicine*, 2(7), p.a007070.

Casartelli, N. et al., 2010. Tetherin restricts productive HIV-1 cell-to-cell transmission. *PLoS pathogens*, 6(6), p.e1000955.

Cavrois, M. et al., 2004. HIV-1 virion fusion assay: uncoating not required and no effect of Nef on fusion. *Virology*, 328(1), pp.36–44.

Celestino, M. et al., 2012. Feline tetherin is characterized by a short N-terminal region and is counteracted by the feline immunodeficiency virus envelope glycoprotein. *Journal of virology*, 86(12), pp.6688–700.

Cerboni, C. et al., 2007. Human immunodeficiency virus 1 Nef protein downmodulates the ligands of the activating receptor NKG2D and inhibits natural killer cell-mediated cytotoxicity. *The Journal of general virology*, 88(Pt 1), pp.242–50.

Cerwenka, A. & Lanier, L.L., 2001. Ligands for natural killer cell receptors: redundancy or specificity. *Immunological reviews*, 181, pp.158–69.

Chan, D.C. et al., 1997. Core structure of gp41 from the HIV envelope glycoprotein. *Cell*, 89(2), pp.263–73.

Charneau, P., Alizon, M. & Clavel, F., 1992. A second origin of DNA plus-strand synthesis is required for optimal human immunodeficiency virus replication. *Journal of virology*, 66(5), pp.2814–20.

Chaudhuri, R. et al., 2007. Downregulation of CD4 by human immunodeficiency virus type 1 Nef is dependent on clathrin and involves direct interaction of Nef with the AP2 clathrin adaptor. *Journal of virology*, 81(8), pp.3877–90.

Chazal, N. et al., 2001. Human immunodeficiency virus type 1 particles pseudotyped with envelope proteins that fuse at low pH no longer require Nef for optimal infectivity. *Journal of virology*, 75(8), pp.4014–8.

Chen, Y.L., Trono, D. & Camaur, D., 1998. The proteolytic cleavage of human immunodeficiency virus type 1 Nef does not correlate with its ability to stimulate virion infectivity. *Journal of virology*, 72(4), pp.3178–84.

Chen, Z. et al., 1996. Genetic characterization of new West African simian immunodeficiency virus SIVsm: geographic clustering of household-derived SIV strains with human immunodeficiency virus type 2 subtypes and genetically diverse viruses from a single feral sooty mangabey t. *Journal of virology*, 70(6), pp.3617–27.

Cherepanov, P. et al., 2003. HIV-1 integrase forms stable tetramers and associates with LEDGF/p75 protein in human cells. *The Journal of biological chemistry*, 278(1), pp.372–81.

Chowers, M.Y. et al., 1994. Optimal infectivity in vitro of human immunodeficiency virus type 1 requires an intact nef gene. *Journal of virology*, 68(5), pp.2906–14.

Chowers, M.Y. et al., 1995. The growth advantage conferred by HIV-1 nef is determined at the level of viral DNA formation and is independent of CD4 downregulation. *Virology*, 212(2), pp.451–7.

Chung, H.-Y. et al., 2008. NEDD4L overexpression rescues the release and infectivity of human immunodeficiency virus type 1 constructs lacking PTAP and YPXL late domains. *Journal of virology*, 82(10), pp.4884–97.

Clavel, F. et al., 1986. Isolation of a new human retrovirus from West African patients with AIDS. *Science (New York, N.Y.)*, 233(4761), pp.343–6.

Coadou, G. et al., 2002. HIV-1 encoded virus protein U (Vpu) solution structure of the 41-62 hydrophilic region containing the phosphorylated sites Ser52 and Ser56. *International journal of biological macromolecules*, 30(1), pp.23–40.

Coadou, G. et al., 2003. NMR studies of the phosphorylation motif of the HIV-1 protein Vpu bound to the F-box protein beta-TrCP. *Biochemistry*, 42(50), pp.14741–51.

Cocka, L.J. & Bates, P., 2012. Identification of Alternatively Translated Tetherin Isoforms with Differing Antiviral and Signaling Activities C. Aiken, ed. *PLoS Pathogens*, 8(9), p.12.

Coffin, J. & Swanstrom, R., 2013. HIV Pathogenesis: Dynamics and Genetics of Viral Populations and Infected Cells. *Cold Spring Harbor Perspectives in Medicine*, 3(1), pp.a012526–a012526.

Coffin, J.M., 1995. HIV population dynamics in vivo: implications for genetic variation, pathogenesis, and therapy. *Science (New York, N.Y.)*, 267(5197), pp.483–9.

Cohen, E.A. et al., 1988. Identification of a protein encoded by the vpu gene of HIV-1. *Nature*, 334(6182), pp.532–4.

Cohen, F.S. & Melikyan, G.B., 2004. The energetics of membrane fusion from binding, through hemifusion, pore formation, and pore enlargement. *The Journal of membrane biology*, 199(1), pp.1–14.

Cohen, G.B. et al., 1999. The selective downregulation of class I major histocompatibility complex proteins by HIV-1 protects HIV-infected cells from NK cells. *Immunity*, 10(6), pp.661–71.

Cohen, M.S. et al., 2011. Acute HIV-1 Infection. *The New England journal of medicine*, 364(20), pp.1943–54.

Collins, K.L. et al., 1998. HIV-1 Nef protein protects infected primary cells against killing by cytotoxic T lymphocytes. *Nature*, 391(6665), pp.397–401.

Compton, A.A. et al., 2014. IFITM proteins incorporated into HIV-1 virions impair viral fusion and spread. *Cell host & microbe*, 16(6), pp.736–47.

Compton, A.A. & Emerman, M., 2013. Convergence and divergence in the evolution of the APOBEC3G-Vif interaction reveal ancient origins of simian immunodeficiency viruses. *PLoS pathogens*, 9(1), p.e1003135.

Connor, R.I. et al., 1997. Change in coreceptor use correlates with disease progression in HIV-1--infected individuals. *The Journal of experimental medicine*, 185(4), pp.621–8.

Connor, R.I. et al., 1995. Vpr is required for efficient replication of human immunodeficiency virus type-1 in mononuclear phagocytes. *Virology*, 206(2), pp.935–44.

Côté, M., Zheng, Y.-M. & Liu, S.-L., 2012. Membrane fusion and cell entry of XMRV are pH-independent and modulated by the envelope glycoprotein's cytoplasmic tail. *PloS one*, 7(3), p.e33734.

Cowan, S. et al., 2002. Cellular inhibitors with Fv1-like activity restrict human and simian immunodeficiency virus tropism. *Proceedings of the National Academy of Sciences of the United States of America*, 99(18), pp.11914–9.

Craig, H.M., Pandori, M.W. & Guatelli, J.C., 1998. Interaction of HIV-1 Nef with the cellular dileucine-based sorting pathway is required for CD4 down-regulation and optimal viral infectivity. *Proceedings of the National Academy of Sciences of the United States of America*, 95(19), pp.11229–34.

Crow, Y.J. & Rehwinkel, J., 2009. Aicardi-Goutieres syndrome and related phenotypes: linking nucleic acid metabolism with autoimmunity. *Human molecular genetics*, 18(R2), pp.R130–6.

D'arc, M. et al., 2015. Origin of the HIV-1 group O epidemic in western lowland gorillas. *Proceedings of the National Academy of Sciences of the United States of America*, 112(11), pp.E1343–52.

D'Souza, V. & Summers, M.F., 2005. How retroviruses select their genomes. *Nature reviews. Microbiology*, 3(8), pp.643–55.

Dalgleish, A.G. et al., 1984. The CD4 (T4) antigen is an essential component of the receptor for the AIDS retrovirus. *Nature*, 312(5996), pp.763–7.

Van Damme, N. et al., 2008. The interferon-induced protein BST-2 restricts HIV-1 release and is downregulated from the cell surface by the viral Vpu protein. *Cell host & microbe*, 3(4), pp.245–52.

Dang, Q. et al., 2004. Nonrandom HIV-1 infection and double infection via direct and cell-mediated pathways. *Proceedings of the National Academy of Sciences of the United States of America*, 101(2), pp.632–7.

Dave, V.P. et al., 2013. Efficient BST2 antagonism by Vpu is critical for early HIV-1 dissemination in humanized mice. *Retrovirology*, 10(1), p.128.

Day, J.R., Munk, C. & Guatelli, J.C., 2004. The Membrane-Proximal Tyrosine-Based Sorting Signal of Human Immunodeficiency Virus Type 1 gp41 Is Required for Optimal Viral Infectivity. *Journal of Virology*, 78(3), pp.1069–1079.

Deacon, N.J. et al., 1995. Genomic structure of an attenuated quasi species of HIV-1 from a blood transfusion donor and recipients. *Science (New York, N.Y.)*, 270(5238), pp.988–91.

Diaz-Griffero, F. et al., 2006. Rapid turnover and polyubiquitylation of the retroviral restriction factor TRIM5. *Virology*, 349(2), pp.300–15.

Dicks, M.D.J. et al., 2015. Oligomerization requirements for MX2 mediated suppression of HIV-1 infection. *Journal of virology*.

Dietrich, I., McMonagle, E.L., et al., 2011. Feline tetherin efficiently restricts release of feline immunodeficiency virus but not spreading of infection. *Journal of virology*, 85(12), pp.5840–52.

Dietrich, I., Hosie, M.J. & Willett, B.J., 2011. The role of BST2/tetherin in feline retrovirus infection. *Veterinary immunology and immunopathology*, 143(3-4), pp.255–64.

Dittmann, M. et al., 2015. A serpin shapes the extracellular environment to prevent influenza A virus maturation. *Cell*, 160(4), pp.631–43.

Doitsh, G. et al., 2010. Abortive HIV infection mediates CD4 T cell depletion and inflammation in human lymphoid tissue. *Cell*, 143(5), pp.789–801.

Doitsh, G. et al., 2014. Cell death by pyroptosis drives CD4 T-cell depletion in HIV-1 infection. *Nature*, 505(7484), pp.509–14.

Douglas, J.L. et al., 2009. Vpu directs the degradation of the human immunodeficiency virus restriction factor BST-2/Tetherin via a {beta}TrCP-dependent mechanism. *Journal of virology*, 83(16), pp.7931–47.

Dubé, M., Roy, B.B., et al., 2010. Antagonism of tetherin restriction of HIV-1 release by Vpu involves binding and sequestration of the restriction factor in a perinuclear compartment. *PLoS pathogens*, 6(4), p.e1000856.

Dubé, M. et al., 2011. HIV-1 Vpu antagonizes BST-2 by interfering mainly with the trafficking of newly synthesized BST-2 to the cell surface. *Traffic (Copenhagen, Denmark)*, 12(12), pp.1714–29.

Dubé, M., Bego, M.G., et al., 2010. Modulation of HIV-1-host interaction: role of the Vpu accessory protein. *Retrovirology*, 7, p.114.

Dubé, M. et al., 2009. Suppression of Tetherin-restricting activity upon human immunodeficiency virus type 1 particle release correlates with localization of Vpu in the trans-Golgi network. *Journal of virology*, 83(9), pp.4574–90.

Duncan, L.M. et al., 2006. Lysine-63-linked ubiquitination is required for endolysosomal degradation of class I molecules. *The EMBO journal*, 25(8), pp.1635–45.

Engelman, A. & Cherepanov, P., 2012. The structural biology of HIV-1: mechanistic and therapeutic insights. *Nature reviews. Microbiology*, 10(4), pp.279–90.

Erikson, E. et al., 2011. In vivo expression profile of the antiviral restriction factor and tumor-targeting antigen CD317/BST-2/HM1.24/tetherin in humans. *Proceedings of the National Academy of Sciences of the United States of America*, 108(33), pp.13688–93.

Etienne, L. et al., 2013. Gene loss and adaptation to hominids underlie the ancient origin of HIV-1. *Cell host & microbe*,

14(1), pp.85–92.

Evans, D.T. et al., 2010. BST-2/tetherin: a new component of the innate immune response to enveloped viruses. *Trends in microbiology*, 18(9), pp.388–96.

Exline, C.M. et al., 2015. Determinants in HIV-2 Env and tetherin required for functional interaction. *Retrovirology*, 12, p.67.

Fackler, O.T. et al., 1999. Activation of Vav by Nef induces cytoskeletal rearrangements and downstream effector functions. *Molecular cell*, 3(6), pp.729–39.

Faria, N.R. et al., 2014. The early spread and epidemic ignition of HIV-1 in human populations. *Science*, 346(6205), pp.56–61.

Farnet, C.M. & Haseltine, W.A., 1991. Circularization of human immunodeficiency virus type 1 DNA in vitro. *Journal of virology*, 65(12), pp.6942–52.

Fassati, A. & Goff, S.P., 2001. Characterization of intracellular reverse transcription complexes of human immunodeficiency virus type 1. *Journal of virology*, 75(8), pp.3626–35.

Fischer, U. et al., 1995. The HIV-1 Rev activation domain is a nuclear export signal that accesses an export pathway used by specific cellular RNAs. *Cell*, 82(3), pp.475–83.

Fitzpatrick, K. et al., 2010. Direct restriction of virus release and incorporation of the interferon-induced protein BST-2 into HIV-1 particles. *PLoS pathogens*, 6(3), p.e1000701.

Fletcher, A.J. et al., 2015. TRIM5α requires Ube2W to anchor Lys63-linked ubiquitin chains and restrict reverse transcription. *The EMBO journal*, 34(15), pp.2078–95.

Franzolin, E. et al., 2013. The deoxynucleotide triphosphohydrolase SAMHD1 is a major regulator of DNA precursor pools in mammalian cells. *Proceedings of the National Academy of Sciences of the United States of America*, 110(35), pp.14272–7.

Friborg, J. et al., 1995. Functional analysis of the phosphorylation sites on the human immunodeficiency virus type 1 Vpu protein. *Journal of acquired immune deficiency syndromes and human retrovirology : official publication of the International Retrovirology Association*, 8(1), pp.10–22.

Fribourgh, J.L. et al., 2014. Structural Insight into HIV-1 Restriction by MxB. *Cell Host & Microbe*.

Fricke, T. et al., 2014. MxB binds to the HIV-1 core and prevents the uncoating process of HIV-1. *Retrovirology*, 11, p.68.

Fujii, K. et al., 2009. Functional role of Alix in HIV-1 replication. *Virology*, 391(2), pp.284–92.

Fujinaga, K. et al., 2004. Dynamics of human immunodeficiency virus transcription: P-TEFb phosphorylates RD and dissociates negative effectors from the transactivation response element. *Molecular and cellular biology*, 24(2), pp.787–95.

Gaddis, N.C. et al., 2004. Further investigation of simian immunodeficiency virus Vif function in human cells. *Journal of virology*, 78(21), pp.12041–6.

Galão, R.P. et al., 2012. Innate sensing of HIV-1 assembly by Tetherin induces NFκB-dependent proinflammatory responses. *Cell host & microbe*, 12(5), pp.633–44.

Galão, R.P. et al., 2014. Retroviral Retention Activates a Syk-Dependent HemITAM in Human Tetherin. *Cell host & microbe*, 16(3), pp.291–303.

Gallo, R.C. et al., 1983. Isolation of human T-cell leukemia virus in acquired immune deficiency syndrome (AIDS). *Science (New York, N.Y.)*, 220(4599), pp.865–7.

Ganser, B.K. et al., 1999. Assembly and analysis of conical models for the HIV-1 core. *Science (New York, N.Y.)*, 283(5398), pp.80–3.

Ganser-Pornillos, B.K. et al., 2011. Hexagonal assembly of a restricting TRIM5alpha protein. *Proceedings of the National Academy of Sciences of the United States of America*, 108(2), pp.534–9.

Ganser-Pornillos, B.K., Yeager, M. & Sundquist, W.I., 2008. The structural biology of HIV assembly. *Current opinion in structural biology*, 18(2), pp.203–17.

Gao, D. et al., 2013. Cyclic GMP-AMP synthase is an innate immune sensor of HIV and other retroviruses. *Science (New York, N.Y.)*, 341(6148), pp.903–6.

Gao, F. et al., 1992. Human infection by genetically diverse SIVSM-related HIV-2 in west Africa. *Nature*, 358(6386), pp.495–9.

Gao, S. et al., 2010. Structural basis of oligomerization in the stalk region of dynamin-like MxA. *Nature*, 465(7297), pp.502–6.

Gao, S. et al., 2011. Structure of myxovirus resistance protein a reveals intra- and intermolecular domain interactions required for the antiviral function. *Immunity*, 35(4), pp.514–25.

Garcia, J.A. et al., 1989. Human immunodeficiency virus type 1 LTR TATA and TAR region sequences required for transcriptional regulation. *The EMBO journal*, 8(3), pp.765–78.

Garcia, J.V. & Miller, A.D., 1991. Serine phosphorylation-independent downregulation of cell-surface CD4 by nef. *Nature*, 350(6318), pp.508–511.

Garrus, J.E. et al., 2001. Tsg101 and the vacuolar protein sorting pathway are essential for HIV-1 budding. *Cell*, 107(1),

pp.55–65.

Geijtenbeek, T.B. et al., 2000. DC-SIGN, a dendritic cell-specific HIV-1-binding protein that enhances trans-infection of T cells. *Cell*, 100(5), pp.587–97.

Gerhard, D.S. et al., 2004. The status, quality, and expansion of the NIH full-length cDNA project: the Mammalian Gene Collection (MGC). *Genome research*, 14(10B), pp.2121–7.

Giese, S. & Marsh, M., 2014. Tetherin Can Restrict Cell-Free and Cell-Cell Transmission of HIV from Primary Macrophages to T Cells. *PLoS pathogens*, 10(7), p.e1004189.

Gilbert, M.T.P. et al., 2007. The emergence of HIV/AIDS in the Americas and beyond. *Proceedings of the National Academy of Sciences of the United States of America*, 104(47), pp.18566–70.

Gnirß, K. et al., 2015. Tetherin Sensitivity of Influenza A Viruses Is Strain Specific: Role of Hemagglutinin and Neuraminidase. *Journal of virology*, 89(18), pp.9178–88.

Goffinet, C. et al., 2010. Antagonism of CD317 restriction of human immunodeficiency virus type 1 (HIV-1) particle release and depletion of CD317 are separable activities of HIV-1 Vpu. *Journal of virology*, 84(8), pp.4089–94.

Goffinet, C. et al., 2009. HIV-1 antagonism of CD317 is species specific and involves Vpu-mediated proteasomal degradation of the restriction factor. *Cell host & microbe*, 5(3), pp.285–97.

Goh, W.C. et al., 1998. HIV-1 Vpr increases viral expression by manipulation of the cell cycle: a mechanism for selection of Vpr in vivo. *Nature medicine*, 4(1), pp.65–71.

Goldsmith, M.A. et al., 1995. Dissociation of the CD4 downregulation and viral infectivity enhancement functions of human immunodeficiency virus type 1 Nef. *Journal of virology*, 69(7), pp.4112–21.

Goldstone, D.C. et al., 2011. HIV-1 restriction factor SAMHD1 is a deoxynucleoside triphosphate triphosphohydrolase. *Nature*, 480(7377), pp.379–82.

Goncalves, A. et al., 2012. SAMHD1 is a nucleic-acid binding protein that is mislocalized due to aicardi-goutières syndrome-associated mutations. *Human mutation*, 33(7), pp.1116–22.

Goto, T. et al., 1994. A novel membrane antigen selectively expressed on terminally differentiated human B cells. *Blood*, 84(6), pp.1922–30.

Gottlieb, M.S. et al., 1981. Pneumocystis carinii pneumonia and mucosal candidiasis in previously healthy homosexual men: evidence of a new acquired cellular immunodeficiency. *The New England journal of medicine*, 305(24), pp.1425–31.

Göttlinger, H.G. et al., 1993. Vpu protein of human immunodeficiency virus type 1 enhances the release of capsids produced by gag gene constructs of widely divergent retroviruses. *Proceedings of the National Academy of Sciences of the United States of America*, 90(15), pp.7381–5.

Götz, N. et al., 2012. Reacquisition of Nef-mediated tetherin antagonism in a single in vivo passage of HIV-1 through its original chimpanzee host. *Cell host & microbe*, 12(3), pp.373–80.

Goujon, C. et al., 2015. A triple-arginine motif in the amino-terminal domain and oligomerization are required for HIV-1 inhibition by human MX2. *Journal of virology*, 89(8), pp.4676–80.

Goujon, C. et al., 2008. Characterization of simian immunodeficiency virus SIVSM/human immunodeficiency virus type 2 Vpx function in human myeloid cells. *Journal of virology*, 82(24), pp.12335–45.

Goujon, C. et al., 2013. Human MX2 is an interferon-induced post-entry inhibitor of HIV-1 infection. *Nature*, 502(7472), pp.559–62.

Goujon, C. et al., 2014. Transfer of the amino-terminal nuclear envelope targeting domain of human MX2 converts MX1 into an HIV-1 resistance factor. *Journal of virology*, 88(16), pp.9017–26.

Gray, R.R. et al., 2009. Spatial phylodynamics of HIV-1 epidemic emergence in east Africa. *AIDS (London, England)*, 23(14), pp.F9–F17.

Greenberg, M.E. et al., 1997. Co-localization of HIV-1 Nef with the AP-2 adaptor protein complex correlates with Nef-induced CD4 down-regulation. *The EMBO journal*, 16(23), pp.6964–76.

Grzesiek, S. et al., 1996. The CD4 determinant for downregulation by HIV-1 Nef directly binds to Nef. Mapping of the Nef binding surface by NMR. *Biochemistry*, 35(32), pp.10256–61.

Guenzel, C.A., Hérate, C. & Benichou, S., 2014. HIV-1 Vpr-a still “enigmatic multitasker”. *Frontiers in microbiology*, 5, p.127.

Guha, D. & Ayyavoo, V., 2013. Innate immune evasion strategies by human immunodeficiency virus type 1. *ISRN AIDS*, 2013, p.954806.

Gummuluru, S., Kinsey, C.M. & Emerman, M., 2000. An in vitro rapid-turnover assay for human immunodeficiency virus type 1 replication selects for cell-to-cell spread of virus. *Journal of virology*, 74(23), pp.10882–91.

Gupta, R.K., Hué, S., et al., 2009. Mutation of a single residue renders human tetherin resistant to HIV-1 Vpu-mediated depletion. *PLoS pathogens*, 5(5), p.e1000443.

Gupta, R.K., Mlcochova, P., et al., 2009. Simian immunodeficiency virus envelope glycoprotein counteracts tetherin/BST-2/CD317 by intracellular sequestration. *Proceedings of the National Academy of Sciences of the United States of America*, 106(49), pp.20889–94.

Gustin, J.K. et al., 2012. Ubiquitination of BST-2 protein by HIV-1 Vpu protein does not require lysine, serine, or threonine

residues within the BST-2 cytoplasmic domain. *The Journal of biological chemistry*, 287(18), pp.14837–50.

Haller, O. et al., 2010. Dynamin-like MxA GTPase: structural insights into oligomerization and implications for antiviral activity. *The Journal of biological chemistry*, 285(37), pp.28419–24.

Haller, O. et al., 2015. Mx GTPases: dynamin-like antiviral machines of innate immunity. *Trends in microbiology*, 23(3), pp.154–63.

Hammes, S.R. et al., 1989. Nef protein of human immunodeficiency virus type 1: evidence against its role as a transcriptional inhibitor. *Proceedings of the National Academy of Sciences of the United States of America*, 86(23), pp.9549–53.

Hammonds, J. et al., 2010. Immunoelectron microscopic evidence for Tetherin/BST2 as the physical bridge between HIV-1 virions and the plasma membrane. *PLoS pathogens*, 6(2), p.e1000749.

Hansen, E.C. et al., 2014. GTP activator and dNTP substrates of HIV-1 restriction factor SAMHD1 generate a long-lived activated state. *Proceedings of the National Academy of Sciences of the United States of America*, 111(18), pp.E1843–51.

Harris, R.S. et al., 2003. DNA deamination mediates innate immunity to retroviral infection. *Cell*, 113(6), pp.803–9.

Hartley, O. et al., 2005. V3: HIV's switch-hitter. *AIDS research and human retroviruses*, 21(2), pp.171–89.

Hatziioannou, T. et al., 2006. Generation of Simian-Tropic HIV-1 by Restriction Factor Evasion. *Science*, 314(5796), pp.95–95.

Hatziioannou, T. et al., 2004. Retrovirus resistance factors Ref1 and Lv1 are species-specific variants of TRIM5alpha. *Proceedings of the National Academy of Sciences of the United States of America*, 101(29), pp.10774–9.

Hauser, H. et al., 2010. HIV-1 Vpu and HIV-2 Env counteract BST-2/tetherin by sequestration in a perinuclear compartment. *Retrovirology*, 7, p.51.

He, N. et al., 2010. HIV-1 Tat and host AFF4 recruit two transcription elongation factors into a bifunctional complex for coordinated activation of HIV-1 transcription. *Molecular cell*, 38(3), pp.428–38.

Hemelaar, J. et al., 2011. Global trends in molecular epidemiology of HIV-1 during 2000-2007. *AIDS (London, England)*, 25(5), pp.679–89.

Henderson, B.R. & Percipalle, P., 1997. Interactions between HIV Rev and nuclear import and export factors: the Rev nuclear localisation signal mediates specific binding to human importin-beta. *Journal of molecular biology*, 274(5), pp.693–707.

Henne, W.M., Buchkovich, N.J. & Emr, S.D., 2011. The ESCRT pathway. *Developmental cell*, 21(1), pp.77–91.

Heusinger, E. et al., 2015. Early Vertebrate Evolution of the Host Restriction Factor Tetherin. *J. Virol.*, pp.JVI.02149–15–.

Van Heuverswyn, F. & Peeters, M., 2007. The origins of HIV and implications for the global epidemic. *Current infectious disease reports*, 9(4), pp.338–46.

Hilditch, L. et al., 2011. Ordered assembly of murine leukemia virus capsid protein on lipid nanotubes directs specific binding by the restriction factor, Fv1. *Proceedings of the National Academy of Sciences of the United States of America*, 108(14), pp.5771–6.

Hilditch, L. & Towers, G.J., 2014. A model for cofactor use during HIV-1 reverse transcription and nuclear entry. *Current opinion in virology*, 4, pp.32–6.

Hinz, A. et al., 2010. Structural basis of HIV-1 tethering to membranes by the BST-2/tetherin ectodomain. *Cell host & microbe*, 7(4), pp.314–23.

Hirsch, V.M. et al., 1989. An African primate lentivirus (SIVsm) closely related to HIV-2. *Nature*, 339(6223), pp.389–92.

Hirst, J. et al., 2011. The fifth adaptor protein complex. *PLoS biology*, 9(10), p.e1001170.

Hladik, F. & McElrath, M.J., 2008. Setting the stage: host invasion by HIV. *Nature reviews. Immunology*, 8(6), pp.447–57.

Hoch, J. et al., 1995. vpr deletion mutant of simian immunodeficiency virus induces AIDS in rhesus monkeys. *Journal of virology*, 69(8), pp.4807–13.

Hofmann, W. et al., 1999. Species-specific, postentry barriers to primate immunodeficiency virus infection. *Journal of virology*, 73(12), pp.10020–8.

Homann, S. et al., 2011. Upregulation of BST-2/Tetherin by HIV infection in vivo. *Journal of virology*, 85(20), pp.10659–68.

Hotter, D., Kirchhoff, F. & Sauter, D., 2013. HIV-1 Vpu does not degrade interferon regulatory factor 3. *Journal of virology*, 87(12), pp.7160–5.

Hrecka, K. et al., 2007. Lentiviral Vpr usurps Cul4-DDB1[VprBP] E3 ubiquitin ligase to modulate cell cycle. *Proceedings of the National Academy of Sciences of the United States of America*, 104(28), pp.11778–83.

Hrecka, K. et al., 2011. Vpx relieves inhibition of HIV-1 infection of macrophages mediated by the SAMHD1 protein. *Nature*, 474(7353), pp.658–61.

Hu, W.S. & Temin, H.M., 1990. Retroviral recombination and reverse transcription. *Science (New York, N.Y.)*, 250(4985), pp.1227–33.

Huang, Y. et al., 1997. Primer tRNA3Lys on the viral genome exists in unextended and two-base extended forms within mature human immunodeficiency virus type 1. *Journal of virology*, 71(1), pp.726–8.

Huet, T. et al., 1990. Genetic organization of a chimpanzee lentivirus related to HIV-1. *Nature*, 345(6273), pp.356–9.

Hulme, A.E. et al., 2015. Complementary Assays Reveal a Low Level of CA Associated with Viral Complexes in the Nuclei of HIV-1-Infected Cells. *Journal of virology*, 89(10), pp.5350–61.

Hurley, J.H. & Hanson, P.I., 2010. Membrane budding and scission by the ESCRT machinery: it's all in the neck. *Nature reviews. Molecular cell biology*, 11(8), pp.556–66.

Huthoff, H. et al., 2009. RNA-dependent oligomerization of APOBEC3G is required for restriction of HIV-1. *PLoS pathogens*, 5(3), p.e1000330.

Igakura, T. et al., 2003. Spread of HTLV-I between lymphocytes by virus-induced polarization of the cytoskeleton. *Science (New York, N.Y.)*, 299(5613), pp.1713–6.

Ilinskaya, A. et al., 2013. Cell-cell transmission allows human T-lymphotropic virus 1 to circumvent tetherin restriction. *Virology*, 436(1), pp.201–9.

Inuzuka, M., Hayakawa, M. & Ingi, T., 2005. Serinc, an activity-regulated protein family, incorporates serine into membrane lipid synthesis. *The Journal of biological chemistry*, 280(42), pp.35776–83.

Isel, C. & Karn, J., 1999. Direct evidence that HIV-1 Tat stimulates RNA polymerase II carboxyl-terminal domain hyperphosphorylation during transcriptional elongation. *Journal of molecular biology*, 290(5), pp.929–41.

Ishido, S. et al., 2000. Downregulation of major histocompatibility complex class I molecules by Kaposi's sarcoma-associated herpesvirus K3 and K5 proteins. *Journal of virology*, 74(11), pp.5300–9.

Ishikawa, J. et al., 1995. Molecular cloning and chromosomal mapping of a bone marrow stromal cell surface gene, BST2, that may be involved in pre-B-cell growth. *Genomics*, 26(3), pp.527–34.

Iwabu, Y. et al., 2009. HIV-1 accessory protein Vpu internalizes cell-surface BST-2/tetherin through transmembrane interactions leading to lysosomes. *The Journal of biological chemistry*, 284(50), pp.35060–72.

Iwatani, Y. et al., 2007. Deaminase-independent inhibition of HIV-1 reverse transcription by APOBEC3G. *Nucleic acids research*, 35(21), pp.7096–108.

Jacobo-Molina, A. et al., 1993. Crystal structure of human immunodeficiency virus type 1 reverse transcriptase complexed with double-stranded DNA at 3.0 A resolution shows bent DNA. *Proceedings of the National Academy of Sciences of the United States of America*, 90(13), pp.6320–4.

Jafari, M., Guatelli, J. & Lewinski, M.K., 2014. Activities of Transmitted/Founder and Chronicå Clade B HIV-1 Vpu and a C-terminal Polymorphism Specifically Affecting Virion Release. *Journal of virology*.

Jäger, S. et al., 2012. Vif hijacks CBF-β to degrade APOBEC3G and promote HIV-1 infection. *Nature*, 481(7381), pp.371–5.

Jakobsen, M.R. et al., 2013. IFI16 senses DNA forms of the lentiviral replication cycle and controls HIV-1 replication. *Proceedings of the National Academy of Sciences of the United States of America*, 110(48), pp.E4571–80.

Jakobsen, M.R., Olagnier, D. & Hiscott, J., 2015. Innate immune sensing of HIV-1 infection. *Current opinion in HIV and AIDS*, 10(2), pp.96–102.

Janvier, K. et al., 2003. Recognition of dileucine-based sorting signals from HIV-1 Nef and LIMP-II by the AP-1 gamma-sigma1 and AP-3 delta-sigma3 hemicomplexes. *The Journal of cell biology*, 163(6), pp.1281–90.

Janvier, K. et al., 2011. The ESCRT-0 component HRS is required for HIV-1 Vpu-mediated BST-2/tetherin down-regulation. *PLoS pathogens*, 7(2), p.e1001265.

Ji, X. et al., 2013. Mechanism of allosteric activation of SAMHD1 by dGTP. *Nature structural & molecular biology*, 20(11), pp.1304–9.

Jia, B. et al., 2009. Species-specific activity of SIV Nef and HIV-1 Vpu in overcoming restriction by tetherin/BST2. *PLoS pathogens*, 5(5), p.e1000429.

Jia, X. et al., 2012. Structural basis of evasion of cellular adaptive immunity by HIV-1 Nef. *Nature structural & molecular biology*, 19(7), pp.701–6.

Jia, X. et al., 2014. Structural basis of HIV-1 Vpu-mediated BST2 antagonism via hijacking of the clathrin adaptor protein complex 1. *eLife*, 3, p.e02362.

Johnson, W.E. & Sawyer, S.L., 2009. Molecular evolution of the antiretroviral TRIM5 gene. *Immunogenetics*, 61(3), pp.163–76.

Jolly, C. et al., 2004. HIV-1 cell to cell transfer across an Env-induced, actin-dependent synapse. *The Journal of experimental medicine*, 199(2), pp.283–93.

Jolly, C., Booth, N.J. & Neil, S.J.D., 2010. Cell-cell spread of human immunodeficiency virus type 1 overcomes tetherin/BST-2-mediated restriction in T cells. *Journal of virology*, 84(23), pp.12185–99.

Jones, K.A. et al., 1986. Activation of the AIDS retrovirus promoter by the cellular transcription factor, Sp1. *Science (New York, N.Y.)*, 232(4751), pp.755–9.

Jones, P.H. et al., 2012. Bone marrow stromal cell antigen 2 (BST-2) restricts mouse mammary tumor virus (MMTV) replication in vivo. *Retrovirology*, 9, p.10.

Jones, P.H. et al., 2013. BST-2/tetherin-mediated restriction of chikungunya (CHIKV) VLP budding is counteracted by CHIKV

non-structural protein 1 (nsP1). *Virology*, 438(1), pp.37–49.

Jouvenet, N. et al., 2009. Broad-spectrum inhibition of retroviral and filoviral particle release by tetherin. *Journal of virology*, 83(4), pp.1837–44.

Kaletsky, R.L. et al., 2009. Tetherin-mediated restriction of filovirus budding is antagonized by the Ebola glycoprotein. *Proceedings of the National Academy of Sciences of the United States of America*, 106(8), pp.2886–91.

Kane, M. et al., 2013. MX2 is an interferon-induced inhibitor of HIV-1 infection. *Nature*, 502(7472), pp.563–6.

Kao, S.Y. et al., 1987. Anti-termination of transcription within the long terminal repeat of HIV-1 by tat gene product. *Nature*, 330(6147), pp.489–93.

Karn, J. & Stoltzfus, C.M., 2012. Transcriptional and posttranscriptional regulation of HIV-1 gene expression. *Cold Spring Harbor perspectives in medicine*, 2(2), p.a006916.

Kasper, M.R. et al., 2005. HIV-1 Nef disrupts antigen presentation early in the secretory pathway. *The Journal of biological chemistry*, 280(13), pp.12840–8.

Katzmann, D.J., Babst, M. & Emr, S.D., 2001. Ubiquitin-dependent sorting into the multivesicular body pathway requires the function of a conserved endosomal protein sorting complex, ESCRT-I. *Cell*, 106(2), pp.145–55.

Keckesova, Z., Ylinen, L.M.J. & Towers, G.J., 2006. Cyclophilin A renders human immunodeficiency virus type 1 sensitive to Old World monkey but not human TRIM5 alpha antiviral activity. *Journal of virology*, 80(10), pp.4683–90.

Keckesova, Z., Ylinen, L.M.J. & Towers, G.J., 2004. The human and African green monkey TRIM5alpha genes encode Ref1 and Lv1 retroviral restriction factor activities. *Proceedings of the National Academy of Sciences of the United States of America*, 101(29), pp.10780–5.

Keele, B.F. et al., 2006. Chimpanzee reservoirs of pandemic and nonpandemic HIV-1. *Science (New York, N.Y.)*, 313(5786), pp.523–6.

Keele, B.F. et al., 2008. Identification and characterization of transmitted and early founder virus envelopes in primary HIV-1 infection. *Proceedings of the National Academy of Sciences of the United States of America*, 105(21), pp.7552–7.

Kestler, H. et al., 1990. Induction of AIDS in rhesus monkeys by molecularly cloned simian immunodeficiency virus. *Science*, 248(4959), pp.1109–1112.

Kestler, H.W. et al., 1991. Importance of the nef gene for maintenance of high virus loads and for development of AIDS. *Cell*, 65(4), pp.651–62.

Kim, E.-Y. et al., 2010. Human APOBEC3G-mediated editing can promote HIV-1 sequence diversification and accelerate adaptation to selective pressure. *Journal of virology*, 84(19), pp.10402–5.

Kim, S. et al., 1989. Lack of a negative influence on viral growth by the nef gene of human immunodeficiency virus type 1. *Proceedings of the National Academy of Sciences of the United States of America*, 86(23), pp.9544–8.

Kirchhoff, F. et al., 1995. Brief report: absence of intact nef sequences in a long-term survivor with nonprogressive HIV-1 infection. *The New England journal of medicine*, 332(4), pp.228–32.

Klatzmann, D. et al., 1984. Selective tropism of lymphadenopathy associated virus (LAV) for helper-inducer T lymphocytes. *Science (New York, N.Y.)*, 225(4657), pp.59–63.

Klimkait, T. et al., 1990. The human immunodeficiency virus type 1-specific protein vpu is required for efficient virus maturation and release. *Journal of virology*, 64(2), pp.621–9.

Kluge, S.F. et al., 2014. Nef Proteins of Epidemic HIV-1 Group O Strains Antagonize Human Tetherin. *Cell Host & Microbe*, 16(5), pp.639–650.

Kobayashi, T. et al., 2011. Identification of amino acids in the human tetherin transmembrane domain responsible for HIV-1 Vpu interaction and susceptibility. *Journal of virology*, 85(2), pp.932–45.

Kohleisen, B. et al., 1992. Cellular localization of Nef expressed in persistently HIV-1-infected low-producer astrocytes. *AIDS (London, England)*, 6(12), pp.1427–36.

Köhler, A. & Hurt, E., 2007. Exporting RNA from the nucleus to the cytoplasm. *Nature reviews. Molecular cell biology*, 8(10), pp.761–73.

Kohlstaedt, L.A. et al., 1992. Crystal structure at 3.5 A resolution of HIV-1 reverse transcriptase complexed with an inhibitor. *Science (New York, N.Y.)*, 256(5065), pp.1783–90.

König, R. et al., 2008. Global analysis of host-pathogen interactions that regulate early-stage HIV-1 replication. *Cell*, 135(1), pp.49–60.

Koning, F.A. et al., 2009. Defining APOBEC3 expression patterns in human tissues and hematopoietic cell subsets. *Journal of virology*, 83(18), pp.9474–85.

Korber, B. et al., 2000. Timing the ancestor of the HIV-1 pandemic strains. *Science (New York, N.Y.)*, 288(5472), pp.1789–96.

Krummheuer, J. et al., 2007. A minimal uORF within the HIV-1 vpu leader allows efficient translation initiation at the downstream env AUG. *Virology*, 363(2), pp.261–71.

Kueck, T. et al., 2015. Serine Phosphorylation of HIV-1 Vpu and Its Binding to Tetherin Regulates Interaction with Clathrin Adaptors. *PLoS pathogens*, 11(8), p.e1005141.

Kueck, T. & Neil, S.J.D., 2012. A Cytoplasmic Tail Determinant in HIV-1 Vpu Mediates Targeting of Tetherin for Endosomal Degradation and Counteracts Interferon-Induced Restriction. *PLoS pathogens*, 8(3), p.e1002609.

Kühl, A. et al., 2011. The Ebola virus glycoprotein and HIV-1 Vpu employ different strategies to counteract the antiviral factor tetherin. *The Journal of infectious diseases*, 204 Suppl , pp.S850–60.

Kuhl, B.D. et al., 2010. Tetherin restricts direct cell-to-cell infection of HIV-1. *Retrovirology*, 7, p.115.

Kupzig, S. et al., 2003. Bst-2/HM1.24 is a raft-associated apical membrane protein with an unusual topology. *Traffic (Copenhagen, Denmark)*, 4(10), pp.694–709.

Kusunoki, Y. et al., 2000. NK-Mediated Elimination of Mutant Lymphocytes that Have Lost Expression of MHC Class I Molecules. *The Journal of Immunology*, 165(7), pp.3555–3563.

Kutluay, S.B. et al., 2014. Global changes in the RNA binding specificity of HIV-1 gag regulate virion genesis. *Cell*, 159(5), pp.1096–109.

Kutluay, S.B., Perez-Caballero, D. & Bieniasz, P.D., 2013. Fates of retroviral core components during unrestricted and TRIM5-restricted infection. *PLoS pathogens*, 9(3), p.e1003214.

Kwong, P.D. et al., 1998. Structure of an HIV gp120 envelope glycoprotein in complex with the CD4 receptor and a neutralizing human antibody. *Nature*, 393(6686), pp.648–59.

Lafer, E.M., 2002. Clathrin-protein interactions. *Traffic (Copenhagen, Denmark)*, 3(8), pp.513–20.

Laguette, N. et al., 2014. Premature activation of the SLX4 complex by Vpr promotes G2/M arrest and escape from innate immune sensing. *Cell*, 156(1-2), pp.134–45.

Laguette, N. et al., 2011. SAMHD1 is the dendritic- and myeloid-cell-specific HIV-1 restriction factor counteracted by Vpx. *Nature*, 474(7353), pp.654–657.

Lahaye, X. et al., 2013. The capsids of HIV-1 and HIV-2 determine immune detection of the viral cDNA by the innate sensor cGAS in dendritic cells. *Immunity*, 39(6), pp.1132–42.

Lahaye, X. & Manel, N., 2015. Viral and cellular mechanisms of the innate immune sensing of HIV. *Current opinion in virology*, 11, pp.55–62.

Lahouassa, H. et al., 2012. SAMHD1 restricts the replication of human immunodeficiency virus type 1 by depleting the intracellular pool of deoxynucleoside triphosphates. *Nature Immunology*.

Lai, R.P.J. et al., 2011. Nef Decreases HIV-1 Sensitivity to Neutralizing Antibodies that Target the Membrane-proximal External Region of TMgp41 B. R. Cullen, ed. *PLoS Pathogens*, 7(12), p.e1002442.

Lamb, R.A., 1993. Paramyxovirus fusion: a hypothesis for changes. *Virology*, 197(1), pp.1–11.

Lang, S.M. et al., 1993. Importance of vpr for infection of rhesus monkeys with simian immunodeficiency virus. *Journal of virology*, 67(2), pp.902–12.

Laplana, M. et al., 2013. Association of BST-2 gene variants with HIV disease progression underscores the role of BST-2 in HIV type 1 infection. *The Journal of infectious diseases*, 207(3), pp.411–9.

Lau, D., Kwan, W. & Guatelli, J., 2011. Role of the endocytic pathway in the counteraction of BST-2 by human lentiviral pathogens. *Journal of virology*, 85(19), pp.9834–46.

Lehmann, M. et al., 2011. Quantitative multicolor super-resolution microscopy reveals tetherin HIV-1 interaction. *PLoS pathogens*, 7(12), p.e1002456.

Lehmann, M.J. et al., 2005. Actin- and myosin-driven movement of viruses along filopodia precedes their entry into cells. *The Journal of cell biology*, 170(2), pp.317–25.

Lehner, P.J. et al., 2005. Downregulation of cell surface receptors by the K3 family of viral and cellular ubiquitin E3 ligases. *Immunological reviews*, 207, pp.112–25.

Lemaître, C. et al., 2014. The HERV-K human endogenous retrovirus envelope protein antagonizes Tetherin antiviral activity. *Journal of virology*, 88(23), pp.13626–37.

Lepelley, A. et al., 2011. Innate sensing of HIV-infected cells. *PLoS pathogens*, 7(2), p.e1001284.

Lewinski, M.K. et al., 2015. Membrane Anchoring by a C-terminal Tryptophan Enables HIV-1 Vpu to Displace Bone Marrow Stromal Antigen 2 (BST2) from Sites of Viral Assembly. *The Journal of biological chemistry*, 290(17), pp.10919–33.

Leyva-Grado, V.H. et al., 2014. Modulation of an ectodomain motif in the influenza A virus neuraminidase alters tetherin sensitivity and results in virus attenuation in vivo. *Journal of molecular biology*, 426(6), pp.1308–21.

Li, S.X. et al., 2014. Tetherin promotes the innate and adaptive cell-mediated immune response against retrovirus infection in vivo. *Journal of immunology (Baltimore, Md. : 1950)*, 193(1), pp.306–16.

Liao, C.-H. et al., 2007. A novel fusion gene, TRIM5-Cyclophilin A in the pig-tailed macaque determines its susceptibility to HIV-1 infection. *AIDS (London, England)*, 21 Suppl 8, pp.S19–26.

Liberatore, R.A. & Bieniasz, P.D., 2011. Tetherin is a key effector of the antiretroviral activity of type I interferon in vitro and in vivo. *Proceedings of the National Academy of Sciences of the United States of America*, 108(44), pp.18097–101.

Lightfoote, M.M. et al., 1986. Structural characterization of reverse transcriptase and endonuclease polypeptides of the acquired immunodeficiency syndrome retrovirus. *Journal of virology*, 60(2), pp.771–5.

Lim, E.S. et al., 2012. The Ability of Primate Lentiviruses to Degrade the Monocyte Restriction Factor SAMHD1 Preceded the Birth of the Viral Accessory Protein Vpx. *Cell Host & Microbe*, 11(2), pp.194–204.

Lim, E.S., Malik, H.S. & Emerman, M., 2010. Ancient adaptive evolution of tetherin shaped the functions of Vpu and Nef in human immunodeficiency virus and primate lentiviruses. *Journal of virology*, 84(14), pp.7124–34.

Lindwasser, O.W. et al., 2008. A diacidic motif in human immunodeficiency virus type 1 Nef is a novel determinant of binding to AP-2. *Journal of virology*, 82(3), pp.1166–74.

Liu, J. et al., 1992. Specific NF-kappa B subunits act in concert with Tat to stimulate human immunodeficiency virus type 1 transcription. *Journal of virology*, 66(6), pp.3883–7.

Liu, Y. et al., 2014. Tetherin restricts HSV-2 release and is counteracted by multiple viral glycoproteins. *Virology*, 475C, pp.96–109.

Liu, Z. et al., 2015. The highly polymorphic cyclophilin A-binding loop in HIV-1 capsid modulates viral resistance to MxB. *Retrovirology*, 12, p.1.

Liu, Z. et al., 2013. The interferon-inducible MxB protein inhibits HIV-1 infection. *Cell host & microbe*, 14(4), pp.398–410.

Llano, M. et al., 2006. An essential role for LEDGF/p75 in HIV integration. *Science (New York, N.Y.)*, 314(5798), pp.461–4.

Lock, M. et al., 1999. Two elements target SIV Nef to the AP-2 clathrin adaptor complex, but only one is required for the induction of CD4 endocytosis. *The EMBO Journal*, 18(10), pp.2722–2733.

Londrigan, S.L. et al., Endogenous Murine BST-2/Tetherin Is Not a Major Restriction Factor of Influenza A Virus Infection. *PloS one*, 10(11), p.e0142925.

Lopez, C.F. et al., 2002. Molecular dynamics investigation of membrane-bound bundles of the channel-forming transmembrane domain of viral protein U from the human immunodeficiency virus HIV-1. *Biophysical journal*, 83(3), pp.1259–67.

Lopez, L.A. et al., 2012. Anti-tetherin activities of HIV-1 Vpu and Ebola virus glycoprotein do not involve removal of tetherin from lipid rafts. *Journal of virology*, 86(10), pp.5467–80.

Lopez, L.A. et al., 2010. Ebola virus glycoprotein counteracts BST-2/Tetherin restriction in a sequence-independent manner that does not require tetherin surface removal. *Journal of virology*, 84(14), pp.7243–55.

Lori, F. et al., 1992. Viral DNA carried by human immunodeficiency virus type 1 virions. *Journal of virology*, 66(8), pp.5067–74.

Lu, J. et al., 2011. The IFITM proteins inhibit HIV-1 infection. *Journal of virology*, 85(5), pp.2126–37.

Luciw, P.A., Cheng-Mayer, C. & Levy, J.A., 1987. Mutational analysis of the human immunodeficiency virus: the orf-B region down-regulates virus replication. *Proceedings of the National Academy of Sciences of the United States of America*, 84(5), pp.1434–8.

Luo, T. et al., 1998. Infectivity Enhancement by HIV-1 Nef Is Dependent on the Pathway of Virus Entry: Implications for HIV-Based Gene Transfer Systems. *Virology*, 241(2), pp.224–233.

Lv, M. et al., 2015. Identification of BST-2/tetherin-induced hepatitis B virus restriction and hepatocyte-specific BST-2 inactivation. *Scientific reports*, 5, p.11736.

Maddon, P.J. et al., 1986. The T4 gene encodes the AIDS virus receptor and is expressed in the immune system and the brain. *Cell*, 47(3), pp.333–48.

Maertens, G.N., Hare, S. & Cherepanov, P., 2010. The mechanism of retroviral integration from X-ray structures of its key intermediates. *Nature*, 468(7321), pp.326–9.

Magadán, J.G. et al., 2010. Multilayered Mechanism of CD4 Downregulation by HIV-1 Vpu Involving Distinct ER Retention and ERAD Targeting Steps M. Emerman, ed. *PLoS Pathogens*, 6(4), p.e1000869.

Magadán, J.G. & Bonifacino, J.S., 2012. Transmembrane domain determinants of CD4 Downregulation by HIV-1 Vpu. *Journal of virology*, 86(2), pp.757–72.

Mahauad-Fernandez, W.D., Jones, P.H. & Okeoma, C.M., 2014. Critical role for BST-2 in acute Chikungunya virus infection. *The Journal of general virology*.

Maldarelli, F. et al., 1993. Human immunodeficiency virus type 1 Vpu protein is an oligomeric type I integral membrane protein. *Journal of virology*, 67(8), pp.5056–61.

Mali, P., Esvelt, K.M. & Church, G.M., 2013. Cas9 as a versatile tool for engineering biology. *Nature methods*, 10(10), pp.957–63.

Malim, M.H., 2009. APOBEC proteins and intrinsic resistance to HIV-1 infection. *Philosophical transactions of the Royal Society of London. Series B, Biological sciences*, 364(1517), pp.675–87.

Malim, M.H. et al., 1989. The HIV-1 rev trans-activator acts through a structured target sequence to activate nuclear export of unspliced viral mRNA. *Nature*, 338(6212), pp.254–7.

Malim, M.H. & Bieniasz, P.D., 2012. HIV Restriction Factors and Mechanisms of Evasion. *Cold Spring Harbor perspectives in medicine*, 2(5), p.a006940.

Malim, M.H. & Cullen, B.R., 1991. HIV-1 structural gene expression requires the binding of multiple Rev monomers to the viral RRE: implications for HIV-1 latency. *Cell*, 65(2), pp.241–8.

Mangeat, B. et al., 2003. Broad antiretroviral defence by human APOBEC3G through lethal editing of nascent reverse transcripts. *Nature*, 424(6944), pp.99–103.

Mangeat, B. et al., 2009. HIV-1 Vpu neutralizes the antiviral factor Tetherin/BST-2 by binding it and directing its beta-TrCP2-dependent degradation. *PLoS pathogens*, 5(9), p.e1000574.

Mangeat, B. et al., 2012. Influenza virus partially counteracts restriction imposed by tetherin/BST-2. *The Journal of biological chemistry*, 287(26), pp.22015–29.

Mansky, L.M. & Temin, H.M., 1995. Lower in vivo mutation rate of human immunodeficiency virus type 1 than that predicted from the fidelity of purified reverse transcriptase. *Journal of virology*, 69(8), pp.5087–94.

Mansouri, M. et al., 2009. Molecular mechanism of BST2/tetherin downregulation by K5/MIR2 of Kaposi's sarcoma-associated herpesvirus. *Journal of virology*, 83(19), pp.9672–81.

Margolis, L. & Shattock, R., 2006. Selective transmission of CCR5-utilizing HIV-1: the "gatekeeper" problem resolved? *Nature reviews. Microbiology*, 4(4), pp.312–7.

Margottin, F. et al., 1998. A novel human WD protein, h-beta TrCp, that interacts with HIV-1 Vpu connects CD4 to the ER degradation pathway through an F-box motif. *Molecular cell*, 1(4), pp.565–74.

Marini, B. et al., 2015. Nuclear architecture dictates HIV-1 integration site selection. *Nature*, 521(7551), pp.227–31.

Martin-Serrano, J. & Neil, S.J.D., 2011. Host factors involved in retroviral budding and release. *Nature reviews. Microbiology*, 9(7), pp.519–31.

Martin-Serrano, J., Zang, T. & Bieniasz, P.D., 2001. HIV-1 and Ebola virus encode small peptide motifs that recruit Tsg101 to sites of particle assembly to facilitate egress. *Nature medicine*, 7(12), pp.1313–9.

Martinelli, E. et al., 2007. HIV-1 gp120 inhibits TLR9-mediated activation and IFN-{alpha} secretion in plasmacytoid dendritic cells. *Proceedings of the National Academy of Sciences of the United States of America*, 104(9), pp.3396–401.

Masuyama, N. et al., 2009. HM1.24 is internalized from lipid rafts by clathrin-mediated endocytosis through interaction with alpha-adaptin. *The Journal of biological chemistry*, 284(23), pp.15927–41.

Matheson, N.J. et al., 2015. Cell Surface Proteomic Map of HIV Infection Reveals Antagonism of Amino Acid Metabolism by Vpu and Nef. *Cell host & microbe*.

Matreyek, K.A. et al., 2014. Host and viral determinants for MxB restriction of HIV-1 infection. *Retrovirology*, 11, p.90.

Matreyek, K.A. et al., 2013. Nucleoporin NUP153 phenylalanine-glycine motifs engage a common binding pocket within the HIV-1 capsid protein to mediate lentiviral infectivity. *PLoS pathogens*, 9(10), p.e1003693.

Matreyek, K.A. & Engelman, A., 2011. The requirement for nucleoporin NUP153 during human immunodeficiency virus type 1 infection is determined by the viral capsid. *Journal of virology*, 85(15), pp.7818–27.

Matsuda, A. et al., 2003. Large-scale identification and characterization of human genes that activate NF-kappaB and MAPK signaling pathways. *Oncogene*, 22(21), pp.3307–18.

Mauclère, P. et al., 1997. Serological and virological characterization of HIV-1 group O infection in Cameroon. *AIDS (London, England)*, 11(4), pp.445–53.

Mauxion, F. et al., 1996. A casein kinase II phosphorylation site in the cytoplasmic domain of the cation-dependent mannose 6-phosphate receptor determines the high affinity interaction of the AP-1 Golgi assembly proteins with membranes. *The Journal of biological chemistry*, 271(4), pp.2171–8.

McClure, M.O., Marsh, M. & Weiss, R.A., 1988. Human immunodeficiency virus infection of CD4-bearing cells occurs by a pH-independent mechanism. *The EMBO journal*, 7(2), pp.513–8.

McDonald, D. et al., 2003. Recruitment of HIV and its receptors to dendritic cell-T cell junctions. *Science (New York, N.Y.)*, 300(5623), pp.1295–7.

McDougal, J.S. et al., 1986. Binding of HTLV-III/LAV to T4+ T cells by a complex of the 110K viral protein and the T4 molecule. *Science (New York, N.Y.)*, 231(4736), pp.382–5.

McNatt, M.W. et al., 2009. Species-specific activity of HIV-1 Vpu and positive selection of tetherin transmembrane domain variants. *PLoS pathogens*, 5(2), p.e1000300.

McNatt, M.W., Zang, T. & Bieniasz, P.D., 2013. Vpu Binds Directly to Tetherin and Displaces It from Nascent Virions D. T. Evans, ed. *PLoS Pathogens*, 9(4), p.e1003299.

McNatt, M.W., Zang, T. & Bieniasz, P.D., 2013. Vpu binds directly to tetherin and displaces it from nascent virions. *PLoS pathogens*, 9(4), p.e1003299.

Means, R.E., Lang, S.M. & Jung, J.U., 2007. The Kaposi's sarcoma-associated herpesvirus K5 E3 ubiquitin ligase modulates targets by multiple molecular mechanisms. *Journal of virology*, 81(12), pp.6573–83.

Melén, K. et al., 1996. Human MxB protein, an interferon-alpha-inducible GTPase, contains a nuclear targeting signal and is localized in the heterochromatin region beneath the nuclear envelope. *The Journal of biological chemistry*, 271(38), pp.23478–86.

Melikyan, G.B., 2008. Common principles and intermediates of viral protein-mediated fusion: the HIV-1 paradigm. *Retrovirology*, 5, p.111.

Miazzi, C. et al., 2014. Allosteric regulation of the human and mouse deoxyribonucleotide triphosphohydrolase sterile α-

motif/histidine-aspartate domain-containing protein 1 (SAMHD1). *The Journal of biological chemistry*, 289(26), pp.18339–46.

Miller, M.D. et al., 1995. Expression of the human immunodeficiency virus type 1 (HIV-1) nef gene during HIV-1 production increases progeny particle infectivity independently of gp160 or viral entry. *Journal of virology*, 69(1), pp.579–84.

Mitchell, R.S. et al., 2009. Vpu antagonizes BST-2-mediated restriction of HIV-1 release via beta-TrCP and endo-lysosomal trafficking. *PLoS pathogens*, 5(5), p.e1000450.

Miyagi, E. et al., 2009. Vpu enhances HIV-1 virus release in the absence of Bst-2 cell surface down-modulation and intracellular depletion. *Proceedings of the National Academy of Sciences of the United States of America*, 106(8), pp.2868–73.

Miyakawa, K. et al., 2009. BCA2/Rabring7 promotes tetherin-dependent HIV-1 restriction. *PLoS pathogens*, 5(12), p.e1000700.

Miyakawa, K. et al., 2012. Interferon-induced SCYL2 limits release of HIV-1 by triggering PP2A-mediated dephosphorylation of the viral protein Vpu. *Science signaling*, 5(245), p.ra73.

Miyakawa, K. et al., 2015. Molecular dissection of HBV evasion from restriction factor tetherin: A new perspective for antiviral cell therapy. *Oncotarget*, 6(26), pp.21840–52.

Miyauchi, K. et al., 2009. HIV enters cells via endocytosis and dynamin-dependent fusion with endosomes. *Cell*, 137(3), pp.433–44.

Mizutani, S., Boettiger, D. & Temin, H.M., 1970. A DNA-depenent DNA polymerase and a DNA endonuclease in virions of Rous sarcoma virus. *Nature*, 228(5270), pp.424–7.

Moll, M. et al., 2010. Inhibition of lipid antigen presentation in dendritic cells by HIV-1 Vpu interference with CD1d recycling from endosomal compartments. *Blood*, 116(11), pp.1876–84.

Monroe, K.M. et al., 2013. IFI16 DNA Sensor Is Required for Death of Lymphoid CD4 T Cells Abortively Infected with HIV. *Science (New York, N.Y.)*, 343(6169), pp.428–432.

Moore, M.D. et al., 2009. Probing the HIV-1 genomic RNA trafficking pathway and dimerization by genetic recombination and single virion analyses. *PLoS pathogens*, 5(10), p.e1000627.

Morita, E. et al., 2011. ESCRT-III protein requirements for HIV-1 budding. *Cell host & microbe*, 9(3), pp.235–42.

Morrison, J.H. et al., 2014. Feline immunodeficiency virus envelope glycoproteins antagonize tetherin through a distinctive mechanism that requires virion incorporation. *Journal of virology*, 88(6), pp.3255–72.

Muesing, M.A. et al., 1985. Nucleic acid structure and expression of the human AIDS/lymphadenopathy retrovirus. *Nature*, 313(6002), pp.450–8.

Münch, J. et al., 2007. Nef-mediated enhancement of virion infectivity and stimulation of viral replication are fundamental properties of primate lentiviruses. *Journal of virology*, 81(24), pp.13852–64.

Murakami, T. et al., 2004. Regulation of human immunodeficiency virus type 1 Env-mediated membrane fusion by viral protease activity. *Journal of virology*, 78(2), pp.1026–31.

Nabel, G. & Baltimore, D., 1987. An inducible transcription factor activates expression of human immunodeficiency virus in T cells. *Nature*, 326(6114), pp.711–3.

Nakamura, N. et al., 1997. Expression cloning of PIG-L, a candidate N-acetylglucosaminyl-phosphatidylinositol deacetylase. *The Journal of biological chemistry*, 272(25), pp.15834–40.

Neil, S.J.D. et al., 2007. An interferon-alpha-induced tethering mechanism inhibits HIV-1 and Ebola virus particle release but is counteracted by the HIV-1 Vpu protein. *Cell host & microbe*, 2(3), pp.193–203.

Neil, S.J.D. et al., 2006. HIV-1 Vpu promotes release and prevents endocytosis of nascent retrovirus particles from the plasma membrane. *PLoS pathogens*, 2(5), p.e39.

Neil, S.J.D., 2013. The antiviral activities of tetherin. *Current topics in microbiology and immunology*, 371, pp.67–104.

Neil, S.J.D., Zang, T. & Bieniasz, P.D., 2008. Tetherin inhibits retrovirus release and is antagonized by HIV-1 Vpu. *Nature*, 451(7177), pp.425–430.

Newman, R.M. et al., 2008. Evolution of a TRIM5-CypA splice isoform in old world monkeys. *PLoS pathogens*, 4(2), p.e1000003.

Niederman, T.M., Thielan, B.J. & Ratner, L., 1989. Human immunodeficiency virus type 1 negative factor is a transcriptional silencer. *Proceedings of the National Academy of Sciences of the United States of America*, 86(4), pp.1128–32.

Nisole, S., Stoye, J.P. & Saïb, A., 2005. TRIM family proteins: retroviral restriction and antiviral defence. *Nature reviews. Microbiology*, 3(10), pp.799–808.

Noble, B. et al., 2006. Recruitment of the adaptor protein 2 complex by the human immunodeficiency virus type 2 envelope protein is necessary for high levels of virus release. *Journal of virology*, 80(6), pp.2924–32.

O'Neil, P.K. et al., 2002. Mutational analysis of HIV-1 long terminal repeats to explore the relative contribution of reverse transcriptase and RNA polymerase II to viral mutagenesis. *The Journal of biological chemistry*, 277(41), pp.38053–61.

Onafuwa, A. et al., 2003. Human immunodeficiency virus type 1 genetic recombination is more frequent than that of Moloney

murine leukemia virus despite similar template switching rates. *Journal of virology*, 77(8), pp.4577–87.

Ono, A. et al., 2004. Phosphatidylinositol (4,5) bisphosphate regulates HIV-1 Gag targeting to the plasma membrane. *Proceedings of the National Academy of Sciences of the United States of America*, 101(41), pp.14889–94.

Ono, A. & Freed, E.O., 2001. Plasma membrane rafts play a critical role in HIV-1 assembly and release. *Proceedings of the National Academy of Sciences of the United States of America*, 98(24), pp.13925–30.

Ooi, Y.S., Dubé, M. & Kielian, M., 2015. BST2/tetherin inhibition of alphavirus exit. *Viruses*, 7(4), pp.2147–67.

Ota, T. et al., 2004. Complete sequencing and characterization of 21,243 full-length human cDNAs. *Nature genetics*, 36(1), pp.40–5.

Pandori, M.W. et al., 1996. Producer-cell modification of human immunodeficiency virus type 1: Nef is a virion protein. *Journal of virology*, 70(7), pp.4283–90.

Papkalla, A. et al., 2002. Nef enhances human immunodeficiency virus type 1 infectivity and replication independently of viral coreceptor tropism. *Journal of virology*, 76(16), pp.8455–9.

Paprotka, T. et al., 2011. Recombinant origin of the retrovirus XMRV. *Science (New York, N.Y.)*, 333(6038), pp.97–101.

Pardieu, C. et al., 2010. The RING-CH ligase K5 antagonizes restriction of KSHV and HIV-1 particle release by mediating ubiquitin-dependent endosomal degradation of tetherin. *PLoS pathogens*, 6(4), p.e1000843.

Park, S.H. et al., 2003. Three-dimensional structure of the channel-forming trans-membrane domain of virus protein “u” (Vpu) from HIV-1. *Journal of molecular biology*, 333(2), pp.409–24.

Park, S.H. & Opella, S.J., 2005. Tilt angle of a trans-membrane helix is determined by hydrophobic mismatch. *Journal of molecular biology*, 350(2), pp.310–8.

Pawlak, E.N. & Dikeakos, J.D., 2015. HIV-1 Nef: a master manipulator of the membrane trafficking machinery mediating immune evasion. *Biochimica et biophysica acta*, 1850(4), pp.733–41.

Peeters, M. et al., 1997. Geographical distribution of HIV-1 group O viruses in Africa. *AIDS (London, England)*, 11(4), pp.493–8.

Peeters, M. et al., 2002. Risk to human health from a plethora of simian immunodeficiency viruses in primate bushmeat. *Emerging infectious diseases*, 8(5), pp.451–7.

Peng, K. et al., 2014. Quantitative microscopy of functional HIV post-entry complexes reveals association of replication with the viral capsid. *eLife*, 3, p.e04114.

Perez-Caballero, D. et al., 2005. Human tripartite motif 5alpha domains responsible for retrovirus restriction activity and specificity. *Journal of virology*, 79(14), pp.8969–78.

Perez-Caballero, D. et al., 2009. Tetherin inhibits HIV-1 release by directly tethering virions to cells. *Cell*, 139(3), pp.499–511.

Perreira, J.M. et al., 2013. IFITMs Restrict the Replication of Multiple Pathogenic Viruses. *Journal of Molecular Biology*, 425(24), pp.4937–4955.

Perron, M.J. et al., 2004. TRIM5alpha mediates the postentry block to N-tropic murine leukemia viruses in human cells. *Proceedings of the National Academy of Sciences of the United States of America*, 101(32), pp.11827–32.

Pertel, T. et al., 2011. TRIM5 is an innate immune sensor for the retrovirus capsid lattice. *Nature*, 472(7343), pp.361–5.

Pham, T.N. et al., 2014. HIV Nef and Vpu protect HIV-infected CD4+ T cells from antibody-mediated cell Lysis through down-modulation of CD4 and BST2. *Retrovirology*, 11(1), p.15.

Pickering, S. et al., 2014. Preservation of tetherin and CD4 counter-activities in circulating Vpu alleles despite extensive sequence variation within HIV-1 infected individuals. *PLoS pathogens*, 10(1), p.e1003895.

Pillai, S.K. et al., 2012. Role of retroviral restriction factors in the interferon- -mediated suppression of HIV-1 in vivo. *Proceedings of the National Academy of Sciences*, p.1111573109–.

Pinter, A. et al., 2004. The V1/V2 domain of gp120 is a global regulator of the sensitivity of primary human immunodeficiency virus type 1 isolates to neutralization by antibodies commonly induced upon infection. *Journal of virology*, 78(10), pp.5205–15.

Pitossi, F. et al., 1993. A functional GTP-binding motif is necessary for antiviral activity of Mx proteins. *Journal of virology*, 67(11), pp.6726–32.

Pizzato, M. et al., 2007. Dynamin 2 is required for the enhancement of HIV-1 infectivity by Nef. *Proceedings of the National Academy of Sciences of the United States of America*, 104(16), pp.6812–7.

Pizzato, M., 2010. MLV glycosylated-Gag is an infectivity factor that rescues Nef-deficient HIV-1. *Proceedings of the National Academy of Sciences of the United States of America*, 107(20), pp.9364–9.

Pizzato, M., Popova, E. & Göttlinger, H.G., 2008. Nef can enhance the infectivity of receptor-pseudotyped human immunodeficiency virus type 1 particles. *Journal of virology*, 82(21), pp.10811–9.

Pizzato, N., Derrien, M. & Lenfant, F., 2004. The short cytoplasmic tail of HLA-G determines its resistance to HIV-1 Nef-mediated cell surface downregulation. *Human immunology*, 65(11), pp.1389–96.

Plantier, J.-C. et al., 2009. A new human immunodeficiency virus derived from gorillas. *Nature medicine*, 15(8), pp.871–2.

Ponten, A. et al., 1997. Dominant-negative mutants of human MxA protein: domains in the carboxy-terminal moiety are important for oligomerization and antiviral activity. *Journal of virology*, 71(4), pp.2591–9.

Popov, S. et al., 2008. Human immunodeficiency virus type 1 Gag engages the Bro1 domain of ALIX/AIP1 through the nucleocapsid. *Journal of virology*, 82(3), pp.1389–98.

Pornillos, O. et al., 2003. HIV Gag mimics the Tsg101-recruiting activity of the human Hrs protein. *The Journal of cell biology*, 162(3), pp.425–34.

Powell, R.D. et al., 2011. Aicardi-Goutieres Syndrome Gene and HIV-1 Restriction Factor SAMHD1 Is a dGTP-regulated Deoxynucleotide Triphosphohydrolase. *Journal of Biological Chemistry*, 286(51), pp.43596–43600.

Prabu-Jeyabalan, M., Nalivaika, E. & Schiffer, C.A., 2002. Substrate shape determines specificity of recognition for HIV-1 protease: analysis of crystal structures of six substrate complexes. *Structure (London, England : 1993)*, 10(3), pp.369–81.

Pullen, K.A., Ishimoto, L.K. & Champoux, J.J., 1992. Incomplete removal of the RNA primer for minus-strand DNA synthesis by human immunodeficiency virus type 1 reverse transcriptase. *Journal of virology*, 66(1), pp.367–73.

Radoshitzky, S.R. et al., 2010. Infectious Lassa virus, but not filoviruses, is restricted by BST-2/tetherin. *Journal of virology*, 84(20), pp.10569–80.

Raiborg, C. et al., 2006. Flat clathrin coats on endosomes mediate degradative protein sorting by scaffolding Hrs in dynamic microdomains. *Journal of cell science*, 119(Pt 12), pp.2414–24.

Rasaiyaah, J. et al., 2013. HIV-1 evades innate immune recognition through specific cofactor recruitment. *Nature*.

Rasmussen, T.A., Tolstrup, M. & Søgaard, O.S., 2015. Reversal of Latency as Part of a Cure for HIV-1. *Trends in Microbiology*.

Ratner, L. et al., 1985. Complete nucleotide sequence of the AIDS virus, HTLV-III. *Nature*, 313(6000), pp.277–84.

Raulet, D.H., 2003. Roles of the NKG2D immunoreceptor and its ligands. *Nature reviews. Immunology*, 3(10), pp.781–90.

Refsland, E.W. et al., 2010. Quantitative profiling of the full APOBEC3 mRNA repertoire in lymphocytes and tissues: implications for HIV-1 restriction. *Nucleic acids research*, 38(13), pp.4274–84.

Rein, A., 2010. Nucleic acid chaperone activity of retroviral Gag proteins. *RNA biology*, 7(6), pp.700–5.

Ren, X. et al., 2014. How HIV-1 Nef hijacks the AP-2 clathrin adaptor to downregulate CD4. *eLife*, 3, p.e01754.

Ren, X. & Hurley, J.H., 2011. Proline-rich regions and motifs in trafficking: from ESCRT interaction to viral exploitation. *Traffic (Copenhagen, Denmark)*, 12(10), pp.1282–90.

Rhee, S.S. & Marsh, J.W., 1994. Human immunodeficiency virus type 1 Nef-induced down-modulation of CD4 is due to rapid internalization and degradation of surface CD4. *Journal of virology*, 68(8), pp.5156–63.

Rice, G.I. et al., 2009. Mutations involved in Aicardi-Goutières syndrome implicate SAMHD1 as regulator of the innate immune response. *Nature genetics*, 41(7), pp.829–32.

Rittner, K. et al., 1995. The human immunodeficiency virus long terminal repeat includes a specialised initiator element which is required for Tat-responsive transcription. *Journal of molecular biology*, 248(3), pp.562–80.

Roa, A. et al., 2012. RING domain mutations uncouple TRIM5α restriction of HIV-1 from inhibition of reverse transcription and acceleration of uncoating. *Journal of virology*, 86(3), pp.1717–27.

Rollason, R. et al., 2009. A CD317/tetherin-RICH2 complex plays a critical role in the organization of the subapical actin cytoskeleton in polarized epithelial cells. *The Journal of cell biology*, 184(5), pp.721–36.

Rollason, R. et al., 2007. Clathrin-mediated endocytosis of a lipid-raft-associated protein is mediated through a dual tyrosine motif. *Journal of cell science*, 120(Pt 21), pp.3850–8.

Rosa, A. et al., 2015. HIV-1 Nef promotes infection by excluding SERINC5 from virion incorporation. *Nature*, advance on.

Ruiz, A. et al., 2008. Requirements of the membrane proximal tyrosine and dileucine-based sorting signals for efficient transport of the subtype C Vpu protein to the plasma membrane and in virus release. *Virology*, 378(1), pp.58–68.

Ryoo, J. et al., 2014. The ribonuclease activity of SAMHD1 is required for HIV-1 restriction. *Nature medicine*, 20(8), pp.936–41.

Sadler, H.A. et al., 2010. APOBEC3G contributes to HIV-1 variation through sublethal mutagenesis. *Journal of virology*, 84(14), pp.7396–404.

Saksela, K., Cheng, G. & Baltimore, D., 1995. Proline-rich (PxxP) motifs in HIV-1 Nef bind to SH3 domains of a subset of Src kinases and are required for the enhanced growth of Nef+ viruses but not for down-regulation of CD4. *The EMBO journal*, 14(3), pp.484–91.

Sakuma, T. et al., 2009. Inhibition of Lassa and Marburg virus production by tetherin. *Journal of virology*, 83(5), pp.2382–5.

Salazar-Gonzalez, J.F. et al., 2009. Genetic identity, biological phenotype, and evolutionary pathways of transmitted/founder viruses in acute and early HIV-1 infection. *The Journal of experimental medicine*, 206(6), pp.1273–89.

Saphire, A.C. et al., 2001. Syndecans serve as attachment receptors for human immunodeficiency virus type 1 on macrophages. *Journal of virology*, 75(19), pp.9187–200.

Sato, K. et al., 2012. Vpu augments the initial burst phase of HIV-1 propagation and downregulates BST2 and CD4 in

humanized mice. *Journal of virology*, 86(9), pp.5000–13.

Sattentau, Q., 2008. Avoiding the void: cell-to-cell spread of human viruses. *Nature reviews. Microbiology*, 6(11), pp.815–26.

Sauter, D. et al., 2015. Differential Regulation of NF-κB-Mediated Proviral and Antiviral Host Gene Expression by Primate Lentiviral Nef and Vpu Proteins. *Cell reports*.

Sauter, D., Hué, S., et al., 2011. HIV-1 Group P is unable to antagonize human tetherin by Vpu, Env or Nef. *Retrovirology*, 8, p.103.

Sauter, D., Unterweger, D., Vogl, M., Usmani, S.M., et al., 2012. Human Tetherin Exerts Strong Selection Pressure on the HIV-1 Group N Vpu Protein C. Aiken, ed. *PLoS Pathogens*, 8(12), p.e1003093.

Sauter, D., Unterweger, D., Vogl, M., Usmani, S.M., et al., 2012. Human tetherin exerts strong selection pressure on the HIV-1 group N Vpu protein. *PLoS pathogens*, 8(12), p.e1003093.

Sauter, D. et al., 2009. Tetherin-driven adaptation of Vpu and Nef function and the evolution of pandemic and nonpandemic HIV-1 strains. *Cell host & microbe*, 6(5), pp.409–21.

Sauter, D. & Kirchhoff, F., 2011. Tetherin antagonism by primate lentiviral nef proteins. *Current HIV research*, 9(7), pp.514–23.

Sauter, D., Specht, A. & Kirchhoff, F., 2010. Tetherin: holding on and letting go. *Cell*, 141(3), pp.392–8.

Sauter, D., Vogl, M. & Kirchhoff, F., 2011. Ancient origin of a deletion in human BST2/Tetherin that confers protection against viral zoonoses. *Human mutation*, 32(11), pp.1243–5.

Sawyer, S.L. et al., 2005. Positive selection of primate TRIM5alpha identifies a critical species-specific retroviral restriction domain. *Proceedings of the National Academy of Sciences of the United States of America*, 102(8), pp.2832–7.

Sayah, D.M. et al., 2004. Cyclophilin A retrotransposition into TRIM5 explains owl monkey resistance to HIV-1. *Nature*, 430(6999), pp.569–73.

Scarlatti, G. et al., 1997. In vivo evolution of HIV-1 co-receptor usage and sensitivity to chemokine-mediated suppression. *Nature Medicine*, 3(11), pp.1259–1265.

Schaefer, M.R. et al., 2008. HIV-1 Nef targets MHC-I and CD4 for degradation via a final common beta-COP-dependent pathway in T cells. *PLoS pathogens*, 4(8), p.e1000131.

Schaeffer, E., Geleziunas, R. & Greene, W.C., 2001. Human Immunodeficiency Virus Type 1 Nef Functions at the Level of Virus Entry by Enhancing Cytoplasmic Delivery of Virions. *Journal of Virology*, 75(6), pp.2993–3000.

Schindler, M. et al., 2006. Nef-Mediated Suppression of T Cell Activation Was Lost in a Lentiviral Lineage that Gave Rise to HIV-1. *Cell*, 125(6), pp.1055–1067.

Schmidt, S. et al., 2011. HIV-1 Vpu blocks recycling and biosynthetic transport of the intrinsic immunity factor CD317/tetherin to overcome the virion release restriction. *mBio*, 2(3), pp.e00036–11.

Schrager, J.A. & Marsh, J.W., 1999. HIV-1 Nef increases T cell activation in a stimulus-dependent manner. *Proceedings of the National Academy of Sciences of the United States of America*, 96(14), pp.8167–72.

Schubert, H.L. et al., 2010. Structural and functional studies on the extracellular domain of BST2/tetherin in reduced and oxidized conformations. *Proceedings of the National Academy of Sciences of the United States of America*, 107(42), pp.17951–6.

Schubert, U. et al., 1992. Human-immunodeficiency-virus-type-1-encoded Vpu protein is phosphorylated by casein kinase II. *European journal of biochemistry / FEBS*, 204(2), pp.875–83.

Schubert, U. et al., 1996. The two biological activities of human immunodeficiency virus type 1 Vpu protein involve two separable structural domains. *Journal of virology*, 70(2), pp.809–19.

Schubert, U., Clouse, K.A. & Strebel, K., 1995. Augmentation of virus secretion by the human immunodeficiency virus type 1 Vpu protein is cell type independent and occurs in cultured human primary macrophages and lymphocytes. *Journal of virology*, 69(12), pp.7699–711.

Schubert, U. & Strebel, K., 1994. Differential activities of the human immunodeficiency virus type 1-encoded Vpu protein are regulated by phosphorylation and occur in different cellular compartments. *Journal of virology*, 68(4), pp.2260–71.

Schuitemaker, H. et al., 1992. Biological phenotype of human immunodeficiency virus type 1 clones at different stages of infection: progression of disease is associated with a shift from monocytotropic to T-cell-tropic virus population. *Journal of virology*, 66(3), pp.1354–60.

Schulte, B. et al., 2015. Restriction of HIV-1 Requires the N-Terminal Region of MxB as a Capsid-Binding Motif but Not as a Nuclear Localization Signal. *Journal of virology*, 89(16), pp.8599–610.

Schwartz, O. et al., 1996. Endocytosis of major histocompatibility complex class I molecules is induced by the HIV-1 Nef protein. *Nature medicine*, 2(3), pp.338–42.

Schwartz, S. et al., 1990. Env and Vpu proteins of human immunodeficiency virus type 1 are produced from multiple bicistronic mRNAs. *Journal of virology*, 64(11), pp.5448–56.

Selby, M.J. et al., 1989. Structure, sequence, and position of the stem-loop in tar determine transcriptional elongation by tat through the HIV-1 long terminal repeat. *Genes & development*, 3(4), pp.547–58.

Serra-Moreno, R. et al., 2011. Compensatory changes in the cytoplasmic tail of gp41 confer resistance to tetherin/BST-2 in a pathogenic nef-deleted SIV. *Cell host & microbe*, 9(1), pp.46–57.

Serra-Moreno, R. et al., 2013a. Tetherin/BST-2 antagonism by Nef depends on a direct physical interaction between Nef and tetherin, and on clathrin-mediated endocytosis. *PLoS pathogens*, 9(7), p.e1003487.

Serra-Moreno, R. et al., 2013b. Tetherin/BST-2 antagonism by Nef depends on a direct physical interaction between Nef and tetherin, and on clathrin-mediated endocytosis. *PLoS pathogens*, 9(7), p.e1003487.

Shah, A.H. et al., 2010. Degranulation of natural killer cells following interaction with HIV-1-infected cells is hindered by downmodulation of NTB-A by Vpu. *Cell host & microbe*, 8(5), pp.397–409.

Shalem, O. et al., 2014. Genome-scale CRISPR-Cas9 knockout screening in human cells. *Science (New York, N.Y.)*, 343(6166), pp.84–7.

Sharp, P.M. & Hahn, B.H., 2011. Origins of HIV and the AIDS pandemic. *Cold Spring Harbor perspectives in medicine*, 1(1), p.a006841.

Sheehy, A.M. et al., 2002. Isolation of a human gene that inhibits HIV-1 infection and is suppressed by the viral Vif protein. *Nature*, 418(6898), pp.646–650.

Sherer, N.M., Jin, J. & Mothes, W., 2010. Directional spread of surface-associated retroviruses regulated by differential virus-cell interactions. *Journal of virology*, 84(7), pp.3248–58.

Shun, M.-C. et al., 2007. LEDGF/p75 functions downstream from preintegration complex formation to effect gene-specific HIV-1 integration. *Genes & development*, 21(14), pp.1767–78.

Simmons, A., Aluvihare, V. & McMichael, A., 2001. Nef triggers a transcriptional program in T cells imitating single-signal T cell activation and inducing HIV virulence mediators. *Immunity*, 14(6), pp.763–77.

Simon, F. et al., 1998. Identification of a new human immunodeficiency virus type 1 distinct from group M and group O. *Nature medicine*, 4(9), pp.1032–7.

Simon, J.H. et al., 1998. Evidence for a newly discovered cellular anti-HIV-1 phenotype. *Nature medicine*, 4(12), pp.1397–400.

Singh, S.K. et al., 2012. Mapping the interaction between the cytoplasmic domains of HIV-1 viral protein U and human CD4 with NMR spectroscopy. *The FEBS journal*, 279(19), pp.3705–14.

Skasko, M. et al., 2011. BST-2 is rapidly down-regulated from the cell surface by the HIV-1 protein Vpu: evidence for a post-ER mechanism of Vpu-action. *Virology*, 411(1), pp.65–77.

Skasko, M. et al., 2012. HIV-1 Vpu protein antagonizes innate restriction factor BST-2 via lipid-embedded helix-helix interactions. *The Journal of biological chemistry*, 287(1), pp.58–67.

Smith, J.S. & Roth, M.J., 1992. Specificity of human immunodeficiency virus-1 reverse transcriptase-associated ribonuclease H in removal of the minus-strand primer, tRNA(Lys3). *The Journal of biological chemistry*, 267(21), pp.15071–9.

Sobhian, B. et al., 2010. HIV-1 Tat assembles a multifunctional transcription elongation complex and stably associates with the 7SK snRNP. *Molecular cell*, 38(3), pp.439–51.

Solis, M. et al., 2011. RIG-I-mediated antiviral signaling is inhibited in HIV-1 infection by a protease-mediated sequestration of RIG-I. *Journal of virology*, 85(3), pp.1224–36.

Song, B. et al., 2005. The B30.2(SPRY) domain of the retroviral restriction factor TRIM5alpha exhibits lineage-specific length and sequence variation in primates. *Journal of virology*, 79(10), pp.6111–21.

Specht, A. et al., 2008. Selective downmodulation of HLA-A and -B by Nef alleles from different groups of primate lentiviruses. *Virology*, 373(1), pp.229–37.

Srivastava, S. et al., 2008. Lentiviral Vpx accessory factor targets VprBP/DCAF1 substrate adaptor for cullin 4 E3 ubiquitin ligase to enable macrophage infection. *PLoS pathogens*, 4(5), p.e1000059.

Stein, B.S. et al., 1987. pH-independent HIV entry into CD4-positive T cells via virus envelope fusion to the plasma membrane. *Cell*, 49(5), pp.659–68.

Stolp, B. et al., 2009. HIV-1 Nef interferes with host cell motility by deregulation of Cofilin. *Cell host & microbe*, 6(2), pp.174–86.

Strack, B. et al., 2003. AIP1/ALIX is a binding partner for HIV-1 p6 and EIAV p9 functioning in virus budding. *Cell*, 114(6), pp.689–99.

Strebel, K. et al., 1989. Molecular and biochemical analyses of human immunodeficiency virus type 1 vpu protein. *Journal of virology*, 63(9), pp.3784–91.

Strebel, K., Klimkait, T. & Martin, M.A., 1988. A novel gene of HIV-1, vpu, and its 16-kilodalton product. *Science (New York, N.Y.)*, 241(4870), pp.1221–3.

Stremlau, M., Song, B., et al., 2006. Cyclophilin A: an auxiliary but not necessary cofactor for TRIM5alpha restriction of HIV-1. *Virology*, 351(1), pp.112–20.

Stremlau, M. et al., 2005. Species-specific variation in the B30.2(SPRY) domain of TRIM5alpha determines the potency of human immunodeficiency virus restriction. *Journal of virology*, 79(5), pp.3139–45.

Stremlau, M., Perron, M., et al., 2006. Specific recognition and accelerated uncoating of retroviral capsids by the TRIM5alpha restriction factor. *Proceedings of the National Academy of Sciences of the United States of America*, 103(14), pp.5514–9.

Stremlau, M. et al., 2004. The cytoplasmic body component TRIM5alpha restricts HIV-1 infection in Old World monkeys. *Nature*, 427(6977), pp.848–53.

Sundquist, W.I. & Kräusslich, H.-G., 2012. HIV-1 assembly, budding, and maturation. *Cold Spring Harbor perspectives in medicine*, 2(7), p.a006924.

Suspène, R. & Meyerhans, A., 2012. Quantification of unintegrated HIV-1 DNA at the single cell level in vivo. *PloS one*, 7(5), p.e36246.

Swanson, C.M. & Malim, M.H., 2008. SnapShot: HIV-1 proteins. *Cell*, 133(4), pp.742, 742.e1.

Swanson, C.M., Sherer, N.M. & Malim, M.H., 2010. SRp40 and SRp55 promote the translation of unspliced human immunodeficiency virus type 1 RNA. *Journal of virology*, 84(13), pp.6748–59.

Swiecki, M. et al., 2012. Cutting Edge: Paradoxical Roles of BST2/Tetherin in Promoting Type I IFN Response and Viral Infection. *Journal of immunology (Baltimore, Md. : 1950)*.

Swiecki, M. et al., 2011. Structural and biophysical analysis of BST-2/tetherin ectodomains reveals an evolutionary conserved design to inhibit virus release. *The Journal of biological chemistry*, 286(4), pp.2987–97.

Swiecki, M., Omattage, N.S. & Brett, T.J., 2013. BST-2/tetherin: structural biology, viral antagonism, and immunobiology of a potent host antiviral factor. *Molecular immunology*, 54(2), pp.132–9.

Tahirov, T.H. et al., 2010. Crystal structure of HIV-1 Tat complexed with human P-TEFb. *Nature*, 465(7299), pp.747–51.

Tang, C. et al., 2004. Entropic switch regulates myristate exposure in the HIV-1 matrix protein. *Proceedings of the National Academy of Sciences of the United States of America*, 101(2), pp.517–22.

Tang, C. et al., 2008. Visualizing transient events in amino-terminal autoprocessing of HIV-1 protease. *Nature*, 455(7213), pp.693–6.

Tartour, K. et al., 2014. IFITM proteins are incorporated onto HIV-1 virion particles and negatively imprint their infectivity. *Retrovirology*, 11, p.103.

Tavano, B. et al., 2013. Ig-like Transcript 7, but Not Bone Marrow Stromal Cell Antigen 2 (Also Known as HM1.24, Tetherin, or CD317), Modulates Plasmacytoid Dendritic Cell Function in Primary Human Blood Leukocytes. *Journal of immunology (Baltimore, Md. : 1950)*.

Taylor, J.K. et al., 2015. Severe Acute Respiratory Syndrome Coronavirus ORF7a Inhibits Bone Marrow Stromal Antigen 2 Virion Tethering through a Novel Mechanism of Glycosylation Interference. *Journal of virology*, 89(23), pp.11820–33.

Tervo, H.-M. et al., 2011. β-TrCP is dispensable for Vpu's ability to overcome the CD317/Tetherin-imposed restriction to HIV-1 release. *Retrovirology*, 8, p.9.

Terwilliger, E.F. et al., 1989. Functional role of human immunodeficiency virus type 1 vpu. *Proceedings of the National Academy of Sciences of the United States of America*, 86(13), pp.5163–7.

Thibault, S. et al., 2009. TLR2 and TLR4 triggering exerts contrasting effects with regard to HIV-1 infection of human dendritic cells and subsequent virus transfer to CD4+ T cells. *Retrovirology*, 6, p.42.

Tiganos, E. et al., 1997. Putative alpha-helical structures in the human immunodeficiency virus type 1 Vpu protein and CD4 are involved in binding and degradation of the CD4 molecule. *Journal of virology*, 71(6), pp.4452–60.

Tobiume, M. et al., 2003. Nef Does Not Affect the Efficiency of Human Immunodeficiency Virus Type 1 Fusion with Target Cells. *Journal of Virology*, 77(19), pp.10645–10650.

Tokarev, A. et al., 2013. Stimulation of NF-κB activity by the HIV restriction factor BST2. *Journal of virology*, 87(4), pp.2046–57.

Tokarev, A.A., Munguia, J. & Guatelli, J.C., 2011. Serine-threonine ubiquitination mediates downregulation of BST-2/tetherin and relief of restricted virion release by HIV-1 Vpu. *Journal of virology*, 85(1), pp.51–63.

Le Tortorec, A. & Neil, S.J.D., 2009. Antagonism to and intracellular sequestration of human tetherin by the human immunodeficiency virus type 2 envelope glycoprotein. *Journal of virology*, 83(22), pp.11966–78.

Le Tortorec, A., Willey, S. & Neil, S.J.D., 2011. Antiviral Inhibition of Enveloped Virus Release by Tetherin/BST-2: Action and Counteraction. *Viruses*, 3(5), pp.520–540.

Towers, G. et al., 2000. A conserved mechanism of retrovirus restriction in mammals. *Proceedings of the National Academy of Sciences of the United States of America*, 97(22), pp.12295–9.

Trono, D., 1992. Partial reverse transcripts in virions from human immunodeficiency and murine leukemia viruses. *Journal of virology*, 66(8), pp.4893–900.

Uchil, P.D. et al., 2013. TRIM protein-mediated regulation of inflammatory and innate immune signaling and its association with antiretroviral activity. *Journal of virology*, 87(1), pp.257–72.

Uchil, P.D. & Mothes, W., 2009. HIV Entry Revisited. *Cell*, 137(3), pp.402–4.

Usami, Y. & Göttlinger, H., 2013. HIV-1 Nef responsiveness is determined by Env variable regions involved in trimer association and correlates with neutralization sensitivity. *Cell reports*, 5(3), pp.802–12.

Usami, Y., Popov, S. & Göttlinger, H.G., 2014. The Nef-like effect of murine leukemia virus glycosylated gag on HIV-1 infectivity is mediated by its cytoplasmic domain and depends on the AP-2 adaptor complex. *Journal of virology*, 88(6), pp.3443–54.

Usami, Y., Wu, Y. & Göttlinger, H.G., 2015. SERINC3 and SERINC5 restrict HIV-1 infectivity and are counteracted by Nef. *Nature*, advance on.

Vallari, A. et al., 2011. Confirmation of putative HIV-1 group P in Cameroon. *Journal of virology*, 85(3), pp.1403–7.

Vallari, A. et al., 2010. Four new HIV-1 group N isolates from Cameroon: Prevalence continues to be low. *AIDS research and human retroviruses*, 26(1), pp.109–15.

Varthakavi, V. et al., 2003. Viral protein U counteracts a human host cell restriction that inhibits HIV-1 particle production. *Proceedings of the National Academy of Sciences of the United States of America*, 100(25), pp.15154–9.

Veillette, M., Désormeaux, A., et al., 2014. Interaction with cellular CD4 exposes HIV-1 envelope epitopes targeted by antibody-dependent cell-mediated cytotoxicity. *Journal of virology*, 88(5), pp.2633–44.

Veillette, M., Coutu, M., et al., 2014. The HIV-1 gp120 CD4-bound conformation is preferentially targeted by ADCC-mediating antibodies in sera from HIV-1-infected individuals. *Journal of virology*.

Venkatesh, S. & Bieniasz, P.D., 2013. Mechanism of HIV-1 virion entrapment by tetherin. *PLoS pathogens*, 9(7), p.e1003483.

VerPlank, L. et al., 2001. Tsg101, a homologue of ubiquitin-conjugating (E2) enzymes, binds the L domain in HIV type 1 Pr55(Gag). *Proceedings of the National Academy of Sciences of the United States of America*, 98(14), pp.7724–9.

Vigan, R. & Neil, S.J.D., 2010. Determinants of tetherin antagonism in the transmembrane domain of the human immunodeficiency virus type 1 Vpu protein. *Journal of virology*, 84(24), pp.12958–70.

Vigan, R. & Neil, S.J.D., 2011. Separable determinants of subcellular localization and interaction account for the inability of group O HIV-1 Vpu to counteract tetherin. *Journal of virology*, 85(19), pp.9737–48.

Virgen, C.A. et al., 2008. Independent genesis of chimeric TRIM5-cyclophilin proteins in two primate species. *Proceedings of the National Academy of Sciences of the United States of America*, 105(9), pp.3563–8.

Viswanathan, K. et al., 2011. BST2/Tetherin enhances entry of human cytomegalovirus. *PLoS pathogens*, 7(11), p.e1002332.

Waheed, A.A. & Freed, E.O., 2010. The Role of Lipids in Retrovirus Replication. *Viruses*, 2(5), pp.1146–1180.

Wain-Hobson, S. et al., 1985. Nucleotide sequence of the AIDS virus, LAV. *Cell*, 40(1), pp.9–17.

van Wamel, J.L. & Berkhout, B., 1998. The first strand transfer during HIV-1 reverse transcription can occur either intramolecularly or intermolecularly. *Virology*, 244(2), pp.245–51.

Wang, G.P. et al., 2007. HIV integration site selection: analysis by massively parallel pyrosequencing reveals association with epigenetic modifications. *Genome research*, 17(8), pp.1186–94.

Wang, S.-M., Huang, K.-J. & Wang, C.-T., 2014. BST2/CD317 counteracts human coronavirus 229E productive infection by tethering virions at the cell surface. *Virology*, 449, pp.287–96.

Ward, J. et al., 2009. HIV-1 Vpr triggers natural killer cell-mediated lysis of infected cells through activation of the ATR-mediated DNA damage response. *PLoS pathogens*, 5(10), p.e1000613.

Watanabe, R., Leser, G.P. & Lamb, R.A., 2011. Influenza virus is not restricted by tetherin whereas influenza VLP production is restricted by tetherin. *Virology*, 417(1), pp.50–6.

Wei, P. et al., 1998. A novel CDK9-associated C-type cyclin interacts directly with HIV-1 Tat and mediates its high-affinity, loop-specific binding to TAR RNA. *Cell*, 92(4), pp.451–62.

Weidner, J.M. et al., 2010. Interferon-induced cell membrane proteins, IFITM3 and tetherin, inhibit vesicular stomatitis virus infection via distinct mechanisms. *Journal of virology*, 84(24), pp.12646–57.

Weinelt, J. & Neil, S.J.D., 2014. Differential sensitivities of tetherin isoforms to counteraction by primate lentiviruses. *Journal of virology*.

Weissenhorn, W. et al., 1997. Atomic structure of the ectodomain from HIV-1 gp41. *Nature*, 387(6631), pp.426–30.

Welbourn, S. et al., 2013. Restriction of virus infection but not catalytic dNTPase activity is regulated by phosphorylation of SAMHD1. *Journal of virology*, 87(21), pp.11516–24.

Welker, R. et al., 1996. Human immunodeficiency virus type 1 Nef protein is incorporated into virus particles and specifically cleaved by the viral proteinase. *Virology*, 219(1), pp.228–36.

Wen, X. et al., 2007. The HIV1 protein Vpr acts to promote G2 cell cycle arrest by engaging a DDB1 and Cullin4A-containing ubiquitin ligase complex using VprBP/DCAF1 as an adaptor. *The Journal of biological chemistry*, 282(37), pp.27046–57.

White, T.E. et al., 2013. The retroviral restriction ability of SAMHD1, but not its deoxynucleotide triphosphohydrolase activity, is regulated by phosphorylation. *Cell host & microbe*, 13(4), pp.441–51.

Wildum, S. et al., 2006. Contribution of Vpu, Env, and Nef to CD4 down-modulation and resistance of human immunodeficiency virus type 1-infected T cells to superinfection. *Journal of virology*, 80(16), pp.8047–59.

Wilen, C.B., Tilton, J.C. & Doms, R.W., 2012. HIV: Cell Binding and Entry. *Cold Spring Harbor Perspectives in Medicine*,

2(8), pp.a006866–a006866.

Wilen, C.B., Tilton, J.C. & Doms, R.W., 2012. Molecular mechanisms of HIV entry. *Advances in experimental medicine and biology*, 726, pp.223–42.

van Wilgenburg, B. et al., 2014. The productive entry pathway of HIV-1 in macrophages is dependent on endocytosis through lipid rafts containing CD4. *PloS one*, 9(1), p.e86071.

Willbold, D., Hoffmann, S. & Rösch, P., 1997. Secondary structure and tertiary fold of the human immunodeficiency virus protein U (Vpu) cytoplasmic domain in solution. *European journal of biochemistry / FEBS*, 245(3), pp.581–8.

Willey, R.L. et al., 1992. Human immunodeficiency virus type 1 Vpu protein induces rapid degradation of CD4. *Journal of virology*, 66(12), pp.7193–200.

Wilson, S.J. et al., 2008. Independent evolution of an antiviral TRIMCyp in rhesus macaques. *Proceedings of the National Academy of Sciences of the United States of America*, 105(9), pp.3557–62.

Winkler, M. et al., 2012. Influenza A virus does not encode a tetherin antagonist with Vpu-like activity and induces IFN-dependent tetherin expression in infected cells. *PloS one*, 7(8), p.e43337.

Wittlich, M. et al., 2009. NMR structural characterization of HIV-1 virus protein U cytoplasmic domain in the presence of dodecylphosphatidylcholine micelles. *The FEBS journal*, 276(22), pp.6560–75.

Wittlich, M., Koenig, B.W. & Willbold, D., 2008. Structural consequences of phosphorylation of two serine residues in the cytoplasmic domain of HIV-1 VpU. *Journal of peptide science : an official publication of the European Peptide Society*, 14(7), pp.804–10.

Wood, N. et al., 2009. HIV evolution in early infection: selection pressures, patterns of insertion and deletion, and the impact of APOBEC. *PLoS pathogens*, 5(5), p.e1000414.

Worobey, M. et al., 2008. Direct evidence of extensive diversity of HIV-1 in Kinshasa by 1960. *Nature*, 455(7213), pp.661–4.

Wu, X. et al., 2006. Proteasome inhibitors uncouple rhesus TRIM5alpha restriction of HIV-1 reverse transcription and infection. *Proceedings of the National Academy of Sciences of the United States of America*, 103(19), pp.7465–70.

Wyma, D.J. et al., 2004. Coupling of human immunodeficiency virus type 1 fusion to virion maturation: a novel role of the gp41 cytoplasmic tail. *Journal of virology*, 78(7), pp.3429–35.

Yamada, T. et al., 2006. P-TEFb-mediated phosphorylation of hSpt5 C-terminal repeats is critical for processive transcription elongation. *Molecular cell*, 21(2), pp.227–37.

Yamashita, M. et al., 2007. Evidence for Direct Involvement of the Capsid Protein in HIV Infection of Nondividing Cells. *PLoS Pathogens*, 3(10), p.e156.

Yamashita, M. & Emerman, M., 2004. Capsid is a dominant determinant of retrovirus infectivity in nondividing cells. *Journal of virology*, 78(11), pp.5670–8.

Yan, J. et al., 2015. CyclinA2-Cyclin-dependent Kinase Regulates SAMHD1 Protein Phosphohydrolase Domain. *The Journal of biological chemistry*, 290(21), pp.13279–92.

Yan, N. et al., 2010. The cytosolic exonuclease TREX1 inhibits the innate immune response to human immunodeficiency virus type 1. *Nature Immunology*, 11(11), pp.1005–1013.

Yang, H. et al., 2010. Structural insight into the mechanisms of enveloped virus tethering by tetherin. *Proceedings of the National Academy of Sciences of the United States of America*, 107(43), pp.18428–32.

Yang, O.O. et al., 2002. Nef-Mediated Resistance of Human Immunodeficiency Virus Type 1 to Antiviral Cytotoxic T Lymphocytes. *Journal of Virology*, 76(4), pp.1626–1631.

Yang, S.J. et al., 2010. Anti-tetherin activities in Vpu-expressing primate lentiviruses. *Retrovirology*, 7, p.13.

Yang, S.J. et al., 2011. Lack of adaptation to human tetherin in HIV-1 group O and P. *Retrovirology*, 8, p.78.

Yao, X.J. et al., 1992. Envelope glycoprotein and CD4 independence of vpu-facilitated human immunodeficiency virus type 1 capsid export. *Journal of virology*, 66(8), pp.5119–26.

Yin, X. et al., 2014. Equine tetherin blocks retrovirus release and its activity is antagonized by equine infectious anemia virus envelope protein. *Journal of virology*, 88(2), pp.1259–70.

Yondola, M.A. et al., 2011. Budding capability of the influenza virus neuraminidase can be modulated by tetherin. *Journal of virology*, 85(6), pp.2480–91.

Yu, J. et al., 2015. IFITM Proteins Restrict HIV-1 Infection by Antagonizing the Envelope Glycoprotein. *Cell reports*.

Yu, Q. et al., 2004. Single-strand specificity of APOBEC3G accounts for minus-strand deamination of the HIV genome. *Nature structural & molecular biology*, 11(5), pp.435–42.

Yu, X. et al., 2003. Induction of APOBEC3G ubiquitination and degradation by an HIV-1 Vif-Cul5-SCF complex. *Science (New York, N.Y.)*, 302(5647), pp.1056–60.

Zapp, M.L. et al., 1991. Oligomerization and RNA binding domains of the type 1 human immunodeficiency virus Rev protein: a dual function for an arginine-rich binding motif. *Proceedings of the National Academy of Sciences of the United States of America*, 88(17), pp.7734–8.

Zenner, H.L. et al., 2013. Herpes simplex virus type-1 counteracts tetherin restriction via its virion host shutoff activity.

Journal of virology.

Zennou, V. et al., 2004. APOBEC3G incorporation into human immunodeficiency virus type 1 particles. *Journal of virology*, 78(21), pp.12058–61.

Zhang, C. et al., 2005. Imbalance of NKG2D and its inhibitory counterparts: how does tumor escape from innate immunity? *International immunopharmacology*, 5(7-8), pp.1099–111.

Zhang, F. et al., 2009. Nef proteins from simian immunodeficiency viruses are tetherin antagonists. *Cell host & microbe*, 6(1), pp.54–67.

Zhang, F. et al., 2011. SIV Nef proteins recruit the AP-2 complex to antagonize Tetherin and facilitate virion release. *PLoS pathogens*, 7(5), p.e1002039.

Zhang, H. et al., 2015. Structural determination of Virus protein U from HIV-1 by NMR in membrane environments. *Biochimica et biophysica acta*.

Zhang, H. et al., 2003. The cytidine deaminase CEM15 induces hypermutation in newly synthesized HIV-1 DNA. *Nature*, 424(6944), pp.94–8.

Zhang, W. et al., 2012. T-cell differentiation factor CBF-β regulates HIV-1 Vif-mediated evasion of host restriction. *Nature*, 481(7381), pp.376–9.

Zhong, P. et al., 2013. Cell-to-cell transmission can overcome multiple donor and target cell barriers imposed on cell-free HIV. *PloS one*, 8(1), p.e53138.

Zhou, J. & Aiken, C., 2001. Nef enhances human immunodeficiency virus type 1 infectivity resulting from intervirion fusion: evidence supporting a role for Nef at the virion envelope. *Journal of virology*, 75(13), pp.5851–9.

Zhu, P. et al., 2006. Distribution and three-dimensional structure of AIDS virus envelope spikes. *Nature*, 441(7095), pp.847–52.

Appendix A. Publications

JVI Journals.ASM.org

Differential Sensitivities of Tetherin Isoforms to Counteraction by Primate Lentiviruses

Julia Weinelt, Stuart J. D. Neil

Department of Infectious Disease, King's College London School of Medicine, Guy's Hospital, London, United Kingdom

ABSTRACT

The mammalian antiviral membrane protein tetherin (BST2/CD317) can be expressed as two isoforms derived from differential translational initiation. The shorter isoform of the human protein (S-tetherin) lacks the first 12 amino acids of the longer (L-tetherin) cytoplasmic tail, which includes a tyrosine motif that acts as both an endocytic recycling signal and a determinant of virus-induced NF-κB activation. S-tetherin is also reported to be less sensitive to the prototypic viral antagonist human immunodeficiency virus type 1 (HIV-1) Vpu. Here we analyzed the relative sensitivities of L- and S-tetherins to primate lentiviral countermeasures. We show that the reduced sensitivity of S-tetherin to HIV-1 Vpu is a feature of all group M proteins, including those of transmitted founder viruses, primarily because it cannot be targeted for endosomal degradation owing to the truncation of its cytoplasmic tail. In contrast, both isoforms of the human and rhesus macaque tetherins display the same sensitivity to non-degradative lentiviral countermeasures of HIV-2 and SIVmac, respectively. Surprisingly, however, the Vpu proteins encoded by simian immunodeficiency viruses (SIVs) of African guenons, as well as that from recently isolated highly pathogenic HIV-1 group N, do not discriminate between tetherin isoforms. Together, these data suggest that the group M HIV-1 Vpu primarily adapted to target L-tetherin upon zoonotic transmission from chimpanzees, and further, we speculate that functions specifically associated with this isoform, such as proinflammatory signaling, play key roles in human tetherin's antiviral function *in vivo*.

IMPORTANCE

The ability of HIV-1 and related viruses to counteract a host antiviral protein, tetherin, is strictly maintained. The adaptation of the HIV-1 Vpu protein to counteract human tetherin is thought to have been one of the key events in the establishment of the HIV/AIDS pandemic. Recent evidence shows that tetherin is expressed as two isoforms and that Vpu preferentially targets the longer form. Here we show that unlike other virus-encoded countermeasures, such as those from primate viruses related to HIV-1, the enhanced ability to counteract the long tetherin isoform is conserved among HIV-1 strains that make up the majority of the human pandemic. This correlates with the ability of Vpu to induce long tetherin degradation. We speculate that functions associated with the human version of this isoform, such as an inflammatory signaling capacity, selected for Vpu's enhanced targeting of long tetherin during its adaptation to humans.

The interferon (IFN)-induced transmembrane (TM) protein tetherin (BST2/CD317/HM1.24) displays antiviral activity *in vitro* and *in vivo* (reviewed in reference 1). It has been shown to potently restrict the release of diverse enveloped viruses, including the members of the families *Retroviridae* (2, 3) and *Herpesviridae* (4–7) and negative-strand RNA viruses (8), from infected cells by cross-linking them to the plasma membrane (PM). Tetherin is a dimeric glycoprotein that consists of an N-terminal cytoplasmic tail, a conventional TM helix, a coiled-coil extracellular domain, and a C-terminal glycosylphosphatidylinositol (GPI) anchor (1). This structural arrangement is essential for tetherin's antiviral activity (9); the dual-anchor conformation allows predominantly the GPI linkage to partition into budding virions, resulting in stable cross-links of parallel tetherin dimers when viral and cellular membranes separate (10). Thus, tetherin does not need to interact with any virus-encoded structure, which accounts for its wide activity against enveloped viruses. Virions retained by tetherin cross-links can subsequently be endocytosed and trafficked to late endosomes (2). Recent data also demonstrate that human tetherin can mediate signal transduction upon virion retention that activates NF-κB and promotes proinflammatory gene expression, thereby acting as an innate sensor of viral release (11–13).

There are now several examples of virus-encoded proteins that have evolved to counteract tetherin, often in a species-specific manner, highlighting an important selective pressure imposed by tetherin on viral evolution (1). These viral proteins include the primate lentiviral accessory proteins human immunodeficiency virus type 1 (HIV-1) Vpu (2, 14) and simian immunodeficiency virus (SIV) Nef (15, 16); the envelope glycoproteins encoded by HIV-2 and SIVtan (Env) (17, 18), Ebola virus (EBOV-G) (19), and herpes simplex virus 1 (gM) (7); and K5, a membrane-bound ubiquitin ligase encoded by Kaposi's sarcoma-associated herpesvirus (KSHV) (5, 6). Among the primate lentiviruses, genetic evidence strongly suggests that the ability to counteract tetherin is an essential attribute for viral spread *in vivo* (20). Furthermore, adaptation to target human tetherin efficiently by the Vpu proteins of the HIV-1 group M is thought to have been a key event in determining its spread to become the major agent of the HIV/AIDS pandemic (21).

Received 24 December 2013 **Accepted** 5 March 2014
Published ahead of print 12 March 2014
Editor: R. W. Doms
Address correspondence to Stuart J. D. Neil, stuart.neil@kcl.ac.uk.

doi:10.1128/JVI.03818-13

Recently it was shown that tetherin is expressed as a long (L-tetherin) or short (S-tetherin) isoform because of leaky ribosomal scanning of its mRNA that results in translational initiations at two AUG codons (11). S-tetherin lacks the first 12 amino acids of its cytoplasmic tail (11). Within these 12 residues lies a conserved tyrosine-based motif that acts both as an endocytic recycling sequence (22) and as the determinant of signal transduction in the human protein (11–13). HIV-1 Vpu, a small membrane phosphoprotein, interacts with human and chimpanzee tetherins via direct TM domain interactions (23–26) and blocks the transit of newly synthesized and recycling tetherin to the PM (27, 28). This is then coupled to tetherin's endosomal degradation by a clathrin-dependent transport event that requires both an acidic/dileucine motif in the Vpu cytoplasmic tail and the tyrosine-based sequence in L-tetherin (29). Endosomal degradation of tetherin is ubiquitin and ESCRT dependent (30, 31) and is determined by the recruitment the $SCF^{\beta TRCP1/2}$ E3 ligase to a conserved phosphoserine motif (DSGNES) in the Vpu cytoplasmic tail (32, 33). Tetherin can be ubiquitinated on multiple residues in its cytoplasmic tail, but the exact requirements for counteraction and/or degradation are unclear (34, 35). However, a serine-threonine motif found only in L-tetherin has been highlighted as important (35). In contrast, other lentiviral tetherin antagonists do not mediate its degradation but rather promote its endocytosis from the PM for intracellular sequestration (15, 18, 36–38).

Human S-tetherin has been reported to be less sensitive to Vpu of the prototypic HIV-1 molecular clone NL4.3 (11). However, it is not yet known whether such differences in Vpu sensitivity are observable at physiological expression levels. Also, recent findings by our group indicate that the majority of primary Vpu isolate alleles from patients infected with clade B HIV-1 display activity superior to that of NL4.3 Vpu both for counteraction of tetherin's antiviral activity and for suppression of its signaling activity, indicating that it may not be fully representative of wild-type (WT) Vpu function (39). We therefore characterized the sensitivities of the L- and S-tetherins to a diverse panel of Vpu proteins, as well as countermeasures from HIV-2, SIVmac, and KSHV. We found that differential sensitivity of L- and S-tetherins was a conserved feature of all of the group M Vpu proteins tested but not SIVmac Nef, HIV-2 Env, KSHV K5, or the Vpu proteins of SIVs from African guenons, which represent descendants of the viruses from which the 5′ half of the SIVcpz genome is derived (40).

MATERIALS AND METHODS

Cell lines and plasmids. WT HIV-1 NL4.3 and HIV-1 NL4.3ΔVpu have been described previously (41). The HIV-2 molecular clone pRod10 was obtained from the Centre for AIDS Research (National Institute for Biological Standards and Control, Potters Bar, United Kingdom), and envelope mutants and Env-internal ribosome entry site-green fluorescent protein (Env-IRES-GFP) were described previously (18). SIVmac239 and SIVmacΔNef proviral plasmids were kindly provided by Theodora Hatziioannou, Aaron Diamond AIDS Research Center, New York, NY (16). Tetherin isoforms and species orthologues were made in pCR3.1, pLHCX (Clontech), and pCMS28 by standard molecular biological methods. Vpu proteins from different clades of HIV-1 or clade B transmitted/founder viruses (42) were cloned into a rev-dependent expression vector, pCRV1, as described previously (39). SIVgsn Vpu, SIVmon Vpu, and group N Vpu YBF30 or N1FR2011 (43) were synthesized and cloned into pCRV1. Mona and greater spot-nosed monkey tetherins (21) were similarly synthesized and cloned into pCR3.1.

HEK293T, HEK293, HT1080, and Jurkat cells were obtained from the American Type Culture Collection; the HIV reporter TZM-bl HeLa cell line was kindly provided by John Kappes through the NIH AIDS Reagents Repository Program (ARRP). Jurkat-TAg cells were kindly provided by Marie-Jose Bijlmakers, King's College London. All adherent cells were maintained in Dulbecco's modified Eagle medium (Invitrogen) supplemented with 10% fetal calf serum and gentamicin. Derivatives of cell lines stably expressing human tetherin or mutant forms thereof were produced by transducing the cells with murine leukemia virus-based retroviral vectors packaging a pLHCX or pCMS28 vector genome encoding the tetherin construct and selecting the cells in hygromycin (Invitrogen) or puromycin, respectively. Jurkat and Jurkat-TAg cells were maintained in Roswell Park Memorial Institute medium supplemented with 10% fetal calf serum and gentamicin.

Production of vector and virus stocks. For full-length vesicular stomatitis virus G protein (VSV-G)-pseudotyped HIV-1 stocks, 293T cells were transfected with 2 μg proviral plasmid and 200 ng pCMV-VSV-G by using polyethylenimine (PEI; 1 mg/ml; Polysciences Europe GmbH). At 48 h posttransfection, supernatants were harvested and endpoint titers were determined in TZM-bl HeLa cells as described previously (18). For KSHV K5 and HIV-1 Vpu vectors, cells were transfected with a 3:2:1 ratio of the pCMS28 K5/Vpu vector plasmid, pMLV-Gag-Pol, and pCMV-VSV-G and supernatants were harvested 48 h posttransfection and used to transduce HT1080 or 293 cells expressing tetherin isoforms.

Virus release assays. Subconfluent 293T cells were plated on 24-well plates and transfected with 500 ng HIV-1 NL4.3 WT or ΔVpu mutant provirus and various amounts of tetherin expression vector or a constant amount (50 ng) of tetherin and various inputs of Vpu plasmid by using 1 μg/ml PEI. Similarly, 500 ng SIVmac or SIVmacΔNef provirus was cotransfected with various amounts of rhesus macaque tetherin expression vectors. The medium was replaced 6 or 16 h posttransfection, and the supernatants were harvested after 48 h. The infectivity of viral supernatants was determined by infecting TZM-bl HeLa cells, which were assayed 48 h later for β-galactosidase activity with the Tropix GalactoStar chemiluminescence kit (Applied Biosystems). For the analysis of physical virion release, supernatants were filtered (0.22 mm) and pelleted through a 20% sucrose–phosphate-buffered saline (PBS) cushion at 20,000 × *g* for 90 min at 4°C, and pellets were lysed in SDS-PAGE loading buffer. All HIV-1, HIV-2, and SIVmac virion and cell lysates were then subjected to SDS-PAGE and Western blotted for HIV-1 p24 CA (monoclonal antibody 183-H12-5C; kindly provided by B. Chesebro through the NIH ARRP), rabbit anti-Hsp90 (Santa Cruz Biotechnologies), or polyclonal rabbit antitetherin (kindly provided by K. Strebel through the NIH ARRP) (44) and visualized with a LiCor apparatus by using fluorophore-conjugated secondary antibodies (IRDye 800 goat anti-rabbit, IRDye 680 goat anti-mouse).

Flow cytometry. Jurkat-TAg cells expressing tetherin isoforms were infected with VSV-G-pseudotyped HIV-1 NL4.3 WT or ΔVpu virus at a multiplicity of infection (MOI) of 2. Cells were washed at 6 or 16 h postinfection. At 48 h postinfection, cells were stained for surface tetherin with a specific anti-BST2 IgG2a monoclonal antibody (Abnova) and a goat anti-mouse IgG2a Alexa 633-conjugated secondary antibody (Molecular Probes, Invitrogen), fixed and permeabilized for 20 min (Cytofix/Cytoperm fixation/permeabilization kit; BD Biosciences), and then stained for intracellular HIV-1 Gag with the KC57 antibody conjugated to phycoerythrin (PE) (Beckman-Coulter). Cells were then analyzed with a FACSCalibur flow cytometer (Becton Dickinson) and FlowJo software. 293 cells expressing tetherin isoforms were plated in 24-well plates and transfected with 500 ng pCRV1-HIV-2-IRES-GFP vector with PEI. At 48 h posttransfection, the cells were harvested in PBS–5 mM EDTA, stained for surface tetherin, and analyzed as described above. HT1080 or 293 cells expressing tetherin isoforms were transduced with K5/K5NTR or different Vpu proteins, respectively. After puromycin selection, cells were stained for surface tetherin with an anti-human CD317-PE antibody (eBioscience) and analyzed as described above.

Immunoprecipitation. Jurkat cells treated with IFN (1,000 U/ml) or left untreated, Jurkat-TAg L-tetherin, Jurkat-TAg S-tetherin, and Jurkat-TAg empty-vector control cells were lysed on ice for 20 min in buffer containing 50 mM Tris (pH 7.4), 150 mM NaCl, 200 μM sodium orthovanadate, 1% NP-40, 0.5% sodium deoxycholate, 5 mM *N*-ethylmaleimide, and complete protease inhibitors (Roche). Lysates were cleared by centrifugation, and supernatants were incubated with 5 μg/ml mouse anti-BST2 monoclonal antibody (eBioscience) for 1.5 h at 4°C. Sepharose-protein G beads were washed in lysis buffer before they were added to the samples and incubated for another 3 h. Beads were washed five times in lysis buffer before the peptide–*N*-glycosidase mixture for deglycosylation was added (New England BioLabs). Samples were incubated at 37°C overnight and resuspended in SDS-PAGE loading buffer. Cell lysates and immunoprecipitates were subjected to SDS-PAGE and Western blotting for tetherin and Hsp90. Blots were visualized with a LiCor apparatus. The secondary antibodies used are described above.

RESULTS

The L- and S-tetherin isoforms are differentially sensitive to HIV-1 Vpu. To characterize the roles of the recently identified L- and S-tetherin isoforms (11), we generated constructs encoding human tetherin with its authentic Kozak consensus (WT tetherin), the +1 ATG mutated (S-tetherin), or a semiconservative M13I mutation (L-tetherin) (Fig. 1A). We first sought to confirm the data of Cocka and Bates that S-tetherin displayed reduced sensitivity to HIV-1 Vpu in transient-transfection assays (11). 293T cells were transfected with WT HIV-1 (NL4.3) or a Vpu-defective proviral plasmid in combination with increasing doses of each tetherin expression vector. As expected, increasing the expression of all of the tetherin constructs resulted in an equivalent dose-dependent inhibition of Vpu-defective HIV-1 release, as measured both by infectious titer and by physical virus yield (Fig. 1B and C). All tetherin constructs were well expressed, with the WT tetherin construct apparently expressing similar amounts of both isoforms. The WT virus was essentially resistant to L-tetherin at all expression levels. In contrast, above moderate expression levels, S-tetherin partially restricted the release of WT virus, indicating that Vpu incompletely antagonized it. For the WT tetherin construct, a milder phenotype was observed, with appreciable restriction of WT viral release seen at the highest tetherin input. Therefore, consistent with the previous report (11), S-tetherin homodimers are less sensitive to counteraction by Vpu. Furthermore, since L- and S-tetherins should be able to independently assort to give heterodimers, the approximately 4-fold increased input of WT tetherin required for restriction of WT HIV-1 release implies that L-S heterodimers are as sensitive to Vpu as L-tetherin homodimers assuming a 1:2:1 ratio because of independent assortment (compare 50- and 200-ng inputs in Fig. 1B). Finally, we asked whether S-tetherin displays any evidence of Vpu-induced degradation. Stable 293–L-tetherin or 239–S-tetherin cells that express equivalent levels of the respective isoforms (Fig. 1D) were infected with VSV-G-pseudotyped WT or Vpu-defective virus at an MOI of 2, and cell lysates were analyzed by Western blotting 48 h later (Fig. 1E). As expected, L-tetherin levels were degraded in the presence of the WT virus. However, S-tetherin was not degraded under the same conditions. Interestingly, in cells infected with the WT virus, the apparent molecular mass of S-tetherin increased. This may suggest that a Vpu-induced modification, potentially ubiquitination, may underlie the residual antagonistic effect of Vpu.

Determinants of Vpu antagonism in the human tetherin cytoplasmic tail have suggested both a role for the tyrosine-based sorting (YDYCRV) motif (29) and a serine-threonine (STS) motif that may be ubiquitinated (35), both of which are absent from S-tetherin. Mutation of either of these motifs to alanines (STS→AAA or YDY→ADA) (Fig. 2A) reduced the sensitivity of WT human tetherin to Vpu (Fig. 2B), and simultaneous disruption had an additive effect with the caveat that this protein is more highly expressed, probably because it lacks sequences important for its natural turnover. Interestingly, mutation of the tyrosine residues to phenylalanines (YDY→FDF) retained sensitivity to Vpu, likely because Phe residues can, to a certain extent, substitute for tyrosines in endocytic sorting motifs (Fig. 2B and C). This site is known to be required for maximal counteraction by Vpu (29). Of note, the reduced sensitivity of these mutants to Vpu did not correlate with overall surface tetherin expression (Fig. 2D).

To determine whether tetherin isoforms affect WT virus release in a relevant cell type, we took advantage of a derivative of $CD4^+$ Jurkat cells, Jurkat-TAg cells, that has been shown to have no detectable tetherin on its surface (Fig. 3A) (45). Expression of L- or S-tetherin in these cells resulted in bulk populations whose surface tetherin expression levels were equivalent to those of parental Jurkat cells after type 1 IFN treatment (Fig. 3A). Immunoprecipitation of the tetherin from these cell lines revealed that while Jurkat cells express equivalent levels of both tetherin isoforms and IFN treatment upregulated both equivalently, J-TAg–L-tetherin and J-TAg–S-tetherin cells expressed only the desired isoform (Fig. 3B). Thus, we could use these cells to compare the isoforms in relevant target cells at approximately physiological expression levels. J-TAg–L-tetherin and J-TAg–S-tetherin cells were infected with WT and Vpu-defective HIV-1 and analyzed for surface tetherin and HIV-1 Gag expression 48 h later. As expected, neither tetherin was downregulated in cells infected with Vpu-defective virus, with surface levels enhanced in the p24-high cells probably because of tethered virion accumulation on the surface (Fig. 3C). While L-tetherin was efficiently downmodulated from the surface of cells infected with the WT virus, S-tetherin was not, in keeping with Vpu-mediated targeting for endosomal degradation. Infectious viral release and physical virion yield from the same cultures revealed a significant 3- to 4-fold defect in WT virion release from J-TAg-S-tetherin, demonstrating that at relevant expression levels, the S-tetherin isoform is poorly antagonized (Fig. 3D and E). Since L-tetherin is both induced by pattern recognition (46) and itself capable of proinflammatory signaling (11), a potential confounding issue here is whether WT expression (i.e., expression of both isoforms) is induced in infected cells. While this is a possibility in primary cells, we saw no evidence of tetherin upregulation in infected J-TAg cells (Fig. 3E). Neither did we see any expression of S-tetherin in 293T–L-tetherin cells transfected with Vpu-defective HIV-1 provirus (Fig. 3F), which under these conditions triggers NF-κB activation (12; data not shown). Thus, because of a lack of the cytoplasmic tail residues required for subcellular trafficking and ubiquitination (29, 35), the S-tetherin isoform cannot be degraded or downregulated in $CD4^+$ T cells and this accounts for its reduced sensitivity to HIV-1 Vpu. Furthermore, the residual activity of Vpu against S-tetherin in the absence of surface removal is in keeping with the ability of Vpu to exclude tetherin from virions at the surface to some extent (26, 44).

Differential sensitivity of human tetherin isoforms is a feature of HIV-1 group M Vpu proteins. We have recently found that most Vpu alleles from primary isolates display tetherin coun-

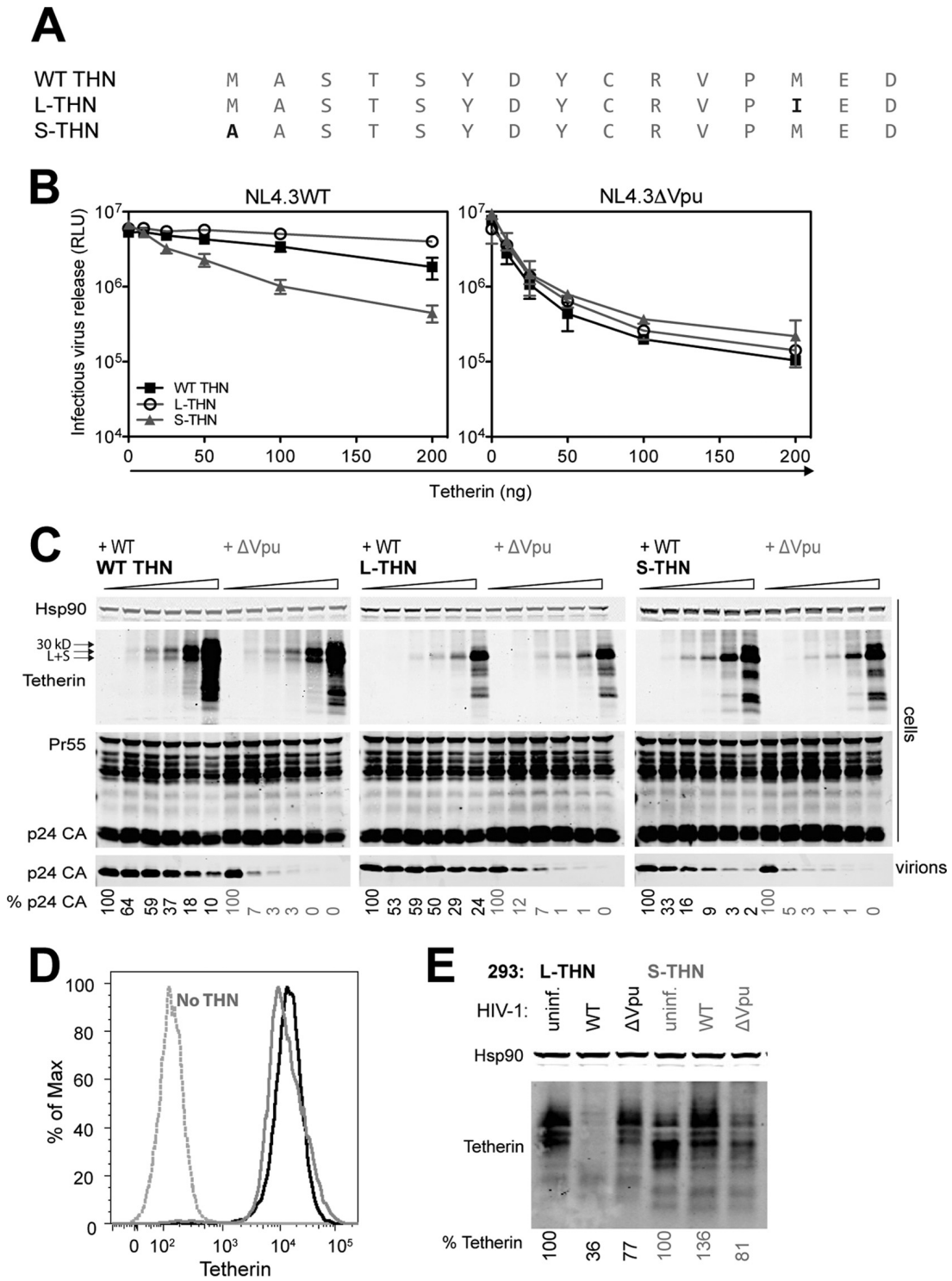

FIG 1 The L- and S-tetherin isoforms are differentially sensitive to HIV-1 Vpu. (A) Schematic representation of the amino acid sequences of WT tetherin (WT THN), L-tetherin (L-THN), and S-tetherin (S-THN). (B and C) 293T cells were transfected with increasing amounts of WT tetherin, L-tetherin, or S-tetherin and NL4.3 WT or ΔVpu proviral plasmid. (B) At 48 h posttransfection, infectious virus release was determined with TZM-bl HeLa reporter cells. Error bars represent standard deviations of the means of three independent experiments. RLU, relative light units. (C) Cell lysates and pelleted viral supernatants from panel B were subjected to SDS-PAGE and analyzed by Western blotting for Hsp90, tetherin, and p24 CA. The percentages of p24 release into the supernatant indicated at the bottom are relative to the release of WT NL4.3 or NL4.3ΔVpu in the absence of tetherin. (D) 293 cells stably expressing the tetherin isoforms were analyzed for surface tetherin expression (L-tetherin, solid black line; S-tetherin, solid gray line; empty-vector 293 cells, dashed gray line [No THN]). (E) 293 cells stably expressing tetherin isoforms were infected with VSV-G-pseudotyped WT NL4.3 or NL4.3ΔVpu virus at an MOI of 2. At 48 h postinfection, cells were harvested and subjected to SDS-PAGE, analyzed by Western blotting for tetherin and Hsp90, and analyzed with a LiCor quantitative imager. The percentages of tetherin levels indicated below the lanes are relative to the tetherin levels in the corresponding uninfected cell lines. Uninf., uninfected.

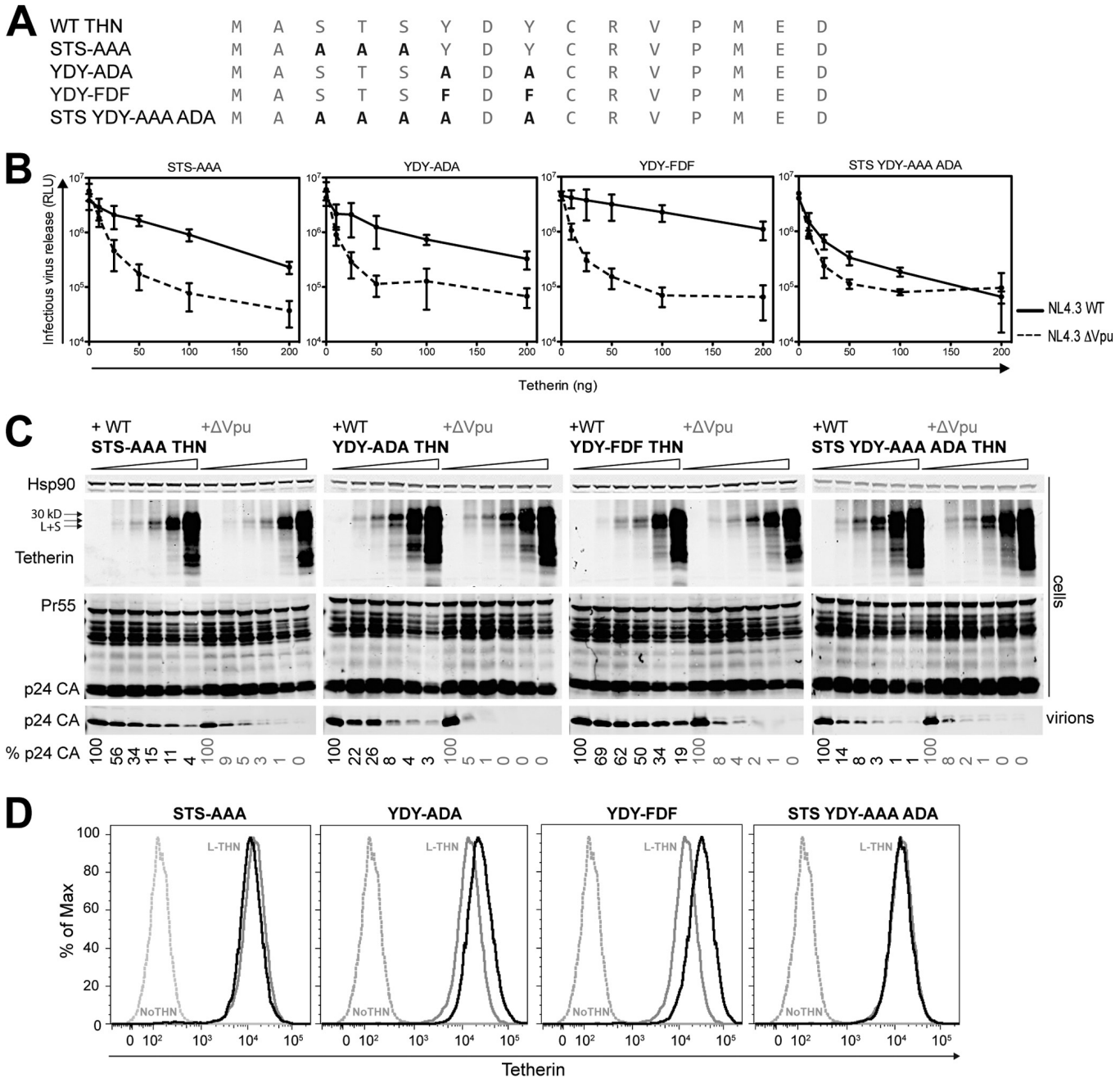

FIG 2 Tetherin's sensitivity to Vpu is dependent on serines, a threonine, and tyrosines. (A) Cytoplasmic tail amino acid sequences of mutant tetherins (THNs) used to determine the residues required for sensitivity to HIV-1 NL4.3 Vpu. (B and C) 293T cells were transfected with increasing amounts of different mutant tetherins and a HIV-1 NL4.3 WT or ΔVpu proviral plasmid. (B) At 48 h posttransfection, infectious virus release was determined with TZM-bl HeLa reporter cells. Error bars represent standard deviations of the means of three independent experiments. Solid lines, NL4.3 WT provirus; dashed lines, NL4.3 ΔVpu provirus. RLU, relative light units. (C) Cell lysates and pelleted viral supernatants from panel B were subjected to SDS-PAGE and analyzed by Western blotting for Hsp90, tetherin, and p24 CA. The percentages of p24 release into the supernatant indicated at the bottom are relative to the release of NL4.3 WT or ΔVpu provirus in the absence of tetherin. (D) 293 cells stably expressing the mutant tetherins were analyzed for surface tetherin expression and are shown in comparison to 293 cells expressing L-tetherin (solid gray line) and empty-vector 293 cells (dashed gray line).

teraction activity superior to that encoded by NL4.3, suggesting that accessory gene alleles from lab-adapted strains of HIV-1 may not be representative because of functional drift after prolonged *ex vivo* passage (39). We therefore examined the sensitivities of human tetherin isoforms to a panel of Vpu alleles from transmitted/founder viruses (42) of HIV-1 subtype B (Fig. 4A) and additional examples from clades A1, A2, C, F, and H (Fig. 4B). In this case, 293T cells were transfected with a Vpu-defective HIV-1 proviral plasmid in the presence of a fixed dose (50 ng) of tetherin and increasing Vpu-encoding plasmid inputs in *trans*. In all cases where the Vpu displayed antitetherin activity (C MJ4 and F Vpu appeared defective against all tetherin isoforms), L-tetherin was robustly counteracted at low Vpu expression levels. However, as with NL4.3 Vpu, S-tetherin sensitivity to counteraction was much

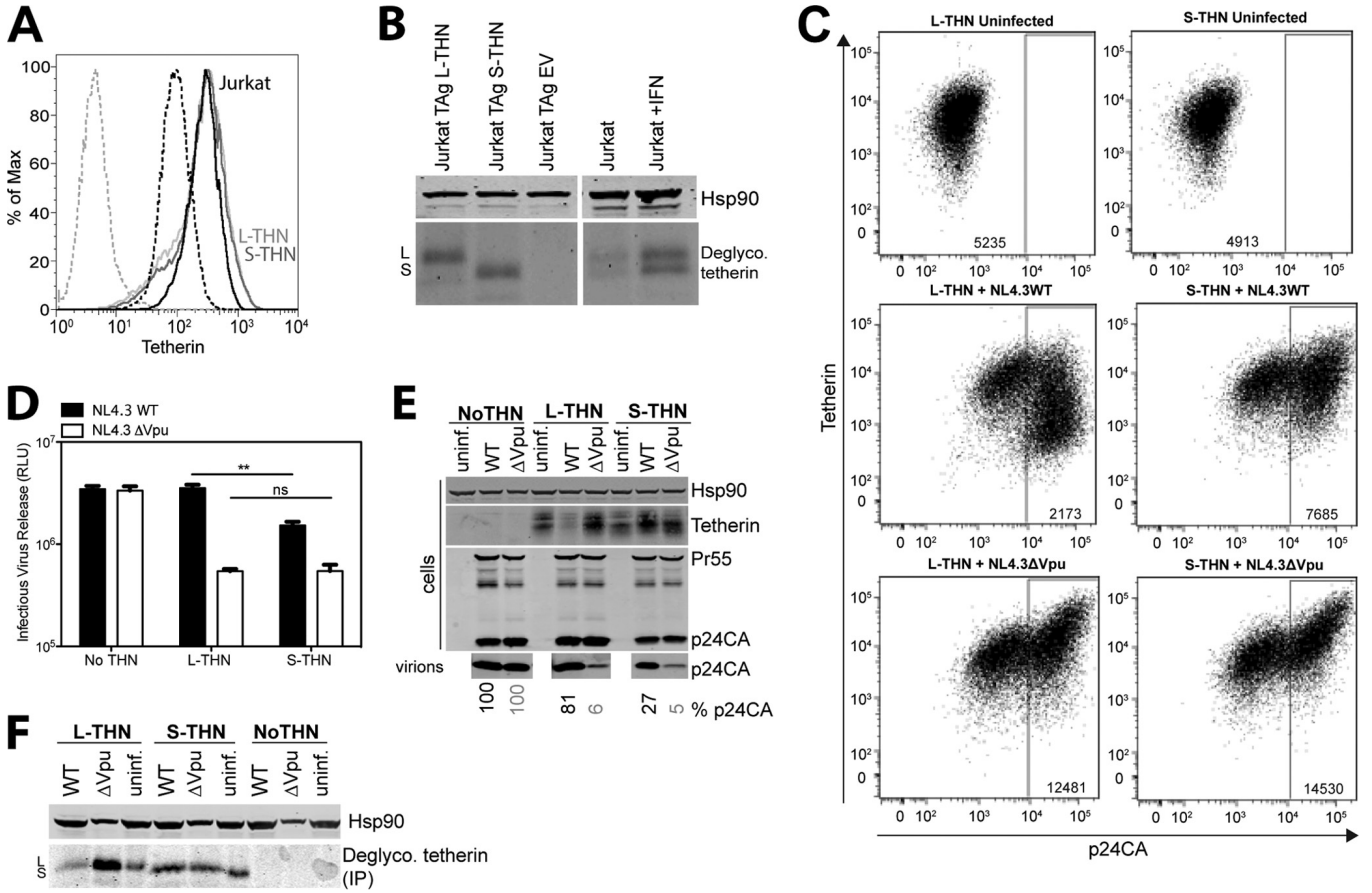

FIG 3 Differential sensitivity of tetherin (THN) isoforms to Vpu in CD4$^+$ T cell lines. (A) Jurkat-TAg cells stably expressing L-tetherin (solid light gray line) or S-tetherin (solid dark gray line) were analyzed for surface tetherin expression compared to Jurkat cells treated with IFN for 24 h (solid black line) or left untreated (dashed black line) and to Jurkat-TAg cells (dashed gray line) not expressing tetherin. (B) Jurkat-TAg cells expressing tetherin isoforms and Jurkat cells treated with IFN or left untreated were lysed and immunoprecipitated with antitetherin antibody and deglycosylated (Deglyco.). Lysates and precipitates were subjected to SDS-PAGE and analyzed by Western blotting for Hsp90 and tetherin. (C and D) Jurkat-TAg cells expressing L- or S-tetherin were infected with VSV-G-pseudotyped HIV-1 NL4.3 WT or ΔVpu at an MOI of 2 for 48 h. (C) Cells were analyzed by flow cytometry for intracellular p24 and surface tetherin expression. Median fluorescence intensities (MFI) are indicated. (D) Titers of infectious virus in supernatants from infected cells were determined on TZM-bl cells. Data are from four different experiments, and error bars show the standard errors of the means. **, $P < 0.01$ (determined by two-tailed t test); ns, no statistically significant difference. RLU, relative light units. (E) Cell lysates and pelleted viral supernatants from panel C were subjected to SDS-PAGE and analyzed by Western blotting for HIV-1 Hsp90, tetherin, and p24 CA. Percent p24 release relative to WT NL4.3 or NL4.3ΔVpu release in the absence of tetherin is indicated at the bottom. uninf., uninfected. (F) 293 cells expressing no tetherin, L-tetherin, or S-tetherin were infected at an MOI of 2. At 48 h postinfection, cells were lysed and immunoprecipitated (IP) with antitetherin antibody and deglycosylated. Lysates and precipitates were subjected to SDS-PAGE and analyzed by Western blotting for Hsp90 and tetherin.

reduced in comparison. In particular, clade A1 and A2 Vpu proteins displayed only marginal activity against S-tetherin, and the weak antagonism of L-tetherin by a clade F Vpu suggests that it may be defective for promotion of degradation. As expected, constructs expressing WT tetherin gave an intermediate phenotype consistent with mixed-isoform expression. Thus, the differential sensitivity of L- and S-tetherins is a feature of the HIV-1 Vpu proteins from group M.

Targeting of both tetherin isoforms by an HIV-1 group N Vpu from Togo and Vpu proteins from SIVgsn and SIVmon. The Vpu proteins of HIV-1 group N display variably weak tetherin counteractivity and are unable to degrade CD4 (21). However, Vpu from a strain isolated from a French national returning from Togo with acute HIV infection revealed evidence of further adaptation to human tetherin in HIV-1 group N (43). In particular, acquisition of a trafficking motif (ExxxLV) found in M-Vpu proteins that is required for promotion of tetherin degradation was associated with tetherin counteraction. While this Vpu (N1.FR.2011) potently targeted L-tetherin in comparison to that from another group N strain, YBF30 (Fig. 5A and B), at higher Vpu expression levels, it could also completely counteract S-tetherin, in contrast to HIV-1 group M Vpu proteins. This enhanced ability to counteract S-tetherin prompted us to examine whether N1.FR.2011 Vpu could downmodulate and degrade S-tetherin. However, expression of N1.FR.2011 Vpu was unable to induce the degradation of S-tetherin (Fig. 5C) and neither did it lead to more than the 2-fold reduction of cell surface S-tetherin that was seen with NL4.3 Vpu (Fig. 5D and E). Thus, N1.FR.2011 Vpu's enhanced activity against S-tetherin may indicate that it is more efficient than group M Vpu proteins at excluding it from budding virions at the cell surface.

A similar result was obtained with Vpu proteins from SIVgsn and SIVmon that target tetherin in their host species, as well as other primate tetherins, including that from rhesus macaques

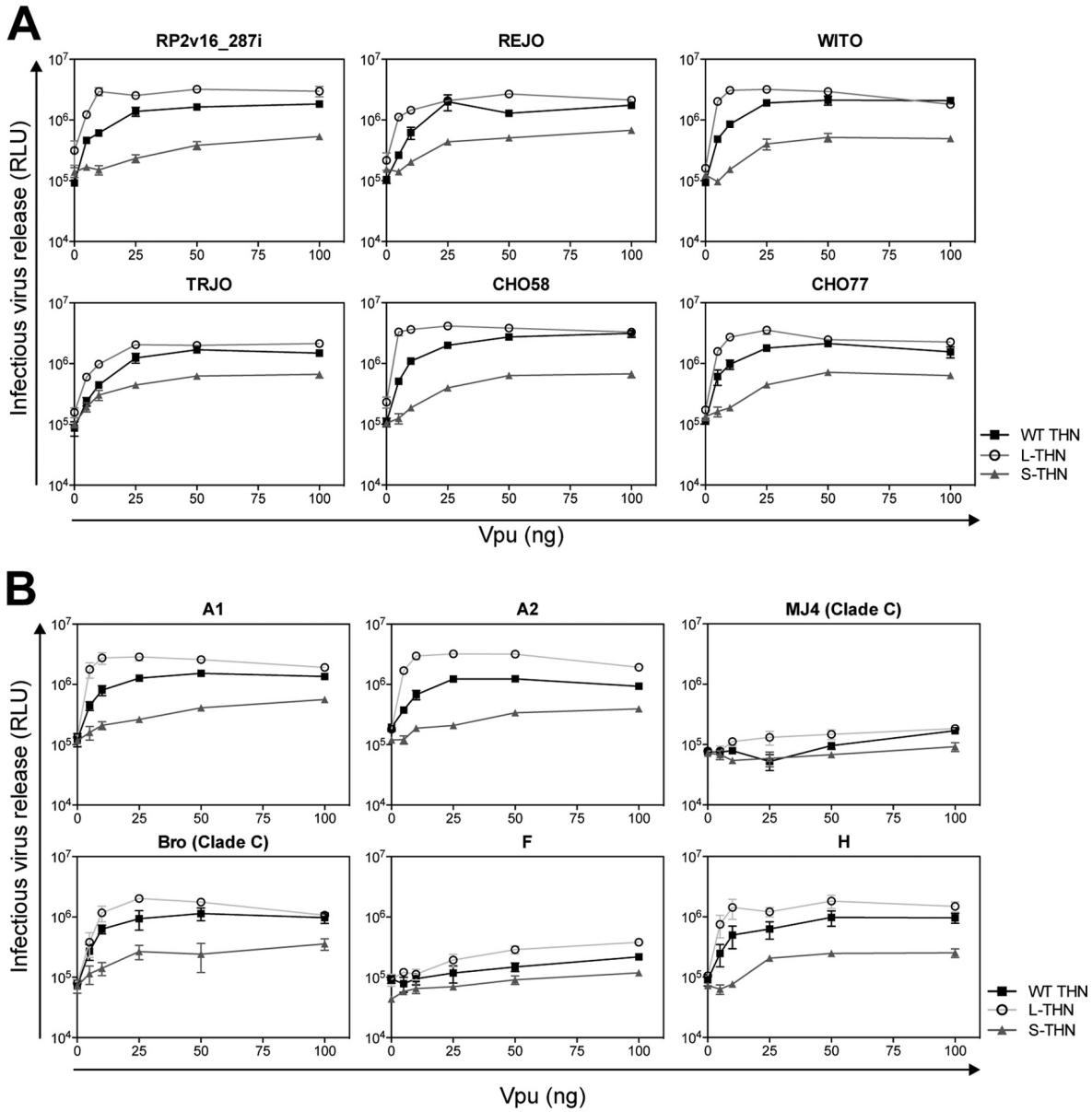

FIG 4 Differential sensitivity of human tetherin (THN) isoforms to Vpu is a feature of group M. (A and B) 293T cells were transfected with increasing amounts of Vpu, ΔVpu proviral plasmid, and 50 ng of human WT tetherin, L-tetherin, or S-tetherin. At 48 h posttransfection, infectious virus release was determined with TZM-bl HeLa reporter cells. Error bars represent standard deviations of the means of three independent experiments. RLU, relative light units.

(21). These are descendants of the ancestral *vpu* alleles from which SIVcpz and HIV-1 Vpu is derived (40). Again, unlike HIV-1 M Vpu, these proteins equally counteracted the rhesus L- and S-tetherin isoforms, whereas the Vpu from SIVcpzUS, which completely lacks tetherin counteractivity (47), had no effect (Fig. 6A and B). Again, neither SIVgsn nor SIVmon Vpu displayed any degradative activity against either isoform of rhesus tetherin (Fig. 6C). Furthermore, to rule out species-specific effects on tetherin counteraction, we tested these Vpu proteins against their cognate species tetherin isoforms. Although the expression levels of the L isoforms of the greater spot-nosed and mona monkey tetherins were lower than those of the WT and short isoforms, the level of counteraction across Vpu expression levels was equivalent (Fig. 6D to G), again demonstrating equal isoform sensitivity. Thus, the proteins in the guenon SIV lineage that contributed Vpu to HIV-1 are capable of counteracting both isoforms of tetherin equally. This suggests that the readaptation of Vpu to target human tetherin during the zoonotic spread of SIVcpz to become HIV-1 group M resulted in a countermeasure that targeted only one isoform for degradation. The apparently higher potency of the guenon SIV Vpu proteins against S-tetherin suggests that there may be cell biological differences in the mechanisms of action of these proteins that account for this.

HIV-2 envelope, SIVmac Nef, and KSHV K5 target tetherin isoforms with equal efficiency. We then examined the sensitivities of human or rhesus L- and S-tetherins to other virus-encoded countermeasures. Most SIVs that lack a *vpu* gene antagonize their species' tetherins with Nef (15, 16). SIVmac Nef binds to the cytoplasmic tail of macaque tetherin and likely forms a ternary complex with clathrin adaptor protein complex 2 (AP2) (36, 37) to

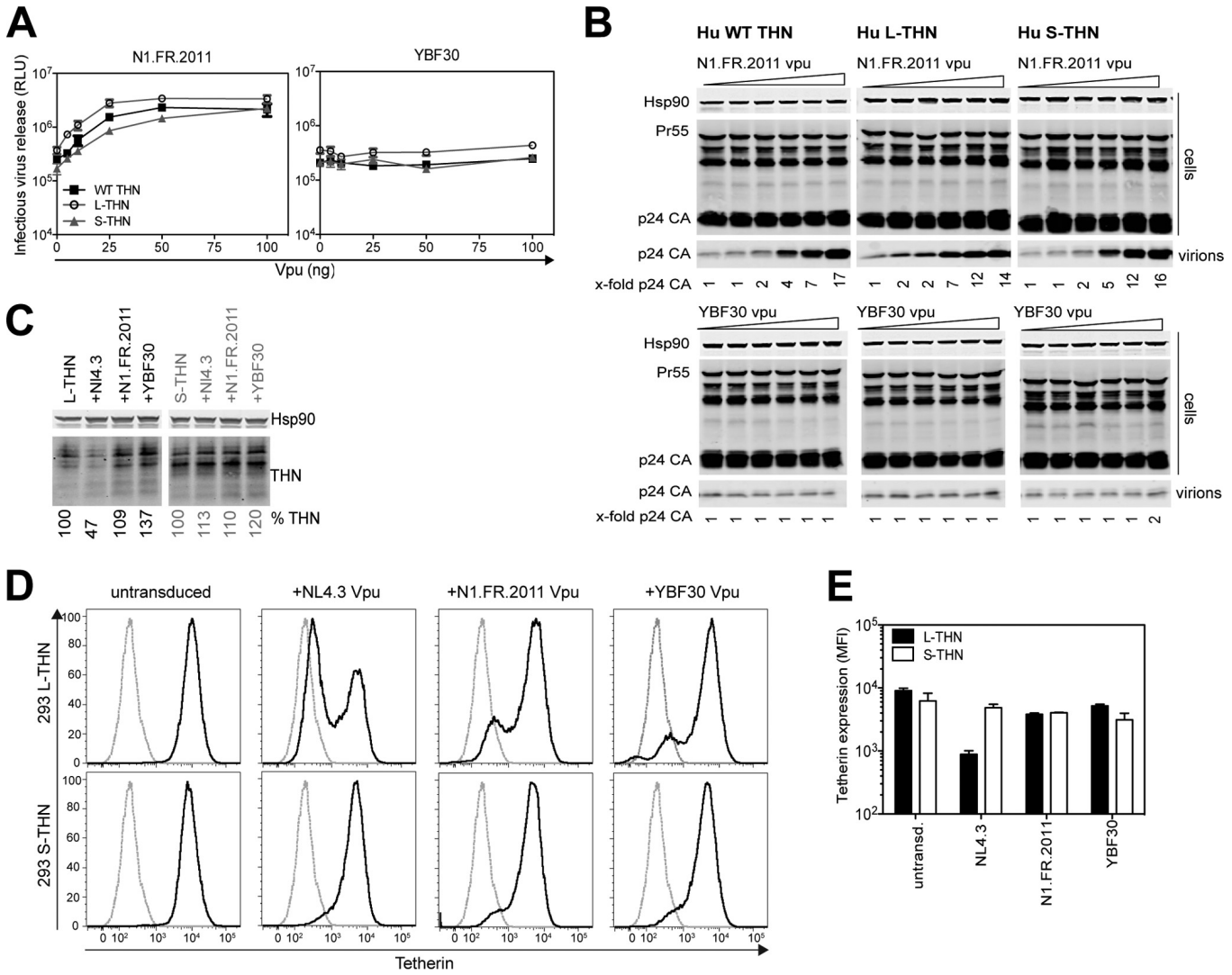

FIG 5 Targeting of both tetherin (THN) isoforms by group N HIV-1 Vpu from Togo. (A) 293T cells were transiently transfected with increasing amounts of Vpu; ΔVpu proviral plasmid; and 50 ng of human WT tetherin, L-tetherin, or S-tetherin. At 48 h posttransfection, infectious virus release was determined with TZM-bl HeLa reporter cells. Error bars represent standard deviations of the means of three independent experiments. RLU, relative light units. (B) Cell lysates and pelleted viral supernatants from panel A were subjected to SDS-PAGE and analyzed by Western blotting for Hsp90 and p24 CA. The fold increases in p24 release into the supernatant indicated at the bottom are relative to the release of NL4.3ΔVpu in the absence of Vpu. (C) 293 cells stably expressing L- or S-tetherin were transduced with retroviral vectors encoding different Vpu proteins. Cell lysates were analyzed for tetherin expression by SDS-PAGE and Western blotting. (D) Vpu-transduced cells from panel C were stained for surface tetherin and analyzed by flow cytometry. Empty-vector 293 cells (not expressing tetherin), dashed gray line. (E) Median fluorescence intensity (MFI) of tetherin in cells from panel D.

stimulate tetherin endocytosis and intracellular sequestration. Nef's specificity for primate tetherins depends on a (G/D)DIWK motif that is absent from human tetherin. Therefore, rhesus macaque L-tetherin (rhL-tetherin) and rhS-tetherin were tested for the ability to restrict the release of WT or Nef-defective SIVmac239 from transiently transfected 293T cells. To overcome the reduced infectivity of Nef-defective viruses, we cotransfected VSV-G. As with Vpu-defective HIV-1, the release of Nef-defective SIVmac239 was equally sensitive to restriction by either isoform of rh-tetherin (Fig. 7A and B). However, in contrast, the WT virus was resistant to all rh-tetherin isoforms, indicating that the absence of the first 12 amino acids of the tetherin cytoplasmic tail has no effect on its sensitivity to Nef-mediated antagonism. This was also the case for HIV-2, which uses its envelope to target tetherin, again in an AP2-dependent manner (18, 38). Despite being a relatively weak tetherin antagonist, the release of WT HIV-2 Rod10 particles from cells transfected with L-tetherin and S-tetherin was equally superior to a viral Env mutant lacking the major AP2 binding site GYXXV (HIV-2 Rod10 GY-AA) in its cytoplasmic tail (Fig. 7C). Furthermore, expression of the HIV-2 Rod10 envelope protein in 293–L- or 293–S-tetherin cells could reduce cell surface tetherin levels dependent on the AP2-binding site (Fig. 7D). Thus, tetherin counteraction and surface downregulation by both SIVmac Nef and HIV-2 Env are independent of trafficking and ubiquitination motifs that are required for Vpu to target human tetherin for degradation.

We finally asked whether the K5 ubiquitin ligase encoded by KSHV could also target both tetherin isoforms. K5 targets a single lysine residue (K18) in human tetherin to promote ESCRT-dependent endosomal degradation (5). However, because K5 cannot

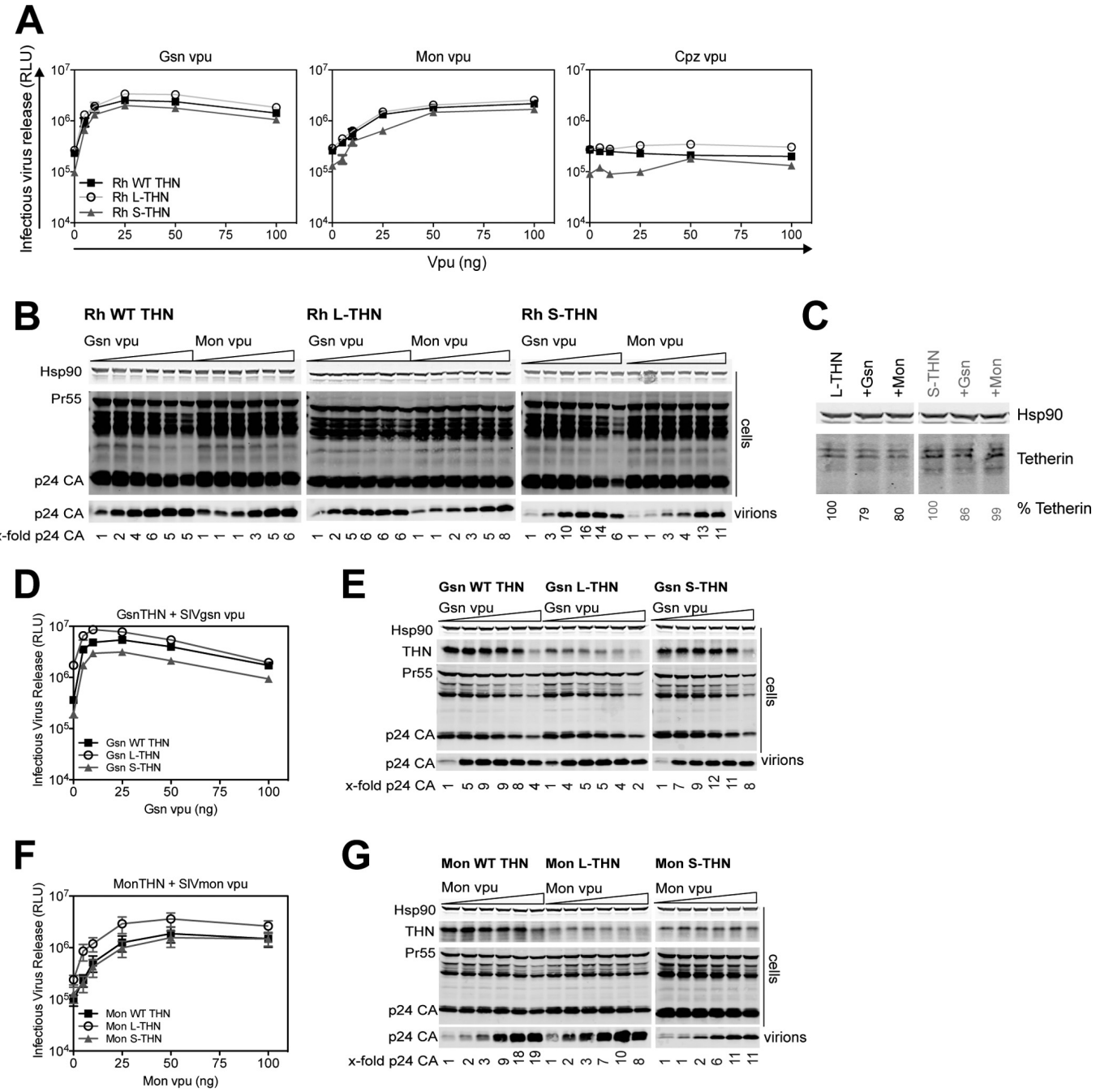

FIG 6 Targeting of both tetherin (THN) isoforms by ancestral Vpu proteins from SIVgsn and SIVmon. (A) 293T cells were transiently transfected with increasing amounts of Vpu; ΔVpu proviral plasmid; and 50 ng of rhesus macaque WT tetherin, L-tetherin, or S-tetherin. At 48 h posttransfection, infectious virus release was determined with TZM-bl HeLa reporter cells. Error bars represent standard deviations of the means of three independent experiments. RLU, relative light units. Rh, rhesus. (B) Cell lysates and pelleted viral supernatants from panel A were subjected to SDS-PAGE and analyzed by Western blotting for Hsp90 and p24 CA. The fold increases in p24 release into the supernatant indicated at the bottom are relative to the release of NL4.3ΔVpu in the absence of Vpu. (C) 293 cells stably expressing L- or S-tetherin were transduced with retroviral vectors encoding different Vpu proteins. Cell lysates were analyzed for tetherin expression by SDS-PAGE and Western blotting. (D and F) 293T cells were transiently transfected with increasing amounts of greater spot-nosed monkey (Gsn) Vpu (D) or mona monkey (Mon) Vpu (F); ΔVpu proviral plasmid; and 50 ng of Gsn (D) or Mon (F) WT tetherin, L-tetherin, or S-tetherin. At 48 h posttransfection, infectious virus release was determined with TZM-bl HeLa reporter cells. Error bars represent standard deviations of the means of three independent experiments. (E and G) Cell lysates and pelleted viral supernatants from panels D and F were subjected to SDS-PAGE and analyzed by Western blotting for Hsp90, tetherin, and p24 CA. The fold increases in p24 release into the supernatant indicated at the bottom are relative to the release of NL4.3ΔVpu in the absence of Vpu.

target rhesus tetherin, it is possible that cytoplasmic tail residues play a role in this specificity. Since 293T cells do not support efficient K5 function (5), HT1080 cells encoding human tetherin isoforms were transduced with puromycin-selective retroviral vectors encoding K5 or a mutant form, K5NTR, bearing a lesion in its C-terminal cytoplasmic tail that abolishes its activity (48). Puromycin-resistant cells expressing K5, but not K5NTR, displayed a marked reduction in the cell surface expression levels of both teth-

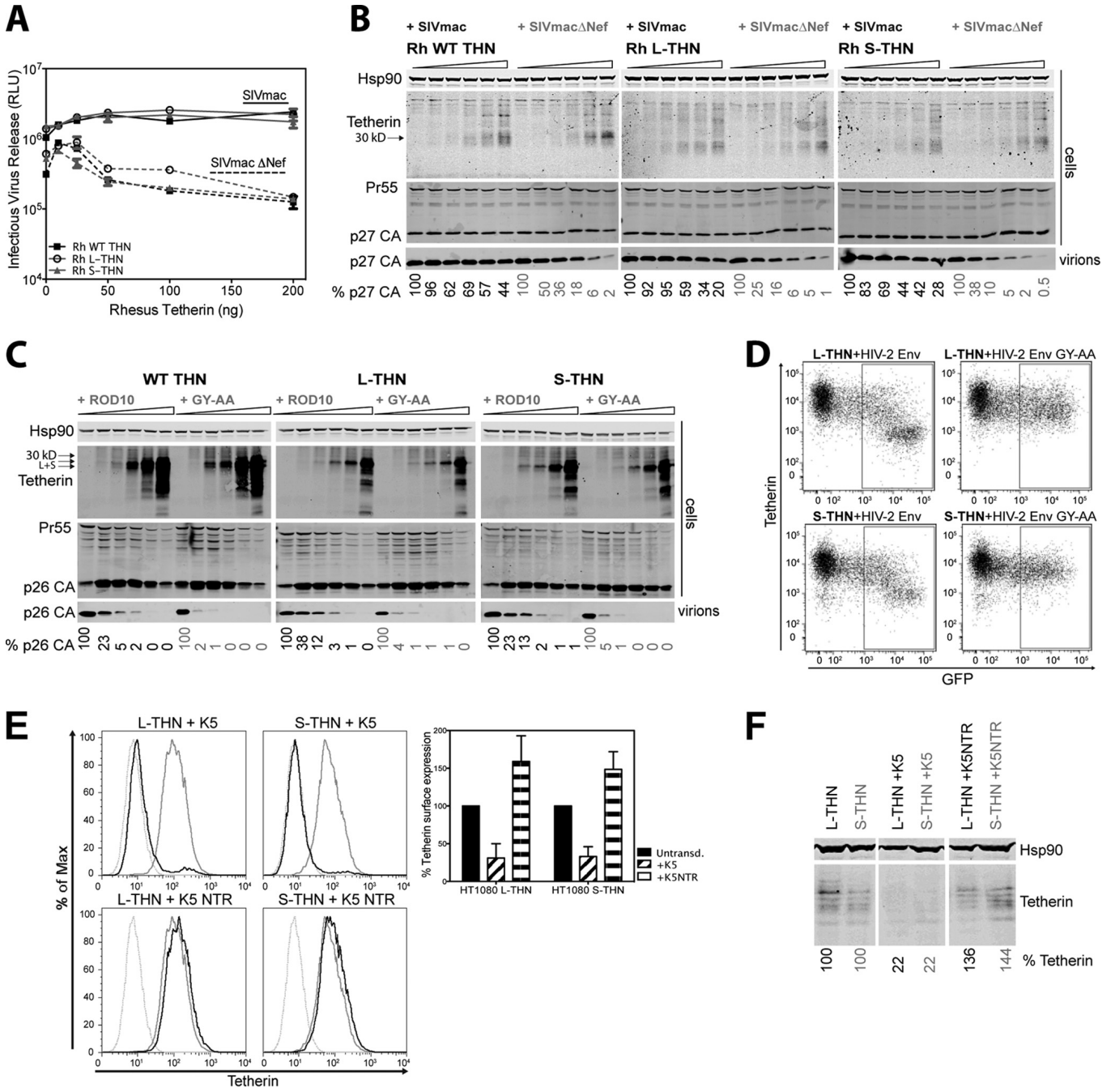

FIG 7 HIV-2 envelope, SIVmac Nef, and KSHV K5 target tetherin (THN) isoforms with equal efficiency. (A and B) 293T cells were transfected with increasing amounts of rhesus (Rh) macaque WT, L-, or S-tetherin and SIVmac or SIVmacΔNef proviral plasmid. (A) Titers of infectious virus released from transfected cells were determined on TZM-bl HeLa reporter cells. Solid lines, SIVmac; dashed lines, SIVmacΔNef. RLU, relative light units. (B) Cell lysates and pelleted supernatant virions were subjected to SDS-PAGE and analyzed by Western blotting for Hsp90, rhesus tetherin, and p27 CA expression. The percentages of p27 CA in the supernatant, relative to virus release in the absence of tetherin, are indicated at the bottom. (C) 293T cells were transfected with increasing amounts of human WT, L-, or S-tetherin and HIV-2 ROD10 or the ROD10 GY-AA mutant proviral plasmid. Cell lysates and pelleted supernatant virions were subjected to SDS-PAGE and analyzed by Western blotting for Hsp90, tetherin, and p26 CA expression. The percentages of p26 CA in the supernatant, relative to virus release in the absence of tetherin, are indicated at the bottom. (D) 293 cells stably expressing L- or S-tetherin were transfected with HIV-2 ROD10 Env-IRES-GFP or HIV-2 ROD10 GY-AA mutant Env-IRES-GFP. At 48 h posttransfection, cells were analyzed by flow cytometry for surface GFP and tetherin expression. (E) HT1080 cells stably expressing tetherin isoforms were transduced with K5 or mutant K5 (K5NTR) defective for tetherin antagonism and selected. Cells were then analyzed by flow cytometry for surface tetherin expression. Dotted gray lines, tetherin-negative HT1080 cells; gray lines, nontransduced tetherin-expressing HT1080 cells; black lines, tetherin-expressing cells transduced with WT K5 (top) or a mutant form (K5NTR; bottom). The graph indicates the surface tetherin expression on transduced cell lines, shown as percentages of the fluorescence of the corresponding nontransduced (Untransd.) tetherin-expressing cell line. (F) Lysates of transduced and nontransduced cells were subjected to SDS-PAGE and analyzed by Western blotting for Hsp90 and tetherin expression. Tetherin expression in lysates as a percentage of that in nontransduced cells is shown at the bottom.

erin isoforms, indicating equal sensitivity to K5 (Fig. 7E). Total tetherin levels in the lysates of the same cells revealed evidence that both tetherin isoforms are sensitive to K5-mediated degradation (Fig. 7F). Together, these data indicate that, unlike Vpu, the first 12 amino acids of the tetherin cytoplasmic tail are dispensable for counteraction by other viral antagonists, thus rendering both isoforms equally sensitive, and further suggest that trafficking determinants in these countermeasures act independently of tetherin's normal recycling mechanism.

DISCUSSION

In this study, we have examined the sensitivities of the L- and S-tetherin isoforms to lentiviral antagonists and found that, uniquely among those studied, the Vpu proteins of HIV-1 group M differ in the potency with which they target isoforms of human tetherin. For the most part, this parallels the ability of M-Vpu to reduce cell surface levels of tetherin and target it for ESCRT-dependent degradation (1). Similarly to a recent study (11), this is determined by the lack of both a clathrin-dependent recycling sequence (YDYCRV) and a putative serine-threonine motif previously reported to act as a ubiquitin acceptor site (35). These data are consistent with the notion that for maximal counteraction of tetherin, Vpu blocks its transit from the trans-Golgi network to the PM and routes it to late endosomes, which requires trafficking motifs in the cytoplasmic tails of both proteins (1). In contrast, SIV Nef and HIV-2 Env do not mediate tetherin degradation but rather lead to tetherin's intracellular sequestration following enhanced internalization from the surface. This is dependent on AP2 binding sites in both viral proteins (18, 36–38, 49). For Nef (36) and also for Env, as shown here, this does not require the presence of the endocytic signal in tetherin itself.

Most of the mammalian tetherins so far sequenced have a second ATG in their first exon that can act as a translation initiation site in the mRNA, leading to the potential to express the L- and S-tetherin isoforms (11). The data so far indicate that both isoforms are expressed equally, and since tetherin is a dimer, independent assembly could give rise to a distribution of homodimers and heterodimers in a 1:2:1 ratio (11). This is borne out in our data showing that approximately 4-fold more expression of WT tetherin than of the short isoform is required to restrict WT HIV-1 release. Polymorphisms in the +1 ATG site have been observed three times so far in different mammalian species. Both the domestic cat (50, 51) and horse (52) tetherin genes lack the +1 ATG, and a similar defect exists in at least one inbred mouse strain, NZW (53). In the latter case, this has been shown to lead to higher tetherin expression levels on lymphocytes and correlates with a better control of murine leukemia virus viremia (53). The facts that both isoforms are equally potent at restricting virion release and that none of the other lentiviral tetherin antagonists tested here differentiate between the isoforms therefore raise the question of why tetherin counteraction and the determinants of L-tetherin degradation are so strictly conserved in group M Vpu.

Key issues are whether the expression of L- and S-tetherin can be differentially regulated and the importance of additional functions associated with the long isoform. The lack of the YDYCRV motif reduces tetherin endocytosis and recycling (22), and in keeping with this, HIV-1 virions do not accumulate in late endosomes in cells expressing either tyrosine mutant or human S-tetherin (12; data not shown). The delivery of retained virions to endosomes for degradation may have immunological consequences in addition to the physical removal of virions from the cell surface. Virion components may be targeted for enhanced antigen presentation in some cell types, or liberation of virion associated pathogen-associated molecular patterns in endosomes may further stimulate cognate pattern recognition receptors in *cis* (1, 12). In contrast, surface accumulation of virions mediated by S-tetherin may enhance the opsonization of infected cells and debris for clearance by phagocytes (1). In support of this notion, very recent data indicate that tetherin-mediated virion retention sensitizes infected cells to antibody-dependent cellular cytotoxicity (54). Furthermore, tetherin itself may directly regulate pattern recognition receptor function in plasmacytoid dendritic cells through the inhibitory leukocyte receptor ILT-7 (55), although this has been recently challenged (56). Thus, other physiological roles of S-tetherin and L-tetherin bear further investigation. Finally, the ability of tetherin to physically restrict cell-to-cell transmission at virological synapses (VS) of HIV-1 has been controversial (57–59). Given the differential sensitivity of the L and S isoforms to Vpu, it will be important to know whether they partition differently to the VS in a manner that may account for these discrepant observations.

Since most of these attributes should be features of all mammalian tetherins, why only the HIV-1 tetherin countermeasure differentiates between the isoforms so markedly still requires explanation. One further function of tetherin that is limited to the long isoform is the ability to mediate an NF-κB-dependent signal upon virion retention (12, 13). This again requires the YDYCRV motif, and the current data suggest that virion aggregation of tetherin at the cell surface upon restriction of release leads to the recruitment of a TRAF2/TRAF6/TAK1 complex that activates NF-κB (11–13). In keeping with this, human $CD4^+$ T cells infected with Vpu-defective HIV-1 express enhanced levels of proinflammatory cytokines in a tetherin-dependent manner (12). This activity is so far limited to the human and chimpanzee proteins (12). Species-specific changes in the cytoplasmic tails of great ape and hominid tetherins are the determinants of its signaling capacity, with the human protein showing considerably more potent activity (12). Importantly, evidence that S-tetherin dominantly interferes with human tetherin signaling suggests that only homodimers of L-tetherin can signal (11). Since the threshold for such a signaling event may be less than efficient virion retention, we suggest that this function fits well with a further selective pressure exerted specifically by human L-tetherin.

The ability of HIV-1 Vpu to counteract tetherin is a reacquisition of an ancestral guenon SIV function that was lost in SIVcpz Vpu proteins (40). This was probably due to redundancy with Nef, which in SIVcpz acts as the tetherin antagonist (21). SIVcpz derives from a recombination between two lineages of SIV with Vpu- and Nef-mediated tetherin counteraction, respectively (40). However, because Nef associates directly with tetherin, dependent in part on a G/DDIWK motif in the cytoplasmic tail (37) that has been deleted from hominids (60), SIVcpz was without a tetherin antagonist upon zoonotic transfer to humans. Thus, Vpu, which still retained CD4 targeting, adapted to target human tetherin (21). Sequence divergence in SIVcpz Vpu proteins is associated with whether the individual zoonotic transfers that gave rise to groups M, N, O, and P adapted to target human tetherin (40, 43). In particular, (i) the development of an AxxxAxxxAxxxW binding interface in the Vpu TM domain (24, 25), (ii) acidic-dileucine trafficking motifs (29), and (iii) a well-characterized ubiquitin ligase binding site (DSGNES) in the cytoplasmic tail (33, 43) are

the key features of the M-Vpu protein that endowed it with tetherin counteractivity. The latter two are essential for L-tetherin degradation by M-Vpu (29, 32, 33). In contrast, O-Vpu lacks tetherin binding in the TM domain and fails to target human tetherin at all, whereas all N-Vpu proteins (save one) have readapted to bind tetherin but fail to counteract it efficiently or degrade it (21, 61, 62). Thus, it has been proposed that efficient tetherin counteraction by Vpu was a key feature in the establishment of the human HIV/AIDS pandemic by group M HIV-1 (40). Coincidentally, the deletion that abolished the Nef sensitivity of human tetherin also gave rise to the enhanced signaling capacity of the long isoform (12), the form that all of the M-Vpu proteins tested herein preferentially target. Thus, we speculate that enhanced targeting of L-tetherin owing to its increased signaling capacity, in addition to its direct antiviral activity, may have contributed to the successful spread of HIV-1 group M in humans, whereas groups N and O remain geographically restricted. In this regard, the increased potency of Vpu from a highly pathogenic group N HIV-1 from Togo is interesting. While it has acquired two cytoplasmic tail attributes important for counteraction (43), in our studies, it did not degrade tetherin. Also, although it is still better at counteracting L-tetherin, it appears to be superior to many M-Vpu proteins at counteracting S-tetherin. Therefore, there may be cell biological differences in its mode of action that account for this. In some experimental systems, Vpu can counteract tetherin to a certain extent at the cell surface by physically excluding it from budding virions without removal from the PM (26). This requires the ExxxLV trafficking motif in Vpu but not the YDYCRV motif in tetherin. Since N1.FR.2011 Vpu has acquired this motif (43), future work will determine if this surface exclusion activity is more potent in this Vpu. Moreover, this may also account for the activity of the SIVgsn and SIVmon Vpu proteins against their cognate species' tetherins, although these do not have equivalent acidic dileucine motifs in their cytoplasmic tails (21). However, given that surface tetherin levels are not reduced by N1.FR.2011, it will also be important to examine the capacity of this Vpu, and other nondegradative tetherin countermeasures such as HIV-2 Env, for the ability to block tetherin-induced signaling.

ACKNOWLEDGMENTS

We thank Theodora Hatziioannou for the kind gift of reagents, Claire Jolly for helpful advice, and Suzanne Pickering and other members of the Neil lab for reagents and support. We are also continually indebted to the NIH AIDS Research Reagents Program and the investigators who make their valuable material available through it.

J.W. performed all the experiments and analyzed the data. J.W. and S.J.D.N. planned the work and wrote the paper.

This work was supported by European Research Council starter grant 281598 and Wellcome Trust senior fellowship WT098049AIA to S.J.D.N.

REFERENCES

1. **Neil SJ.** 2013. The antiviral activities of tetherin. Curr. Top. Microbiol. Immunol. **371:**67–104. http://dx.doi.org/10.1007/978-3-642-37765-5_3.
2. **Neil SJ, Zang T, Bieniasz PD.** 2008. Tetherin inhibits retrovirus release and is antagonized by HIV-1 Vpu. Nature **451:**425–430. http://dx.doi.org/10.1038/nature06553.
3. **Jouvenet N, Neil SJ, Zhadina M, Zang T, Kratovac Z, Lee Y, McNatt M, Hatziioannou T, Bieniasz PD.** 2009. Broad-spectrum inhibition of retroviral and filoviral particle release by tetherin. J. Virol. **83:**1837–1844. http://dx.doi.org/10.1128/JVI.02211-08.
4. **Zenner HL, Mauricio R, Banting G, Crump CM.** 2013. Herpes simplex virus 1 counteracts tetherin restriction via its virion host shutoff activity. J. Virol. **87:**13115–13123. http://dx.doi.org/10.1128/JVI.02167-13.
5. **Pardieu C, Vigan R, Wilson SJ, Calvi A, Zang T, Bieniasz P, Kellam P, Towers GJ, Neil SJ.** 2010. The RING-CH ligase K5 antagonizes restriction of KSHV and HIV-1 particle release by mediating ubiquitin-dependent endosomal degradation of tetherin. PLoS Pathog. **6:**e1000843. http://dx.doi.org/10.1371/journal.ppat.1000843.
6. **Mansouri M, Viswanathan K, Douglas JL, Hines J, Gustin J, Moses AV, Fruh K.** 2009. Molecular mechanism of BST2/tetherin downregulation by K5/MIR2 of Kaposi's sarcoma-associated herpesvirus. J. Virol. **83:**9672–9681. http://dx.doi.org/10.1128/JVI.00597-09.
7. **Blondeau C, Pelchen-Matthews A, Mlcochova P, Marsh M, Milne RS, Towers GJ.** 2013. Tetherin restricts herpes simplex virus 1 and is antagonized by glycoprotein m. J. Virol. **87:**13124–13133. http://dx.doi.org/10.1128/JVI.02250-13.
8. **Sakuma T, Noda T, Urata S, Kawaoka Y, Yasuda J.** 2009. Inhibition of Lassa and Marburg virus production by tetherin. J. Virol. **83:**2382–2385. http://dx.doi.org/10.1128/JVI.01607-08.
9. **Perez-Caballero D, Zang T, Ebrahimi A, McNatt MW, Gregory DA, Johnson MC, Bieniasz PD.** 2009. Tetherin inhibits HIV-1 release by directly tethering virions to cells. Cell **139:**499–511. http://dx.doi.org/10.1016/j.cell.2009.08.039.
10. **Venkatesh S, Bieniasz PD.** 2013. Mechanism of HIV-1 virion entrapment by tetherin. PLoS Pathog. **9:**e1003483. http://dx.doi.org/10.1371/journal.ppat.1003483.
11. **Cocka LJ, Bates P.** 2012. Identification of alternatively translated tetherin isoforms with differing antiviral and signaling activities. PLoS Pathog. **8:**e1002931. http://dx.doi.org/10.1371/journal.ppat.1002931.
12. **Galão RP, Le Tortorec A, Pickering S, Kueck T, Neil SJ.** 2012. Innate sensing of HIV-1 assembly by tetherin induces NFkappaB-dependent proinflammatory responses. Cell Host Microbe **12:**633–644. http://dx.doi.org/10.1016/j.chom.2012.10.007.
13. **Tokarev A, Suarez M, Kwan W, Fitzpatrick K, Singh R, Guatelli J.** 2013. Stimulation of NF-kappaB activity by the HIV restriction factor BST2. J. Virol. **87:**2046–2057. http://dx.doi.org/10.1128/JVI.02272-12.
14. **Van Damme N, Goff D, Katsura C, Jorgenson RL, Mitchell R, Johnson MC, Stephens EB, Guatelli J.** 2008. The interferon-induced protein BST-2 restricts HIV-1 release and is downregulated from the cell surface by the viral Vpu protein. Cell Host Microbe **3:**245–252. http://dx.doi.org/10.1016/j.chom.2008.03.001.
15. **Jia B, Serra-Moreno R, Neidermyer W, Rahmberg A, Mackey J, Fofana IB, Johnson WE, Westmoreland S, Evans DT.** 2009. Species-specific activity of SIV Nef and HIV-1 Vpu in overcoming restriction by tetherin/BST2. PLoS Pathog. **5:**e1000429. http://dx.doi.org/10.1371/journal.ppat.1000429.
16. **Zhang F, Wilson SJ, Landford WC, Virgen B, Gregory D, Johnson MC, Munch J, Kirchhoff F, Bieniasz PD, Hatziioannou T.** 2009. Nef proteins from simian immunodeficiency viruses are tetherin antagonists. Cell Host Microbe **6:**54–67. http://dx.doi.org/10.1016/j.chom.2009.05.008.
17. **Gupta RK, Mlcochova P, Pelchen-Matthews A, Petit SJ, Mattiuzzo G, Pillay D, Takeuchi Y, Marsh M, Towers GJ.** 2009. Simian immunodeficiency virus envelope glycoprotein counteracts tetherin/BST-2/CD317 by intracellular sequestration. Proc. Natl. Acad. Sci. U. S. A. **106:**20889–20894. http://dx.doi.org/10.1073/pnas.0907075106.
18. **Le Tortorec A, Neil SJ.** 2009. Antagonism to and intracellular sequestration of human tetherin by the human immunodeficiency virus type 2 envelope glycoprotein. J. Virol. **83:**11966–11978. http://dx.doi.org/10.1128/JVI.01515-09.
19. **Kaletsky RL, Francica JR, Agrawal-Gamse C, Bates P.** 2009. Tetherin-mediated restriction of filovirus budding is antagonized by the Ebola glycoprotein. Proc. Natl. Acad. Sci. U. S. A. **106:**2886–2891. http://dx.doi.org/10.1073/pnas.0811014106.
20. **Sauter D, Specht A, Kirchhoff F.** 2010. Tetherin: holding on and letting go. Cell **141:**392–398. http://dx.doi.org/10.1016/j.cell.2010.04.022.
21. **Sauter D, Schindler M, Specht A, Landford WN, Munch J, Kim KA, Votteler J, Schubert U, Bibollet-Ruche F, Keele BF, Takehisa J, Ogando Y, Ochsenbauer C, Kappes JC, Ayouba A, Peeters M, Learn GH, Shaw G, Sharp PM, Bieniasz P, Hahn BH, Hatziioannou T, Kirchhoff F.** 2009. Tetherin-driven adaptation of Vpu and Nef function and the evolution of pandemic and nonpandemic HIV-1 strains. Cell Host Microbe **6:**409–421. http://dx.doi.org/10.1016/j.chom.2009.10.004.
22. **Rollason R, Korolchuk V, Hamilton C, Schu P, Banting G.** 2007. Clathrin-mediated endocytosis of a lipid-raft-associated protein is mediated through a dual tyrosine motif. J. Cell Sci. **120:**3850–3858. http://dx.doi.org/10.1242/jcs.003343.

23. **Dubé M, Roy BB, Guiot-Guillain P, Binette J, Mercier J, Chiasson A, Cohen EA.** 2010. Antagonism of tetherin restriction of HIV-1 release by Vpu involves binding and sequestration of the restriction factor in a perinuclear compartment. PLoS Pathog. **6:**e1000856. http://dx.doi.org/10.1371/journal.ppat.1000856.
24. **Skasko M, Wang Y, Tian Y, Tokarev A, Munguia J, Ruiz A, Stephens EB, Opella SJ, Guatelli J.** 2012. HIV-1 Vpu protein antagonizes innate restriction factor BST-2 via lipid-embedded helix-helix interactions. J. Biol. Chem. **287:**58–67. http://dx.doi.org/10.1074/jbc.M111.296772.
25. **Vigan R, Neil SJ.** 2010. Determinants of tetherin antagonism in the transmembrane domain of the human immunodeficiency virus type 1 Vpu protein. J. Virol. **84:**12958–12970. http://dx.doi.org/10.1128/JVI.01699-10.
26. **McNatt MW, Zang T, Bieniasz PD.** 2013. Vpu binds directly to tetherin and displaces it from nascent virions. PLoS Pathog. **9:**e1003299. http://dx.doi.org/10.1371/journal.ppat.1003299.
27. **Dubé M, Paquay C, Roy BB, Bego MG, Mercier J, Cohen EA.** 2011. HIV-1 Vpu antagonizes BST-2 by interfering mainly with the trafficking of newly synthesized BST-2 to the cell surface. Traffic **12:**1714–1729. http://dx.doi.org/10.1111/j.1600-0854.2011.01277.x.
28. **Schmidt S, Fritz JV, Bitzegeio J, Fackler OT, Keppler OT.** 2011. HIV-1 Vpu blocks recycling and biosynthetic transport of the intrinsic immunity factor CD317/tetherin to overcome the virion release restriction. mBio **2:**e00036–00011. http://dx.doi.org/10.1128/mBio.00036-11.
29. **Kueck T, Neil SJ.** 2012. A cytoplasmic tail determinant in HIV-1 Vpu mediates targeting of tetherin for endosomal degradation and counteracts interferon-induced restriction. PLoS Pathog. **8:**e1002609. http://dx.doi.org/10.1371/journal.ppat.1002609.
30. **Agromayor M, Soler N, Caballe A, Kueck T, Freund SM, Allen MD, Bycroft M, Perisic O, Ye Y, McDonald B, Scheel H, Hofmann K, Neil SJ, Martin-Serrano J, Williams RL.** 2012. The UBAP1 subunit of ESCRT-I interacts with ubiquitin via a SOUBA domain. Structure **20:**414–428. http://dx.doi.org/10.1016/j.str.2011.12.013.
31. **Janvier K, Pelchen-Matthews A, Renaud JB, Caillet M, Marsh M, Berlioz-Torrent C.** 2011. The ESCRT-0 component HRS is required for HIV-1 Vpu-mediated BST-2/tetherin down-regulation. PLoS Pathog. **7:**e1001265. http://dx.doi.org/10.1371/journal.ppat.1001265.
32. **Douglas JL, Viswanathan K, McCarroll MN, Gustin JK, Fruh K, Moses AV.** 2009. Vpu directs the degradation of the human immunodeficiency virus restriction factor BST-2/tetherin via a {beta}TrCP-dependent mechanism. J. Virol. **83:**7931–7947. http://dx.doi.org/10.1128/JVI.00242-09.
33. **Mitchell RS, Katsura C, Skasko MA, Fitzpatrick K, Lau D, Ruiz A, Stephens EB, Margottin-Goguet F, Benarous R, Guatelli JC.** 2009. Vpu antagonizes BST-2-mediated restriction of HIV-1 release via beta-TrCP and endo-lysosomal trafficking. PLoS Pathog. **5:**e1000450. http://dx.doi.org/10.1371/journal.ppat.1000450.
34. **Gustin JK, Douglas JL, Bai Y, Moses AV.** 2012. Ubiquitination of BST-2 protein by HIV-1 Vpu protein does not require lysine, serine, or threonine residues within the BST-2 cytoplasmic domain. J. Biol. Chem. **287:**14837–14850. http://dx.doi.org/10.1074/jbc.M112.349928.
35. **Tokarev AA, Munguia J, Guatelli JC.** 2011. Serine-threonine ubiquitination mediates downregulation of BST-2/tetherin and relief of restricted virion release by HIV-1 Vpu. J. Virol. **85:**51–63. http://dx.doi.org/10.1128/JVI.01795-10.
36. **Zhang F, Landford WN, Ng M, McNatt MW, Bieniasz PD, Hatziioannou T.** 2011. SIV Nef proteins recruit the AP-2 complex to antagonize tetherin and facilitate virion release. PLoS Pathog. **7:**e1002039. http://dx.doi.org/10.1371/journal.ppat.1002039.
37. **Serra-Moreno R, Zimmermann K, Stern LJ, Evans DT.** 2013. Tetherin/BST-2 antagonism by Nef depends on a direct physical interaction between Nef and tetherin, and on clathrin-mediated endocytosis. PLoS Pathog. **9:**e1003487. http://dx.doi.org/10.1371/journal.ppat.1003487.
38. **Lau D, Kwan W, Guatelli J.** 2011. Role of the endocytic pathway in the counteraction of BST-2 by human lentiviral pathogens. J. Virol. **85:**9834–9846. http://dx.doi.org/10.1128/JVI.02633-10.
39. **Pickering S, Hue S, Kim EY, Reddy S, Wolinsky SM, Neil SJ.** 2014. Preservation of tetherin and CD4 counter-activities in circulating Vpu alleles despite extensive sequence variation within HIV-1 infected individuals. PLoS Pathog. **10:**e1003895. http://dx.doi.org/10.1371/journal.ppat.1003895.
40. **Sharp PM, Hahn BH.** 2011. Origins of HIV and the AIDS pandemic. Cold Spring Harb. Perspect. Med. **1:**a006841. http://dx.doi.org/10.1101/cshperspect.a006841.
41. **Neil SJ, Eastman SW, Jouvenet N, Bieniasz PD.** 2006. HIV-1 Vpu promotes release and prevents endocytosis of nascent retrovirus particles from the plasma membrane. PLoS Pathog. **2:**e39. http://dx.doi.org/10.1371/journal.ppat.0020039.
42. **Salazar-Gonzalez JF, Salazar MG, Keele BF, Learn GH, Giorgi EE, Li H, Decker JM, Wang S, Baalwa J, Kraus MH, Parrish NF, Shaw KS, Guffey MB, Bar KJ, Davis KL, Ochsenbauer-Jambor C, Kappes JC, Saag MS, Cohen MS, Mulenga J, Derdeyn CA, Allen S, Hunter E, Markowitz M, Hraber P, Perelson AS, Bhattacharya T, Haynes BF, Korber BT, Hahn BH, Shaw GM.** 2009. Genetic identity, biological phenotype, and evolutionary pathways of transmitted/founder viruses in acute and early HIV-1 infection. J. Exp. Med. **206:**1273–1289. http://dx.doi.org/10.1084/jem.20090378.
43. **Sauter D, Unterweger D, Vogl M, Usmani SM, Heigele A, Kluge SF, Hermkes E, Moll M, Barker E, Peeters M, Learn GH, Bibollet-Ruche F, Fritz JV, Fackler OT, Hahn BH, Kirchhoff F.** 2012. Human tetherin exerts strong selection pressure on the HIV-1 group N Vpu protein. PLoS Pathog. **8:**e1003093. http://dx.doi.org/10.1371/journal.ppat.1003093.
44. **Miyagi E, Andrew AJ, Kao S, Strebel K.** 2009. Vpu enhances HIV-1 virus release in the absence of Bst-2 cell surface down-modulation and intracellular depletion. Proc. Natl. Acad. Sci. U. S. A. **106:**2868–2873. http://dx.doi.org/10.1073/pnas.0813223106.
45. **Erikson E, Adam T, Schmidt S, Lehmann-Koch J, Over B, Goffinet C, Harter C, Bekeredjian-Ding I, Sertel S, Lasitschka F, Keppler OT.** 2011. In vivo expression profile of the antiviral restriction factor and tumor-targeting antigen CD317/BST-2/HM1.24/tetherin in humans. Proc. Natl. Acad. Sci. U. S. A. **108:**13688–13693. http://dx.doi.org/10.1073/pnas.1101684108.
46. **Bego MG, Mercier J, Cohen EA.** 2012. Virus-activated interferon regulatory factor 7 upregulates expression of the interferon-regulated BST2 gene independently of interferon signaling. J. Virol. **86:**3513–3527. http://dx.doi.org/10.1128/JVI.06971-11.
47. **Lim ES, Malik HS, Emerman M.** 2010. Ancient adaptive evolution of tetherin shaped the functions of Vpu and Nef in human immunodeficiency virus and primate lentiviruses. J. Virol. **84:**7124–7134. http://dx.doi.org/10.1128/JVI.00468-10.
48. **Means RE, Lang SM, Jung JU.** 2007. The Kaposi's sarcoma-associated herpesvirus K5 E3 ubiquitin ligase modulates targets by multiple molecular mechanisms. J. Virol. **81:**6573–6583. http://dx.doi.org/10.1128/JVI.02751-06.
49. **Noble B, Abada P, Nunez-Iglesias J, Cannon PM.** 2006. Recruitment of the adaptor protein 2 complex by the human immunodeficiency virus type 2 envelope protein is necessary for high levels of virus release. J. Virol. **80:**2924–2932. http://dx.doi.org/10.1128/JVI.80.6.2924-2932.2006.
50. **Celestino M, Calistri A, Del Vecchio C, Salata C, Chiuppesi F, Pistello M, Borsetti A, Palu G, Parolin C.** 2012. Feline tetherin is characterized by a short N-terminal region and is counteracted by the feline immunodeficiency virus envelope glycoprotein. J. Virol. **86:**6688–6700. http://dx.doi.org/10.1128/JVI.07037-11.
51. **Dietrich I, Hosie MJ, Willett BJ.** 2011. The role of BST2/tetherin in feline retrovirus infection. Vet. Immunol. Immunopathol. **143:**255–264. http://dx.doi.org/10.1016/j.vetimm.2011.06.020.
52. **Yin X, Hu Z, Gu Q, Wu X, Zheng YH, Wei P, Wang X.** 2014. Equine tetherin blocks retrovirus release and its activity is antagonized by equine infectious anemia virus envelope protein. J. Virol. **88:**1259–1270. http://dx.doi.org/10.1128/JVI.03148-13.
53. **Barrett BS, Smith DS, Li SX, Guo K, Hasenkrug KJ, Santiago ML.** 2012. A single nucleotide polymorphism in tetherin promotes retrovirus restriction in vivo. PLoS Pathog. **8:**e1002596. http://dx.doi.org/10.1371/journal.ppat.1002596.
54. **Pham TN, Lukhele S, Hajjar F, Routy JP, Cohen EA.** 2014. HIV Nef and Vpu protect HIV-infected $CD4^+$ T cells from antibody-mediated cell lysis through down-modulation of CD4 and BST2. Retrovirology **11:**15. http://dx.doi.org/10.1186/1742-4690-11-15.
55. **Cao W, Bover L, Cho M, Wen X, Hanabuchi S, Bao M, Rosen DB, Wang YH, Shaw JL, Du Q, Li C, Arai N, Yao Z, Lanier LL, Liu YJ.** 2009. Regulation of TLR7/9 responses in plasmacytoid dendritic cells by BST2 and ILT7 receptor interaction. J. Exp. Med. **206:**1603–1614. http://dx.doi.org/10.1084/jem.20090547.
56. **Tavano B, Galão RP, Graham DR, Neil SJ, Aquino VN, Fuchs D, Boasso A.** 2013. Ig-like transcript 7, but not bone marrow stromal cell antigen 2 (also known as HM1.24, tetherin, or CD317), modulates plasmacytoid dendritic cell function in primary human blood leukocytes. J. Immunol. **190:**2622–2630. http://dx.doi.org/10.4049/jimmunol.1202391.

57. **Casartelli N, Sourisseau M, Feldmann J, Guivel-Benhassine F, Mallet A, Marcelin AG, Guatelli J, Schwartz O.** 2010. Tetherin restricts productive HIV-1 cell-to-cell transmission. PLoS Pathog. **6:**e1000955. http://dx.doi.org/10.1371/journal.ppat.1000955.
58. **Jolly C, Booth NJ, Neil SJ.** 2010. Cell-cell spread of human immunodeficiency virus type 1 overcomes tetherin/BST-2-mediated restriction in T cells. J. Virol. **84:**12185–12199. http://dx.doi.org/10.1128/JVI.01447-10.
59. **Kuhl BD, Sloan RD, Donahue DA, Bar-Magen T, Liang C, Wainberg MA.** 2010. Tetherin restricts direct cell-to-cell infection of HIV-1. Retrovirology **7:**115. http://dx.doi.org/10.1186/1742-4690-7-115.
60. **Sauter D, Vogl M, Kirchhoff F.** 2011. Ancient origin of a deletion in human BST2/tetherin that confers protection against viral zoonoses. Hum. Mutat. **32:**1243–1245. http://dx.doi.org/10.1002/humu.21571.
61. **Vigan R, Neil SJ.** 2011. Separable determinants of subcellular localization and interaction account for the inability of group O HIV-1 Vpu to counteract tetherin. J. Virol. **85:**9737–9748. http://dx.doi.org/10.1128/JVI.00479-11.
62. **Yang SJ, Lopez LA, Exline CM, Haworth KG, Cannon PM.** 2011. Lack of adaptation to human tetherin in HIV-1 group O and P. Retrovirology **8:**78. http://dx.doi.org/10.1186/1742-4690-8-78.

PLOS | PATHOGENS

RESEARCH ARTICLE

Serine Phosphorylation of HIV-1 Vpu and Its Binding to Tetherin Regulates Interaction with Clathrin Adaptors

Tonya Kueck[¤☯], Toshana L. Foster[☯], Julia Weinelt[☯], Jonathan C. Sumner, Suzanne Pickering, Stuart J. D. Neil*

Department of Infectious Disease, King's College London School of Life Sciences and Medicine, Guy's Hospital, London, United Kingdom

☯ These authors contributed equally to this work.
¤ Present address: Aaron Diamond AIDS Research Center, The Rockefeller University, New York, New York, United States of America
* stuart.neil@kcl.ac.uk

OPEN ACCESS

Citation: Kueck T, Foster TL, Weinelt J, Sumner JC, Pickering S, Neil SJD (2015) Serine Phosphorylation of HIV-1 Vpu and Its Binding to Tetherin Regulates Interaction with Clathrin Adaptors. PLoS Pathog 11 (8): e1005141. doi:10.1371/journal.ppat.1005141

Editor: David T. Evans, University of Wisconsin, UNITED STATES

Received: December 23, 2015

Accepted: August 11, 2015

Published: August 28, 2015

Data Availability Statement: All relevant data are within the paper and its Supporting Information files.

Funding: This work was funded by a European Research Council Consolidator Grant (281598) and a Wellcome Trust Senior Research Fellowship (WT098049AIA) to SJDN. The funders had no role in study design, data collection and analysis, decision to publish, or preparation of the manuscript.

Competing Interests: The authors have declared that no competing interests exist.

Abstract

HIV-1 Vpu prevents incorporation of tetherin (BST2/ CD317) into budding virions and targets it for ESCRT-dependent endosomal degradation via a clathrin-dependent process. This requires a variant acidic dileucine-sorting motif (ExxxLV) in Vpu. Structural studies demonstrate that recombinant Vpu/tetherin fusions can form a ternary complex with the clathrin adaptor AP-1. However, open questions still exist about Vpu's mechanism of action. Particularly, whether endosomal degradation and the recruitment of the E3 ubiquitin ligase $SCF^{\beta TRCP1/2}$ to a conserved phosphorylated binding site, DSGNES, are required for antagonism. Re-evaluation of the phenotype of Vpu phosphorylation mutants and naturally occurring allelic variants reveals that the requirement for the Vpu phosphoserine motif in tetherin antagonism is dissociable from $SCF^{\beta TRCP1/2}$ and ESCRT-dependent tetherin degradation. Vpu phospho-mutants phenocopy ExxxLV mutants, and can be rescued by direct clathrin interaction in the absence of $SCF^{\beta TRCP1/2}$ recruitment. Moreover, we demonstrate physical interaction between Vpu and AP-1 or AP-2 in cells. This requires Vpu/tetherin transmembrane domain interactions as well as the ExxxLV motif. Importantly, it also requires the Vpu phosphoserine motif and adjacent acidic residues. Taken together these data explain the discordance between the role of $SCF^{\beta TRCP1/2}$ and Vpu phosphorylation in tetherin antagonism, and indicate that phosphorylation of Vpu in Vpu/tetherin complexes regulates promiscuous recruitment of adaptors, implicating clathrin-dependent sorting as an essential first step in tetherin antagonism.

Author Summary

Counteraction of tetherin, a host antiviral protein that blocks viral release from infected cells, is an essential attribute of HIV-1 and its related viruses. The HIV-1 accessory protein Vpu binds to tetherin, preventing its incorporation into viral particles, and targets it for

ubiquitin-dependent degradation. This involves mis-trafficking of tetherin by a Vpu-dependent mechanism through the engagement of clathrin adaptor proteins. Although structural evidence exists for Vpu and tetherin interacting with clathrin adaptor 1 (AP-1), evidence that it is required for Vpu-mediated tetherin counteraction is still lacking. Tetherin degradation by Vpu also requires an E3 ubiquitin ligase, $SCF^{\beta TRCP1/2}$ that binds to phosphorylated serine residues in the Vpu cytoplasmic tail. Again, discrepancies exist about the importance of this interaction in tetherin's counteraction. Here we show that Vpu phosphorylation, in combination with its physical interaction with tetherin, regulates interaction with both AP-1 and the other major cellular clathrin adaptor, AP-2. These interactions can be decoupled from $SCF^{\beta TRCP1/2}$ recruitment, thus indicating clathrin-dependent mis-trafficking as a critical step in tetherin antagonism by Vpu. Additionally, the ability to interact both with AP-1 and AP-2 in a tetherin-dependent manner indicates a redundancy in host cofactors used by Vpu that explains disparate previous observations of its mechanism of action.

Introduction

Counteraction of the antiviral membrane protein tetherin (BST2/ CD317) is an essential attribute of primate lentiviruses, and is mediated by either the Vpu or Nef accessory proteins, or occasionally the viral envelope glycoprotein (reviewed in [1]). In their absence, tetherin restricts the release of virions assembling at the cell surface [2–6]. By virtue of its N-terminal transmembrane (TM) domain and C-terminal GPI anchor, partitioning of tetherin dimers into budding virions allows them to simultaneously span host and viral membranes resulting in accumulation of cross-linked virions on the plasma membrane (PM) [7,8]. In addition to physically limiting virion release, tetherin's activity sensitizes infected cells to antibody-dependent cellular cytotoxicity [9–12], targets virions for endosomal degradation, and in the case of great ape tetherins, can directly induce the activation of proinflammatory NF-κB signaling [13–16].

Tetherin recycles to the PM via the trans-Golgi network (TGN) [17]. This requires a dual tyrosine-based sorting signal (YDYCRV in humans), which can interact with the clathrin adaptor AP-1. Lentiviral countermeasures physically interact with tetherin, often in a highly species-specific manner [1]. Through their action, tetherin incorporation into virions is blocked, and this is associated with its reduced cell surface levels. In the case of HIV-1 Vpu, a small membrane phospho-protein, physical interaction is mediated by the TM domains themselves [18–20]. HIV-1 Vpu targets human tetherin into an ESCRT-dependent endosomal degradation pathway [21,22]. This is an ubiquitin driven process and requires a highly conserved DSGNES motif in the Vpu cytoplasmic tail [23–25]. Phosphorylation of the serine residues (S52/53 and S56/57 in subtype B depending on the isolate) by casein kinase II (CKII) [26,27] recruits the β-TrCP1/2 subunits of a Skp1-Cullin1-F-Box (SCF) E3 ubiquitin ligase [28] that mediates direct ubiquitination of various residues in the tetherin cytoplasmic tail including an STS motif [29]. However, there is still debate as to whether the recruitment of the $SCF^{\beta TRCP1/2}$ to the DSGNES motif in Vpu is required for counteraction of physical retention of virions by tetherin (hereafter also termed antagonism) as well as its final endosomal degradation. Much of this discrepancy may be attributable to whether assays are performed in virally infected cells or those transiently transfected with Vpu, tetherin or both [30]. While ESCRT-I appears to be dispensable in infected cells [21], evidence that the ESCRT-0 component HRS is required for tetherin antagonism suggests targeting to endosomal degradation plays a role [22]. Furthermore, mutations of the Vpu serine residues (so called 2/6 mutations) have intermediate

phenotypes in tetherin antagonism suggesting degradation does not fully explain Vpu function [24,25,31]. Moreover this defect in antagonism is not recapitulated by siRNA depletion of β-TrCP1/2 [32]. Indeed evidence that the DSGNES motif might have a dual function in tetherin trafficking has been proposed [33]. This is consistent with our recent study of Vpu variation in patients where we found that naturally occurring variants in the NE of the DSGNES imparted tetherin-specific defects to Vpu without blocking its other SCF-dependent activity, dislocation of CD4 from the endoplasmic reticulum [34].

Vpu has been shown to block newly synthesized and/or recycling tetherin from trafficking to the cell surface [33,35]. This requires a variant of an acidic dileucine motif, ExxxLV, in the second alpha helix of the cytoplasmic tail of most HIV-1 group M clade Vpu [36]. Acidic dileucine sorting signals bind to the σ subunits of the major cellular clathrin adaptors AP-1 (trafficking from TGN to endosomes and *vice versa*) and AP-2 (clathrin-dependent endocytosis from the PM) (reviewed in [37]). In keeping with this, Vpu-mediated tetherin antagonism is entirely clathrin-dependent [36,38]. Mutation of the ExxxLV motif does not block Vpu/tetherin interactions, but reduces the efficiency of counteraction and inhibits degradation [36]. In particular ExxxLV is essential for counteraction of tetherin in CD4+ T cells upon interferon upregulation, and mutant phenotypes are exacerbated when tetherin lacks the YDYCRV motif [36]. A recent structural and biochemical study has demonstrated that the ExxxLV motif can bind canonically to the σ subunit of AP-1, whereas the YXXθ motif of tetherin can bind to the μ subunit of AP-1 [39]. In fusions of Vpu and tetherin cytoplasmic tails both motifs can occupy their respective binding sites simultaneously [39]. Some density in the structure also indicated other contacts between Vpu and AP-1μ, and together implied a mechanism whereby the formation of this ternary complex would modulate AP-1-dependent trafficking of tetherin to endosomes. However, whilst the localization of Vpu to the TGN suggested AP-1 as the major target, siRNA-mediated knockdown of AP-1 or expression in AP-1 -/- murine fibroblasts did not inhibit Vpu function [36]. Neither has physical interaction between AP-1 and the wild-type Vpu protein been demonstrated in living cells. Expression of tetherin fused at its N-terminus to the second helix of Vpu is excluded from budding virions at the PM in an ExxxLV-dependent manner [18]. Added to this, tetherin can be expressed as two isoforms, one of which lacks the YDYCRV motif and can be antagonized by Vpu to a certain extent without cell surface downregulation [13,40]. Likewise, Vpu has only a modest effect on tetherin endocytosis [25,35], and AP-2 knockdown also has little impact on antagonism, contrasting sharply with SIV Nef and HIV-2 envelopes [38,41,42].

AP1 binding to a non-canonical acidic dileucine motif in CI-M6PR has been associated with upstream serine phosphorylation by CKII previously [43]. Thus we hypothesized that the DSGNES in Vpu might regulate clathrin adaptor interaction independently of SCF recruitment. Here we provide evidence that this is indeed the case.

Results

Vpu does not require ESCRT-I, HRS or β-TrCP to counteract tetherin in HIV-1 infected cells

The importance of the $SCF^{\beta TRCP1/2}$ E3 ligase and the ultimate degradation of tetherin to the counteraction of its physical antiviral activity by Vpu has been controversial. Since the discrepant studies were mostly performed under conditions of transient transfection of tetherin, provirus or both, and which have been shown previously to lead to artifactual effects on tetherin degradation [30], we re-examined these issues in HIV-1 infected 293T cells stably expressing surface tetherin at levels similar to those induced by type 1 interferon (Fig 1A). We have previously shown that an endosomal sorting-specific subunit of ESCRT-I, UBAP1, is essential for

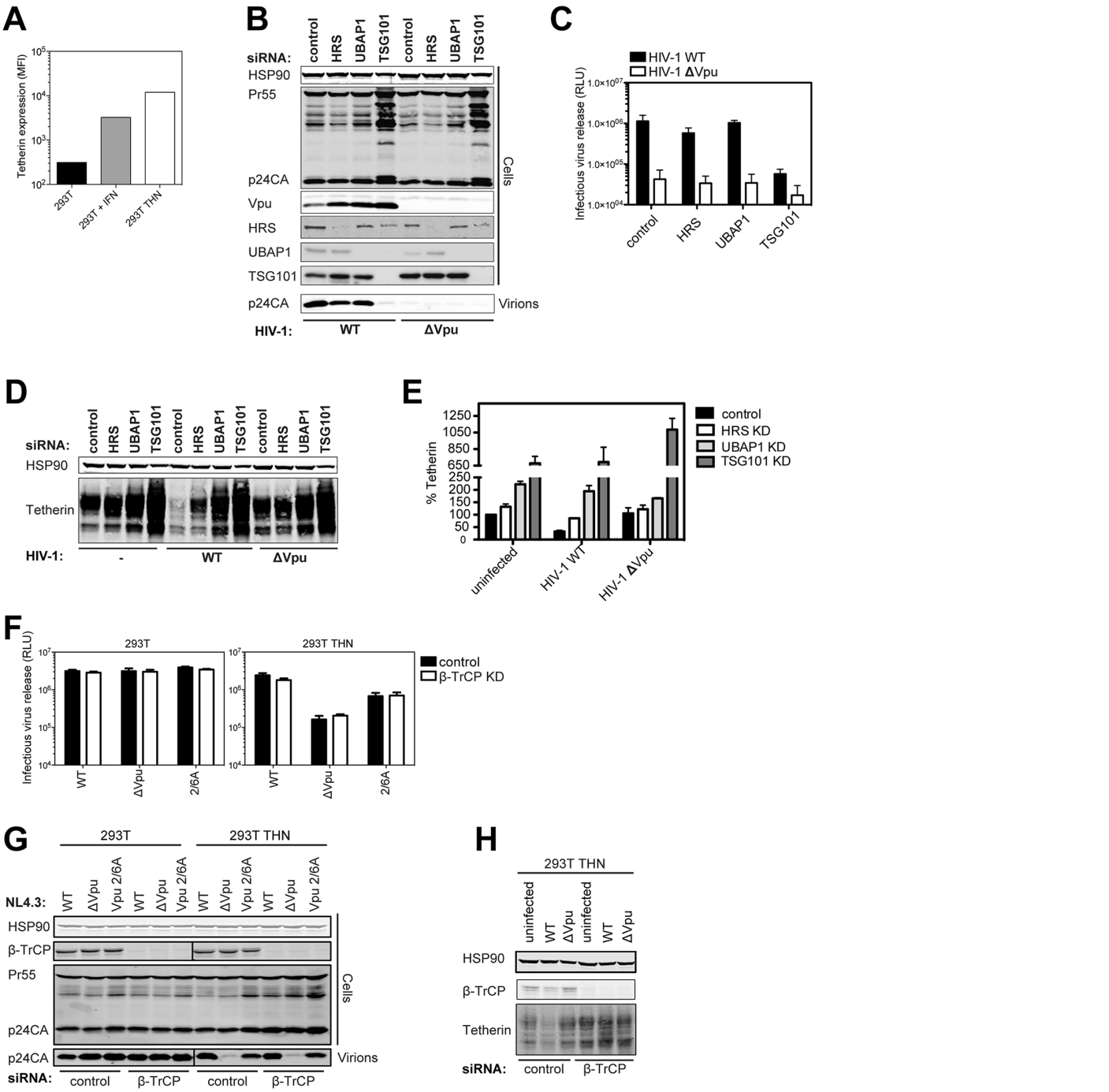

Fig 1. Vpu does not require ESCRT-I, HRS or βTRCP to counteract tetherin in HIV-1 infected cells. (A) The graph indicates the median fluorescence intensity of tetherin surface expression for 293T cells, 293T cells treated with 1000 U/ml universal type-I interferon for 24h or the same cells stably expressing tetherin. (B) 293T tetherin cells were transfected twice over a 48 hour period with siRNA oligonucleotide directed against HRS, UBAP1, TSG101 or non targeting control. Cells were then infected with NL4.3 HIV-1 WT or HIV-1 ΔVpu at an MOI of 0.8. Cell lysates and sucrose purified viral supernatants were subjected to SDS-PAGE and analyzed by Western blotting for HSP90, HIV-1 p24CA and Vpu, and analyzed by LiCor quantitative imager. (C) Infectivity of viral supernatants from (B) was assayed on HeLa-TZMbl reporter cells. Infectious virus release was plotted as β-galactosidase activity in relative light units (RLU). Error bars represent the standard deviation of three independent experiments. (D) Cells were treated as in (B), but infected with an MOI of 2. Cell lysates were subjected to SDS-PAGE and analyzed by Western blotting for HSP90 and tetherin, and analyzed by LiCor quantitative imager. (E) Percent of tetherin in cells transfected with HRS or non-targeting siRNA oligonucleotides and infected with NL4.3 HIV-1 WT or HIV-1 ΔVpu. Error bars represent the standard deviation of three independent experiments. (F-H) 293T or 293T tetherin cells were transfected as in (B) with siRNA oligonucleotide directed

against β-TrCP1 and 2 or non-targeting control. Cells were infected with VSV-G pseudotyped NL4.3 HIV-1 WT, ΔVpu or Vpu 2/6A mutant at an MOI of 0.8 and processed as in (C) and (D). (H) Cells were treated as in (F) but infected at an MOI of 2. Cell lysates were subjected to SDS-PAGE and analyzed by Western blotting for HSP90 and tetherin.

doi:10.1371/journal.ppat.1005141.g001

tetherin's degradation but not for antagonism [21,36]. Despite efficient levels of knockdown, similarly efficient siRNA knockdowns of HRS (ESCRT-0) or UBAP1 had only minor effects on one-round yield of wild-type HIV-1 (HIV-1 wt) from 293T tetherin cells at an MOI of 0.8 (Fig 1B and 1C). As expected, knockdown of the core ESCRT-I subunit TSG101 destablized UBAP1 [44] and blocked all virion release because of its essential late-domain function [45], and all siRNA treatments also stabilized Vpu expression (Fig 1B). In keeping with this, cells infected at an MOI of 2, to ensure at least 90% infection, demonstrated that Vpu-induced degradation was blocked by all siRNA knockdowns (Fig 1D and 1E). These data therefore indicate that in infected cells expressing physiological levels of Vpu from an integrated HIV-1 provirus, the core ESCRT pathway and HRS are essential for Vpu-mediated tetherin degradation, but dispensable for counteraction of tetherin's physical antiviral activity.

A previous study indicated that HRS interacted with Vpu in immuno-precipitates [22]. We confirmed this in transfected cells using myc-tagged HRS, and found that HRS truncations that removed its double-ubiquitin interaction motif (DUIM) inhibited this interaction (S1A and S1B Fig). Furthermore, point mutations in the DUIM that abolish ubiquitin-interaction (A266Q/ A228Q) [46], not putative ubiquitin-binding mutants in the VHS domain, completely abolished HRS/Vpu interactions in co-IPs (S1C Fig). Whilst formally possible that the DUIM is a direct binding site for Vpu, these data likely suggest that Vpu interactions with HRS are mediated indirectly through ubiquitination either of cargo, or associated factors in the degradation pathway.

We next similarly re-evaluated the effect of simultaneously knocking down β-TrCP1 and 2 on Vpu-mediated tetherin-degradation and tetherin-counteraction in infected cells. Again despite efficient knockdown, we saw little effect of this treatment on HIV-1 WT release (Fig 1F–1H). Of note, there was no evidence that β-TrCP1/2 knockdown reduced wild-type release to that of a viral mutant lacking the phosphorylated serines at positions 52 and 56 that are essential for β-TrCP1/2 recruitment (HIV-1 Vpu 2/6A). This was in contrast to a complete reversal of Vpu-mediated tetherin degradation by β-TrCP1/2 siRNAs in cells infected at an MOI of 2 (Fig 1H). Therefore whilst tetherin degradation by Vpu requires the $SCF^{\beta TRCP1/2}$ complex, under conditions when it is sufficiently depleted to block this, there is no effect on Vpu-mediated tetherin antagonism.

Phosphorylation-defective Vpu phenocopies trafficking mutants

Since the phospho-mutant of Vpu, Vpu 2/6A, has been shown to be partially defective for tetherin antagonism [23–25], we revisited whether this impairment could be uncoupled from the ubiquitin ligase. We recently showed that mutants of clade B Vpu lacking a conserved ExxxLV sorting signal (Vpu ELV) were also partially defective for tetherin antagonism because they could not traffic tetherin/Vpu complexes for endosomal degradation [36]. Notably, ELV mutant Vpu loses all residual activity against tetherin lacking the dual-tyrosine recycling motif, and a recent study demonstrated that the tetherin and Vpu cytoplasmic tails can assemble into a ternary complex with clathrin adaptor AP-1 [39]. In addition, hints in the structure suggested that residues 42 and 43 of the first helix of the cytoplasmic tail make a non-canonical contact with AP-1**μ**. We found similar Vpu mutants with tetherin-defective phenotypes in our patient cohort [34], and mutation of conserved $L_{41}I_{42}/L_{45}I_{46}$ in the first alpha helix to alanines in the NL4.3 provirus led to a profound defect in tetherin antagonism and degradation without

preventing interaction (S2A–S2E Fig). Since the DSGNES motif is located in an acidic patch between helix 1 and the ExxxLV site, we hypothesized that Vpu phosphomutants may also be similarly defective for mis-trafficking tetherin. In one round virus infection assays in 293T/tetherin cells, LI/LI, ELV and 2/6A mutants all had similarly defective phenotypes for tetherin antagonism (Fig 2A and 2B). Interestingly, like the ELV mutant [36,39], both LI/LI and 2/6A mutants lost all their residual activity in cells expressing tetherin Y6,8A whereas release of the wild-type virus was only slightly affected. Moreover, as expected, all mutants were defective for tetherin degradation (Fig 2C). Examination of the localization of the three mutants in transfected HeLa cells revealed that, unlike the wild-type, 2/6A and LILI localized prominently to peripheral endosomal structures as well as the TGN (Fig 2D). This was similar to the localization expected for the ELV mutant [36], and quantification of coincidence with TGN46 revealed that all three mutants had a significantly reduced localization to the TGN consistent with a trafficking defect (Fig 2E). Importantly there was no significant additive effect of combined 2/6 and ELV mutations in full-length virus release from either the 293T/tetherin cells or primary CD4+ T cells (S3A–S3C Fig). Also these data could be recapitulated using a highly active primary Vpu (Vpu 2_87) isolate from our previous patient study [34] (S4A–S4D Fig). Treatment of 293T tetherin cells infected with wild-type HIV-1 with a CKII inhibitor, Tyrphostin, to mimic the 2/6A mutation showed a reduction of virus release only in the presence of tetherin, or more prominently, the Y6,8A mutant (Fig 2F and 2G). Western blot analysis of cell lysates transfected with HA-tagged Vpu expression vectors and run on an 8% PhosTag gel showed that in the presence of Tyrphostin, the smear of phosphorylated Vpu was reduced indicating inhibition of Vpu phosphorylation (Fig 2H). Together, these data therefore suggested that the defective tetherin antagonism of Vpu 2/6A may be due to phosphorylation-regulated trafficking of Vpu rather than ubiquitin ligase recruitment and degradation.

Functional rescue of Vpu phospho- and trafficking mutants by direct interaction with clathrin

The current model for Vpu function is that it prevents tetherin trafficking to the PM from the TGN and sorts it into a clathrin-dependent endosomal trafficking pathway [1,47]. If our above hypothesis was the case, we reasoned that bypassing clathrin adaptors and linking Vpu directly to clathrin itself could functionally rescue all ELV, LI/LI and 2/6A mutants. To do this we appended the AQLISFD clathrin box (CB) from HRS or a mutated sequence, AQAASFD, lacking the leucine and isoleucines essential for clathrin interaction, to the C-termini of Vpu and the respective mutants (Fig 3A). Transient transfection of increasing doses of Vpu into 293T tetherin cells effectively rescued Vpu-defective HIV-1 viral release, and neither the clathrin box nor its mutant impaired wild-type Vpu function (Fig 3B and 3C). Remarkably, however, Vpu 2/6A, Vpu ELV or Vpu LI/LI function was almost fully restored by fusion of the clathrin box, whereas grafting the mutated sequence had no effect. All Vpu chimeras were well expressed, although as shown in Fig 3C, the apparent molecular weight of Vpu and its chimeras in SDS-PAGE did not reflect amino acid length. Similar results were obtained for a heterologous clathrin box (RNLLDLL) derived from GGA2 (available on request). The clathrin box also fully restored downregulation of tetherin from the surface of transiently transfected HeLa-TZMbl cells to all the mutants (Figs 3D and S5A–S5D). To show that this rescue of function was clathrin-dependent, we depleted clathrin membrane binding with the C-terminal fragment of the neuronal clathrin-adaptor AP180 (AP180c). As expected, rescue of wild-type Vpu-dependent virus release was inhibited by AP180c whereas residual viral release in the presence of tetherin was not [36]. In all cases, the same held true for clathrin box fusions (Fig 4A). Thus, direct linkage to the clathrin machinery was sufficient to rescue both Vpu 2/6A and the

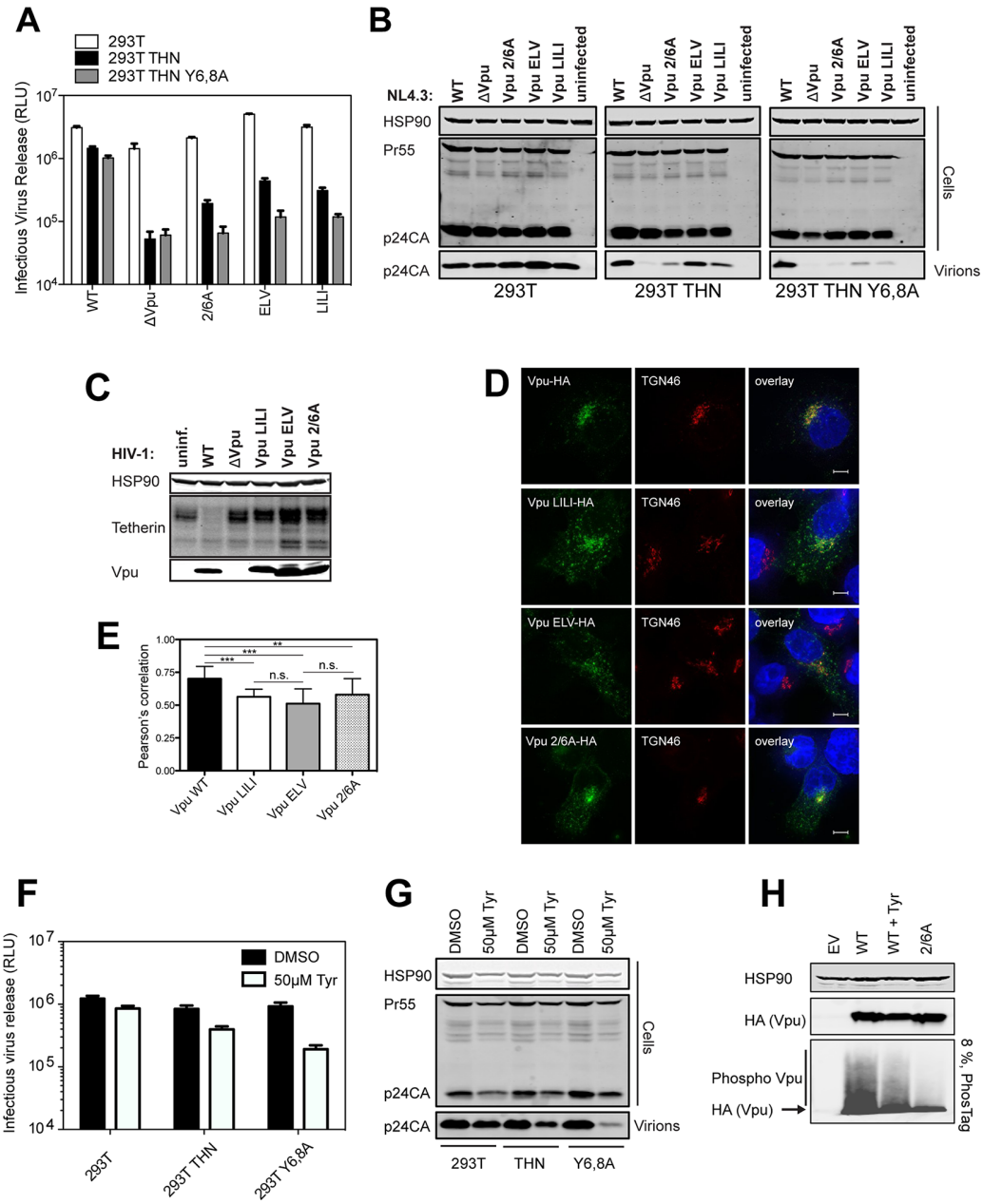

Fig 2. Phosphorylation-defective Vpu phenocopies trafficking mutants. (A-B) 293T, 293T tetherin or Y6,8A tetherin cells were infected with VSV-G pseudotyped NL4.3 WT or mutant virus at an MOI of 0.8. (A) 48 hours post infection viral supernatants were assayed for infectivity using HeLa-TZMbl reporter cells as in Fig 1. Error bars represent the standard deviation of three independent experiments. (B) Cell lysates and sucrose purified viral supernatants were subjected to SDS-PAGE and analyzed by Western blotting as in Fig 1. (C) 293T tetherin cells were infected with NL4.3 HIV-1 WT, ΔVpu, Vpu LILI, Vpu ELV or Vpu 2/6A mutants at an MOI of 2. 48 hours post infection cell lysates were subjected to SDS-PAGE and analyzed by Western blotting for HSP90 and tetherin, and analyzed by LiCor quantitative imager. (D) 293T tetherin expressing cells were transfected with 50 ng of pCR3.1 Vpu-HA or indicated mutants. 16 hours post transfection cells were fixed and stained for HA (green) and the TGN marker TGN46 (red) and examined by widefield fluorescent microscopy. Panels are of representative examples. Bars = 10 μm. (E) Z stacks were taken of all cells (n = 15), images were deconvolved using the AutoQuant X3 software and Pearson's correlations were calculated for all Z stacks using ImageJ. Results were analyzed by unpaired 2-tailed t-test—*** P = 10–5 or lower. (F) 293T, 293T tetherin or Y6,8A tetherin cells were infected with VSV-G pseudotyped NL4.3 WT at an MOI of 0.8. 6 hours post infection DMSO or 50 μM Tyrphostin was added to the medium. 48 hours post infection supernatants were assayed as in (A). (G) Cell lysates and sucrose purified viral supernatants were processed as in (B). (H) 293T tetherin cells were transfected with 2 μg pCR3.1 Vpu-HA or 2/6 Vpu-HA and treated with DMSO or 50 μM Tyrphostin for 24 h. Cell lysates were electrophoresed as before, or on a 8%, 50 μM Phos-tag gel to separate the phosphorylated species.

doi:10.1371/journal.ppat.1005141.g002

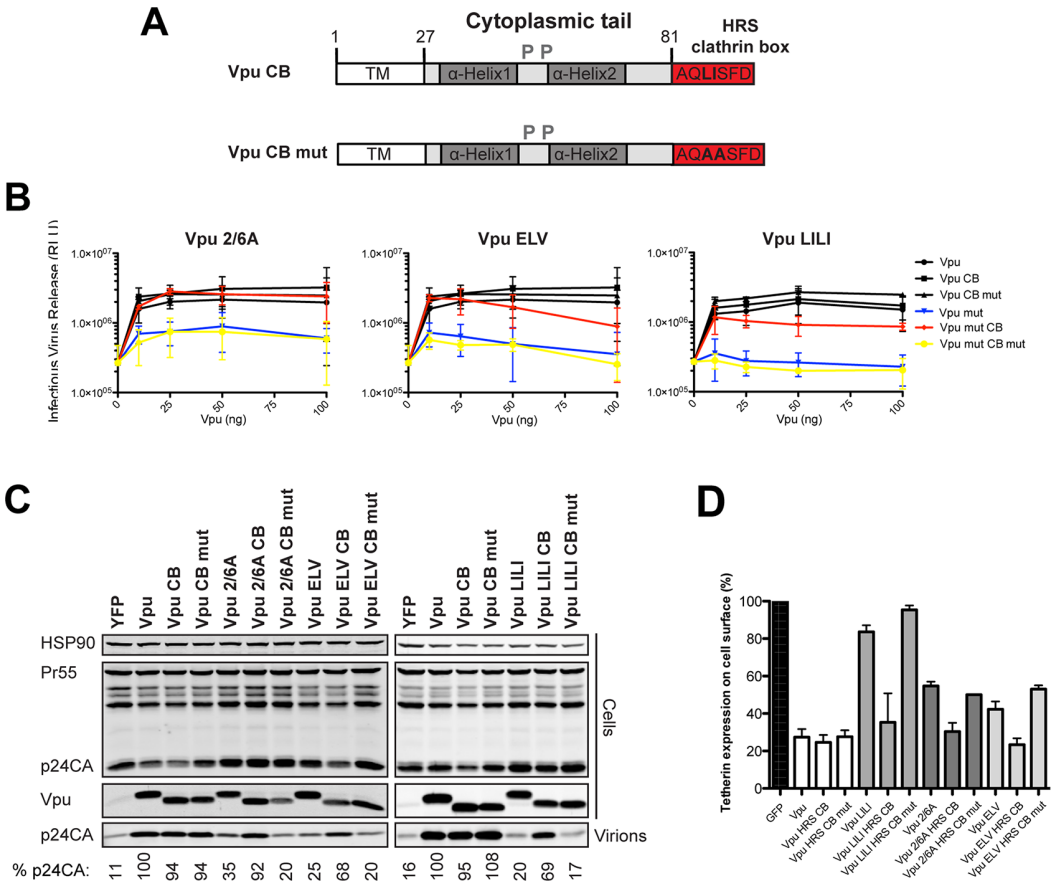

Fig 3. Functional rescue of Vpu phospho- and trafficking mutants by direct interaction with clathrin. (A) Schematic representation of Vpu CB chimera constructs. (B) 293T tetherin cells were transfected with NL4.3 ΔVpu proviral plasmid in combination with YFP expression vector and pCR3.1 Vpu, pCR3.1 Vpu CB or Vpu CB mut or Vpu mutants thereof. 48 hours post transfection infectivity of viral supernatants was determined on HeLa-TZMbl cells as in Fig 1. Error bars represent standard deviation of three independent experiments. (C) Cell lysates and pelleted supernatant virions from (B) were harvested and subjected to SDS-PAGE and analyzed by Western blotting for HIV-1 p24CA, Vpu and HSP90, and analyzed by LiCor quantitative imager. (D) HeLa-TZMbl cells were co-transfected with pCR3.1 Vpu or indicated mutant and a GFP expression vector. Cell-surface tetherin levels were analyzed 48 hours post transfection by flow cytometry in the GFP positive cells. The percentages of tetherin surface expression levels are calculated from median fluorescence intensities.

doi:10.1371/journal.ppat.1005141.g003

trafficking mutants. Moreover, in cells stably expressing the Vpu chimeras, no reduction of tetherin steady state levels was observed upon CB fusion to any of the chimeras (Fig 4B), nor was β-TrCP interaction restored to the 2/6A mutant fusion (Fig 4C), indicating this was independent of SCF and ESCRT function. Wild-type subcellular localization was restored to all mutants; 2/6A, ELV and LI/LI localization was significantly restored to TGN-associated compartments upon CB fusion (Fig 4D and 4E).

To further characterize these Vpu chimeras, we next examined whether they were functional against tetherin bearing tyrosine (trafficking) and serine/threonine (the proposed $SCF^{\beta TRCP}$ ubiquitination site [29]) mutations in the cytoplasmic tail. In the case of 293T tetherin-STS-AAA cells, the Vpu CB chimeras behaved as they did against the wild-type protein, effectively fully rescuing the 2/6A, LILI or ELV lesion (Fig 5A). Importantly, stable expression of an STS mutant tetherin had no detectable effect on the efficiency of counteraction by wild-type Vpu, and the CB addition had no effect, indicating that there is no reduction in Vpu antagonism when tetherin lacks the residues proposed to be important for ubiquitination.

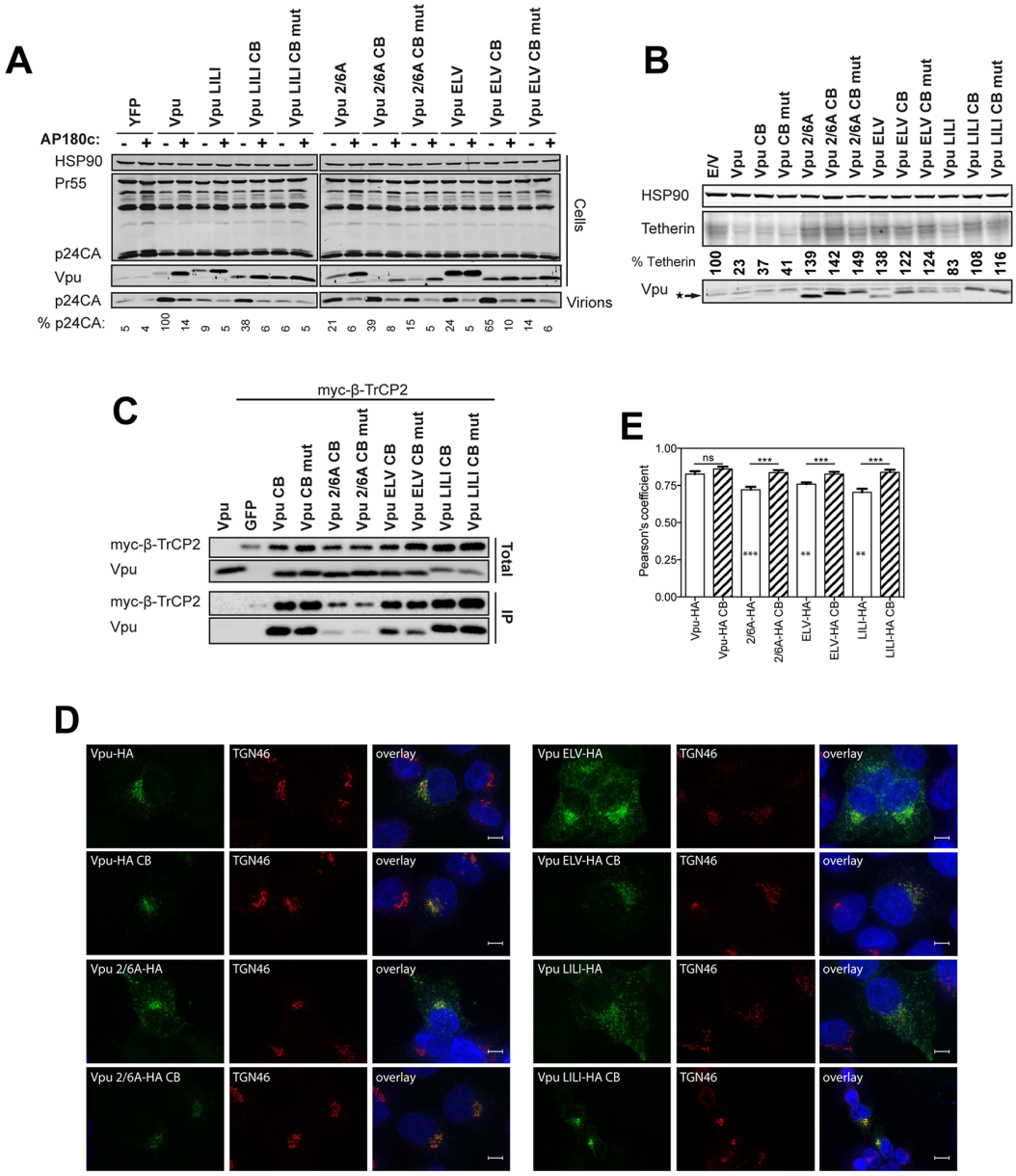

Fig 4. Clathrin binding rescues Vpu localization without restoring β-TrCP binding or tetherin degradation. (A) 293T tetherin expressing cells were co-transfected with NL4.3 ΔVpu proviral plasmid and YFP, pCR3.1 Vpu, Vpu CB, Vpu CB mut expression vector or indicated mutant in combination with AP180c. 48 hours post transfection cell lysates and pelleted supernatant virions were harvested and subjected to SDS-PAGE and analyzed by Western blotting for HIV-1 p24CA, Vpu and HSP90, and analyzed by LiCor quantitative imager. (B) 293T tetherin cells were transfected with pCR3.1 Vpu or indicated mutant. 48 hours post infection cell lysates were subjected to SDS-PAGE and analyzed by Western blotting for HSP90, tetherin and Vpu, and analyzed by LiCor quantitative imager. (C) 293T cells were transfected with pCR3.1 Vpu or indicated mutant in combination with a pCR3.1 myc-β-TrCP2 expression vector. 48 hours post transfection cells were lysed and immunoprecipitated with anti-myc antibody, using PFA (0.05% w/v) as a cross-linking agent. Total cell lysates and precipitates were subjected to SDS-PAGE and analyzed by Western blotting for myc-β-TrCP2 and Vpu-HA, and analyzed by ImageQuant. (D-E) Hela cells were transfected with 100 ng of pCR3.1 Vpu-HA or Vpu-HA CB or indicated mutants and processed as in Fig 2. Vpu-HA (green); TGN marker TGN46 (red). (G) Bars = 10 μm. (E) Asterisks inside the bars represent significant localization differences between the mutant and WT Vpu, those above between mutant and mutant clathrin box fusion.

doi:10.1371/journal.ppat.1005141.g004

However, in the case of 293T tetherin Y6,8A cells, whilst Vpu wild-type and CB fusions remained active, the mutant chimeras remained completely defective (Fig 5B). These data

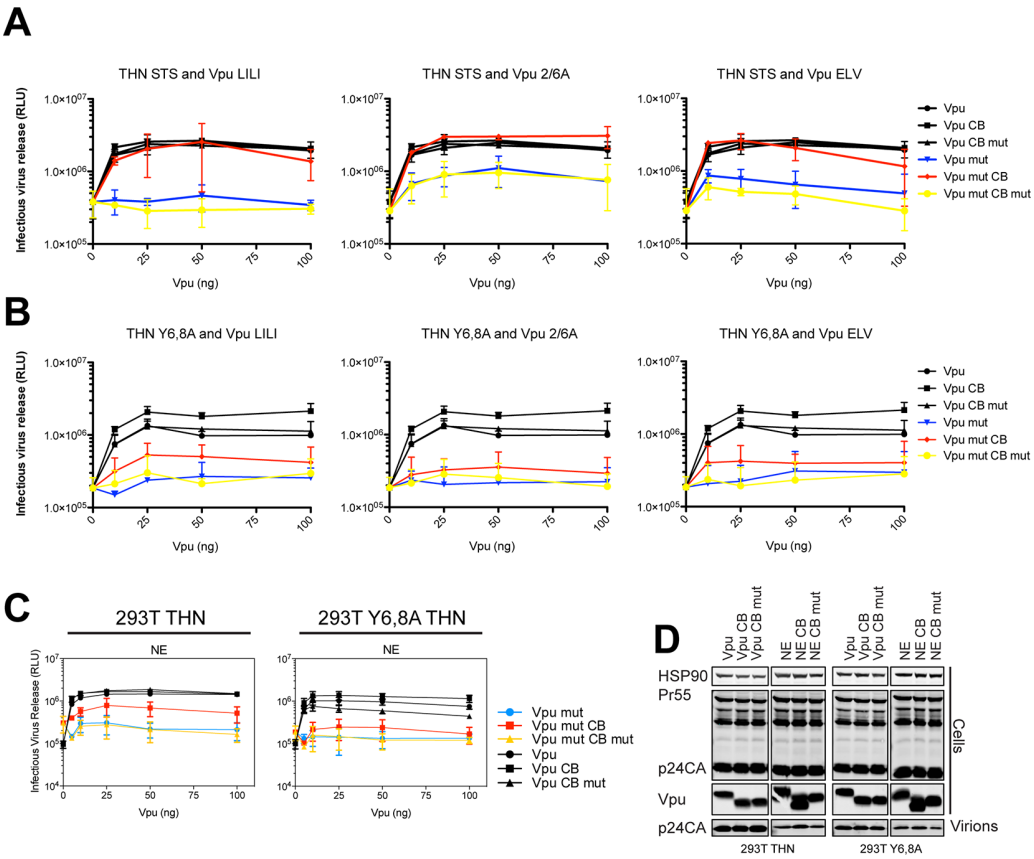

Fig 5. Clathrin box rescue of Vpu mutants is dependent on tetherin's Y6,8 sorting signal. (A-B) 293T tetherin STS or 293T tetherin Y6,8A cells were transfected with NL4.3 ΔVpu proviral plasmid in combination with YFP expression vector and increasing concentrations of pCR3.1 Vpu or indicated mutant. 48 hours post transfection infectivity of viral supernatants was determined on HeLa-TZMbl cells as in Fig 1. (C) 293T tetherin or 293T tetherin Y6,8A cells were transfected as in (A) with pCR3.1 Vpu or the N54H,E55G (NE) mutant. 48 hours post transfection infectivity of viral supernatants was determined on HeLa-TZMbl cells as in Fig 1. Error bars represent standard deviation of three independent experiments. (D) Cell lysates and pelleted supernatant virions from (A) were harvested and subjected to SDS-PAGE and analyzed by Western blotting for HIV-1 p24CA, Vpu and HSP90, and analyzed by LiCor quantitative imager.

doi:10.1371/journal.ppat.1005141.g005

imply that unlike the ExxxLV motif, the clathrin box addition is not dominant over the tetherin tyrosine-based sorting motif. This therefore suggests that tetherin sorting into clathrin-rich domains in the recycling compartment is essential for clathrin box chimera rescue, which then anchors the Vpu/tetherin complex. Subsequent endosomal trafficking, and importantly, any requirement for serine/threonine ubiquitination are downstream of this event. It also further reinforces the notion that the primary lesion in tetherin antagonism of the 2/6A mutant, like ELV and LI/LI, is at the level of clathrin-dependent sorting, not ubiquitin ligase recruitment.

Finally we examined mutations within the DSGNES motif itself. The consensus for a β-TrCP-binding site is DSGxxS, yet the N55/E56 in group M Vpu is almost universally conserved. We found rare mutations (N55H/E56G) in patients that displayed impaired tetherin antagonism despite retaining β-TrCP interaction [34]. Similarly, examination of a Vpu N55H/E56G mutation in the context of the NL4.3 Vpu revealed defects in tetherin counteraction in 293T tetherin cells (S3 and S4 Figs), which again could be rescued by a clathrin box fusion unless tetherin itself contained tyrosine mutations (Fig 5C and 5D). Together with the above data, these observations suggest that structural constraints or flexibility within the

phosphoserine motif may underlie the reason why the 2/6A mutant is defective for tetherin mis-trafficking.

Vpu interacts with clathrin adaptors AP-1 and AP-2 in tetherin-expressing cells

Our previous characterization of the ExxxLV motif and the data presented herein indicate that clathrin-dependent sorting of Vpu/tetherin complexes is an essential step in tetherin antagonism, prior to ubiquitin-dependent degradation. The demonstration that the ExxxLV motif of Vpu and the YDYCRV site in tetherin can form a ternary complex with AP-1 [39] is consistent with the cell biological observations that Vpu primarily blocks tetherin recycling and transit to the PM rather than stimulating its endocytosis [33,35]. However, demonstration that Vpu can interact with AP-1 in cells is lacking, and neither siRNA depletion of AP-1, nor deletion of γ-adaptin in murine fibroblasts, affects tetherin antagonism [36]. Clathrin adaptor interactions with their cargoes can sometimes (but not universally) be detected in yeast 2 or 3-hybrid assays or with recombinant proteins, but the relative weakness of their affinities often precludes direct demonstration of their interactions *in vivo* by conventional immunoprecipitations. To examine Vpu interaction with AP-1, we initially employed a proximity-based biotin ligase assay (S6A Fig). A consenus clade B Vpu or indicated mutant (note the phosphomutant S53,57A is labeled S3/7A), was fused to a myc-tagged E coli biotin ligase BirA-R113G, which itself does not compromise Vpu activity (S6B Fig). These constructs were then transfected into 293T or 293T tetherin cells. 6 hours after transfection the cells were incubated with free-biotin overnight in the presence of concanamycin A to block any tetherin degradation by the wild-type Vpu protein. Cell lysates were precipitated with streptavidin beads, and recovered proteins analyzed by Western blotting. Such treatment will lead to promiscuous biotinylation of proteins in close proximity with Vpu, potentially allowing us to detect interacting factors with weak affinities. As shown in S6C Fig, addition of biotin led to an accumulation of biotinylated proteins in cell lysates, including a strong band that is auto-biotinylation Vpu-BirA fusion itself. Importantly, β-TrCP was detected for all mutants tested in both 293T and 293T tetherin cells except the 2/6A mutant. Interestingly AP-1 γ-adaptin was detected only in streptavidin precipitates from 293T tetherin cells transfected with wild-type Vpu-BirA fusion, and not cells lacking tetherin expression. Furthermore, in 293T tetherin cells both ELV and LI/LI mutants failed to biotinylate AP-1. Interestingly, this was observed for the 2/6A mutant and also a Vpu A14L/W22A mutant that lacks tetherin binding. Thus, proximity-based tagging suggested Vpu does indeed interact with AP-1 in living cells. This appears to be dependent on tetherin binding and requires both the predicted AP-1σ binding site in Vpu, ExxxLV, and the non-canonical AP-1μ contact proposed to imparted by LI/LI. Furthermore, the lack of the 2/6A mutant to biotinylate AP-1γ suggests that Vpu phosphorylation is required to promote interaction, consistent with its cellular phenotype.

Whilst this data is strongly suggestive, it does not rule out that conformational changes in the mutants position the BirA in a context where AP-1 cannot be biotinylated. To strengthen these observations, we performed cross-linking immunoprecipitations in 293T tetherin cells transfected with HA-tagged Vpu or all of the above Vpu mutants. This revealed that AP-1γ could be detected in immunoprecipitates of Vpu-HA (Fig 6A). This was not detected for the A14L/W22A mutant, again indicating a requirement for tetherin interaction. A reduced amount of AP-1γ was detected in the 2/6A and ELV mutant immunoprecipitates, and this varied between replicates (see histogram below blot). Since tetherin's YDYCRV motif also binds to AP-1 (Jia et al., 2014), we repeated the immunoprecipitations in 293T tetherin Y6,8A cells (Fig 6B). Whilst AP-1 precipitation was preserved for the wild-type protein, this effectively

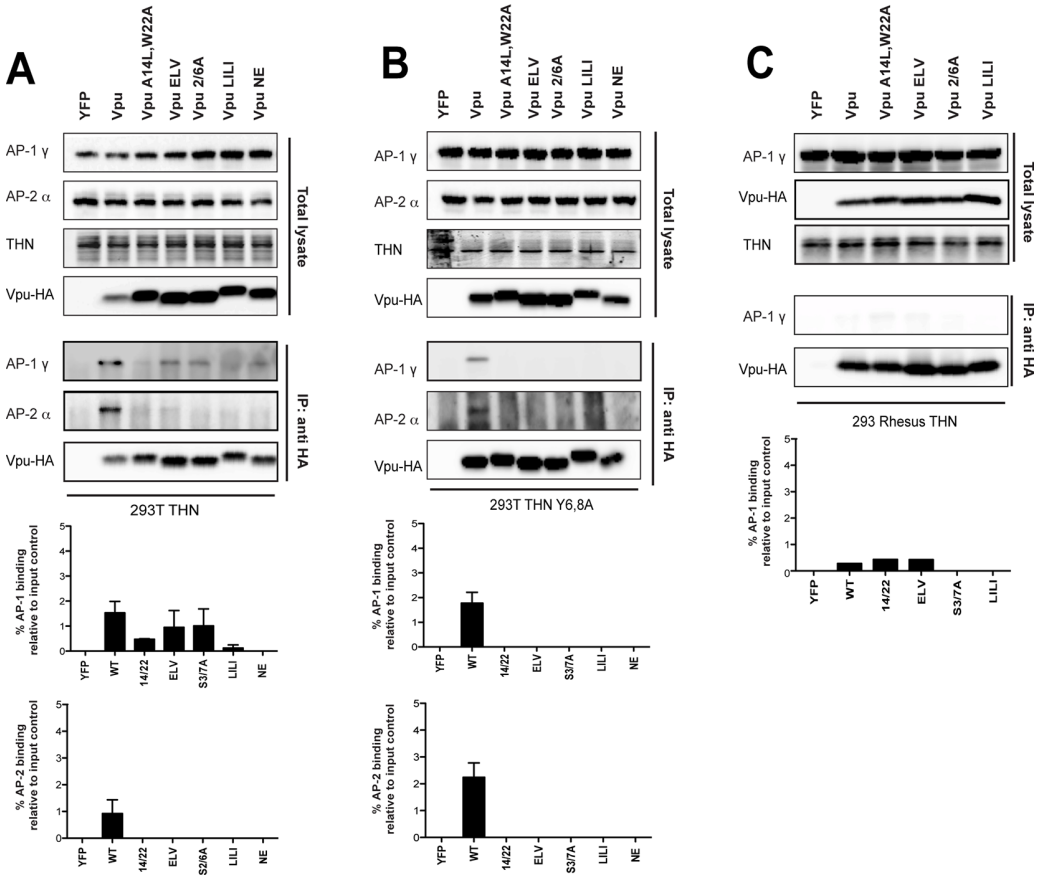

Fig 6. Vpu interacts with clathrin adaptors AP-1 and AP-2 in tetherin-expressing cells. (A-C) 293T tetherin (A), 293T tetherin Y6,8A (B) or 293 rhesus tetherin (C) cells were transfected with pCR3.1 Vpu-HA, Vpu A14L/W22A-HA, Vpu ELV-HA, Vpu 2/6A-HA, Vpu LILI-HA or Vpu NE-HA mutants. 48 h post transfection, cells were lysed and cross-linked using PFA (0.05% w/v) and immunoprecipitated with anti-HA antibody. Total cell lysates and precipitates were subjected to SDS-PAGE and analyzed by Western blotting for Vpu-HA, tetherin, AP-1γ or AP-2α. Panels are of representative experiments. Histograms represent western blot quantification of the relative AP-1 or AP-2 binding normalized to input control. Error bars represent the standard deviation of three independent experiments.

doi:10.1371/journal.ppat.1005141.g006

removed all detectable AP-1 interactions with any of the mutants, including the NE mutation between the two serines, indicating the reduced detection was due to tetherin/AP-1 interactions. To confirm these data, we also performed the same precipitations in 293T cells expressing a rhesus macaque tetherin to which HIV-1 Vpu cannot bind (Fig 6C), or parental 293T cells (S7A Fig) and found that no AP-1 could be detected under any conditions. These data also held true for the patient isolate Vpu 2_87 (S7B Fig). Therefore, these data demonstrate for the first time that Vpu does interact with AP-1 *in vivo*. Tetherin/Vpu TM-domain interactions are essential for this interaction, as are the predicted AP-1 binding sites in Vpu. Moreover, the lack of interaction of the 2/6A mutant indicates that phosphorylation of Vpu upstream of the ExxxLV regulates AP-1 interaction, and these data correlate well will the clathrin dependency presented in Fig 4.

The ExxxLV motif has the potential to bind to other clathrin adaptor σ subunits[39]. Since AP-1 depletion does not block Vpu function, we wondered whether Vpu interaction with the clathrin machinery might also occur through AP-2. We therefore analyzed the precipitations from cells expressing tetherin Y6,8A for the AP-2α adaptin subunit (Figs 6A, 6B and S7B). Surprisingly this could also be detected with the wild-type protein, but was absent for all the

mutants, indicating ExxxLV also regulates this interaction. Thus, Vpu interacts promiscuously with both major cellular clathrin adaptors in a manner dependent on its ability to bind to tetherin. This is likely to account for why individual adaptor knockdowns fail to block Vpu function, and suggest that AP-2 might represent a compensatory clathrin-dependent trafficking mechanism for counteracting tetherin.

Finally, to provide direct evidence that it was phosphorylation of Vpu that permitted AP1/AP2 interactions, we repeated these immunoprecipitations in 293T tetherin Y6,8A cells treated with Tyrphostin (Fig 7). Under these conditions the ability of wildtype Vpu to interact with AP1 or AP2 was abolished, indicating that CKII-mediated phosphorylation for Vpu is required for recruitment of clathrin transport machinery.

Discussion

In this study we have re-evaluated discrepancies in the literature regarding the role of $SCF^{\beta TRCP1/2}$ and ESCRT in Vpu-mediated tetherin degradation and antagonism of its physical antiviral activity. We find that whilst essential for the former, they are dispensable for the latter in HIV-1 infected cells. We further show that phospho-serine mutants of Vpu have a distinct phenotype, displaying defects in tetherin antagonism because they cannot engage with clathrin-dependent trafficking pathways. We demonstrate that *in cellulo* Vpu/tetherin TM interactions induce Vpu binding to either clathrin adaptors AP-1 or AP-2. This interaction requires the ExxxLV trafficking motif, validating the recent structural study [39]. Importantly, phosphomutants of Vpu are also defective for clathrin adaptor engagement, implying that CKII-mediated phosphorylation not only regulates $SCF^{\beta TRCP1/2}$ recruitment, but also regulates Vpu trafficking. Together these data clarify the role of the Vpu DSGNES motif in tetherin counteraction and provide strong evidence that sorting of Vpu/tetherin complexes into clathrin-rich domains of the endocytic pathway is the critical event in efficient tetherin antagonism. Furthermore, the observation that Vpu can interact both with AP-1 or AP-2 suggests a redundancy in adaptor protein requirement for tetherin counteraction that provides a plausible explanation for why depletion of either AP-1 or AP-2 is not sufficient to compromise Vpu function[36]. Thus potentially, tetherin/Vpu complexes that escape AP-1 in the TGN, and which traffic to the PM, can be retrieved by AP-2. Such a model would also rationalize why in some cases tetherin counteraction by Vpu can be observed with minimal evidence of surface downregulation [18,48].

Much of the discrepant literature regarding the mechanism of Vpu-mediated tetherin antagonism comes from experiments where tetherin, provirus and/or Vpu are transiently transfected into cells. Whilst these experiments are useful for understanding much of the biology of tetherin/HIV interactions, they are prone to artifacts when interpreting the cell biology and importance of Vpu-mediated degradation. Overexpression of tetherin or Vpu at non-physiological levels has been shown to induce ER-associated degradation [30]. This is not observed in infected cells, where tetherin is degraded in endosomes. Also, because of the nature of transient transfections, there is a huge variability of expression levels of the transfected components between cells within the culture. Under these conditions strong blocks to degradation may lead to tetherin accumulation, and an overwhelming of the endosomal system, giving the appearance of a direct inhibition of counteraction. By infecting tetherin-expressing cells at relevant multiplicities of infection, to ensure each cell has on average one productive infection event, these issues can be mitigated and this has allowed us to separate the requirement of the phospho-serine motif in counteraction from the recruitment of $SCF^{\beta TRCP1/2}$ and the ESCRT machinery for degradation.

Our *in cellulo* data validates the structural and biochemical studies by Jia et al [39], in which AP-1 interaction requires the ExxxLV motif that occupies the acidic-dileucine binding site in

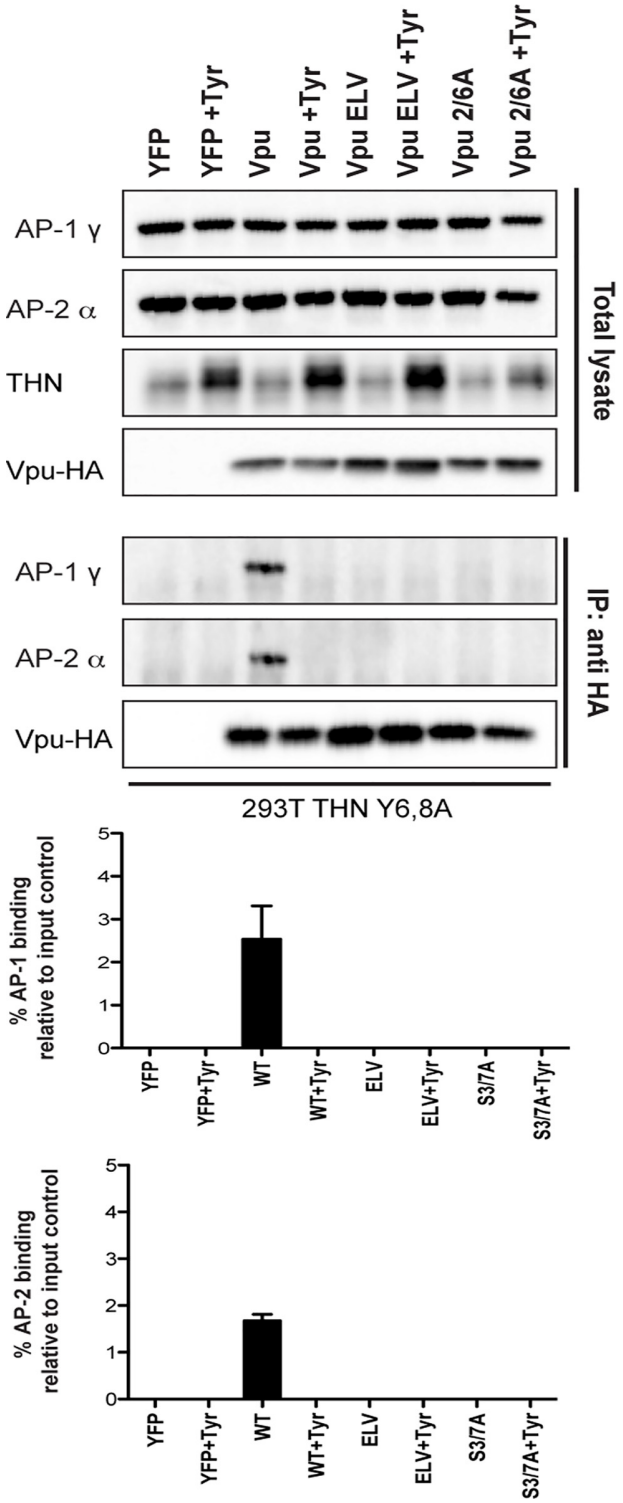

Fig 7. Vpu interaction with clathrin adaptors AP-1 and AP-2 is abrogated following treatment with CKII inhibitor, Tyrphostin. 293T tetherin Y6,8A cells were transfected with pCR3.1 Vpu-HA, Vpu A14L/W22A-HA, Vpu ELV-HA, Vpu 2/6A-HA, Vpu LILI-HA or Vpu NE-HA mutants. 24h post-transfection cells were treated with DMSO or 50 μM Tyrphostin. Cells were lysed and cross-linked, 48 h post transfection, using PFA (0.05% w/v) and immunoprecipitated with anti-HA antibody. Total cell lysates and precipitates were subjected to SDS-PAGE

and analyzed by Western blotting for Vpu-HA, tetherin, AP-1γ or AP-2α. Panels are of representative experiments. Histograms represent quantification of the relative AP-1 or AP-2 binding normalized to input control. Error bars represent the standard deviation of three independent experiments.

doi:10.1371/journal.ppat.1005141.g007

AP-1σ. We also provide evidence that in cells, this motif can also bind to AP-2. Furthermore, the phenotype of our LI/LI mutant is consistent with the proposed non-canonical interaction of R44/L45 with AP-1μ suggested by densities in the crystal. However, because the constructs used by the authors to determine the structural requirements for AP-1/tetherin/Vpu interaction required artificial Vpu/tetherin fusions, they may not faithfully represent how AP-1 is initially recruited. Thus, the requirements for the DSGNES and Vpu/tetherin transmembrane domain interactions that we have uncovered in cells were not previously observed.

We propose a model whereby phosphorylation of Vpu regulates the AP interaction with the ELV motif (Fig 8). Whilst we cannot formally rule out that the phosphoserine directly contributes to AP-1 interaction itself, the lack of a significant additive phenotype in terms of virus release and AP-1 interaction makes this the most consistent explanation of our data. Furthermore there is precedence for phosphorylation upstream of certain acidic dileucine motifs interactions with the clathrin transport machinery [43]. In particular, a CKII phosphorylation upstream of a non-canonical RDDHLL site in the cation-independent mannose-6-phosphate receptor regulates its interaction with AP1. Another context-dependent feature of acidic dileucine signals is an adjacent acidic patch [37]. Interestingly, this feature is present in HIV-1 Vpu. Furthermore, the laboratory strain NL4.3 Vpu, which has a reduced anti-tetherin activity compared to most primary isolates, has a shorter acidic patch between the DSGNES and ExxxLV motifs [34]. The requirement for TM interactions in addition to the phospho-serines in "priming" Vpu for clathrin adaptor interaction would imply that tetherin binding contributes to conformational changes that are required for antagonism. Since β-TrCP binding does not require the presence of tetherin (or CD4), phosphorylation must be an independent event. However, whether β-TrCP and AP-1/2 binding can occur simultaneously or are mutually exclusive is unknown. Another interesting point to note is that the LI/LI mutation is more severely compromised than either the 2/6 or the ELV mutations in some contexts. As it also compromises

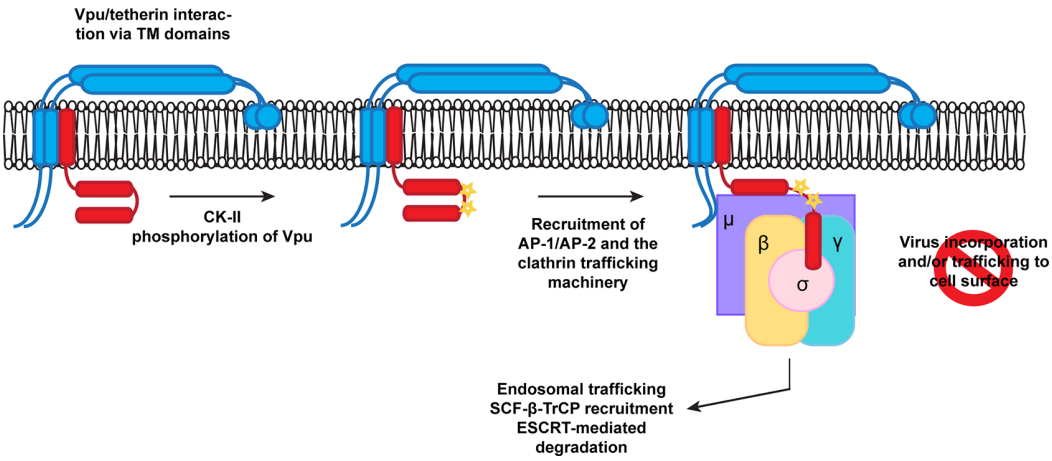

Fig 8. A proposed model for Vpu engagement of clathrin adaptors during tetherin counteraction. Vpu and tetherin interactions via TM/TM domain interactions and casein kinase II phosphorylation promote Vpu recruitment of AP-1 or AP-2. This allows the EXXXLV motif to bind to the σ subunit, and potentially through non-canonical interactions between its first alpha helix with the AP-1 or 2 μ subunits. In addition the YCRV motif in tetherin binds to the AP1μ. Thus tetherin/Vpu complexes are sorted into clathrin rich domains of the TGN or PM for subsequent trafficking and ubiquitination.

doi:10.1371/journal.ppat.1005141.g008

AP binding, the non-canonical interaction of the R45,L46 with AP-1μ may also play an essential contextual role in positioning the ELV motif. This interaction may also explain why the residual activities of 2/6 and ELV mutations are sensitive to clathrin depletion.

Structural information on the Vpu cytoplasmic tail is limited at present. Partial NMR structures in solution and associated with lipids have been determined [49–52]. In a lipid environment, the ExxxLV is embedded within helix 2 of the cytoplasmic tail [52], but adopts an extended conformation in solution [51]. To bind to AP-1, the ExxxLV site cannot be helical. However, the lipid-associated structure has a very interesting feature: a highly conserved C-terminal tryptophan residue appears to pack against the DSGNES, almost as if locking the structure. Mutations in the W residue have context-dependent defects in tetherin antagonism depending on the Vpu used [34,53]. Importantly, NMR studies on the effects of serine phosphorylation suggests that it leads to conformational changes within the C-terminal region of the Vpu cytoplasmic tail that promotes βTRCP binding. In some studies [49,50], but not others [54], these conformational changes are consistent with an opening up of the ELV site. However, all these studies have thusfar been performed in the absence of target binding using soluble Vpu cytoplasmic tails, and so how representative they are of the wildtype protein is unclear. Furthermore, upregulation of SCYL2, a clathrin associated protein that modulates protein phosphatase 2A (PP2A), induces Vpu de-phosphorylation and reduces tetherin antagonism [55]. Thus, there is scope for regulated phosphorylation and subsequent dephosphorylation cycles in regulation of Vpu activity. We suggest that this would occur at the level of clathrin-dependent transport rather than $SCF^{\beta TRCP1/2}$ interactions.

There is much indirect evidence consistent with AP-1 being the major clathrin adaptor used by Vpu. The block to tetherin transport to the surface, the predominant localization to the TGN, and of course the recent structure discussed above [33,35,36,39]. However, AP-1 knockdown is difficult to efficiently achieve and does not compromise Vpu function [36]. AP-1 has multiple orthologs for some of its subunits, and there is potential redundancy in the adaptor machinery allowing the cell to compensate for its absence [37]. Our observation that Vpu can interact also with AP-2 in an ExxxLV-dependent manner is therefore an important observation for several reasons. Firstly, it suggests that Vpu is promiscuous and if one adaptor is compromised, another can be used, explaining why neither AP-1 nor AP-2 have been unambiguously identified as Vpu cofactors [25,36]. Secondly, it might explain why in some studies, Vpu has been observed to induce a weak enhancement of tetherin endocytosis [35]. Artificial tetherin/Vpu linked chimeric proteins are excluded from budding virions, and this is dependent on the ExxxLV motif [18], which would be consistent with anchoring by AP-2 into clathrin-rich domains at the plasma membrane. The YDYCRV motif of tetherin cannot interact with AP-2μ as a YXXθ signal because of a steric clash of Y6 in the binding pocket [39]. The YDYCRV motif is essential for the "slow", AP-1-dependent recycling of tetherin to the PM via the TGN [17,33]. Therefore, Vpu is likely to meet the majority of its target (newly synthesized and recycling tetherin) in the TGN. Since AP-1 has been proposed to regulate bidirectional traffic between the TGN and endosomal compartments [37], AP-1 is likely to be the major player in tetherin counteraction. However, the ExxxLV motif is dominant over the tetherin recycling motif [36]. Therefore we would predict that tetherin/Vpu complexes that escape re-routing in the TGN and make it to the PM would be excluded from virions and AP-2 would promote their endocytosis, much in the same way that SIV Nef proteins and HIV-2 envelopes antagonize tetherin [6,38,56]. More importantly, it also accounts for why Vpu still has some activity against the short tetherin isoform without appreciable cell surface downregulation [13,40]. The relative role of AP-1 and AP-2 will reflect the kinetics of their respective activities in different cell types. We suggest the combination of some or all of the above accounts for the variable importance that downregulation of tetherin from the PM has been given to its antagonism.

The requirement for the ExxxLV and DSGNES motifs is not absolute when tetherin levels are low. At higher expression levels, such as upon IFN treatment of primary CD4+ T cells, they become essential for tetherin antagonism [36]. This residual function requires tetherin's sorting motif, suggestive of competition between the clathrin-dependent trafficking and virion retention. Tetherin/Vpu interaction may simply tip this balance, reducing tetherin partitioning into virions sufficiently when its expression levels are low. It is this that we propose to augment via our clathrin box fusion rescue, locking the tetherin/Vpu complex into clathrin-rich domains in the recycling pathway from where they cannot be transited to the PM.

Decoupling tetherin degradation (which amongst primate lentiviruses is so far peculiar to HIV-1 group M Vpu) from subversion of trafficking (counteraction) suggests that the importance of the former might reflect downstream consequences of tetherin restriction. Enhanced antagonism of the long tetherin isoform by Vpu could be required because of its signal transduction or its ability to deliver retained virions to endosomes [14,40]. Our data shows that in stable tetherin expressing cells, STS mutations impart little resistance to Vpu and that they are still sensitive to Vpu-clathrin box fusions. Since neither LI/LI nor ELV mutations block binding of Vpu to β-TrCP or tetherin, ubiquitination may still occur on serine and threonine residues. However, its effect is likely to be subsequent to antagonism by clathrin-dependent mis-trafficking. Strong reduction of tetherin at the cell surface by Vpu coupled to endosomal degradation would therefore be a potent way of suppressing signal transduction, or blocking the routing of virions for degradation where they may encounter other host pattern recognition receptors or antigen processing machinery. These will be important attributes to maintain *in vivo* without necessarily being essential for physical antagonism of tetherin.

Materials and Methods

Cells, plasmids and reagents

HEK293T cells were obtained from ATCC (American Tissue Culture Collection). 293T tetherin cell lines stably expressing human tetherin and mutants were previously described [4,57]. The HeLa-TZMbl reporter cell line, was kindly provided by John Kappes through the NIH AIDS Reagents Repository Program (ARRP). Cells were maintained in Dulbecco's modified Eagle medium (DMEM) supplemented with 10% fetal calf serum and Gentamycin (Invitrogen, UK). Wildtype HIV-1 NL4.3 (obtained from NIH-ARRP), a Vpu-defective counterpart and a codon optimized pCR3.1 Vpu-HA has been described previously [58]. The Vpu A14L/W22A, ELV, 2/6A, LILI and NE mutants in pCR3.1 Vpu-HA and in the NL4.3 proviral genome were generated by Quick-change site-directed mutagenesis PCR according to standard protocols using Phusion-II polymerase (New England Biolabs). A codon-optimised version of the previously described primary wild-type HIV-1 Vpu 2_87 [34] was HA-tagged and cloned into pCR3.1. The Vpu A15L/W23A, ELV, 2/6A, LILI and NE mutants were generated in pCR3.1 Vpu 2_87-HA by Quick-change site-directed mutagenesis as described above. Consensus B codon-optimised Vpu-myc-BirA-R188G fusion was synthesized (Life Technologies) and cloned into the lentiviral vector pAIP (kindly provided by A Cimarelli). The Vpu A15L/W23A, ELV, 2/6A and LILI mutants were generated by Quick-change site-directed mutagenesis as described above. The pCR3.1 myc-β-TrCP2 was previously described by [36] and the pCR3.1 myc-HRS expression vector was kindly provided by Juan Martin-Serrano [59].

Primary human CD4+ T cells were isolated from fresh venous blood drawn from healthy volunteers. CD4+ T cells were purified from total peripheral blood mononuclear cells (PBMC) isolated by lymphoprep (AXIS-SHIELD) gradient centrifugation using a CD4+ T cell Dynabeads isolation kit (Invitrogen). T cells were then activated for 48 h using anti-CD3/anti-CD28

magnetic beads (Invitrogen). The beads were then removed cells were then maintained in rhIL-2 (20 U/ml) (Roche).

Production of VSV-G pseudotyped viral stocks

For full-length HIV-1 WT, HIV-1 ΔVpu, HIV-1 Vpu LILI, HIV-1 Vpu ELV, HIV-1 Vpu LILI/ELV, HIV-1 Vpu 2/6A, HIV-1 Vpu 2/6A/ELV virus stocks pseudotyped with the Vesicular Stomatitis Virus Glycoprotein (VSV-G), 293T cells were transfected with 2 μg of proviral plasmid in combination with 200 ng of pCMV VSV-G. 48 hours post-transfection, the supernatant containing virions was harvested and endpoint titers were determined on HeLa-TZMbl cells as described previously [3].

Virus release assay

For virus release assays using transient transfection, subconfluent 293T cells or derivatives were plated in 24 well plates and transfected with 500 ng of NL4.3 proviral plasmid, in combination with increasing concentrations of tetherin (0 ng, 25 ng, 50 ng and 100 ng) and fixed 25 ng of Vpu-HA or mutants using 1 μg/ml polyethyleneimine (Polysciences). Medium was replaced 8 hours post-transfection and cells and supernatants were harvested after 48 hours. The infectivity of viral supernatants was determined by infecting HeLa-TZMbl and assayed for β-galactosidase activity as previously described [36]. For biochemical analysis of physical virus particle release, supernatants were filtered (0.22 μm) (Merck Millipore) and pelleted through a 20% sucrose/ PBS cushion at 20,000 x g for 90 min at 4°C. Virion and cell lysates were subjected to SDS-PAGE and Western blotted for rabbit anti-HSP90 (Santa Cruz Biotechnologies), HIV-1 p24CA (monoclonal antibody 183-H12-5C; kindly provided by B Chesebro through the NIH ARRP), monoclonal mouse anti-HA.11 (Covance), polyclonal rabbit anti-HA (Rockland) and/ or Vpu (rabbit polyclonal; kindly provided by K. Strebel through the NIH ARRP [60]. For CK-II inhibition, we used Tyrphostin AG1112 (Sigma) reconstituted in DMSO at a concentration of 50 μM. Where indicated, Phos-tag (Wako Chemicals, Japan) and $MnCl_2$ (Sigma) were added to the composition of 8% polyacrylamide gels to induce mobility shifts in phosphorylated proteins, to final concentrations of 25 μM and 50 μM, respectively.

Tetherin degradation assay

1.5 x 10^5 293T tetherin cells were infected with VSV-G-pseudotyped HIV-1 WT, HIV-1 ΔVpu, HIV-1 Vpu LILI, HIV-1 Vpu ELV or HIV-1 Vpu 2/6A at an MOI of 2. The medium was replaced 4 hours after infection. 48 hours post infection cell lysates were harvested and subjected to SDS-PAGE and Western blotted for rabbit anti-HSP90 (Santa Cruz Biotechnologies) and polyclonal rabbit anti-tetherin antibody (kindly provided by K Strebel through the NIH ARRP) [48], and processed as described above.

siRNA mediated protein knockdown

293T tetherin cells were seeded at a density of 2 x 10^5 cells per well in a 12 well plate. After 6 hours, the first transfection was performed. For each well, 2 μl Dharmafect (Thermo Scientific) was added to 98 μl of Opti-MEM (Life Technologies), this solution was added to 5 μl of 20 μM siRNA in 95 μl of Opti-MEM according to manufactures protocol. For HRS knockdown, siRNA oligonucleotide against HGS targeting the CCGGAACGAGCCCAAGTACAA sequence (Qiagen) was used. For UBAP1 knockdown, siRNA oligonucleotide against UBAP1 targeting CTCGACTATCTCTTTGCACAT (Qiagen) was used. For TSG101 knockdown, siRNA oligonucleotide sequence CCUCCAGUCUUCUCUCGUCUU (Thermo Scientific) was

used. For β-TrCP1 and 2 knockdown, SMARTpool siRNA against human BTRC and FBXW11 (Thermo Scientific) were used. A non-targeting siRNA was used as control (Thermo Scientific). The cells were re-seeded into a 24 well plate on day 2 and a second transfection was performed according to manufactures protocol. The cells were infected 3 hours post transfection with VSV-G-pseudotyped HIV-1 WT, HIV-1 ΔVpu at an MOI of 0.8. The infectivity of viral supernatants was determined by infecting HeLa-TZMbl as described above. Cell lysates and viral particles were subjected to SDS-PAGE, and Western blot assays were performed using a rabbit polyclonal anti-HRS (HGS) antibody (Millipore), a polyclonal rabbit anti-UBAP1 antibody (Proteintech) and a monoclonal mouse anti-TSG101 antibody (Abcam).

Flow cytometry

HeLa-TZMbl cells were transfected with 400 ng of pCR3.1 GFP and 400 ng of pCR3.1 Vpu-HA or indicated mutants. 48 hours post transfection the cells were harvested and stained for surface tetherin using a monoclonal anti-BST2 IgG2a antibody (Abnova) and a goat-anti-mouse IgG2a-Alexa633 conjugated secondary antibody (Molecular Probes, Invitrogen, UK). Tetherin expression on GFP positive cells was then analyzed using a BD FACSCanto II flow-cytometer (Becton Dickinson) and the FlowJo software.

Immunoprecipitation

For Vpu/HRS coIP, 293T tetherin cells were transfected with 700 ng of pCR3.1 myc-HRS or indicated mutants/truncations in combination with pCR3.1 Vpu-HA or indicated mutant or pCR3.1 GFP expression plasmids. 48 hours post transfection the cells were lysed in buffer containing 50 mM Tris pH 7.4, 150 mM NaCl, 200 μM sodium ortho-vanadate, 5 mM NEM, complete protease inhibitors (Roche) and 1% digitonin. After removal of the nuclei, the supernatants were immunoprecipitated with 5 μg/ml monoclonal mouse anti-myc antibody previously described (Kueck and Neil, 2012). Western blot assays were performed using a polyclonal rabbit anti-HA antibody (Rockland) and rabbit polyclonal anti-HRS (HGS) antibody (Millipore). For Vpu/tetherin coIP, 293T cells were transfected twice over 48 hours with siRNA oligonucleotide against UBAP1 targeting CTCGACTATCTCTTTGCACAT or Non-targeting siRNA was used as control (Dharmacon). The cells were then infected with VSV-G-pseudotyped HIV-1 WT, HIV-1 ΔVpu, HIV-1 Vpu LILI or HIV-1 Vpu A14L W22A at an MOI of 2. 48 hours post infection the cells were lysed on ice for 30 min in buffer containing 50 mM Tris pH 7.4, 150 mM NaCl, complete protease inhibitors (Roche) and 1% digitonin (Calbiochem). Immunoprecipitation was performed as previously described [36] and Western blot assays were performed using a rabbit anti-Vpu antibody polyclonal rabbit anti-tetherin antibody and polyclonal rabbit anti-UBAP1 antibody (Proteintech), and visualized by ImageQuant using corresponding HRP-linked secondary antibodies (New England Biolabs, UK).

Immunofluorescence

Hela cells were grown on coverslips, transfected with 50 ng of pCR3.1 Vpu-HA or indicated mutant. 16 hours later cells were fixed in 4% paraformaldehyde/ PBS, washed with 10 mM glycine/ PBS, and permeabilized in 1% bovine serum albumin/ 0.1% Triton-X100/ PBS for 15 min. Cells were stained using anti-rabbit polyclonal HA antibody (Rockland) in combination with sheep anti-human TGN46 (AbD Serotec), followed by the appropriate secondary antibodies conjugated to Alexa 488 or 594 fluorophores (Molecular Probes, Invitrogen). Cells were mounted on glass slides using ProLong AntiFade- 4',6-diamidino-2-phenylindole (DAPI) mounting solution (Molecular Probes, Invitrogen) and images were captured with a Nikon

ESCLIPSE Ti inverted microscope. Z stacks were taken of all cells, images deconvolved using AutoQuant X3 and analyzed using the ImageJ software.

Cross-linking IP

293T, 293T tetherin, 293T tetherin Y6,8A or 293 Rhesus tetherin cells were transfected with 8 μg GFP expression construct, pCR3.1 Vpu-HA or mutant thereof. Transfection media was changed 6 hours post transfection and cells incubated with 50 nM concanamycin. In the case of CKII inhibitor treatment, cells were treated with 50 μM final Tyrphostin 24 hours prior to harvesting. 48 hours post transfection, cells were trypsinised and washed in PBS. Cells were cross-linked with 0.05% HCHO/PBS for 10 min at 37°C. The cross-linking reaction was then quenched by incubating cells in 0.25 M glycine for 5 min. Cells were washed once in PBS before resuspension in lysis buffer (10 mM Hepes pH 7, 150 mM NaCl, 6 mM MgCl2, 2 mM DTT, 10% glycerol, 0.5% NP40, 200 μM sodium orthvanadate and 1x Complete protease inhibitors (Roche)). Cells were lysed on ice for 10 min followed by repeated sonication (3 x 10 s cycles with 20 s rests). The cell lysates were clarified by centrifugation at 1000 x g for 10 min and supernatants were immunoprecipitated with 5 μg/ml mouse monoclonal anti-HA.11 antibody (Covance) or rabbit polyclonal anti-HA antibody (Rockland) on Dynabeads protein G beads (Life Technologies) for 4 hours at 4°C. Beads were collected post incubation and washed 5 times in lysis buffer before cross-links were reversed in 1% SDS, 10 mM EDTA and 5 mm DTT at 65°C for 45 min. Western blot assays were performed using rabbit polyclonal anti-HA antibody (Rockland), polyclonal rabbit anti-tetherin antibody, mouse monoclonal anti-HA.11 antibody, mouse monoclonal anti-AP-1γ1 antibody (Sigma) and mouse monoclonal anti-AP-2α antibody (Sigma). Vpu/β-TrCP2 cross-linking IP was previously described by [36].

Affinity purification of biotinylated proteins

[61] 293T or 293T tetherin cells were transiently transfected with 8 μg empty BirA vector, Vpu-myc-BirA or relevant mutant constructs using polyethylenimine (PEI). Cells were incubated for 8 hours prior to changing medium and treated overnight with 100 nM Concanamycin A (Invitrogen) and 150 μM biotin (Invitrogen). Cells were washed twice in PBS and lysed in 1 ml lysis buffer (50 mM Tris pH 7.4, 500 mM NaCl, 0.4% SDS, 5 mM EDTA, 1 mM DTT and 1x Complete protease inhibitor (Roche)) before sonication. Triton-X-100 was added to a final concentration of 2% before further sonication and an equal volume of 50 mM Tris pH 7.4 was added to the cell lysates before clarification at 14,000 rpm for 5 minutes. Supernatants were incubated with 200 μl avidin agarose (Pierce) for 4 hours at 4°C. Beads were collected and washed four times in 1 ml lysis buffer before resuspension in 100 μl Laemmli-SDS sample buffer supplemented with free biotin. Cell lysates and precipitates were analysed by Western blot using HRP-conjugated streptavidin (Invitrogen), mouse monoclonal anti-myc antibody (Covance), rabbit monoclonal β-TrCP antibody (Cell signaling Technology) and mouse monoclonal anti-AP-1γ1 antibody (Sigma).

Ethical information

Permission to isolate primary human CD4+ T cells from healthy consenting donors was provided by the KCL Infectious Disease BioBank Local Research Ethics Committee, reference SN-1/6/7/9.

Supporting Information

S1 Fig. Vpu/HRS interaction is dependent on residues in the DUIM of HRS that bind ubiquitin. (A) Schematic representation of HRS C-terminal truncations. (B) 293T cells were transfected with pCR3.1 Vpu-HA in combination with a pCR3.1 myc-HRS or myc-HRS truncation expression vector. 48 hours post transfection cells were lysed and immunoprecipitated with anti-myc antibody. Total cell lysates and precipitates were subjected to SDS-PAGE and analysed by Western blotting for myc-HRS and Vpu, and analyzed by ImageQuant. Asterisk: anti-HA antibody heavy chain (C) Immunoprecipitation was performed as in (B) but with myc-HRS W25A L29D and myc-HRS A266Q A268Q mutants.
(TIF)

S2 Fig. Vpu LI/LI mutant exhibits impaired tetherin counteractivity. (A) LogoPlots of the first alpha helix of the Vpu cytoplasmic tail from HIV-1 subgroup M clades A, B, C, D, G and H generated from sequences obtained from the Los Alamos database (www.hiv.lanl.gov). (B) 293T cells were transfected with NL4.3 HIV-1 WT, ΔVpu, Vpu LILI, Vpu ELV or Vpu 2/6A mutant together with increasing concentrations of pCR3.1 tetherin-HA expression plasmid. Cell lysates and sucrose purified viral supernatants from 50 ng tetherin input were subjected to SDS-PAGE and analyzed by Western blotting for HSP90, HIV-1 p24CA and Vpu, and analyzed by LiCor quantitative imager. Asterisk: non-specific band. (C) Infectivity of viral supernatants was assayed on HeLa-TZMbl reporter cells. Infectious virus release was plotted as β-galactosidase activity in relative light units (RLU). Error bars represent the standard deviation of three independent experiments. (D) HeLa-TZMbl cells were co-transfected with pCR3.1 Vpu-HA or indicated mutant and a GFP expression vector. Cell-surface tetherin levels were analysed 48 hours post transfection by flow cytometry. GFP positive cells were gated and tetherin levels (solid lines) were compared to un-transfected cells or transfected with indicated Vpu (dotted lines). Numbers indicate median fluorescence intensities of endogenous tetherin surface levels. The solid peak in the upper histogram in the middle of the panel represents binding of the isotype control. (E) 293T tetherin expressing cells were transfected twice over a 48 hour period with siRNA oligonucleotides directed against UBAP1 or non-targeting control. The cells were then infected with HIV-1 WT, HIV-1 Vpu LILI, HIV-1 Vpu A14L W22A or HIV-1 ΔVpu at an MOI of 2. 48 hours later, cells were lysed and immunoprecipitated with anti-tetherin antibody. Total cell lysates and precipitates were subjected to SDS-PAGE and analyzed by Western blotting for tetherin, UBAP1 and Vpu, and analyzed by ImageQuant.
(TIF)

S3 Fig. Further Vpu mutants show similar phenotypes in infected primary CD4+ T cells and in 293T cells. (A-B) 293T, 293T tetherin or Y6,8A tetherin cells were infected with VSV-G pseudotyped NL4.3 wt or mutant virus at an MOI of 0.8. (A) 48 hours post infection viral supernatants were assayed for infectivity using HeLa-TZMbl reporter cells as in Fig 1. Error bars represent the standard deviation of three independent experiments. (B) Cell lysates and sucrose purified viral supernatants were subjected to SDS-PAGE and analyzed by Western blotting as in Fig 1. (C) Primary human CD4+ T cells were infected with the indicated HIV-1 mutant at an MOI of 0.8. 16 h later the cells were treated or not with 5000 U/ml universal type-I interferon. Cell lysates and viral supernatants were harvested a further 24 h later and analyzed for infectivity on HeLa-TZMbl cells (A) or physical particle yield and cellular viral expression by quantitative Western blotting.
(TIF)

S4 Fig. A primary isolate Vpu allele and its mutants exhibit a comparable phenotype to NL4.3 Vpu. (A) 293T tetherin cells were transfected with NL4.3 ΔVpu proviral plasmid in combination with YFP expression vector and pCR3.1 2_87 Vpu or mutants thereof. 48 hours

post transfection infectivity of viral supernatants was determined on HeLa-TZMbl cells as in Fig 1. (B) Cell lysates and pelleted supernatant virions from (A) were harvested and subjected to SDS-PAGE and analyzed by Western blotting for HIV-1 p24CA, Vpu and HSP90, and analyzed by LiCor quantitative imager. (C) Hela cells were transfected with 100 ng of pCR3.1 2_87 Vpu-HA or indicated mutants. 16 hours post transfection cells were fixed and stained for HA (green) and the TGN marker TGN46 (red) and examined by widefield fluorescent microscopy. Panels are of representative examples. Bars = 10 μm. (D) Z stacks were taken of all cells (n = 15), images were deconvolved using the AutoQuant X3 software and Pearson's correlations were calculated for all Z stacks using ImageJ. Results were analyzed by unpaired 2-tailed t-test—*** P = 10–5 or lower.
(TIF)

S5 Fig. Clathrin binding restores the tetherin downregulation capacity of Vpu mutants. (A to D) HeLa-TZMbl cells were co-transfected with pCR3.1 Vpu-HA or indicated mutant and a GFP expression vector. Cell-surface tetherin levels were analyzed 48 hours post transfection by flow cytometry. GFP positive cells were gated and tetherin levels (solid lines) were compared to un-transfected cells or transfected with indicated Vpu (dotted lines). Numbers indicate median fluorescence intensities of endogenous tetherin surface levels. The solid peak in the upper histogram in the middle of the panel represents binding of the isotype control.
(TIF)

S6 Fig. Proximity-based biotin ligase assay suggests Vpu/AP-1 interaction. (A) Schematic representation of proximity-based biotin ligase assay. (B) 293T tetherin cells were transfected with NL4.3 ΔVpu proviral plasmid in combination with YFP expression vector and pCR3.1 Vpu or indicated mutant thereof. 48 hours post transfection infectivity of viral supernatants was determined on HeLa-TZMbl cells as in Fig 1. (C) 293T or 293T tetherin cells were transfected with Vpu-myc-BirA, B Vpu ELV-myc-BirA, B Vpu A15L/W23A-myc-BirA, B Vpu S3/7A- myc-BirA (phospho-mutant), B Vpu LILI-myc-BirA or empty vector control. 6 hours post transfection, cells were treated with 100 nM concanamycin A in the presence of 150 μM free biotin. 16 hours later, cells were washed, lysed, sonicated and biotinylated proteins were recovered on streptavidin-conjugated beads and analysed by Western blot for avidin, Vpu-myc-BirA, β-TrCP or AP-1 γ. Asterisk: Vpu-myc-BirA band.
(TIF)

S7 Fig. Vpu binding to clathrin adaptors AP-1 and AP-2 is dependent on tetherin binding (A) and binding to AP-1 and AP-2 is conserved by primary Vpu 2_87 in tetherin expressing cells (B). (A) 293T cells were transfected with pCR3.1 Vpu-HA, Vpu ELV-HA, Vpu 3/7A-HA, Vpu LILI-HA or Vpu NE-HA mutants. (B) 293T tetherin Y6,8A were transfected with pCR3.1 Vpu-HA, Vpu A15L/W23A-HA, Vpu ELV-HA, Vpu 3/7A-HA, Vpu LILI-HA or Vpu NE-HA mutants. 48 h post transfection, cells were lysed and cross-linked using PFA (0.05% w/v) and immunoprecipitated with anti-HA antibody. Total cell lysates and precipitates were subjected to SDS-PAGE and analyzed by Western blotting for Vpu-HA, AP-1 γ or AP-2 α. Panels are of representative experiments. Histograms represent quantification of the relative AP-1 or AP-2 binding normalized to input control. Error bars represent the standard deviation of three independent experiments.
(TIF)

Acknowledgments

We thank Juan Martin-Serrano for ESCRT reagents, and Mark Marsh for generous advice.

Author Contributions

Conceived and designed the experiments: TK TLF JW SJDN. Performed the experiments: TK TLF JW JCS. Analyzed the data: TK TLF JW SJDN. Contributed reagents/materials/analysis tools: SP. Wrote the paper: TK TLF JW SJDN.

References

1. Neil SJ (2013) The antiviral activities of tetherin. Curr Top Microbiol Immunol 371: 67–104. doi: 10.1007/978-3-642-37765-5_3 PMID: 23686232
2. Jia B, Serra-Moreno R, Neidermyer W, Rahmberg A, Mackey J, et al. (2009) Species-specific activity of SIV Nef and HIV-1 Vpu in overcoming restriction by tetherin/BST2. PLoS Pathog 5: e1000429. doi: 10.1371/journal.ppat.1000429 PMID: 19436700
3. Le Tortorec A, Neil SJ (2009) Antagonism to and intracellular sequestration of human tetherin by the human immunodeficiency virus type 2 envelope glycoprotein. J Virol 83: 11966–11978. doi: 10.1128/JVI.01515-09 PMID: 19740980
4. Neil SJ, Zang T, Bieniasz PD (2008) Tetherin inhibits retrovirus release and is antagonized by HIV-1 Vpu. Nature 451: 425–430. doi: 10.1038/nature06553 PMID: 18200009
5. Van Damme N, Goff D, Katsura C, Jorgenson RL, Mitchell R, et al. (2008) The interferon-induced protein BST-2 restricts HIV-1 release and is downregulated from the cell surface by the viral Vpu protein. Cell Host Microbe 3: 245–252. doi: 10.1016/j.chom.2008.03.001 PMID: 18342597
6. Zhang F, Landford WN, Ng M, McNatt MW, Bieniasz PD, et al. (2011) SIV Nef proteins recruit the AP-2 complex to antagonize Tetherin and facilitate virion release. PLoS Pathog 7: e1002039. doi: 10.1371/journal.ppat.1002039 PMID: 21625568
7. Perez-Caballero D, Zang T, Ebrahimi A, McNatt MW, Gregory DA, et al. (2009) Tetherin inhibits HIV-1 release by directly tethering virions to cells. Cell 139: 499–511. doi: 10.1016/j.cell.2009.08.039 PMID: 19879838
8. Venkatesh S, Bieniasz PD (2013) Mechanism of HIV-1 virion entrapment by tetherin. PLoS Pathog 9: e1003483. doi: 10.1371/journal.ppat.1003483 PMID: 23874200
9. Alvarez RA, Hamlin RE, Monroe A, Moldt B, Hotta MT, et al. (2014) HIV-1 Vpu antagonism of tetherin inhibits antibody-dependent cellular cytotoxic responses by natural killer cells. J Virol 88: 6031–6046. doi: 10.1128/JVI.00449-14 PMID: 24623433
10. Arias JF, Heyer LN, von Bredow B, Weisgrau KL, Moldt B, et al. (2014) Tetherin antagonism by Vpu protects HIV-infected cells from antibody-dependent cell-mediated cytotoxicity. Proc Natl Acad Sci U S A 111: 6425–6430. doi: 10.1073/pnas.1321507111 PMID: 24733916
11. Pham TN, Lukhele S, Hajjar F, Routy JP, Cohen EA (2014) HIV Nef and Vpu protect HIV-infected CD4 + T cells from antibody-mediated cell lysis through down-modulation of CD4 and BST2. Retrovirology 11: 15. doi: 10.1186/1742-4690-11-15 PMID: 24498878
12. Veillette M, Desormeaux A, Medjahed H, Gharsallah NE, Coutu M, et al. (2014) Interaction with cellular CD4 exposes HIV-1 envelope epitopes targeted by antibody-dependent cell-mediated cytotoxicity. J Virol 88: 2633–2644. doi: 10.1128/JVI.03230-13 PMID: 24352444
13. Cocka LJ, Bates P (2012) Identification of alternatively translated Tetherin isoforms with differing antiviral and signaling activities. PLoS Pathog 8: e1002931. doi: 10.1371/journal.ppat.1002931 PMID: 23028328
14. Galao RP, Le Tortorec A, Pickering S, Kueck T, Neil SJ (2012) Innate sensing of HIV-1 assembly by Tetherin induces NFkappaB-dependent proinflammatory responses. Cell Host Microbe 12: 633–644. doi: 10.1016/j.chom.2012.10.007 PMID: 23159053
15. Galao RP, Pickering S, Curnock R, Neil SJ (2014) Retroviral Retention Activates a Syk-Dependent HemITAM in Human Tetherin. Cell Host Microbe 16: 291–303. doi: 10.1016/j.chom.2014.08.005 PMID: 25211072
16. Tokarev A, Suarez M, Kwan W, Fitzpatrick K, Singh R, et al. (2013) Stimulation of NF-kappaB Activity by the HIV Restriction Factor BST2. J Virol 87: 2046–2057. doi: 10.1128/JVI.02272-12 PMID: 23221546
17. Rollason R, Korolchuk V, Hamilton C, Schu P, Banting G (2007) Clathrin-mediated endocytosis of a lipid-raft-associated protein is mediated through a dual tyrosine motif. J Cell Sci 120: 3850–3858. PMID: 17940069
18. McNatt MW, Zang T, Bieniasz PD (2013) Vpu binds directly to tetherin and displaces it from nascent virions. PLoS Pathog 9: e1003299. doi: 10.1371/journal.ppat.1003299 PMID: 23633949

19. Skasko M, Wang Y, Tian Y, Tokarev A, Munguia J, et al. (2012) HIV-1 Vpu protein antagonizes innate restriction factor BST-2 via lipid-embedded helix-helix interactions. J Biol Chem 287: 58–67. doi: 10.1074/jbc.M111.296772 PMID: 22072710

20. Vigan R, Neil SJ (2010) Determinants of tetherin antagonism in the transmembrane domain of the human immunodeficiency virus type 1 Vpu protein. J Virol 84: 12958–12970. doi: 10.1128/JVI.01699-10 PMID: 20926557

21. Agromayor M, Soler N, Caballe A, Kueck T, Freund SM, et al. (2012) The UBAP1 subunit of ESCRT-I interacts with ubiquitin via a SOUBA domain. Structure 20: 414–428. doi: 10.1016/j.str.2011.12.013 PMID: 22405001

22. Janvier K, Pelchen-Matthews A, Renaud JB, Caillet M, Marsh M, et al. (2011) The ESCRT-0 component HRS is required for HIV-1 Vpu-mediated BST-2/tetherin down-regulation. PLoS Pathog 7: e1001265. doi: 10.1371/journal.ppat.1001265 PMID: 21304933

23. Douglas JL, Viswanathan K, McCarroll MN, Gustin JK, Fruh K, et al. (2009) Vpu directs the degradation of the human immunodeficiency virus restriction factor BST-2/Tetherin via a {beta}TrCP-dependent mechanism. J Virol 83: 7931–7947. doi: 10.1128/JVI.00242-09 PMID: 19515779

24. Mangeat B, Gers-Huber G, Lehmann M, Zufferey M, Luban J, et al. (2009) HIV-1 Vpu neutralizes the antiviral factor Tetherin/BST-2 by binding it and directing its beta-TrCP2-dependent degradation. PLoS Pathog 5: e1000574. doi: 10.1371/journal.ppat.1000574 PMID: 19730691

25. Mitchell RS, Katsura C, Skasko MA, Fitzpatrick K, Lau D, et al. (2009) Vpu antagonizes BST-2-mediated restriction of HIV-1 release via beta-TrCP and endo-lysosomal trafficking. PLoS Pathog 5: e1000450. doi: 10.1371/journal.ppat.1000450 PMID: 19478868

26. Schubert U, Schneider T, Henklein P, Hoffmann K, Berthold E, et al. (1992) Human-immunodeficiency-virus-type-1-encoded Vpu protein is phosphorylated by casein kinase II. Eur J Biochem 204: 875–883. PMID: 1541298

27. Schubert U, Henklein P, Boldyreff B, Wingender E, Strebel K, et al. (1994) The human immunodeficiency virus type 1 encoded Vpu protein is phosphorylated by casein kinase-2 (CK-2) at positions Ser52 and Ser56 within a predicted alpha-helix-turn-alpha-helix-motif. J Mol Biol 236: 16–25. PMID: 8107101

28. Margottin F, Bour SP, Durand H, Selig L, Benichou S, et al. (1998) A novel human WD protein, h-beta TrCp, that interacts with HIV-1 Vpu connects CD4 to the ER degradation pathway through an F-box motif. Mol Cell 1: 565–574. PMID: 9660940

29. Tokarev AA, Munguia J, Guatelli JC (2011) Serine-threonine ubiquitination mediates downregulation of BST-2/tetherin and relief of restricted virion release by HIV-1 Vpu. J Virol 85: 51–63. doi: 10.1128/JVI.01795-10 PMID: 20980512

30. Andrew AJ, Miyagi E, Strebel K (2011) Differential effects of human immunodeficiency virus type 1 Vpu on the stability of BST-2/tetherin. J Virol 85: 2611–2619. doi: 10.1128/JVI.02080-10 PMID: 21191020

31. Schubert U, Strebel K (1994) Differential activities of the human immunodeficiency virus type 1-encoded Vpu protein are regulated by phosphorylation and occur in different cellular compartments. J Virol 68: 2260–2271. PMID: 8139011

32. Tervo HM, Homann S, Ambiel I, Fritz JV, Fackler OT, et al. (2011) beta-TrCP is dispensable for Vpu's ability to overcome the CD317/Tetherin-imposed restriction to HIV-1 release. Retrovirology 8: 9. doi: 10.1186/1742-4690-8-9 PMID: 21310048

33. Schmidt S, Fritz JV, Bitzegeio J, Fackler OT, Keppler OT (2011) HIV-1 Vpu blocks recycling and biosynthetic transport of the intrinsic immunity factor CD317/tetherin to overcome the virion release restriction. MBio 2: e00036–00011. doi: 10.1128/mBio.00036-11 PMID: 21610122

34. Pickering S, Hue S, Kim EY, Reddy S, Wolinsky SM, et al. (2014) Preservation of tetherin and CD4 counter-activities in circulating Vpu alleles despite extensive sequence variation within HIV-1 infected individuals. PLoS Pathog 10: e1003895. doi: 10.1371/journal.ppat.1003895 PMID: 24465210

35. Dube M, Paquay C, Roy BB, Bego MG, Mercier J, et al. (2011) HIV-1 Vpu antagonizes BST-2 by interfering mainly with the trafficking of newly synthesized BST-2 to the cell surface. Traffic 12: 1714–1729. doi: 10.1111/j.1600-0854.2011.01277.x PMID: 21902775

36. Kueck T, Neil SJ (2012) A cytoplasmic tail determinant in HIV-1 Vpu mediates targeting of tetherin for endosomal degradation and counteracts interferon-induced restriction. PLoS Pathog 8: e1002609. doi: 10.1371/journal.ppat.1002609 PMID: 22479182

37. Bonifacino JS, Traub LM (2003) Signals for sorting of transmembrane proteins to endosomes and lysosomes. Annu Rev Biochem 72: 395–447. PMID: 12651740

38. Lau D, Kwan W, Guatelli J (2011) Role of the endocytic pathway in the counteraction of BST-2 by human lentiviral pathogens. J Virol 85: 9834–9846. doi: 10.1128/JVI.02633-10 PMID: 21813615

39. Jia X, Weber E, Tokarev A, Lewinski M, Rizk M, et al. (2014) Structural basis of HIV-1 Vpu-mediated BST2 antagonism via hijacking of the clathrin adaptor protein complex 1. Elife 3: e02362. doi: 10.7554/eLife.02362 PMID: 24843023

40. Weinelt J, Neil SJ (2014) Differential sensitivities of tetherin isoforms to counteraction by primate lentiviruses. J Virol 88: 5845–5858. doi: 10.1128/JVI.03818-13 PMID: 24623426

41. Serra-Moreno R, Jia B, Breed M, Alvarez X, Evans DT (2011) Compensatory changes in the cytoplasmic tail of gp41 confer resistance to tetherin/BST-2 in a pathogenic nef-deleted SIV. Cell Host Microbe 9: 46–57. doi: 10.1016/j.chom.2010.12.005 PMID: 21238946

42. Zhang F, Wilson SJ, Landford WC, Virgen B, Gregory D, et al. (2009) Nef proteins from simian immunodeficiency viruses are tetherin antagonists. Cell Host Microbe 6: 54–67. doi: 10.1016/j.chom.2009.05.008 PMID: 19501037

43. Mauxion F, Le Borgne R, Munier-Lehmann H, Hoflack B (1996) A casein kinase II phosphorylation site in the cytoplasmic domain of the cation-dependent mannose 6-phosphate receptor determines the high affinity interaction of the AP-1 Golgi assembly proteins with membranes. J Biol Chem 271: 2171–2178. PMID: 8567675

44. McDonald B, Martin-Serrano J (2008) Regulation of Tsg101 expression by the steadiness box: a role of Tsg101-associated ligase. Mol Biol Cell 19: 754–763. PMID: 18077552

45. Martin-Serrano J, Neil SJ (2011) Host factors involved in retroviral budding and release. Nat Rev Microbiol 9: 519–531. doi: 10.1038/nrmicro2596 PMID: 21677686

46. Hirano S, Kawasaki M, Ura H, Kato R, Raiborg C, et al. (2006) Double-sided ubiquitin binding of Hrs-UIM in endosomal protein sorting. Nat Struct Mol Biol 13: 272–277. PMID: 16462748

47. Tokarev A, Guatelli J (2011) Misdirection of membrane trafficking by HIV-1 Vpu and Nef: Keys to viral virulence and persistence. Cell Logist 1: 90–102. PMID: 21922073

48. Miyagi E, Andrew AJ, Kao S, Strebel K (2009) Vpu enhances HIV-1 virus release in the absence of Bst-2 cell surface down-modulation and intracellular depletion. Proc Natl Acad Sci U S A 106: 2868–2873. doi: 10.1073/pnas.0813223106 PMID: 19196977

49. Coadou G, Evrard-Todeschi N, Gharbi-Benarous J, Benarous R, Girault JP (2002) HIV-1 encoded virus protein U (Vpu) solution structure of the 41–62 hydrophilic region containing the phosphorylated sites Ser52 and Ser56. Int J Biol Macromol 30: 23–40. PMID: 11893391

50. Coadou G, Gharbi-Benarous J, Megy S, Bertho G, Evrard-Todeschi N, et al. (2003) NMR studies of the phosphorylation motif of the HIV-1 protein Vpu bound to the F-box protein beta-TrCP. Biochemistry 42: 14741–14751. PMID: 14674748

51. Willbold D, Hoffmann S, Rosch P (1997) Secondary structure and tertiary fold of the human immunodeficiency virus protein U (Vpu) cytoplasmic domain in solution. Eur J Biochem 245: 581–588. PMID: 9182993

52. Wittlich M, Koenig BW, Stoldt M, Schmidt H, Willbold D (2009) NMR structural characterization of HIV-1 virus protein U cytoplasmic domain in the presence of dodecylphosphatidylcholine micelles. FEBS J 276: 6560–6575. doi: 10.1111/j.1742-4658.2009.07363.x PMID: 19804408

53. Jafari M, Guatelli J, Lewinski MK (2014) Activities of transmitted/founder and chronic clade B HIV-1 Vpu and a C-terminal polymorphism specifically affecting virion release. J Virol 88: 5062–5078. doi: 10.1128/JVI.03472-13 PMID: 24574397

54. Wittlich M, Koenig BW, Willbold D (2008) Structural consequences of phosphorylation of two serine residues in the cytoplasmic domain of HIV-1 VpU. J Pept Sci 14: 804–810. doi: 10.1002/psc.1004 PMID: 18186541

55. Miyakawa K, Sawasaki T, Matsunaga S, Tokarev A, Quinn G, et al. (2012) Interferon-induced SCYL2 limits release of HIV-1 by triggering PP2A-mediated dephosphorylation of the viral protein Vpu. Sci Signal 5: ra73. doi: 10.1126/scisignal.2003212 PMID: 23047923

56. Serra-Moreno R, Zimmermann K, Stern LJ, Evans DT (2013) Tetherin/BST-2 antagonism by Nef depends on a direct physical interaction between Nef and tetherin, and on clathrin-mediated endocytosis. PLoS Pathog 9: e1003487. doi: 10.1371/journal.ppat.1003487 PMID: 23853598

57. Pardieu C, Vigan R, Wilson SJ, Calvi A, Zang T, et al. (2010) The RING-CH ligase K5 antagonizes restriction of KSHV and HIV-1 particle release by mediating ubiquitin-dependent endosomal degradation of tetherin. PLoS Pathog 6: e1000843. doi: 10.1371/journal.ppat.1000843 PMID: 20419159

58. Neil SJ, Eastman SW, Jouvenet N, Bieniasz PD (2006) HIV-1 Vpu promotes release and prevents endocytosis of nascent retrovirus particles from the plasma membrane. PLoS Pathog 2: e39. PMID: 16699598

59. Martin-Serrano J, Yarovoy A, Perez-Caballero D, Bieniasz PD (2003) Divergent retroviral late-budding domains recruit vacuolar protein sorting factors by using alternative adaptor proteins. Proc Natl Acad Sci U S A 100: 12414–12419. PMID: 14519844

60. Maldarelli F, Chen MY, Willey RL, Strebel K (1993) Human immunodeficiency virus type 1 Vpu protein is an oligomeric type I integral membrane protein. J Virol 67: 5056–5061. PMID: 8331740

61. Roux KJ, Kim DI, Raida M, Burke B (2012) A promiscuous biotin ligase fusion protein identifies proximal and interacting proteins in mammalian cells. J Cell Biol 196: 801–810. doi: 10.1083/jcb.201112098 PMID: 22412018

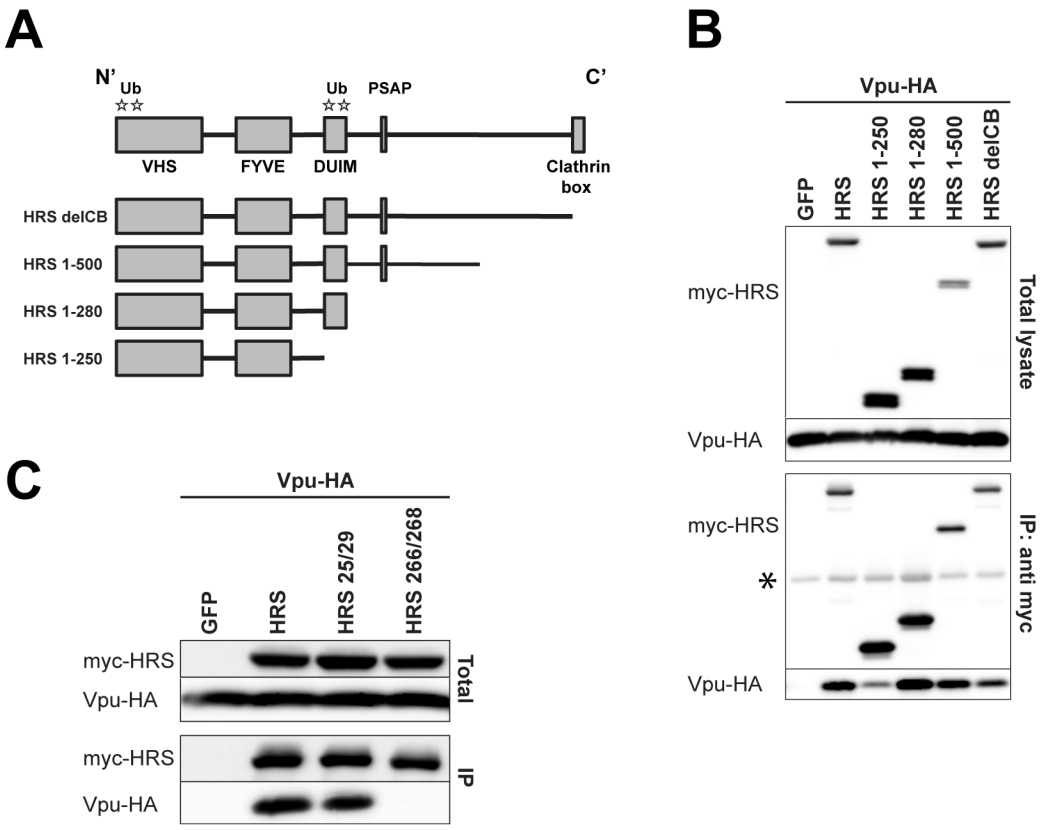

S1 Fig. Vpu/HRS interaction is dependent on residues in the DUIM of HRS that bind ubiquitin. (A) Schematic representation of HRS C-terminal truncations. (B) 293T cells were transfected with pCR3.1 Vpu-HA in combination with a pCR3.1 myc-HRS or myc-HRS truncation expression vector. 48 hours post transfection cells were lysed and immunoprecipitated with anti-myc antibody. Total cell lysates and precipitates were subjected to SDS-PAGE and analysed by Western blotting for myc-HRS and Vpu, and analyzed by ImageQuant. Asterisk: anti-HA antibody heavy chain (C) Immunoprecipitation was performed as in (B) but with myc-HRS W25A L29D and myc-HRS A266Q A268Q mutants.

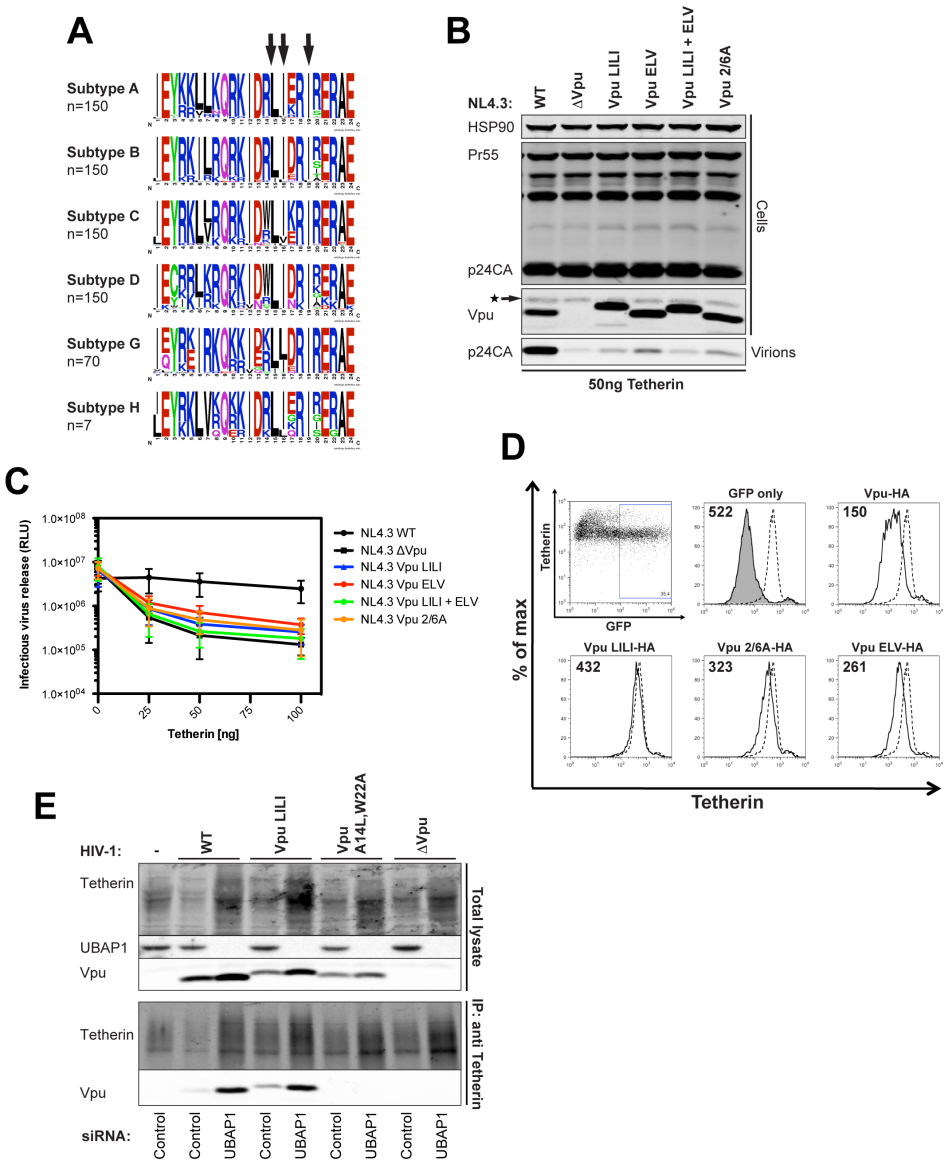

S2 Fig. Vpu LI/LI mutant exhibits impaired tetherin counteractivity. (A) LogoPlots of the first alpha helix of the Vpu cytoplasmic tail from HIV-1 subgroup M clades A, B, C, D, G and H generated from sequences obtained from the Los Alamos database (www.hiv.lanl.gov). (B) 293T cells were transfected with NL4.3 HIV-1 WT, ΔVpu, Vpu LILI, Vpu ELV or Vpu 2/6A mutant together with increasing concentrations of pCR3.1 tetherin-HA expression plasmid. Cell lysates and sucrose purified viral supernatants from 50 ng tetherin input were subjected to SDS-PAGE and analyzed by Western blotting for HSP90, HIV-1 p24CA and Vpu, and analyzed by LiCor quantitative imager. Asterisk: non-specific band. (C) Infectivity of viral supernatants was assayed on HeLa-TZMbl reporter cells. Infectious virus release was plotted as β-galactosidase activity in relative light units (RLU). Error bars represent the standard deviation of three independent experiments. (D) HeLa-TZMbl cells were co-transfected with pCR3.1 Vpu-HA or indicated mutant and a GFP expression vector. Cell-surface tetherin levels were analysed 48 hours post transfection by flow cytometry. GFP positive cells were gated and tetherin levels (solid lines) were compared to un-transfected cells or transfected with indicated Vpu (dotted lines). Numbers indicate median fluorescence intensities of endogenous tetherin surface levels. The solid peak in the upper histogram in the middle of the panel represents binding of the isotype control. (E) 293T tetherin expressing cells were transfected twice over a 48 hour period with siRNA oligonucleotides directed against UBAP1 or non-targeting control. The cells were then infected with HIV-1 WT, HIV-1 Vpu LILI, HIV-1 Vpu A14L W22A or HIV-1 ΔVpu at an MOI of 2. 48 hours later, cells were lysed and immunoprecipitated with anti-tetherin antibody. Total cell lysates and precipitates were subjected to SDS-PAGE and analyzed by Western blotting for tetherin, UBAP1 and Vpu, and analyzed by ImageQuant.

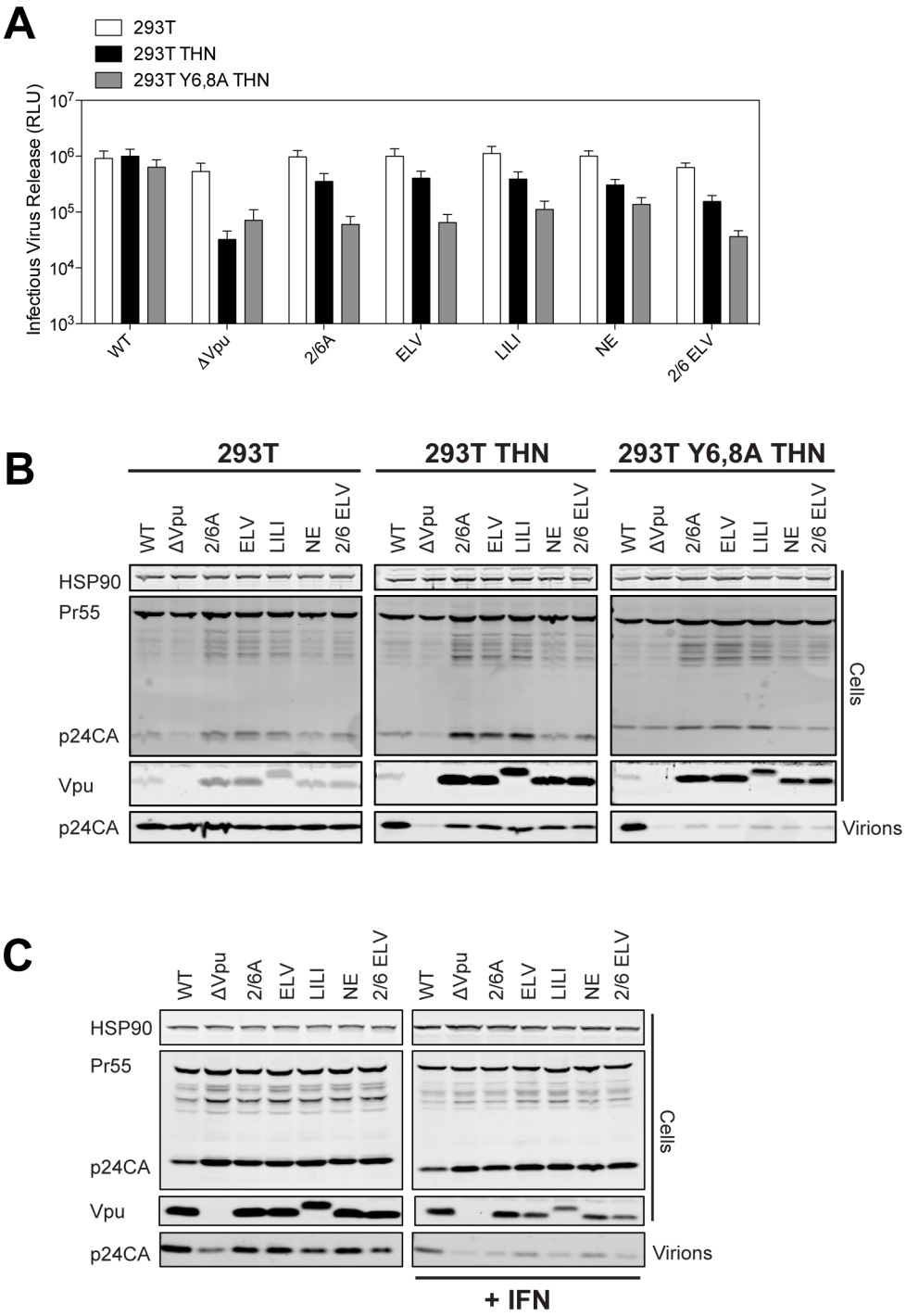

S3 Fig. Further Vpu mutants show similar phenotypes in infected primary CD4+ T cells and in 293T cells. (A-B) 293T, 293T tetherin or Y6,8A tetherin cells were infected with VSV-G pseudotyped NL4.3 wt or mutant virus at an MOI of 0.8. (A) 48 hours post infection viral supernatants were assayed for infectivity using HeLa-TZMbl reporter cells as in Fig 1. Error bars represent the standard deviation of three independent experiments. (B) Cell lysates and sucrose purified viral supernatants were subjected to SDS-PAGE and analyzed by Western blotting as in Fig 1. (C) Primary human CD4+ T cells were infected with the indicated HIV-1 mutant at an MOI of 0.8. 16 h later the cells were treated or not with 5000 U/ml universal type-I interferon. Cell lysates and viral supernatants were harvested a further 24 h later and analyzed for infectivity on HeLa-TZMbl cells (A) or physical particle yield and cellular viral expression by quantitative Western blotting.

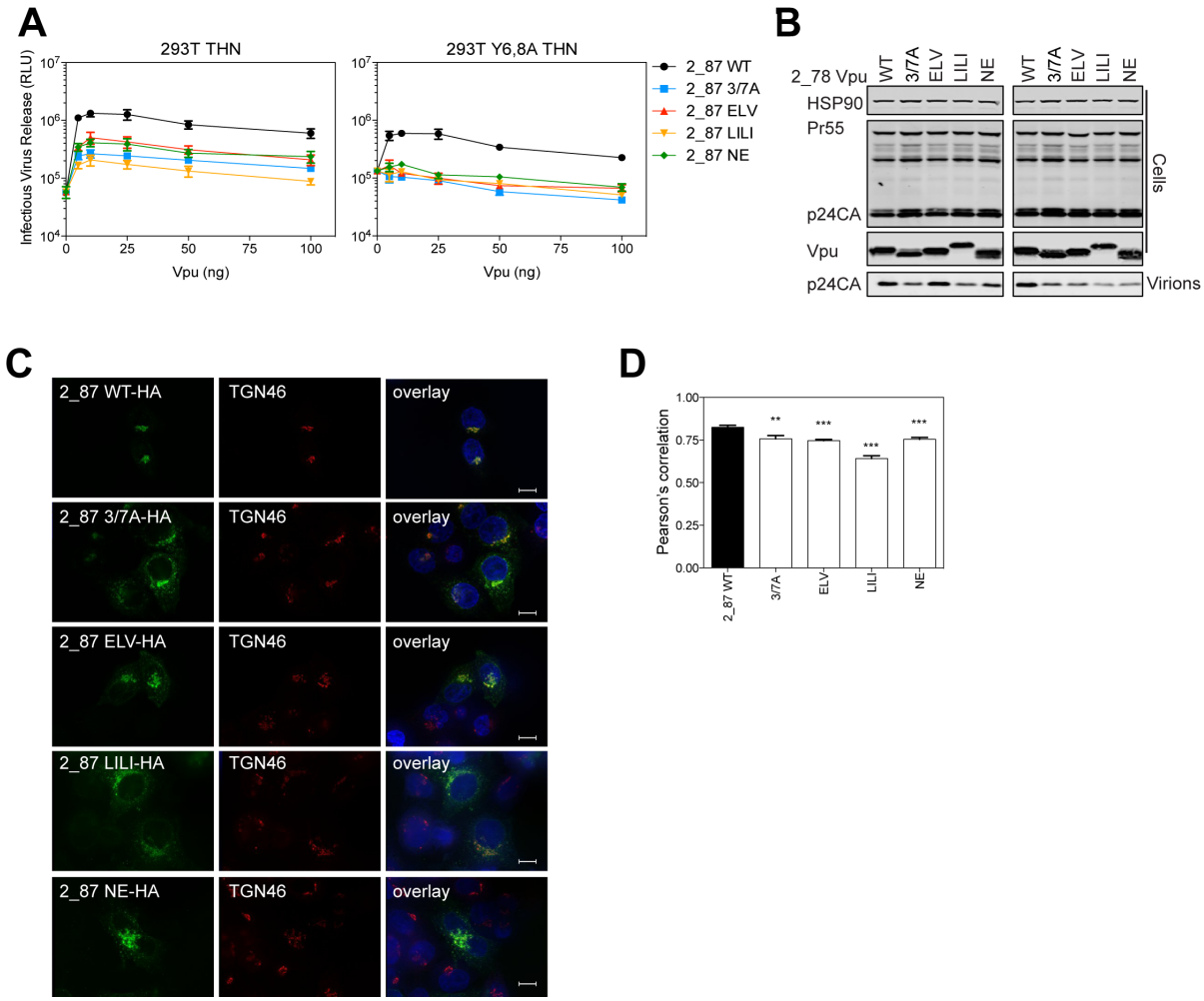

S4 Fig. A primary isolate Vpu allele and its mutants exhibit a comparable phenotype to NL4.3 Vpu. (A) 293T tetherin cells were transfected with NL4.3 ΔVpu proviral plasmid in combination with YFP expression vector and pCR3.1 2_87 Vpu or mutants thereof. 48 hours post transfection infectivity of viral supernatants was determined on HeLa-TZMbl cells as in Fig 1. (B) Cell lysates and pelleted supernatant virions from (A) were harvested and subjected to SDS-PAGE and analyzed by Western blotting for HIV-1 p24CA, Vpu and HSP90, and analyzed by LiCor quantitative imager. (C) Hela cells were transfected with 100 ng of pCR3.1 2_87 Vpu-HA or indicated mutants. 16 hours post transfection cells were fixed and stained for HA (green) and the TGN marker TGN46 (red) and examined by widefield fluorescent microscopy. Panels are of representative examples. Bars = 10 μm. (D) Z stacks were taken of all cells (n = 15), images were deconvolved using the AutoQuant X3 software and Pearson's correlations were calculated for all Z stacks using ImageJ. Results were analyzed by unpaired 2-tailed t-test—*** P = 10–5 or lower.

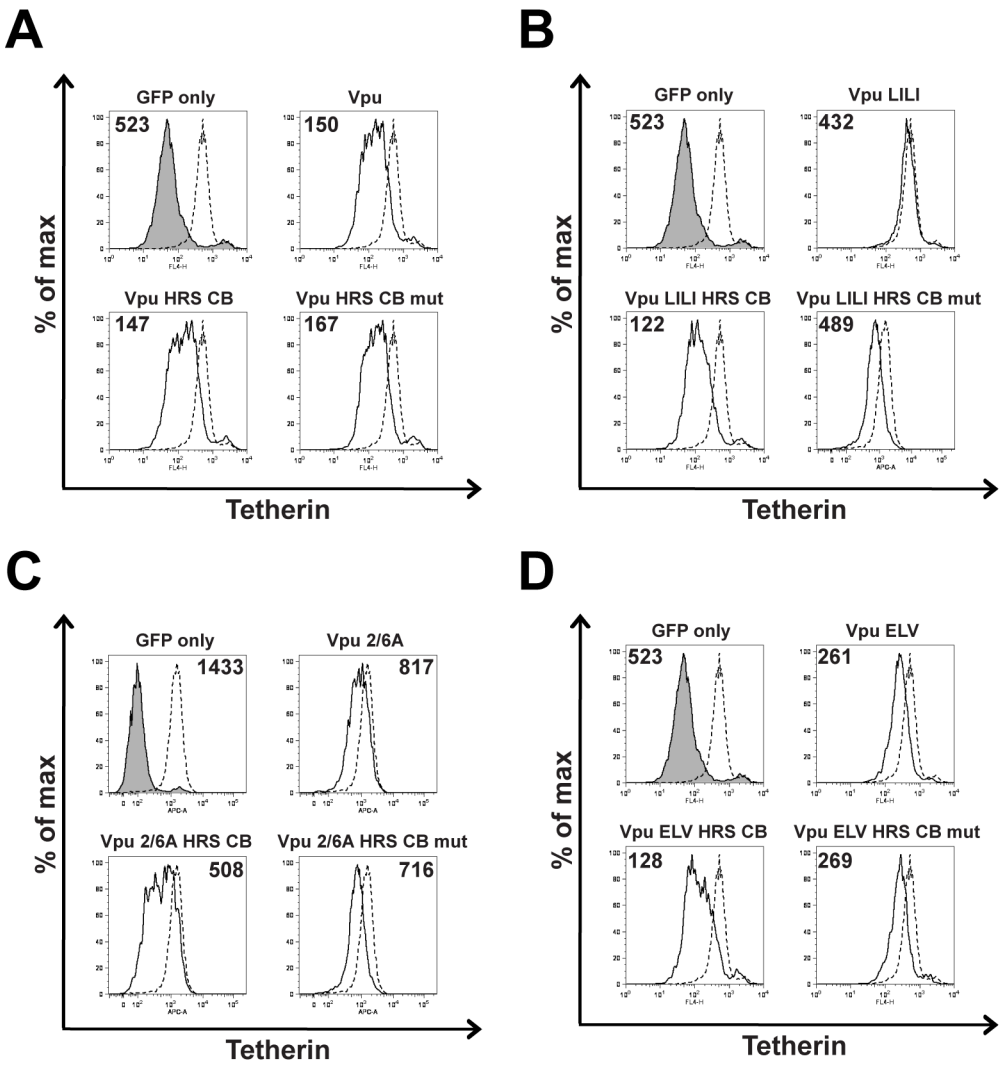

S5 Fig. Clathrin binding restores the tetherin downregulation capacity of Vpu mutants. (A to D) HeLa-TZMbl cells were co-transfected with pCR3.1 Vpu-HA or indicated mutant and a GFP expression vector. Cell-surface tetherin levels were analyzed 48 hours post transfection by flow cytometry. GFP positive cells were gated and tetherin levels (solid lines) were compared to un-transfected cells or transfected with indicated Vpu (dotted lines). Numbers indicate median fluorescence intensities of endogenous tetherin surface levels. The solid peak in the upper histogram in the middle of the panel represents binding of the isotype control.

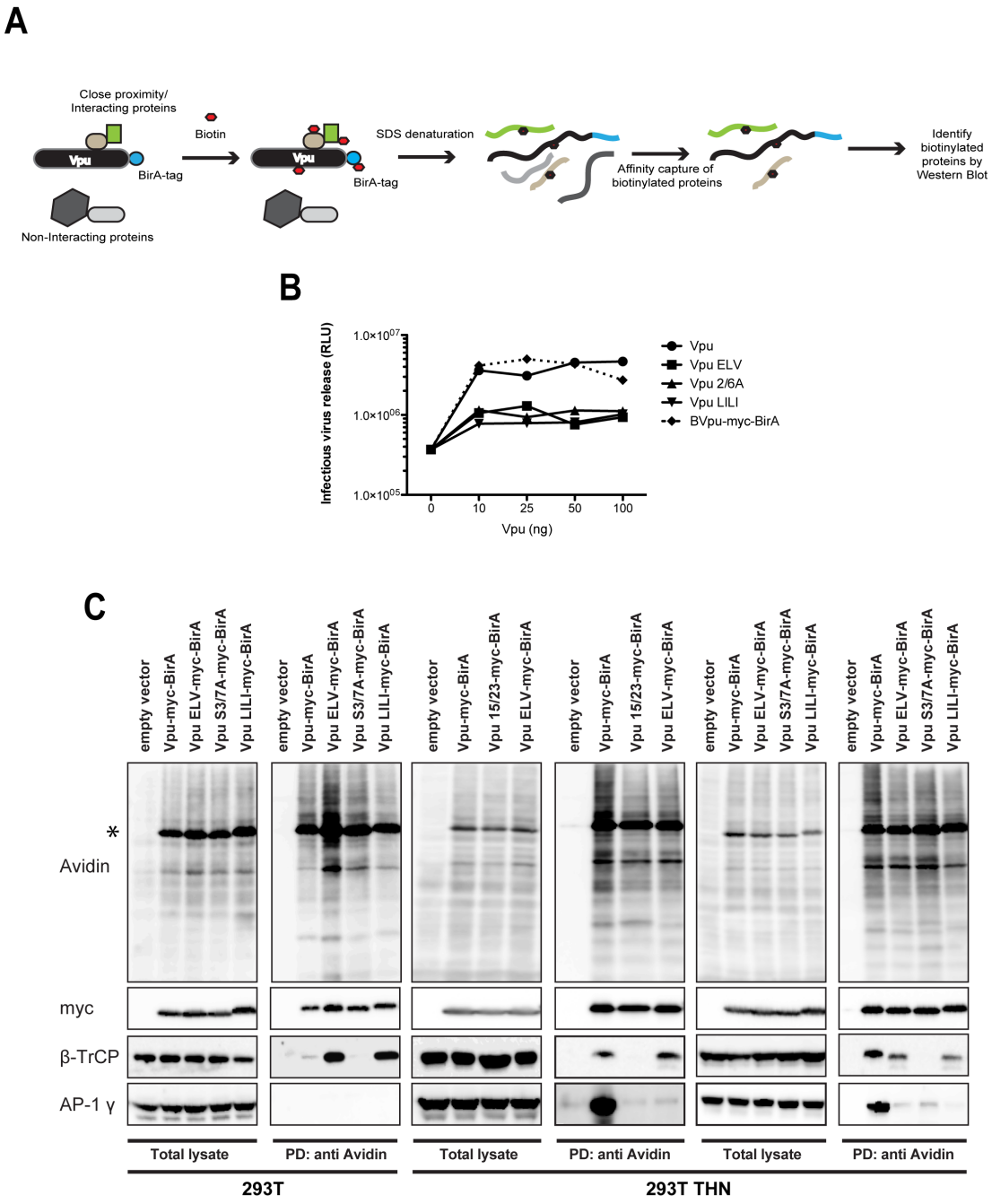

S6 Fig. Proximity-based biotin ligase assay suggests Vpu/AP-1 interaction. (A) Schematic representation of proximity-based biotin ligase assay. (B) 293T tetherin cells were transfected with NL4.3 ΔVpu proviral plasmid in combination with YFP expression vector and pCR3.1 Vpu or indicated mutant thereof. 48 hours post transfection infectivity of viral supernatants was determined on HeLa-TZMbl cells as in Fig 1. (C) 293T or 293T tetherin cells were transfected with Vpu-myc-BirA, B Vpu ELV-myc-BirA, B Vpu A15L/W23A-myc-BirA, B Vpu S3/7A- myc-BirA (phospho-mutant), B Vpu LILI-myc-BirA or empty vector control. 6 hours post transfection, cells were treated with 100 nM concanamycin A in the presence of 150 μM free biotin. 16 hours later, cells were washed, lysed, sonicated and biotinylated proteins were recovered on streptavidin-conjugated beads and analysed by Western blot for avidin, Vpu-myc-BirA, β-TrCP or AP-1 γ. Asterisk: Vpu-myc-BirA band.

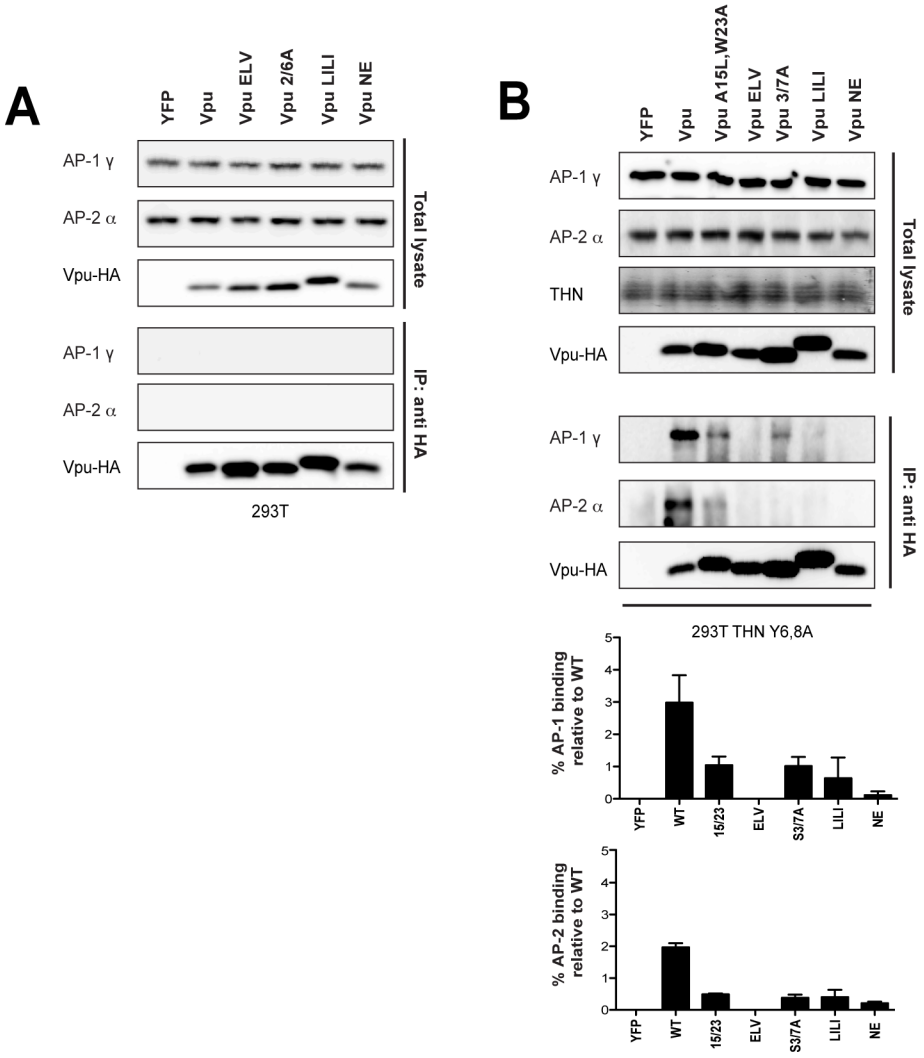

S7 Fig. Vpu binding to clathrin adaptors AP-1 and AP-2 is dependent on tetherin binding (A) and binding to AP-1 and AP-2 is conserved by primary Vpu 2_87 in tetherin expressing cells (B). (A) 293T cells were transfected with pCR3.1 Vpu-HA, Vpu ELV-HA, Vpu 3/7A-HA, Vpu LILI-HA or Vpu NE-HA mutants. (B) 293T tetherin Y6,8A were transfected with pCR3.1 Vpu-HA, Vpu A15L/W23A-HA, Vpu ELV-HA, Vpu 3/7A-HA, Vpu LILI-HA or Vpu NE-HA mutants. 48 h post transfection, cells were lysed and cross-linked using PFA (0.05% w/v) and immunoprecipitated with anti-HA antibody. Total cell lysates and precipitates were subjected to SDS-PAGE and analyzed by Western blotting for Vpu-HA, AP-1 ɣ or AP-2 α. Panels are of representative experiments. Histograms represent quantification of the relative AP-1 or AP-2 binding normalized to input control. Error bars represent the standard deviation of three independent experiments.

Article

Cell Host & Microbe

Cell Surface Proteomic Map of HIV Infection Reveals Antagonism of Amino Acid Metabolism by Vpu and Nef

Graphical Abstract

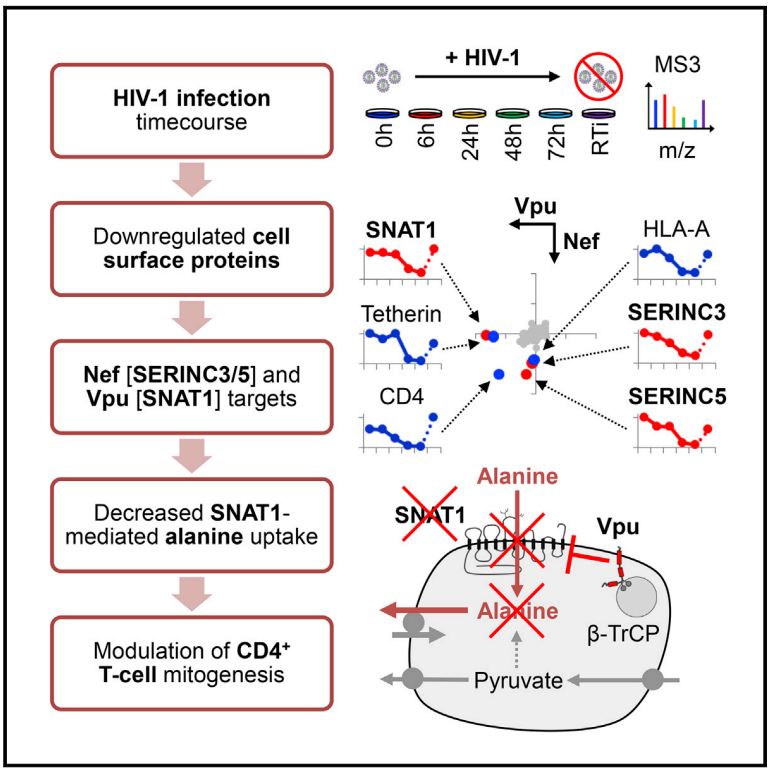

Authors

Nicholas J. Matheson, Jonathan Sumner, Kim Wals, ..., Clary B. Clish, Stuart J.D. Neil, Paul J. Lehner

Correspondence

njm25@cam.ac.uk (N.J.M.), pjl30@cam.ac.uk (P.J.L.)

In Brief

Viruses manipulate host factors to enhance their replication. Matheson et al. use functional proteomics to analyze plasma membrane proteins downregulated during HIV-1 infection. Serine carriers SERINC3/5 and alanine transporter SNAT1 were identified as Nef and Vpu targets, respectively. Antagonism of SNAT1-mediated alanine transport enables viral interference with T cell immunometabolism

Highlights

- Unbiased global analysis of T cell surface proteome remodeling during HIV infection
- >100 proteins downregulated, including Nef targets SERINC3/5 and Vpu target SNAT1
- β-TrCP-dependent SNAT1 downregulation acquired by pandemic SIVcpz/HIV-1 viruses
- Uptake of exogenous alanine by SNAT1 critical for primary CD4+ T cell mitogenesis

Matheson et al., 2015, Cell Host & Microbe *18*, 409–423
October 14, 2015
http://dx.doi.org/10.1016/j.chom.2015.09.003

Cell Host & Microbe
Article

Cell Surface Proteomic Map of HIV Infection Reveals Antagonism of Amino Acid Metabolism by Vpu and Nef

Nicholas J. Matheson,[1,*] Jonathan Sumner,[2] Kim Wals,[1] Radu Rapiteanu,[1] Michael P. Weekes,[1] Raphael Vigan,[2] Julia Weinelt,[2] Michael Schindler,[3,4] Robin Antrobus,[1] Ana S.H. Costa,[5] Christian Frezza,[5] Clary B. Clish,[6] Stuart J.D. Neil,[2] and Paul J. Lehner[1,*]

[1]Cambridge Institute for Medical Research, University of Cambridge, Cambridge Biomedical Campus, Cambridge CB2 0XY, UK
[2]Department of Infectious Diseases, King's College London School of Medicine, Guy's Hospital, London SE1 9RT, UK
[3]Helmholtz Center Munich, Institute of Virology, 85764 Neuherberg, Germany
[4]Institute of Medical Virology and Epidemiology of Viral Diseases, University Clinic Tübingen, 72076 Tübingen, Germany
[5]MRC Cancer Unit, Hutchison/MRC Research Centre, University of Cambridge, Cambridge Biomedical Campus, Cambridge CB2 0XZ, UK
[6]The Broad Institute of the Massachusetts Institute of Technology and Harvard, Cambridge, MA 02142, USA
*Correspondence: njm25@cam.ac.uk (N.J.M.), pjl30@cam.ac.uk (P.J.L.)
http://dx.doi.org/10.1016/j.chom.2015.09.003

SUMMARY

Critical cell surface immunoreceptors downregulated during HIV infection have previously been identified using non-systematic, candidate approaches. To gain a comprehensive, unbiased overview of how HIV infection remodels the T cell surface, we took a distinct, systems-level, quantitative proteomic approach. >100 plasma membrane proteins, many without characterized immune functions, were downregulated during HIV infection. Host factors targeted by the viral accessory proteins Vpu or Nef included the amino acid transporter SNAT1 and the serine carriers SERINC3/5. We focused on SNAT1, a β-TrCP-dependent Vpu substrate. SNAT1 antagonism was acquired by Vpu variants from the lineage of SIVcpz/HIV-1 viruses responsible for pandemic AIDS. We found marked SNAT1 induction in activated primary human CD4+ T cells, and used Consumption and Release (CoRe) metabolomics to identify alanine as an endogenous SNAT1 substrate required for T cell mitogenesis. Downregulation of SNAT1 therefore defines a unique paradigm of HIV interference with immunometabolism.

INTRODUCTION

HIV-1 viruses of the AIDS pandemic encode four "accessory proteins" (Vif, Vpr, Vpu, and Nef) dispensable for viral replication in vitro, but essential for viral pathogenesis in vivo (Malim and Emerman, 2008). Vpu and Nef are multifunctional adaptors that downregulate cell surface proteins to counteract host-cell restriction and evade the immune response (Haller et al., 2014; Tokarev and Guatelli, 2011). Targets have typically been identified using non-systematic, candidate approaches and include the HIV receptor CD4, the restriction factor tetherin, and the MHC I molecules HLA-A/B (Tokarev and Guatelli, 2011).

Among primate lentiviruses, a correlation is observed between viral pathogenicity and expression of Vpu, with CD4+ T cell decline and progression to AIDS markedly faster in HIV-1 than HIV-2, and increased mortality in chimpanzees infected with SIVcpz (Keele et al., 2009). Vpu induces substrate-specific ubiquitination of CD4 and tetherin through recruitment of the SCF-β-TrCP E3 ligase complex via a constitutively phosphorylated phosphodegron in its cytoplasmic tail (Douglas et al., 2009; Margottin et al., 1998; Mitchell et al., 2009). In the SIV-HIV (SHIV) macaque model of HIV, CD4+ T cell loss is abrogated by deletion of Vpu, scrambling of its transmembrane domain, or mutation of its β-TrCP-binding phosphodegron (Hout et al., 2005; Singh et al., 2003; Stephens et al., 2002). This effect is unlikely to be attributable to loss of Vpu-mediated downregulation of macaque CD4 or tetherin because CD4 is also efficiently downregulated by Nef, and pig-tailed macaque tetherin is antagonized by SIVmac Nef, but not by HIV-1 Vpu (Zhang et al., 2009). Together, these data point to the existence of additional, biologically important, β-TrCP-dependent Vpu substrates.

In this study, we combine plasma membrane enrichment through selective aminooxy-biotinylation (Plasma Membrane Profiling; PMP) with Tandem Mass Tag (TMT) and Stable Isotope Labeling by Amino Acids in Cell Culture (SILAC)-based quantitative proteomics to describe global changes in the cell surface landscape of an HIV-infected T cell, including expression time courses of >800 plasma membrane proteins (Weekes et al., 2013, 2014). Our unbiased, comprehensive analysis reveals downregulation of >100 HIV-1 targets, particularly proteins involved in cell adhesion, leukocyte activation, and transmembrane transport, and is presented as a searchable database to facilitate data mining.

In addition to their known substrates, we show that Vpu is necessary and sufficient for β-TrCP-dependent degradation of the amino acid transporter SNAT1, and Nef is sufficient for downregulation of the serine carriers SERINC3 and SERINC5. We apply an unbiased, CoRe metabolomic approach to identify the non-essential amino acid alanine as an endogenous SNAT1

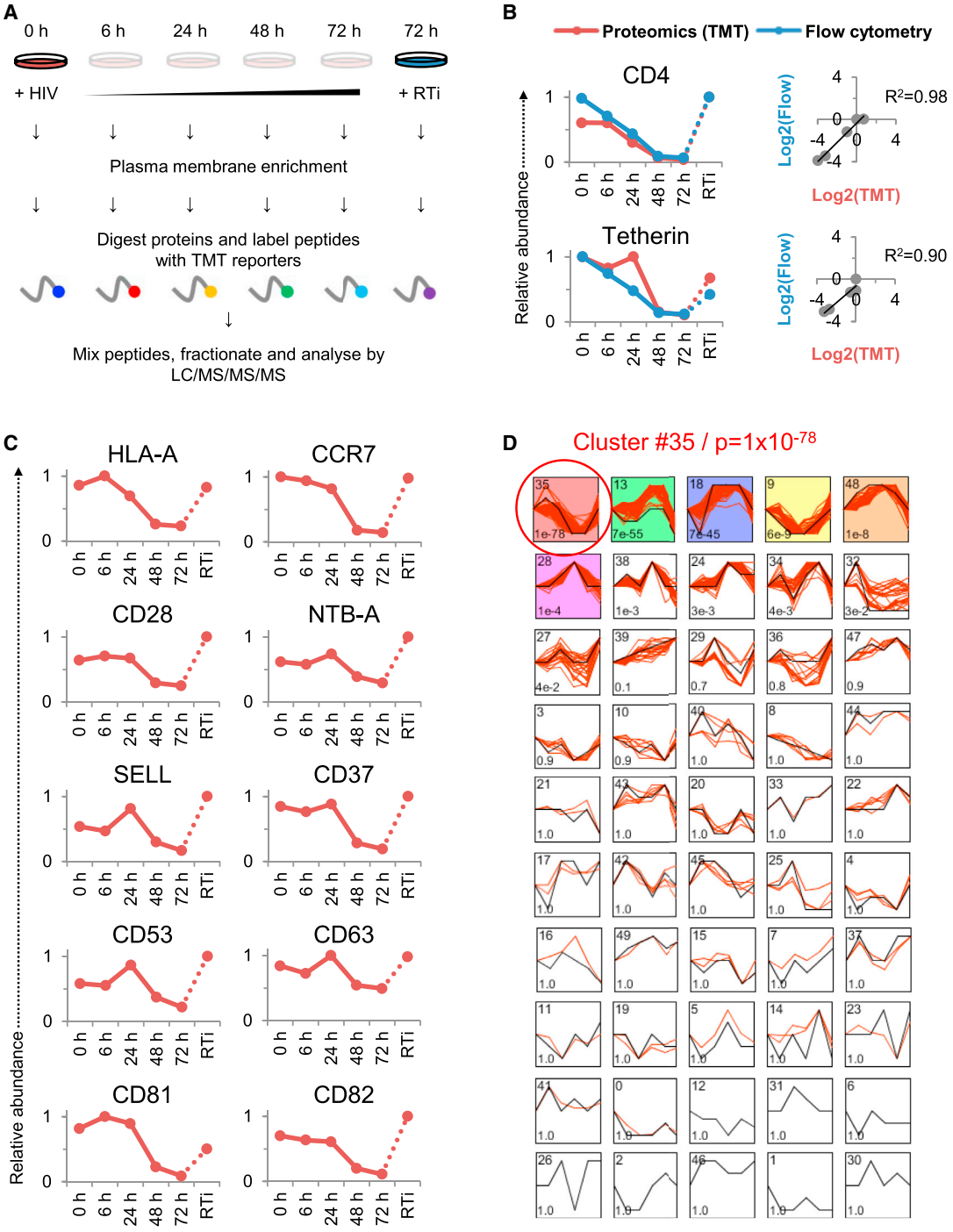

Figure 1. TMT-Based Proteomic Time Course of Plasma Membrane Protein Expression in HIV-1-Infected Cells

(A) Workflow of TMT-based 6-plex PMP time course experiment. In subsequent figures, time points 1–5 show plasma membrane protein expression 0, 6, 24, 48, and 72 hr after HIV-1 infection (where 0 hr = uninfected cells), and time point 6 shows plasma membrane protein expression 72 hr after HIV-1 infection in the presence of reverse transcriptase inhibitors (RTi). NL4-3-deltaE-EGFP HIV-1 viruses at an MOI of 10 were used for all proteomic experiments.

(B) Comparison of temporal profiles of CD4 and tetherin obtained by proteomic (TMT) versus flow cytometric quantitation. Cells from (A) were stained with anti-CD4 and anti-tetherin antibodies at the indicated time points and analyzed by flow cytometry. Relative abundance is expressed as a fraction of maximum TMT reporter ion or fluorescence intensity. For linear regression, log2(fold change compared with uninfected cells) is shown.

(C) Temporal profiles of previously reported targets for HIV-mediated downregulation.

(legend continued on next page)

substrate in primary human CD4+ T cells, and show that extracellular alanine is critical for T cell mitogenesis. Restricting alanine uptake through Vpu-mediated downregulation of SNAT1 therefore represents a viral strategy to regulate immune cell activation.

RESULTS

Systematic Time Course Analysis of T Cell Surface Protein Expression during HIV-1 Infection

To gain a comprehensive, unbiased overview of plasma membrane protein regulation by HIV-1, we used PMP to measure expression levels of cell surface proteins in CEM-T4 T cells infected with HIV-1 (Figure 1A) (Weekes et al., 2013, 2014). By spinoculating cells with Env-deficient, VSVg-pseudotyped virus, we ensured a synchronous, single-round infection, and by using a multiplicity of infection (MOI) sufficient to infect >90% of cells, we minimized confounding effects from bystander (uninfected) cells (Figure S1A). We exploited 6-plex TMT quantitation to compare plasma membrane protein abundance in uninfected cells (0 hr), at 4 time points following HIV-1 infection (6, 24, 48, and 72 hr) and, to control for cellular changes occurring in the absence of de novo viral gene expression, in cells infected for 72 hr in the presence of reverse transcriptase inhibitors (RTi). In total, 2,320 proteins were quantitated, including 804 proteins previously reported to localize to the plasma membrane (Figure S1B). The complete dataset is shown in interactive Table S1, which allows generation of temporal profiles for any quantitated genes of interest.

We observed a strong correlation between expression time courses determined by mass spectrometry and flow cytometry for CD4 (R^2 = 0.98) and tetherin (R^2 = 0.90) (Figure 1B), saw marked time-dependent depletion of cell surface HLA-A, and confirmed progressive downregulation of other known HIV-1 targets (CCR7, CD28, NTB-A, SELL, and the tetraspanins CD37/53/63/81/82) (Figure 1C) (Haller et al., 2014; Lambelé et al., 2015; Ramirez et al., 2014; Shah et al., 2010; Swigut et al., 2001; Vassena et al., 2015). Downregulation of CD71 and the chemokine receptors is controversial, with our data suggesting depletion of cell surface CD71, CXCR4, and CCR5 (Figure S1C). As expected, VSVg levels increased immediately after infection, then rapidly declined (Figure S1D).

Discovery of Cell Surface Targets Depleted by HIV-1

To identify host factors regulated by HIV-1 without observer bias based on known biological function, we used the Short Time Series Expression Miner (STEM) to cluster proteins according to patterns of temporal expression and identify profiles occurring more frequently than expected by chance (Figure 1D). The most enriched profile comprised 134 proteins showing progressive time-dependent downregulation, abolished by reverse transcriptase inhibitors (Cluster #35; $p = 10^{-78}$). Proteins in this cluster, which include CD4, tetherin, and HLA-A, represent candidate HIV-1 cell surface targets (Table S2).

We validated these candidates in an independent infection time course experiment using SILAC as an alternative quantitative proteomic approach (Figures 2A and 2B) and confirmed downregulation of a functionally and structurally diverse set of proteins with available antibody reagents (CD43/47/162 and NOTCH1) by flow cytometry in CEM-T4s and primary human CD4+ T cells infected with HIV-1 (Figure S2A).

Functional Analysis of Progressively Downregulated HIV-1 Targets

To identify biological functions targeted by HIV-1 in an unbiased fashion, we used the Database for Annotation, Visualization and Integrated Discovery (DAVID) to determine gene ontology "molecular function" and "biological process" annotations over-represented in Cluster #35 compared with other quantitated proteins. The cluster was enriched for terms relating to cell adhesion, leukocyte activation, and transmembrane transport. These categories intersect processes known to be modulated by HIV-1 and provide a framework for interpreting both previously identified and novel HIV-1 targets. We therefore mined our data for downregulated proteins with closely related functions (Figures 2C–2F and Table S3).

Cell adhesion molecules regulate leukocyte trafficking and NK cell killing. Modulation of lymphocyte migration through targeting of SELL and CCR7 (Figure 1C) is proposed to facilitate HIV-1 immune avoidance (Ramirez et al., 2014; Vassena et al., 2015), and downregulation of NTB-A (Figure 1C) protects HIV-infected cells from NK cell lysis (Shah et al., 2010). We now show that HIV-1 also downregulates NCR3LG1 (B7H6; Figure 2D), a ligand for the NK activating receptor NKp30 found on activated monocytic cells in vivo (Brandt et al., 2009; Matta et al., 2013). Flow cytometry confirmed reduced Ig-NKp30 binding to HIV-1-infected CEM-T4 cells (Figure S2B).

HIV-1 replication is critically dependent on the activation state of infected cells, and the virus employs multiple strategies to modulate T cell activation and maximize replication in vivo (Abraham and Fackler, 2012). Attention has focused on downregulation of CD3 by Nef variants of non-pathogenic SIVs, attenuated in HIV-1 Nef (Schindler et al., 2006). Conversely, our data revealed downregulation of numerous other immunoreceptors with important functions in T cell activation (Figure 2E), along with a range of transmembrane transporters with no known roles in the immune system, particularly amino acid transporters (Figure 2F). Since T cell activation requires profound upregulation in amino acid metabolism (Wang et al., 2011), we predict that these proteins have important, but unrecognized, functions in T cell biology.

Systematic Plasma Membrane Proteomic Analysis of HIV-1 Accessory Proteins Vpu and Nef

Depletion of most known HIV-1 cell surface targets has been attributed to Vpu and/or Nef (Haller et al., 2014; Tokarev and Guatelli, 2011). To assign downregulation of proteins in Cluster #35 to particular viral genes, we applied an unbiased,

(D) Identification of enriched temporal profiles by STEM. Model temporal profiles (black) and matched experimental protein expression profiles (red) are shown. Each box includes a profile identification number (top left) and an unadjusted p value (bottom left). Colored boxes indicate model profiles assigned more proteins than expected by chance alone (Bonferroni-adjusted p values < 0.05).
See also Figure S1 and Tables S1 and S2.

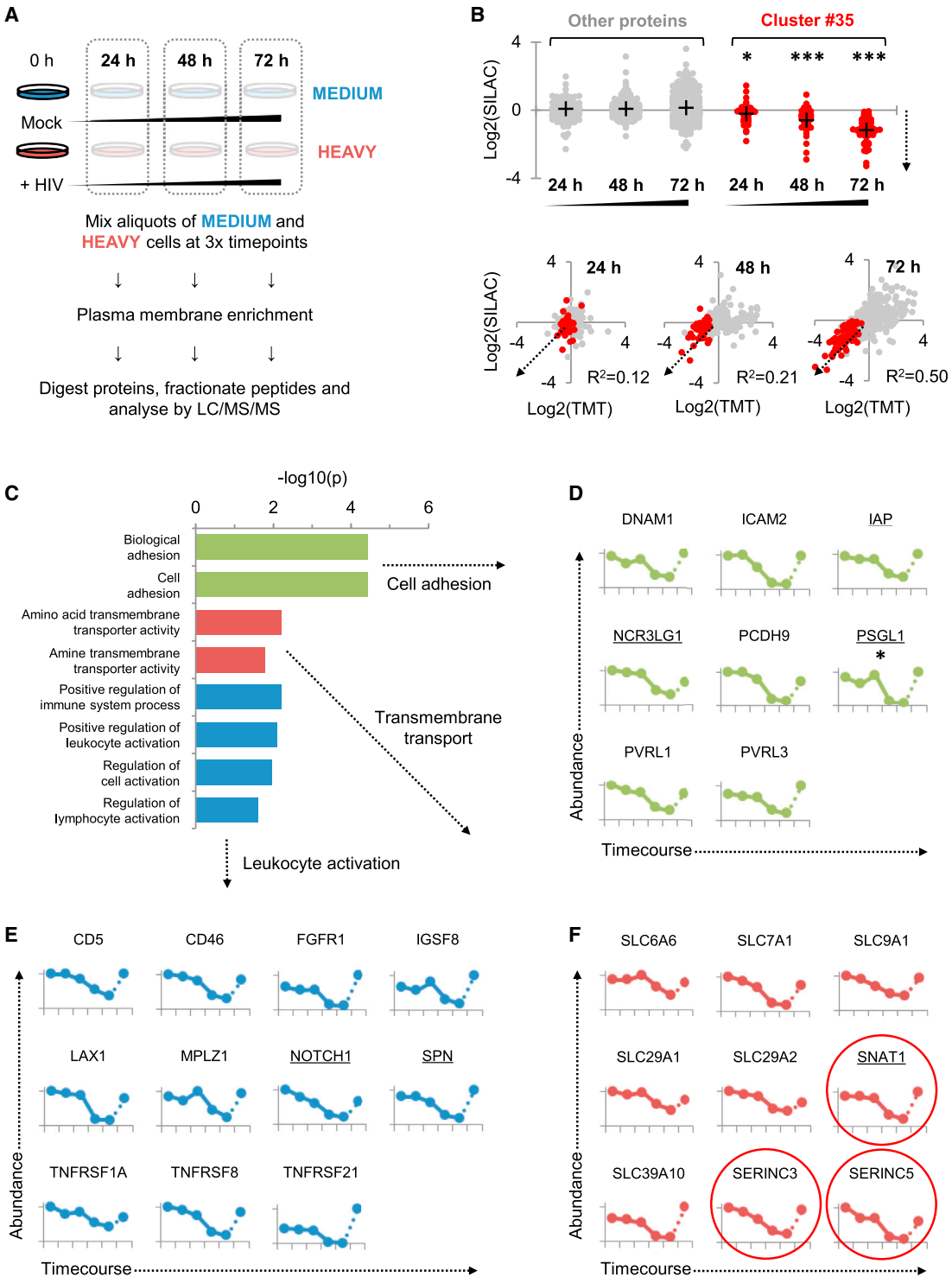

Figure 2. SILAC-Based Proteomic Validation and Functional Analysis of Cell Surface Targets Downregulated by HIV-1

(A) Workflow of SILAC-based 3-way PMP time course experiment.

(B) Validation of HIV-1 targets (upper panel) and comparison between SILAC- and TMT-based time course experiments (lower panel). Log2(fold change compared with mock/uninfected cells) at 24, 48, and 72 hr is shown for proteins from Cluster #35 (red) versus all other quantitated proteins (gray). Downregulation by HIV-1 is indicated by dotted arrows. Proteins identified by >1 unique peptide in both TMT and SILAC experiments are shown. Crosses indicate mean values. *p < 0.05; ***p < 0.001.

(legend continued on next page)

systematic approach to define Vpu and Nef substrates. SILAC-based PMP was used to compare expression levels of cell surface proteins in CEM-T4s infected with either Vpu- or Nef-deficient viruses (Figures 3A and S3A), or transduced with Vpu or Nef as single genes (Figures 3B and S3B). As positive controls, we found that Vpu depleted cell surface CD4 and tetherin, while Nef depleted cell surface CD4 and HLA-A (Figures 3A and 3B). Surprisingly, many HIV-1 cell surface targets were downregulated efficiently by both Vpu- and Nef-deficient viruses and not by overexpression of Vpu and Nef as single genes, suggesting Vpu- and Nef-independent mechanisms.

Targeting of Amino Acid Metabolism by Vpu and Nef

As well as their known targets, we found Vpu to be both necessary and sufficient for downregulation of the amino acid transporter SNAT1 (Figures 2F and 3A–3B), and Nef to be sufficient for downregulation of the serine carriers SERINC3 and SERINC5 (Figures 2F and 3A–3B). This effect was specific within the SERINC family, because SERINC1 was induced rather than downregulated (Figure S1E). While this manuscript was in preparation, SERINC3 and SERINC5 were independently identified as HIV-1 restriction factors using orthogonal approaches (M. Pizzato, personal communication; H. Gottlinger, personal communication). We confirmed restriction of infectious HIV-1 viral production by SERINC5, antagonized by Nef (Figure S3C). Conversely, SNAT1 does not act as an HIV-1 restriction factor (Figure S3D). Instead, we hypothesized that antagonism of SNAT1-dependent amino acid transport by Vpu may modulate T cell activation.

We confirmed Vpu-dependent depletion of endogenous SNAT1 from the plasma membrane of transduced cells by confocal and total internal reflection (TIRF) microscopy (Figures S4A and S4B). As well as decreased expression at the cell surface, depletion of total SNAT1 was seen by immunoblot of CEM-T4s infected with WT or Nef-deficient HIV-1, but not with Vpu-deficient virus (Figures 3C, lanes 2–4, 3D, lanes 2 and 4, and S4C), and by immunoblot of CEM-T4s transduced with Vpu, but not Nef (Figure 3E, lane 5).

Previous studies have suggested that SNAT1 is predominantly expressed in the CNS (Gu et al., 2001; Varoqui et al., 2000). We found SNAT1 protein to be poorly expressed in resting primary human CD4+ T cells but dramatically induced following mitogenic T cell stimulation (Figures 3F, lanes 2–5, and 3G, panel 2). Furthermore, Vpu depletes SNAT1 from activated primary human CD4+ T cells both in the context of viral infection (Figures S4D and S4E) and as a single gene in transduced cells purified by Antibody-Free Magnetic Cell Sorting (AFMACS; Figures 3G, panel 5, 3H, lane 5, and S4F) (Matheson et al., 2014).

Ubiquitination and β-TrCP-Dependent Endolysosomal Degradation of SNAT1

To probe the mechanism of Vpu-mediated SNAT1 depletion, we confirmed that Vpu binds endogenous SNAT1 (Figure 4A, lanes 2 and 4) and leads to SNAT1 ubiquitination (Figure 4B, lane 5). As with CD4 and tetherin, downregulation of SNAT1 is rescued by mutation of the Vpu phosphodegron responsible for β-TrCP recruitment (S52, 56A) (Figures 3G, panel 6, 3H, lane 6, 4F, and S5A) and by RNAi-mediated depletion of β-TrCP (Figure 4C, lane 3).

Vpu mediates degradation of CD4 by hijacking the endoplasmic reticulum-associated degradation (ERAD) pathway (Margottin et al., 1998; Schubert et al., 1998) and antagonizes tetherin by co-opting the endolysosomal degradative pathway (Douglas et al., 2009; Mitchell et al., 2009). SNAT1 degradation is rescued by incubation with vacuolar ATPase inhibitors, but not proteasome inhibitors (Figure 4D, lanes 5 and 6), and by RNAi-mediated depletion of TSG101 (Figure 4E, lane 3), suggesting that, as for tetherin, SNAT1 is degraded in endolysosomes by the ESCRT machinery.

Downregulation of tetherin is abolished by substitution of conserved amino acid residues W22 or A14 in the transmembrane domain of Vpu, and W22 is also critical for downregulation of CD4 (Vigan and Neil, 2010). While the W22A mutation abolished downregulation of all 3 Vpu substrates, SNAT1 and CD4 downregulation were preserved in the presence of the A14L mutation (Figure 4F, lane 4, and Figure S4A). The same pattern of SNAT1 downregulation was observed with equivalent mutations in a patient-derived Vpu (Figure S5B) and with Vpu mutants in the context of viral infection (Figure S5C). The pathway for SNAT1 degradation by Vpu therefore shares the cellular machinery used for antagonism of tetherin but occurs independently of tetherin downregulation and may be dissociated from it by the A14L mutation.

CoRe Metabolomic Analysis of SNAT1-Depleted Primary Human CD4+ T Cells

When overexpressed in vitro, SNAT1 mediates uptake of a range of small neutral amino acids (Gu et al., 2001; Varoqui et al., 2000). Transport by SNAT1 is Na dependent and sensitive to competition by the model substrate α-methylaminoisobutyric acid (MeAIB), a specific inhibitor of amino acid transport System A (Mackenzie and Erickson, 2004). Based on its functional characteristics and pattern of expression, SNAT1 has primarily been considered a neuronal glutamine transporter (Chaudhry et al., 2002).

To identify endogenous SNAT1 substrates in primary human CD4+ T cells in an unbiased fashion, we combined an "activation-rest" strategy for shRNA knockdown (Monroe et al., 2014) with Consumption and Release (CoRe) metabolomics (Jain et al., 2012) (Figure 5A). Pure populations of transduced cells expressing control or SNAT1-specific shRNAs were generated by AFMACS (Figures 5B and S6A) (Matheson et al., 2014). After resting for 7–10 days, control and SNAT1-depleted cells were re-stimulated using CD3/CD28 Dynabeads. A marked reduction

(C) Gene ontology "molecular function" and "biological process" terms enriched among proteins from Cluster #35. DAVID functional annotation clusters with adjusted p values < 0.05 and containing terms with Bonferroni-adjusted p values < 0.05 are shown. Further details are included in Table S3.
(D–F) Temporal profiles of downregulated proteins associated with cell adhesion (D), leukocyte activation (E), and transmembrane transport (F). Proteomic quantitation and time points are as for Figures 1B–1C. Proteins exhibiting >2-fold downregulation compared with uninfected cells in both TMT and SILAC experiments are shown, and proteins subsequently validated using flow cytometry or immunoblot are underlined.
See also Figure S2 and Table S2.

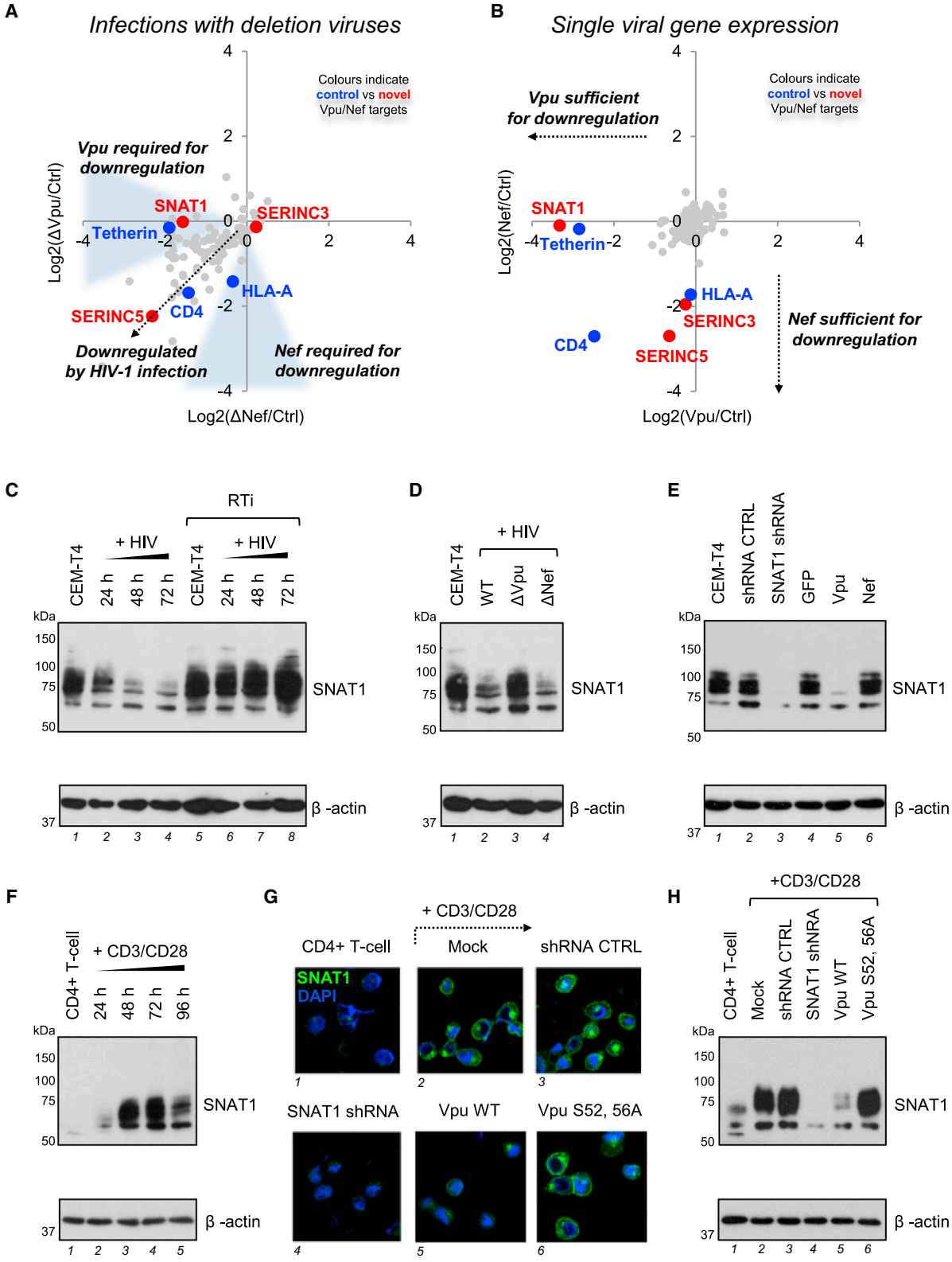

Figure 3. Proteomic Analysis of Vpu and Nef Targets and Identification of SNAT1 as a Vpu Substrate

(A and B) SILAC-based quantitation of plasma membrane proteins in cells infected with Vpu-deficient (y axis) versus Nef-deficient (x axis) HIV-1 viruses (A) and cells transduced with Vpu (x axis) versus Nef (y axis) as single genes (B). Log2(fold change compared with uninfected [A] or GFP-transduced [B] cells)

(legend continued on next page)

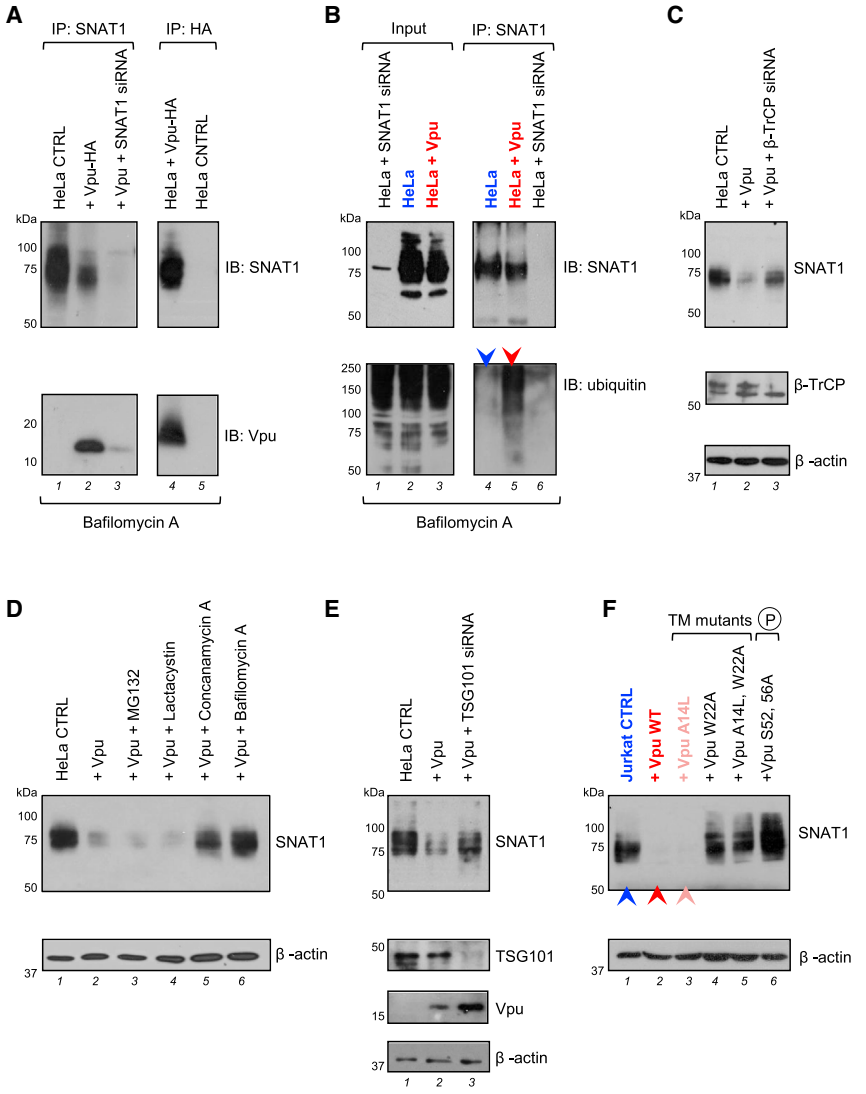

Figure 4. Mechanism of SNAT1 Depletion by Vpu

(A) Interaction of SNAT1 with Vpu. HeLa cells stably transduced with Vpu-HA were immunoprecipitated with anti-SNAT1 (G63; first panel) or anti-HA (second panel) antibodies and immunoblotted with anti-SNAT1 (H60) or anti-Vpu antibodies. Untransduced HeLas transfected with SNAT1-specific siRNA were included as controls.

(B) Ubiquitination of SNAT1 by Vpu. HeLa cells stably transduced with Vpu-HA were either immunoblotted with anti-SNAT1 (H60) and anti-ubiquitin antibodies (first panel) or immunoprecipitated with anti-SNAT1 (G63) antibody, re-immunoprecipitated with anti-SNAT1 (H60) antibody, and immunoblotted with anti-SNAT1 (H60) and anti-ubiquitin antibodies (second panel). Untransduced HeLas transfected with SNAT1-specific siRNA were included as controls. Ubiquitinated SNAT1 in control (blue arrow) and Vpu-expressing (red arrow) HeLas is highlighted.

(C) β-TrCP-dependent depletion of SNAT1. HeLa cells stably transduced with Vpu-HA were transfected with control or β-TrCP-specific siRNA then immunoblotted.

(D and E) SNAT1 depletion via an endolysosomal pathway. HeLa cells stably transduced with Vpu-HA were either treated with MG132, lactacystin, concanamycin, or bafilomycin (D) or transfected with control or TSG101-specific siRNA (E) then immunoblotted.

(F) Molecular determinants of SNAT1 down-regulation. Jurkats stably expressing Vpu WT or indicated Vpu mutants were immunoblotted. Cells transduced with empty vector (blue), Vpu WT (red), and Vpu A14L (pink) are highlighted. The same cells stained with anti-CD4 or anti-tetherin antibodies and analyzed by flow cytometry are shown in Figure S5A.

See also Figure S5.

in proliferation of SNAT1-depleted cells was observed (Figures 5C and S6A). Culture supernatants were sampled at baseline, 24, and 48 hr, and extracellular metabolite fluxes were calculated on a per-cell basis. In total, data for consumption and release of 126 metabolites, including 19 natural amino acids, were used to derive CoRe metabolomic profiles of control and SNAT1-depleted cells. Principal component analysis readily distinguished these profiles, particularly at 48 hr (Figure 5D, upper panels). Surprisingly, across all measured metabolites, the most significant difference was in net alanine release, with no difference in net glutamine consumption (Figure 5D, middle and lower panels).

is shown for proteins from Cluster #35. Figures S3A and S3B selectively enlarge the lower left quadrant of each scatterplot. Proteins identified by >1 unique peptide are shown.

(C) SNAT1 depletion by HIV-1 infection. CEM-T4s infected with WT NL4-3-deltaE-EGFP HIV-1 virus in the presence or absence of RTi were immunoblotted at the indicated time points. An MOI of 10 was used, and infection controls are shown in Figure S4C.

(D) Rescue of SNAT1 in the absence of Vpu. CEM-T4s infected with WT, Vpu-deficient, or Nef-deficient HIV-1 NL4-3-deltaE-EGFP viruses were immunoblotted at 48 hr. An MOI of 10 was used, and infection controls are shown in Figure S4C.

(E) SNAT1 depletion by Vpu. CEM-T4s stably transduced with GFP, Vpu, or Nef were immunoblotted. Untransduced CEM-T4s and CEM-T4s stably transduced with control or SNAT1-specific shRNAs were included as controls.

(F) SNAT1 induction in activated primary T cells. Primary human $CD4^+$ T cells activated with CD3/CD28 Dynabeads were immunoblotted at the indicated time points.

(G and H) SNAT1 depletion by Vpu in activated primary T cells. Primary human $CD4^+$ T cells were activated with CD3/CD28 Dynabeads and mock transduced or transduced with the indicated shRNA or Vpu constructs. After purification by AFMACS (Figure S4F), cells were either rested or re-stimulated with CD3/CD28 Dynabeads and immunoblotted (G) or analyzed by confocal microscopy (H) at 48 hr.

See also Figures S3 and S4.

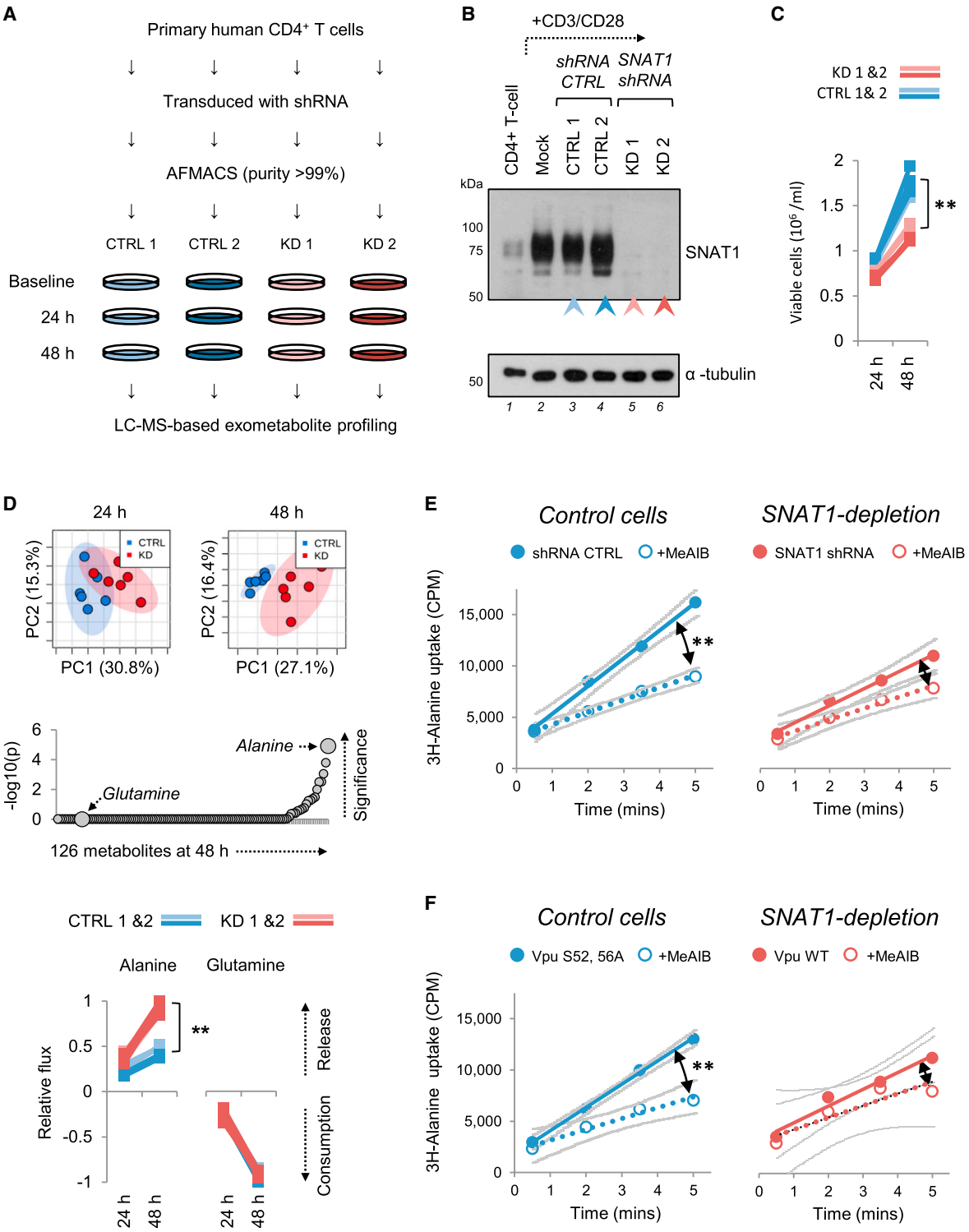

Figure 5. CoRe Metabolomics of Proliferating T Cells and Identification of Alanine Transport by SNAT1

(A) Workflow of CoRe metabolomics experiment.

(B) SNAT1 knockdown for CoRe metabolomics experiment. Primary human CD4+ T cells were activated with CD3/CD28 Dynabeads and mock transduced or transduced with the indicated shRNAs. After purification by AFMACS (Figure S6A), cells were either rested or re-stimulated with CD3/CD28 Dynabeads, then immunoblotted at 48 hr.

(legend continued on next page)

Alanine Transport by Endogenous SNAT1 in T Cells

While attention has focused on glutamine, alanine is the paradigmatic substrate for System A amino acid transport (Oxender and Christensen, 1963) and has consistently been found to be a high-affinity substrate for SNAT1 in overexpression studies (Gu et al., 2001; Mackenzie and Erickson, 2004; Varoqui et al., 2000). We therefore hypothesized that the increase in net alanine release caused by SNAT1 depletion may be explained by a decrease in SNAT1-mediated alanine uptake. To test this, 3H-alanine transport was measured directly in AFMACS-purified primary human CD4+ T cells depleted of SNAT1 by expression of a SNAT1-specific shRNA (Figure 5E) or wild-type Vpu (Figure 5F). Whereas alanine uptake in control T cells was markedly reduced by the System A transport inhibitor MeAIB, this effect was abolished in SNAT1-depleted T cells (Figures 5E and 5F), confirming alanine transport by endogenous SNAT1.

Critical Requirement for Extracellular Alanine in T Cell Mitogenesis

Since alanine is both a non-essential amino acid and excreted by proliferating cells (Jain et al., 2012), including lymphocytes (Figure 5D, lower panels), it appears paradoxical to suggest that a reduction in alanine uptake could result in the mitogenic defect observed in T cells depleted of SNAT1. Nonetheless, we observed a dose-dependent increase in proliferation of CEM-T4 and Jurkat T cells cultured in increasing alanine concentrations (Figure S7A), and a supply of exogenous alanine is required for optimal lymphocyte proliferation in response to PHA (Chuang et al., 1990; Rotter et al., 1979).

We investigated this requirement in primary human CD4+ T cells by activating cells with CD3/CD28 Dynabeads in media supplemented with increasing alanine concentrations. A clear dose response in proliferation from 0 to 0.1 mM was observed (Figure 6A). Furthermore, the effect of increasing alanine concentration was inhibited by MeAIB in a dose-dependent fashion, supporting a role for System A transport in alanine uptake (Figure 6B). Interestingly, exogenous alanine had no effect on the expression of the early T cell activation markers CD69 and CD25 (Figure S7B). The same dissociation of proliferation from early activation has been reported for T cells stimulated in the absence of glutamine (Carr et al., 2010).

Contribution of Extracellular Alanine to the Free Intracellular Amino Acid Pool

To explain the requirement for exogenous alanine in T cell mitogenesis, we hypothesized that bidirectional transport of alanine at the plasma membrane could result in both uptake of extracellular alanine and net alanine excretion (Figure S7C). We therefore measured the size of the free intracellular alanine pool of primary human CD4+ T cells re-stimulated with CD3/CD28 Dynabeads and resuspended in media either lacking alanine or supplemented with a physiological alanine concentration (Figures 6C and S7D). Intracellular alanine levels were markedly reduced by extracellular alanine depletion, but increased by extracellular alanine supplementation, an effect abolished in the presence of MeAIB. These observations confirm bidirectional flux of alanine across the plasma membrane, resulting in equilibration of intracellular and extracellular alanine concentrations, with alanine uptake mediated by System A transport.

The free intracellular alanine pool may be filled by de novo synthesis through transamination of pyruvate, by release of alanine from proteins by proteasomal or lysosomal degradation, or by uptake of extracellular alanine. To formally distinguish these possibilities, and assess their relative contributions, we resuspended washed cells in media supplemented with physiological levels of heavy isotopologue-labeled 13C6-glucose and 15N-alanine (Figure 6D). The free intracellular alanine pool was rapidly reconstituted by extracellular 15N-alanine, an effect markedly inhibited by MeAIB, with little contribution from unlabeled alanine or alanine generated from 13C-glucose-derived pyruvate (Figures 6E and S7D). Conversely, almost all lactate released from cells was derived from glycolysis of 13C6-glucose (Figures 6F). Finally, MeAIB-inhibitable transamination of 15N-alanine to 15N-glutamate was observed (Figure S7E). Extracellular alanine is therefore rapidly taken up by System A transport in primary human CD4+ T cells and incorporated into the wider cellular metabolite pool.

Modulation of T Cell Mitogenesis by SNAT1 Downregulation in HIV-1 Infection

As a functional readout for SNAT1 downregulation in the context of viral infection, we examined the effect of Vpu expression on proliferation of primary human CD4+ T cells. Similar to transduction with SNAT1 shRNA, lentiviral delivery of WT Vpu (but not the Vpu S53, 57A phosphodegron mutant) retarded T cell proliferation (Figure S7F). Remarkably, despite antagonism of cell-cycle progression by Vpr (Malim and Emerman, 2008), and Vpu-independent modulation of a range of mitogenic cell surface proteins (Figure 2E), we also observed a significant reduction in proliferation of T cells infected with WT HIV-1, as compared with Vpu-deficient or Vpu S53, 57A phosphodegron mutant viruses (Figure 6G).

(C) Defective proliferation of SNAT1-depleted primary T cells. Re-stimulated cells from (B) were seeded at equal densities and viable cells enumerated at the indicated time points using CytoCount beads. Data were obtained in triplicate. **$p < 0.01$. No difference in cell size between the two populations was seen by flow cytometry (Figure S6B).

(D) CoRe metabolomic analysis of control and SNAT1-depleted primary T cells. Metabolite compositions of culture supernatants from (C) were determined by LC-MS at baseline, 24, and 48 hr. Data were obtained in triplicate, and Principal component analysis was used to compare net consumption or release of metabolites by control and SNAT1-depleted cells (upper panels). 95% confidence regions are shown. p values for differences in consumption or release of individual metabolites at 48 hr are shown on a negative log scale (middle panel). Net consumption or release of alanine and glutamine is shown scaled to a maximum change of 1 (lower panels). **$p < 0.01$.

(E and F) Impaired alanine uptake by primary T cells depleted of SNAT1 by shRNA (E) or Vpu (F). Cells from Figures 3G–3H were re-stimulated for 48 hr with CD3/CD28 Dynabeads and uptake (counts per minutes; CPM) of 3H-alanine measured at time points from 30 s to 5 min. 3H-alanine transport in the presence of MeAIB is included as a control, and MeAIB-inhibitable uptake is highlighted (black arrows). 95% confidence bands on linear regression lines (indicating rates of uptake) are shown in gray. **$p < 0.01$.

See also Figure S6.

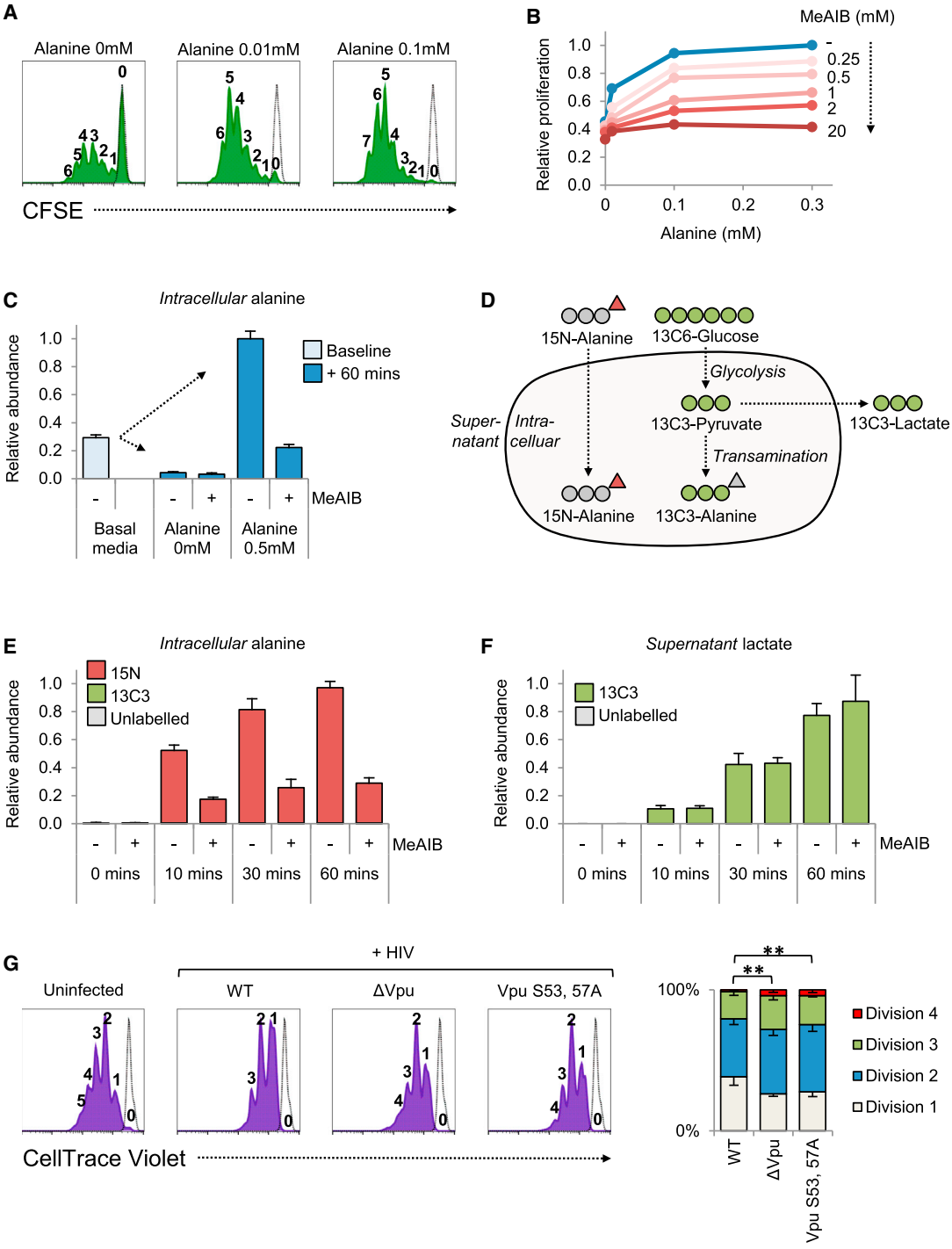

Figure 6. Requirement for Extracellular Alanine in T Cell Mitogenesis

(A) Dose-dependent proliferation of primary T cells in response to exogenous alanine. Primary human CD4+ T cells were stained with CFSE, stimulated with CD3/CD28 Dynabeads in media supplemented with alanine at the concentrations indicated, and analyzed by flow cytometry after 120 hr (green filled histograms). Peaks are labeled by division number, and unstimulated cells were included as a control (black dotted lines). Representative data from three independent experiments are shown.

(B) Dose-dependent inhibition of primary T cell proliferation by MeAIB. Primary human CD4+ T cells were stimulated with CD3/CD28 Dynabeads in media supplemented with alanine and MeAIB at the concentrations indicated. Viable cells were enumerated using CytoCount beads after 72 hr and numbers expressed as a fraction of the maximum.

(C) Regulation of free intracellular alanine pool by System A-dependent alanine uptake. Primary human CD4+ T cells were expanded, rested, and re-stimulated for 48 hr with CD3/CD28 Dynabeads. Cells were then resuspended in media supplemented with alanine at the concentrations indicated in the presence or absence

(legend continued on next page)

SNAT1 Downregulation by Vpu Variants of Pandemic HIV-1 Viruses

HIV-1 viruses form three main groups, each representing a separate transmission of chimpanzee SIVcpz or gorilla SIVgor to humans: M (or Main, responsible for the AIDS pandemic), O (or Outlier), and N (or New or Non-M, Non-O). Group M viruses are responsible for greater than 90% of all HIV infections and cluster into genetically distinct clades, of which the most widespread are A (East Africa), B (Europe and North America), and C (Southern Africa) (Hemelaar et al., 2011). Among non-human primates, Vpu is found in viruses of the SIVcpz lineage (including HIV-1 and SIVgor), as well as more distantly related guenon monkey viruses (SIVgsn, SIVmus, and SIVmon).

To explore the phylogenetic history of Vpu-mediated SNAT1 downregulation, we generated a stable 293T cell line expressing SNAT1-FLAG and CD4 and compared the effects of different Vpu-IRES-GFP constructs. CD4 downregulation is widely conserved and therefore represents a positive control for functional Vpu expression (Sauter et al., 2009). As expected, whereas NL4-3 Vpu (but not Vpu S52A) downregulated both CD4 and SNAT1-FLAG, Nef only downregulated CD4 (Figure 7A). Depletion of cell surface SNAT1-FLAG was conserved across all 6 HIV-1 clade A, B, and C Vpu variants tested (Figures 7A and 7B), but restricted to the SIVcpz *Ptt* lineage giving rise to pandemic HIV-1 group M viruses (Figure 7C). The ability of Vpu to downregulate SNAT1 has therefore been acquired recently and may be critical for the in vivo replication or enhanced pathogenicity of HIV-1 viruses.

DISCUSSION

In this study, we provide a comprehensive, unbiased temporal map of the cell surface of an HIV-1-infected T cell. Our plasma membrane proteomic approach captures transcriptional and post-transcriptional effects, including protein sequestration and redistribution, and is not limited to known T cell immunoreceptors (Weekes et al., 2014). The study of cell surface proteins downregulated by viruses has uncovered important areas of immunobiology, and manipulation by HIV-1 therefore suggests host factors with unsuspected functions in both viral pathogenesis and cellular physiology. Downregulation is unlikely to reflect a non-specific cellular response to productive viral infection because plasma membrane proteins depleted by HIV-1 exhibit contrasting temporal regulation in cells infected with human cytomegalovirus, even within protein families (Figures S1F and S1G) (Weekes et al., 2014).

Along with CD4 and tetherin, our data identify SNAT1 as the third β-TrCP-dependent Vpu substrate. Other Vpu targets have been proposed, based on candidate approaches: NTB-A, CCR7, CD1d, PVR, SELL, and the tetraspanins CD37/53/63/81/82 (Haller et al., 2014; Lambelé et al., 2015; Matusali et al., 2012; Moll et al., 2010; Ramirez et al., 2014; Shah et al., 2010; Vassena et al., 2015). In general, the mechanisms are not β-TrCP dependent, remain poorly characterized, and may be indirect. Furthermore, the magnitude of downregulation reported has been modest, which may contribute to less-robust phenotypes (Sato et al., 2012). Compared with these targets, our systematic analysis suggests that downregulation of CD4, tetherin, and SNAT1 is qualitatively distinct (Figure S3E), reflecting recruitment of β-TrCP and hijack of enzymatic ubiquitin-mediated degradation. Together with downregulation of CD4, MHC-I, SERINC3, and SERINC5 by Nef, we therefore define a more limited group of highly downregulated HIV-1 accessory protein targets.

Vpu and Nef co-operate in the downregulation of CD4 and tetherin, and loss of function in one gene may be compensated by gain of function in the other (Sauter et al., 2009). The Nef proteins of HIV-2 and most SIVs are able to modulate T cell activation by downregulating CD3 from the surface of infected cells, but Nef has lost this ability in most Vpu-containing viruses. Vpu has therefore been suspected to modulate T cell activation via an alternative pathway (Kirchhoff, 2009). We focused on downregulation of SNAT1 both because it is a direct Vpu target and because the importance of amino acid transport in regulating T cell activation is increasingly recognized (Nakaya et al., 2014; Sinclair et al., 2013). Furthermore, while many transporters are poorly characterized multi-pass transmembrane proteins with few reliable reagents, their plasma membrane location makes them potentially druggable therapeutic targets, and inhibitors already exist for many biochemically defined transport systems.

Induction of SNAT1 mRNA correlates with increased glutamine uptake during activation of murine T cells (Carr et al., 2010), but other candidate glutamine transporters are also induced (Nakaya et al., 2014; Wang et al., 2011), and pre-genomic studies attributed lymphocyte glutamine transport to Systems ASC, L, and N, not System A (Segel, 1992). We therefore used an unbiased systematic approach to identify SNAT1 substrates in primary human CD4+ T cells. Measured differences between alanine fluxes of control and SNAT1-depleted cells could potentially reflect both direct transport effects and secondary effects on synthesis or utilization. Alanine may be synthesized by transamination of pyruvate and glutamine-derived glutamate, and re-analysis of data from a previous

of MeAIB. Abundance of free intracellular alanine at baseline and 60 min is expressed as a fraction of the maximum. Mean values and 95% confidence intervals are shown for data obtained in triplicate. No difference in cell size was observed between 0 and 0.5 mM alanine (Figure S7D, left panel).

(D–F) Reconstitution of free intracellular alanine pool by extracellular alanine. Washed cells prepared as in (C) were resuspended in media supplemented with 5.6 mM 13C6-glucose and 0.5 mM 15N-alanine (D) in the presence or absence of MeAIB. Abundances of labeled and unlabeled free intracellular alanine (E) and supernatant lactate (F) at the indicated time points are expressed as a fraction of the maximum. Mean values and 95% confidence intervals are shown for data obtained in triplicate. No difference in cell size was observed in the presence or absence of MeAIB (Figure S7D, right panel).

(G) Defective proliferation of primary T cells depleted of SNAT1 by HIV-1. Primary human CD4+ T cells were stained with CellTrace Violet, stimulated with CD3/CD28 Dynabeads, infected with the indicated NL4-3 Vpu 2_87 HIV-1 viruses at an MOI of 3, and analyzed by flow cytometry after 120 hr (violet filled histograms). Peaks are labeled by division number, and unstimulated cells are included as a control (black dotted lines). Representative data for infected (p24+) and uninfected (p24−) cells are shown. Mean percent of infected cells in each generation from four independent experiments are depicted as stacked columns. Error bars indicate SEM. $^{**}p < 0.01$.

See also Figure S7.

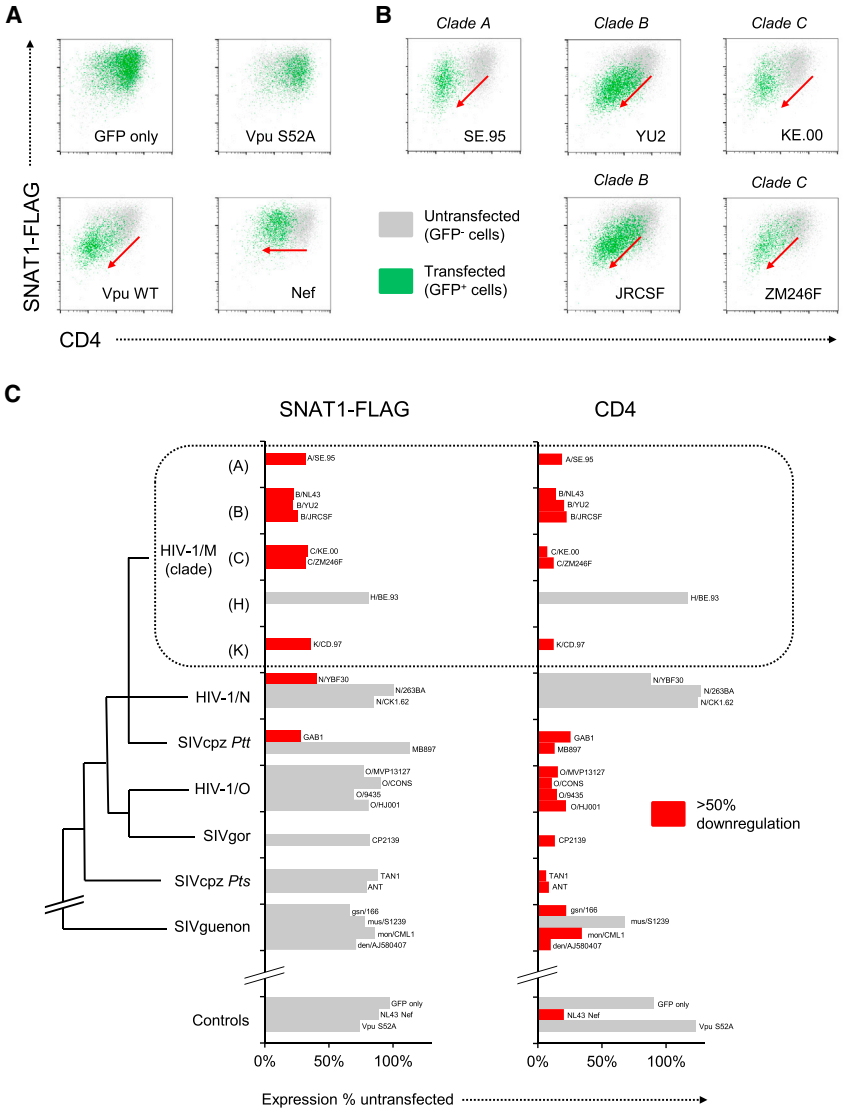

Figure 7. SNAT1 Downregulation by Vpu Variants from Pandemic HIV-1 Viruses

(A) Screening strategy for SNAT1 downregulation by naturally occurring Vpu variants. 293Ts stably expressing SNAT1-FLAG and CD4 were transfected with the indicated pCG-IRES-GFP constructs (all based on HIV-1 group M, clade B, strain NL4-3 virus) and analyzed by flow cytometry at 36 hr. Target downregulation is indicated by a shift in the transfected (GFP^+) cells toward the lower left quadrant (red arrows).

(B) SNAT1-FLAG downregulation by Vpu variants from pandemic HIV-1 group M clade A/B/C viruses. As for (A), but cells were transfected with pCG-IRES-GFP constructs encoding Vpu variants from the indicated strains of HIV-1.

(C) Phylogenetic analysis of SNAT1-FLAG downregulation by Vpu variants of HIV-1 and SIV viruses. As for (A) and (B), but cells were transfected with pCG-IRES-GFP constructs encoding Vpu variants from the indicated strains of HIV-1 or SIV and downregulation of SNAT1-FLAG or CD4 expressed as ratio of geomean fluorescence intensity between transfected (GFP^+) and untransfected (GFP^-) cells. Illustrative phylogenetic relationships are shown, and branch lengths are arbitrary (further details are included in Supplemental Experimental Procedures). HIV-1/M/N/O (HIV-1 group M, N, or O viruses); SIVcpz *Ptt* (SIVs infecting central *P. t. troglodytes* chimpanzees); SIVcpz *Pts* (SIVs infecting eastern *P. t. schweinfruthii* chimpanzees); SIVgor (gorilla SIV); SIVguenon (SIVs infecting guenon monkeys).

CoRe metabolomic screen of NCI-60 cancer cell lines confirmed that release of alanine typically correlates with release of lactate and consumption of glucose and glutamine (Jain et al., 2012). Conversely, we saw no difference between control and SNAT1-depleted cells in release of lactate or consumption of glucose and glutamine (Figures 5D and S6C), suggesting similar rates of alanine synthesis, and confirmed alanine uptake by SNAT1 in primary human CD4+ T cells using a formal transport assay and a concentration of alanine approximating that seen in vivo.

Alanine is the second most abundant amino acid in human plasma, but absent from standard media such as RPMI, and contributed to in vitro cell culture systems by serum supplementation (Rotter et al., 1979). Despite net excretion, we show that the concentration of extracellular alanine dramatically impacts T cell mitogenesis, and uptake of exogenous alanine by System A transport is critical to maintain the free intracellular alanine pool. Alanine is a major constituent of mammalian proteins and may be incorporated into the wider cellular metabolite pool by transamination. In addition, bidirectional transport of alanine at the plasma membrane may be used to drive tertiary active transport of other amino acids (Nicklin et al., 2009). The relative significance of these effects remains to be determined. While amino acid availability is known to regulate immune activation in multiple settings, antagonism of SNAT1 by HIV-1 Vpu is a specific example of viral interference with amino acid immunometabolism.

Modulation of cell surface targets by viruses may enhance viral replication directly, in a cell-autonomous fashion, or indirectly, through effects on non-infected cells or the immune response. It is difficult to account for indirect effects on virus production in vivo using in vitro models. For example, tetherin restricts (Neil et al., 2008) or enhances (Jolly et al., 2010) HIV-1 replication, depending on the assay used. The significance of tetherin as a restriction factor is instead proven by conservation of antagonism across a range of HIV and SIV viruses, and we therefore sought analagous genetic evidence for the importance of SNAT1 in the host-HIV interaction. SNAT1 antagonism was observed for HIV-1 group M Vpu variants from laboratory-adapted viruses and primary patient isolates, including a founder virus strain, X4 and R5 tropic viruses, and related HIV-1 group N and SIVcpz *Ptt* Vpu variants. Remarkably, despite the extraordinary sequence diversity of HIV-1, and the potential to dissociate SNAT1 downregulation from that of CD4 and tetherin, the ability

of Vpu to target SNAT1 is therefore conserved across pandemic HIV-1 viruses, suggesting a significant selective advantage. Furthermore, the restriction of SNAT1 downregulation to Vpu variants from the SIVcpz/HIV-1 lineage suggests a specific role in the pathogenesis of these viruses.

EXPERIMENTAL PROCEDURES

HIV-1 Infections

For proteomic time course analysis, CEM-T4 T cells were spinoculated with VSVg-pseudotyped NL4-3-dE-EGFP HIV-1 virus at an MOI of 10, aliquots of infected cells harvested sequentially at the indicated time points, and dead cells removed by immunomagnetic depletion prior to PMP.

Plasma Membrane Enrichment and Peptide Labeling

PMP was performed as previously described (Weekes et al., 2013, 2014) using 2×10^7 viable cells per condition and a "one pot" oxidation and aminooxy-biotinylation reaction to selectively biotinylate plasma membrane glycoproteins before immunoprecipitation with streptavidin beads and on-bead tryptic digestion. For TMT quantitation, cells from each condition were processed separately, and peptide samples were labeled with TMT reagents before pooling. For SILAC quantitation, cells were pre-labeled by propagation in SILAC media and pooled prior to processing together.

Proteomics and Data Analysis

Peptide samples were fractionated by high-pH reverse-phase high-pressure liquid chromatography (HpRP-HPLC) and analyzed by liquid chromatography coupled to triple-stage (TMT) or tandem (SILAC) mass spectrometry using an Orbitrap Fusion Tribrid (TMT) or Q Exactive (SILAC) mass spectrometer. Reporter ions from TMT-labeled peptides were quantitated from an MS3 scan using Proteome Discoverer. SILAC-labeled peptides were quantitated using MaxQuant.

Primary Cell Knockdowns

Primary human CD4+ T cells were activated with CD3/CD28 Dynabeads and transduced with lentiviral constructs encoding U6-shRNA knockdown and SFFV-SBP-ΔLNGFR streptavidin-binding affinity tag cassettes. Transduced cells were selected with streptavidin Dynabeads then released by incubation with excess biotin as previously described (AFMACS) (Matheson et al., 2014). Ethical permission for this project was granted by the Cambridgeshire 2 Research Ethics Committee (REC reference 97/092). Informed written consent was obtained from all of the volunteers included in this study prior to providing blood samples.

CoRe Metabolomics and Data Analysis

AFMACS-purified primary human CD4+ T cells expressing control or SNAT1-specific shRNAs were re-stimulated using CD3/CD28 Dynabeads. After 24 hr, cells were resuspended in 20% conditioned media at equal densities and supernatant samples at baseline, 24, and 48 hr were analyzed by liquid chromatography coupled to mass spectrometry (LC-MS) as previously described (Jain et al., 2012). To account for differential proliferation, viable cells were enumerated at each time point and changes in metabolite concentrations normalized based on average cell numbers.

3H-Alanine Uptake

AFMACS-purified primary human CD4+ T cells expressing control or SNAT1-specific shRNAs were re-stimulated using CD3/CD2 min8 Dynabeads. After 48 hr, cells were starved to reduce *trans*-inhibition then resuspended at 37°C in Tyrode's buffer supplemented with 3H-alanine at a final concentration of 0.5 mM. Aliquots of cells were harvested sequentially over 5 min and uptake terminated by filtering centrifugation through silicone oil before liquid scintillation counting.

Free Intracellular Amino Acids

Primary human CD4+ T cells were expanded once and then re-stimulated using CD3/CD28 Dynabeads. After 48 hr, cells were resuspended in media supplemented with dialyzed FCS and either unlabeled alanine and glucose or (for stable isotopologue-resolved metabolomics) 15N-alanine and 13C6-glucose at concentrations of 0.5 mM and 5.6 mM, respectively. Aliquots of cells were harvested sequentially over 1 hr, and free intracellular amino acids were extracted from washed cells using dry ice-cold 50% methanol 30% acetonitrile before analysis by LC-MS. Please see Supplemental Experimental Procedures for further details.

SUPPLEMENTAL INFORMATION

Supplemental Information includes Supplemental Experimental Procedures, seven figures, and three tables and can be found with this article online at http://dx.doi.org/10.1016/j.chom.2015.09.003.

AUTHOR CONTRIBUTIONS

N.J.M. and P.J.L. conceived the project and wrote the manuscript; N.J.M., J.S., K.W., R.R., M.P.W., R.V., and J.W. performed experiments; M.P.W. and N.J.M. developed proteomic methods; M.S. supplied essential reagents; R.A. conducted proteomic mass spectrometry; A.S.H.C., C.F., and C.B.C. conducted metabolomic mass spectrometry; and S.J.D.N. and P.J.L. supervised the project. J.S., K.W., and R.R. contributed equally to the final manuscript.

ACKNOWLEDGMENTS

This work was supported by a Wellcome Trust PRF (WT101835) to P.J.L. and SRF (WT098049) to S.J.D.N., the NIHR Cambridge BRC, a Wellcome Trust Strategic Award to CIMR, and the Addenbrooke's Charitable Trust. M.P.W. is a Wellcome Trust Fellow (093966/Z/10/Z), and N.J.M. is a Wellcome Trust Training Fellow (093964/Z/10/Z) and Raymond and Beverly Sackler student. The authors thank Dr. Jenny Ho (Thermo) for help with proteomics, Dr. Jo Glazier (University of Manchester) and Dr. Richard Boyd (University of Oxford) for advice on amino acid transport assays, Dr. Reiner Schulte and his team for FACS, Matthew Gratian and Mark Bowen for microscopy, and the Lehner laboratory for critical discussion.

Received: July 2, 2015
Revised: August 30, 2015
Accepted: September 10, 2015
Published: October 1, 2015

REFERENCES

Abraham, L., and Fackler, O.T. (2012). HIV-1 Nef: a multifaceted modulator of T cell receptor signaling. Cell Commun. Signal. *10*, 39.

Brandt, C.S., Baratin, M., Yi, E.C., Kennedy, J., Gao, Z., Fox, B., Haldeman, B., Ostrander, C.D., Kaifu, T., Chabannon, C., et al. (2009). The B7 family member B7-H6 is a tumor cell ligand for the activating natural killer cell receptor NKp30 in humans. J. Exp. Med. *206*, 1495–1503.

Carr, E.L., Kelman, A., Wu, G.S., Gopaul, R., Senkevitch, E., Aghvanyan, A., Turay, A.M., and Frauwirth, K.A. (2010). Glutamine uptake and metabolism are coordinately regulated by ERK/MAPK during T lymphocyte activation. J. Immunol. *185*, 1037–1044.

Chaudhry, F.A., Reimer, R.J., and Edwards, R.H. (2002). The glutamine commute: take the N line and transfer to the A. J. Cell Biol. *157*, 349–355.

Chuang, J.C., Yu, C.L., and Wang, S.R. (1990). Modulation of human lymphocyte proliferation by amino acids. Clin. Exp. Immunol. *81*, 173–176.

Douglas, J.L., Viswanathan, K., McCarroll, M.N., Gustin, J.K., Früh, K., and Moses, A.V. (2009). Vpu directs the degradation of the human immunodeficiency virus restriction factor BST-2/Tetherin via a betaTrCP-dependent mechanism. J. Virol. *83*, 7931–7947.

Gu, S., Roderick, H.L., Camacho, P., and Jiang, J.X. (2001). Characterization of an N-system amino acid transporter expressed in retina and its involvement in glutamine transport. J. Biol. Chem. *276*, 24137–24144.

Haller, C., Müller, B., Fritz, J.V., Lamas-Murua, M., Stolp, B., Pujol, F.M., Keppler, O.T., and Fackler, O.T. (2014). HIV-1 Nef and Vpu are functionally

redundant broad-spectrum modulators of cell surface receptors, including tetraspanins. J. Virol. *88*, 14241–14257.

Hemelaar, J., Gouws, E., Ghys, P.D., and Osmanov, S.; WHO-UNAIDS Network for HIV Isolation and Characterisation (2011). Global trends in molecular epidemiology of HIV-1 during 2000-2007. AIDS *25*, 679–689.

Hout, D.R., Gomez, M.L., Pacyniak, E., Gomez, L.M., Inbody, S.H., Mulcahy, E.R., Culley, N., Pinson, D.M., Powers, M.F., Wong, S.W., and Stephens, E.B. (2005). Scrambling of the amino acids within the transmembrane domain of Vpu results in a simian-human immunodeficiency virus (SHIVTM) that is less pathogenic for pig-tailed macaques. Virology *339*, 56–69.

Jain, M., Nilsson, R., Sharma, S., Madhusudhan, N., Kitami, T., Souza, A.L., Kafri, R., Kirschner, M.W., Clish, C.B., and Mootha, V.K. (2012). Metabolite profiling identifies a key role for glycine in rapid cancer cell proliferation. Science *336*, 1040–1044.

Jolly, C., Booth, N.J., and Neil, S.J. (2010). Cell-cell spread of human immunodeficiency virus type 1 overcomes tetherin/BST-2-mediated restriction in T cells. J. Virol. *84*, 12185–12199.

Keele, B.F., Jones, J.H., Terio, K.A., Estes, J.D., Rudicell, R.S., Wilson, M.L., Li, Y., Learn, G.H., Beasley, T.M., Schumacher-Stankey, J., et al. (2009). Increased mortality and AIDS-like immunopathology in wild chimpanzees infected with SIVcpz. Nature *460*, 515–519.

Kirchhoff, F. (2009). Is the high virulence of HIV-1 an unfortunate coincidence of primate lentiviral evolution? Nat. Rev. Microbiol. *7*, 467–476.

Lambelé, M., Koppensteiner, H., Symeonides, M., Roy, N.H., Chan, J., Schindler, M., and Thali, M. (2015). Vpu is the main determinant for tetraspanin downregulation in HIV-1-infected cells. J. Virol. *89*, 3247–3255.

Mackenzie, B., and Erickson, J.D. (2004). Sodium-coupled neutral amino acid (System N/A) transporters of the SLC38 gene family. Pflugers Arch. *447*, 784–795.

Malim, M.H., and Emerman, M. (2008). HIV-1 accessory proteins–ensuring viral survival in a hostile environment. Cell Host Microbe *3*, 388–398.

Margottin, F., Bour, S.P., Durand, H., Selig, L., Benichou, S., Richard, V., Thomas, D., Strebel, K., and Benarous, R. (1998). A novel human WD protein, h-beta TrCp, that interacts with HIV-1 Vpu connects CD4 to the ER degradation pathway through an F-box motif. Mol. Cell *1*, 565–574.

Matheson, N.J., Peden, A.A., and Lehner, P.J. (2014). Antibody-free magnetic cell sorting of genetically modified primary human CD4+ T cells by one-step streptavidin affinity purification. PLoS ONE *9*, e111437.

Matta, J., Baratin, M., Chiche, L., Forel, J.M., Cognet, C., Thomas, G., Farnarier, C., Piperoglou, C., Papazian, L., Chaussabel, D., et al. (2013). Induction of B7-H6, a ligand for the natural killer cell-activating receptor NKp30, in inflammatory conditions. Blood *122*, 394–404.

Matusali, G., Potestà, M., Santoni, A., Cerboni, C., and Doria, M. (2012). The human immunodeficiency virus type 1 Nef and Vpu proteins downregulate the natural killer cell-activating ligand PVR. J. Virol. *86*, 4496–4504.

Mitchell, R.S., Katsura, C., Skasko, M.A., Fitzpatrick, K., Lau, D., Ruiz, A., Stephens, E.B., Margottin-Goguet, F., Benarous, R., and Guatelli, J.C. (2009). Vpu antagonizes BST-2-mediated restriction of HIV-1 release via beta-TrCP and endo-lysosomal trafficking. PLoS Pathog. *5*, e1000450.

Moll, M., Andersson, S.K., Smed-Sörensen, A., and Sandberg, J.K. (2010). Inhibition of lipid antigen presentation in dendritic cells by HIV-1 Vpu interference with CD1d recycling from endosomal compartments. Blood *116*, 1876–1884.

Monroe, K.M., Yang, Z., Johnson, J.R., Geng, X., Doitsh, G., Krogan, N.J., and Greene, W.C. (2014). IFI16 DNA sensor is required for death of lymphoid CD4 T cells abortively infected with HIV. Science *343*, 428–432.

Nakaya, M., Xiao, Y., Zhou, X., Chang, J.H., Chang, M., Cheng, X., Blonska, M., Lin, X., and Sun, S.C. (2014). Inflammatory T cell responses rely on amino acid transporter ASCT2 facilitation of glutamine uptake and mTORC1 kinase activation. Immunity *40*, 692–705.

Neil, S.J., Zang, T., and Bieniasz, P.D. (2008). Tetherin inhibits retrovirus release and is antagonized by HIV-1 Vpu. Nature *451*, 425–430.

Nicklin, P., Bergman, P., Zhang, B., Triantafellow, E., Wang, H., Nyfeler, B., Yang, H., Hild, M., Kung, C., Wilson, C., et al. (2009). Bidirectional transport of amino acids regulates mTOR and autophagy. Cell *136*, 521–534.

Oxender, D.L., and Christensen, H.N. (1963). Evidence for two types of mediation of neutral and amino-acid transport in Ehrlich cells. Nature *197*, 765–767.

Ramirez, P.W., Famiglietti, M., Sowrirajan, B., DePaula-Silva, A.B., Rodesch, C., Barker, E., Bosque, A., and Planelles, V. (2014). Downmodulation of CCR7 by HIV-1 Vpu results in impaired migration and chemotactic signaling within $CD4^+$ T cells. Cell Rep. *7*, 2019–2030.

Rotter, V., Yakir, Y., and Trainin, N. (1979). Role of L-alanine in the response of human lymphocytes to PHA and Con A. J. Immunol. *123*, 1726–1731.

Sato, K., Misawa, N., Fukuhara, M., Iwami, S., An, D.S., Ito, M., and Koyanagi, Y. (2012). Vpu augments the initial burst phase of HIV-1 propagation and downregulates BST2 and CD4 in humanized mice. J. Virol. *86*, 5000–5013.

Sauter, D., Schindler, M., Specht, A., Landford, W.N., Münch, J., Kim, K.A., Votteler, J., Schubert, U., Bibollet-Ruche, F., Keele, B.F., et al. (2009). Tetherin-driven adaptation of Vpu and Nef function and the evolution of pandemic and nonpandemic HIV-1 strains. Cell Host Microbe *6*, 409–421.

Schindler, M., Münch, J., Kutsch, O., Li, H., Santiago, M.L., Bibollet-Ruche, F., Müller-Trutwin, M.C., Novembre, F.J., Peeters, M., Courgnaud, V., et al. (2006). Nef-mediated suppression of T cell activation was lost in a lentiviral lineage that gave rise to HIV-1. Cell *125*, 1055–1067.

Schubert, U., Antón, L.C., Bacík, I., Cox, J.H., Bour, S., Bennink, J.R., Orlowski, M., Strebel, K., and Yewdell, J.W. (1998). CD4 glycoprotein degradation induced by human immunodeficiency virus type 1 Vpu protein requires the function of proteasomes and the ubiquitin-conjugating pathway. J. Virol. *72*, 2280–2288.

Segel, G.B. (1992). Amino Acid Transport in Lymphocytes. In Mammalian Amino Acid Transport, M.S. Kilberg and D. Haussinger, eds. (Springer), pp. 261–274.

Shah, A.H., Sowrirajan, B., Davis, Z.B., Ward, J.P., Campbell, E.M., Planelles, V., and Barker, E. (2010). Degranulation of natural killer cells following interaction with HIV-1-infected cells is hindered by downmodulation of NTB-A by Vpu. Cell Host Microbe *8*, 397–409.

Sinclair, L.V., Rolf, J., Emslie, E., Shi, Y.B., Taylor, P.M., and Cantrell, D.A. (2013). Control of amino-acid transport by antigen receptors coordinates the metabolic reprogramming essential for T cell differentiation. Nat. Immunol. *14*, 500–508.

Singh, D.K., Griffin, D.M., Pacyniak, E., Jackson, M., Werle, M.J., Wisdom, B., Sun, F., Hout, D.R., Pinson, D.M., Gunderson, R.S., et al. (2003). The presence of the casein kinase II phosphorylation sites of Vpu enhances the CD4(+) T cell loss caused by the simian-human immunodeficiency virus SHIV(KU-1bMC33) in pig-tailed macaques. Virology *313*, 435–451.

Stephens, E.B., McCormick, C., Pacyniak, E., Griffin, D., Pinson, D.M., Sun, F., Nothnick, W., Wong, S.W., Gunderson, R., Berman, N.E., and Singh, D.K. (2002). Deletion of the vpu sequences prior to the env in a simian-human immunodeficiency virus results in enhanced Env precursor synthesis but is less pathogenic for pig-tailed macaques. Virology *293*, 252–261.

Swigut, T., Shohdy, N., and Skowronski, J. (2001). Mechanism for down-regulation of CD28 by Nef. EMBO J. *20*, 1593–1604.

Tokarev, A., and Guatelli, J. (2011). Misdirection of membrane trafficking by HIV-1 Vpu and Nef: Keys to viral virulence and persistence. Cell. Logist. *1*, 90–102.

Varoqui, H., Zhu, H., Yao, D., Ming, H., and Erickson, J.D. (2000). Cloning and functional identification of a neuronal glutamine transporter. J. Biol. Chem. *275*, 4049–4054.

Vassena, L., Giuliani, E., Koppensteiner, H., Bolduan, S., Schindler, M., and Doria, M. (2015). HIV-1 Nef and Vpu Interfere with L-Selectin (CD62L) Cell Surface Expression To Inhibit Adhesion and Signaling in Infected CD4+ T Lymphocytes. J. Virol. *89*, 5687–5700.

Vigan, R., and Neil, S.J. (2010). Determinants of tetherin antagonism in the transmembrane domain of the human immunodeficiency virus type 1 Vpu protein. J. Virol. *84*, 12958–12970.

Wang, R., Dillon, C.P., Shi, L.Z., Milasta, S., Carter, R., Finkelstein, D., McCormick, L.L., Fitzgerald, P., Chi, H., Munger, J., and Green, D.R. (2011). The transcription factor Myc controls metabolic reprogramming upon T lymphocyte activation. Immunity *35*, 871–882.

Weekes, M.P., Tan, S.Y., Poole, E., Talbot, S., Antrobus, R., Smith, D.L., Montag, C., Gygi, S.P., Sinclair, J.H., and Lehner, P.J. (2013). Latency-associated degradation of the MRP1 drug transporter during latent human cytomegalovirus infection. Science *340*, 199–202.

Weekes, M.P., Tomasec, P., Huttlin, E.L., Fielding, C.A., Nusinow, D., Stanton, R.J., Wang, E.C., Aicheler, R., Murrell, I., Wilkinson, G.W., et al. (2014). Quantitative temporal viromics: an approach to investigate host-pathogen interaction. Cell *157*, 1460–1472.

Zhang, F., Wilson, S.J., Landford, W.C., Virgen, B., Gregory, D., Johnson, M.C., Munch, J., Kirchhoff, F., Bieniasz, P.D., and Hatziioannou, T. (2009). Nef proteins from simian immunodeficiency viruses are tetherin antagonists. Cell Host Microbe *6*, 54–67.

Cell Host & Microbe, Volume *18*

Supplemental Information

Cell Surface Proteomic Map of HIV Infection Reveals Antagonism of Amino Acid Metabolism by Vpu and Nef

Nicholas J. Matheson, Jonathan Sumner, Kim Wals, Radu Rapiteanu, Michael P. Weekes, Raphael Vigan, Julia Weinelt, Michael Schindler, Robin Antrobus, Ana S.H. Costa, Christian Frezza, Clary B. Clish, Stuart J.D. Neil, and Paul J. Lehner

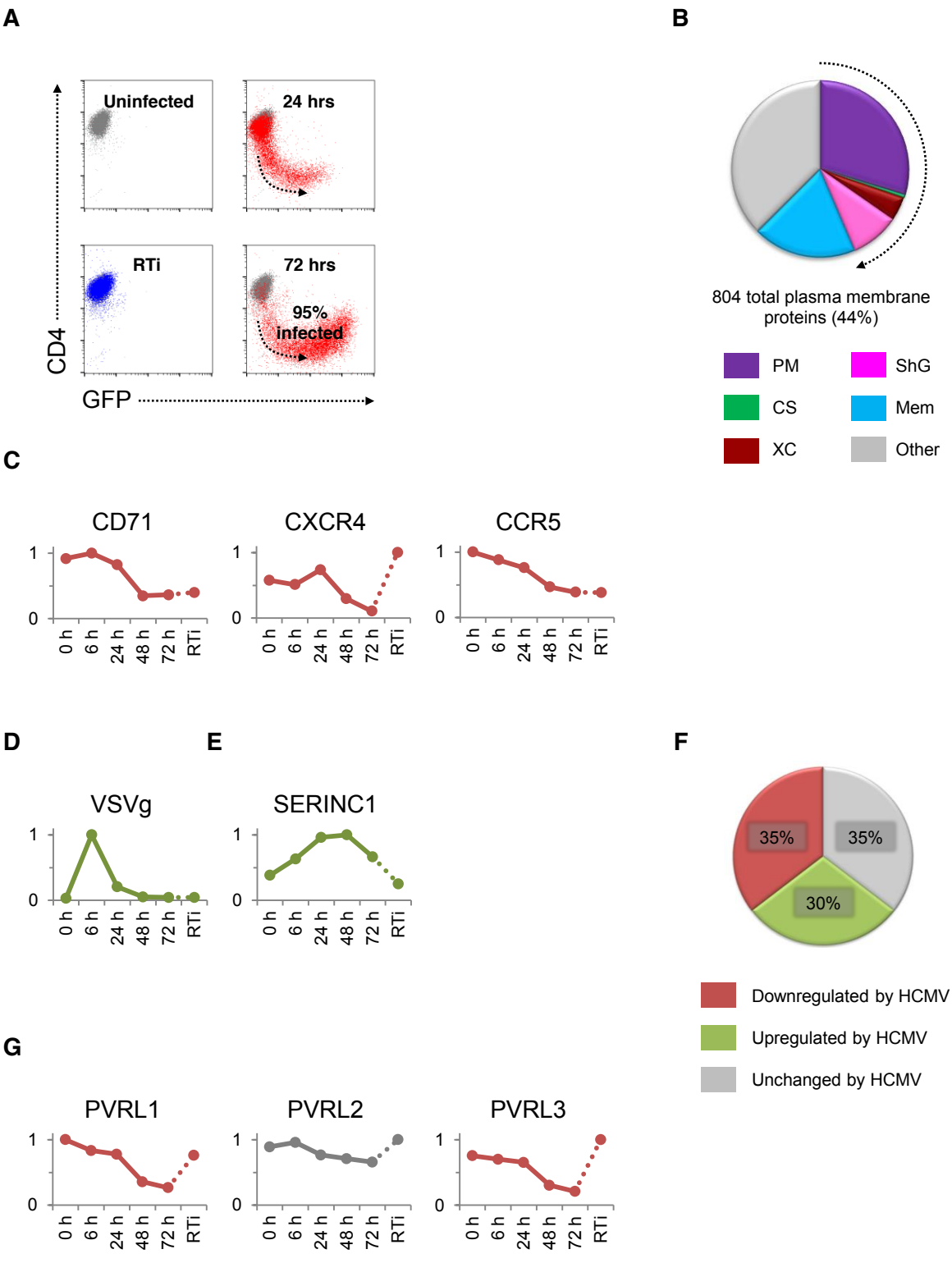

Figure S1. Controls for TMT-based Proteomic Timecourse and Comparison with HCMV Infection, Related to Figure 1

(A) Identification of HIV-infected cells. Cells from **Figure 1A** were stained with anti-CD4 antibody and analysed by flow cytometry. Productive infection with VSVg-pseudotyped NL4-

3-deltaE-EGFP virus results in expression of GFP and downregulation of CD4 by Nef and Vpu. Uninfected cells (grey), cells infected for 24 and 72 hrs (red) and cells infected for 72 hrs in the presence of reverse transcriptase inhibitors (blue) are shown.

(B) Gene Ontology Cellular Compartment (GOCC) annotation of quantitated proteins. PM, plasma membrane; CS, cell surface; XC, extracellular; ShG, short GOCC (a subset of proteins with short membrane-specific GOCC terms but no subcellular assignment (Weekes et al., 2012); Mem, membrane. 1,846 of 2,320 quantitated proteins had GOCC annotations, of which 804 (44%) were indicative of plasma membrane localisation.

(C) Temporal profiles of other reported targets for HIV-mediated downregulation (Drakesmith et al., 2005; Koppensteiner et al., 2014; Michel et al., 2006; Ramirez et al., 2014).

(D) Temporal profile of VSVg.

(E) Temporal profile of SERINC1.

(F) Differential regulation of cell surface proteins by HIV and HCMV infection. 79 proteins from Cluster #35 (cell surface proteins progressively downregulated by HIV) were previously quantitated in HCMV-infected fibroblasts (Weekes et al., 2014) and found to be variably upregulated, downregulated, or unchanged by HCMV infection.

(G) Temporal profiles of nectins (PVRL1-3) revealing differential regulation by HIV and HCMV. Nectin-2 (PVRL2, CD112) is targeted for proteasomal degradation by co-operation between the HCMV proteins UL141 and US2. Conversely, in HIV-1-infected cells (as shown), we observed downregulation of nectin-1 (PVRL1, CD111) and nectin-3 (PVRL3, CD113), but not nectin-2.

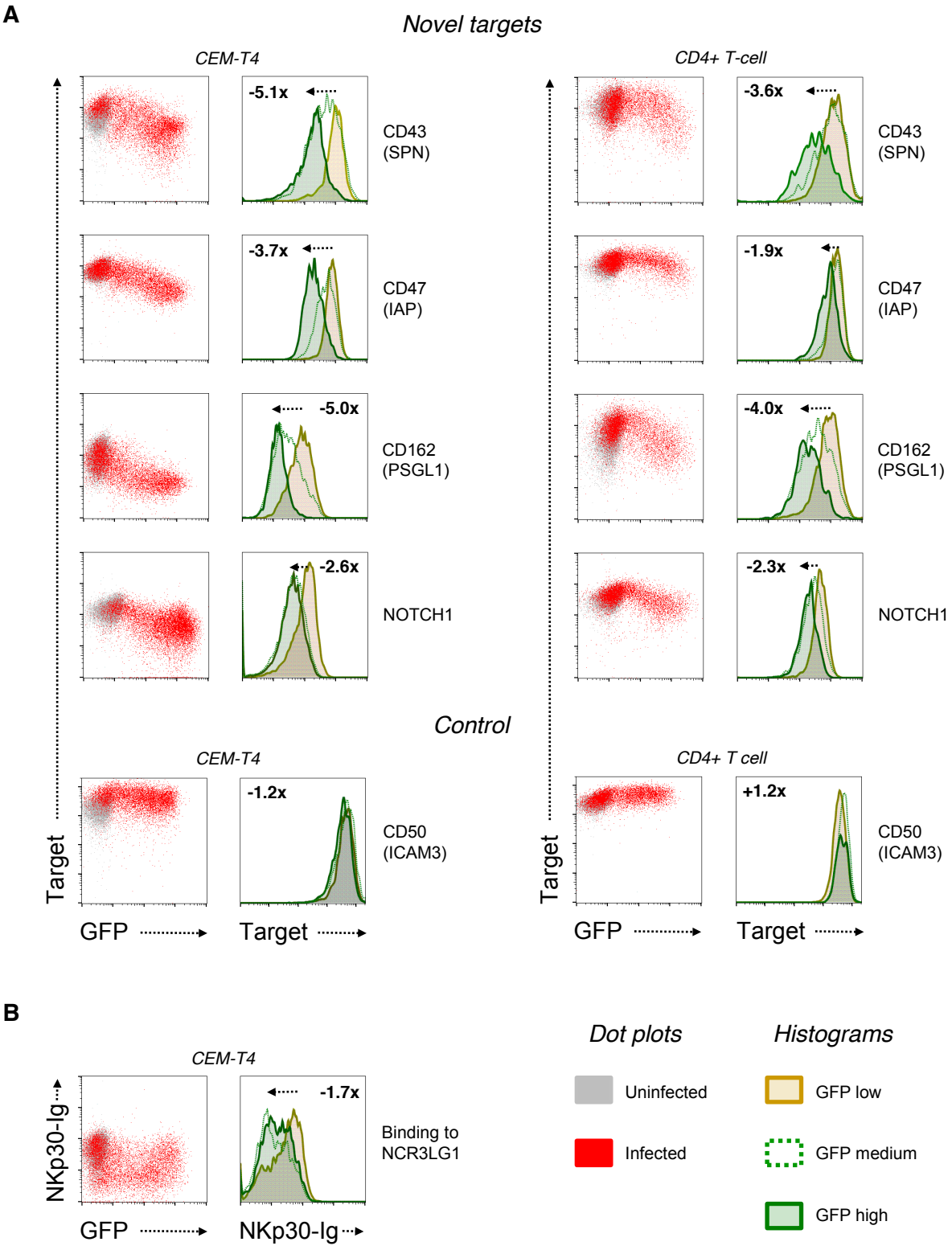

Figure S2. Flow Cytometric Validation of Novel HIV-1 Targets, Related to Figure 2

(A) Validation of novel HIV-1 targets by flow cytometry in CEM-T4s and primary T-cells. CEM-T4s or primary human CD4+ T-cells stimulated with CD3/CD28 Dynabeads were stained with antibodies against the indicated targets 48 hrs after infection with NL4-3-deltaE-

EGFP HIV-1 virus typically at an MOI of 1. Target expression is shown for GFP low, medium and high cells and fold-change in geomean fluorescence intensity high/low is indicated. Negative values denote downregulation in productively infected (GFP-expressing) cells. CD50 abundance was unchanged by HIV-infection in the TMT dataset and is included as a control.

(B) Downregulation of NCR3LG1. CEM-T4s were stained with NKp30-Ig fusion protein (endogenous NCR3LG1 ligand) 48 hrs after infection with NL4-3-deltaE-EGFP HIV-1 virus at an MOI of 1. As in (A) NKp30-Ig binding is shown for GFP low, medium and high cells and fold-change high/low is indicated.

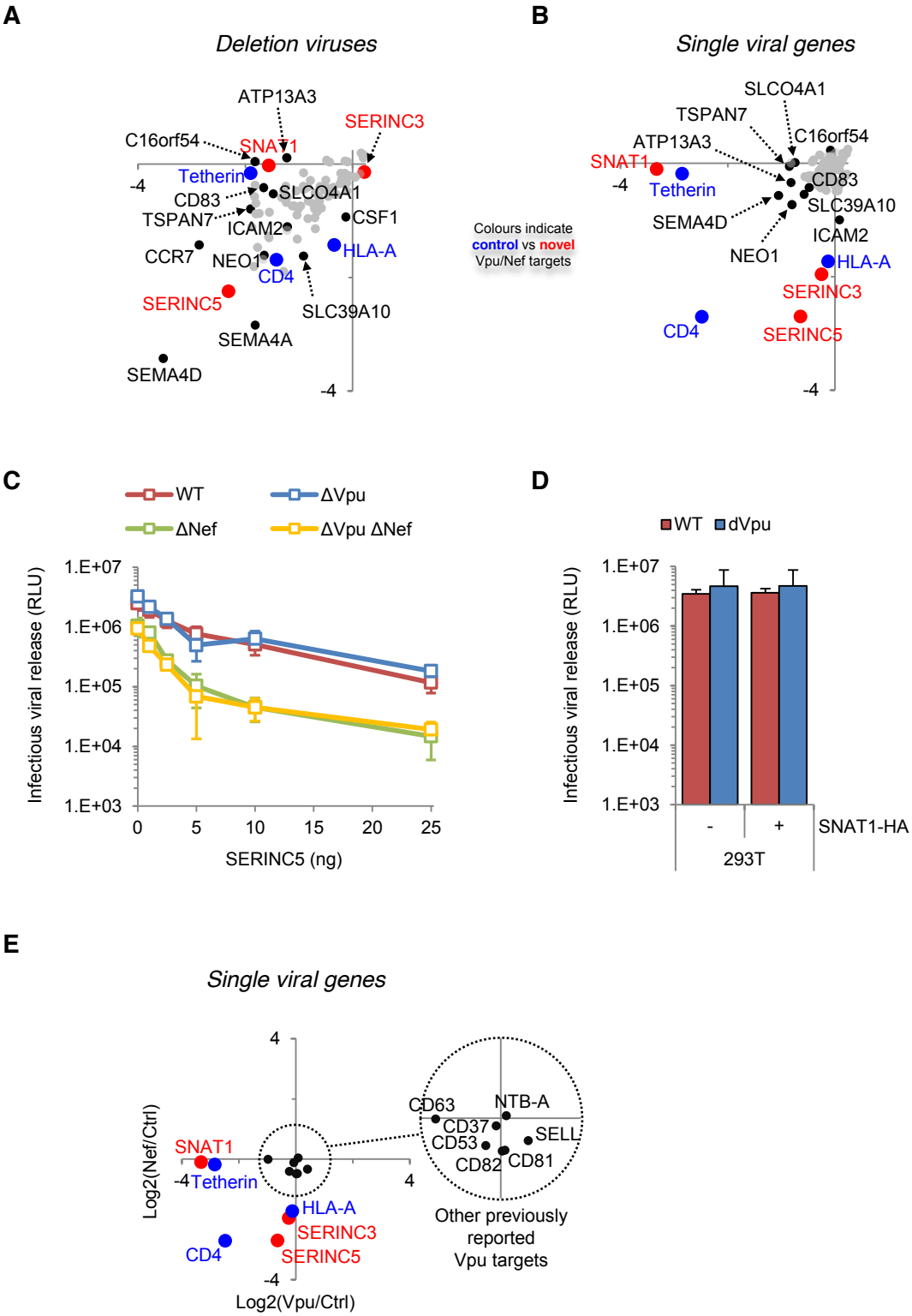

Figure S3. Novel Vpu and Nef targets, Related to Figure 3

(A-B) SILAC-based quantitation of plasma membrane proteins in cells infected with Vpu-deficient (y-axis) versus Nef-deficient (x-axis) viruses (A; enlarged left lower quadrant of scatterplot shown in **Figure 3A**) or transduced with Vpu (x-axis) versus Nef (y-axis) as single

genes (B; enlarged left lower quadrant of scatterplot shown in **Figure 3B**). Outliers of potential interest are labelled.

(C) Restriction of HIV-1 virus production by SERINC5. 293Ts were co-transfected with the indicated pNL4-3 HIV-1 molecular clones plus increasing concentrations of pCR3.1-SERINC5 and 48 hr culture supernatants assayed for infectious viral release using HeLa-TZM-bl cells. Mean values and 95% confidence intervals are shown.

(D) No effect on HIV-1 virus production by SNAT1. Control and SNAT1-HA-expressing 293Ts were infected with the indicated VSVg-pseudotyped NL4-3 HIV-1 viruses at an MOI of 2 and 48 hr culture supernatants assayed for infectious virus release using HeLa-TZM-bl cells. Mean values and 95% confidence intervals are shown.

(E) Comparison of SNAT1 with known Vpu targets. As for (B) and Figure 3B, but showing downregulation of SNAT1, CD4 and tetherin compared with previously reported Vpu targets NTB-A, SELL, CD37, CD53, CD63, CD81 and CD82. HLA-A (downregulated by Nef) is also shown. CCR7, CD1d and PVR (CD155) were not quantitated in this experiment, but CCR7 was downregulated by both ΔVpu and ΔNef viruses. CD53 was quantitated on the basis of a single PSM.

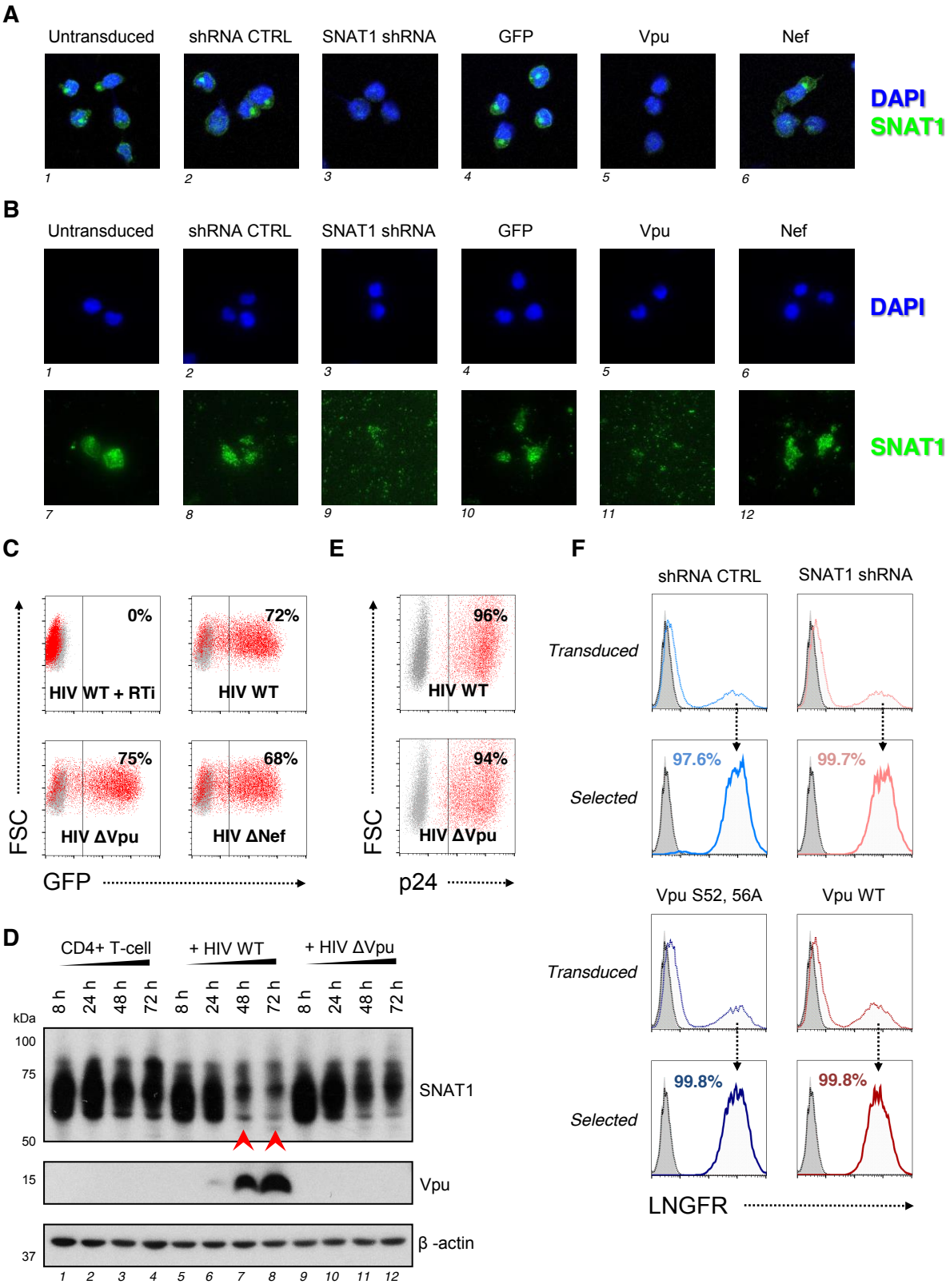

Figure S4. Validation of SNAT1 Depletion, Related to Figure 3

(A-B) Cell surface SNAT1 depletion by Vpu. Cells from **Figure 3E** were stained with anti-SNAT1 antibody (green) and DAPI (blue) and analysed by confocal microscopy (A) or TIRF

microscopy (B). TIRF microscopy enables selective visualisation of the plasma membrane (SNAT1; lower panels) with widefield images (DAPI; upper panels) included as controls.

(C) Infection controls for **Figures 3C-D**. Cells from **Figures 3C-D** were analysed by flow cytometry 48 hrs after infection with the indicated NL4-3-deltaE-EGFP HIV-1 viruses. In each case % productively infected (GFP+) cells is indicated. Uninfected cells (grey) are also shown.

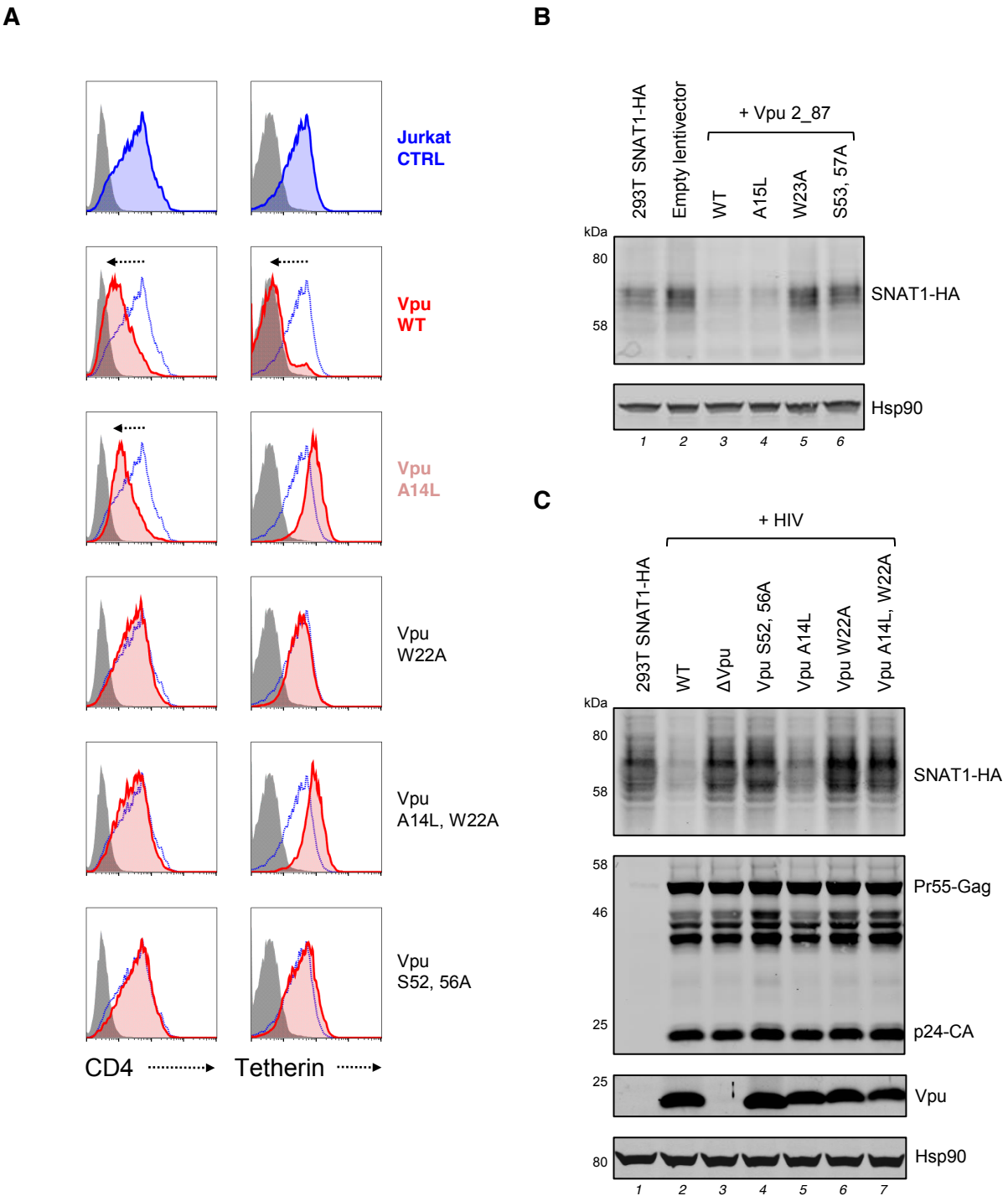

Figure S5. Controls for Mechanism of SNAT1 Depletion, Related to Figure 4

(A) Molecular determinants of CD4 and tetherin downregulation. Cells from **Figure 4F** were stained with anti-CD4 or anti-tetherin antibodies and analysed by flow cytometry. Jurkats transduced with empty vector (blue) or Vpu variants (red) are shown. Unstained cells (CD4) or cells stained with secondary antibody only (tetherin) are included as controls (grey).

(B) Depletion of SNAT1 by Vpu 2_87. 293Ts stably expressing SNAT1-HA were transduced with the indicated Vpu constructs at an MOI of 2 then immunoblotted with anti-HA and HSP90 (loading control) antibodies.

(C) Molecular determinants of SNAT1 depletion by HIV-1. 293Ts stably expressing SNAT1-HA were infected with the indicated VSVg-pseudotyped NL4-3 HIV-1 viruses at an MOI of 2 then immunoblotted with anti-HA, anti-p24, anti-Vpu and anti-HSP90 (loading control) antibodies.

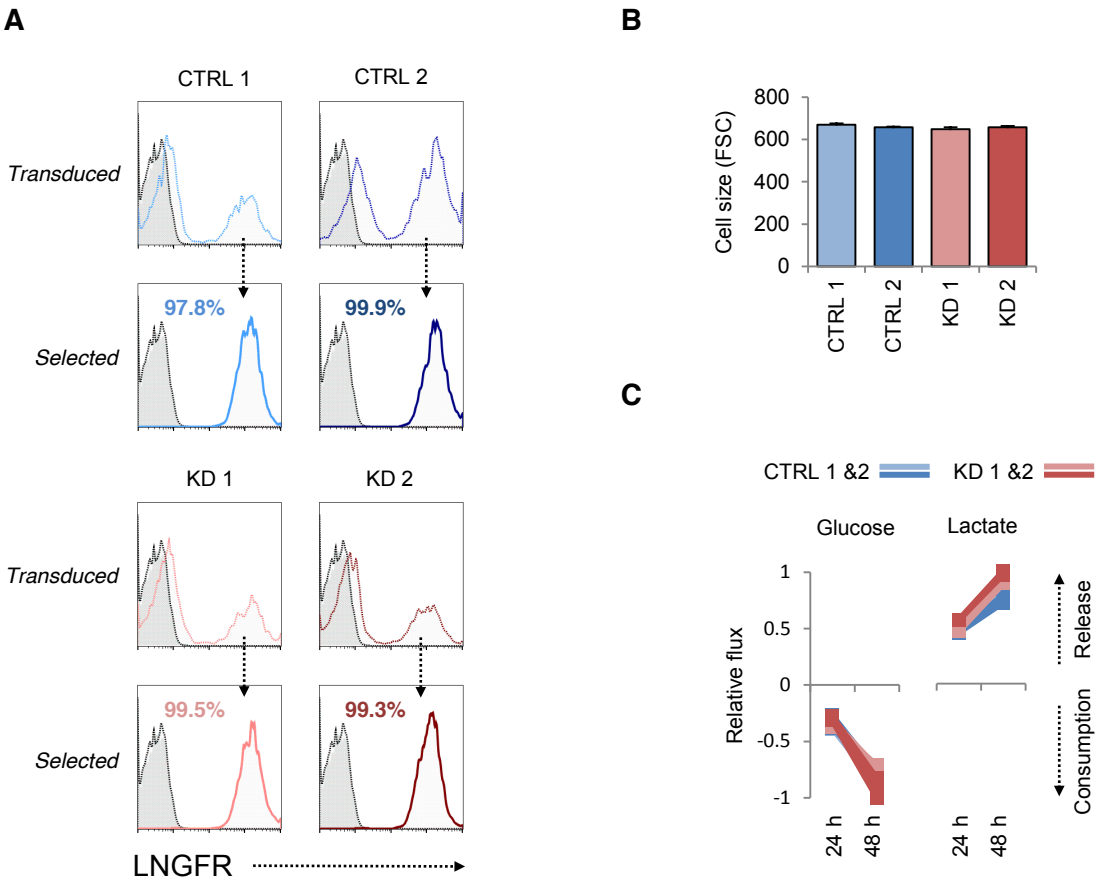

Figure S6. Controls for CoRe Metabolomics, Related to Figure 5

(A) Enrichment of transduced cells by AFMACS. Transduced cells from **Figures 5A-D** were stained with anti-LNGFR antibody before and after selection by AFMACS (red and blue lines). In each case, unstained cells (grey) and control cells stained with anti-LNGFR antibody (dotted line) are included and % LNGFR positive cells after selection are shown.

(B) No change in size of T-cells in response to SNAT1 depletion. Cells from **Figure 5B** were analysed by flow cytometry 48 hrs after re-stimulation with CD3/CD28 Dynabeads. Cell size is indicated by intensity of forward-scattered light (FSC). Mean values and 95% confidence intervals are shown for data obtained in triplicate.

(C) No change in glucose uptake or lactate release by SNAT1 depleted T-cells. As for **Figure 5D**, but net consumption or release of glucose and lactate by control and SNAT1-depleted cells is shown, scaled to a maximum change of 1.

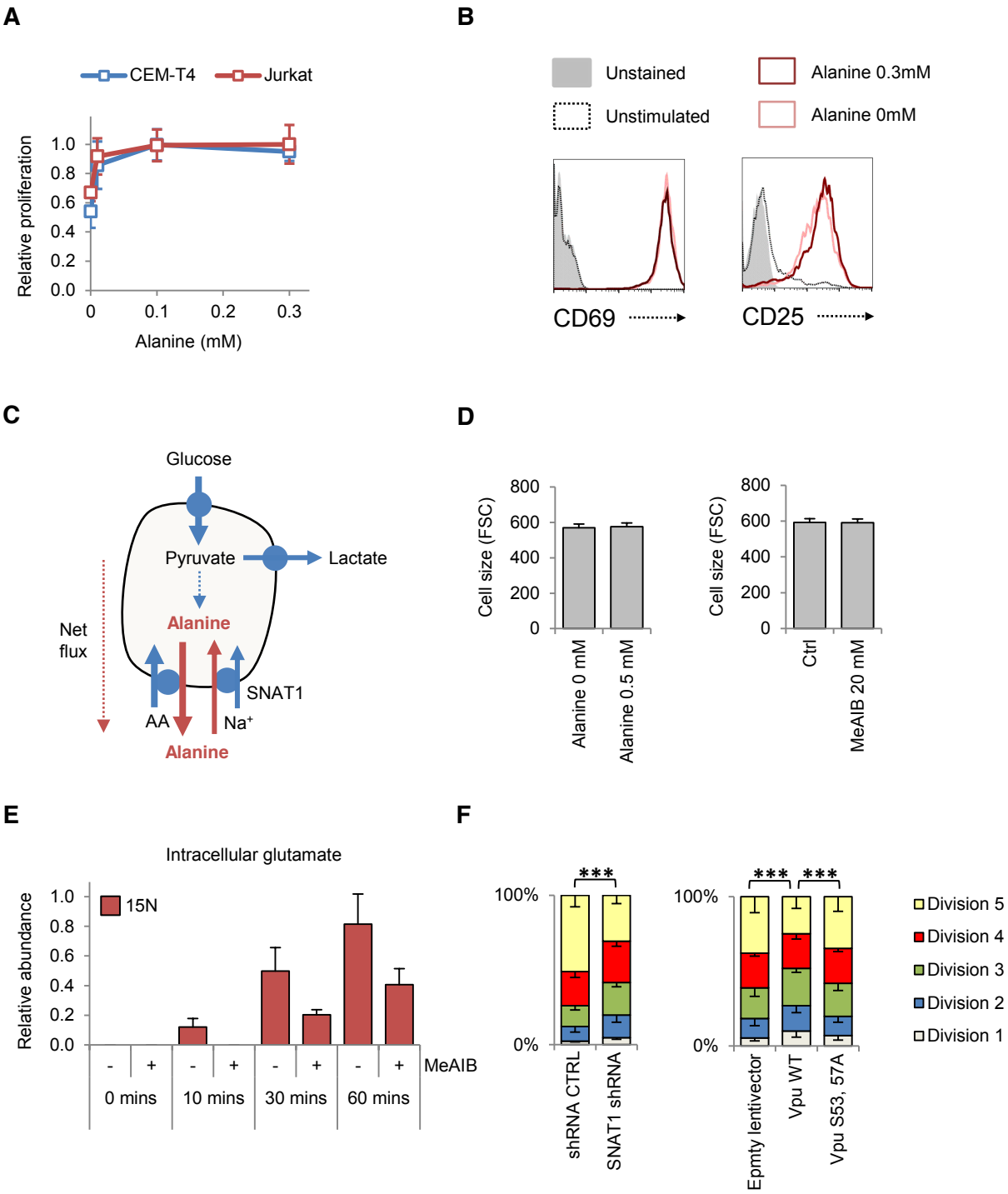

Figure S7. Controls for Free Intracellular Amino Acids, Related to Figure 6

(A) Dose-dependent proliferation of CEM-T4s and Jurkats in response to exogenous alanine. CEM-T4 and Jurkat T-cells were seeded in phenol red-free media supplemented with alanine at the concentrations indicated. Viable cells were enumerated using an MTT assay after 72 hrs and optical density expressed as fraction of maximum.

(B) Preserved CD69 and CD25 expression in the absence of alanine. As for **Figure 6A** but cells were stained with conjugated antibodies against CD69 and CD25 and analysed by flow cytometry after 24 hrs.